

THIS VERSION OF DIABLO CANYON POWER PLANT FINAL SAFETY ANALYSIS REPORT UPDATE (UFSAR) CONTAINS SECTIONS 2.5, 3.7 AND 3.10 OF THE LICENSEE'S REVISION 21, ISSUED SEPTEMBER 2013, WITH CERTAIN REDACTIONS OF SENSITIVE INFORMATION BY STAFF OF THE NUCLEAR REGULATORY COMMISSION (nrc) TO ALLOW RELEASE TO THE PUBLIC. THE REDACTIONS ARE MADE UNDER 10 CFR 2.390(d)(1). THE MATERIAL INCLUDED WITH IS CLASSIFIED AS PUBLICLY AVAILABLE INFORMATION. AS OF SEPTEMBER 2014, THIS IS THE LATEST UFSAR REVISION SUBMITTED TO NRC. THE REDACTIONS WERE MADE DUE TO MEETING THE NRC'S CRITERIA ON SENSITIVE INFORMATION, AS SPECIFIED IN SECY-04-0191, "WITHHOLDING SENSITIVE UNCLASSIFIED INFORMATION CONCERNING NUCLEAR POWER REACTORS FROM PUBLIC DISCLOSURE," DATED OCTOBER 19, 2004, ADAMS ACCESSION NO. ML042310663, AS MODIFIED BY THE NRC COMMISSIONERS STAFF REQUIREMENTS MEMORANDUM ON SECY-04-0191, DATED NOVEMBER 9, 2004, ADAMS ACCESSION NO. 043140175.



***Pacific Gas and
Electric Company***[®]

Diablo Canyon Power Plant Units 1 and 2 Final Safety Analysis Report Update



Revision 21 September 2013

Docket No. 50-275

Docket No. 50-323

DIABLO CANYON POWER PLANT
UNITS 1 AND 2

FSAR UPDATE CONTENTS

Chapter 1 - INTRODUCTION AND GENERAL DESCRIPTION OF PLANT

- 1.1 Introduction
- 1.2 General Plant Description
- 1.3 Comparison Tables
- 1.4 Identification of Agents and Contractors
- 1.5 Requirements for Further Technical Information
- 1.6 Material Incorporated by Reference

Tables for Chapter 1
Figures for Chapter 1

Chapter 2 - SITE CHARACTERISTICS

- 2.1 Geography and Demography
- 2.2 Nearby Industrial, Transportation, and Military Facilities
- 2.3 Meteorology
- 2.4 Hydrologic Engineering
- 2.5 Geology and Seismology

Tables for Chapter 2
Figures for Chapter 2

Chapter 3 - DESIGN OF STRUCTURES, COMPONENTS, EQUIPMENT, AND SYSTEMS

- 3.1 Conformance with AEC General Design Criteria
- 3.2 Classification of Structures, Systems, and Components
- 3.3 Wind and Tornado Loadings
- 3.4 Water Level (Flood) Design
- 3.5 Missile Protection
- 3.6 Protection Against Dynamic Effects Associated with the Postulated Rupture of Piping
- 3.7 Seismic Design
- 3.8 Design of Design Class I Structures
- 3.9 Mechanical Systems and Components
- 3.10 Seismic Design of Design Class I Instrumentation, HVAC, and Electrical Equipment
- 3.11 Environmental Design of Mechanical and Electrical Equipment

Tables for Chapter 3
Figures for Chapter 3
Appendices for Chapter 3

DIABLO CANYON POWER PLANT
UNITS 1 AND 2

FSAR UPDATE CONTENTS

Chapter 4 - REACTOR

- 4.1 Summary Description
- 4.2 Mechanical Design
- 4.3 Nuclear Design
- 4.4 Thermal and Hydraulic Design

Tables for Chapter 4
Figures for Chapter 4

Chapter 5 - REACTOR COOLANT SYSTEM

- 5.1 Summary Description
- 5.2 Integrity of the Reactor Coolant Pressure Boundary
- 5.3 Thermal Hydraulic System Design
- 5.4 Reactor Vessel and Appurtenances
- 5.5 Component and Subsystem Design
- 5.6 Instrumentation Requirements

Tables for Chapter 5
Figures for Chapter 5
Appendices for Chapter 5

Chapter 6 - ENGINEERED SAFETY FEATURES

- 6.1 General
- 6.2 Containment Systems
- 6.3 Emergency Core Cooling System
- 6.4 Habitability Systems
- 6.5 Auxiliary Feedwater System

Tables for Chapter 6
Figures for Chapter 6
Appendices for Chapter 6

Chapter 7 - INSTRUMENTATION AND CONTROLS

- 7.1 Introduction
- 7.2 Reactor Trip System
- 7.3 Engineered Safety Features Actuation System
- 7.4 Systems Required for Safe Shutdown
- 7.5 Safety-Related Display Instrumentation
- 7.6 All Other Instrumentation Systems Required for Safety
- 7.7 Control Systems Not Required for Safety

DIABLO CANYON POWER PLANT
UNITS 1 AND 2

FSAR UPDATE CONTENTS

Chapter 7 (continued)

Tables for Chapter 7
Figures for Chapter 7

Chapter 8 - ELECTRIC POWER

- 8.1 Introduction
- 8.2 Offsite Power System
- 8.3 Onsite Power Systems

Tables for Chapter 8
Figures for Chapter 8
Appendices for Chapter 8

Chapter 9 - AUXILIARY SYSTEMS

- 9.1 Fuel Storage and Handling
- 9.2 Water Systems
- 9.3 Process Auxiliaries
- 9.4 Heating, Ventilation, and Air-Conditioning (HVAC) Systems
- 9.5 Other Auxiliary Systems

Tables for Chapter 9
Figures for Chapter 9
Appendices for Chapter 9

Chapter 10 - STEAM AND POWER CONVERSION SYSTEM

- 10.1 Summary Description
- 10.2 Turbine-Generator
- 10.3 Main Steam System
- 10.4 Other Features of Steam and Power Conversion System

Tables for Chapter 10
Figures for Chapter 10

Chapter 11 - RADIOACTIVE WASTE MANAGEMENT

- 11.1 Source Terms
- 11.2 Liquid Waste System
- 11.3 Gaseous Waste System
- 11.4 Process and Effluent Radiological Monitoring System
- 11.5 Solid Waste System

DIABLO CANYON POWER PLANT
UNITS 1 AND 2

FSAR UPDATE CONTENTS

Chapter 11 (continued)

11.6 Offsite Radiological Monitoring Program

Tables for Chapter 11
Figures for Chapter 11

Chapter 12 - RADIATION PROTECTION

12.1 Shielding
12.2 Ventilation
12.3 Health Physics Program

Tables for Chapter 12
Figures for Chapter 12

Chapter 13 - CONDUCT OF OPERATIONS

13.1 Organizational Structure
13.2 Training Program
13.3 Emergency Planning
13.4 Review and Audit
13.5 Plant Procedures and Programs
13.6 Plant Records
13.7 Physical Security

Tables for Chapter 13
Figures for Chapter 13

Chapter 14 - INITIAL TESTS AND OPERATION

14.1 Test Program
14.2 Augmentation of Applicant's Staff for Initial Tests and Operation
14.3 Postcommercial Operational Test Program

Tables for Chapter 14
Figures for Chapter 14

DIABLO CANYON POWER PLANT
UNITS 1 AND 2

FSAR UPDATE CONTENTS

Chapter 15 - ACCIDENT ANALYSES

- 15.1 Condition I - Normal Operation and Operational Transients
- 15.2 Condition II - Faults of Moderate Frequency
- 15.3 Condition III - Infrequent Faults
- 15.4 Condition IV - Limiting Faults
- 15.5 Environmental Consequences of Plant Accidents

Tables for Chapter 15
Figures for Chapter 15

Chapter 16 - TECHNICAL SPECIFICATIONS AND EQUIPMENT CONTROL GUIDELINES

- 16.1 Technical Specifications and Equipment Control Guidelines

Table for Chapter 16

Chapter 17 - QUALITY ASSURANCE

- 17.1 Organization
- 17.2 Quality Assurance Program
- 17.3 Design Control
- 17.4 Procurement Document Control
- 17.5 Instructions, Procedures, and Drawings
- 17.6 Document Control
- 17.7 Control of Purchased Material, Equipment, and Services
- 17.8 Identification and Control of Materials, Parts, and Components
- 17.9 Special Processes
- 17.10 Inspection
- 17.11 Test Control
- 17.12 Control of Measuring and Test Equipment
- 17.13 Handling, Storage, and Shipping
- 17.14 Inspection, Test, and Operating Status
- 17.15 Control of Nonconforming Conditions
- 17.16 Corrective Action
- 17.17 Quality Assurance Records
- 17.18 Audits

Tables for Chapter 17
Figures for Chapter 17

2.5 GEOLOGY AND SEISMOLOGY

This section presents the findings of the regional and site-specific geologic and seismologic investigations of the Diablo Canyon Power Plant (DCPP) site. Information presented is in compliance with the criteria in Appendix A of 10 CFR Part 100, as described below, and meets the format and content recommendations of Regulatory Guide 1.70, Revision 1 (Reference 39). Because the development of the seismic inputs for DCPP predates the issuance of 10 CFR Part 100, Appendix A, "Seismic and Geologic Siting Criteria for Nuclear Power Plants," the DCPP earthquakes are plant specific.

To capture the historical progress of the geotechnical and seismological investigations associated with the DCPP site, information pertaining to the following three time periods is described herein:

- (1) Original Design Phase: investigations performed in support of the Preliminary Safety Analysis Report, prior to the issuance of the Unit 1 construction permit (1967), through the early stages of the construction of Unit 1 (1971). The Design Earthquake and Double Design Earthquake ground motions are associated with this phase. These earthquakes are similar to the regulatory ground motion level that the NRC subsequently developed in 10 CFR Part 100 Appendix A as the "Operating Basis Earthquake (OBE)" ground motion and the "Safe Shutdown Earthquake (SSE)" ground motion, respectively.
- (2) Hosgri Evaluation Phase: investigations performed in response to the identification of the offshore Hosgri fault zone (1971) through the issuance of the Unit 1 operating license (1984). The 1977 Hosgri Earthquake ground motions are associated with this phase. The Hosgri Evaluation Phase does not affect or change the investigations and conclusions of the Original Design Phase.
- (3) Long Term Seismic Program (LTSP) Evaluation Phase: investigations performed in response to the License Condition Item No. 2.C.(7) of the Unit 1 operating license (1984) through the removal of the License Condition (1991), including current on-going investigations. The 1991 LTSP ground motion is associated with this phase. The LTSP Evaluation Phase does not affect or change the investigations and conclusions of either the Original Design Phase or the Hosgri Evaluation Phase.

Overview

Locations of earthquake epicenters within 200 miles of the plant site, and faults and earthquake epicenters within 75 miles of the plant site for either magnitudes or intensities, respectively, are shown in Figures 2.5-2, 2.5-3, and 2.5-4 (through 1972). A geologic and tectonic map of the region surrounding the site is shown in Figure 2.5-5,

DCPP UNITS 1 & 2 FSAR UPDATE

and detailed information about site geology is presented in Figures 2.5-8 through 2.5-16. Geology and seismology are discussed in detail in Sections 2.5.2 through 2.5.5. Additional information on site geology is contained in References 1 and 2.

Detailed supporting data pertaining to this section are presented in Appendices 2.5A, 2.5B, 2.5C, and 2.5D of Reference 27 in Section 2.3. Geologic and seismic information from investigations that responded to Nuclear Regulatory Commission (NRC) licensing review questions are presented Appendices 2.5E and 2.5F of the same reference. A brief synopsis of the information presented in Reference 27 (Section 2.3) is given below. The DCPP site is located in San Luis Obispo County approximately 190 miles south of San Francisco and 150 miles northwest of Los Angeles, California. It is adjacent to the Pacific Ocean, 12 miles west-southwest of the city of San Luis Obispo, the county seat. The plant site location and topography are shown in Figure 2.5-1.

The site is located near the mouth of Diablo Creek which flows out of the San Luis Range, the dominant feature to the northeast. The Pacific Ocean is southwest of the site. Facilities for the power plant are located on a marine terrace that is situated between the mountain range and the ocean.

The terrace is bedrock overlain by surficial deposits of marine and nonmarine origin. PG&E Design Class I structures at the site are situated on bedrock that is predominantly stratified marine sedimentary rocks and volcanics, all of Miocene age. A more extensive discussion of the regional geology is presented in Section 2.5.2.1 and site geology in Section 2.5.2.2.

Several investigations were performed at the site and in the vicinity of the site to determine: potential vibratory ground motion characteristics, existence of surface faulting, and stability of subsurface materials and cut slopes adjacent to Seismic Category I structures. Details of these investigations are presented in Sections 2.5.2 through 2.5.5. Consultants retained to perform these studies included: Earth Science Associates (geology and seismicity), John A. Blume and Associates (seismic design and foundation materials dynamic response), Harding-Lawson and Associates (stability of cut slope), Woodward-Clyde-Sherard and Associates (soil testing), and Geo-Recon, Incorporated (rock seismic velocity determinations). The findings of these consultants are summarized in this section and the detailed reports are included in Appendices 2.5A, 2.5B, 2.5C, 2.5D, 2.5E, and 2.5F of Reference 27 in Section 2.3.

Geologic investigation of the Diablo Canyon coastal area, including detailed mapping of all natural exposures and exploratory trenches, yielded the following basic conclusions:

- (1) The area is underlain by sedimentary and volcanic bedrock units of Miocene age. Within this area, the power plant site is underlain almost wholly by sedimentary strata of the Monterey Formation, which dip northward at moderate to very steep angles. More specifically, the reactor site is underlain by thick-bedded to almost massive Monterey sandstone

DCPP UNITS 1 & 2 FSAR UPDATE

that is well indurated and firm. Where exposed on the nearby hillslope, this rock is markedly resistant to erosion.

- (2) The bedrock beneath the main terrace area, within which the power plant site has been located, is covered by 3 to 35 feet of surficial deposits. These include marine sediments of Pleistocene age and nonmarine sediments of Pleistocene and Holocene age. In general, they are thickest in the vicinity of the reactor site.
- (3) The interface between the unconsolidated terrace deposits and the underlying bedrock comprises flat to moderately irregular surfaces of Pleistocene marine planation and intervening steeper slopes that also represent erosion in Pleistocene time.
- (4) The bedrock beneath the power plant site occupies the southerly flank of a major syncline that trends west to northwest. No evidence of a major fault has been recognized within or near the coastal area, and bedrock relationships in the exploratory trenches positively indicate that no such fault is present within the area of the power plant site.
- (5) Minor surfaces of disturbance, some of which plainly are faults, are present within the bedrock that underlies the power plant site. None of these breaks offsets the interface between bedrock and the cover of terrace deposits, and none of them extends upward into the surficial cover. Thus, the latest movements along these small faults must have antedated erosion of the bedrock section in Pleistocene time.
- (6) No landslide masses or other gross expressions of ground instability are present within the power plant site or on the main hillslope east of the site. Some landslides have been identified in adjacent ground, but these are minor features confined to the naturally oversteepened walls of Diablo Canyon.
- (7) No water of subsurface origin was encountered in the exploratory trenches, and the level of permanent groundwater beneath the main terrace area probably is little different from that of the adjacent lower reaches of the deeply incised Diablo Creek.

2.5.1. DESIGN BASIS

2.5.1.1 General Design Criterion 2, 1967 Performance Standards

DCPP systems, structures, and components have been located, designed and analyzed to withstand those forces that might result from the most severe natural earthquake phenomena.

2.5.1.2 License Condition 2.C(7) of DCPP Facility Operating License DPR-80 Rev. 44 (LTSP), Elements (1), (2) and (3)

DCPP developed and implemented a program to re-evaluate the seismic design bases used for the Diablo Canyon Power Plant.

The program included the following three Elements that were completed and accepted by the NRC (References 40, 41, and 43):

- (1) The identification, examination, and evaluation of all relevant geologic and seismic data, information, and interpretations that have become available since the 1979 ASLB hearing in order to update the geology, seismology and tectonics in the region of the Diablo Canyon Nuclear Power Plant. If needed to define the earthquake potential of the region as it affects the Diablo Canyon Plant, PG&E has also re-evaluated the earlier information and acquired additional data.
- (2) DCPP has re-evaluated the magnitude of the earthquakes used to determine the seismic basis of the Diablo Canyon Nuclear Plant using the information from Element 1.
- (3) DCPP has re-evaluated the ground motion at the site based on the results obtained from Element 2 with full consideration of site and other relevant effects.

As a condition of the NRC's closeout of License Condition 2.C.(7), PG&E committed to several ongoing activities in support of the LTSP, as discussed in a public meeting between PG&E and the NRC on March 15, 1991 (Reference 53), described as the "Framework for the Future," in a letter to the NRC, dated April 17, 1991 (Reference 50), and affirmed by the NRC in SSER 34 (Reference 43). These ongoing activities are discussed in Section 2.5.7.

2.5.1.3 10 CFR Part 100, March 1966- Reactor Site Criteria

During the determination of the location of the Diablo Canyon Power Plant, consideration was given to the physical characteristics of the site, including seismology and geology.

2.5.2 BASIC GEOLOGIC AND SEISMIC INFORMATION

This section presents the basic geologic and seismic information for DCPP site and surrounding region. Information contained herein has been obtained from literature studies, field investigations, and laboratory testing and is to be used as a basis for evaluations required to provide a safe design for the facility. The basic data contained in this section and in Reference 27 of Section 2.3 are referenced in several other

sections of this FSAR Update. Additional information, developed during the Hosgri and LTSP evaluations, is described in Sections 2.5.3.9.3 and 2.5.3.9.4, respectively.

2.5.2.1 Regional Geology

2.5.2.1.1 Regional Physiography

Diablo Canyon is in the southern Coast Range which is a part of the California Coast Ranges section of the Pacific Border physiographic province (refer to Figure 2.5-1). The region surrounding the power plant site consists of mountains, foothills, marine terraces, and valleys. The dominant features are the San Luis Range adjacent to the site to the northeast, the Santa Lucia Range farther inland, the lowlands of the Los Osos and San Luis Obispo Valleys separating the San Luis and Santa Lucia Ranges, and the marine terrace along the coastal margin of the San Luis Range.

Landforms of the San Luis Range and the adjacent marine terrace produce the physiography at the site and in the region surrounding the site. The westerly end of the San Luis Range is a mass of rugged high ground that extends from San Luis Obispo Creek and San Luis Obispo Bay on the east and is bounded by the Pacific Ocean on the south and west. Except for its narrow fringe of coastal terraces, the range is featured by west-northwesterly-trending ridge and canyon topography. Ridge crest altitudes range from about 800 to 1800 feet. Nearly all of the slopes are steep, and they are modified locally by extensive slump and earthflow landslides.

Most of the canyons have narrow-bottomed, V-shaped cross sections. Alluvial fans and talus aprons are prominent features along the bases of many slopes and at localities where ravines debouch onto relatively gentle terrace surfaces. The coastal terrace belt extends between a steep mountain-front backscarp and a near-vertical sea cliff 40 to 200 feet in height. Both the bedrock benches of the terraces and the present offshore wave-cut bench are irregular in detail, with numerous basins and rock projections.

The main terrace along the coastal margin of the San Luis Range is a gently to moderately sloping strip of land as much as 2000 feet in maximum width. The more landward parts of its surface are defined by broad aprons of alluvial deposits. This cover thins progressively in a seaward direction and is absent altogether in a few places along the present sea cliff. The main terrace represents a series of at least three wave-cut rock benches that have approximate shoreline-angle elevations of 70, 100, and 120 feet.

Owing to both the prevailing seaward slopes of the rock surfaces and the variable thickness of overlying marine and nonmarine cover, the present surface of the main terrace ranges from 70 to more than 200 feet in elevation. Remnants of higher terraces exist at scattered locations along upper slopes and ridge crests. The most extensive among these is a series of terrace surfaces at altitudes of 300+, 400+, and 700+ feet at the west end of the ridge between Coon and Islay Creeks, north of Point Buchon. A surface described by Headlee (Reference 19) as a marine terrace at an altitude of about

700 feet forms the top of San Luis Hill. Remnants of a lower terrace at an altitude of 30 to 45 feet are preserved at the mouth of Diablo Canyon and at several places farther north.

Owing to contrasting resistance to erosion among the various bedrock units of the San Luis Range, the detailed topography of the wave-cut benches commonly is very irregular. As extreme examples, both modern and fossil sea stacks rise as much as 100 feet above the general levels of adjacent marine-eroded surfaces at several localities.

2.5.2.1.2 Regional Geologic and Tectonic Setting

2.5.2.1.2.1 Geologic Setting

The San Luis Range is underlain by a synclinal section of Tertiary sedimentary and volcanic rocks, which have been downfolded into a basement of Mesozoic rocks now exposed along its southwest and northeast sides. Two zones of faulting have been recognized within the range. The Edna fault zone trends along its northeast side, and the Miguelito fault zone extends into the range from the vicinity of Avila Bay. Minor faults and bedding-plane shears can be seen in the parts of the section that are well exposed along the sea cliff fringing the coastal terrace benches. None of these faults shows evidence of geologically recent activity, and the most recent movements along those in the rocks underlying the youngest coastal terraces can be positively dated as older than 80,000 to 120,000 years. Geologic and tectonic maps of the region surrounding the site are shown in Figures 2.5-5 (2 sheets), 2.5-6, 2.5-8, and 2.5-9.

2.5.2.1.2.2 Tectonic Features of the Central Coastal Region

DCPP site lies within the southern Coast Ranges structural province, and approximately upon the centerline axis of the northwest-trending block of crust that is bounded by the San Andreas fault on the northeast and the continental margin on the southwest. This crustal block is characterized by northwest-trending structural and geomorphic features, in contrast to the west-trending features of the Transverse Ranges to the south. A major geologic boundary within the block is associated with the Sur-Nacimiento and Rinconada faults, which separate terrains of contrasting basement rock types. The ground southwest of the Sur-Nacimiento zone and the southerly half of the Rinconada fault, referred to as the Coastal Block, is underlain by Franciscan basement rocks of dominantly oceanic types, whereas that to the northeast, referred to as the Salinia Block, is underlain by granitic and metamorphic basement rocks of continental types. Page (Reference 10) outlined the geology of the Coast Ranges, describing it generally in terms of "core complexes" of basement rocks and surrounding sections of younger sedimentary rocks. The principal Franciscan core complex of the southern Coast Range crops out on the coastal side of the Santa Lucia Range from the vicinity of San Luis Obispo to Point Sur, a distance of 120 miles. Its complex features reflect numerous episodes of deformation that evidently included folding, faulting, and the tectonic emplacement of extensive bodies of ultrabasic rocks. Other core complexes

DCPP UNITS 1 & 2 FSAR UPDATE

consisting of granitic and metamorphic basement rocks are exposed in the southern Coast Ranges in the ground between the Sur-Nacimiento and Rinconada and in the San Andreas fault zones. The locations of these areas of basement rock exposure are shown in Figure 2.5-6 and in Figure 1 of Appendix 2.5D of Reference 27 in Section 2.3.

Younger structural features include thick folded basins of Tertiary strata and the large faults that form structural boundaries between and within the core complexes and basins.

The structure of the southern Coast Ranges has evolved during a lengthy history of deformation extending from the time when the ancestral Sur-Nacimiento zone was a site for subduction (a Benioff zone) along the then-existing continental margin, through subsequent parts of Cenozoic time when the San Andreas fault system was the principal expression of the regional stress-strain system. The latest episodes of major deformation involved folding and faulting of Pliocene and older sediments during mid-Pliocene time, and renewed movements along preexisting faults during early or mid-Pliocene time. Present tectonic activity within the region is dominated by interaction between the Pacific and American crustal plates on opposite sides of the San Andreas fault and by continuing vertical uplift of the Coast Ranges. In the regional setting of DCPP site, the major structural features addressed during the original design phase are the San Andreas, Rinconada-San Marcos-Jolon, Sur-Nacimiento, and Santa Lucia Bank faults. Additional faults were identified during the Hosgri evaluation and LTSP evaluation phases, discussed in Sections 2.5.3.9.3 and 2.5.3.9.4, respectively. The San Simeon fault may also be included with this group. These original design phase faults are described as follows:

1. San Andreas Fault

The San Andreas fault is recognized as a major transform fault of regional dimensions that forms an active boundary between the Pacific and North American crustal plates. Cumulative slip along the San Andreas fault may have amounted to several hundred miles, and a substantial fraction of the total slip has occurred during late Cenozoic time. The fault has spectacular topographic expression, generally lying within a rift valley or along an escarpment mountain front, and having associated sag ponds, low scarps, right-laterally deflected streams, and related manifestations of recent activity.

The most recent episode of large-scale movement along the reach of the San Andreas fault that is closest to the San Luis Range occurred during the great Fort Tejon earthquake of 1857. Geologic evidence pertinent to the behavior of the fault during this and earlier seismic events was studied in great detail by Wallace (Reference 15 and 32) who reported in terms of infrequent great earthquakes accompanied by ground rupture of 10 to 30 feet, with intervening periods of near total quiescence. Allen (Reference 16) suggested that such behavior has been typical for this reach of the San Andreas fault and has been fundamentally different from the behavior of the fault along the reach farther northwest, where creep and numerous small earthquakes have occurred. He further suggested that release of accumulating strain energy might have been facilitated

by the presence of large amounts of serpentine in the fault zone to the northwest, and retarded by the locking effect of the broad bend of the fault zone where it crosses the Transverse Ranges to the southeast.

Movement is currently taking place along large segments of the San Andreas fault. The active reach of the fault between Parkfield and San Francisco is currently undergoing relative movement of at least 3 to 4 cm/yr, as determined geodetically and analyzed by Savage and Burford (Reference 33). When the movement that occurs during the episodes of fault displacement in the western part of the Basin and Ranges Province is added to the minimum of 3 to 4 cm/yr of continuously and intermittently released strain, the total probably amounts to at least 5 to 6 cm/yr. This may account for essentially all of the relative motion between the Pacific and North American plates at present. In the Transverse Ranges to the south, this strain is distributed between lateral slip along the San Andreas system and east-west striking lateral slip faulting, thrust faulting, and folding. North of the latitude of Monterey Bay and south of the Transverse Ranges, transcurrent movement is again concentrated along the San Andreas system, but in those regions, it is distributed among several major strands of the system.

2. Sur-Nacimiento Fault Zone

The Sur-Nacimiento fault zone has been regarded as the system of faults that extends from the vicinity of Point Sur, near the northwest end of the Santa Lucia Range, to the Big Pine fault in the western Transverse Ranges, and that separates the granitic-metamorphic basement of the Salinian Block from the Franciscan basement of the Coastal Block. The most prominent faults that are included within this zone are, from northwest to southeast, the Sur, Nacimiento, Rinconada, and (south) Nacimiento faults. The Sur fault, which extends as far northward as Point Sur on land, continues to the northwest in the offshore continental margin. At its southerly end, the zone terminates where the (south) Nacimiento fault is cut off by the Big Pine fault. The overall length of the Sur-Nacimiento fault zone between Point Sur and the Transverse Ranges is about 180 miles. The 60 mile long Nacimiento fault, between points of juncture with the Sur and Rinconada faults, forms the longest segment within this zone. Page (Reference 11) stated that:

"It is unlikely that the Nacimiento fault proper has displaced the ground surface in Late Quaternary time, as there are no indicative offsets of streams, ridges, terrace deposits, or other topographic features. The Great Valley-type rocks on the northeast side must have been down-dropped against the older Franciscan rocks on the southwest, yet they commonly stand higher in the topography. This implies relative quiescence of the Late Quaternary time, allowing differential erosion to take place. In a few localities, the northeast side is the low side, and this inconsistency favors the same conclusion. In addition to the foregoing circumstances, the fault is offset by minor cross-faults in a manner suggesting that little, if any, Late Quaternary near-surface movement had occurred along the main fracture."

Hart (Reference 14), on the other hand, stated that: ". . . youthful topographic features (offset streams, sag ponds, possible fault scarplets, and apparently oversteepened slopes) suggest movement along both (Sur-Nacimiento and Rinconada) fault zones." The map compiled by Jennings (Reference 23), however, shows only the Rinconada with a symbol indicating "Quaternary fault displacement."

The results of photogeologic study of the region traversed by the Sur-Nacimiento fault zone tend to support Page's view. A pronounced zone of fault-controlled topographic lineaments can be traced from the northwest end of the Nacimiento fault southeastward to the Rinconada (south Nacimiento), East Huasna, and West Huasna faults. Only along the Rinconada, however, are there topographic features that seem to have originated through fault disturbances of the ground surface rather than through differential erosion along zones of shearing and juxtaposition of differing rocks. Richter (Reference 13) noted that some historic seismicity, particularly the 1952 Bryson earthquake, appears to have originated along the Nacimiento fault. This view is supported by recent work of S. W. Smith (Reference 30) that indicates that the Bryson shock and the epicenters of several smaller, more recent earthquakes were located along or near the trace of the Nacimiento.

3. Rinconada (Nacimiento)-San Marcos-Jolon-San Antonio Fault System

A system of major faults extends northwestward, parallel to the San Andreas fault, from a point of junction with the Big Pine fault in the western Transverse Ranges. This system includes several faults that have been mapped as separate features and assigned individual names. Dibblee (Reference 27) however, has suggested that these faults are part of a single system, provisionally termed the Rinconada fault zone after one of its more prominent members. He also proposed abandoning the name Nacimiento for the large fault that constitutes the most southerly part of this system, as it is not continuous with the Nacimiento fault to the north, near the Nacimiento River. The newly defined Rinconada fault system comprises the old (south) Nacimiento, Rinconada, and San Marcos faults. Dibblee proposed that the system also include the Espinosa and Reliz faults, to the north, but detailed work by Durham (Reference 28) does not seem to support this interpretation. Instead, the system may extend into Lockwood Valley and die out there along the Jolon and San Antonio faults. All the faults of the Rinconada system have undergone significant movement during middle and late Cenozoic time, though the entire system did not behave as a unit. Dibblee pointed out that: "Relative vertical displacements are controversial, inconsistent, reversed from one segment to another; the major movement may be strike slip, as on the San Andreas fault."

Regarding the structural relationship of the Rinconada fault to nearby faults, Dibblee wrote as follows:

"Thrust or reverse faults of Quaternary age are associated with the Rinconada fault along much of its course on one or both sides, within 9 miles, especially in areas of intense folding. In the northern part several, including the San Antonio fault, are

DCPP UNITS 1 & 2 FSAR UPDATE

present along both margins of the range of hills between the Salinas and Lockwood Valleys . . . along which this range was elevated in part. Near the southern part are the major southwest-dipping South Cuyama and Ozena faults along which the Sierra Madre Range was elevated against Cuyama Valley, with vertical displacements possibly up to 8000 feet. All these thrust or reverse faults dip inward toward the Rinconada fault and presumably either splay from it at depth, or are branches of it. These faults, combined with the intense folding between them, indicated that severe compression accompanied possible transcurrent movement along the Rinconada fault."

"The La Panza fault along which the La Panza Range was elevated in Quaternary time, is a reverse fault that dips northeast under the range, and is not directly related to the Rinconada fault.

"The Big Pine fault against which the Rinconada fault abuts . . . is a high angle left-lateral transcurrent fault active in Quaternary time (Reference 35). The Pine Mountain fault south of it . . . is a northeast-dipping reverse fault along which the Pine Mountain Range was elevated in Quaternary time. This fault may have been reactivated along an earlier fault that may have been continuous with the Rinconada fault, but displaced about 8 miles from it by left slip on the Big Pine fault (Reference 12) in Quaternary time."

"The Rinconada and Reliz faults were active after deposition of the Monterey Shale and Pancho Rico Formation, which are severely deformed adjacent and near the faults. The faults were again active after deposition of the Paso Robles Formation but to a lesser degree. These faults do not affect the alluvium or terrace deposits. There are no offset stream channels along these faults. However, in two areas several canyons and streams are deviated, possibly by right-lateral movement on the (Espinosa and San Marcos segments of the) Rinconada fault. There are no indications that these faults are presently active."

4. San Simeon Fault

The fault here referred to as the San Simeon fault trends along the base of the peninsula that lies north of the settlement of San Simeon. This fault is on land for a distance of 12 miles between its only outcrop, north of Ragged Point, and Point San Simeon. It may extend as much as 16 miles farther to the southeast, to the vicinity of Point Estero. This possibility is suggested by the straight reach of coastline between Cambria and Point Estero, which is directly aligned with the onshore trend of the fault; its linear form may well have been controlled by a zone of structural weakness associated with the inferred southerly part of the fault. South of Port Estero, however, there is no evidence of faulting observable in the seismic reflection profiles across Estero Bay, and the trend defined by the Los Osos Valley-Estero Bay series of lower Miocene or Oligocene intrusives extends across the San Simeon trend without deviation.

DCPP UNITS 1 & 2 FSAR UPDATE

North of Point Piedras Blancas, Silver (Reference 26) reports a fault with about 5 kilometers of vertical separation between the 4-kilometer-thick Tertiary section in the offshore basin and the nearby 1-kilometer-high exposure of Franciscan basement rocks in the coastline mountain front. The existence of a fault in this region is also indicated by the 30- milligal gravity anomaly between the offshore basin and the onshore ranges (Plate II of Appendix 2.5D of Reference 27 in Section 2.3). This postulated fault may well be a northward extension of the San Simeon fault. If this is the case, the San Simeon fault may have a total length of as much as 60 miles.

Between Point San Simeon and Ragged Point, the San Simeon fault lies along the base of a broad peninsula, the surface of which is characterized by elevated marine terraces and younger, steep-walled ravines and canyons. The low, terraced topography of the peninsula contrasts sharply with that of the steep mountain front that rises immediately behind it. Clearly, the ground west of the main fault represents a part of the sea floor that has been locally arched up.

This has resulted in exposure of the fault, which elsewhere is concealed underwater off the shoreline.

The ground between the San Simeon fault and the southwest coastline of the Piedras Blancas peninsula is underlain by faulted blocks and slivers of Franciscan rocks, serpentinites, Tertiary sedimentary breccia and volcanic rocks, and Miocene shale. The faulted contacts between these rock masses trend somewhat more westerly than the trend of the San Simeon fault. One north-dipping reverse fault, which separates serpentinite from graywacke, has broken marine terrace deposits in at least two places, one of them in the basal part of the lowest and youngest terrace. Movement along this branch fault has therefore occurred less than 130,000 years before the present, although the uppermost, youngest Pleistocene deposits are apparently not broken. Prominent topographic lineations defined by northwest-aligned ravines that incise the upper terrace surface, on the other hand, apparently have originated through headward gully erosion along faults and faulted contacts, rather than through the effects of surface faulting.

The characteristics of the San Simeon fault can be summarized as follows: The fault may be related to a fault along the coast to the north that displays some 5 kilometers of vertical displacement. Near San Simeon, it exhibits probable Pleistocene right-lateral strike-slip movement of as much as 1500 feet near San Simeon, although it apparently does not break dune sand deposits of late Pleistocene or early Holocene age. A branch reverse fault, however, breaks upper Pleistocene marine terrace deposits. The San Simeon fault may extend as far south as Point Estero, but it dies out before crossing the northern part of Estero Bay.

5. Santa Lucia Bank Fault

South of the latitude of Point Piedras Blancas, the western boundary of the main offshore Santa Maria Basin is defined by the east-facing scarp along the east side of the

DCPP UNITS 1 & 2 FSAR UPDATE

Santa Lucia Bank. This scarp is associated with the Santa Lucia Bank fault, the structure that separates the subsided block under the basin from the structural high of the bank. The escarpment that rises above the west side of the fault trace has a maximum height of about 450 feet, as shown on U.S. Coast and Geodetic Survey (USC&GS) Bathymetric Map 1306N-20.

The Santa Lucia Bank fault can be traced on the sea floor for a distance of about 65 miles. Extensions that are overlapped by upper Tertiary strata continue to the south for at least another 10 miles, as well as to the north. The northern extension may be related to another, largely buried fault that crosses and may intersect the trend of the Santa Lucia Bank fault. This second fault extends to the surface only at points north of the latitude of Point Piedras Blancas.

West of the Santa Lucia Bank fault, between N latitudes 34°30' and 30°, several subparallel faults are characterized by apparent surface scarps. The longest of these faults trends along the upper continental slope for a distance of as much as 45 miles, and generally exhibits a west-facing scarp. Other faults are present in a zone about 30 miles long lying between the 45 mile fault and the Santa Lucia Bank fault. These faults range from 5 to 15 or more miles in length, and have both east-and west-facing scarps.

This zone of faulting corresponds closely in space with the cluster of earthquake epicenters around N latitude 34°45' and 121°30'W longitude, and it probably represents the source structure for those shocks (Figure 2.5-3).

2.5.2.1.2.3 Tectonic Features in the Vicinity of the DCPP Site

Geologic relationships between the major fold and fault structures in the vicinity of Diablo Canyon are shown in Figures 2.5-5, 2.5-6, and 2.5-7, and are described and illustrated in Appendix 2.5D of Reference 27 of Section 2.3. The San Luis Ranges-Estero Bay area is characterized structurally by west-northwest-trending folds and faults. These include the San Luis-Pismo syncline and the bordering Los Osos Valley and Point San Luis antiformal highs, and the West Huasna, Edna, and San Miguelito faults. A few miles offshore, the structural features associated with this trend merge into a north-northwest-trending zone of folds and faults that is referred to herein as the offshore Santa Maria Basin East Boundary zone of folding and faulting. The general pattern of structural highs and lows of the onshore area is warped and stepped downward to the west across this boundary zone, to be replaced by more northerly-trending folds in the lower part of the offshore basin section. The overall relationship between the onshore Coast Ranges and the offshore continental margin is one of differential uplift and subsidence. The East Boundary zone represents the structural expression of the zone of inflection between these regions of contrasting vertical movement.

DCPP UNITS 1 & 2 FSAR UPDATE

In terms of regional relationships, structural style, and history of movement, the faults in the San Luis Ranges-Estero Bay vicinity, identified during the original design phase, may be characterized as follows:

1. *West Huasna Fault*

This fault zone separates the large downwarp of the Huasna syncline on the northeast from Franciscan assemblage rocks of the Los Osos Valley antiform and the Tertiary section of the southerly part of the San Luis-Pismo syncline on the southwest. The West Huasna fault is thought to join with the Suey fault to the south. Differences in thicknesses and facies relationships between units of apparently equivalent age on opposite sides of the fault are interpreted as indicating lateral movement along the fault; however, the available evidence regarding the amount and even the relative sense of displacement is not consistent. The West Huasna shows no evidence of late Quaternary activity.

2. *Edna Fault Zone*

The Edna fault zone lies along a west-northwesterly trend that extends obliquely from the West Huasna fault at its southeast end to the hills of the San Luis Range south of Morro Bay. Several isolated breaks that lie on a line with the trend are present in the Tertiary strata beneath the south part of Estero Bay, east of the Santa Maria Basin East Boundary fault zone across the mouth of the bay.

The Edna fault is typically a zone of two or more anastomosing branches that range in width from 1/2 mile to as much as 1-1/2 miles. Although individual strands are variously oriented and exhibit various senses of amounts of movement, the zone as a whole clearly expresses high-angle dip-slip displacement (down to the southwest). The irregular traces of major strands suggest that little, if any, strike-slip movement has occurred. Preliminary geologic sections shown by Hall and Surdam (Reference 21) and Hall (Reference 20) imply that the total amount of vertical separation ranges from 1500 to a few thousand feet along the central part of the fault zone. The amount of displacement across the main fault trend evidently decreases to the northwest, where the zone is mostly overlapped by upper Tertiary strata.

It may be, however, that most of the movement in the Baywood Park vicinity has been transferred to the north-trending branch of the Edna, which juxtaposes Pliocene and Franciscan rocks where last exposed. In the northwesterly part of the San Luis Range, the Edna fault forms much of the boundary between the Tertiary and basement rock sections. Most of the measurable displacements along this zone of rupture occurred during or after folding of the Pliocene Pismo Formation but prior to deposition of the lower Pleistocene Paso Robles Formation. Some additional movement has occurred during or since early Pleistocene time, however, because Monterey strata have been faulted against Paso Robles deposits along at least one strand of the Edna near the head of Arroyo Grande valley. This involved steep reverse fault movement, with the

DCPP UNITS 1 & 2 FSAR UPDATE

southwest side raised, in contrast to the earlier normal displacement down to the southwest.

Search has failed to reveal dislocation of deposits younger than the Paso Robles Formation, disturbance of late Quaternary landforms, or other evidence of Holocene or late Pleistocene activity.

3. *San Miguelito Fault Zone*

Northwesterly-trending faults have been mapped in the area between Pismo Beach and Arroyo Grande, and from Avila Beach to the vicinity of the west fork of Vineyard Canyon, north of San Luis Hill. Because these faults lie on the same trend, appear to reflect similar senses of movement, and are "separated" only by an area of no exposure along the shoreline between Pismo Beach and Avila Beach, they may well be part of a more or less continuous zone about 10 miles long. As on the Edna fault, movements along the San Miguelito fault appear to have been predominantly dip-slip, but with displacement down on the northeast. Hall's preliminary cross section indicates total vertical separation of about 1400 feet. The fault is mapped as being overlain by unbroken deposits of the Paso Robles Formation near Arroyo Grande.

Field checking of the ground along the projected trend of the San Miguelito fault zone northwest of Vineyard Canyon in the San Luis Range has substantiated Hall's note that the fault cannot be traced west of that area.

Detailed mapping of the nearly continuous sea cliff exposures extending across this trend northeast of Point Buchon has shown there is no faulting along the San Miguelito trend at the northwesterly end of the range. Like the Edna fault zone, the San Miguelito fault zone evidently represents a zone of high-angle dip-slip rupturing along the flank of the San Luis-Pismo syncline.

4. *East Boundary Zone of the Offshore Santa Maria Basin*

The boundary between the offshore Santa Maria Basin and the onshore features of the southern Coast Ranges is a 4 to 5 wide zone of generally north-northwest-trending folds, faults, and onlap unconformities referred to as the "Hosgri fault zone" by Wagner (Reference 31). The geology of this boundary zone has been investigated in detail by means of extensive seismic reflection profiling, high resolution surface profiling, and side scan sonar surveying.

More general information about structural relationships along the boundary zone has been obtained from the pattern of Bouguer Gravity anomaly values that exist in its vicinity. These data show the East Boundary zone to consist of a series of generally parallel north-northwest-trending faults and folds, developed chiefly in upper Pliocene strata that flank upwarped lower Pliocene and older rocks. The zone extends from south of the latitude of Point Sal to north of Point Piedras Blancas. Within the zone, individual fault breaks range in length from less than 1000 feet up to a maximum of

about 30 miles. The overall length of the zone is approximately 90 miles, with about 60 miles of relatively continuous faulting.

The apparent vertical component of movement is down to the west across some faults and down to the east across others. Along the central reach of the zone, opposite the San Luis Range, a block of ground has been dropped between the two main strands of the fault to form a graben structure. Within the graben, and at other points along the East Boundary zone, bedding in the rock has been folded down toward the upthrown side of the west side down fault. This feature evidently is an expression of "reverse drag" phenomena.

The axes of folds in the ground on either side of the principal fault breaks can be traced for distances of as much as 22 miles. The fold axes typically are nearly horizontal; maximum axial plunges seem to be 5° or less. The structure and onlap relationships of the upper Pliocene, as reflected in the configuration of the unconformity at its base, are such that it consistently rises from the offshore basin and across the boundary zone via a series of upwarps, asymmetric folds, and faults. This configuration seems to correspond generally to a zone of warping and partial disruption along the boundary between relatively uplifting and subsiding regions.

2.5.2.1.3 Geologic History

The geologic history reflected by the rocks, structural features, and landforms of the San Luis Range is typical of that of the southern Coast Ranges of California in its length and complexity. Six general episodes for which there is direct evidence can be tabulated as follows:

<u>Age</u>	<u>Episode</u>	<u>Evidence</u>
Late Mesozoic	Development of Franciscan and Upper Cretaceous rock assemblages	Franciscan and other Mesozoic rocks
Late Mesozoic - Early Tertiary	Early Coast Ranges deformation	Structural features pre-served in the Mesozoic rocks
Mid-Tertiary	Uplift and erosion	Erosion surface at the base of the Tertiary section
Mid- and late-Tertiary	Accumulation of Miocene and Pliocene sedimentary and volcanic rocks	Vaqueros, Rincon, Obispo, Point Sal, Monterey, and Pismo Formation and associated volcanic intrusive, and brecciated rocks
Pliocene	Folding and faulting associated with the Pliocene Coast Ranges deformation	Folding and faulting of the Tertiary and basement rocks

DCPP UNITS 1 & 2 FSAR UPDATE

Pleistocene	Uplift and erosion, development of successive tiers of wave-cut-benches alluvial fan, talus, and landslide deposition.	Pleistocene and Holocene deposits, present land-forms.
-------------	--	--

The earliest recognizable geologic history of the southern Coast Ranges began in Mesozoic time, during the Jurassic period when eugeosynclinal deposits (graywacke sandstone, shale, chert, and basalt) accumulated in an offshore trench developed in oceanic crust.

Some time after the initiation of Franciscan sedimentation, deposition of a sequence of miogeosynclinal or shelf sandstones and shales, known as the Great Valley Sequence, began on the continental crust, at some distance to the east of the Franciscan trench. Deposition of both sequences continued into Cretaceous time, even while the crustal basement section on which the Great Valley strata were being deposited was undergoing plutonism involving emplacement of granitic rocks. Subsequently, the Franciscan assemblage, the Great Valley Sequence, and the granite-intruded basement rocks were tectonically juxtaposed. The resulting terrane consisted generally of granitic basement thrust over intensely deformed Franciscan, with Great Valley Sequence strata overlying the basement, but thrust over and faulted into the Franciscan.

The processes that were involved in the tectonic juxtaposition evidently were active during the Mesozoic, and continued into the early Tertiary. Page (Reference 25) has shown that they were completed by no later than Oligocene time, so that the dual core complex basement of the southern Coast Ranges was formed by then.

The Miocene and later geologic history of the southern Coast Ranges region began with deposition of the Vaqueros and Rincon Formations on a surface eroded on the Franciscan and Great Valley core complex rocks.

Following deposition and some deformation and erosion of these formations, the stratigraphic unit that includes the Point Sal and Obispo Formations as approximately contemporaneous facies was laid down. The Obispo consists of a section of tuffaceous sandstone and mudstone, with lesser amounts of shale, and lensing layers of vitric and lithic-crystal tuff. Locally, the unit is featured by masses of clastic-textured tuffaceous rock that exhibit cross-cutting intrusive relations with the bedded parts of the formation. The Obispo and Point Sal were folded and locally eroded prior to initiation of the main episode of upper Miocene and Pliocene marine sedimentation.

During late middle Miocene to late Miocene time, deposition of the thick sections of silica-rich shale of the Monterey Formation began. Deposition of this formation and equivalent strata took place throughout much of the coastal region of California, but apparently was centered in a series of offshore basins that all developed at about the same time, some 10 to 12 million years ago. Local volcanism toward the latter part of this time is shown by the presence of diabase dikes and sills in the Monterey. Near the end of the Miocene, the Monterey strata were subjected to compressional deformation resulting in folding, in part with great complexity, and in faulting. Near the old

DCPP UNITS 1 & 2 FSAR UPDATE

continental margin, represented by the Sur-Nacimiento fault zone, the deformation was most intense, and was accompanied by uplift. This apparently resulted in the first development of many of the large folds of the southern Coast Ranges including the Huasna and San Luis-Pismo synclines, and in the partial erosion of the folded Monterey section in areas of uplift. The pattern of regional uplift of the Coast Ranges and subsidence of the offshore basins, with local upwarping and faulting in a zone of inflection along the boundary between the two regions, apparently became well established during the episode of late Miocene and Mio-Pliocene diastrophism.

Sedimentation resumed in Pliocene time throughout much of the region of the Miocene basins, and several thousand feet of siltstone and sandstone was deposited. This was the last significant episode of marine sedimentation in the region of the present Coast Ranges. Pliocene deposits in the region of uplift were then folded, and there was renewed movement along most of the preexisting larger faults.

Differential movements between the Coast Ranges uplift and the offshore basins were again concentrated along the boundary zone of inflection, resulting in upwarping and faulting of the basement, Miocene, and Pliocene sections. Relative displacement across parts of this zone evidently was dominantly vertical, because the faulting in the Pliocene has definitely extensional character, and Miocene structures can be traced across the zone without apparent lateral offset. The basement and Tertiary sections step down seaward, away from the uplift, along a system of normal faults having hundreds to nearly a thousand feet of dip-slip offset. A second, more seaward system of normal faults is antithetic to the master set and exhibits only tens to a few hundreds of feet of displacement. Strata between these faults locally exhibit reverse drag downfolding toward the edge of the Pliocene basin, whereas the section is essentially undeformed farther offshore. This style of deformation indicates a passive response, through gravity tectonics, to the onshore uplift.

The Plio-Pleistocene uplift was accompanied by rapid erosion, with consequent nearby deposition of clastic sediments such as the Paso Robles Formation in valleys throughout the southern Coast Ranges. The high-angle reverse and normal faulting observed by Compton (Reference 38) in the northern Santa Lucia Range also occurred farther south, probably more or less contemporaneously with accumulation of the continental deposits. Much of the Quaternary faulting other than that related to the San Andreas right lateral stress-strain system may well have occurred at this time.

Tectonic activity during the Quaternary has involved continued general uplift of the southern Coast Ranges, with superimposed local downwarping and continued movement along faults of the San Andreas system. The uplift is shown by the general high elevation and steep youthful topography that characterizes the Coast Ranges and by the widespread uplifted marine and stream terraces. Local downwarping can be seen in valleys, such as the Santa Maria Valley, where thick sections of Plio-Pleistocene and younger deposits have accumulated. Evidence of significant late Quaternary fault movement is seen in the topography along the Rinconada-San Marcos, Espinosa, San Simeon, and Santa Lucia Bank faults, as well

as along the San Andreas itself. Only along the San Andreas, however, is there evidence of Holocene or contemporary movement.

The latest stage in the evolution of the San Luis Range has extended from mid-Pleistocene time to the present, and has involved more or less continuous interaction between apparent uplift of the range and alternating periods of erosion or deposition, especially along the coast, during times of relatively rising, falling, or unchanging sea level. The development of wave-cut benches and the accumulation of marine deposits on these benches have provided a reliable guide to the minimum age of latest displacements along breaks in the underlying bedrock. Detailed exploration of the interfaces between wave-cut benches and overlying marine deposits at the site of DCPP has shown that no breaks extend across these interfaces. This demonstrates that the youngest faulting or other bedrock breakage in that area antedated the time of terrace cutting, which is on the order of 80,000 to 120,000 years before the present.

The bedrock section and the surficial deposits that formerly capped this bedrock on which the power plant facilities are located have been studied in detail to determine whether they express any evidence of deformation or dislocation ascribable to earthquake effects.

The surficial geologic materials at the site consisted of a thin, discontinuous basal section of rubbly marine sand and silty sand, and an overlying section of nonmarine rocky sand and sandy clay alluvial and colluvial deposits. These deposits were extensively exposed by exploratory trenches, and were examined and mapped in detail. No evidence of earthquake-induced effects such as lurching, slumping, fissuring, and liquefaction was detected during this investigation.

The initial movement of some of the landslide masses now present in Diablo Canyon upstream from the switchyard area may have been triggered by earthquake shaking. It is also possible that some local talus deposits may represent earthquake-triggered rock falls from the sea cliff or other steep slopes in the vicinity.

Deformation of the rock substrata in the site area may well have been accompanied by earthquake activity at the time of its occurrence in the geologic past. There is no evidence, however, of post-terrace earthquake effects in the bedrock where the power plant is being constructed.

2.5.2.1.4 Stratigraphy of the San Luis Range and Vicinity

The geologic section exposed in the San Luis Range comprises sedimentary, igneous, and tectonically emplaced ultrabasic rocks of Mesozoic age, sedimentary, pyroclastic, and hypabyssal intrusive rocks of Tertiary age, and a variety of surficial deposits of Quaternary age. The lithology, age, and distribution of these rocks were studied by Headlee and more recently have been mapped in detail by Hall. The geology of the San Luis Range is shown in Figure 2.5-6 with a geologic cross section constructed using exploratory oil wells shown in Figure 2.5-7. The geologic events that resulted in

the stratigraphic units described in this section are discussed in Section 2.5.2.1.3, Geologic History.

2.5.2.1.4.1 Basement Rocks

An assemblage of rocks typical of the Coast Ranges basement terrane west of the Nacimiento fault zone is exposed along the south and northeast sides of the San Luis Range. As described by Headlee, this assemblage includes quartzose and greywacke sandstone, shale, radiolarian chert, intrusive serpentine and diabase, and pillow basalt. Some of these rocks have been dated as Upper Cretaceous from contained microfossils, including pollen and spores, and Headlee suggested that they may represent dislocated parts of the Great Valley Sequence. There is contrasting evidence, however, that at least the pillow basalt and associated cherty rocks may be more typically Franciscan. Certainly, such rocks are characteristic of the Franciscan terrane. Further, a potassium-argon age of 156 million years, equivalent to Upper Jurassic, has been determined for a core of similar rocks obtained from the bottom of the Montodoro Well No. 1 near Point Buchon.

2.5.2.1.4.2 Tertiary Rocks

Five formational units are represented in the Tertiary section of the San Luis Range. The lower part of this section comprises rocks of the Vaqueros, Rincon, and Obispo Formations, which range in age from lower Miocene through middle Miocene. These strata crop out in the vicinity of Hazard Canyon, at the northwest end of the range, and in a broad band along the south coastal margin of the range. In both areas the Vaqueros rests directly on Mesozoic basement rocks. The core of the western San Luis Range is underlain by the Upper Miocene Monterey Formation, which constitutes the bulk of the Tertiary section. The Upper Miocene to Lower Pliocene Pismo Formation crops out in a discontinuous band along the southwest flank and across the west end of the range, resting with some discordance on the Monterey section and elsewhere directly on older Tertiary or basement rocks.

The coastal area in the vicinity of Diablo Canyon is underlain by strata that have been variously correlated with the Obispo, Point Sal, and Monterey Formations. Headlee, for example, has shown the Point Sal as overlying the Obispo, whereas Hall has considered these two units as different facies of a single time-stratigraphic unit. Whatever the exact stratigraphic relationships of these rocks might prove to be, it is clear that they lie above the main body of tuffaceous sedimentary rocks of the Obispo Formation and below the main part of the Monterey Formation. The existence of intrusive bodies of both tuff breccia and diabase in this part of the section indicates either that local volcanic activity continued beyond the time of deposition of the Obispo Formation, or that the section represents a predominantly sedimentary facies of the upper part of the Obispo Formation. In either case, the strata underlying the power plant site range downward through the Obispo Formation and presumably include a few hundred feet of the Rincon and Vaqueros Formations resting upon a basement of Mesozoic rocks.

DCPP UNITS 1 & 2 FSAR UPDATE

A generalized description of the major units in the Tertiary section follows, and a more detailed description of the rocks exposed at the power plant site is included in a later section.

The Vaqueros Formation has been described by Headlee as consisting of 100 to 400 feet of resistant, massive, coarse-grained, calcareously cemented bioclastic sandstone. The overlying Rincon Formation consists of 200 to 300 feet of dark gray to chocolate brown calcareous shale and mudstone.

The Obispo Formation (or Obispo Tuff) is 800 to 2000 feet thick and comprises alternating massive to thick-bedded, medium to fine grained vitric-lithic tuffs, finely laminated black and brown marine siltstone and shale, and medium grained light tan marine sandstone. Headlee assigned to the Point Sal Formation a section described as consisting chiefly of medium to fine grained silty sandstone, with several thin silty and fossiliferous limestone lenses; it is gradational upward into siliceous shale characteristic of the Monterey Formation. The Monterey Formation itself is composed predominantly of porcelaneous and finely laminated siliceous and cherty shales.

The Pismo Formation consists of massive, medium to fine grained arkosic sandstone, with subordinate amounts of siltstone, sandy shale, mudstone, hard siliceous shale, and chert.

2.5.2.1.4.3 Quaternary Deposits

Deposits of Pleistocene and Holocene age are widespread on the coastal terrace benches along the southwest margin of the San Luis Range, and they exist farther onshore as local alluvial and stream-terrace deposits, landslide debris, and various colluvial accumulations. The coastal terrace deposits include discontinuous thin basal sections of marine silt, sand, gravel, and rubble, some of which are highly fossiliferous, and generally much thicker overlying sections of talus, alluvial-fan debris, and other deposits of landward origin. All of the marine deposits and most of the overlying nonmarine accumulations are of Pleistocene age, but some of the uppermost talus and alluvial deposits are Holocene. Most of the alluvial and colluvial materials consist of silty clayey sand with irregularly distributed fragments and blocks of locally exposed rock types. The landslide deposits include chaotic mixtures of rock fragments and fine-grained matrix debris, as well as some large masses of nearly intact to thoroughly disrupted bedrock.

A more detailed description of surficial deposits that are present in the vicinity of the power plant site is included in a later section.

2.5.2.1.5 Structure of the San Luis Range and Vicinity

2.5.2.1.5.1 General Features

The geologic structure of the San Luis Range-Estero Bay and adjacent offshore area is characterized by a complex set of folds and faults (Figures 2.5-5, 2.5-6, and 2.5-7). Tectonic events that produced these folds and faults are discussed in Section 2.5.2.1.3, Geologic History. The San Luis Range-Estero Bay and adjacent offshore area lies within the zone of transition from the west-trending Transverse Range structural province to the northwest-trending Coast Ranges province. Major structural features are the long narrow downfold of the San Luis-Pismo syncline and the bordering antiformal structural highs of Los Osos Valley on the northeast, and of Point San Luis and the adjacent offshore area on the southwest. This set of folds trends obliquely into a north-northwest aligned zone of basement upwarping, folding, and high-angle normal faulting that lies a few miles off the coast. The main onshore folds can be recognized, by seismic reflection and gravity techniques, in the structure of the buried, downfaulted Miocene section that lies across (west of) this zone.

Lesser, but yet important structural features in this area include smaller zones of faulting and trends of volcanic intrusives. The Edna and San Miguelito fault zones disrupt parts of the northeast and southwest flanks of the San Luis-Pismo syncline. A southward extension of the San Simeon fault, the existence of which is inferred on the basis of the linearity of the coastline between Cambria and Point Estero, and of the gravity gradient in that area, may extend into, and die out within, the northern part of Estero Bay. An aligned series of plugs and lensoid masses of Tertiary volcanic rocks that intrude the Franciscan Formation along the axis of the Los Osos Valley antiform extends from the outer part of Estero Bay southeastward for 22 miles (Figure 2.5-6).

These features define the major elements of geologic structure in the San Luis Range-Estero Bay area. Other structural elements include the complex fold and fault structures within the Franciscan core complex rocks and the numerous smaller folds within the Tertiary section.

2.5.2.1.5.2 San Luis-Pismo Syncline

The main synclinal fold of the San Luis Range, referred to here as the San Luis-Pismo syncline, trends about N60°W and forms a structural trend more than 15 miles in length. The fold system comprises several parallel anticlines and synclines across its maximum onshore width of about 5 miles. Individual folds of the system typically range in length from hundreds of feet to as much as 10,000 feet. The folds range from zero to more than 30° in plunge, and have flank dips as steep as 90°. Various kinds of smaller folds exist locally, especially flexures and drag folds associated with tuff intrusions and with zones of shear deformation.

Near Estero Bay, the major fold extends to a depth of more than 6000 feet. Farther south, in the central part of the San Luis Range, it is more than 11,000 feet deep. Parts

of the northeast flank of the fold are disrupted by faults associated with the Edna fault zone. Local breaks along the central part of the southwest flank have been referred to as the San Miguelito fault zone.

2.5.2.1.5.3 Los Osos Valley Antiform

The body of Franciscan and Great Valley Sequence rocks that crops out between the San Luis-Pismo and Huasna synclines is here referred to as the Los Osos Valley antiform. This composite structure extends southward from the Santa Lucia Range, across the central and northern part of Estero Bay, and thence southeastward to the point where it is faulted out at the juncture of the Edna and the West Huasna fault zones.

Notable structural features within this core complex include northwest- and west-northwest- trending-faults that separate Franciscan melange, graywacke, metavolcanic, and serpentinite units. The serpentinites have been intruded or dragged within faults, apparently over a wide range of scales. One of the more persistent zones of serpentinite bodies occurs along a trend which extends west-northwestward from the West Huasna fault. It has been suggested that movement from this fault may have taken place within this serpentine belt. The range of hills that lies between the coast and Highway 1 between Estero Bay and Cambria is underlain by sandstone and minor shale of the Great Valley Sequence, referred to as the Cambria slab, which has been underthrust by Franciscan rocks. The thrust contact extends southeastward under Estero Bay near Cayucos. This contact is probably related to the fault contact between Great Valley and Franciscan rocks located just north of San Luis Obispo, which Page has shown to be overlain by unbroken lower Miocene strata.

A prominent feature of the Los Osos Valley antiform is the line of plugs and lensoid masses of intrusive Tertiary volcanic rocks. These distinctive bodies are present at isolated points along the approximate axis of the antiform over a distance of 22 miles, extending from the center of outer Estero Bay to the upper part of Los Osos Valley (Figure 2.5-6). The consistent trend of the intrusives provides a useful reference for assessing the possibility of northwest-trending lateral slip faulting within Estero Bay. It shows that such faulting has not extended across the trend from either the inferred San Simeon fault offshore south extension, or from faults in the ground east of the San Simeon trend.

2.5.2.1.5.4 Edna and San Miguelito Fault Zones

These fault zones are described in Section 2.5.2.1.2.3.

2.5.2.1.5.5 Adjacent Offshore Area and East Boundary of the Offshore Santa Maria Basin

The stratigraphy and west-northwest-trending structure that characterize the onshore region from Point Sal to north of Point Estero have been shown by extensive marine

DCPP UNITS 1 & 2 FSAR UPDATE

geophysical surveying to extend into the adjacent offshore area as far as the north-northwest trending structural zone that forms a boundary with the main offshore Santa Maria Basin. Owing to the irregular outline of the coast, the width of the offshore shelf east of this boundary zone ranges from 2-1/2 to as much as 12 miles. The shelf area is narrowest opposite the reach of coast between Point San Luis and Point Buchon, and widest in Estero Bay and south of San Luis Bay.

The major geologic features that underlie the near-shore shelf include, from south to north, the Casmalia Hills anticline, the broad Santa Maria Valley downwarp, the anticlinal structural high off Point San Luis, the San Luis-Pismo syncline, and the Los Osos Valley antiform.

The form of these features is defined by the outcrop pattern and structure of the older Pliocene, Miocene, and basement core complex rocks. The younger Pliocene strata that constitute the upper 1000 to 2000 feet of section in the adjacent offshore Santa Maria Basin are partly buttressed and partly faulted against the rocks that underlie the near-shore shelf, and they unconformably overlap the boundary zone and parts of the shelf in several areas.

The boundaries between the San Luis-Pismo syncline and the adjacent Los Osos Valley and Point San Luis antiforms can be seen in the offshore area to be expressed chiefly as zones of inflection between synclinal and anticlinal folds, rather than as zones of fault rupture such as occurs farther south along the Edna and San Miguelito faults. Isolated west-northwest-trending faults of no more than a few hundred feet displacement are located along the northeast flank of the syncline in Estero Bay. These faults evidently are the northwesternmost expressions of breakage along the Edna fault trend.

The main San Luis-Pismo synclinal structure opens to the northwest, attaining a maximum width of 8 or 9 miles in the southerly part of Estero Bay. The Point San Luis high, on the other hand, is a domal structure, the exposed basement rock core of which is about 10 miles long and 5 miles wide.

The general characteristics of the Santa Maria Basin East Boundary zone have been described in Section 2.5.2.1.2.3. As was noted there, the zone is essentially an expression of the boundary between the synclinorial downwarp of the offshore basin and the regional uplift of the southern Coast Ranges. In the vicinity of the San Luis Range, the zone is characterized by pronounced upwarping and normal faulting of the basement and overlying Tertiary rock sections. Both modes of deformation have contributed to the structural relief of about 500 feet in the Pliocene section, and of 1500 feet or more in the basement rocks, across this boundary. Successively younger strata are banked unconformably against the slopes that have formed from time to time in response to the relative uplifting of the ground east of the boundary zone.

A series of near-surface structural troughs forms prominent features within the segment of the boundary zone structure that extends between the approximate latitudes of

DCPP UNITS 1 & 2 FSAR UPDATE

Arroyo Grande and Estero Bay. This trough structure apparently has formed through the extension and subsidence of a block of ground in the zone where the downwarp of the offshore basin has pulled away from the Santa Lucia uplift. Continued subsidence of this block has resulted in deformation and partial disruption of the buttress unconformity between the offshore Pliocene section and the near-shore Miocene and older rocks. This deformation is expressed by normal faulting and reverse drag type downfolding of the Pliocene strata adjacent to the contact, along the east side of the trough.

On the opposite, seaward side of the trough, a series of antithetic down-to-the-east normal faults of small displacement has formed in the Pliocene strata west of the contact zone. These faults exhibit only a few tens of feet displacement, and they seem to exhibit constant or even decreasing displacement downward.

The structural evolution of the offshore area near Estero Bay and the San Luis Range involved episodes of compressional deformation that affected the upper Tertiary section similarly on opposite sides of the boundary zone. The section on either side exhibits about the same intensity and style of folding. Major folds, such as the San Luis-Pismo syncline and the Piedras Blancas anticline, can be traced into the ground across the boundary zone.

The internal structure of the zone, including the presence of several on-lap unconformities in the adjacent Pliocene section, shows that, at least during Pliocene and early Pleistocene time, the boundary zone has been the inflection line between the Coast Ranges uplift and the offshore Santa Maria Basin downwarp.

Evidence that uplift has continued through late Pleistocene time, at least in the vicinity of the San Luis Range, is given by the presence of successive tiers of marine terraces along the seaward flank of the range. The wave-cut benches and back scarps of these terraces now exist at elevations ranging from about -300 feet (below sea level) to more than 300 feet above sea level.

The ground within which the East Boundary zone lies has been beveled by the post-Wisconsin marine transgression, and so the zone generally is not expressed topographically. Small topographic features, such as a seaward topographic step-up of the sea floor surface across the east-down fault at the BBN (Reference 37) (offshore) survey line 27 crossing, in Estero Bay, and several possible fault-line notch back scarps, however, may represent minor topographic expressions of deformation within the zone.

2.5.2.1.6 Structural Stability

The potential for surface or subsurface subsidence, uplift, or collapse at the site or in the region surrounding the site, is discussed in Section 2.5.5, Stability of Subsurface Materials.

2.5.2.1.7 Regional Groundwater

Groundwater in the region surrounding the site is used as a backup source due to its poor quality and the lack of a significant groundwater reservoir. Section 2.4.13 states that most of the groundwater at the site or in the area around the site is either in the alluvial deposits of Diablo Creek or seeps from springs encountered in excavations at the site.

2.5.2.2 Site Geology

2.5.2.2.1 Site Physiography

The site consists of approximately 750 acres near the mouth of Diablo Creek and is located on a sloping coastal terrace, ranging from 60 to 150 feet above sea level. The terrace terminates at the Pacific Ocean on the southwest and extends toward the San Luis Mountains on the northeast. The terrace consists of bedrock overlain by surficial deposits of marine and nonmarine origin.

The remainder of this section presents a detailed description of site geology.

2.5.2.2.2 General Features

The area of the DCP site is a coastal tract in San Luis Obispo County approximately 6.5 miles northwest of Point San Luis. It lies immediately southeast of the mouth of Diablo Canyon, a major westward-draining feature of the San Luis Range, and about a mile southeast of Lion Rock, a prominent offshore element of the highly irregular coastline.

The ground being developed as a power plant site occupies an extensive topographic terrace about 1000 feet in average width. In its pregrading, natural state, the gently undulating surface of this terrace sloped gradually southwestward to an abrupt termination along a cliff fronting the ocean; in a landward, or northeasterly, direction, it rose with progressively increasing slope to merge with the much steeper front of a foothill ridge of the San Luis Range. The surface ranged in altitude from 65 to 80 feet along the coastline to a maximum of nearly 300 feet along the base of the hillslope to the northeast, but nowhere was its local relief greater than 10 feet. Its only major interruption was the steep-walled canyon of lower Diablo Creek, a gash about 75 feet in average depth.

The entire subject area is underlain by a complex sequence of stratified marine sedimentary rocks and tuffaceous volcanic rocks, all of Tertiary (Miocene) age. Diabasic intrusive rocks are locally exposed high on the walls of Diablo Canyon at the edge of the area. Both the sedimentary and volcanic rocks have been folded and otherwise disturbed over a considerable range of scales.

DCPP UNITS 1 & 2 FSAR UPDATE

Surficial deposits of Quaternary age are widespread. In a few places, they are as thick as 50 feet, but their average thickness probably is on the order of 20 feet over the terrace areas and 10 feet or less over the entire mapped ground. The most extensive deposits underlie the main topographic terrace.

Like many other parts of the California coast, the Diablo Canyon area is characterized by several wave-cut benches of Pleistocene age. These surfaces of irregular but generally low relief were developed across bedrock by marine erosion, and they are ancient analogues of the benches now being cut approximately at sea level along the present coast. They were formed during periods when the sea level was higher, relative to the adjacent land, than it is now. Each is thinly and discontinuously mantled with marine sand, gravel, and rubble similar to the beach and offshore deposits that are accumulating along the present coastline. Along its landward margin each bears thicker and more localized coarse deposits similar to the modern talus along the base of the present sea cliff.

Both the ancient wave-cut benches and their overlying marine and shoreline deposits have been buried beneath silty to gravelly detritus derived from landward sources after the benches were, in effect, abandoned by the ocean. This nonmarine cover is essentially an apron of coalescing fan deposits and other alluvial debris that is thickest adjacent to the mouths of major canyons.

Where they have been deeply trenched by subsequent erosion, as along Diablo Canyon in the map areas, these deposits can be seen to have buried some of the benches so deeply that their individual identities are not reflected by the present (pregrading) rather smooth terrace topography. Thus, the surface of the main terrace is defined mainly by nonmarine deposits that conceal both the older benches of marine erosion and some of the abruptly rising ground that separates them (refer to Figures 2.5-8 and 2.5-10).

The observed and inferred relationships among the terrace surfaces and the wave-cut benches buried beneath them can be summarized as follows:

<u>Wave-cut Bench</u>		<u>Terrace Surface</u>	
<u>Altitude, feet</u>	<u>Location</u>	<u>Altitude, feet</u>	<u>Location</u>
170-175	Small remnants on sides of Diablo Canyon	Mainly 170-190	Sides of Diablo Canyon and upper parts of main terrace; in places separated from
145-155	Very small remnants on sides of Diablo Canyon	Mainly 150-170	lower parts of terrace by scarps
120-130	Subparallel benches elongate in a northwest-southeast direction but with considerable	Mainly 70-160	Most of main terrace, a wide-spread surface on a composite section of nonmarine deposits; no well-defined scarps
90-100	aggregate width; wholly		
65-80			

DCPP UNITS 1 & 2 FSAR UPDATE

	beneath main terrace surface	50-100	Small remnants above modern sea cliff
30-45	Small remnants above modern sea cliff		No depositional terrace
Approx. 0	Small to moderately large areas along present coastline.		

Within the subject area the wave-cut benches increase progressively in age with increasing elevation above present sea level; hence, their order in the above list is one of decreasing age. By far, the most extensive of these benches slopes gently seaward from a shoreline angle that lies at an elevation of 100 feet above present sea level.

The geology of the power plant site is shown in the site geologic maps, Figures 2.5-8 and 2.5-9, and geologic section, Figure 2.5-10.

2.5.2.2.3 Stratigraphy

2.5.2.2.3.1 Obispo Tuff

The Obispo Tuff, which has been classified either as a separate formation or as a member of the Miocene Monterey Formation, is the oldest bedrock unit exposed in the site area. Its constituent rocks generally are well exposed, appear extensively in the coastward parts of the area, and form nearly all of the offshore prominences and shoals. They are dense to highly porous, and thinly layered to almost massive. Their color ranges from white to buff in fresh exposures, and from yellowish to reddish brown on weathered surfaces, many of which are variegated in shades of brown. Outcrop surfaces have a characteristic "punky" to crusty appearance, but the rocks in general are tough, cohesive, and relatively resistant to erosion.

Several pyroclastic rock types constitute the Obispo Tuff ("To" on map, Figure 2.5-8) in and near the subject area. By far, the most widespread is fine-grained vitric tuff with rare to moderately abundant tabular crystals of sodic plagioclase. The constituent glass commonly appears as fresh shards, but in many places it has been partly or completely devitrified. Crystal tuffs are locally prominent, and some of these are so crowded with 1/8 to 3/8 inch crystals of plagioclase that they superficially resemble granitoid plutonic rocks. Other observed rock types include pumiceous tuffs, pumice-pellet tuff breccias, perlitic vitreous tuffs, tuffaceous siltstones and mudstones, and fine-grained tuff breccias with fragments of glass and various Monterey rocks. No massive flow rocks were recognized anywhere in the exposed volcanic section.

In terms of bulk composition, the pyroclastic rocks appear to be chiefly soda rhyolites and soda quartz latites. Their plagioclase, which ranges from calcic albite to sodic oligoclase, commonly is accompanied by lesser amounts of quartz as small rounded

crystals and irregular crystal fragments. Biotite, zircon, and apatite also are present in many of the specimens that were examined under the microscope. Most of the tuffaceous rocks, and especially the more vitreous ones, have been locally to pervasively altered. Products of silicification, zeolitization, and pyritization are readily recognizable in many exposures, where the rocks generally are traversed by numerous thin, irregular veinlets and layers of cherty to opaline material. Veinlets and thin, pod-like concentrations of gypsum also are widespread. Where pyrite is present, the rocks weather yellowish to brownish and are marked by gossan-like crusts.

The various contrasting rock types are simply interlayered in only a few places; much more typical are abutting, intertonguing, and irregularly interpenetrating relationships over a wide range of scales. Septa and inclusions of Monterey rocks are abundant, and a few of them are large enough to be shown separately on the accompanying geologic map (Figure 2.5-8). Highly irregular inclusions, a few inches to several feet in maximum dimension, are so densely packed together in some places that they form breccias with volcanic matrices.

The Obispo Tuff is underlain by mudstones of early Miocene (pre-Monterey) age, on which it rests with a highly irregular contact that appears to be in part intrusive. This contact lies offshore in the vicinity of the power plant site, but it is exposed along the seacoast to the southeast.

In a gross way, the Obispo underlies the basal part of the Monterey formation, but many of its contacts with these sedimentary strata are plainly intrusive. Moreover, individual sills and dikes of slightly to thoroughly altered tuffaceous rocks appear here and there in the Monterey section, not uncommonly at stratigraphic levels well above its base (refer to Figures 2.5-8 and 2.5-13). The observed physical relationships, together with the local occurrence of diatoms and foraminifera within the principal masses of volcanic rocks, indicate that much of the Obispo Tuff in this area probably was emplaced at shallow depths beneath the Miocene sea floor during accumulation of the Monterey strata. The tuff unit does not appear to represent a single, well-defined eruptive event, nor is it likely to have been derived from a single source conduit.

2.5.2.2.3.2 Monterey Formation

Stratified marine rocks variously correlated with the Monterey Formation, Point Sal Formation, and Obispo Tuff underlie most of the subject area, including all of that portion intended for power plant location. They are almost continuously exposed along the crescentic sea cliff that borders Diablo Cove, and elsewhere they appear in much more localized outcrops. For convenience, they are here assigned to the Monterey Formation ("Tm" on map, Figure 2.5-8) in order to delineate them from the adjacent more tuffaceous rocks so typical of the Obispo Tuff.

The observed rock types, listed in general order of decreasing abundance, are silty and tuffaceous sandstone, siliceous shale, shaly siltstone and mudstone, diatomaceous shale, sandy to highly tuffaceous shale, calcareous shale and impure limestone,

bituminous shale, fine- to coarse-grained sandstone, impure vitric tuff, silicified limestone and shale, and tuff-pellet sandstone. Dark colored and relatively fine-grained strata are most abundant in the lowest part of the section, as exposed along the east side of Diablo Cove, whereas lighter colored sandstones and siliceous shales are dominant at stratigraphically higher levels farther north. In detail, however, the different rock types are interbedded in various combinations, and intervals of uniform lithology rarely are thicker than 30 feet. Indeed, the closely-spaced alternations of contrasting strata yield a prominent rib-like pattern of outcrop along much of the sea cliff and shoreline bench forming the margin of Diablo Cove.

The sandstones are mainly fine- to medium-grained, and most are distinctly tuffaceous. Shards of volcanic glass generally are recognizable under the microscope, and the very fine-grained siliceous matrix may well have been derived largely through alteration of original glassy material. Some of the sandstone contains small but megascopically visible fragments of pumice, perlitic glass, and tuff, and a few beds grade along strike into submarine tuff breccia. The sandstones are thinly to very thickly layered; individual beds 6 inches to 4 feet thick are fairly common, and a few appear to be as thick as 15 feet. Some of them are hard and very resistant to erosion, and they typically form subdued but nearly continuous elongated projections on major hillslopes (Figure 2.5-8).

The siliceous shales are buff to light gray platy rocks that are moderately hard to extremely hard according to their silica content, but they tend to break readily along bedding and fracture surfaces. The bituminous rocks and the siltstones and mudstones are darker colored, softer, and grossly more compact. Some of them are very thinly bedded or laminated, others appear almost massive or form matrices for irregularly ellipsoidal masses of somewhat sandier material. The diatomaceous, tuffaceous, and sandy rocks are lighter colored. The more tuffaceous types are softer, and the diatomaceous ones are soft to the degree of punkiness; both kinds of rocks are easily eroded, but are markedly cohesive and tend to retain their gross positions on even the steepest of slopes.

The siliceous shale and most of the hardest, highly silicified rocks weather to very light gray, and the dark colored, fine-grained rocks tend to bleach when weathered. The other types, including the sandstones, weather to various shades of buff and light brown. Stains of iron oxides are widespread on exposures of nearly all the Monterey rocks, and are especially well developed on some of the finest-grained shales that contain disseminated pyrite. All but the hardest and most thick-bedded rocks are considerably broken to depths of as much as 6 feet in the zone of weathering on slopes other than the present sea cliff, and the broken fragments have been separated and displaced by surface creep to somewhat lesser depths.

2.5.2.2.3.3 Diabasic Intrusive Rocks

Small, irregular bodies of diabasic rocks are poorly exposed high on the walls of Diablo Canyon at and beyond the northeasterly edge of the map area. Contact relationships are readily determined at only a few places where these rocks evidently are intrusive

into the Monterey Formation. They are considerably weathered, but an ophitic texture is recognizable. They consist chiefly of calcic plagioclase and augite, with some olivine, opaque minerals, and zeolitic alteration products.

2.5.2.2.3.4 Masses of Brecciated Rocks

Highly irregular masses of coarsely brecciated rocks, a few feet to many tens of feet in maximum dimension, are present in some of the relatively siliceous parts of the Monterey section that adjoin the principal bodies of Obispo Tuff. The fracturing and dislocation is not genetically related to any recognizable faults, but instead seems to have been associated with emplacement of the volcanic rocks; it evidently was accompanied by, or soon followed by, extensive silicification. Many adjacent fragments in the breccias are closely juxtaposed and have matching opposed surfaces, so that they plainly represent no more than coarse crackling of the brittle rocks. Other fragments, though angular or subangular, are not readily matched with adjacent fragments and hence may represent significant translation within the entire rock masses.

The ratio of matrix materials to coarse fragments is very low in most of the breccias and nowhere was it observed to exceed about 1:3. The matrices generally comprise smaller angular fragments of the same Monterey rocks that are elsewhere dominant in the breccias, and they characteristically are set in a siliceous cement. Tuffaceous matrices, with or without Monterey fragments, also are widespread and commonly show the effects of pervasive silicification. All the exposed breccias are firmly cemented, and they rank among the hardest and most resistant units in the entire bedrock section.

A few 3 to 18 inch beds of sandstone have been pulled apart to form separate tabular masses along specific stratigraphic horizons in higher parts of the Monterey sequence. Such individual tablets, which are boudins rather than ordinary breccia fragments, are especially well exposed in the sea cliff at the northern corner of Diablo Cove. They are flanked by much finer-grained strata that converge around their ends and continue essentially unbroken beyond them. This boudinage or separation and stringing out of sandstone beds that lie within intervals of much softer and more shaly rocks has resulted from compression during folding of the Monterey section. Its distribution is stratigraphically controlled and is not systematically related to recognizable faults in the area.

2.5.2.2.3.5 Surficial Deposits

1. Coastal Terrace Deposits

The coastal wave-cut benches of Pleistocene age, as described in a foregoing section, are almost continuously blanketed by terrace deposits (Qter in Figure 2.5-8) of several contrasting types and modes of origin. The oldest of these deposits are relatively thin and patchy in their occurrence, and were laid down along and adjacent to ancient beaches during Pleistocene time. They are covered by considerably thicker and more

DCPP UNITS 1 & 2 FSAR UPDATE

extensive nonmarine accumulations of detrital materials derived from various landward sources.

The marine deposits consist of silt, sand, gravel, and cobbly to bouldery rubble. They are approximately 2 feet in average thickness over the entire terrace area and reach a maximum observed thickness of about 8 feet. They rest directly upon bedrock, some of which is marked by numerous holes attributable to the action of boring marine mollusks, and they commonly contain large rounded cobbles and boulders of Monterey and Obispo rocks that have been similarly bored. Lenses and pockets of highly fossiliferous sand and gravel are present locally.

The marine sediments are poorly to very well sorted and loose to moderately well consolidated. All of them have been naturally compacted; the degree of compaction varies according to the material, but it is consistently greater than that observed in any of the associated surficial deposits of other types. Near the inner margins of individual wave-cut benches the marine deposits merge landward into coarser and less well-sorted debris that evidently accumulated along the bases of ancient sea cliffs or other shoreline slopes. This debris is locally as much as 12 feet thick; it forms broad but very short aprons, now buried beneath younger deposits, that are ancient analogues of the talus accumulations along the inner margin of the present beach in Diablo Cove. One of these occurrences, identified as "fossil Qtz" in the geologic map of Figure 2.5-8, is well exposed high on the northerly wall of Diablo Canyon.

A younger, thicker, and much more continuous nonmarine cover is present over most of the coastal terrace area. It consistently overlies the marine deposits noted above, and, where these are absent, it rests directly upon bedrock. It is composed in part of alluvial detritus contributed during Pleistocene time from Diablo Canyon and several smaller drainage courses, and it thickens markedly as traced sourceward toward these canyons. The detritus represents a series of alluvial fans, some of which appear to have partly coalesced with adjacent ones. It is chiefly fine- to moderately-coarse-grained gravel and rubble characterized by tabular fragments of Monterey rocks in a rather abundant silty to clayey matrix. Most of it is thinly and regularly stratified, but the distinctness of this layering varies greatly from place to place.

Slump, creep, and slope-wash deposits, derived from adjacent hillsides by relatively slow downhill movement over long periods of time, also form major parts of the nonmarine terrace cover. All are loose and uncompact. They comprise fragments of Monterey rocks in dark colored clayey matrices, and their internal structure is essentially chaotic. In some places they are crudely interlayered with the alluvial fan deposits, and elsewhere they overlie these bedded sediments. On parts of the main terrace area not reached by any of the alluvial fans, a cover of slump, creep, and slope-wash deposits, a few inches to nearly 10 feet thick, rests directly upon either marine terrace deposits or bedrock.

Thus, the entire section of terrace deposits that caps the coastal benches of Pleistocene marine erosion is heterogeneous and internally complex; it includes contributions of

detritus from contrasting sources, from different directions at different times, and via several basically different modes of transport and deposition.

2. Stream-terrace Deposits

Several narrow, irregular benches along the walls of Diablo Canyon are veneered by a few inches to 6 feet of silty gravels that are somewhat coarser but otherwise similar to the alluvial fan deposits described above. These stream-terrace deposits (Qst) originally occupied the bottom of the canyon at a time when the lower course of Diablo Creek had been cut downward through the alluvial fan sediments of the main terrace and well into the underlying bedrock. Subsequent deepening of the canyon left remnants of the deposits as cappings on scattered small terraces.

3. Landslide Deposits

The walls of Diablo Canyon also are marked by tongue- and bench-like accumulations of loose, rubbly landslide debris (Qls), consisting mainly of highly broken and jumbled masses of Monterey rocks with abundant silty and soily matrix materials. These landslide bodies represent localized failure on naturally oversteepened slopes, generally confined to fractured bedrock in and immediately beneath the zone of weathering. Individual bodies within the mapped area are small, with probable maximum thicknesses no greater than 20 feet. All of them lie outside the area intended for power plant construction.

Landslide deposits along the sea cliff have been recognized at only one locality, on the north side of Diablo Cove about 400 feet northwest of the mouth of Diablo Canyon. Here slippage has occurred along bedding and fracture surfaces in siliceous Monterey rocks, and it has been confined essentially to the axial region of a well-defined syncline (refer to Figure 2.5-8). Several episodes of sliding are attested by thin, elongate masses of highly broken ground separated from one another by well-defined zones of dislocation. Some of these masses are still capped by terrace deposits. The entire composite accumulation of debris is not more than 35 feet in maximum thickness, and ground failure at this locality does not appear to have resulted in major recession of the cliff. Elsewhere within the mapped area, landsliding along the sea cliff evidently has not been a significant process.

Large landslides, some of them involving substantial thickness of bedrock, are present on both sides of Diablo Canyon not far northeast of the power plant area. These occurrences need not be considered in connection with the plant site, but they have been regarded as significant factors in establishing a satisfactory grading design for the switchyard and other up-canyon installations. They are not dealt with in this section.

4. Slump, Creep, and Slope-wash Deposits

As noted earlier, slump, creep, and slope-wash deposits (Qsw) form parts of the nonmarine sedimentary blanket on the main terrace. These materials are shown separately on the geologic map only in those limited areas where they have been considerably concentrated along well-defined swales and are readily distinguished from other surficial deposits. Their actual distribution is much wider, and they undoubtedly are present over a large fraction of the areas designated as Qter; their average thickness in such areas, however, is probably less than 5 feet.

Angular fragments of Monterey rocks are sparsely to very abundantly scattered through the slump, creep, and slope-wash deposits, whose most characteristic feature is a fine-grained matrix that is dark colored, moderately rich in clay minerals, and extremely soft when wet. Internal layering is rarely observable and nowhere is sharply expressed. The debris seems to have been rather thoroughly intermixed during its slow migration down hillslopes in response to gravity. That it was derived mainly from broken materials in the zone of weathering is shown by several exposures in which it grades downward through soily debris into highly disturbed and partly weathered bedrock, and thence into progressively fresher and less broken bedrock.

5. Talus and Beach Deposits

Much of the present coastline in the subject area is marked by bare rock, but Diablo Cove and a few other large indentations are fringed by narrow, discontinuous beaches and irregular concentrations of sea cliff talus. These deposits (Qtb) are very coarse grained. Their total volume is small, and they are of interest mainly as modern analogues of much older deposits at higher levels beneath the main terrace surface.

The beach deposits consist chiefly of well-rounded cobbles. They form thin veneers over bedrock, and in Diablo Cove they grade seaward into patches of coarse pebbly sand. The floors of both Diablo Cove and South Cove probably are irregular in detail and are featured by rather hard, fresh bedrock that is discontinuously overlain by irregular thin bodies of sand and gravel. The distribution and abundance of kelp suggest that bedrock crops out over large parts of these cove areas where the sea bottom cannot be observed from onshore points.

6. Stream-laid Alluvium

Stream-laid alluvium (Qal) occurs as a strip along the present narrow floor of Diablo Canyon, where it is only a few feet in average thickness. It is composed of irregularly intertongued silt, sand, gravel, and rubble. It is crudely to sharply stratified, poorly to well sorted, and, in general, somewhat compacted. Most of it is at least moderately porous.

7. Other Deposits

Earlier inhabitation of the area by Indians is indicated by several midden deposits that are rich in charcoal and fragments of shells and bones. The most extensive of these occurrences marks the site of a long-abandoned village along the edge of the main terrace immediately northwest of Diablo Canyon. Others have been noted on the main terrace just east of the mouth of Diablo Canyon, on the shoreward end of South Point, and at several places in and near the plant site.

2.5.2.2.4 Structure

2.5.2.2.4.1 Tectonic Structures Underlying the Region Surrounding the Site

The dominant tectonic structure in the region of the power plant site is the San Luis-Pismo downwarp system of west-northwest-trending folds. This structure is bounded on the northeast by the antiformal basement rock structure of the Los Osos and San Luis Valley trend. The west-northwest-trending Edna fault zone lies along the northeast flank of the range, and the parallel Miguelito fault extends into the southeasterly end of the range. A north-northwest-trending structural discontinuity that may be a fault has been inferred or interpolated from widely spaced traverses in the offshore, extending within about 5 miles of the site at its point of closest approach. To the west of this discontinuity, the structure is dominated by north to north-northwest-trending folds in Tertiary rocks. These features are illustrated in Figure 2.5-3 and described in this section.

Tectonic structures underlying the site and region surrounding the site are identified in the above and following sections, and they are shown in Figures 2.5-3, 2.5-5, 2.5-8, 2.5-10, 2.5-15, and 2.5-16. They are listed as follows:

2.5.2.2.4.2 Tectonic Structures Underlying the Site

The rocks underlying the DCPD site have been subjected to intrusive volcanic activity and to later compressional deformation that has given rise to folding, jointing and fracturing, minor faulting, and local brecciation. The site is situated in a section of moderately to steeply north-dipping strata, about 300 feet south of an east-west-trending synclinal fold axis (Figures 2.5-8 and 2.5-10). The rocks are jointed throughout, and they contain local zones of closely spaced high-angle fractures (Figure 2.5-16).

A minor fault zone extends into the site from the west, but dies out in the vicinity of the Unit 1 turbine building. Two other minor faults were mapped for distances of 35 to more than 200 feet in the bedrock section exposed in the excavation for the Unit 1 containment structure. In addition to these features, cross-cutting bodies of tuff and tuff breccia, and cemented "crackle breccia" could be considered as tectonic structures.

DCPP UNITS 1 & 2 FSAR UPDATE

Exact ages of the various tectonic structures at the site are not known. It has been clearly demonstrated, however, that all of them are truncated by, and therefore antedate, the principal marine erosion surface that underlies the coastal terrace bench. This terrace can be correlated with coastal terraces to the north and south that have been dated as 80,000 to 120,000 years old. The tectonic structures probably are related to the Pliocene-lower Pleistocene episode of Coast Ranges deformation, which occurred more than 1 million years ago.

The bedrock units within the entire subject area form part of the southerly flank of a very large syncline that is a major feature of the San Luis Range. The northerly-dipping sequence of strata is marked by several smaller folds with subparallel trends and flank-to-flank dimensions measured in hundreds of feet. One of these, a syncline with gentle to moderate westerly plunge, is the largest flexure recognized in the vicinity of the power plant site. Its axis lies a short distance north of the site and about 450 feet northeast of the mouth of Diablo Canyon (Figures 2.5-8 and 2.5-10). East of the canyon this fold appears to be rather open and simple in form, but farther west it probably is complicated by several large wrinkles and may well lose its identity as a single feature. Some of this complexity is clearly revealed along the northerly margin of Diablo Cove, where the beds exposed in the sea cliff have been closely folded along east to northeast trends. Here a tight syncline (shown in Figure 2.5-8) and several smaller folds can be recognized, and steep to near-vertical dips are dominant in several parts of the section.

The southerly flank of the main syncline within the map area steepens markedly as traced southward away from the fold axis. Most of this steepening is concentrated within an across-strike distance of about 300 feet as revealed by the strata exposed in the sea cliff southeastward from the mouth of Diablo Canyon; farther southward the beds of sandstone and finer-grained rocks dip rather uniformly at angles of 70° or more. A slight overturning through the vertical characterizes the several hundred feet of section exposed immediately north of the Obispo Tuff that underlies South Point and the north shore of South Cove (refer to Figure 2.5-8). Thus the main syncline, though simple in gross form, is distinctly asymmetric. The steepness of its southerly flank may well have resulted from buttressing, during the folding, by the relatively massive and competent unit of tuffaceous rocks that adjoins the Monterey strata at this general level of exposure.

Smaller folds, corrugations, and highly irregular convolutions are widespread among the Monterey rocks, especially the finest-grained and most shaley types. Some of these flexures trend east to southeast and appear to be drag features systematically related to the larger-scale folding in the area. Most, however, reflect no consistent form or trend, range in scale from inches to only a few feet, and evidently are confined to relatively soft rocks that are flanked by intervals of harder and more massive strata. They constitute crudely tabular zones of contortion within which individual rock layers can be traced for short distances but rarely are continuous throughout the deformed ground.

Some of this contortion appears to have derived from slumping and sliding of unconsolidated sediments on the Miocene sea floor during accumulation of the

Monterey section. Most of it, in contrast, plainly occurred at much later times, presumably after conversion of the sediments to sedimentary rocks, and it can be most readily attributed to highly localized deformation during the ancient folding of a section that comprises rocks with contrasting degrees of structural competence.

2.5.2.2.4.3 Faults

Numerous faults with total displacements ranging from a few inches to several feet cut the exposed Monterey rocks. Most of these occur within, or along the margins of, the zones of contortion noted above. They are sharp, tight breaks with highly diverse attitudes, and they typically are marked by 1/16-inch or less of gouge or microbreccia. Nearly all of them are curving or otherwise somewhat irregular surfaces, and many can be seen to terminate abruptly or to die out gradually within masses of tightly folded rocks. These small faults appear to have been developed as end products of localized intense deformation caused by folding of the bedrock section. Their unsystematic attitudes, small displacements, and limited effects upon the host rocks identify them as second-order features, i.e., as results rather than causes of the localized folding and convolution with which they are associated.

Three distinctly larger and more continuous faults also were recognized within the mapped area. They are well exposed on the sea cliff that fringes Diablo Cove (refer to Figure 2.5-8), and each lies within a zone of moderately to severely contorted fine-grained Monterey strata. Each is actually a zone, 6 inches to several feet wide, within which two or more subparallel tight breaks are marked by slickensides, 1/4-inch or less of gouge, and local stringers of gypsum. None of these breaks appears to be systematically related to individual folds within the adjoining rocks. None of them extends upward into the overlying blanket of Quaternary terrace deposits.

One of these faults, exposed on the north side of the cove, trends north-northwest essentially parallel to the flanking Monterey beds, but it dips more steeply than these beds. Another, exposed on the east side of the cove, trends east-southeast and is essentially vertical; thus, it is essentially parallel to the structure of the host Monterey section. Neither of these faults projects toward the ground intended for power plant construction. The third fault, which appears on the sea cliff at the mouth of Diablo Canyon, trends northeast and projects toward the ground in the northernmost part of the power plant site. It dips northward somewhat more steeply than the adjacent strata.

Total displacement is not known for any of these three faults on the basis of natural exposures, but it could amount to as much as tens of feet. That these breaks are not major features, however, is strongly suggested by their sharpness, by the thinness of gouge along individual surfaces of slippage, and by the essential lack of correlation between the highly irregular geometry of deformation in the enclosing strata and any directions of movement along the slip surfaces.

The possibility that these surfaces are late-stage expressions of much larger-scale faulting at this general locality was tested by careful examination of the deformed rocks

that they transect. On megascopic scales, the rocks appear to have been deformed much more by flexing than by rupture and slippage, as evidenced by local continuity of numerous thin beds that denies the existence of pervasive faulting within much of the ground in question. That the finer-grained rocks are not themselves fault gouged was confirmed by examination of 34 samples under the microscope.

Sedimentary layering, recognized in 27 of these samples, was observed to be grossly continuous even though dislocated here and there by tiny fractures. Moreover, nearly all the samples were found to contain shards of volcanic glass and/or the tests of foraminifera; some of these delicate components showed effects of microfracturing and a few had been offset a millimeter or less along tiny shear surfaces, but none appeared to have been smeared out or partially obliterated by intense shearing or grinding. Thus, the three larger faults in the area evidently were superimposed upon ground that already had been deformed primarily by small-scale and locally very intense folding rather than by pervasive grinding and milling.

It is not known whether these faults were late-stage results of major folding in the region or were products of independent tectonic activity. In either case, they are relatively ancient features, as they are capped without break by the Quaternary terrace deposits exposed along the upper part of the sea cliff. They probably are not large-scale elements of regional structure, as examination of the nearest areas of exposed bedrock along their respective landward projections revealed no evidence of substantial offsets among recognizable stratigraphic units.

Seaward projection of one or more of these faults might be taken to explain a possible large offset of the Obispo Tuff units exposed on North Point and South Point. The notion of such an offset, however, would rest upon the assumption that these two units are displaced parts of an originally continuous body, for which there is no real evidence. Indeed, the two tuff units are bounded on their northerly sides by lithologically different parts of the Monterey Formation; hence, they were clearly originally emplaced at different stratigraphic levels and are not directly correlative.

2.5.2.2.5 Geological Relationships at the Units 1 and 2 Power Plant Site

2.5.2.2.5.1 Geologic Investigations at the Site

The geologic relationships at DCPP site have been studied in terms of both local and regional stratigraphy and structure, with an emphasis on relationships that could aid in dating the youngest tectonic activity in the area. Geologic conditions that could affect the design, construction, and performance of various components of the plant installation also were identified and evaluated. The investigations were carried out in three main phases, which spanned the time between initial site selection and completion of foundation construction.

2.5.2.2.5.2 Feasibility Investigation Phase

Work directed toward determining the pertinent general geologic conditions at the plant site comprised detailed mapping of available exposures, limited hand trenching in areas with critical relationships, and petrographic study of the principal rock types. The results of this feasibility program were presented in a report that also included recommendations for determining suitability of the site in terms of geologic conditions. Information from this early phase of studies is included in the preceding four sections and illustrated in Figures 2.5-8, 2.5-9, and 2.5-10.

2.5.2.2.5.3 Suitability Investigation Phase

The record phase of investigations was directed toward testing and confirming the favorable judgments concerning site feasibility. Inasmuch as the principal remaining uncertainties involved structural features in the local bedrock, additional effort was made to expose and map these features and their relationships. This was accomplished through excavation of large trenches on a grid pattern that extended throughout the plant area, followed by photographing the trench walls and logging the exposed geologic features. Large-scale photographs were used as a mapping base, and the recorded data were then transferred to controlled vertical sections at a scale of 1 inch = 20 feet. The results of this work were reported in three supplements to the original geologic report (Reference 1). Supplementary Reports I and III presented data and interpretation based on trench exposures in the areas of the Unit 1 and Unit 2 installations, respectively. Supplementary Report II described the relationships of small bedrock faults exposed in the exploratory trenches and in the nearby sea cliff. During these suitability investigations, special attention was given to the contact between bedrock and overlying terrace deposits in the plant site area. It was determined that none of the discontinuities present in the bedrock section displaces either the erosional surface developed across the bedrock or the terrace deposits that rest upon this surface. The pertinent data are presented farther on in this section and illustrated in Figures 2.5-11, 2.5-12, 2.5-13, and 2.5-14.

2.5.2.2.5.4 Construction Geology Investigation Phase

Geologic work done during the course of construction at the plant site spanned an interval of 5 years, which encompassed the period of large-scale excavation. It included detailed mapping of all significant excavations, as well as special studies in some areas of rock bolting and other work involving rock reinforcement and temporary instrumentation. The mapping covered essentially all parts of the area to be occupied by structures for Units 1 and 2, including the excavations for the circulating water intake and outlet, the turbine-generator building, the auxiliary building, and the containment structures. The results of this mapping are described farther on and illustrated in Figures 2.5-15 and 2.5-16.

2.5.2.2.5.5 Exploratory Trenching Program, Unit 1 Site

Four exploratory trenches were cut beneath the main terrace surface at the power plant site, as shown in Figures 2.5-8, 2.5-11, 2.5-12, and 2.5-13. Trench AF (Trench A), about 1080 feet long, extended in a north-northwesterly direction and thus was roughly parallel to the nearby margin of Diablo Cove. Trench BE (Trench B), 380 feet long, was parallel to Trench A and lay about 150 feet east of the northerly one-third of the longer trench. Trenches C and D, 450 and 490 feet long, respectively were nearly parallel to each other, 130 to 150 feet apart, and lay essentially normal to Trenches A and B. The two pairs of trenches crossed each other to form a "#" pattern that would have been symmetrical were it not for the long southerly extension of Trench A. They covered the area intended for Unit 1 power plant construction, and the intersection of Trenches B and C coincided in position with the center of the Unit 1 nuclear reactor structure.

All four trenches, throughout their aggregate length of approximately 2400 feet, revealed a section of surficial deposits and underlying bedrock that corresponds to the two-ply sequence of surficial deposits and Monterey strata exposed along the sea cliff in nearby Diablo Cove. The trenches ranged in depth from 10 feet to nearly 40 feet, and all had sloping sides that gave way downward to essentially vertical walls in the bedrock encountered 3 to 8 feet above their floors.

To facilitate detailed geologic mapping, the easterly walls of Trenches A and B and the southerly walls of Trenches C and D were trimmed to near-vertical slopes extending upward from the trench floors to levels well above the top of bedrock. These walls subsequently were scaled back by means of hand tools in order to provide fresh, clean exposures prior to mapping of the contact between bedrock and overlying unconsolidated materials.

1. *Bedrock*

The bedrock that was continuously exposed in the lowest parts of all the exploratory trenches lies within a portion of the Monterey Formation characterized by a preponderance of sandstone. It corresponds to the part of the section that crops out in lower Diablo Canyon and along the sea cliff southeasterly from the canyon mouth. The sandstone ranges from light gray through buff to light reddish brown, from silty to markedly tuffaceous, and from thin-bedded and platy to massive. The distribution and thickness of beds can be readily appraised from sections along Trenches A and B (Figure 2.5-12) that show nearly all individual bedding surfaces that could be recognized on the ground.

The sandstone ranges from very hard to moderately soft, and some of it feels slightly punky when struck with a pick. All of it is, however, firm and very compact. In general, the most platy parts of the sequence are also the hardest, but the soundest rock in the area is almost massive sandstone of the kind that underlies the site of the intended reactor structure. This rock is well exposed on the nearby hillslope adjoining the main

terrace area, where it has been markedly resistant to erosion and stands out as distinct low ridges.

Tuff, consisting chiefly of altered volcanic glass, forms irregular sills and dikes in several parts of the bedrock section. This material, generally light gray to buff, is compact but distinctly softer than the enclosing sandstone. Individual bodies are 1/2 inch to 4 feet thick. They are locally abundant in Trench C west of Trench A, and in Trench A southward beyond the end of the section in Figure 2.5-12. They are very rare or absent in Trenches B and D, and in the easterly parts of Trench C and the northerly parts of Trench A. These volcanic rocks probably are related to the Obispo Tuff as described earlier, but all known masses of typical Obispo rocks in this area lie at considerable distances west and south of the ground occupied by the trenches.

2. Bedrock Structure

The stratification of the Monterey rocks dips northward wherever it was observable in the trenches, in general, at angles of 35 to 55°. Thus, the bedrock beneath the power plant site evidently lies on the southerly flank of the major syncline noted and described earlier. Zones of convolution and other expressions of locally intense folding were not recognized, and probably are much less common in this general part of the section than in other, previously described parts that include intervals of softer and more shaley rocks.

Much of the sandstone is traversed by fractures. Planar, curving, and irregular surfaces are well represented, and, in places, they are abundant and closely spaced. All prominent fractures and many of the minor and discontinuous ones are shown in the sections of Figure 2.5-12. Also shown in these sections are all recognized slip joints, shear surfaces, and faults, i.e., all surfaces along which the bedrock has been displaced. Such features are most abundant in Trenches A and C near their intersection, in Trench D west of the intersection with Trench A, and near the northerly end of Trench B.

Most of the surfaces of movement are hairline features with or without thin films of clay and/or gypsum. Displacements range from a small fraction of an inch to several inches. The other surfaces are more prominent, with well-defined zones of gouge and fine-grained breccia ordinarily 1/8 inch or less in thickness. Such zones were observed to reach a maximum thickness of nearly 1/2 inch along two small faults, but only as local lenses or pockets. Exposures were not sufficiently extensive in three dimensions for definitely determining the magnitude of slip along the more prominent faults, but all of these breaks appeared to be minor features. Indeed, no expressions of major faulting were recognized in any of the trenches despite careful search, and the continuous bedrock exposures precluded the possibility that such features could have been readily overlooked.

A northeast-trending fault that appears on the sea cliff at the mouth of Diablo Canyon projects toward the ground in the northernmost part of the power plant site, as noted in

a foregoing section. No zone of breaks as prominent as this one was identified in the trench exposures, and any distinct northeastward continuation of the fault would necessarily lie north of the trenched ground. Alternatively, this fault might well separate northeastward into several smaller faults; some or all of these could correspond to some or all of the breaks mapped in the northerly parts of Trenches A and B.

3. Terrace Deposits

Marine terrace deposits of Pleistocene age form a cover, generally 2 to 5 feet thick, over the bedrock that lies beneath the power plant site. This cover was observed to be continuous in Trench C and the northerly part of Trench A, and to be nearly continuous in the other two trenches. Its lithology is highly variable, and includes bouldery rubble, loose beach sand, pebbly silt, silty to clayey sand with abundant shell fragments, and soft clay derived from underlying tuffaceous rocks. Nearly all of these deposits are at least sparsely fossiliferous, and, in a few places, they consist mainly of shells and shell fragments. Vertebrate fossils, chiefly vertebral and rib materials representing large marine mammals, are present locally; recognized occurrences are designated by the symbol X in the sections of Figure 2.5-12.

At the easterly ends of Trenches C and D, the marine deposits intergrade and intertongue in a landward direction with thicker and coarser accumulations of poorly sorted debris. This material evidently is talus that was formed along the base of an ancient sea cliff or other shoreline slope. In some places, the marine deposits are overlain by nonmarine terrace sediments with a sharp break, but elsewhere the contact between these two kinds of deposits is a dark colored zone, a few inches to as much as 2 feet thick, that appears to represent a soil developed on the marine section. Fragments of these soily materials appear here and there in the basal parts of the nonmarine section.

The nonmarine sediments that were exposed in Trenches B, C, and D and in the northerly part of Trench A are mainly alluvial deposits derived in ancient times from Diablo Canyon. They consist of numerous tabular fragments of Monterey rocks in a relatively dark colored silty to clayey matrix, and, in general, they are distinctly bedded and moderately to highly compact. As indicated in the sections of Figure 2.5-12, they thicken progressively in a north-northeastward direction, i.e., toward their principal source, the ancient mouth of Diablo Canyon.

Slump, creep, and slope-wash deposits, which constitute the youngest major element of the terrace section, overlie the alluvial fan gravels and locally are interlayered with them. Where the gravels are absent, as in the southerly part of Trench A, this younger cover rests directly upon bedrock. It is loose and uncompacted, internally chaotic, and is composed of fragments of Monterey rocks in an abundant dark colored clayey matrix.

All the terrace deposits are soft and unconsolidated, and hence are much less resistant to erosion than is the underlying bedrock. Those appearing along the walls of exploratory trenches were exposed to heavy rainfall during two storms, and showed

some tendency to wash and locally to rill. Little slumping and no gross failure were noted in the trenches, however, and it was not anticipated that these materials would cause special problems during construction of a power plant.

4. Interface Between Bedrock and Surficial Deposits

As once exposed continuously in the exploratory trenches, the contact between bedrock and overlying terrace deposits represents a broad wave-cut platform of Pleistocene age. This buried surface of ancient marine erosion ranges in altitude between extremes of 82 and 100 feet, and more than three-fourths of it lies within the more limited range of 90 to 100 feet. It terminates eastward against a moderately steep shoreline slope, the lowest parts of which were encountered at the extreme easterly ends of Trenches C and D, and beyond this slope is an older buried bench at an altitude of 120 to 130 feet.

Available exposures indicate that the configuration of the erosional platform is markedly similar, over a wide range of scales, to that of the platform now being cut approximately at sea level along the present coast. Grossly viewed, it slopes very gently in a seaward (westerly) direction and is marked by broad, shallow channels and by upward projections that must have appeared as low spines and reefs when the bench was being formed (Figures 2.5-12 and 2.5-13). The most prominent reef, formerly exposed in Trenches B and D at and near their intersection, is a wide, westerly-trending projection that rises 5 to 15 feet above neighboring parts of the bench surface. It is composed of massive sandstone that was relatively resistant to the ancient wave erosion.

As shown in the sections and sketches of Figure 2.5-12, the surface of the platform is nearly planar in some places but elsewhere is highly irregular in detail. The small-scale irregularities, generally 3 feet or less in vertical extent, including knob, spine, and rib like projections and various wave-scoured pits, crevices, notches, and channels. The upward projections clearly correspond to relatively hard, resistant beds or parts of beds in the sandstone section. The depressions consistently mark the positions of relatively soft silty or shaley sandstone, of very soft tuffaceous rocks, or of extensively jointed rocks. The surface traces of most faults and some of the most prominent joints are in sharp depressions, some of them with overhanging walls. All these irregularities of detail have modern analogues that can be recognized on the bedrock bench now being cut along the margins of Diablo Cove.

The interface between bedrock and overlying surficial deposits is of particular interest in the trenched area because it provides information concerning the age of youngest fault movements within the bedrock section. This interface is nowhere offset by faults revealed in the trenches, but instead has been developed irregularly across these faults after their latest movements. The consistency of this general relationship was established by highly detailed tracing and inspection of the contact as freshly exhumed by scaling of the trench walls. Gaps in exposure of the interface necessarily were developed at the four intersections of trenches; at these localities, the bedrock was carefully laid bare so that all joints and faults could be recognized and traced along the

trench floors to points where their relationships with the exposed interface could be determined.

Corroborative evidence concerning the age of the most recent fault displacements stems from the marine deposits that overlie the bedrock bench and form the basal part of the terrace section. That these deposits rest without break across the traces of faults in the underlying bedrock was shown by the continuity of individual sedimentary beds and lenses that could be clearly recognized and traced.

Further, some of the faults are directly capped by individual boulders, cobbles, pebbles, shells, and fossil bones, none of which have been affected by fault movements. Thus, the most recent fault displacements in the plant site area occurred prior to marine planation of the bedrock and deposition of the overlying terrace sediments. As pointed out earlier, the age of the most recent faulting in this area is therefore at least 80,000 years and more probably at least 120,000 years. It might be millions of years.

2.5.2.2.5.6 Exploratory Trenching Program, Unit 2 Site

Eight additional trenches were cut beneath the main terrace surface south of Diablo Canyon (Figure 2.5-13) in order to extend the scope of subsurface exploration to include all ground in the Unit 2 plant site. As in the area of the Unit 1 plant site, the trenches formed two groups; those in each group were parallel with one another and were oriented nearly normal to those of the other group. The excavations pertinent to the Unit 2 plant site can be briefly identified as follows:

1. North-northwest Alignment

- a. Trench EJ, 240 feet long, was a southerly extension of older Trench BE (originally designated as Trench B).
- b. Trench WU, 1300 feet long, extended southward from Trench DG (originally designated as Trench D), and its northerly part lay about 65 feet east of Trench EJ. The northernmost 485 feet of this trench was mapped in connection with the Unit 2 trenching program.
- c. Trench MV, 700 feet long, lay about 190 feet east of Trench WU. The northernmost 250 feet of this trench was mapped in connection with the Unit 2 trenching program.
- d. Trench AF (originally designated as Trench A) was mapped earlier in connection with the detailed study of the Unit 1 plant site. A section for this trench, which lay about 140 feet west of Trench EJ, was included with others in the report on the Unit 1 trenching program.

2. *East-northeast Alignment*

- a. Trench KL, about 750 feet long, lay 180 feet south of Trench DG (originally designated as Trench D) and crossed Trenches AF, EJ, and WU.
- b. Trench NO, about 730 feet long, lay 250 feet south of Trench KL and crossed Trenches AF, WU, and MV.

These trenches, or parts thereof, covered the area intended for the Unit 2 power plant construction, and the intersection of Trenches WU and KL coincided in position with the center of the Unit 2 nuclear reactor structure.

All five additional trenches, throughout their aggregate length of nearly half a mile, revealed a section of surficial deposits and underlying Monterey bedrock that corresponded to the two-ply sequence of surficial deposits and Monterey strata exposed in the older trenches and along the sea cliff in nearby Diablo Cove. The trenches ranged in depth from 10 feet (or less along their approach ramps) to nearly 35 feet, and all had sloping sides that gave way downward to essentially vertical walls in the bedrock encountered 3 to 22 feet above their floors. To facilitate detailed geologic mapping, the easterly walls of Trenches EJ, WU, and MV and the southerly walls of Trenches KL and NO were trimmed to near-vertical slopes extending upward from the trench floors to levels well above the top of bedrock. These walls subsequently were scaled back by means of hand tools in order to provide fresh, clean exposures prior to mapping of the contact between bedrock and overlying unconsolidated materials.

The geologic sections shown in Figures 2.5-12 and 2.5-13 correspond in position to the vertical portions of the mapped trench walls. Relationships exposed at higher levels on sloping portions of the trench walls have been projected to the vertical planes of the sections. Centerlines of intersecting trenches are shown for convenience, but the planes of the geologic sections do not contain the centerlines of the respective trenches.

3. *Bedrock*

The bedrock that was continuously exposed in the lowest parts of all the exploratory trenches lies within a part of the Monterey Formation characterized by a preponderance of sandstone. It corresponds to the portion of the section that crops out along the sea cliff southward from the mouth of Diablo Canyon. The sandstone is light to medium gray where fresh, and light gray to buff and reddish brown where weathered. It ranges from silty to markedly tuffaceous, with tuffaceous units tending to dominate southward and southwestward from the central parts of the trenched area (refer to geologic section in Figure 2.5-13). Much of the sandstone is thin-bedded and platy, but the most siliceous parts of the section are characterized by a strata a foot or more in thickness. Individual beds commonly are well defined by adjacent thin layers of more silty material.

DCPP UNITS 1 & 2 FSAR UPDATE

Bedding is less distinct in the more tuffaceous parts of the section, some of which seem to be almost massive. These rocks typically are broken by numerous tight fractures disposed at high angles to one another so that, where weathered, their appearance is coarsely blocky rather than layered.

As broadly indicated in the geologic sections, the sandstone ranges from very hard to moderately soft, and some of it feels slightly punky when struck with a pick. All of it, however, is firm and very compact. In general, the most platy parts of the sequence are relatively hard, but the hardest and soundest rock in the area is thick-bedded to almost massive sandstone of the kind at and immediately north of the site for the intended reactor structure. This resistant rock is well exposed as distinct low ridges on the nearby hillside adjoining the main terrace area.

Tuff, consisting chiefly of altered volcanic glass, is abundant within the bedrock section. Also widely scattered, but much less abundant, is tuff breccia, consisting typically of small fragments of older tuff, pumice, or Monterey rocks in a matrix of fresh to altered volcanic glass. These materials, which form sills, dikes, and highly irregular intrusive masses, are generally light gray to buff, gritty, and compact but distinctly softer than much of the enclosing sandstone. Individual bodies range from stringers less than a quarter of an inch thick to bulbous or mushroom-shaped masses with maximum exposed dimensions measured in tens of feet. As shown on the geologic sections, they are abundant in all the trenches.

These volcanic rocks probably are related to the Obispo Tuff, large masses of which are well exposed west and south of the trenched ground. The bodies exposed in the trenches doubtless represent a rather lengthy period of Miocene volcanism, during which the Monterey strata were repeatedly invaded by both tuff and tuff breccia. Indeed, several of the mapped tuff units were themselves intruded by dikes of younger tuff, as shown, for example, in Sections KL and NO.

4. Bedrock Structure

The stratification of the Monterey rocks dips northward wherever it was observable in the trenches, in general, at angles of 45 to 85°. The steepness of dip increases progressively from north to south in the trenched ground, a relationship also noted along the sea cliff southward from the mouth of Diablo Canyon. Thus, the bedrock beneath the power plant site evidently lies on the southerly flank of the major syncline that was described previously. Zones of convolution and other expressions of locally intense folding were not recognized, and they probably are much less common in this general part of the section than in other (previously described) parts that include intervals of softer and more shaley rocks.

Much of the sandstone is traversed by fractures. Planar, curving, and irregular surfaces are well represented, and in places they are abundant and closely spaced. All prominent fractures and nearly all of the minor and discontinuous ones are shown on the geologic sections (Figure 2.5-13). Also shown in these sections are all recognized

DCPP UNITS 1 & 2 FSAR UPDATE

shear surfaces, faults, and other discontinuities along which the bedrock has been displaced. Such features are nowhere abundant in the trench exposures.

Most of the surfaces of movement are hairline breaks with or without thin films of clay, calcite, and/or gypsum. Displacements range from a small fraction of an inch to several inches. A few other surfaces are more prominent, with well-defined zones of fine-grained breccia and/or infilling mineral material ordinarily 1/8 inch or less in thickness. Such zones were observed to reach maximum thicknesses of 3/8 to 1/2 inch along three small faults, but only as local lenses or pockets.

Exposures are not sufficiently extensive in three dimensions for definitely determining the magnitude of slip along all the faults, but for most of them it is plainly a few inches or less. None of them appears to be more than a minor break in a bedrock section that has been folded on a large scale. Indeed, no expressions of major faulting were recognized in any of the trenches despite careful search, and the continuous bedrock exposures preclude the possibility that such features could be readily overlooked.

Most surfaces of past movement probably were active during times when the Monterey rocks were being deformed by folding, when rupture and some differential movements would be expected in a section comprising such markedly differing rock types. Some of the fault displacements may well have been older, as attested in two places by relationships involving small faults, the Monterey rocks, and tuff.

In Trench WU south of Trench KL, for example, sandstone beds were seen to have been offset about a foot along a small fault. A thin sill of tuff occupies the same stratigraphic horizon on opposite sides of this fault, but the sill has not been displaced by the fault. Instead, the tuff occupies a short segment of the fault to effect the slight jog between its positions in the strata on either side. Intrusion of the tuff plainly postdated all movements along this fault.

5. Terrace Deposits

Marine terrace deposits of Pleistocene age form covers, generally 2 to 5 feet thick, but locally as much as 12 feet thick, over the bedrock that lies beneath the Unit 2 plant site. These covers were observed to be continuous in some parts of all the trenches, and thin and discontinuous in a few other parts. Elsewhere, the marine sediments were absent altogether, as in the lower and more southerly parts of Trenches EJ and WU and in the lower and more westerly parts of Trenches KL and NO.

The range in lithology of these deposits is considerable, and includes bouldery rubble, gravel composed of well-rounded fragments of shells and/or Monterey rocks, beach sand, loose accumulations of shells, pebbly silt, silty to clayey sand with abundant shell fragments, and soft clay derived from underlying tuffaceous rocks. Nearly all of the deposits are at least sparsely fossiliferous, and many of them contain little other than shell material. Vertebrate fossils, chiefly vertebral and rib materials representing large marine mammals, are present locally.

DCPP UNITS 1 & 2 FSAR UPDATE

The trenches in and near the site of the reactor structure exposed a buried narrow ridge of hard bedrock that once projected westward as a bold promontory along an ancient sea coast, probably at a time when sea level corresponded approximately to the present 100 foot contour (refer to Figure 2.5-11). Along the flanks of this promontory and the face of an adjoining buried sea cliff that extends southeastward through the area in which Trenches MV and NO intersected, the marine deposits intergrade and intertongue with thicker and coarser accumulations of poorly sorted debris. This rubbly material evidently is talus that was formed and deposited along the margins of the ancient shoreline cliff.

Similar gradations of older marine deposits into older talus deposits were observable at higher levels in the easternmost parts of Trenches KL and NO, where the rubbly materials doubtless lie against a more ancient sea cliff that was formed when sea level corresponded to the present 140 foot contour. The cliff itself was not exposed, however, as it lies slightly beyond the limits of trenching.

In many places, the marine covers are overlain by younger nonmarine terrace sediments with a sharp break, but elsewhere the contact between these two kinds of deposits is a zone of dark colored material, a few inches to as much as 6 feet thick, that represents weathering and development of soils on the marine sections. Fragments of these soily materials are present here and there in the basal parts of the nonmarine section. Over large areas, the porous marine deposits have been discolored through infiltration by fine-grained materials derived from the overlying ancient soils.

The nonmarine accumulations, which form the predominant fraction of the entire terrace cover, consist mainly of slump, creep, and slope-wash debris that is characteristically loose, uncompacted, and internally chaotic. These relatively dark colored deposits are fine grained and clayey, but they contain sparse to very abundant fragments of Monterey rocks generally ranging from less than an inch to about 2 feet in maximum dimension. Toward Diablo Canyon they overlie and, in places, intertongue with silty to clayey gravels that are ancient contributions from Diablo Creek when it flowed at levels much higher than its present one. These "dirty" alluvial deposits appeared only in the most northerly parts of the more recently trenched terrace area, and they are not distinguished from other parts of the nonmarine cover on the geologic sections (Figure 2.5-13).

All the terrace deposits are soft and unconsolidated, and hence are much less resistant to erosion than is the underlying bedrock. Those appearing along the walls of the exploratory trenches showed some tendency to wash and locally to rill when exposed to heavy rainfall, but little slumping and no gross failure were noted in the trenches.

6. Interface Between Bedrock and Surficial Deposits

As exposed continuously in the exploratory trenches, the contact between bedrock and overlying terrace deposits represents two wave-cut platforms and intervening slopes, all of Pleistocene age. The broadest surface of ancient marine erosion ranges in altitude

DCPP UNITS 1 & 2 FSAR UPDATE

from 80 to 105 feet, and its shoreward margin, at the base of an ancient sea cliff, lies uniformly within 5 feet of the 100 foot contour. A higher, older, and less extensive marine platform ranges in altitude from 130 to 145 feet, and most of it lies within the ranges of 135 to 140 feet. As noted previously, these are two of several wave-cut benches in this coastal area, each of which terminates eastward against a cliff or steep shoreline slope and westward at the upper rim of a similar but younger slope.

Available exposures indicate that the configurations of the erosional platforms are markedly similar, over a wide range of scales, to that of the platform now being cut approximately at sea level along the present coast. Grossly viewed, they slope very gently in a seaward (westerly) direction and are marked by broad, shallow channels and by upward projections that must have appeared as low spines and reefs when the benches were being formed. The most prominent reefs, which rise from a few inches to about 5 feet above neighboring parts of the bench surfaces, are composed of hard, thick-bedded sandstone that was relatively resistant to ancient wave erosion.

As shown in the geologic sections (Figure 2.5-13), the surfaces of the platforms are nearly planar in some places but elsewhere are highly irregular in detail. The small scale irregularities, generally 3 feet or less in vertical extent, include knob-, spine-, and rib-like projections and various wave-scoured pits, notches, crevices, and channels. Most of the upward projections closely correspond to relatively hard, resistant beds or parts of beds in the sandstone section. The depressions consistently mark the positions of relatively soft silty or shaley sandstone, of very soft tuffaceous rocks, or of extensively jointed rocks. The surface traces of most faults and some of the most prominent joints are in sharp depressions, some of them with overhanging walls. All these irregularities of detail have modern analogues that can be recognized on the bedrock bench now being cut along the margins of Diablo Cove.

The interface between bedrock and overlying surficial deposits provides information concerning the age of youngest fault movements within the bedrock section. This interface is nowhere offset by faults that were exposed in the trenches, but instead has been developed irregularly across the faults after their latest movements. The consistency of this general relationship was established by highly detailed tracing and inspection of the contact as freshly exhumed by scaling of the trench walls. Gaps in exposure of the interface necessarily were developed at the intersections of trenches as in the exploration at the Unit 1 site. At such localities, the bedrock was carefully laid bare so that all joints and faults could be recognized and traced along the trench floors to points where their relationships with the exposed interface could be determined.

Corroborative evidence concerning the age of the most recent fault displacements stems from the marine deposits that overlie the bedrock bench and form a basal part of the terrace section. That these deposits rest without break across the traces of faults in the underlying bedrock was shown by the continuity of individual sedimentary beds and lenses that could be clearly recognized and traced. As in other parts of the site area, some of the faults are directly capped by individual boulders, cobbles, pebbles, shells, and fossil bones, none of which have been affected by fault movements. Thus, the

DCPP UNITS 1 & 2 FSAR UPDATE

most recent fault displacements in the plant site area occurred before marine planation of the bedrock and deposition of the overlying terrace sediments.

The age of the most recent faulting in this area is therefore at least 80,000 years. More probably, it is at least 120,000 years, the age most generally assigned to these terrace deposits along other parts of the California coastline. Evidence from the higher bench in the plant site area indicates a much older age, as the unfaulted marine deposits there are considerably older than those that occupy the lower bench corresponding to the 100 foot terrace. Moreover, it can be noted that ages thus determined for most recent fault displacements are minimal rather than absolute, as the latest faulting actually could have occurred millions of years ago.

During the Unit 2 exploratory trenching program, special attention was directed to those exposed parts of the wave-cut benches where no marine deposits are present, and hence where there are no overlying reference materials nearly as old as the benches themselves. At such places, the bedrock beneath each bench has been weathered to depths ranging from less than 1 inch to at least 10 feet, a feature that evidently corresponds to a lengthy period of surface exposure from the time when the bench was abandoned by the sea to the time when it was covered beneath encroaching nonmarine deposits derived from hillslopes to the east.

Stratification and other structural features are clearly recognizable in the weathered bedrock, and they obviously have exercised some degree of control over localization of the weathering. Moreover, in places where upward projections of bedrock have been gradually bent or rotationally draped in response to weathering and creep, their contained fractures and surfaces of movement have been correspondingly bent. Nowhere in such a section that has been disturbed by weathering have the materials been cut by younger fractures that would represent straight upward projections of breaks in the underlying fresh rocks. Nor have such fractures been observed in any of the overlying nonmarine terrace cover.

Thus, the minimum age of any fault movement in the plant site area is based on compatible evidence from undisplaced reference features of four kinds: (a) Pleistocene wave-cut benches developed on bedrock, (b) immediately overlying marine deposits that are very slightly younger, (c) zones of weathering that represent a considerable span of subsequent time, and (d) younger terrace deposits of nonmarine origin.

2.5.2.2.5.7 Bedrock Geology of the Plant Foundation Excavations

Bedrock was continuously exposed in the foundation excavations for major structural components of Units 1 and 2. Outlines and invert elevations of these large openings, which ranged in depth from about 5 to nearly 90 feet below the original ground surface, are shown in Figures 2.5-15 and 2.5-16. The complex pattern of straight and curved walls with various positions and orientations provided an excellent three-dimensional representation of bedrock structure. These walls were photographed at large scales as construction progressed, and the photographs were used directly as a geologic

DCPP UNITS 1 & 2 FSAR UPDATE

mapping base. The largest excavations also were mapped in detail on a surveyed planimetric base.

Geologic mapping of the plant excavations confirmed the conclusions based on earlier investigations at the site. The exposed section of Monterey strata was found to correspond in lithology and structure to what had been predicted from exposures at the mouth of Diablo Canyon, along the sea cliffs in nearby Diablo Cove, and in the test trenches. Thus, the plant foundation is underlain by a moderately to steeply north-dipping sequence of thin to thick bedded sandy mudstone and fine-grained sandstone. The rocks at these levels are generally fresh and competent, as they lie below the zone of intense near-surface weathering.

Several thin interbeds of claystone were exposed in the southwestern part of the plant site in the excavations for the Unit 2 turbine-generator building, intake conduits, and outlet structure. These beds, which generally are less than 6 inches thick, are distinctly softer than the flanking sandstone. Some of them show evidence of internal shearing.

Layers of tuffaceous sandstone and sills, dikes, and irregular masses of tuff and tuff breccia are present in most parts of the foundation area. They tend to increase in abundance and thickness toward the south, where they are relatively near the large masses of Obispo Tuff exposed along the coast south of the plant site.

Some of the tuff bodies are conformable with the enclosing sandstone, but others are markedly discordant. Most are clearly intrusive. Individual masses, as exposed in the excavations, range in thickness from less than 1 inch to about 40 feet. The tuff breccia, which is less abundant than the tuff, consists typically of small fragments of older tuff, pumice, or Monterey rocks in a matrix of fresh to highly altered volcanic glass. At the levels of exposure in the excavations, both the tuff and tuff breccia are somewhat softer than the enclosing sandstone.

The stratification of the Monterey rocks dips generally northward throughout the plant foundation area. Steepness of dips increases progressively and, in places, sharply from north to south, ranging from 10 to 15° on the north side of Unit 1 to 75 to 80° in the area of Unit 2. A local reversal in direction of dip reflects a small open fold or warp in the Unit 1 area. The axis of this fold is parallel to the overall strike of the bedding, and strata on the north limb dip southward at angles of 10 to 15°. The more general steepening of dips from north to south may reflect buttressing by the large masses of Obispo Tuff south of the plant site.

The bedrock of the plant area is traversed throughout by fractures, including various planar, broadly curving, and irregular breaks. A dominant set of steeply dipping to vertical joints trends northerly, nearly normal to the strike of bedding. Other joints are diversely oriented with strikes in various directions and dips ranging from 10° to vertical. Many fractures curve abruptly, terminate against other breaks, or die out within single beds or groups of beds.

Most of the joints are widely spaced, ranging from about 1 to 10 feet apart, but within several northerly trending zones, ranging in width from 10 to 20 feet, closely spaced near vertical fractures give the rocks a blocky or platy appearance. The fracture and joint surfaces are predominantly clean and tight, although some irregular ones are thinly coated with clay or gypsum. Others could be traced into thin zones of breccia with calcite cement.

Several small faults were mapped in the foundation excavations for Unit 1 and the outlet structure. A detailed discussion of these breaks and their relationship to faults that were mapped earlier along the sea cliff and in the exploratory trenches is included in the following section.

2.5.2.2.5.8 Relationships of Faults and Shear Surfaces

Several subparallel breaks are recognizable on the sea cliff immediately south of Diablo Canyon, where they transect moderately thick-bedded sandstone of the kind exposed in the exploratory trenches to the east. These breaks are nearly concordant with the bedrock stratification but, in general, they dip more steeply (refer to detailed structure section, Figure 2.5-14) and trend more northerly than the stratification. Their trend differs significantly from much of their mapped trace, as the trace of each inclined surface is markedly affected by the local steep topography. The indicated trend, which projects eastward toward ground north of the Unit 1 reactor site, has been summed from numerous individual measurements of strike on the sea cliff exposures, and it also corresponds to the trace of the main break as observed in nearly horizontal outcrop within the tidal zone west of the cliff.

The structure section shows all recognizable surfaces of faulting and shearing in the sea cliff that are continuous for distances of 10 feet or more. Taken together, they represent a zone of dislocation along which rocks on the north have moved upward with respect to those on the south as indicated by the attitude and roughness sense of slickensides. The total amount of movement cannot be determined by any direct means, but it probably is not more than a few tens of feet and could well be less than 10 feet. This is suggested by the following observed features:

- (1) All individual breaks are sharp and narrow, and the strata between them are essentially undeformed except for their gross inclination.
- (2) Some breaks plainly die out as traced upward along the cliff surface, and others merge with adjoining breaks. At least one well-defined break butts downward against a cross-break, which in turn butts upward against a break that branches and dies out approximately 20 feet away (refer to structure section, Figure 2.5-14, for details).
- (3) Nearly all the breaks curve moderately to abruptly in the general direction of movement along them.

DCPP UNITS 1 & 2 FSAR UPDATE

- (4) Most of the breaks are little more than knife-edge features along which rock is in direct contact with rock, and others are marked by thin films of gouge. Maximum thickness of gouge anywhere observed is about 1/2 inch, and such exceptional occurrences are confined to short curving segments of the main break at the southerly margin of the zone.
- (5) No fault breccia is present; instead, the zone represents transection of otherwise undeformed rocks by sharply-defined breaks. No bedrock unit is cut off and juxtaposed against a unit of different lithology along any of the breaks.
- (6) Local prominence of the exposed breaks, and especially the main one, is due to slickensides, surface coatings of gypsum, and iron-oxide stains rather than to any features reflecting large-scale movements.

This zone of faulting cannot be regarded as a major tectonic element, nor is it the kind of feature normally associated with the generation of earthquakes. It appears instead to reflect second-order rupturing related to a marked change in dip of strata to the south, and its general sense of movement is what one would expect if the breaks were developed during folding of the Monterey section against what amounts to a broad buttress of Obispo Tuff farther south (refer to geologic map, Figure 2.5-8). That the fault and shear movements were ancient is positively indicated by upward truncation of the zone at the bench of marine erosion along the base of the overlying terrace deposits.

As indicated earlier, bedrock was continuously exposed along several exploratory trenches. This bedrock is traversed by numerous fractures, most of which represent no more than rupture and very small amounts of simple separation. The others additionally represent displacement of the bedrock, and the map in Figure 2.5-14 shows every exposed break in the initial set of trenches along which any amount of displacement could be recognized or inferred.

That the surfaces of movement constitute no more than minor elements of the bedrock structure was verified by detailed mapping of the large excavations for the plant structures. Detailed examination of the excavation walls indicated that the faults exposed in the sea cliff south of Diablo Canyon continue through the rock under the Unit 1 turbine-generator building, where they are expressed as three subparallel breaks with easterly trend and moderately steep northerly dips (Figure 2.5-15). Stratigraphic separation along these breaks ranges from a few inches to nearly 5 feet, and, in general, decreases eastward on each of them. They evidently die out in the ground immediately west of the containment excavation, and their eastward projections are represented by several joints along which no offsets have occurred. Such joints, with eastward trend and northward dip, also are abundant in some of the ground adjacent to the faults on the south (Figure 2.5-15).

The easterly reach of the Diablo Canyon sea cliff faults apparently corresponds to the two most northerly of the north-dipping faults mapped in Trench A (Figure 2.5-14).

Dying out of these breaks, as established from subsequent large excavations in the ground east of where Trench A was located, explains and verifies the absence of faults in the exposed rocks of Trenches B and C. Other minor faults and shear surfaces mapped in the trench exposures could not be identified in the more extensive exposures of fresher rocks in the Unit 1 containment and turbine-generator building excavations. The few other minor faults that were mapped in these large excavations evidently are not sufficiently continuous to have been present in the exploratory trenches.

2.5.2.2.6 Site Engineering Properties

2.5.2.2.6.1 Field and Laboratory Investigations

In order to determine anticipated ground accelerations at the site, it was necessary to conduct field surveys and laboratory testing to evaluate the engineering properties of the materials underlying the site.

Bore holes were drilled into the rock upon which PG&E Design Class 1 structures are founded. The borings were located at or near the intersection of the then existing Unit 1 exploration trenches. (refer to Figures 2.5-11, 2.5-12, and 2.5-13 for exploratory trenching programs and boring locations.) These holes were cored continuously and representative samples were taken from the cores and submitted for laboratory testing.

The field work also included a reconnaissance to evaluate physical condition of the rocks that were exposed in trenches, and samples were collected from the ground surface in the trenches for laboratory testing. These investigations included seismic refraction measurements across the ground surface and uphole seismic measurements in the various drill holes to determine shear and compressional velocities of vertically propagated waves.

Laboratory testing, performed by Woodward-Clyde-Sherard & Associates, included unconfined compression tests, dynamic elastic moduli tests under controlled stress conditions, density and water content determinations, and Poisson's ratio tests. Tests were also carried out by Geo-Recon, Incorporated, to determine seismic velocities on selected rock samples in the laboratory. The results of seismic measurements in the field were used to construct a three-dimensional model of the subsurface materials beneath the plant site showing variations of shear wave velocity and compressional wave velocity both laterally and vertically. The seismic velocity data and elastic moduli determined from laboratory testing were correlated to determine representative values of elastic moduli necessary for use in dynamic analyses of structures.

Details of field investigations and results of laboratory testing and correlation of data are contained in Appendices 2.5A and 2.5B of Reference 27 in Section 2.3.

2.5.2.2.6.2 Summary and Correlation of Data

The foundation material at the site can be categorized as a stratified sequence of fine to very fine grained sandstone deeply weathered to an average elevation of 75 to 80 feet, mean sea level (MSL). The rock is closely fractured, with tightly closed or healed fractures generally present below elevation 75 feet. Compressional and shear wave velocity interfaces generally are at an average elevation of 75 feet, correlating with fracture conditions.

Time-distance plots and seismic velocity profiles presenting results of each seismic refraction line and time depth plots with results for each uphole seismic survey are included in Appendices 2.5A and 2.5B of Reference 27 in Section 2.3. Compressional wave velocities range from 2350 to 5700 feet per second and shear wave velocities from 1400 to 3600 feet per second as determined by the refraction survey. These same parameters range from 2450 to 9800 and 1060 to 6050 feet per second as determined by the uphole survey. For the Hosgri Evaluation an average shear wave velocity of 3600 feet per second is used at the foundation grade. An isometric diagram summarizing results of the refraction survey for Unit 1 is also included in Appendix 2.5A of Reference 27 in Section 2.3.

Table 1 of Appendix 2.5A of Reference 27 of Section 2.3 shows calculations of Poisson's ratio and Young's Modulus based on representative compressional and shear wave velocities from the field geophysical investigations and laboratory measurements of compressional wave velocities. Table 2 of Appendix 2.5A of the same reference presents laboratory test results including density, unconfined compressive strength, Poisson's ratio and calculated values for compressional and shear wave velocities, shear modulus, and constrained modulus. Secant modulus values in Table 2 were determined from cyclic stress-controlled laboratory tests.

Compressional wave velocity measurements were made in the laboratory of four selected core samples and three hand specimens from exposures in the trench excavations. Measured values ranged from 5700 to 9500 feet per second. A complete tabulation of these results can be found in Appendix 2.5A of Reference 27 of Section 2.3.

2.5.2.2.6.3 Dynamic Elastic Moduli and Poisson's Ratio

Laboratory test results are considered to be indicative of intact specimens of foundation materials. Field test results are considered to be indicative of the gross assemblage of foundation materials, including fractures and other defects. Load stress conditions are obtained by evaluating cyclic load tests. In-place load stress conditions and confinement of the material at depth are also influential in determining elastic behavior. Because of these considerations, originally recommended representative values for Young's Modulus of Elasticity and Poisson's ratio for the site were:

DCPP UNITS 1 & 2 FSAR UPDATE

<u>Depth Below Bottom of Trench</u>	<u>E</u>	<u>δ</u>
0 to approximately 15 feet	$44 \times 10^6 \text{ lb/ft}^2$	0.20
Below 15 feet	$148 \times 10^6 \text{ lb/ft}^2$	0.18

A single value was selected for Young's Modulus below 15 feet because the initial analyses of the seismic response of the structures utilized a single value that was considered representative of the foundation earth materials as a whole.

More detailed seismic analyses were performed subsequent to the initial analyses. These analyses, discussed in Section 3.7.2, incorporated the finite element method and made it possible to model the rock beneath the plant site in a more refined manner by accounting for changes in properties with increasing depth. To determine the refined properties of the founding materials for these analyses, the test data were reviewed and consideration was given to: (a) strain range of the materials at the site, (b) overburden pressure and confinement, (c) load imposed by the structure, (d) observation of fracture condition and geometry of the founding rock in the open excavation, (e) decreases in Poisson's ratio with depth, and (f) significant advances in state-of-the-art techniques of testing and analysis in rock mechanics that had been made and which resulted in considerably more being known about the behavior of rock under seismic strains in 1970 than in 1968 or 1969.

For the purposes of developing the mathematical models that represented the rock mass, the foundation was divided into horizontal layers based on: (a) the estimated depth of disturbance of the foundation rock below the base of the excavation, (b) changes in rock type and physical condition as determined from bore hole logs, (c) velocity interfaces as determined by refraction geophysical surveys, and (d) estimated depth limit of fractures across which movement cannot take place because of confinement and combined overburden and structural load. Based on these considerations, the founding material properties as shown in Figure 2.5-19 were selected as being representative of the physical conditions in the founding rock.

2.5.2.2.6.4 Engineered Backfill

Backfill operations were carefully controlled to ensure stability and safety. All engineered backfill was placed in lifts not exceeding 8 inches in loose depth. Yard areas and roads were compacted to 95 percent relative compaction as determined by the method specified in ASTM D1557. Rock larger than 8 inches in its largest dimension that would not break down under the compactors was not permitted. Figures 2.5-17 and 2.5-18 show the plan and profile view of excavation and backfill for major plant structures.

2.5.2.2.6.5 Foundation Bearing Pressures

PG&E Design Class I structures were analyzed to determine the foundation pressures resulting from the combination of dead load, live load, and the double design

earthquake (DDE). The maximum pressure was found to be 158 ksf and occurs under the containment structure foundation slab. This analysis assumed that the lateral seismic shear force will be transferred to the rock at the base of the slab which is embedded 11 feet into rock. This computed bearing pressure is considered conservative in that no passive lateral pressure was assumed to act on the sides of the slab. Based on the results of the laboratory tests of unconfined compressive strength of representative samples of rock at the site, which ranged from 800 to 1300 ksf, the calculated foundation pressure is well below the ultimate in situ rock bearing capacity.

Adverse hydrologic effects on the foundations of PG&E Design Class I structures (there are no PG&E Design Class I embankments) can be safely neglected at this site, since PG&E Design Class I structures are founded on a substantial layer of bedrock, and the groundwater level lies well below grade, at a level corresponding to that of Diablo Creek. Additionally, the computed factors of safety (minimum of 5 under DDE) of foundation pressures versus unconfined compressive strength of rock are sufficiently high to ensure foundation integrity in the unlikely event groundwater levels temporarily rose to foundation grade.

Soil properties such as grain size, Atterberg limits, and water content need not be considered since PG&E Design Class I structures and PG&E Design Class II structures housing PG&E Design Class I equipment are founded on rock.

2.5.3 VIBRATORY GROUND MOTION

2.5.3.1 Geologic Conditions of the Site and Vicinity

DCPP is situated at the coastline on the southwest flank of the San Luis Range, in the southern Coast Ranges of California. The San Luis Range branches from the main coastal mountain chain, the Santa Lucia Range, in the area north of the Santa Maria Valley and southeast of the plant site, and thence follows an alignment that curves toward the west. Owing to this divergence in structural grain, the range juts out from the regional coastline as a broad peninsula and is separated from the Santa Lucia Range by an elongated lowland that extends southeasterly from Morro Bay and includes Los Osos and San Luis Obispo Valleys. It is characterized by rugged west-northwesterly trending ridges and canyons, and by a narrow fringe of coastal terraces along its southwesterly flank.

Diablo Canyon follows a generally west-southwesterly course from the central part of the range to the north-central part of the terraced coastal strip. Detailed discussions of the lithology, stratigraphy, structure, and geologic history of the plant site and surrounding region are presented in Section 2.5.2.

2.5.3.2 Underlying Tectonic Structures

Evidence pertaining to tectonic and seismic conditions in the region of the DCPP site, developed during the original design phase, is summarized later in the section, and is

illustrated in Figures 2.5-2, 2.5-3, 2.5-4, and 2.5-5. Table 2.5-1 includes a summary listing of the nature and effects of all significant historic earthquakes within 75 miles of the site that have been reported through the end of 1972. Table 2.5-2 shows locations of 19 selected earthquakes that have been investigated by S. W. Smith. Table 2.5-3 lists the principal faults in the region that were identified during the original design phase and indicates major elements of their histories of displacement, in geological time units.

Prior to the start of construction of DCPP, Benioff and Smith (reference 5) assessed the maximum earthquakes to be expected at the site, and John A. Blume and Associates (references 6 and 7) derived the site vibratory motions that could result from these maximum earthquakes, which form the basis of the Design Earthquake. An extensive discussion of the geology of the southern Coast Ranges, the western Transverse Ranges, and the adjoining offshore region is presented in Appendix 2.5D of Reference 27 of Section 2.3. Tectonic features of the central coastal region are discussed in Section 2.5.2.1.2, Regional Geologic and Tectonic Setting.

Additional information about the tectonic and seismic conditions was gathered during the Hosgri evaluation and LTSP evaluation phases, as discussed in Sections 2.5.3.9.3 and 2.5.3.9.4, respectively.

2.5.3.3 Behavior During Prior Earthquakes

Physical evidence that indicates the behavior of subsurface materials, strata, and structure during prior earthquakes is presented in Section 2.5.2.2.5. The section presents the findings of the exploratory trenching programs conducted at the site.

2.5.3.4 Engineering Properties of Materials Underlying the Site

A description of the static and dynamic engineering properties of the materials underlying the site is presented in Section 2.5.2.2.6, Site Engineering Properties.

2.5.3.5 Earthquake History

The seismicity of the southern Coast Ranges region is known from scattered records extending back to the beginning of the 19th century, and from instrumental records dating from about 1900. Detailed records of earthquake locations and magnitudes became available following installation of the California Institute of Technology and University of California (Berkeley) seismograph arrays in 1932.

A plot of the epicenters for all large historical earthquakes and for all instrumentally recorded earthquakes of Magnitude 4 or larger that have occurred within 200 miles of DCPP site, through the end of 1972, is given in Figure 2.5-2. Plots of all historically and instrumentally recorded epicenters and all mapped faults within about 75 miles of the site, known through the end of 1972, are shown in Figures 2.5-3 and 2.5-4.

A tabulated list of seismic events through the end of 1972, representing the computer printout from the Berkeley Seismograph Station records, supplemented with records of individual shocks of greater than Magnitude 4 that appear only in the Caltech records, is included as Table 2.5-1. Table 2.5-2 gives a summary of revised epicenters of a representative sample of earthquakes off the coast of California near San Luis Obispo, as determined by S. W. Smith.

2.5.3.6 Correlation of Epicenters With Geologic Structures

Studies of particular aspects of the seismicity of the southern Coast Ranges region have been made by Benioff and Smith, Richter, and Allen. From results of these studies, together with data pertaining to the broader aspects of the geology and seismicity of central and eastern California, it can be concluded that, although the southern Coast Ranges region may be subjected to vibratory ground motion from earthquakes originating along faults as distant as 200 miles or more, the region itself is traversed by faults capable of producing large earthquakes, and that the strongest shaking possible for sites within the region probably would be caused by earthquakes no more than a few tens of miles away. Therefore, only the seismicity of the southern Coast Ranges, the adjacent offshore area, and the western Transverse Ranges is reviewed in detail.

Figure 2.5-3 shows three principal concentrations of earthquake epicenters, three smaller or more diffuse areas of activity, and a scattering of other epicenters, for earthquakes recorded through 1972. The most active areas, in terms of numbers of shocks, are the reach of the San Andreas fault north of about 35°7' latitude, the offshore area near Santa Barbara, and the offshore Santa Lucia Bank area. Notable concentrations of epicenters also are located as occurring in Salinas Valley, at Point San Simeon, and near Point Conception. The scattered epicenters are most numerous in the general vicinities of the most active areas, but they also occur at isolated points throughout the region.

The reliability of the position of instrumentally located epicenters of small shocks in the central California region has been relatively poor in the past, owing to its position between the areas covered by the Berkeley and Caltech seismograph networks. A recent study by Smith, however, resulted in relocation of nineteen epicenters in the coastal and offshore region between the latitudes of Point Arguello and Point Sur. Studies by Gawthrop (reference 29) and reported in Wagner have led to results that seem to accord generally with those achieved by Smith.

The epicenters relocated by Smith and those recorded by Gawthrop are plotted in Figure 2.5-3. This plot shows that most of the epicenters recorded in the offshore region seem to be spatially associated with faults in the Santa Lucia Bank region, the East Boundary zone, and the San Simeon fault. Other epicenters, including ones for the 1952 Bryson shock, and several smaller shocks originally located in the offshore area, were determined to be centered on or near the Sur-Nacimiento fault north of the latitude of San Simeon.

2.5.3.7 Identification of Active Faults

Faults that have evidence of recent activity and have portions passing within 200 miles of the site, as known through the end of 1972, are identified in Section 2.5.2.1.2.

2.5.3.8 Description of Active Faults

Active faults that have any part passing within 200 miles of the site, as known through the end of 1972, are described in Section 2.5.2.1.2. Additional active faults were identified during the Hosgri and LTSP evaluation phases, as described in Sections 2.5.3.9.3 and 2.5.3.9.4, respectively.

2.5.3.9 Design and Licensing Basis Earthquakes

The seismic design and evaluation of DCPP is based on the earthquakes described in the following four subsections. Refer to Section 3.7 for the design criteria associated with the application of these earthquakes to the structures, systems, and components. The DE, DDE, and HE are design bases earthquakes and the LTSP is a licensing bases earthquake.

2.5.3.9.1 Design Earthquake

During the original design phase, Benioff and Smith, in reviewing the seismicity of the region around DCPP site, determined the maximum earthquakes that could reasonably be expected to affect the site. Their conclusions regarding the maximum size earthquakes that can be expected to occur during the life of the reactor are listed below:

- (1) Earthquake A: A great earthquake may occur on the San Andreas fault at a distance from the site of more than 48 miles. It would be likely to produce surface rupture along the San Andreas fault over a distance of 200 miles with a horizontal slip of about 20 feet and a vertical slip of 3 feet. The duration of strong shaking from such an event would be about 40 seconds, and the equivalent magnitude would be 8.5.
- (2) Earthquake B: A large earthquake on the Nacimiento (Rinconada) fault at a distance from the site of more than 20 miles would be likely to produce a 60 mile surface rupture along the Nacimiento fault, a slip of 6 feet in the horizontal direction, and have a duration of 10 seconds. The equivalent magnitude would be 7.25.
- (3) Earthquake C: Possible large earthquakes occurring on offshore fault systems that may need to be considered for the generation of seismic sea waves are listed below:

DCPP UNITS 1 & 2 FSAR UPDATE

<u>Location</u>	<u>Length of Fault Break</u>	<u>Slip, feet</u>	<u>Magnitude</u>	<u>Distance to Site</u>
Santa Ynez Extension	80 miles	10 horizontal	7.5	50 miles
Cape Mendocino, NW Extension of San Andreas fault	100 miles	10 horizontal	7.5	420 miles
Gorda Escarpment	40 miles	5 vertical or horizontal	7	420 miles

- (4) Earthquake D: Should a great earthquake occur on the San Andreas fault, as described in "A" above, large aftershocks may occur out to distances of about 50 miles from the San Andreas fault, but those aftershocks which are not located on existing faults would not be expected to produce new surface faulting, and would be restricted to depths of about 6 miles or more and magnitudes of about 6.75 or less. The distance from the site to such aftershocks would thus be more than 6 miles.

The available information suggests that the faults in this region can be associated with contrasting general levels of seismic potential. These are as follows:

- (1) Level I: Potential for great earthquakes involving surface faulting over distances on the order of 100 miles: seismic activity at this level should occur only on the reach of the San Andreas fault that extends between the locales of Cajon Pass and Parkfield. This was the source of the 1857 Fort Tejon earthquake, estimated to have been of Magnitude 8.
- (2) Level II: Potential for large earthquakes involving faulting over distances on the order of tens of miles: seismic activity at this level can occur along offshore faults in the Santa Lucia Bank region (the likely source of the Magnitude 7.3 earthquake of 1927), and possibly along the Big Pine and Santa Ynez faults in the Transverse Ranges.

Although the Rinconada-San Marcos-Jolon, Espinosa, Sur-Nacimiento, and San Simeon faults do not exhibit historical or even Holocene activity indicating this level of seismic potential, the fault dimensions, together with evidence of late Pleistocene movements along these faults, suggest that they may be regarded as capable of generating similarly large earthquakes.

- (3) Level III: Potential for earthquakes resulting chiefly from movement at depth with no surface faulting, but at least with some possibility of surface faulting of as much as a few miles strike length and a few feet of slip:

DCPP UNITS 1 & 2 FSAR UPDATE

Seismic activity at this level probably could occur on almost any major fault in the southern Coast Ranges and adjacent regions.

From the observed geologic record of limited fault activity extending into Quaternary time, and from the historical record of apparently associated seismicity, it can be inferred that both the greater frequency of earthquake activity and larger shocks from earthquake source structures having this level of seismic potential probably will be associated with one of the relatively extensive faults. Faults in the vicinity of the San Luis Range that may be considered to have such seismic potential include the West Huasna, Edna, and offshore Santa Maria Basin East Boundary zone.

- (4) Level IV: Potential for earthquakes and aftershocks resulting from crustal movements that cannot be associated with any near-surface fault structures: such earthquakes apparently can occur almost anywhere in the region.

This information forms the basis of the Design Earthquake, described in section 2.5.3.10.1.

2.5.3.9.2 Double Design Earthquake

During the original design phase, in order to assure adequate reserve seismic resisting capability of safety related structures, systems, and components, an earthquake producing two-times the acceleration values of the Design Earthquake was also considered (Reference 51).

2.5.3.9.3 Hosgri Earthquake

In 1976, subsequent to the issuance of the construction permit of Unit 1, PG&E was requested by the NRC to evaluate the plant's capability to withstand a postulated Richter Magnitude 7.5 earthquake centered along an offshore zone of geologic faulting, approximately 3 miles offshore, generally referred to as the "Hosgri fault." Details of the investigations associated with this fault are provided in Appendices 2.5D, 2.5E, and 2.5F of Reference 27 in Section 2.3. An overview is provided in Section 2.5.3.10.3. Note that the Shoreline Fault Zone (refer to Section 2.5.7.1) is considered to be a lesser included case under the Hosgri evaluation (Reference 55).

A further assessment of the seismic potential of faults mapped in the region of DCP site was made following the extensive additional studies of on and offshore geology and is reported in Appendix 2.5D of Reference 27 of Section 2.3. This was done in terms of observed Holocene activity, to achieve assessment of what seismic activity is reasonably probable, in terms of observed late Pleistocene activity, fault dimensions, and style of deformation.

2.5.3.9.4 1991 Long Term Seismic Program Earthquake

PG&E performed a reevaluation of the seismic design bases of DCPP in response to License Condition No. 2.C.(7) of the Unit 1 Operating License. Details of this reevaluation, referred to as the Long Term Seismic Program, are provided in Section 2.5.7.

PG&E's evaluations included the development of significant additional data applicable to the geology, seismology, and tectonics of the DCPP region, including characterization of the Hosgri, Los Osos, San Luis Bay, Olson, San Simeon, and Wilmar Avenue faults. These faults were evaluated as potential seismic sources (Reference 40, Chapter 3). However, PG&E determined that the potential seismic sources of significance to the ground motions at the site are: the Hosgri and Los Osos fault zones, and the San Luis Bay fault, based on the probabilistic seismic hazard analysis; and the Hosgri fault zone, based on the deterministic analysis. Details are provided in Reference 40, Chapters 2 and 3, and summarized in SSER 34, Section 2.5.1, "Geology" and 2.5.2, "Seismology".

The NRC's review of PG&E's evaluations is documented in References 42 and 43.

2.5.3.10 Ground Accelerations and Response Spectra

The seismic design and evaluation of DCPP is based on the earthquakes described in the following four subsections. Refer to Section 3.7 for the design criteria associated with the application of the DE, DDE, and HE to the structures, systems, and components and the seismic margin assessment of the LTSP.

2.5.3.10.1 Design Earthquake

During the original design phase, the maximum ground acceleration that would occur at the DCPP site was estimated for each of the postulated earthquakes listed in Section 2.5.3.9, using the methods set forth in References 12 and 24. The plant site acceleration was primarily dependent on the following parameters: Gutenberg-Richter magnitude and released energy, distance from the earthquake focus to the plant site, shear and compressional velocities of the rock media, and density of the rock. Rock properties are discussed under Section 2.5.2.2.6, Site Engineering Properties.

The maximum rock accelerations that would occur at the DCPP site were estimated as:

Earthquake A	0.10 g	Earthquake C	0.05 g
Earthquake B	0.12 g	Earthquake D	0.20 g

In addition to the maximum acceleration, the frequency distribution of earthquake motions is important for comparison of the effects on plant structures and equipment. In general, the parameters affecting the frequency distribution are distance, properties of the transmitting media, length of faulting, focus depth, and total energy release. Earthquakes that might reach the site after traveling over great distances would tend to

DCPP UNITS 1 & 2 FSAR UPDATE

have their high frequency waves filtered out. Earthquakes that might be centered close to the site would tend to produce wave forms at the site having minor low frequency characteristics.

In order to evaluate the frequency distribution of earthquakes, the concept of the response spectrum is used.

For nearby earthquakes, the resulting response spectra accelerations would peak sharply at short periods and would decay rapidly at longer periods. Earthquake D would produce such response spectra. The March 1957 San Francisco earthquake as recorded in Golden Gate Park (S80°E component) was the same type. It produced a maximum recorded ground acceleration of 0.13 g (on rock) at a distance of about 8 miles from the epicenter. Since Earthquake D has an assigned hypocentral distance of 12 miles, it would be expected to produce response spectra similar in shape to those of the 1957 event.

Large earthquakes centered at some distance from the plant site would tend to produce response spectra accelerations that peak at longer periods than those for nearby smaller shocks. Such spectra maintain a higher spectral acceleration throughout the period range beyond the peak period. Earthquakes A and C are events that would tend to produce this type of spectra. The intensity of shaking as indicated by the maximum predicted ground acceleration shows that Earthquake C would always have lower spectral accelerations than Earthquake A.

Since the two shocks would have approximately the same shape spectra, Earthquake C would always have lower spectral accelerations than Earthquake A, and it is therefore eliminated from further consideration. The north-south component of the 1940 El Centro earthquake produced response spectra that emphasized the long period characteristics described above. Earthquake A, because of its distance from the plant site, would be expected to produce response spectra similar in shape to those produced by the El Centro event. Smoothed response spectra for Earthquake A were constructed by normalizing the El Centro spectra to 0.10 g. These spectra, however, show smaller accelerations than the corresponding spectra for Earthquake B (discussed in the next paragraph) for all building periods, and thus Earthquake A is also eliminated from further consideration.

Earthquake B would tend to produce response spectra that emphasize the intermediate period range inasmuch as the epicenter is not close enough to the plant site to produce large high frequency (short-period) effects, and it is too close to the site and too small in magnitude to produce large low frequency (long-period) effects. The N69°W component to the 1952 Taft earthquake produced response spectra having such characteristics. That shock was therefore used as a guide in establishing the shape of the response spectra that would be expected for Earthquake B.

Following several meetings with the AEC staff and their consultants, the following two modifications were made in order to make the criteria more conservative:

DCPP UNITS 1 & 2 FSAR UPDATE

- (1) The Earthquake D time-history was modified in order to obtain better continuity of frequency distribution between Earthquakes D and B.
- (2) The accelerations of Earthquake B were increased by 25 percent in order to provide the required margin of safety to compensate for possible uncertainties in the basic earthquake data.

Accordingly, Earthquake D-modified was derived by modifying the S80°E component of the 1957 Golden Gate Park, San Francisco earthquake, and then normalizing to a maximum ground acceleration of 0.20 g. Smoothed response spectra for this earthquake are shown in Figure 2.5-21. Likewise, Earthquake B was derived by normalizing the N69°W component of the 1952 Taft earthquake to a maximum ground acceleration of 0.15 g. Smoothed response spectra for Earthquake B are shown in Figure 2.5-20. The maximum vibratory motion at the plant site would be produced by either Earthquake D-modified or Earthquake B, depending on the natural period of the vibrating body.

2.5.3.10.2 Double Design Earthquake

The maximum ground acceleration and response spectra for the Double Design Earthquake are twice those associated with the design earthquake, as described in Section 2.5.3.10.1 (Reference 51).

2.5.3.10.3 Hosgri Earthquake

As mentioned earlier, based on a review of the studies presented in Appendices 2.5D and 2.5E (of Reference 27 in Section 2.3) by the NRC and the United States Geologic Survey (USGS) (acting as the NRC's geological consultant), the NRC issued SSER 4 in May 1976. This supplement included the USGS conclusion that a magnitude 7.5 earthquake could occur on the Hosgri fault at a point nearest to the Diablo Canyon site. The USGS further concluded that such an earthquake should be described in terms of near fault horizontal ground motion using techniques and conditions presented in Geological Survey Circular 672. The USGS also recommended that an effective, rather than instrumental, acceleration be derived for seismic analysis.

The NRC adopted the USGS recommendation of the seismic potential of the Hosgri fault. In addition, based on the recommendation of Dr. N. M. Newmark, the NRC prescribed that an effective horizontal ground acceleration of 0.75g be used for the development of response spectra to be employed in a seismic evaluation of the plant. The NRC outlined procedures considered appropriate for the evaluation including an adjustment of the response spectra to account for the filtering effect of the large building foundations. An appropriate allowance for torsion and tilting was to be included in the analysis. A guideline for the consideration of inelastic behavior, with an associated ductility ratio, was also established.

DCPP UNITS 1 & 2 FSAR UPDATE

The NRC issued SSER 5 in September 1976. This supplement included independently-derived response spectra and the rationale for their development. Parameters to be used in the foundation filtering calculation were delineated for each major structure. The supplement prescribed that either the spectra developed by Blume or Newmark would be acceptable for use in the evaluation with the following conditions:

- (1) In the case of the Newmark spectra no reduction for nonlinear effects would be taken except in certain specific areas on an individual case basis.
- (2) In the case of the Blume spectra a reduction for nonlinear behavior using a ductility ratio of up to 1.3 may be employed.
- (3) The Blume spectra would be adjusted so as not to fall below the Newmark spectra at any frequency.

The development of the Blume ground response spectra, including the effect of foundation filtering, is briefly discussed below. The rationale and derivation of the Newmark ground response spectra is discussed in Appendix C to Supplement No. 5 of the SER.

The time-histories of strong motion for selected earthquakes recorded on rock close to the epicenters were normalized to a 0.75g peak acceleration. Such records provide the best available models for the Diablo Canyon conditions relative to the Hosgri fault zone. The eight earthquake records used are listed in the table below.

<u>Earthquake</u>	<u>M</u>	<u>Depth, km</u>	<u>Recorded at</u>	<u>Epicentral Distance, km</u>	<u>Component</u>	<u>Peak Acceleration g</u>
Helena 1935	6	5	Helena	3 to 8	EW	0.16
Helena 1935	6	5	Helena	3 to 8	NS	0.13
Daly City 1957	5.3	9	Golden Gate Park	8	N80W	0.13
Daly City 1957	5.3	9	Golden Gate Park	8	N10E	0.11
Parkfield 1966	5.6	7	Temblor 2	7	S25W	0.33
Parkfield 1966	5.6	7	Temblor 2	7	N65W	0.28
San Fernando 1971	6.6	13	Pacoima Dam	3	S14W	1.17
San Fernando 1971	6.6	13	Pacoima	3	N76W	1.08

The magnitudes are the greatest recorded thus far (September 1985) close in on rock stations and range from 5.3 to 6.6. Adjustments were made subsequently in the period range of the response spectrum above 0.40 sec for the greater long period energy expected in a 7.5M shock as compared to the model magnitudes.

The procedure followed was to develop 7 percent damped response spectra for each of the eight records normalized to 0.75g and then to treat the results statistically according

to period bands to obtain the mean, the median, and the standard deviations of spectral response. At this stage, no adjustments for the size of the foundation or for ductility were made. The 7 percent damped response spectra were used as the basis for calculating spectra at other damping values.

Figures 2.5-29 and 2.5-30 show free-field horizontal ground response spectra as determined by Blume and Newmark, respectively, at damping levels from two to seven percent.

Figures 2.5-31 and 2.5-32 show vertical ground response spectra as determined by Blume and Newmark, respectively, for two to seven percent damping. The ordinates of vertical spectra are taken as two-thirds of the corresponding ordinates of the horizontal spectra. These response spectra, finalized in 1977, are described as the "1977 Hosgri response spectra." Note that the Shoreline Fault Zone (refer to Section 2.5.7.1) is considered to be a lesser included case under the Hosgri evaluation (Reference 55).

2.5.3.10.4 1991 Long Term Seismic Program Earthquake

As discussed in Section 2.5.3.9.4, the Long Term Seismic Program, in response to License Condition No. 2.C.(7) determined that the governing earthquake source for the deterministic seismic margins evaluation of DCPP (84th percentile ground motion response spectrum) is the Hosgri fault. Ground motions, and the corresponding free-field response spectra for a Richter Magnitude 7.2 earthquake centered along the Hosgri fault, approximately 4.5 km from DCPP, were developed by PG&E, as documented in Reference 40. This event is referred to as the "LTSP Earthquake." As part of their review of Reference 40, the NRC concluded that spectra developed by PG&E could underestimate the ground motion (Reference 42). As a result, the final spectra, applicable to the LTSP evaluation of DCPP, is an envelope of that developed by PG&E and that developed by the NRC. Figures 2.5-33 and 2.5-34 show the 84th percentile ground motion response spectrum at 5% damping for the horizontal and vertical directions, respectively, described as the "1991 LTSP response spectra". These spectra define the current licensing basis for the LTSP.

Figure 2.5-35 shows a comparison of the horizontal 1991 LTSP response spectrum with the 1977 Newmark Hosgri spectrum (based on Reference 40, Figure 7-2). This comparison indicates that the 1977 Hosgri spectrum is greater than the 1991 LTSP spectrum at all frequencies less than about 15 Hz, but the 1991 LTSP spectrum exceeds the 1977 Hosgri spectrum by approximately 10 percent for frequencies above 15 Hz. This exceedance was accepted by the NRC in SSER 34 (Reference 42), Section 3.8.1.1 (Ground-Motion Input for Deterministic Evaluations):

"On the basis of PG&E's margins evaluation discussed in Section 3.8.1.7 of this SSER, the staff concludes that these high-frequency spectral exceedances are not significant."

In addition, the NRC states in SSER 34 (Reference 42), Section 1.4 (Summary of Staff Conclusions):

"The staff notes that the seismic qualification basis for Diablo Canyon will continue to be the original design basis plus the Hosgri evaluation basis, along with the associated analytical methods, initial conditions, etc. The LTSP has served as a useful check of the adequacy of the seismic margins and has generally confirmed that the margins are acceptable."

Therefore, the 1991 LTSP ground motion response spectra does not replace or modify, the DE, DDE, or 1977 Hosgri response spectra described above.

2.5.4 SURFACE FAULTING

2.5.4.1 Geologic Conditions of the Site

The geologic history and lithologic, stratigraphic, and structural conditions of the site and the surrounding area are described in Section 2.5.2 and are illustrated in the various figures included in Section 2.5.

2.5.4.2 Evidence for Fault Offset

Substantive geologic evidence, described under Section 2.5.2.2, Site Geology, indicates that the ground at and near the site has not been displaced by faulting for at least 80,000 to 120,000 years. It can be inferred, on the basis of regional geologic history, that minor faults in the site bedrock date from the mid-Pliocene or, at the latest, from mid-Pleistocene episodes of tectonic activity.

2.5.4.3 Identification of Active Faults

Three zones that include faults greater than 1000 feet in length were mapped within about 5 miles of the site. Two of these, the Edna and San Miguelito fault zones, were mapped on land in the San Luis Range. The third, consisting of several breaks associated with the offshore Santa Maria Basin East Boundary zone of folding and faulting, is described in Sections 2.5.2.1.2.3 and 2.5.2.1.5.5 under Regional Geologic and Tectonic Setting. The mapped trace of each of these structures is shown in Figures 2.5-3 and 2.5-4. Additional active faults that were identified through the studies associated with the Hosgri Evaluation and LTSP are discussed in Sections 2.5.3.9.3 and 2.5.3.9.4, respectively.

2.5.4.4 Earthquakes Associated With Active Faults

The earthquakes discussions are limited to those identified during the original design phase and do not include any earthquakes recorded since 1971.

DCPP UNITS 1 & 2 FSAR UPDATE

The Edna fault or fault zone has been active at some time since the deposition of the Plio-Pleistocene Paso Robles Formation, which it displaces. It has no morphologic expression suggestive of late Pleistocene activity, nor is it known to displace late Pleistocene or younger deposits. Four epicenters of small (3.9 to 3M) shocks and 42 other epicenters for shocks of "small" or "unknown" intensity have been reported as occurring in the approximate vicinity of the Edna fault (Figures 2.5-3 and 2.5-4). Owing to the small size of the earthquakes that they represent, however, all of these epicenters are only approximately located. Further, they fall in the energy range of shocks that can be generated by fairly large construction blasts. At present, no conclusive evidence is available to determine whether the Edna fault could be classified as seismically active, or as geologically active in the sense of having undergone multiple movements within the last 500,000 years.

The San Miguelito fault has been mapped as not displacing the Plio-Pleistocene Paso Robles Formation. No instrumental epicenter has been reliably recorded from its vicinity, but the Berkeley Seismological Laboratory indicates Avila Bay as the presumed epicentral location for a moderately damaging (Intensity VII at Avila) earthquake that occurred on December 1, 1916. It seems likely, however, that this shock occurred along the offshore East Boundary zone rather than on the San Miguelito fault zone.

The East Boundary zone has an overall length of about 70 miles. Individual breaks within the zone are as much as 30 miles long, though the varying amount of displacement that occurs along specific breaks indicates that movement along them is not uniform, and it suggests that breakage may have occurred on separate, limited segments of the faults. The reach of the zone that is opposite DCPP site contains four fault breaks. These breaks range from 1 to 15 miles in length, and they have minimum distances of 2.1 to 4.5 miles from the site. The East Boundary zone is considered to be seismically active, since at least five instrumentally well located epicenters and as many as ten less reliably located other epicenters are centered along or near the zone. One of the breaks (located 3-1/2 miles offshore from the site) exhibits topographic expression that may represent a tectonic offset of the sea floor surface at a point along its trace 6 miles north of the site. Other faults in the East Boundary zone have associated erosion features, a few of which could possibly be partly of faultline origin.

The earthquake of December 1, 1916, though listed as having an epicentral location at Avila Bay, is considered more probably to have originated along either the East Boundary zone or, possibly, the Santa Lucia Bank fault. Effects of this shock at Avila included landsliding in Dairy Canyon, 2 miles north of town, and "...disturbance of waters in the Bay of San Luis Obispo." "...plaster in several cottages...was jarred loose...while some of the smokestacks on the (Union Oil Company) refinery were toppled over." It is apparently on this basis that the Berkeley listing of earthquakes assigns this shock a "large" intensity and places its approximate epicentral location at Port San Luis.

A small (Magnitude 2.9) shock that apparently originated near the East Boundary zone a short distance south of DCPP site was lightly felt at the site on September 24, 1974.

DCPP UNITS 1 & 2 FSAR UPDATE

This shock, like most of those recorded along the East Boundary zone, was not damaging.

The minor fault zone that was mapped in the sea cliff at the mouth of Diablo Creek and in the excavation for the Unit 1 turbine building has an onshore length of about 550 feet, and it probably continues for some distance offshore. It has been definitely determined to be not active.

2.5.4.5 Correlation of Epicenters With Active Faults

Earthquake epicenters located within 50 miles of DCPP site, for earthquakes recorded through 1972, have been approximately located in the vicinity of each of the faults. The reported earthquakes are listed in Table 2.5-1 and as follows, and their indicated epicentral locations are shown in Figures 2.5-3 and 2.5-4:

Earthquake Epicenters Reported as Being Located Approximately in the Vicinities of San Luis Obispo, Avila, and Arroyo Grande

<u>Date</u>	<u>Geographic N Latitude</u>	<u>Coordinates W Longitude</u>	<u>Magni- tude</u>	<u>Inten- sity</u>	<u>Notes and Greenwich Mean Time (GMT)</u>
7.10.1889	35.17°	120.58°			Arroyo Grande. Shocks for several days.
12.1.1916	35.17°	120.75°		VII	VII at Avila. Considerable glass broken and goods in stores thrown from shelves at San Luis Obispo. Water in bay disturbed, plaster in cottages jarred loose, smoke stacks of Union Oil refinery toppled over at Avila. Severe at Port San Luis. III at Santa Maria: 22:53:00
4.26.1950	35.20°	120.60°	3.5	V	V at Santa Maria. Also felt at Orcutt: 7:23:29
1.26.1971	35.20°	120.70°	3		Near San Luis Obispo: 21:53:53
1830 to 7.21.1931	35.25°	120.67°			42 epicenters

DCPP UNITS 1 & 2 FSAR UPDATE

Earthquake Epicenters Reported as Being Located Approximately in the Vicinity of the Offshore Santa Maria Basin East Boundary Zone

<u>Date</u>	<u>Geographic Coordinates</u>		<u>Magni-</u>	<u>Inten-</u>	<u>Notes and Greenwich</u>
	<u>N Latitude</u>	<u>W Longitude</u>	<u>tude</u>	<u>sity</u>	<u>Mean Time (GMT)</u>
5.27.1935 ⁽³⁰⁻¹⁾	35.62°	121.64°	3	III	Felt at Templeton: 16:08:00
9.7.1939 ⁽³⁰⁻⁶⁾	35.46°	121.50°	3		Off San Luis Obispo County; felt at Cambria: 2:50:30
1.27.1945	34.75°	120.67°	3.9		17:50:31
12.31.1948 ⁽³⁰⁻¹⁰⁾	35.60°	121.23°	4.6		Felt along coast from Lompoc to Moss Landing. VI at San Simeon. V at Cayucos, Creston, Moss Landing, Piedras Blancas Light Station: 14:35:46
11.17.1949	34.80°	120.70°	2.8		IV at Santa Maria. Near Priest: 5:06:60
2.5.1955 ⁽³⁰⁻²³⁾	35.86°	121.15°	3.3		West of San Simeon: 7:10:19
6.21.1957 ^(30-25A)	35.23°	120.95°	3.7		Off Coast. Felt in San Luis Obispo, Morro Bay: 20:46:42
8.18.1958	35.60°	121.30	3.4		Near San Simeon: 5:30:42
10.25.1967	35.73°	121.45°	2.6		Near San Simeon: 23:05:39.5

(Figures in parentheses refer to events relocated by S. W. Smith, refer to Table 2.5-2).

2.5.4.6 Description of Active Faults

Data pertaining to faults with lengths greater than 1000 feet and reaches within 50 miles of the site, as identified during the original design phase, are included in Section 2.5.2.1.5, Structure of the San Luis Range and Vicinity, and in Figures 2.5-3 and 2.5-4. These data indicate the fault lengths, relationship of the faults to regional tectonic structures, known history of displacements, outer limits, and whether the faults can be considered as active.

2.5.4.7 Results of Faulting Investigation

The site for Units 1 and 2 of DCPD was investigated in detail for faulting and other possibly detrimental geologic conditions. From studies made prior to design of the plant, it was determined that there was need to take into account the possibility of surface faulting in such design. The data on which this determination was based are presented in Section 2.5.2.2, Site Geology.

2.5.5 Stability of Subsurface Materials

The possibility of past or potential surface or subsurface ground subsidence, uplift, or collapse in the vicinity of DCPD was considered during the course of the geologic investigations for Units 1 and 2.

2.5.5.1 Geologic Features

The site is underlain by folded bedrock strata consisting predominantly of sandy mudstone and fine-grained sandstone. The existence of an unbroken and otherwise undeformed section of upper Pleistocene terrace deposits overlying a wave-cut bedrock bench at the site provides positive evidence that all folding and faulting in the bedrock antedated formation of the terrace. Local depressions and other irregularities on the bedrock surface plainly reflect erosion in an ancient surf zone.

The rocks that constitute the bedrock section are not subject to significant solution effects (i.e., development of cavities or channels that could affect the engineering or fluid conducting character of the rock) because the bedrock section does not contain thick or continuous bodies of soluble rock types such as limestone or gypsum. Voids encountered during excavation at the site were limited to thin zones of vuggy breccia and isolated vugs in some beds of calcareous mudstone. Areas where such minor vuggy conditions were present were noted at a few locations in the excavation for the Unit 2 containment and fuel handling structures (at plant grid coordinates N59, N597, E10, E005 and N59, N700, E10, E120).

The maximum size of any individual opening was 3 inches or less, and most were less than 1 inch in maximum dimension. Because of the limited extent and isolated nature of these small voids, they were not considered significant in foundation engineering or slope stability analyses.

DCPP UNITS 1 & 2 FSAR UPDATE

It has been determined by field examination that no sea caves exist in the immediate vicinity of the site. The only cave like natural features in the area are shallow pits and hollows in some of the sea cliff outcrops of resistant tuff. These features generally have dimensions of a few inches to about 10 feet. They are superficial, and have originated through differential weathering of variably cemented rock.

Several exploratory wells have been drilled for petroleum within the San Luis Range, but no production was achieved and the wells were abandoned. The area is not now active in terms of either production or exploration. The location of the abandoned wells is shown in Figure 2.5-6, and the geologic relationships in the Range are illustrated in Section A-A' of Figure 2.5-6 and in Figure 2.5-7, Section D-D'. The nearest oil-producing area is the Arroyo Grande field, about 15 miles to the southeast.

The potential for future problems of ground instability at the site, because of nearby petroleum production, can be assessed in terms of the geologic potential for the occurrence of oil within, or offshore from, the San Luis Range. In addition, assessment can be made in terms of the geologic relationships in the site as contrasted with geologic conditions in places where oil field exploitation has resulted in deformation of the ground surface.

As shown in Figures 2.5-6 and 2.5-7, the San Luis Range has the structural form of a broad synclinal fold, which in turn is made up of several tightly compressed anticlines and synclines of lesser order. The configuration is not conducive to entrapment of hydrocarbon fluids, as such fluids tend to migrate upward through bedding and fracture-controlled zones of higher primary and secondary permeability until they reach a local trap or escape into the near surface or surface environment.

Within the San Luis Range, the only recognizable structural traps are in local zones where plunge reversals exist along the crests of the second-order anticlines. Such structures evidently were the actual or hoped-for targets for most of the exploratory wells that have been drilled in the San Luis Range, but none of these wells has produced enough oil or gas to record; thus, the traps have not been effective, or perhaps the strata are essentially lacking in hydrocarbon fluids. Other conditions that indicate poor petroleum prospects for the Range include the general absence of good reservoir rocks within the section and the relatively shallow basement of non petroliferous Franciscan rocks.

In the offshore, adjacent to the southerly flank of the San Luis Range, subsurface conditions are not well known, but are probably generally similar. Scattered data suggest that a structural high, perhaps defined by a west-northwest plunging anticline, may exist a few miles offshore from DCPP site. Such a feature could conceivably serve as a structural trap, if local closure were present along its axis; however, it seems unlikely that it would contain significant amounts of petroleum.

Available data pertaining to exploratory oil wells drilled in the region of the site are given here:

DCPP UNITS 1 & 2 FSAR UPDATE

Exploratory Oil Wells in the Vicinity of DCPP Site

Data from exploratory wells drilled outside of oil and gas fields in California to December 31, 1963: Division of Oil and Gas, San Francisco.

Mount Diablo B. & M.				Elev,	Date	Total	Stratigraphy
<u>T</u>	<u>R</u>	<u>Sec</u>	<u>Operator</u>	<u>ft</u>	<u>Started</u>	<u>ft</u>	(depth in ft) Age <u>at Bottom of Hole</u>
31S	10E	3	Tidewater Oil Co.	"Montadoro" 1	365	April 1954	6,146 Monterey 0-3800; Obispo Tuff 3800; Franciscan; U. Jurassic
30S	10E	24	Gretna Corp.	"Maino- Gonzales" 1	275	March 1937	1,575 Franciscan; Jurassic
		24	Wm. H. Provost	"Spooner" 1	325	July 1952	1,749 Jurassic
		24	Shell Oil Co.	"Buchon"	-	-	-
		34	A. O. Lewis	"Pecho" 1	177	May 1937	2,745 Monterey 0-2612; U. Miocene
30S	11E	9	Van Stone and Dallaston	"Souza" 1	42	Oct 1951	1,233 Franciscan; Jurassic
31S	11E	15	Tidewater Oil Co.	"Honolulu- Tidewater- U.S.L.- Heller "Lease" 1	1,614	Jan 1958	10,788 Monterey 0-4363; Pt. Sal 4363; Obispo Tuff 4722; Rincon Shale 5370; 2nd Tuff 5546; 2nd Rincon Shale 6354; 3rd Tuff 10,174; L. Miocene

For the purpose of assessing the potential for the occurrence of adverse oil field related ground deformation effects at DCPP site, in the unlikely event that petroleum should be discovered and produced at a nearby location, it is useful to review the nature and causes of such ground deformation, and the types of geologic conditions at places where it has been observed.

DCPP UNITS 1 & 2 FSAR UPDATE

The general subject of surface deformation associated with oil and gas field operations has been reviewed by Yerkes and Castle (Reference 22), among others. Such deformation includes differential subsidence, development of horizontally compressive strain effects within the central parts of subsidence bowls and horizontally extensive strain effects around their margins, and development or activation of cracks and faults. Pull-apart cracks and normal faults may develop in the marginal zone of extensive strain, while reverse and thrust faults sometimes occur in the central, compressive part of subsidence bowls. These effects all can develop when extraction of petroleum, water, and sand, plus lowering of fluid pressures, result in compression within and adjacent to producing zones, and attendant subsidence of the overlying ground. Other effects, including rebound of the ground surface, fault activation, and earthquake generation, have resulted from injection of fluid into the ground for purposes of secondary recovery, subsidence control, and disposal of fluid waste.

In virtually all instances of ground-surface deformation associated with petroleum production, the producing field has been centered on an anticlinal structure, in general relatively broad and internally faulted. The strata in the producing and overlying parts of the section typically are poorly consolidated sandstone, siltstone, claystone, and shale of low structural competence. The field generally is one with relatively large production, with significant decline of fluid pressure in the producing zones.

The conditions just cited can be contrasted with those obtained in the vicinity of DCPP site, where the rocks lie along the flank of a major syncline. They consist of tight sandstone, tuffaceous sandstone, mudstone, and shale, together with large resistant masses of tuff and diabase. Bedding dips range from near horizontal to vertical and steeply overturned, as shown in Section D-D' of Figure 2.5-7 and Section A-B of Figure 2.5-10. This structural setting is unlike any reported from areas where oil-field-associated surface deformation has occurred.

The foregoing discussion leads to the following conclusions: (a) future development of a producing oil field in the vicinity of DCPP site is highly unlikely because of unfavorable geologic conditions, and (b) geologic conditions in the site vicinity are not conducive to the occurrence of surface deformation, even if nearby petroleum production could be achieved.

As was noted in Section 2.4, the rocks underlying the site do not constitute a significant groundwater reservoir, so that future development of deep rock water wells in the vicinity is not a reasonable possibility. The considerations pertaining to surface deformation resulting from water extraction are about the same as for petroleum extraction, so there is no likelihood that DCPP site could experience artificially induced and potentially damaging subsidence, uplift, collapse, or changes in subsurface effective stress related to pore pressure phenomena.

There are no mineral deposits of economic significance in the ground underlying the site.

DCPP UNITS 1 & 2 FSAR UPDATE

Although some regional warping and uplift may well be taking place in the southern Coast Ranges, such deformation cannot be sufficiently rapid and local to impose significant effects on coastal installations. Apparent elevation of the San Luis Range has increased about 100 feet relative to sea level since the cutting of the main terrace bench at least 80,000 years ago.

Expressions of deformation preserved in the bedrock at the site include minor faults, folds, and zones of blocky fracturing in sandstone and intra-bed shearing in claystone. Zones of cemented breccia also are present, as is widespread evidence of disturbance adjacent to intrusive bodies of tuff. Local weakening of the rocks in some of these zones led to some problems during construction, but these were handled by conventional techniques such as overexcavation and rock bolting. No observed features of deformation are large or continuous enough to impose significant effects on the overall performance of the site foundation.

The foundation excavations for Units 1 and 2 were extended below the zone of intense near surface weathering so that the exposed bedrock was found to be relatively fresh and firm. The principal zones of structural weakness are associated with small bodies of altered tuff and with internally sheared beds of claystone. The claystone intra-bed shear was expressed by the development of numerous slickensided shear surfaces within parts of the beds, especially in places where the claystone had locally been squeezed into pod like masses. The shearing and local squeezing clearly are expressions of the preferential occurrence of differential adjustments in the relatively weaker claystone beds during folding of the section.

The claystone beds are localized in a part of the rock section that underlies the discharge structure and extends across the southerly part of the Unit 2 turbine-generator building, thence continuing easterly, along a strike through the ground south of the Unit 2 containment. The bedding dips 48 to 75° north within this zone. Individual claystone beds range from 1/2 inch to about 6 inches in thickness, and they occur as interbeds in the sandstone-mudstone rock section.

The relationship of the claystone layers to the foundation excavation is such that they crop out in several narrow bands across the floor and walls (refer to Figures 2.5-15 and 2.5-16). Thus, the claystone bed remains confined within the rock section, except in a narrow strip at the face of the excavation. Because of the small amount of claystone mass and the geometric relationship of the steeply dipping claystone interbeds to the foundation structures, it was determined that the finished structure would not be affected by any tendency of the claystone to undergo further changes in volume.

The only area in which claystone swelling was monitored was along the north wall of the lower part of the large slot cut for the cooling water discharge structure. There are several thin (6 inches or less) claystone interbeds in the sandstone-mudstone section. Because the orientation of the bedding and the plane of the cut face differ by only about 30°, and the bedding dips steeply into the face, opening of the cut served both to remove lateral support from the rock behind the face, and also to expose the clay beds

to rainfall and runoff. This apparently resulted in both load relief and hydration swelling of the newly exposed claystone, which in turn caused some outward movement of the cut face. The movement then continued as gravity creep of the locally destabilized mass of rock between the claystone beds and the free face. The movement was finally controlled by installation of drilled-in lateral tie-backs, prior to placement of the reinforced concrete wall of the discharge structure.

No evidence of unrelieved residual stresses in the bedrock was noted during the excavation or subsequent construction of the plant foundation. Isolated occurrences of temporary slope instability clearly were related to locally weathered and fractured rock, hydration swelling of claystone interbeds, and local saturation by surface runoff. The Units 1 and 2 power plant facilities are founded on physically and chemically stable bedrock.

2.5.5.2 Properties of Underlying Materials

Static and dynamic engineering properties of materials in the subsurface at the site are presented in Section 2.5.2.2.6, Site Engineering Properties.

2.5.5.3 Plot Plan

Plan views of the site indicating exploratory boring and trenching locations are presented in Figures 2.5-8 and 2.5-11 through 2.5-15. Profiles illustrating the subsurface conditions relative to the PG&E Design Class I structures are furnished in Figures 2.5-12 through 2.5-16. Discussions of engineering properties of materials and groundwater conditions are included in Section 2.5.2.2.6, Site Engineering Properties.

2.5.5.4 Soil and Rock Characteristics

Information on compressional and shear wave velocity surveys performed at the site are included in Appendices 2.5A and 2.5B of Reference 27 of Section 2.3. Values of soil modulus of elasticity and Poisson's ratio calculated from seismic measurements are presented in Table 1 of Appendix 2.5A of Reference 27 of Section 2.3, and in Figure 2.5-19. Boring and trench logs are presented in Figures 2.5-23 through 2.5-28.

2.5.5.5 Excavations and Backfill

Plan and profile drawings of excavations and backfill at the site are presented in Figures 2.5-17 and 2.5-18. The engineered backfill placement operations are discussed in Section 2.5.2.2.6.4, Engineered Backfill.

2.5.5.6 Groundwater Conditions

Groundwater conditions at the site are discussed in Section 2.4.13. The effect on foundations of PG&E Design Class I structures is discussed in Section 2.5.2.2.6, Site Engineering Properties.

2.5.5.7 Response of Soil and Rock to Dynamic Loading

Details of dynamic testing on site materials are contained in Appendices 2.5A and 2.5B of Reference 27 in Section 2.3.

2.5.5.8 Liquefaction Potential

As stated in Section 2.5.2.2.6.5, adverse hydrologic effects on foundations of PG&E Design Class I structures can be neglected due to the structures being founded on bedrock and the groundwater level lying well below final grade.

There is a small local zone of medium dense sand located northeast of the intake structure and beneath a portion of buried ASW piping that is not attached to the circulating water tunnels. This zone is susceptible to liquefaction during design basis seismic events (References 45 and 46). The associated liquefaction-induced settlements from seismic events are considered in the design of the buried ASW piping. (References 48 and 49)

2.5.5.9 Earthquake Design Basis

The earthquake design bases for the DCPD site are discussed in Section 2.5.3.9, a discussion of the design response spectra is provided in Section 2.5.3.10, and the application of the earthquake ground motions to the seismic analysis of structures, systems, and components is provided in Section 3.7. Response acceleration curves for the site resulting from Earthquake B and Earthquake D-modified are shown in Figures 2.5-20 and 2.5-21, respectively. Response spectrum curves for the Hosgri earthquake are shown in Figures 2.5-29 through 2.5-32.

2.5.5.10 Static Analysis

A discussion of the analyses performed on materials at the site is presented in Section 2.5.2.2.6, Site Engineering Properties.

2.5.5.11 Criteria and Design Methods

The criteria and methods used in evaluating subsurface material stability are presented in Section 2.5.2.2.6, Site Engineering Properties.

2.5.5.12 Techniques to Improve Subsurface Conditions

Due to the bearing of in situ rock being well in excess of the foundation pressure, no treatment of the in situ rock is necessary. Compaction specifications for backfill are presented in Section 2.5.2.2.6.4, Engineered Backfill.

2.5.6 SLOPE STABILITY

2.5.6.1 Slope Characteristics

The only slope whose failure during a DDE could adversely affect the nuclear power plant is the slope east of the building complex (refer to Figures 2.5-17, 2.5-18, and 2.5-22). To evaluate the stability of this slope, the soil and rock conditions were investigated by exploratory borings, test pits, and a thorough geological reconnaissance by the soil consultant, Harding-Lawson Associates, and was in addition to the overall geologic investigation performed by other consultants.

The slope configuration and representative locations of the subsurface conditions determined from the exploration are shown on Plates 2, 3, and 4 of Appendix 2.5C of Reference 27 of Section 2.3. Reference 44 provides further information compiled in 1997 in response to NRC questions on landslide potential.

Bedrock is exposed along the lower portions of the cut slope up to about the lower bench at elevation 115 feet. It consists of tuffaceous siltstone and fine-grained sandstone of the Monterey Formation. Terrace gravel overlies bedrock and extends to an approximate elevation of 145 feet. Stiff clays and silty soils with gravel and rock fragments constitute the upper material on the site. The upper few feet of fine-grained soils are dark brown and expansive.

No free groundwater was observed in any of the borings which were drilled in April 1971, nor was any evidence of groundwater observed in this slope during the previous years of investigation and construction of the project.

In response to an NRC request in early 1997, PG&E conducted further investigations of slope stability at the site (Reference 44). The results of the investigations showed that earthquake loading, as a result of an earthquake on the Hosgri fault zone, following periods of prolonged precipitation will not produce any significant slope failure that can impact Design Class I structures and equipment. In addition, potential slope failures under such conditions will not adversely impact other important facilities, including the raw water reservoirs, the 230 kV and 500 kV switchyards, and the intake and discharge structures. Potential landslides may temporarily block the access road at several locations. However, there is considerable room adjacent to and north of the road to reroute emergency traffic. The investigation of the cut slope included geologic mapping of the soil and rock conditions exposed on the surface of slope and existing benches. Subsurface conditions were investigated by drilling test borings and by excavating test pits in the natural slope above the plant site (refer to Figure 2.5-22). The test borings were drilled with a truck mounted, 24 inch flight auger drill rig, and the test pits were excavated with a track-mounted backhoe. Boring and Log of Test Pits 1, 2, and 3 were logged by the soil consultant; borings 2 and 3 were logged by PG&E engineering personnel. The logs of all borings were verified by the soil consultant, who examined all samples obtained from each boring. Undisturbed samples were obtained from boring 2 and each of the test pits. Because of the stiffness of the soil, hardness of the rock, and

type of drilling equipment used, the undisturbed samples were obtained by pushing an 18-inch steel tube that measured 2.5 inches in outside diameter. A Sprague & Henwood split-barrel sampler containing brass liners was used to obtain undisturbed soil samples from the test pits. The brass liners measured 2.5 inches in outside diameter and 6 inches in height. Logs of the borings and pits are shown in Figures 2.5-23 through 2.5-27. The soils were classified in accordance with the Unified Soil Classification System presented in Figure 2.5-28.

2.5.6.2 Design Criteria and Analyses

Undisturbed samples of the materials encountered in pits and borings were examined by the soil consultant in the laboratory and were subsequently tested to determine the shear strength, moisture content, and dry density. Strain controlled, unconsolidated, undrained triaxial tests at field moisture were performed on the clay to evaluate the shear strength of the materials penetrated. (The samples were maintained at field moisture since adverse moisture or seepage conditions were not encountered during this investigation nor previous investigations.) The confining stress was varied in relation to depth at which the undisturbed sample was taken. The test results are presented on the boring logs and are explained by the Key to Test Data, Figure 2.5-28.

The results of strength tests were correlated with the results developed during earlier investigations of DCPP site. Mohr circles of stresses at failure (6 to 7 percent strain) were drawn for each strength test result, and failure lines were developed through points representing one-half the deviator stresses. An average $C-\theta$ strength equal to a cohesion (C) value of 1000 psf and an angle of internal friction (θ) of 29° was selected for the slope stability analysis. The analysis was checked by maintaining the angle of internal friction (θ) constant at 19° and varying the cohesion (C) from 950 psf (weakest layer) to 3400 psf (deepest and strongest layer).

Because of the presence of large gravel sizes, it was not possible to accurately determine the strength of the sand and gravel lense. However, based on tests on sand samples from other parts of the site, an angle of internal friction of 35° was selected as being the minimum available. An assumed rock strength of 5000 psf was used. This value is consistent with strength tests performed on remold rock samples from other areas of the site.

The stability of the slope was analyzed for the forces of gravity using a static method that is, the conventional method of slices. This analysis was checked using Bishop's modified method. The static method of analysis was chosen because, for the soil conditions at the site, it was judged to be more conservative than a dynamic analysis.

Because the overall strength of the rock would preclude a stability failure except along a plane of weakness which was not encountered in the borings or during the many geologic mappings of the slope, only the stability of the soil over the rock was analyzed. The strength parameters were varied as previously discussed to determine the minimum factor of safety under the most critical strength condition. For the static

analysis excluding horizontal forces, the factor of safety was computed to be 3. When the additional unbalanced horizontal force of 0.4 times the weight of the soil within the critical surface combined with a vertical force of 0.26 times the weight was included, the minimum computed factor of safety was 1.1.

On the basis of the investigation and analysis, it was concluded that the slope adjacent to DCPP site would not experience instability of sufficient magnitude to damage adjacent safety-related structures.

The above conclusion is substantiated by additional field exploration, laboratory tests, and dynamic analyses using finite element techniques. Refer to Appendix 2.5C of Reference 27 in Section 2.3, Harding-Lawson Associates' report on this work.

2.5.6.3 Slope Stability for Buried Auxiliary Saltwater System Piping

A portion of the buried ASW piping for Unit 1 ascends an approximate 2:1 (horizontal/vertical) slope to the parking area near the meteorology tower (Plates 1 and 2 of Reference 47). To ensure the stability of this slope in which the ASW piping is buried, a geotechnical evaluation, considering various design basis seismic events, was performed by Harding Lawson Associates. This evaluation is described in Reference 47. Based on this evaluation, it was concluded that this slope will be stable during seismic events and that additional loads resulting from permanent deformation of the slope will not impact the buried ASW piping.

2.5.7 LONG TERM SEISMIC PROGRAM

On November 2, 1984, the NRC issued the Diablo Canyon Unit 1 Facility Operating License DPR-80. In DPR-80, License Condition Item 2.C.(7), the NRC stated, in part:

"PG&E shall develop and implement a program to reevaluate the seismic design bases used for the Diablo Canyon Power Plant."

PG&E's reevaluation effort in response to the license condition was titled the "Long Term Seismic Program" (LTSP). PG&E prepared and submitted to the NRC the "Final Report of the Diablo Canyon Long Term Seismic Program" in July 1988 (Reference 40). Between 1988 and 1991, the NRC performed an extensive review of the Final Report, and PG&E prepared and submitted written responses to formal NRC questions. In February 1991, PG&E issued the "Addendum to the 1988 Final Report of the Diablo Canyon Long Term Seismic Program" (Reference 41). In June 1991, the NRC issued Supplement Number 34 to the Diablo Canyon Safety Evaluation Report (SSER) (Reference 42) in which the NRC concluded that PG&E had satisfied License Condition 2.C.(7) of Facility Operating License DPR-80. In the SSER the NRC requested certain confirmatory analyses from PG&E, and PG&E subsequently submitted the requested analyses. The NRC's final acceptance of the LTSP is documented in a letter to PG&E dated April 17, 1992 (Reference 43).

DCPP UNITS 1 & 2 FSAR UPDATE

The LTSP contains extensive data bases and analyses that update the basic geologic and seismic information in this section of the FSAR Update. However, the LTSP material does not address or alter the current design licensing basis for the plant. In SSER 34 (Reference 42), the NRC stated, "The Staff notes that the seismic qualification basis for Diablo Canyon will continue to be the original design basis plus the Hosgri Evaluation basis, along with associated analytical methods, initial conditions, etc."

As a condition of the NRC's close out of License Condition 2.C.(7), PG&E committed to several ongoing activities in support of the LTSP, as discussed in a public meeting between PG&E and the NRC on March 15, 1991 (Reference 53), described as the "Framework for the Future," in a letter to the NRC, dated April 17, 1991 (Reference 50), and affirmed by the NRC in SSER 34 (Reference 43). These ongoing activities include the following that are related to geology and seismology (Reference 42, Section 2.5.2.4):

- (1) To continue to maintain a strong geosciences and engineering staff to keep abreast of new geological, seismic, and seismic engineering information and evaluate it with respect to its significance to Diablo Canyon.
- (2) To continue to operate the strong-motion accelerometer array and the coastal seismic network.

A complete listing of bibliographic references to the LTSP reports and other documents may be found in References 40, 41 and 42.

2.5.7.1 Shoreline Fault Zone

In November 2008, as a result of the ongoing activities described in Section 2.5.7, the USGS, working in collaboration with the PG&E Geosciences Department, identified an alignment of microseismicity subparallel to the coastline adjacent to DCPD indicating the possible presence of a previously unidentified fault located approximately 1 km offshore of DCPD. The offshore region associated with this fault was subsequently named the Shoreline fault zone.

PG&E developed estimates of the 84th percentile deterministic ground motion response spectrum for earthquakes associated with the Shoreline fault zone. The results of the study of the Shoreline fault zone are documented in Reference 52. A map showing the location of the Shoreline Fault Zone is provided in Figure 2.5-36. This report includes a comparison of the updated 84th percentile deterministic response spectra with the 1991 LTSP and 1977 Hosgri earthquake response spectra. This comparison indicates that the updated deterministic response spectra are enveloped by both the 1977 Hosgri earthquake spectrum and the 1991 LTSP earthquake spectrum.

The NRC developed an independent assessment of the seismic source characteristics of the Shoreline fault and performed an independent deterministic seismic hazard

assessment (References 54 and 55). The NRC concluded that their conservative estimates for the potential ground motions from the Shoreline fault are at or below the ground motions for which the DCPD has been evaluated previously and demonstrated to have a reasonable assurance of safety (i.e., the 1977 Hosgri earthquake and 1991 LTSP earthquake ground motion response spectra). The NRC stated that the "Shoreline scenario should be considered as a lesser included case under the Hosgri evaluation."

2.5.7.2 Evaluation of Updated Estimates of Ground Motion

As an outcome of the Shoreline fault zone evaluation described in Section 2.5.7.1, the process to be used for the evaluation of new/updated geological/seismological information has been developed (References 55 and 56). The new/updated geological/seismological information, resulting from the activities described in Section 2.5.7, will be evaluated using a process that is consistent with the evaluation process defined by the NRC in Reference 57.

2.5.8 Safety Evaluation

2.5.8.1 General Design Criterion 2, 1967 Performance Standards

The determination of the appropriate earthquake parameters for design of plant SSCs is addressed throughout Section 2.5, and the maximum earthquakes for the plant site are presented in Sections 2.5.3.9.1, 2.5.3.9.2, and 2.5.3.9.3. The associated design basis site free field accelerations and response spectra are presented in Sections 2.5.3.10.1, 2.5.3.10.2, and 2.5.3.10.3. The seismic design of these SSC is addressed in Section 3.7.

2.5.8.2 License Condition 2.C(7) of DCPD Facility Operating License DPR-80 Rev 44 (LTSP), Elements (1), (2) and (3)

PG&E's reevaluation effort in response to the license condition was titled the "Long Term Seismic Program" (LTSP). PG&E prepared and submitted to the NRC the "Final Report of the Diablo Canyon Long Term Seismic Program" in July 1988. Between 1988 and 1991, the NRC performed an extensive review of the Final Report, and PG&E prepared and submitted written responses to formal NRC questions. In February 1991, PG&E issued the "Addendum to the 1988 Final Report of the Diablo Canyon Long Term Seismic Program". In June 1991, the NRC issued Supplement Number 34 to the Diablo Canyon Safety Evaluation Report (SSER) in which the NRC concluded that PG&E had satisfied License Condition 2.C(7) of Facility Operating License DPR-80. In the SSER the NRC requested certain confirmatory analyses from PG&E, and PG&E subsequently submitted the requested analyses. The NRC's final acceptance of the LTSP is documented in a letter to PG&E dated April 17, 1992

The commitments made as a part of the Diablo Canyon Long Term Seismic Program are detailed in Section 2.5.3.9.4 and Section 2.5.7.

2.5.8.3 10 CFR Part 100, March 1966 - Reactor Site Criteria

As described in Sections 2.5.2 through 2.5.6 above, the physical characteristics of the site, including seismology and geology have been considered.

2.5.9 REFERENCES

1. R. H. Jahns, "Geology of the Diablo Canyon Power Plant Site, San Luis Obispo County, California," 1967-Supplementary Reports I and II, 1968-Supplementary Report III, Diablo Canyon PSAR, Docket No. 50-275, (Main Report and Supplementary Report I). Diablo Canyon PSAR, Docket No. 50-323, (All reports, 1966 and 1967).
2. R. H. Jahns, "Guide to the Geology of the Diablo Canyon Nuclear Power Plant Site, San Luis Obispo County, California," Geol. Soc. Amer., Guidebook for 66th Annual Meeting, Cordilleran Section, 1970.
3. Deleted in Revision 1
4. Deleted in Revision 1
5. H. Benioff and S. W. Smith, "Seismic Evaluation of the Diablo Canyon Site," Diablo Canyon Unit 1 PSAR, Docket No. 50-275. Also, Diablo Canyon Unit 2 PSAR Docket No. 50-323, 1967.
6. John A. Blume & Associates, Engineers, "Earthquake Design Criteria for the Nuclear Power Plant - Diablo Canyon Site," Diablo Canyon Unit 1 PSAR, Docket No. 50-275., January 12, 1967. Also, Diablo Canyon Unit 2 PSAR Docket No. 50-323.
7. John A. Blume & Associates, Engineers, "Recommended Earthquake Design Criteria for the Nuclear Power Plant - Unit No. 2, Diablo Canyon Site," Diablo Canyon Unit 2 PSAR, Docket No. 50-323, June 24, 1968.
8. Deleted in Revision 1
9. Deleted in Revision 1
10. B. M. Page, "Geology of the Coast Ranges of California," E. H. Bailey (editor), Geology of Northern California, California Division, Mines and Geology, Bull. 190, 1966, pp 255-276.
11. B. M. Page, "Sur-Nacimiento Fault Zone of California: Continental Margin Tectonics," Geol. Soc. Amer., Bull., Vol. 81, 1970, pp 667-690.

DCPP UNITS 1 & 2 FSAR UPDATE

12. J. G. Vedder and R. D. Brown, "Structural and Stratigraphic Relations Along the Nacimiento Fault in the Santa Lucia Range and San Rafael Mountains, California," W. R. Dickinson and Arthur Grantz (editors), Proceedings of Conference on Geologic Problems of the San Andreas Fault System, Stanford University Publs. in the Geol. Sciences, Vol. XI, 1968, pp 242-258.
13. C. F. Richter, "Possible Seismicity of the Nacimiento Fault, California," Geol. Soc. Amer., Bull., Vol. 80, 1969, pp 1363-1366.
14. E. W. Hart, "Possible Active Fault Movement Along the Nacimiento Fault Zone, Southern Coast Ranges, California," (abs.), Geol. Soc. Amer., Abstracts with Programs for 1969, pt. 3, 1969, pp 22-23.
15. R. E. Wallace, "Notes on Stream Channels Offset by the San Andreas Fault, Southern Coast Ranges, California," W. R. Dickinson and Arthur Grantz (editors), Proceedings of Conference on Geologic Problems of the San Andreas Fault System, Stanford University Publs. in the Geol. Sciences, Vol. XI, 1968, pp 242-258.
16. C. R. Allen, "The Tectonic Environments of Seismically Active and Inactive Areas Along the San Andreas Fault System," W. R. Dickinson and Arthur Grantz (editors), Proceedings of Conference on Geologic Problems of the San Andreas Fault System, Stanford University Publs. in the Geol. Sciences, Volume XI, 1968, pp 70-82.
17. Deleted in Revision 1
18. Deleted in Revision 1
19. L. A. Headlee, Geology of the Coastal Portion of the San Luis Range, San Luis Obispo County, California, Unpublished MS thesis, University of Southern California, 1965.
20. C. A. Hall, "Geologic Map of the Morro Bay South and Port San Luis Quadrangles, San Luis County, California," U.S. Geological Survey Miscellaneous Field Studies Map MF-511, 1973.
21. C. A. Hall and R. C. Surdam, "Geology of the San Luis Obispo-Nipomo Area, San Luis Obispo County, California," Geol. Soc. Amer., Guidebook for 63rd Ann. Meeting, Cordilleran Section, 1967.
22. R. F. Yerkes and R. O. Castle, "Surface Deformation Associated with Oil and Gas Field Operations in the United States in Land Subsidence," Proceedings of the Tokyo Symposium, Vol. 1, IASH/A1HS Unesco, 1969, pp 55-65.

DCPP UNITS 1 & 2 FSAR UPDATE

23. C. W. Jennings, et al., Geologic Map of California, South Half, scale 1:750,000, California Div. Mines and Geology, 1972.
24. John H. Wiggins, Jr., "Effect of Site Conditions on Earthquake Intensity," ASCE Proceedings, Vol. 90, ST2, Part 1, 1964.
25. B. M. Page, "Time of Completion of Underthrusting of Franciscan Beneath Great Valley Rocks West of Salinian Block, California," Geol. Soc. Amer., Bull., Vol. 81, 1970, pp 2825-2834.
26. Eli A. Silver, "Basin Development Along Translational Continental Margins," W. R. Dickinson (editor), Geologic Interpretations from Global Tectonics with Applications for California Geology and Petroleum Exploration, San Joaquin Geological Society, Short Course, 1974.
27. T. W. Dibblee, The Riconada Fault in the Southern Coast Ranges, California, and Its Significance, Unpublished abstract of talk given to the AAPG, Pacific Section, 1972.
28. D. L. Durham, "Geology of the Southern Salinas Valley Area, California," U.S. Geol. Survey Prof. Paper 819, 1974, p 111.
29. William Gawthrop, Preliminary Report on a Short-term Seismic Study of the San Luis Obispo Region, in May 1973 (Unpublished research paper), 1973.
30. S. W. Smith, Analysis of Offshore Seismicity in the Vicinity of the Diablo Canyon Nuclear Power Plant, report to Pacific Gas and Electric Company, 1974.
31. H. C. Wagner, "Marine Geology between Cape San Martin and Pt. Sal, South-Central California Offshore; a Preliminary Report, August 1974," USGS Open File Report 74-252, 1974.
32. R. E. Wallace, "Earthquake Recurrence Intervals on the San Andreas Fault", Geol. Soc. Amer., Bull., Vol. 81, 1970, pp 1875-2890.
33. J. C. Savage and R. O. Burford, "Geodetic Determination of Relative Plate Motion in Central California", Jour. Geophys. Res., Vol. 78, No. 5, 1973, pp 832-845.
34. Deleted in Revision 1
35. Hill, et al., "San Andreas, Garlock, and Big Pine faults, California" - A Study of the character, history, and significance of their displacements, Geol. Soc. Amer., Bull., Vol. 64, No. 4, 1953, pp 443-458.

DCPP UNITS 1 & 2 FSAR UPDATE

36. C.A. Hall and C.E. Corbato, "Stratigraphy and Structure of Mesozoic and Cenozoic Rocks, Nipomo Quadrangle, Southern Coast Ranges, California," Geol. Soc. Amer., Bull., Vol. 78, No. 5, 1969, pp 559-582. (Table 2.5-3, Sheet 1 of 2).
37. Bolt, Beranek, and Newman, Inc., Sparker Survey Line, Plates III and IV, 1973/1974. (Appendix 2.5D, to Diablo Canyon Power Plant Final Safety Analysis Report as amended through August 1980). (See also Reference 27 of Section 2.3.)
38. R. R. Compton, "Quaternary of the California Coast Ranges," E. H. Bailey (editor), Geology of Northern California, California Division Mines and Geology, Bull. 190, 1966, pp 277-287.
39. Regulatory Guide 1.70, Revision 1, Standard Format and Content of Safety Analysis Reports for Nuclear Power Plants, USNRC, October 1972.
40. Pacific Gas and Electric Company, Final Report of the Diablo Canyon Long Term Seismic Program, July 1988.
41. Pacific Gas and Electric Company, Addendum to the 1988 Final Report of the Diablo Canyon Long Term Seismic Program, February 1991.
42. NUREG-0675, Supplement No. 34, Safety Evaluation Report Related to the Operation of Diablo Canyon Nuclear Power Plant, Units 1 and 2, USNRC, June 1991.
43. NRC letter to PG&E, Transmittal of Safety Evaluation Closing Out Diablo Canyon Long-Term Seismic Program, (TAC Nos. M80670 and M80671), April 17, 1992.
44. Pacific Gas and Electric Company, Assessment of Slope Stability Near the Diablo Canyon Power Plant, April 1997.
45. Harding Lawson Associates, Liquefaction Evaluation - Proposed ASW Bypass - Diablo Canyon Power Plant, August 23, 1996.
46. Harding Lawson Associates Letter, "Geotechnical Consultation - Liquefaction Evaluation - Proposed ASW Bypass - Diablo Canyon Power Plant," October 1, 1996.
47. Harding Lawson Associates Report, Geotechnical Slope Stability Evaluation - ASW System Bypass, Unit 1 - Diablo Canyon Power Plant, July 3, 1996.
48. License Amendment Request 97-11, Submitted to the NRC by PG&E Letters DCL-97-150, dated August 26, 1997; DCL-97-177, dated October 14, 1997; DCL-97-191, dated November 13, 1997; and DCL-98-013, dated January 29, 1998.

DCPP UNITS 1 & 2 FSAR UPDATE

49. NRC Letter to PG&E dated March 26, 1999, granting License Amendment No. 131 to Unit 1 and No. 129 to Unit 2.
50. PG&E letter to the NRC, "Benefits and Insights of the Long Term Seismic Program," DCL-91-091, April 17, 1991.
51. John A. Blume and Associates letter to PG&E, "Earthquake Design Criteria for the Nuclear Power Plant - Diablo Canyon Site," January 12, 1967.
52. Pacific Gas and Electric Company, Report on the Analysis of the Shoreline Fault Zone - Central Coastal California, January 2011.
53. NRC Letter to PG&E, "Summary of March 15, 1991 Public Meeting to Discuss Diablo Canyon Long-Term Seismic Program (TAC Nos. 55305 and 68049)", March 22, 1991
54. NRC Office of Nuclear Regulatory Research, "Confirmatory Analysis of Seismic Hazard at the Diablo Canyon Power Plant from the Shoreline Fault Zone," Research Information Letter No. 12-01, September 2012
55. NRC letter to PG&E, "Diablo Canyon Power Plant, Unit Nos. 1 and 2 - NRC Review of Shoreline Fault (TAC Nos. ME5306 and ME5307)," October 12, 2012.
56. Pacific Gas and Electric Company letter to the NRC, "Withdrawal of License Amendment Request 11-05, Evaluation Process for New Seismic Information and Clarifying the Diablo Canyon Power Plant Safe Shutdown Earthquake,": Letter No. DCL-12-103, October 25, 2012.
57. NRC letter to All Power Reactor Licensees and Holders of Construction Permits in Active or Deferred Status, "Request of Information Pursuant to Title 10 of the Code of Federal Regulations 50.54(f) Regarding Recommendations 2.1, 2.3, and 9.3 of the Near-Term Task Force Review of Insights from the Fukushima Dai-Ichi Accident," Marc 12, 2012.

3.7 SEISMIC DESIGN

3.7.1 SEISMIC INPUT

This section describes the DE, the DDE, and the postulated 7.5M HE.

In addition to the above three earthquakes, PG&E conducted, as described below, a program to reevaluate the seismic design for DCP. On November 2, 1984, the NRC issued the DCP Unit 1 Facility Operating License DPR-80. In License Condition 2.C(7) of DPR-80, the NRC stated, in part: "PG&E shall develop and implement a program to reevaluate the seismic design bases used for the Diablo Canyon Power Plant."

PG&E's reevaluation effort in response to the license condition was titled the "Long Term Seismic Program" (LTSP). PG&E prepared and submitted to the NRC the "Final Report of the Diablo Canyon Long Term Seismic Program" in July 1988 (Reference 19). The NRC reviewed the Final Report between 1988 and 1991, and PG&E prepared and submitted written responses to NRC questions resulting from that review. In February 1991, PG&E issued the "Addendum to the 1988 Final Report of the Diablo Canyon Long Term Seismic Program." (Reference 20) In June 1991, the NRC issued Supplement 34 to the Diablo Canyon Safety Evaluation Report (SSER) (Reference 21), in which the NRC concluded that PG&E had satisfied License Condition 2.C(7) of DPR-80. In the SSER the NRC requested certain confirmatory analyses from PG&E, and PG&E subsequently submitted the requested analyses. The NRC's final acceptance of the LTSP is documented in a letter to PG&E dated April 17, 1992 (Reference 22).

The LTSP contains extensive databases and analyses that update the basic geologic and seismic information in this FSAR Update. However, the LTSP material does not alter the design bases for DCP. In SSER 34 (Reference 21), the NRC states, "The Staff notes that the seismic qualification basis for Diablo Canyon will continue to be the original design basis plus the Hosgri evaluation basis, along with associated analytical methods, initial conditions, etc."

PG&E committed to the NRC in a letter dated July 16, 1991 (Reference 23), that certain future plant additions and modifications, as identified in that letter, would be checked against insights and knowledge gained from the LTSP to verify that the plant margins remain acceptable.

A completed listing of bibliographic references to the LTSP reports and other documents are provided in References 19, 20, and 21.

3.7.1.1 Design Response Spectra

Section 2.5.2 provides a discussion of the earthquakes postulated for the DCP site and the effects of these earthquakes in terms of maximum free-field ground motion accelerations and corresponding response spectra at the plant site. The maximum

vibratory accelerations at the plant site would result from either Earthquake B or Earthquake D-modified, depending on the natural period of the vibrating body. Response acceleration spectra curves for horizontal free-field ground motion at the plant site from Earthquake B, Earthquake D-modified, and HE are presented in Figures 2.5-20, 2.5-21, and 2.5-29 through 32, respectively.

For design purposes, the response spectra for each damping value from Earthquake B and Earthquake D-modified are combined to produce an envelope spectrum. The acceleration value for any period on the envelope spectrum is equal to the larger of the two values from the Earthquake B spectrum and the Earthquake D-modified spectrum. Vertical free field ground accelerations, and the vertical free-field ground motion response spectra are assumed to be two-thirds of the corresponding horizontal spectra.

The DE is the hypothetical earthquake that would produce these horizontal and vertical vibratory accelerations. The DE corresponds to the operating basis earthquake (OBE), as described in Appendix A to 10 CFR 100 (Reference 7).

To ensure adequate reserve energy capacity, Design Class I structures and equipment are reviewed for the DDE. The DDE is the hypothetical earthquake that would produce accelerations twice those of the DE. The DDE corresponds to the SSE, as described in Appendix A to 10 CFR 100 (Reference 7).

PG&E was requested by the NRC to evaluate the plant's capability to withstand a postulated Richter magnitude 7.5 earthquake centered along an offshore zone of geologic faulting, generally referred to as the Hosgri Fault. This evaluation is discussed in the various chapters when it is specifically referred to as the Hosgri evaluation or Hosgri event evaluation.

Acceleration response spectra curves for horizontal and vertical free field ground motion at the plant site from the HE are the Newmark and Blume spectra described in Section 2.5. The vertical free field response spectra are two-thirds of the corresponding horizontal spectra.

3.7.1.2 Design Response Spectra Derivation

The free-field ground motion acceleration time-histories used in the dynamic analyses of the containment structure, auxiliary building, turbine building, and intake structure are developed by the following procedure: The response spectra for 2 percent damping for Earthquake B and Earthquake D-modified are enveloped to produce a single response spectrum (DE intensity). A time-history is then developed that produces a spectrum with no significant deviation from the smooth DE-envelope spectrum. This procedure eliminates undesirable peaks and valleys that exist in the response spectrum calculated directly from Earthquake B and Earthquake D-modified records.

A similar procedure is used to obtain a free-field ground motion acceleration time-history for the DDE. The free-field ground motion acceleration time-histories for the DE and

DCPP UNITS 1 & 2 FSAR UPDATE

DDE are shown in Figures 3.7-1 and 3.7-2, respectively. Comparison of the response spectrum computed from the time-history with the smoothed envelope spectrum is shown in Figure 3.7-3 (2 percent damping) and in Figure 3.7-4 (5 percent damping). These spectra are calculated at period intervals of 0.01 seconds, which adequately define the spectra.

For the HE evaluation of containment structure, auxiliary building, turbine building, and intake structure, the horizontal input motions are reduced from free-field motions to account for the presence of the structures that have large foundations. These reduced inputs have been derived by spatial averaging of acceleration across the foundations of each structure by the Tau filtering procedure (Reference 12). The resulting horizontal response spectra for these structures are shown in Figures 3.7-4A through 3.7-4F.

For HE evaluation of outdoor water storage tanks and smaller structures, the horizontal design response spectra are the free-field horizontal response spectra. HE vertical design response spectra are the free-field vertical response spectra. For design purposes, the Newmark spectra are used, or alternately the Blume spectra are used, with adjustment in certain frequency ranges as necessary so that they do not fall below the corresponding Newmark spectra.

Acceleration time-histories used in the analysis of the containment and intake structures, auxiliary building, and turbine building are shown in Figures 3.7-4G through 3.7-4M. Comparison of the response spectrum computed from each time-history with the corresponding design response spectrum for 7 percent damping is shown in Figures 3.7-4N through 3.7-4T.

3.7.1.3 Critical Damping Values

The specific percentages of critical damping used for Design Class I SSCs, and the Design Class II turbine building and intake structure are listed in the following table:

<u>Type of Structure</u>	<u>% of Critical Damping</u>		
	<u>DE</u>	<u>DDE</u>	<u>HE</u>
Containment structures and all internal concrete structures	2.0	5.0	7.0
Other conventionally reinforced concrete structures above ground, such as shear walls or rigid frames	5.0	5.0	7.0
Welded structural steel assemblies	1.0	1.0	4.0
Bolted or riveted steel assemblies	2.0	2.0	7.0
Mechanical components (PG&E purchased)	2.0	2.0	4.0
Vital piping systems (except reactor coolant loop) ^(a)	0.5	0.5	3.0 ^(b)

DCPP UNITS 1 & 2 FSAR UPDATE

<u>Type of Structure</u>	<u>% of Critical Damping</u>		
	<u>DE</u>	<u>DDE</u>	<u>HE</u>
Reactor coolant loop ^{(a)(c)}	1.0	1.0	4.0
Replacement Steam Generators ^(f)	2.0	4.0	4.0
Integrated Head Assembly ^(g)	4.9	6.85	6.85
CRDMs ^(h)	5.0	5.0	5.0
Foundation rocking (containment structure only) ^(d)	5.0	5.0	NA ^(e)

(a) ASME Code Case N-411 damping may be used provided it is applied to all earthquake cases and used in response spectrum modal superposition analysis. When used, pipe displacements are checked for adequacy of clearances and pipe mounted equipment accelerations are verified against project qualification criteria. For equipment and components modeled inline, damping should be consistent with RG 1.61; a composite damping value may be used for the analysis of these piping systems. A log of calculations is kept that indicates which calculations have used Code Case N-411 damping.

Request for NRC approval for the use of ASME Code Case N-411 was made in letter DCL-86-009, dated January 22, 1986. NRC approval was granted by letter on April 7, 1986

- (b) Two percent of critical damping is used for piping less than or equal to 12 inches in diameter.
- (c) Although a damping value of 1 percent is used for the DE and DDE analyses of the reactor coolant loop (RCL), damping values of greater than 4 percent have been measured experimentally for the RCL in full-size power plants (Reference 8). These testing programs have been reviewed and approved by the NRC. The damping values recommended in RG 1.61 are acceptable for use in analysis of mechanical equipment and systems. (References 24-26)
- (d) Five percent of critical damping is used for structures founded on rock for the purpose of computing the response in the rocking mode, and 7 percent of critical damping is used for the purpose of computing the response in the translation mode.
- (e) Analysis utilizes fixed base.
- (f) These values are valid for replacement steam generator (RSG) internals and shell components up to the RSG nozzle to pipe/tube connections in the RCS, MS, and FW systems and the interface between the RSG shell and upper and lower lateral and lower vertical supports. The restrictions imposed by WCAP 7921-AR (Reference 8) shall be observed when applying these values. (Reference 27)

- (g) Damping values for the IHA are based on Regulatory Guide 1.61, Revision 1 (Reference 31), Tables 1 and 2, using a weighted average for "Welded Steel or Bolted Steel with Friction Connections" and "Bolted Steel with Bearing Connections". See PG&E Document 6023227-19 (Reference 30) for computation of weighted average value. Computation of weighted average value was approved in Reference 32.
- (h) Damping values for the CRDMs are based on Regulatory Guide 1.61, Revision 1, (Reference 31) as approved in Reference 33.

3.7.1.4 Bases for Site-Dependent Analysis

Site conditions used to develop the shape of site seismic design response spectra are described in Section 2.5.2.

3.7.1.5 Soil-Supported Design Class I Structures

All Design Class I plant structures are founded on rock or on concrete fill.

3.7.1.6 Soil-Structure Interaction

Soil-structure interaction effects are considered as described in Section 3.7.2.1.7.

3.7.1.7 Hosgri Evaluation

The criteria and methods used to review the major structures for response to the postulated 7.5M HE are discussed in this chapter. A comparison of the DE and the DDE criteria with the HE evaluation criteria is given in Table 3.7-1 for the containment and auxiliary building, Tables 3.7-1A for the turbine building, 3.7-1B for the intake structure, and 3.7-1C for the outdoor water storage tanks, respectively.

3.7.2 SEISMIC SYSTEM ANALYSIS

In accordance with Revision 1 to RG 1.70, paragraphs under the headings below Seismic Analysis Methods and Description of Seismic Analyses, apply to all seismic analysis performed, i.e., both seismic system analysis and seismic subsystem analysis. Paragraphs under subsequent headings in this section provide discussion of specific topics applicable to seismic system analysis. Discussion of specific topics applicable to seismic subsystem analysis is provided in Section 3.7.3. The seismic analysis of Design Class I SSCs is based on input motions of the DE, DDE, and HE described in Section 3.7.1.

3.7.2.1 Seismic Analysis Methods

Four dynamic methods of seismic analysis are used for Design Class I SSCs: time-history modal superposition, response spectrum modal superposition, response spectrum single-degree-of-freedom, and the method for rigid equipment and piping.

The concept of modal analysis and each of the four methods of seismic analysis are discussed in subsequent paragraphs.

3.7.2.1.1 Modal Analysis

The structure, system, or component is represented as a mathematical model that is in the form of lumped masses interconnected by springs or finite elements. The mathematical model typically has one, two, or three degrees of freedom for each lumped mass or node point, but could have as many as six degrees of freedom for each lumped mass or node point.

Each multiple-degree-of-freedom (multidegree) system has the same number of normal modes as it has degrees of freedom. The characteristics of a normal mode of vibration is that, under certain conditions, the multidegree system could vibrate freely in that mode alone, and during such vibration the ratio of displacements of any two masses is constant with time. These ratios define the characteristic shape of the mode. For any vibration of the multidegree system, the motion in any of the individual normal modes can be treated as an independent single-degree-of-freedom system, and the complete motion of the multidegree system can be obtained by superimposing the independent motions of the individual modes.

The natural frequencies and characteristic shapes are determined by solution of the equations of motions for free vibrations.

3.7.2.1.2 Time-History Modal Superposition

The time-history of response in each mode is determined from the acceleration time-history input by integration of the equations of motion. The modal responses are combined by algebraic sum to produce an accurate summation at each step.

3.7.2.1.3 Response Spectrum Modal Superposition

The response spectrum is a plot, for all periods of vibration, of the maximum acceleration experienced by a single-degree-of-freedom vibrating body during a particular earthquake. The response spectrum modal superposition method of analysis applies to multidegree systems and is based on the concept of modal analysis. The modal equation of motion for a multidegree system is analogous to the equation of motion for a single degree of freedom. The maximum response in each mode is calculated, and modal responses (displacements, accelerations, shears, moments, etc.) are combined by the square root of the sum of the squares (SRSS) method.

3.7.2.1.4 Response Spectrum, Single-Degree-of-Freedom

Many components can be accurately represented by a single-degree-of-freedom mathematical model. The response spectrum method of analysis is applicable and the concept of modal analysis is not required.

3.7.2.1.5 Static Equivalent Method

When it can be shown that a sub-system is rigid, a static analysis may be performed. The zero period acceleration obtained from the applicable response spectra curve may be used in static calculations.

3.7.2.1.6 Application

All Design Class I structures, components, systems, and piping are designed by time-history modal superposition, response spectrum modal superposition, response spectrum single-degree-of-freedom, or the method for rigid equipment and piping, except the following:

- (1) Mechanical equipment whose seismic adequacy is verified by testing as described in Section 3.9
- (2) Electrical and instrumentation equipment whose seismic adequacy is verified as described in Section 3.10
- (3) Certain Design Class I piping less than 2-1/2 inches in diameter that is restrained according to criteria described in Section 3.7.2.1.7.4
- (4) Reactor internals, fuel elements, control rod drive assemblies, and control rod drives, as described in Section 3.7.3.15.

3.7.2.1.7 Description of Seismic Analyses

3.7.2.1.7.1 Design Class I Structures

Dynamic analyses by the time-history modal superposition method were performed for the containment structure and the auxiliary building. Acceleration time-histories were obtained at specific points in the structures, and response spectra were calculated from these. In order to provide for possible variations in the parameters used in the dynamic analyses, such as mass values, material properties, and material sections, the calculated spectra were modified. For DE and DDE analyses, it is estimated that the calculated period of the structure could vary by approximately 10 percent, and to account for this the peaks of the spectra were correspondingly widened. Similarly, for HE analyses, peaks of the spectra are widened 5 percent on the low period side and 15 percent on the high period side. The modified spectra, known as "smooth spectra," are used in the design of Design Class I equipment and piping located in the containment structure and auxiliary building.

A detailed analytical static model of the auxiliary building was used to distribute the seismic inertial forces and moments to various walls, diaphragms, and columns, as described in Section 3.8.2.4.

Allowable stresses for Design Class I structures are presented in Section 3.8.

Containment Structure Model

(1) DE and DDE events

The containment structure calculations relative to responses to DE and DDE events are performed with a computer program for analysis of axisymmetric structures by the finite element method. The foundation rock mass and the containment structure are modeled as one structure system to consider the effect of rock-structure interaction, as shown in Figure 3.7-5. The boundary dimensions of the model are selected such that they do not have a significant effect on the response of the structure. The exterior shell and internal structure are modeled using shell elements with four degrees of freedom at each nodal point. There are a total of 156 nodal points and 140 elements in the model. The weight of mechanical equipment in the structure is included in the calculation of equivalent mass density for the structure elements. Values of elastic constants for the rock mass and their variation with depth are based on field measurements made at the plant site (see Section 2.5).

To substantiate that the coupling effect is small at the reactor pressure vessel (RPV) elevation, two floor response spectra were generated for a decoupled interior concrete structure model and a coupled RPV and the interior concrete structure model, respectively. The RPV model is a simplified one-degree-of-freedom system, with its natural frequency matching the fundamental mode of the DCPP vessel. The RPV model is attached to Node 2 of the interior concrete structure model at the vessel support elevation by the spring of the vessel model.

Floor response spectra for the decoupled and the coupled models were very similar, indicating that the coupling effect at this low elevation is very small. More importantly, the response spectra magnitude of the decoupled model is consistently higher than the coupled model between 0.05 to 0.40 seconds, and is equal at all other natural periods. This shows that, indeed, the decoupled model is more conservative.

(2) Hosgri event

The dynamic analysis for HE is performed for exterior shell, interior concrete structures, and the annulus steel structure. The description of these structural components is given in Section 3.8.1.

The elements used in the analysis of exterior shell consist of annular rings of shell elements as shown in Figure 3.7-5A. The model consists of 27 nodal points and 26 elements. A typical shell element has four degrees-of-freedom as shown in Figure 3.7-7. The axisymmetric model is used to compute the translational response of the structure due to the horizontal and vertical ground motion. Since the center of mass and the

DCPP UNITS 1 & 2 FSAR UPDATE

center of rigidity coincide, the translational analysis does not yield any torsional response. The torsional responses are obtained from separate lumped mass models as shown in Figure 3.7-5B. These lumped mass models account for 5 percent and 7 percent accidental eccentricities. The responses from axisymmetric model and the lumped mass models are combined by absolute sum for 5 percent eccentricity and by SRSS for 7 percent eccentricity.

The dynamic analysis of containment internal structure is divided into two parts: concrete interior structure and annulus steel structure.

- (a) Concrete interior structure mainly comprised of reactor cavity walls and crane wall is represented by an axisymmetric model as shown in Figure 3.7-5A. The model as shown in Figure 3.7-5A contains 22 nodal points and 22 elements. Because the center of mass and the center of rigidity coincide, the analysis does not yield torsional modes. Therefore, a separate lumped mass model, as shown in Figure 3.7-5C, is used to consider torsional response. Figure 3.7-5D is used to compute vertical responses of the concrete interior structures due to the HE. The lumped mass stick with model points 1, 7, 18, 29, and 40 represent the concrete walls. The annulus steel is modeled by five frames located along the circumference as shown. This model was developed at an early stage of the project to estimate vertical responses of both annulus steel and concrete structures from the HE. However, subsequently detailed models were developed for the annulus steel as described later and the model of Figure 3.7-5D is used for the vertical analysis of the concrete interior structures only.

The models of Figures 3.7-5A, 3.7-5C, and 3.7-5D represent concrete interiors up to elevation 140 feet which is the operating floor of the containment. The secondary shield walls housing the steam generators do extend above elevation 140 feet; however, the mass of these walls above elevation 140 feet is small compared to the total concrete mass and, therefore, lumping the mass at elevation 140 feet of the walls that extend above elevation 140 feet has little effect on the dynamic behavior of concrete internals below elevation 140 feet.

- (b) Several models are developed for the vertical dynamic analysis of annulus steel. Each model represents a steel frame with a column at the outside perimeter, crane wall at the inside perimeter, and the radial beam. Figure 3.7-5E represents a typical model.

DCPP UNITS 1 & 2 FSAR UPDATE

The horizontal responses of the annulus steel are considered to be the same as the concrete interior structures as computed from model of Figure 3.7-5A. This consideration is supported by:

- The study results showing that the amplification above 20 Hz for the annulus steel is negligible; and
- The modal analysis of steel frames shows that the first mode of vibration, which is the predominant mode, is approximately 20 Hz.

(3) Input boundary motions

In the seismic analysis of the finite element model, for DE and DDE, the motions at the boundary of the rock mass are required as input. These boundary motions are derived using procedures described in the following steps:

- (a) The finite element model of the rock mass only (without the structure) is subjected to a unit impulse acceleration acting at the rock mass boundaries. As a result, the acceleration time-history (impulse response that reflects the rock mass properties) is obtained at the center nodal point on the surface of the rock mass.
- (b) The impulse response function, together with the desired free-field ground motion, is used as input to a deconvolution program. The required boundary motion is obtained as the output. This boundary motion, when used as input to the nodes along the horizontal and vertical boundaries of the rock mass model, produces a time-history at the center nodal point on the surface of the model that is equivalent to the free-field motion. To check the accuracy of the derived boundary motion, the rock mass without the structure is analyzed using this motion as input, and the computed free-field ground motion at the center nodal point on the surface of the rock mass is obtained. The computed free-field spectrum is calculated for this surface motion and compared with the DE- or DDE-smoothed spectrum. Due to approximations involved in the analytical methods used to derive the boundary motions, the computer spectra show slight deviations from the desired smoothed spectra. To account for these deviations, the structural response results are then conservatively scaled upward by appropriate correction factors.

The boundary motions derived from the procedure described above are used to complete the analysis of the containment structure.

DCPP UNITS 1 & 2 FSAR UPDATE

For the HE, the analytical models are considered fixed as shown in Figures 3.7-5A, 3.7-5B, 3.7-5C, and 3.7-5D. The analysis is performed using the input motions as specified in Section 3.7.1.2.

Containment Polar Crane

The polar crane as described in Sections 9.1.4 and 3.8.1 is an overhead gantry crane, supported by the crane wall inside the containment.

A nonlinear time-history analysis is performed for the crane to consider the possibility of wheel uplift and/or slack in the hook cable. The crane structure model is shown in Figure 3.7-7A. Structural members are represented as beam elements; wheel assemblies as nonlinear gap elements with compression stiffness only, and a hook cable is represented as a truss element with no compression capability. A step-by-step integration procedure is employed to determine the response. The time-step for integration is 0.005 sec. Seismic input is provided by simultaneous, independent time-histories in three directions (two horizontal and one vertical). These time-histories are developed at the top of the crane wall from the dynamic analysis described in Section 3.7.2.1.7.1 above.

Pipeway Structure

To obtain seismic responses in the pipeway structure, a combined model is used consisting of containment exterior shell, pipeway-framing members, and the mainsteam and feedwater piping which are supported by the framing members. The three-dimensional pipeway structure model consists of steel platforms supported on structural steel columns, containment shell and auxiliary and turbine buildings. This structure is represented in the model by beam elements (approximately 900). Oversized holes are provided to support pipeway structure beams on the auxiliary and turbine buildings. Accordingly, the model is decoupled from auxiliary and turbine buildings in the horizontal direction. The horizontal coupling between pipeway framing model and containment model is achieved by rigid links. The main steam and feedwater lines are included in the model since they represent significant masses for the pipeway structure.

The combined containment-pipeway structure model was excited by acceleration time-history at the containment base.

(1) DE and DDE events

Equivalent static analyses of the pipeway structure are performed for the DE and DDE events as described in Section 3.8.6. The adequacy of these analyses is confirmed by a time-history dynamic analysis.

(2) Hosgri event

The response spectra are generated using the time-history dynamic analysis method. The effect of accidental torsion is included as discussed for the containment structure model in Section 3.7.2.1.7.1. These response spectra are used for qualification of equipment and components. The structural qualification is performed using the response spectrum dynamic modal superposition method for the Unit 1 pipeway structure and using the equivalent static method for the Unit 2 pipeway structure.

Auxiliary Building

The dynamic time-history analysis of the auxiliary building is performed with a computer program for analysis of a spring and lumped mass model. Two horizontal models and a vertical model, shown in Figure 3.7-13, are used. Each model is fixed at the base (elevation 85 feet). Each horizontal model consists of five lumped masses with two degrees of freedom at each mass point, one translational degree of freedom in the horizontal direction, and one rotational degree of freedom about the vertical axis. The vertical model for HE evaluation consists of five lumped masses with one translational degree of freedom in the vertical direction at each mass point.

The masses are represented as the mass of the slab plus one-half of the walls immediately above and below the slab, with an appropriate live load on each floor to account for the effect of small pieces of equipment, concrete pads for equipment, tanks, pumps, and incidental weight not otherwise considered. Weights of cranes, storage tanks, and other large pieces of equipment are included at the appropriate mass points. Location of the centers of masses and rigidities are calculated to consider torsional modes of vibration. Mass moments of inertia and torsional rigidities are calculated by conventional structural analysis methods.

The soil at elevation 100 feet is represented by soil springs as shown in Figure 3.7-13. The stiffnesses of these foundation springs are derived by considering the case of a rigid plate on a semi-infinite elastic half-space with a horizontal surface (References 2, 3, and 4). The auxiliary building is a broad-based and comparatively low-rise structure, and therefore rocking is insignificant.

For HE evaluation, dynamic time-history analysis of flexible floor slabs is performed using finite element models composed of plate elements. Columns supporting the slabs are represented by springs. In each model, masses of slab, equipment, piping, and other items are concentrated at appropriate nodal points. A typical flexible slab model is shown in Figure 3.7-13A. Input excitation is the vertical acceleration time-history at the slab supports, obtained from the vertical analysis of the auxiliary building model.

Dynamic time-history analysis of the fuel handling area crane support structure is performed using one model to represent six end-bay frames and a second model to represent six middle bay frames. Each model is fixed at its base and uses beam and

DCPP UNITS 1 & 2 FSAR UPDATE

truss elements to represent all significant structural members. Structure masses are concentrated at appropriate nodal points. The model representing the middle bay frames is shown in Figure 3.7-13B. Input excitations are translational and rotational acceleration time-histories at elevation 140 feet obtained from analysis of the auxiliary building model.

Outdoor Water Storage Tanks

The axisymmetric and 3-D SAP IV mathematical models used in the HE finite element analysis are shown in Figures 3.7-14, 3.7-15, 3.7-15A, and 3.7-15B. The axisymmetric model using the AXIDYN computer program is used to analyze the effects of gravity loading, hydrostatic pressure, structure inertial forces, and hydrodynamic loads consisting of impulsive and convective pressures caused by the seismic event. The fluid impulsive effects are modeled as effective fluid inertia masses attached to appropriate concrete elements (see Reference 13). The 3-D SAP IV model is used to assess the effects of the nonaxisymmetric vault opening on the stresses in and around the opening area. The loads determined from dynamic analysis using axisymmetric model are input as static loads in the 3-D SAP IV model. All tanks except the firewater and transfer tank are analyzed as fixed base models.

The exterior tank of the firewater and transfer tank is analyzed as a fixed base, whereas the inner steel tank is pinned at the base in the finite-element analyses.

For horizontal direction, a response spectrum, modal superposition analysis is performed with an axisymmetric model to determine the combined dynamic effects of structure inertial forces and impulsive pressures due to the horizontal earthquake. Gravity, hydrostatic pressure, and convective pressure loads are analyzed statically. The tanks analyzed are refueling water storage tank and firewater and transfer tank. No additional analysis is done for condensate tank since it is similar to refueling water storage tank.

For the SAP IV nonaxisymmetric model, an equivalent, static, lateral load analysis based on accelerations computed from the axisymmetric model analysis is performed for the refueling water storage tank to determine the structure response maxima. The results of this analysis are applicable to other outdoor water storage tanks because they have similar vault openings and are of comparable size. The axisymmetric analyses have shown that responses of these tanks are generally similar to refueling tank.

Since the fundamental period is approximately 0.033 sec in the vertical direction, the empty tanks are determined to be rigid in that direction. Considering the possibility that fluid may not act as a rigid mass during vertical motion, effects of the vertical earthquake are obtained by scaling the results of the analysis for gravity loading and hydrostatic pressure by a factor of 1.0 for the HE ($2/3 \times 0.75 \times$ amplification factor of 2). For the DE and the DDE, HE finite-element analysis results are used as the basis for evaluation. The HE responses are adjusted by the ratio of peak spectral accelerations for the DE, or the DDE, and by appropriate damping ratios.

3.7.2.1.7.2 Turbine Building and Intake Structure

The turbine building and the intake structure are Design Class II. However, Design Class I equipment is located inside: component cooling water (CCW) heat exchangers, 4160V vital switchgear, emergency diesel generators, and other Class I systems in the turbine building, and auxiliary saltwater (ASW) pumps, piping, and instrumentation in the intake structure. In order to provide assurance that the function of Design Class I equipment will not be adversely affected, these structures are reviewed to ensure that they would not collapse in the unlikely event of an HE. The vulnerability of the main turbine steam valves to seismically induced falling debris is reviewed and is described in Section 3.5.

The structural evaluation of the turbine building and intake structure for the HE earthquake was performed using the response spectrum dynamic modal superposition method. In addition, a time-history dynamic analysis is performed to generate DE, DDE, and HE response spectra.

Turbine Building

Turbine building horizontal analyses use one model to represent the Unit 1 portion of the building, which extends from column line 1 to 19, and a second model to represent the Unit 2 portion of the building, which extends from column line 19 to 35. The models are fixed at the base and are composed of truss, beam, and plane stress elements. The Unit 1 horizontal model, shown in Figures 3.7-15C and 3.7-15D, has a total of approximately 500 nodal points and 1000 elements. The Unit 2 horizontal model is similar.

Four models representing different areas of the building are used to represent the building in the vertical direction. The models are fixed at the base and consist of plate, beam, and truss elements. Three of the models are three-dimensional extending the full building height and width, and together represent the building from column lines 1 to 17 and 19 to 35. The fourth model is two-dimensional extending to elevation 140 feet only and represents the building between column lines 17 and 19. The vertical model used to represent the building between lines 1 and 5 and between lines 31 and 35 is shown in Figures 3-7.15E and 3.7-15F. This model has over 500 nodes and over 1100 elements. Additional models are used to represent bridge crane effects. Analyses consider that both the Unit 1 and the Unit 2 bridge cranes may be located in the Unit 1 or the Unit 2 portion of the building with one of the cranes lifting 135 tons.

Structural evaluation of the turbine pedestal for the HE earthquake is performed using the response spectrum dynamic modal superposition method. The possibility of impingement between the turbine building structure and the turbine pedestal is considered in the response calculations, with the assumption that limited local structural damage, such as concrete chipping or spalling, is permissible provided the overall safety of the structures or the Class I equipment is not impaired. Three-dimensional fixed base models are used to evaluate loading of the pedestals in the horizontal and

DCPP UNITS 1 & 2 FSAR UPDATE

vertical directions. The model shown in Figure 3.7-15G represents the Unit 1 turbine pedestal. The Unit 2 model is similar. Pedestal members are modeled as beam elements with rigid joints to account for the stiff zones at beam-column intersections. Pedestal and turbine-generator masses are included at appropriate nodal points. The models each include approximately 270 nodes and 210 elements.

Intake Structure

The seismic analysis of the intake structure was carried out by initially separating the structure into two basic parts: (a) the pump-deck base, consisting of the massive land-side portion of the structure, from elevation -31.5 feet to the -2.1-foot pump-deck level; and (b) the remainder of the structural system. The analysis demonstrated that the massive pump-deck base below the 2.1-foot level would not amplify the ground motion. Hence, the pump-deck base need not be considered in the analysis of the remainder of the structure.

The three-dimensional mathematical model is used for the north-south and east-west/vertical analysis. Figures 3.7-15H and 3.7-15I show a typical finite element model. The model is fixed at the base and uses typical finite-element methods of discretization suitable for the structural system. Floor slabs and walls are modeled as flat-plate elements primarily to capture in-plane behavior. The slabs are shown to be rigid in the vertical direction by a separate simplified analysis. Some thick shear walls near the symmetry plane of the structure in the east-west direction are modeled as three-dimensional solid elements. There are six degrees of freedom for each node - three translational and three rotational degrees of freedom.

For the north-south analysis, the effect of the virtual mass of contained water has been considered by including the total mass of water tributary to the transverse flow straighteners (or piers). This method is considered reasonable because the relatively short distance between piers inhibits the tendency of the water to slosh and thereby reduce its virtual mass. A high-tide condition, with sea level at elevation +3.4 feet (MSL), is assumed for the analysis.

For the east-west/vertical analysis, the effect of water due to an earthquake is considered negligible because it is assumed that the water can flow in and out of the structure and will exert relatively little force on the structure.

Static and dynamic lateral earth pressures on the east wall of the intake structure are considered in the calculation of the in-place shear stress for the east-west walls and roof slabs. The earth pressure influence is combined by SRSS method with the seismic forces.

3.7.2.1.7.3 Design Class I Mechanical Equipment

Reactor Coolant Loop

The RCLs and their support systems are analyzed for seismic loads based on a three-dimensional, multi-mass elastic dynamic model, as discussed in Section 5.2. Table 3.7-24 shows the fundamental mode frequency ranges for RCL primary equipment (steam generator, reactor coolant pump, and reactor pressure vessel). The stress analyses for faulted condition loadings of these components from a Hosgri earthquake are provided in Section 5.2.1.15. The analyses of the reactor internals, fuel elements, control rod drive assemblies, and control rod drives are described in Section 3.7.3.15.

Other Design Class I Mechanical Equipment

Design Class I mechanical equipment is grouped into: (a) equipment purchased directly by PG&E, and (b) equipment supplied by Westinghouse.

(1) Equipment purchased directly by PG&E

Equipment is considered rigid if all natural periods are equal to or less than 0.05 seconds for the DE and the DDE, and 0.03 seconds for the HE. Rigid equipment is designed for the maximum acceleration of the supporting structure at the equipment location. Flexible equipment is analyzed by response spectrum methods. Hydrodynamic analysis of rigid tanks is performed using the methods described in Reference 6. Flexible tanks were analyzed by the methods described in Reference 13.

Load combinations and allowable stresses for Design Class I equipment are given in Section 3.9.

(2) Equipment supplied by Westinghouse Electric Corporation

The seismic response of Design Class I piping and components is determined by response spectrum methods. The system is evaluated for the simultaneous occurrence of one horizontal and the vertical seismic input motions. For each mode, the results for the vertical excitation are added absolutely to the separate results for the north-south or east-west directions. The larger of the two values so determined at each point in the model is considered as the earthquake response. Details of the response spectrum analyses are as follows:

- (a) If a component falls within one of the many categories that has been previously analyzed using a multi-degree-of-freedom model and shown to be relatively rigid, the equipment specification for the component is checked to ensure that the equivalent static g-values specified are larger than the building floor response spectrum

DCPP UNITS 1 & 2 FSAR UPDATE

values and therefore are conservative. Equipment is considered to be rigid relative to the building if its natural frequencies are all greater than 20 cycles per second for the DE and DDE, and 33 cycles per second for HE.

- (b) If the component cannot be categorized as similar to a previously analyzed component that has been shown to be relatively rigid, an analysis is performed as described below.

Design Class I mechanical equipment, including heat exchangers, pumps, tanks, and valves, are analyzed using a multi-degree-of-freedom modal analysis. Appendages, such as motors attached to motor-operated valves, are included in the models. The natural frequencies and normal modes are obtained using analytical techniques developed to solve eigenvalue-eigenvector problems. A response spectrum analysis is then performed using horizontal and vertical umbrella spectra that encompass the appropriate floor response spectra developed from the building time-history analyses.

The simultaneous occurrence of horizontal and vertical motions are included in the analyses. These response spectra are combined with the modal participation factors and the mode shapes to give the structural response for each mode from which the modal stresses are determined. The combined total seismic response is obtained by adding the individual modal responses utilizing the SRSS method.

Under certain conditions, the natural frequency of the equipment is not calculated. Under those conditions, using the appropriate damping value, the peak value of acceleration response curve is used to calculate the inertia forces. This method of calculation is termed the pseudo-dynamic method.

Components and supports of the RCS are designed for the loading combinations given in Section 5.2. Components are designed in complete accordance with the ASME Boiler and Pressure Vessel Code, Section III, Nuclear Vessels, and the USAS Code for Pressure Piping. The allowable stress limits for these components and supports are also given in Section 5.2. The loading combinations and stress limits for other components and supports are given in Section 3.9.

The Hosgri evaluation of the RCS is discussed in Section 5.2. All components and supports of the RCS satisfy criteria demonstrating qualification for the HE.

3.7.2.1.7.4 Design Class I Piping

Criteria

The following criteria determine the type of seismic analysis performed for Design Class I piping:

- (1) 2-1/2 inches in diameter and larger

Seismic analysis is performed by the response spectrum, modal superposition method.

- (2) Less than 2-1/2 inches in diameter

Seismic analysis is performed by the response spectrum modal superposition method for all Unit 2 piping. In Unit 1, piping less than 2-1/2 inches in diameter was analyzed by sampling criteria in which systems representing the worst case configurations or reflecting generic concerns were selected for analysis by the response spectrum modal superposition method. The remainder was qualified by criteria that limit the periods of free vibration to valves that assure only moderate amplification of piping responses.

Model

Three dimensional mathematical models are used in the response spectrum modal superposition analyses. A typical mathematical model is shown in Figure 3.7-26.

Valves and valve operators are included where appropriate in the piping models as eccentric masses. Pipe supports, restraints and equipment having a natural frequency of 20 Hz or greater are modeled as being rigid restraints. Where Design Class II piping connects to Design Class I piping, sufficient Design Class II piping is included in the model to assure qualification of the Design Class I piping and code boundary.

Allowable Stresses

Load combinations and allowable stresses for Design Class I piping are given in Section 3.9.

3.7.2.2 Natural Frequencies and Response Loads

The natural frequencies and seismic response results summarized in the following sections for the major plant structures are representative of the seismic analyses performed for the operating license review (Reference 18), but may not reflect minor changes associated with subsequent plant modifications.

Containment Structure

(1) DE and DDE

The natural periods for all significant modes of the containment structure are listed in Table 3.7-2. The corresponding mode shapes are shown in Figure 3.7-6. The shell forces and moments in a typical element of the model are defined in Figure 3.7-7.

The containment structure seismic analysis provides acceleration time-histories, maximum absolute accelerations, displacements, shell forces and moments, total shears, and total overturning moments. These maximum response values are listed in Tables 3.7-3 through 3.7-8 for the nodal points indicated in Figure 3.7-5.

Acceleration response spectra for the containment are calculated from the acceleration time-histories, and corresponding smooth spectra are prepared. Typical smooth spectra are shown in Figures 3.7-8 through 3.7-12.

(2) HE

The natural periods and significant modes of vibration are listed in Table 3.7-8A. Modes having a period of vibration less than 0.03 sec (frequency greater than 33 Hz) are considered to be insignificant. As shown in Table 3.7-8A three sets of periods are given for the exterior shell:

- (a) Translational mode determined from model of Figure 3.7-5A
- (b) Torsional and translational mode determined from Figure 3.7-5B
- (c) Vertical modes determined from Figure 3.7-5D

Table 3.7-8B gives the horizontal and vertical maximum absolute accelerations and Table 3.7-8C gives the maximum relative horizontal and vertical displacement. Table 3.7-8D gives the maximum shell forces and moments. Tables 3.7-8E and 3.7-8F give the maximum total shear forces, overturning moments, torsional moments, and axial forces for the containment shell.

The horizontal floor response spectra, including the effects of accidental torsion of the structure, at the inside face of the exterior shell are shown in Figures 3.7-12A and 3.7-12B. To develop these spectra, the translational spectra are combined with the torsional spectra from the 5 percent and 7 percent accidental eccentricities.

DCPP UNITS 1 & 2 FSAR UPDATE

The combined translational and torsional spectra are then combined on an SRSS basis with the horizontal component due to the vertical input to yield the spectra shown in Figures 3.7-12A and 3.7-12B.

The vertical floor spectra are shown in Figures 3.7-12C and 3.7-12D. Tables 3.7-8G and 3.7-8H show the accelerations, displacements, stress, and moments for the containment interior structures as a result of the horizontal dynamic analysis.

For the interior structure, the Newmark input generally produces a higher structure response than does the Blume input. Figures 3.7-12E through 3.7-12G show the response spectra for the interior structure at elevation 140 feet, which is the operating floor for the containment. The spectra are for the horizontal, torsional, and vertical response.

For the annulus structural steel frames, a separate vertical dynamic analysis is carried out for each frame as shown in Figures 3.7-12H and 3.7-12I for Units 1 and 2, respectively. Tables 3.7-8I and 3.7-8J list the frequencies and participation factors for frame number 6 which is a typical annulus steel radial frame. After the response spectra are generated in the vertical direction for each radial frame, they are enveloped according to their locations. As shown in Figures 3.7-12H and 3.7-12I, the annulus is divided into the five major sectors (called sector frames) and the response spectra for any sector frame at given elevation are derived from enveloping the response spectra of radial frames located in that sector. Typical enveloped response spectra are shown in Figures 3.7-12J and 3.7-12K. As discussed earlier, the annulus structure does not amplify the horizontal motion of the interior concrete.

Therefore, the horizontal spectra for the concrete interior structures are used for the annulus steel. Table 3.7-8K lists the natural frequencies for horizontal seismic motion. As mentioned in Section 3.7.2.1.7, the first mode frequencies are approximately 20 Hz or higher and, therefore, for the rationale given earlier, the annulus is considered rigid in the horizontal direction.

Containment Polar Crane

Maximum displacements for various nodes for the polar crane are given in Table 3.7-8L. The member forces and bending moments are shown in Tables 3.7-8M and Table 3.7-8N. The typical response spectra are shown in Figures 3.7-12L and 3.7-12M.

Pipeway Structure

The modal analysis indicates that the minimum frequency of the model is 1.6 Hz and there are 100 modes below 33 cps indicating many closely spaced modes. The containment structure and the piping modes are included in the results since a composite model is analyzed as discussed in Section 3.7.2.1.7.1. The mode shapes indicate there are no global structural modes of the pipeway structure itself; instead, there are many local modes.

The input horizontal acceleration time-histories are scaled up by a factor of 1.06 to approximate the accidental eccentricity of masses. Five input cases are considered for the seismic analysis: The Blume horizontal time-history in E-W and N-S direction, the Newmark horizontal time-history in E-W and N-S direction, and the Newmark time-history in the vertical direction. Typical response spectra for pipeway structure are shown in Figures 3.7-12N through 3.7-12S.

Auxiliary Building

The natural periods for all significant modes of the auxiliary building are listed in Tables 3.7-9 through 3.7-11. Frequencies for significant modes of the fuel handling crane support structure are listed in Tables 3.7-11A and 3.7-11B.

Acceleration response spectra for the auxiliary building are calculated from the acceleration time-histories at the mass points and corresponding smooth spectra are developed. Typical spectra are shown in Figures 3.7-16 through 3.7-25 and 3.7-21A through 3.7-21I.

Maximum absolute accelerations, relative displacements, story shears, overturning moments, and torsional moments in the auxiliary building are listed in Tables 3.7-12 through 3.7-23. Maximum absolute accelerations and relative displacements in the fuel handling crane support structure are listed in Tables 3.7-8O and 3.7-8P; the displacements are obtained from static analysis of the detailed model described in Section 3.8.2.4.

Turbine Building

Natural frequencies of vibration in the horizontal direction in all significant modes of the Unit 1 portion of the building, for the condition where two bridge cranes are centered near column line 10.6, are listed on Table 3.7-23A. Corresponding horizontal frequencies for the Unit 2 portion of the building are similar. Natural frequencies of vibration in the vertical direction for all significant modes of the building between column lines 1 and 5 are listed on Table 3.7-23B. Corresponding vertical frequencies for the Unit 2 portion of the building are similar.

DCPP UNITS 1 & 2 FSAR UPDATE

Acceleration response spectra for the turbine building are calculated from acceleration time-histories at the mass points and corresponding smooth spectra are developed. Typical spectra are shown in Figures 3.7-25A through 3.7-25M.

Maximum absolute accelerations and relative displacements in the Unit 1 portion of the building are listed in Tables 3.7-23C and 3.7-23D. Corresponding accelerations and displacements in the Unit 2 end of the building are similar.

Natural periods for all significant modes of the turbine pedestal model are listed in Table 3.7-23E. Maximum relative displacements of the pedestal model are listed in Table 3.7-23F.

Intake Structure

The natural periods and participation factors for all significant modes of the intake structure are listed in Tables 3.7-23G. Acceleration response spectra for the intake structure are calculated from the acceleration time-histories at the selected mass points, and corresponding smooth spectra are developed as specified in Figure 3.7-4A. Typical spectra are shown in Figures 3.7-25N through 3.7-25T. Maximum absolute acceleration, relative maximum displacements are listed in Table 3.7-23H.

Outdoor Water Storage Tanks

The natural periods for significant modes of the refueling water storage tanks and fire water and transfer tank are listed in Tables 3.7-23I and 3.7-23J.

3.7.2.3 Procedures Used to Lump Masses

3.7.2.3.1 Structures

The mass of the structure is assumed to be concentrated at particular locations on the model. These locations coincide with either floor levels, significant points where dynamic response is required as input for piping and equipment, nodal points in the finite element model, or any other points required to accurately define the natural frequencies and mode shapes for the significant modes. The torsional effect for containment, auxiliary building, turbine building, and intake structure is considered as discussed in Section 3.7.2.10.

3.7.2.3.2 Equipment and Piping

The mass of the equipment and piping systems is assumed to be concentrated at particular locations on the model. These locations coincide with either actual masses such as pumps, motors, valve restraints and anchors, or any other points required to accurately define the natural frequencies and mode shapes of the significant modes.

3.7.2.4 Rocking and Translational Response Summary

Methods used to consider soil-structure interaction for Design Class I structures are described in Section 3.7.2.1.7.1.

3.7.2.5 Methods Used to Couple Soil with Seismic-System Structures

The procedures used to represent the containment structure and surrounding rock mass as a finite element model, and the procedures used to derive the stiffnesses of foundation springs for the auxiliary building are described in Section 3.7.2.1.7.1.

3.7.2.6 Development of Floor Response Spectra

Floor response spectra are developed using time-history modal superposition analyses as described in Section 3.7.2.1.7.1.

3.7.2.7 Differential Seismic Movement of Interconnected Components

Components and supports of the RCS are designed for the loading combinations and stress limits given in Section 5.2. The loading combinations and stress limits for other components and supports are given in Section 3.9.

3.7.2.8 Effects of Variations on Floor Response Spectra

Consideration of the effects on floor response spectra of possible variations in the parameters used for the structural analysis is discussed in connection with the development of smooth spectra in Section 3.7.2.1.7.1.

3.7.2.9 Use of Constant Vertical Load Factors

The Design Class I structures are heavy, massive, reinforced concrete, rigid-type structures and are founded on competent hard rock. For such structures, insignificant amplification of vertical motions can be expected, the critical factor in design being the response of the structures to horizontal earthquake motions. The containment structure and auxiliary building including Class I systems and components are designed for DE and DDE, using a vertical static coefficient equal to two-thirds of the peak horizontal ground motion, unless otherwise noted. For the HE, a dynamic analysis in the vertical direction is carried out as discussed in Section 3.7.2.1.7.1.

3.7.2.10 Method Used to Account for Torsional Effects

The containment structure is essentially axisymmetric and therefore has insignificant torsional response. The torsional response of the auxiliary building is calculated by use of a combined translational and torsional mathematical model in the seismic system time-history modal superposition analysis, as described in Section 3.7.2.1.7.1.

For the Hosgri evaluation of Design Class I structures, the effect of accidental torsion is included as an additional eccentricity in the mathematical models. The additional eccentricity is the greater of 5 percent of the building dimension in the direction perpendicular to the applied loads, when torsional and translational effects are

combined together, and the 7 percent of the building dimension in the direction perpendicular to the applied loads, when torsional and translational effects are computed independently and combined by the SRSS method.

For Hosgri evaluation of the Design Class II turbine building, including the turbine pedestal and the intake structure, a torsional response is calculated by the use of finite element models which include both translation and torsion. In addition, the effect of accidental eccentricity is accounted for by a 10 percent increase in the structural responses for the turbine building and intake structure. For the turbine pedestal, a static torsional moment corresponding to a 5 percent eccentricity is added to the dynamic analysis in each horizontal direction.

3.7.2.11 Comparison of Responses

Time-history analyses only are performed for Design Class I structures. Response spectrum analyses are not performed because the time-history produces spectra that represent reasonably the criteria response spectra.

3.7.2.12 Methods for Seismic Analysis of Dams

There are no dams associated with the DCPP.

3.7.2.13 Methods to Determine Design Class I Structure Overturning Moments

The maximum overturning moments for Design Class I structures are determined as part of the time-history modal superposition analyses. Vertical earthquake is considered to act concurrently with the maximum horizontal overturning moments.

3.7.2.14 Analysis Procedure for Damping

Structures are analyzed using modal superposition techniques, and element or material-associated damping ratios are given in Section 3.7.1.3. "Composite" or modal damping ratios in structural systems comprised of different element material types are selected based on an inspection of the significant mode shapes, and on the assumption that the contribution of each material to the composite effective modal damping is proportional to the elastic energy induced in each material. The following criteria and procedures are applied on a-mode-by mode basis to evaluate and conservatively determine composite damping values:

- (1) Where a particular mode primarily indicates response of a single element type, the damping ratio corresponding to that element type is assigned to

that mode. Where all but a negligible amount of the elastic energy is induced in, for example, concrete or rock, the damping ratio appropriate to these materials is applied. Similarly, where a lightly damped material exhibits a major portion of the elastic energy of the mode, a conservative choice is made to use the damping ratio of that material for that mode. In most cases for this plant, the modes are well defined according to material types; composite damping values can be selected on the basis of a visual inspection of mode shapes and no additional numerical computations are required.

- (2) In a few instances, the above criteria cannot be applied because a particular mode indicates response of several element types. The damping ratio for that mode is conservatively estimated based on the degree of participation of the different elements. Table 3.7-10 lists the participation factors for the auxiliary building. The elastic energy induced in the different elements is estimated and the composite damping values assigned in proportion to the elastic energy.
- (3) Mass-weighted composite modal-damping is used for the DE and DDE analysis of the turbine building.

The approach described above is consistent with currently accepted techniques, and in all cases the damping values are selected conservatively. The use of this approach results in design that can conservatively resist the seismic motions postulated for the DCPP.

3.7.2.15 Combination of Components of Earthquake Motion For Structures

For DE and DDE analysis maximum structural response due to one horizontal and the vertical component of earthquake motion are combined by the absolute sum method. For HE analysis the maximum structural responses due to each of the three components of earthquake motion are combined by the SRSS method.

3.7.3 SEISMIC SUBSYSTEM ANALYSIS

3.7.3.1 Determination of Number of Earthquake Cycles

Where fatigue is a criterion, it is assumed that there are 20 occurrences of the DE, each producing 20 cycles of maximum response.

3.7.3.2 Basis for Selection of Forcing Frequencies

Design Class I equipment and piping is analyzed by the response spectrum method or the pseudo-dynamic method, using floor response spectra, unless it can be shown to be rigid, as discussed in Section 3.7.2.1. Accordingly, a special procedure to avoid certain frequencies is not needed.

3.7.3.3 Procedure for Combining Modal Responses

The method and procedure for combining modal responses are described in Sections 3.7.2.1 and 3.7.3.4.

3.7.3.4 Root Mean Square Basis

Closely spaced modes in Design Class I piping are analyzed by the response spectrum modal superposition method where all modal responses are combined by the SRSS method to obtain total response.

A study was conducted to evaluate the effects of combining modes with closely spaced modal frequencies by the absolute sum method. For closely spaced modes, the combined total response was obtained by taking the absolute sum of the closely spaced modes and then taking the SRSS with all other modes. Twenty-nine piping systems were studied, representing approximately 10 percent of the total number of piping systems analyzed. Of these 29 piping systems, 8 systems had no closely spaced frequencies and 8 systems had closely spaced frequencies which were in the rigid period range and therefore required no further study.

The remaining 13 systems had some modal frequencies in the flexible range that could be termed closely spaced. Of these, 5 systems had low seismic stresses with an adequate margin of safety, so that any possible increase in seismic stresses due to a combination of closely spaced frequencies by the absolute sum method would not affect the safety of the piping systems. In addition, 6 systems had closely spaced frequencies, but study of the mode shapes revealed that the seismic stresses would not be significantly affected by the absolute sum of these modal responses.

For the 2 remaining systems, it was not possible to positively conclude that the effects of combining the modes with closely spaced frequencies by absolute sum would be minimal by inspecting the stresses or mode shapes. Therefore, these 2 systems were reanalyzed by computer, and it was found that if the seismic responses of the modes with closely spaced frequencies were combined by the absolute sum method, the increase in stress would be less than 1 percent.

It was therefore concluded that the combination of modal responses of piping systems by the SRSS method is adequate and conservative.

3.7.3.5 Design Criteria and Analytical Procedures for Piping

Stresses induced in Design Class I piping from relative movement of anchor points (points where all degrees of freedom are fixed), whether due to building or equipment movement, are considered with stresses calculated in the piping response spectrum modal superposition analyses.

DCPP UNITS 1 & 2 FSAR UPDATE

PG&E has developed specific guidelines for the design of Class I pipe supports that account for such items as allowable deflections, forces, gaps, and moments imposed on the supports. Allowable stresses and loads are described in more detail in Section 3.9.

A study (Reference 9) has also been performed to evaluate the stresses in piping systems, assuming failure of a single hydraulic or mechanical pipe snubber during a seismic event. Results of the study indicate that the probability of a snubber failing to snub and causing a pipe failure was sufficiently low that no additional design restraints had to be imposed.

As an additional control, hydraulic snubbers are visually inspected and functionally tested. These surveillance requirements are detailed in the DCPP Equipment Control Guidelines (see Chapter 16).

At the request of the NRC in April 18, 1984, in its order to modify Facility Operating License No. DPR-76, PG&E developed a program to review the small and large bore pipe supports for the specific concerns raised by that order.

The specific items requested by the NRC were as follows:

- (1) PG&E shall complete the review of all small-bore piping supports which were reanalyzed and requalified by computer analysis. The review shall include consideration of the additional technical topics, as appropriate, contained in License Condition No. 7 below.
- (2) PG&E shall identify all cases in which rigid supports are placed in close proximity to other rigid supports or anchors. For these cases PG&E shall conduct a program that assures loads shared between these adjacent supports and anchors result in acceptable piping and support stresses. Upon completion of this effort, PG&E shall submit a report to the NRC Staff documenting the results of the program.

Design procedures were revised to address this issue.

- (3) PG&E shall identify all cases in which snubbers are placed in close proximity to rigid supports and anchors. For these cases, utilizing snubber lock-up motion criteria acceptable to the staff, PG&E shall demonstrate that acceptable piping and piping support stresses are met. Upon completion of this effort, PG&E shall submit a report to the NRC Staff documenting the results.

Design procedures were revised to address this issue.

- (4) PG&E shall identify all pipe supports for which thermal gaps have been specifically included in the piping thermal analyses. For these cases the licensee shall develop a program for periodic inservice inspection to

DCPP UNITS 1 & 2 FSAR UPDATE

assure that these thermal gaps are maintained throughout the operating life of the plant. PG&E shall submit to the NRC Staff a report containing the gap-monitoring program.

Rather than establishing a gap-monitoring program, the piping analysis and procedures were modified to eliminate the thermal gaps in the analyses.

- (5) PG&E shall provide to the NRC the procedures and schedules for the hot walkdown of the main steam system piping. PG&E shall document the main steam hot walkdown results in a report to the NRC Staff.
- (6) PG&E shall conduct a review of the "Pipe Support Design Tolerance Clarification" program (PSDTC) and "Diablo Problem" system (DP) activities. The review shall include specific identification of the following:
 - (a) Support changes, which deviated from the defined PSDTC program scope;
 - (b) Any significant deviations between as-built and design configurations stemming from the PSDTC or DP activities; and
 - (c) Any unresolved matters identified by the DP system.

The purpose of this review is to ensure that all design changes and modifications have been resolved and documented in an appropriate manner. Upon completion PG&E shall submit a report to the NRC Staff documenting the results of this review.

- (7) PG&E shall conduct a program to demonstrate that the following technical topics have been adequately addressed in the design of small and large-bore piping supports:
 - (a) Inclusion of warping normal and shear stresses due to torsion in those open sections where warping effects are significant.
 - (b) Resolution of differences between the AISC Code and Bechtel criteria with regard to allowable lengths of unbraced angle sections in bending.
 - (c) Consideration of lateral/torsional buckling under axial loading of angle members.
 - (d) Inclusion of axial and torsional loads due to load eccentricity where appropriate.

DCPP UNITS 1 & 2 FSAR UPDATE

- (e) Correct calculation of pipe support fundamental frequency by Rayleigh's method.
- (f) Consideration of flare bevel weld effective throat thickness as used on structural steel tubing with an outside radius of less than $2T$.

The above considerations were incorporated in the applicable design procedures.

All of the above specific concerns were addressed and resolved to the satisfaction of the NRC.

3.7.3.6 Basis for Computing Combined Response

As a minimum, mechanical equipment is designed for a vertical static coefficient equal to $2/3$ of the peak horizontal ground motion for DE and DDE analysis. For HE analysis, specific vertical floor response spectra are used. Horizontal and vertical responses are combined by absolute sum.

Equipment is reviewed for a vertical force determined from a response spectrum, as described in Section 3.7.2.1.7.3, 3.7.3.15, and 5.2.

The horizontal and vertical responses of Design Class I piping are determined from the two-dimensional response spectrum modal superposition analyses described in Section 3.7.2.1.7.4. Response spectra at the applicable piping support attachment elevations are enveloped to obtain the final design response spectra. The vertical and one horizontal response are combined by absolute sum on the modal level. Modal responses are combined by the SSRS method. The two two-dimensional results are then enveloped to obtain the total response. Figure 3.7-26 shows a typical piping mathematical model. Figure 3.7-29 illustrates the derivation of the design response spectra for a typical piping system.

In many cases, earthquake piping stresses due to DDE are not directly calculated. Instead, the results from the DE piping analysis are doubled to represent the DDE. This approach was chosen because review of the design spectra showed that the DDE accelerations did not exceed twice the DE accelerations. Since pipe stress is linear with accelerations, this approach is conservative.

3.7.3.7 Amplified Seismic Responses

Components that can be adequately characterized as a single-degree-of-freedom system are considered to have a modal participation of one.

3.7.3.8 Use of Simplified Dynamic Analysis

All methods of seismic analysis used for Design Class I structures, components, systems, and piping are described in Section 3.7.2.

Two methods of dynamic seismic analysis are used for Design Class I components and piping that are different than multiple-degree-of-freedom, modal analysis methods. The first of these is the response spectrum, single-degree-of-freedom method used for components whose dynamic behavior can be accurately represented by a single-degree-of-freedom mathematical model. The second of these is the method for rigid components where the component is designed for the maximum acceleration experienced by the supporting structure at the location of support, if all natural periods of the component are less than, or equal to, 0.05 seconds (33 Hz for HE in piping analysis).

The pseudo-dynamic method of analysis is used for certain items of mechanical equipment as described in Section 3.7.2. The basis for this method is described in Section 3.7.2.1.7.3.

Certain Unit 1 Design Class I piping less than 2-1/2 inches in diameter is restrained according to criteria described in Section 3.7.2.1.7.4.

3.7.3.9 Modal Period Variation

Consideration of the effects on floor response spectra of possible variations in the parameters used for structural analysis is discussed in connection with the development of smooth spectra in Section 3.7.2.1.7.1.

3.7.3.10 Torsional Effects of Eccentric Masses

Where appropriate, valves and valve operators are included as eccentric masses in the mathematical models for piping seismic analysis, as described in Section 3.7.2.1.7.4.

3.7.3.11 Piping Outside Containment Structure

The procedures used to determine piping stresses resulting from relative movement between anchor points (points where all degrees-of-freedom are fixed) are discussed in Section 3.7.3.5. The forces exerted by piping on anchor points, including the containment structure penetrations, are included in the evaluation of stresses for Design Class I structures.

Buried Design Class I piping is confined by sand backfill in rock trenches. The piping material is ASTM A-53 or A-106 carbon steel.

3.7.3.12 Interaction of Other Piping With Design Class I Piping

Mathematical models for Design Class I piping seismic analyses normally originate and terminate at anchor points. Where Design Class II piping connects to Design Class I piping sufficient Design Class II piping is included in the mathematical model to assure qualification of the Design Class I piping and code boundary.

3.7.3.13 System Interaction Program

PG&E developed a program to consider seismically-induced physical interactions between nonsafety-related SSCs and Design Class I SSCs. The methodology and results of this interaction study are presented in Reference 10 and are summarized as follows. The objective of the program was to establish confidence that when subjected to seismic events of severity up to and including the HE, SSCs important to safety shall not be prevented from performing their intended safety functions as a result of physical interactions caused by seismically induced failures of nonsafety-related SSCs. In addition, safety-related SSCs shall not lose the redundancy required to compensate for single failures as a result of such interactions.

To accomplish the program, PG&E defined as targets all SSCs required to safely shut down the plant and maintain it in a safe shutdown condition, and certain accident-mitigating systems. Initial plant operating modes of normal operation, shutdown, and refueling were considered in the selection of the target equipment. All nonsafety-related SSCs were defined as sources.

Interactions between source and target equipment were postulated by an interdisciplinary Interaction Team. The Interaction Team postulated interactions during walkdowns of the target equipment, using previously established guidelines and criteria. The Interaction Team also recommended resolutions to the postulated interactions. The findings of the Interaction Team were evaluated during a subsequent office-based technical evaluation. Any modifications deemed necessary were reviewed after completion by the Interaction Team to ensure that no new interactions were created by the modifications themselves.

The program was subjected to an independent audit by PG&E's Quality Assurance Department and a review by an Independent Review Board which reported its findings to a managing consultant who, in turn, reported his findings to PG&E management.

3.7.3.14 Field Location of Supports and Restraints

Seismic supports and restraining devices for Design Class I piping are located as follows:

3.7.3.14.1 Two Inches in Diameter and Less

Field-routed and vendor-furnished piping 2 inches and less in diameter is supported by the piping installation contractor's field personnel in accordance with criteria supplied by PG&E's engineering staff on Approved for Construction drawings. These criteria specify size, type, spacing, and permissible locations for seismic supports and restraining devices. Prior to initial fuel loading, the completed installation of this piping was reviewed by an experienced piping engineer from PG&E's engineering staff to ensure compliance with the criteria and the observance of good design practice.

3.7.3.14.2 Larger Than 2 Inches in Diameter

The size, type, and location of each support or restraining device on each line is shown on Approved for Construction drawings.

The procedures followed during development of the Approved for Construction drawings provide assurance that the field location and the seismic design of supports and restraining devices are consistent with the assumptions made in the seismic analysis. These procedures are:

- (1) The locations of supports and restraining devices are established on preliminary drawings.
- (2) The locations shown on the preliminary drawings are used to develop the mathematical model for the seismic analysis, and the seismic analysis is performed. If the results show piping stresses higher than allowable, adjustments are made in the location, and/or the type of support or restraining device, and the seismic analysis is repeated.
- (3) The reactions calculated as part of the seismic analysis, combined with other loads, are used for final design of piping supports and restraining devices.
- (4) When the design is complete, drawings are issued as Approved for Construction to the piping installation contractor. Installation of supports and restraining devices is in accordance with Approved for Construction drawings.

3.7.3.15 Seismic Analyses for Fuel Elements, Control Rod Assemblies, and Control Rod Drives

3.7.3.15.1 Reactor Vessel Internals Evaluation - DE, DDE, and HE

Nonlinear dynamic seismic analysis of the reactor pressure vessel (RPV) system includes the development of the system finite element model and the synthesized time

history accelerations. Both of these developments for the seismic time history analysis are discussed below.

The basic mathematical model for seismic analysis is essentially similar to a LOCA model in that the seismic model includes the hydrodynamic mass matrices in the vessel/barrel downcomer annulus to account for the fluid-solid interactions. On the other hand, the fluid-solid interactions in the LOCA analysis are accounted through the hydraulic forcing functions generated by Multiflex Code (Reference 3). Another difference between the LOCA and seismic models is the difference in loop stiffness matrices. The seismic model uses the unbroken loop stiffness matrix, whereas the LOCA model uses the broken loop stiffness matrix. Except for these two differences, the RPV system seismic model is identical to that of LOCA model.

The RPV system finite element model for the nonlinear time history dynamic analysis consists of three concentric structural sub-models connected by nonlinear impact elements and linear stiffness matrices. The first sub-model, shown in Figure 3.7-27A, represents the reactor vessel shell and its associated components. The reactor vessel is restrained by four reactor vessel supports (situated beneath alternate nozzles) and by the attached primary coolant piping. Also shown in Figure 3.7-27A is a typical RPV support mechanism.

The second sub-model, shown in Figure 3.7-27B, represents the reactor core barrel, thermal shield, lower support plate, tie plates, and the secondary support components for Unit 1 (PGE); whereas, for Unit 2 (PEG) the second sub-model is shown in Figure 3.7-27C (core barrel with neutron pads instead of thermal shield).

These sub-models are physically located inside the first, and are connected to them by stiffness matrices at the vessel/internals interfaces. Core barrel to reactor vessel shell impact is represented by nonlinear elements at the core barrel flange, upper support plate flange, core barrel outlet nozzles, and the lower radial restraints.

The third and innermost sub-model, shown in Figure 3.7-27D, represents the upper support plate assembly consisting of guide tubes, upper support columns, upper and lower core plates, and the fuel. The fuel assembly simplified structural model incorporated into the RPV system model preserves the dynamic characteristics of the entire core. For each type of fuel design the corresponding simplified fuel assembly model is incorporated into the system model. The third sub-model is connected to the first and second by stiffness matrices and nonlinear elements.

As mentioned earlier, fluid-structure or hydroelastic interaction is included in the reactor pressure vessel model for seismic evaluations. The horizontal hydroelastic interaction is significant in the cylindrical fluid flow region between the core barrel and the reactor vessel annulus. Mass matrices with off-diagonal terms (horizontal degrees-of-freedom only) attach between nodes on the core barrel, thermal shield and the reactor vessel. The mass matrices for the hydroelastic interactions of two concentric cylinders are developed using the work of Reference 36. The diagonal terms of the mass matrix are

DCPP UNITS 1 & 2 FSAR UPDATE

similar to the lumping of water mass to the vessel shell, thermal shield, and core barrel. The off-diagonal terms reflect the fact that all the water mass does not participate when there is no relative motion of the vessel and core barrel. It should be pointed out that the hydrodynamic mass matrix has no artificial virtual mass effect and is derived in a straight-forward, quantitative manner.

The matrices are a function of the properties of two cylinders with the fluid in the cylindrical annulus, specifically, inside and outside radius of the annulus, density of the fluid, and length of the cylinders. Vertical segmentation of the reactor vessel and the core barrel allows inclusion of radii variations along their heights and approximates the effects beam mode deformation. These mass matrices were inserted between the selected nodes on the core barrel, thermal shield, and the reactor vessel as shown in Figure 3.7-27E.

The seismic evaluations are performed by including the effects of simultaneous application of time history accelerations in three orthogonal directions. For the DE, DDE and HE, the Westinghouse generated synthesized time history accelerations at the reactor vessel support were used. The detailed seismic analyses results of the RPV system are documented in Reference 34.

The WECAN computer code, which is used to determine the response of the reactor vessel and its internals, is a general-purpose finite element code. In the finite element approach, the structure is divided into a finite number of discrete members or elements. The inertia and stiffness matrices, as well as the force array, are first calculated for each element in the local coordinates. Employing appropriate transformations, the element global matrices and arrays are assembled into global structural matrices and arrays, and used for dynamic solution of the system equations.

The results of the nonlinear seismic dynamic analyses include the transient displacements and impact loads for various elements of the mathematical model. These displacements, impact loads, and linear component loads (forces and moments) are then used by cognizant organizations for detailed component evaluations to assess the structure of the reactor vessel, reactor internals, and the fuel. Note that the linear component forces and moments are not the direct output from the modal superposition analysis but rather are obtained by post-processing the data saved from the nonlinear time history analysis.

From the modal analysis (free vibration analysis), the system eigenvalues and eigenvectors are stored on a magnetic tape to be used later in the modal superposition analysis. The validity of a complex system structural model is generally verified by comparing the calculated fundamental frequency of the system with the available test data frequency. The fundamental core barrel frequency of a four-loop thermal shield core barrel is known from test data to be approximately 6.6 to 7.0 Hz. The results of Diablo Canyon Unit 1 modal analysis show that the core barrel fundamental beam mode frequency is close to 7.0 Hz, thereby verifying the applicability of the system model for the desired analysis.

Note that the preceding paragraphs describe RPV and internals system dynamic analyses for which the WECAN computer code was used. Current analyses (such as the dynamic analyses performed in support of the replacement vessel head project) utilize the ANSYS computer code. The methodology used to develop the ANSYS system models is consistent with the methodology used to develop historic WECAN models. The direct time integration method is used in ANSYS to solve the dynamic equations of motion for the system; whereas the nonlinear mode superposition method is used in WECAN to solve the dynamic equations of motion for the system.

3.7.3.15.2 Fuel Assembly Evaluation

The fuel assembly design adequacy under DDE and HE conditions was assessed through a combination of mechanical tests and analyses. The information obtained from the fuel assembly and component structural tests provided the fundamental mechanical constants for the finite element model used in the fuel analysis.

The analysis of the fuel is performed in two steps. The first step involves analysis of the detailed reactor core model, which includes the reactor vessel, internals, and a simplified model of the fuel (Figures 3.7-27A thru 3.7-27E). This dynamic analysis uses seismic time history motion at the reactor vessel support elevation (Elevation 102 ft.). The second step of the fuel analysis involves running a detailed fuel assembly model using the WEGAP code. This detailed model (Figure 3.7-27F) conservatively represents an entire row of full-length fuel assemblies (15 total).

The fuel assembly model consists of a series of beam elements with torsional springs located at the various fuel assembly grid elevations to simulate the fuel assembly dynamic characteristics. The values of the mechanical constants such as the rigidity modulus and the torsional stiffness were selected to accurately represent the experimentally determined fuel assembly modal stiffness and natural frequencies.

The time history motion for the upper and lower core plates and core barrel are simultaneously applied to the simulated fuel assembly model as illustrated in Figure 3.7-27F. These input motions were obtained from the time history analysis of the reactor vessel and internals finite element model.

The maximum grid impact forces and the fuel assembly maximum deflection are determined with the reactor core model.

Because of the basic fuel assembly design configuration, the assembly impacting is restricted to the grid locations. The seismic and LOCA loads at each grid were combined using the SRSS method to obtain the design maximum loads. These loads are compared with the allowable grid load, which is determined based on the test data using 95 percent confidence level on the true mean criteria. The results of the Unit 1 and Unit 2 evaluations indicated the possibility of some deformation of fuel grids at a small number of specific locations. An analysis of the effects of this grid deformation has shown the core geometry will remain coolable (Reference 29). Note that with the

acceptance of the DCPP leak-before-break analysis by the NRC, dynamic LOCA loads resulting from pipe rupture events in the main reactor coolant loop piping no longer have to be considered in the design basis structural analyses and included in the loading combinations (see Section 3.6.2.1.1.1). Only the much smaller LOCA loads from RCS branch line breaks have to be considered.

3.7.3.15.3 Control Rod Drive Mechanism Evaluation

The replacement CRDMs were evaluated using a combination of linear and nonlinear finite element models which included the CRDM housings, RPV head adapters, and the integrated head assembly. The following models and analysis methods were employed for the specified earthquakes:

- (1) DE and DDE: The horizontal analyses for the DE and DDE were based on a nonlinear model. The horizontal DE and DDE acceleration time-histories at the seismic plate elevation and the reactor vessel support elevation were used as inputs to the model. The vertical analyses for the DE and DDE were based on a linear model. The vertical DE and DDE response spectra at the reactor vessel head elevation were used as input to the model.
- (2) HE: The horizontal and vertical analyses for the HE were based on a linear model. The horizontal and vertical HE response spectra at the seismic plate elevation and the reactor vessel head elevation were used as input to the model.

3.7.3.15.4 CRDM Support System Evaluation

The integrated head assembly CRDM seismic support structure, tie rods, and head lifting legs were evaluated using linear elastic 3-D finite element models of the support system. Tension-only capability of the tie rods was modeled. The loading from the CRDMs was addressed through the inclusion of a simplified representation of the pressure housings, including the appropriate lumped masses.

In general, the qualification was based on the response spectrum superposition method using the envelope of the spectra at the 140 foot elevation of the containment interior concrete (attachment point for the tie rods for the tie rods to the reactor cavity walls) and on the reactor vessel lifting lugs and pads (attachment point for the integrated head assembly ring beam to the head) for the DE, DDE, HE, and LOCA load cases. These analyses were supplemented with the time history modal superposition method for the determination of DDE loads for selected connections.

3.7.4 SEISMIC INSTRUMENTATION PROGRAM

3.7.4.1 Comparison With NRC Regulatory Guide 1.12, Revision 2

The seismic instrumentation consists of strong motion triaxial accelerometers that sense and record ground motions. This instrumentation meets the intent of RG 1.12, Revision 2. Enhancements to the seismic instrumentation have been made to improve the system effectiveness. The enhancements include supplemental accelerometers and rapid processing of the ground motion data. The enhancements exceed the intent of RG 1.12, Revision 2, and are not considered part of the licensing basis.

3.7.4.2 Location and Description of Instrumentation

Seismic instrumentation is provided in accordance with RG 1.12, Revision 2, paragraph 1.2. All instruments are rigidly mounted so their records can be related to movement of the structures and ground motion. All are accessible for periodic servicing and for obtaining readings.

3.7.4.2.1 Strong Motion Triaxial Accelerometers

Strong motion triaxial accelerometers provide time-histories of acceleration for each of three orthogonal directions. These histories are recorded in the accelerometer housings. The instruments start recording upon actuation of a seismic trigger which has an adjustable threshold. Six strong motion triaxial accelerometers are provided in accordance with RG 1.12, Revision 2, paragraph 1.2. Supplemental accelerometers provide ground motion data beyond the regulatory guidance and are not part of the licensing commitment,

3.7.4.3 Control Room Operator Notification

Operation of the strong motion triaxial accelerometers (ESTA01 or ESTA28) will activate an annunciator in the control room and provide indications on the earthquake force monitor (EFM) in the RSI panel. The EFM will display the acceleration levels for all areas of both the Unit 1 containment base sensor (ESTA01) and the free field sensor (ESTA28). For the Emergency Plan event classification, it also provides a status of level exceedance for any axis on both sensors within a few minutes. The setpoint thresholds are set in accordance with Emergency Plan Action Levels. .

3.7.4.4 Comparison of Measured and Predicted Responses

In the event of an earthquake that produces significant ground motions, all seismic instruments are read and the readings compared to the corresponding design values. This comparison, together with information provided by other plant instrumentation and an inspection of safety-related systems, forms the basis for a judgment on severity, level, and the effects of the earthquake.

3.7.5 SEISMIC DESIGN CONTROL

3.7.5.1 Equipment Purchased Directly by PG&E

The position of PG&E's engineering staff in the corporate structure is shown in Figures 17.1-1 and 17.1-2. The procedures for specifying technical and quality assurance requirements in purchase orders and specifications are included in Sections 17.4, 17.5, and 17.8.

The seismic design requirements developed from the structure seismic system analysis are included in the purchase order or specification for Design Class I equipment. The purchase order or specification requires that the manufacturer submit seismic qualification data of the equipment to be furnished, for review by the responsible PG&E engineer. The procurement is approved only when all seismic design criteria are met.

3.7.5.2 Equipment Supplied by Westinghouse

The following procedure is implemented for Design Class I mechanical equipment that falls within one of the many categories analyzed as described in Section 3.7.2 and shown to be rigid (frequency > 33 Hz).

- (1) Equivalent static acceleration factors for the horizontal and vertical directions must be checked against those in the Design Criteria Memoranda (DCM). Westinghouse must certify the adequacy of the equipment to meet the seismic requirements as described in Section 3.7.2 for DE, DDE, and HE.
- (2) Westinghouse must check to ensure that the given equivalent static acceleration factors are less than or equivalent to those given in the equipment analysis.
- (3) Westinghouse must perform the necessary reanalysis to the procedures and criteria presented herein for those cases, where required, due to revised DE, DDE, and HE seismic response spectra.

All other Design Class I equipment must be analyzed or tested as described in Sections 3.7.2 and 3.10.

Design control measures and design documentation for all Design Class I SSCs are in accordance with formalized quality assurance procedures. These procedures are presented in Chapter 17, Quality Assurance.

3.7.6 SEISMIC EVALUATION TO DEMONSTRATE COMPLIANCE WITH THE HOSGRI EARTHQUAKE REQUIREMENTS UTILIZING A DEDICATED SHUTDOWN FLOWPATH

3.7.6.1 Post-Hosgri Shutdown Requirements and Assumed Conditions

In response to a request from the NRC, PG&E evaluated the ability of DCPP to shut down following the occurrence of a 7.5M earthquake due to a seismic event on the Hosgri fault. This evaluation is presented in Reference 15, which was amended several times after it was first issued in order to respond to questions by the NRC and reflect agreements made at meetings with the NRC. The final document describes the method proposed by PG&E to shut down the plant after the earthquake, assuming a loss of all offsite power, but no concurrent accident, using only equipment qualified to remain operable following such an earthquake.

For this purpose, valves that are required to operate to achieve shutdown following the earthquake were qualified for active function to the Hosgri parameters, whereas other valves, which might have an active function for postaccident mitigation, but were not required to operate to achieve shutdown following the earthquake, were qualified for passive function (pressure boundary integrity) to the Hosgri parameters. This is consistent with the DCPP design basis stated in FSAR Section 3.7.1.1 that the DDE is the SSE for DCPP, and that the guidelines presented in RG 1.29 apply to the DDE.

In addition, pursuant to the NRC request, it was necessary to demonstrate that DCPP could be shut down following an HE in order to protect the health and safety of the public. The Hosgri evaluation presented in Reference 15 demonstrated this. To provide increased conservatism, PG&E has subsequently qualified all active valves for active function for an HE pursuant to a commitment made in Reference 17.

3.7.6.2 Post-Hosgri Safe Shutdown Flowpath

The flowpath qualified to enable shutdown of the plant following an HE is defined in Chapter 5 of Reference 15. For this purpose, safe shutdown was defined as cold shutdown. It assumes concurrent loss of offsite power, a single active failure, but no concurrent accident or fire. Local manual operation of equipment from outside the control room is acceptable for taking the plant from hot standby to cold shutdown.

3.7.6.2.1 Hot Standby

Hot standby is achieved by feeding the steam generators using the auxiliary feedwater system and by release of steam to the atmosphere through the 10 percent steam dump valves. Although other long term cooling water sources may be available, only the seismically qualified condensate storage tank and firewater storage tank are assumed to be available.

3.7.6.2.2 Cold Shutdown

Cold shutdown is achieved by use of the normal charging system flow path. Depressurization is performed using auxiliary spray (alternatively, the PORVs may be used). Boration to cold shutdown concentration is accomplished using boric acid from the boric acid storage tanks via the emergency borate valve 8104 and using a centrifugal charging pump (CCP1 or CCP2) charging through valves FCV-128, HCV-142, 8108, 8107, and 8146 or 8147. Sampling capability to verify boron concentration is available. While reactor coolant pump seal injection flow would be available, the seal water return flow path and the normal letdown flow path are assumed not to be available. Calculations have shown that even with letdown unavailable, by taking credit for shrinkage of the reactor coolant during cooldown, sufficient volume is available in the reactor coolant system to borate to cold shutdown using 4 percent boric acid.

Once the RCS is less than or equal to 390 psig and 350°F, the normal RHR system is placed into service, along with the portions of the component cooling water and auxiliary salt water systems which support RHR operation.

3.7.6.2.3 Single Active Failure

Systems and components used to perform the post-Hosgri shutdown described above have redundant counterparts except for components along the normal charging flowpath, which lacks redundancy since its redundant flow path for emergency boration is the high pressure safety injection flow path. Use of that redundant flow path is not postulated for post-Hosgri shutdown, however, so adequate redundancy had to be incorporated into the normal charging flowpath to enable cold shutdown following the HE. For this purpose, the Hosgri evaluation assumed that manual bypass valves 8387B or 8387C would be used in the event that fail-open valve FCV-128 was to fail closed. Manual bypass valve 8403 would be used in the event that fail-closed valve HCV-142 was to fail closed. Fail-open valve FCV-110A and manual bypass valve 8471 would be used in the event that motor-operated valve 8104 was to fail closed. Valves 8146 and 8147 were assumed redundant for normal charging, and valves 8145 and 8148 were assumed redundant for pressurizer auxiliary spray. Valves with pneumatic operators, which are required to operate to achieve shutdown, were fitted with seismically qualified air or nitrogen accumulators to enable their operation in spite of the loss of their instrument air or nitrogen supply. Although some of these valves do not have safety-related operators since they are not required for accident mitigation, they are seismically qualified to ensure their operability for post-Hosgri shutdown.

3.7.6.2.4 Equipment Required for Post-Hosgri Shutdown

The equipment determined to be required to achieve post-Hosgri cold shutdown in the manner described above is presented in Sections 7.3 and 9.2 of Reference 15. Some minor revisions to the list of valves required have been made, and are reflected in the latest revision of the active valve list, FSAR Table 3.9-9. Instrument Class IA,

DCPP UNITS 1 & 2 FSAR UPDATE

Instrument Class IB, Category 1, and on a case-by-case basis, Instrument Class ID instrumentation are qualified to the Hosgri parameters, and assumed to be operable following an HE. Additional instrumentation determined to be required is presented in Section 7.3 of Reference 15. Some revisions have been made to that list; the revised list of required instrumentation is presented in Reference 16. The electrical Class 1E system is also qualified to the Hosgri parameters, and is assumed to be operable following an HE.

3.7.7 REFERENCES

1. Deleted in Revision 4.
2. Lawrence Livermore Laboratory, Soil-Structure Interaction: The Status of Current Analysis Methods and Research, NUREG/CR-1780, January 1981. (Section by J. M. Roesset.)
3. J. E. Luco, Independence Functions for a Rigid Foundation on a Layered Medium, Nuclear Engineering and Design, Vol. 31, 1974.
4. R. V. Whitman and F. E. Richardt, Design Procedures for Dynamically Loaded Foundations, Journal of Soil Mechanics and Foundations Division, SM6, Nov. 1967.
5. G. Bohm, Seismic Analysis of Reactor Internals for Pressurized Water Reactors, First National Congress of Pressure Vessel and Piping Technology, ASME Panel on Seismic Analysis & Design of Pressure Vessel and Piping Components, San Francisco, May 10-12, 1971.
6. U.S. Atomic Energy Commission (Division of Reactor Development) Publication TID - 7024, Nuclear Reactors and Earthquakes.
7. Appendix A to 10 CFR 100, Seismic and Geologic Siting Criteria for Nuclear Power Plants.
8. Damping Values of Nuclear Power Plant Components, WCAP-7921-AR, May 1974.
9. Stress Evaluation of Piping Systems Assuming Single Snubber Failures, Letter dated January 24, 1978, from P.A. Crane (PG&E) to J.F. Stolz (NRC).
10. Description of the Systems Interaction Program for Seismically Induced Events, Revision 4, August 29, 1980.
11. Answer to the NRC Staff Questions on the Westinghouse Evaluation of the Effect of Grid Deformation on ECCS Performance, transmitted via letter May 11, 1978, P.A. Crane to J.F. Stolz.

DCPP UNITS 1 & 2 FSAR UPDATE

12. Supplement No. 5 to the Safety Evaluation of the Diablo Canyon Nuclear Power Station, Units 1 and 2, Nuclear Regulatory Commission, Division of Reactor Licensing, Washington, DC, September 1976.
13. "Dynamics of Fixed-Base Liquid Storage Tanks," Veletsos, A.S. and T.Y. Yang; Proceedings of U.S.-Japan Seminar on Earthquake Engineering Research with Emphasis on Lifeline Systems, Tokyo, November 1976.
14. Westinghouse 1981 ECCS Evaluation Model Using the BASH Code, WCAP-10266-P-A, Rev. 2, March 1987.
15. Seismic Evaluation for Postulated 7.5M Hosgri Earthquake, DCPP Units 1&2, PG&E.
16. PG&E Design Change Package N-47546.
17. PG&E Letter to the NRC, DCL-92-198 (LER 1-92-015).
18. Phase I Final Report - Design Verification Program, Diablo Canyon Power Plant, Revision 14, transmitted via letter dated October 14, 1983, J. O. Schuyler (PG&E) to D. G. Eisenhut (NRC).
19. Final Report of the Diablo Canyon Long Term Seismic Program, July 1988, PG&E.
20. Addendum to the 1988 Final Report of the Diablo Canyon Long Term Seismic Program, February 1991, PG&E.
21. NUREG-0675, Supplement Number 34, Safety Evaluation Report Related to the Operation of Diablo Canyon Nuclear Power Plant, Units 1 and 2, NRC, June 1991.
22. NRC letter to PG&E, "Transmittal of Safety Evaluation Closing Out Diablo Canyon Long-Term Seismic Program," April 17, 1992.
23. PG&E letter to the NRC, "Long Term Seismic Program - Future Plant Modifications," DCL-91-178, July 16, 1991.
24. Supplement No. 7 to the Safety Evaluation of the Diablo Canyon Nuclear Power Station, Units 1 and 2, Nuclear Regulatory Commission, Division of Reactor Licensing, Washington, DC, May 1978.
25. Supplement No. 8 to the Safety Evaluation of the Diablo Canyon Nuclear Power Station, Units 1 and 2, Nuclear Regulatory Commission, Division of Reactor Licensing, Washington, DC, November 1978.

DCPP UNITS 1 & 2 FSAR UPDATE

26. Damping Values for Seismic Design of Nuclear Power Plants, Regulatory Guide 1.61, USAEC, October 1973.
27. PG&E Licensing Basis Impact Evaluation 2005-03, "Replacement Steam Generator Seismic Damping Values," May 25, 2005.
28. Deleted in Revision 20
29. WCAP-16946-P, Revision 2, Diablo Canyon Vessel Closure Head and Integrated Head Assembly Project - Impact of IHA on Reactor Vessel, Internals, Fuel, and Loop Piping, September 2010.
30. PG&E Document 6023227-19, "Damping Values for Use in the Integrated Head Assembly Seismic Response Analysis at Diablo Canyon Power Plant (DCPP) Units 1 and 2."
31. Damping Values for Seismic Design of Nuclear Power Plants, Regulatory Guide 1.61, Revision 1, USNRC.
32. License Amendment Nos. 208 (DPR-80) and 210 (DPR-82), "Damping Values for the Seismic Design and Analysis of the Reactor Vessel Integrated Head Assembly," USNRC, September 29, 2010.
33. License Amendment Nos. 207 (DPR-80) and 209 (DPR-82), "Critical Damping Values for Control Rod Drive Mechanism Pressure Housings," USNRC, July 30, 2010
34. Bhandari, D. R., et al., System Dynamic Seismic and LOCA Analyses of Reactor Pressure Vessel System for the Pacific Gas and Electric Company Diablo Canyon Power Plants (DCPP) Units 1 & 2, WCAP-14693, Revision 1, February 11, 1997 (Westinghouse Proprietary Class 2).
35. Deleted in Revision 21
36. Fritz, R. J., The Effects of Liquids on the Dynamic Motions of Immersed Solids, Trans. ASME, Journal of Engineering for Industry, 1972, pp. 167-173.
37. PG&E Calculation No. 2252 C-2 (SAP Calc. No. 9000041232), "Polar Crane ANSR Analyses Results and Spectra Generation for DE, DDE, & HE Cases."
38. PG&E Calculation No. 2252 C-3 (SAP Calc. No. 9000041233), "Seismic Evaluation of the Unit 1 Containment Polar Crane Design for 1R17 Modifications and Added Mass."
39. PG&E Calculation No. 2252C-4 (SAP Calc. No. 9000041234), "U2 Polar Crane ANSR Analyses Results & Spectra Gen for DE, DDE & HE Cases."

3.10 SEISMIC DESIGN OF DESIGN CLASS I INSTRUMENTATION, HVAC, AND ELECTRICAL EQUIPMENT

3.10.1 SEISMIC DESIGN CRITERIA

The Design Class I instrumentation, HVAC, and electrical equipment are capable of performing their nuclear safety functions during and after a DDE or the postulated 7.5M HE. The seismic levels for DDE and HE are given in Section 3.7. Instrument Class IA instrumentation is capable of performing its active nuclear safety functions during and after a DDE or HE. Instrument Class IB Category 1 instrumentation is capable of performing its active nuclear safety functions after a DDE or HE. Other Design Class I instrumentation is capable of performing the passive function of maintaining Class I pressure boundary integrity during and after a DDE or HE. In addition, some of the Design Class I instrumentation may have active seismic qualification; these instruments are identified on a case-by-case basis.

Performance criteria for Design Class I instrumentation, HVAC, and electrical equipment are as follows: (a) The reactor protection system shall be able to shut down the unit and maintain it in safe shutdown condition. (b) The electrical equipment is able to perform its required functions of providing electrical power, control, instrumentation, and protection for the ESF. (c) No device shall fail to initiate and maintain its safety function, nor shall it prevent other safety devices from performing their safety function.

The original seismic qualification of most equipment was done in accordance with IEEE 344-1971 (Reference 1) for DDE levels. As a result of changes in spectra the Design Class I equipment has been reevaluated, based on response spectra derived from the HE as well as the DDE levels discussed in Section 3.7. In the process of reevaluation, some equipment had to be requalified because: (a) its previous qualification was not adequate to envelop the HE input, or (b) concerns had been raised about the adequacy of the justification for the previous qualification methods. Requalification of the equipment, according to the guidance contained in IEEE Standard 344-1975 (Reference 2) and NRC RG 1.100 (Reference 3) was performed where necessary.

Tables 3.10-1 and 3.10-2 list instrumentation and electrical equipment that have been seismically qualified. The tables provide references to appropriate sections where qualification is described. Table 3.10-3 lists HVAC equipment that has been seismically qualified.

The seismic qualification of the equipment is based on the free-field ground motions described in Section 3.7.1. Effects of amplification of ground accelerations due to the response of the building at the location of the equipment were derived from the time-history modal superposition analyses made for the structures, as described in Section 3.7.

In addition to direct seismic effects on Design Class I equipment, PG&E has also given consideration to possible seismically induced physical interactions between nonsafety-related SSCs and Design Class I SSCs. The methodology and results of this interaction study are presented in Reference 4, and are provided in summary form in Section 3.7.3.13. Appropriate design modifications were performed where the study indicated safety functions of Design Class I equipment might be affected due to seismic interaction.

3.10.2 SEISMIC ANALYSES, TESTING PROCEDURES, AND RESTRAINT MEASURES

The effects of seismic accelerations were determined either by physical tests, mathematical analyses, or engineering judgment. Mathematical analyses of structural elements were made for Design Class I exposed electrical raceways, for equipment supports, and also for some equipment. Physical tests of equipment were made either on one of the units being supplied or on one of a similar type. Choice of method used to determine seismic capability of the equipment and devices was based on the supplier's judgment of what would be adequate and appropriate.

3.10.2.1 Nuclear Reactor Instrumentation and Protection Systems

The seismic testing of Westinghouse-supplied electrical and control equipment is documented in WCAP-8021 (Reference 5). The testing conforms to the procedures of IEEE-344-1971. The radiation monitoring cabinet and the Tracerlab scintillation detector and liquid sampler equipment are not safety-related, and these portions of WCAP-8021 are not applicable. The radiation monitoring system cabinet at DCPP has been upgraded to Design Class I (see Section 3.10.2.26). Details of the original seismic analysis and testing procedures for Design Class I instruments and electrical equipment are summarized in Table 3.10-1 and the following sections.

Typical items of equipment have been type tested under simulated seismic motion in the form of sine beats. This testing was done with conservatively large accelerations over a range of applicable frequencies and conformed to the procedures given in IEEE 344-1971. The peak test input accelerations used in those tests were checked to verify that they are larger than the requirements derived by structural analyses of DDE and HE levels. Westinghouse Electric Company, the supplier, made dynamic tests of typical samples of this equipment to confirm its seismic adequacy. Included in this test program were the racks for the nuclear instrumentation system; the process control and protection sets; the solid-state protection system cabinets and its safeguards test cabinets and auxiliary safeguards cabinets; the inverters for the power supply; pressure and differential pressure transmitters; the reactor trip switchgear; and main coolant loop resistance temperature detectors. Details of these tests are given in Table 3.10-1 and in Sections 3.10.2.1.1 to 3.10.2.1.9.

3.10.2.1.1 Nuclear Instrumentation

As described in Reference 5, a typical two-cabinet unit of the Westinghouse nuclear instrumentation system (NIS) and radiation monitoring system (RMS) has been seismically tested. The NIS equipment was contained in one cabinet and the RMS equipment was mounted in the other cabinet. The two cabinets were attached and mounted on a two-cabinet base to simulate the support or adjoining cabinets. A typical NIS installation consists of four cabinets.

The NIS cabinet contained one source range channel, one intermediate range channel, and one power range channel located and mounted in the same configuration as the plant installation. Since any DBA described in this FSAR Update can be terminated within acceptable limits by the power range channels, only the power range channel was energized and monitored. The other NIS channels mounted in the cabinet served to simulate the mass distribution and weight in an actual installation.

Shutdown procedures contain the following provisions in the event that the source range channels are rendered inoperative due to a seismic event:

- (1) The operator will take appropriate action to preclude boron dilution
- (2) Prior to cooldown, boric acid will be added to the reactor coolant to ensure that the concentration is sufficient to maintain the reactor in a subcritical state

During seismic testing an external test signal was applied to the equipment so that the power range output signal was 100 percent full power. The test input signals, analog output signals, and bistable output signals were monitored during test. The tripping action of the bistable amplifier circuitry was checked after each series of tests to insure that the simulated earthquake had not impaired this function.

Only one instance of mechanical malfunction occurred as a result of this level of testing. Drawer latch damage occurred during side-to-side testing at higher g levels. A new fastening mechanism has been designed and the design submitted to the NRC (Reference 6). This modification was implemented at DCP. A demonstration test for seismic operability of the NIS equipment was performed with multiple frequency, multiple axis inputs. The test, reported in Reference 7, indicated that the equipment will operate during a seismic event as required.

The neutron detector for the NIS power range channel has been tested using sinusoidal inputs in both the horizontal and vertical directions at accelerations at least equal to those calculated for the DCP. Neutron current measurements were made during the tests, and current, resistance and capacitance checks were made after the tests. No significant changes were found and there was no mechanical damage to the detector.

DCPP UNITS 1 & 2 FSAR UPDATE

In addition, a two-section power range excore neutron detector was tested using multiple frequency, multiple axis inputs in a support assembly which simulated a detector holder. The multiple frequency inputs were developed in accordance with the guidelines set forth in Reference 8. The test response spectra envelope the DDE and HE inputs.

During the multiple frequency test, the detector was energized from a high voltage power supply, and an AC signal was imposed in each of the two signal electrodes to determine proper electrical operability.

At the completion of the tests, there was no observable mechanical damage and the electrical recordings revealed only a transient type electrical disturbance of one of the two signals. The signal perturbations were small in amplitude and would not cause any loss of protection capability of the NIS during normal operation. Subsequent detector acceptance tests performed by the detector manufacturer did not disclose any abnormal permanent change in the electrical or neutron sensitivity characteristics. Thus the NIS Power Range Detector will operate as required during and after the DCPP postulated seismic events.

3.10.2.1.1.1 Radiation Monitoring

Qualification of the radiation monitoring panels in the control room is based on shake table tests performed on the panels for Victoreen. The racks were shaketable tested with the monitoring equipment in place. See Section 3.10.2.26

3.10.2.1.2 Solid-State Protection System

The three-bay, two-train SSPS was seismically tested as described in Section 2.5 of Reference 5. During the seismic test, a typical reactor trip matrix and typical safeguards actuation matrix were energized and monitored. Before each test, the circuitry was placed in a pre-trip condition. During the actual shaking, the circuitry was deliberately tripped and changed to a post-trip condition. The functional integrity of the system was thus demonstrated by observing a satisfactory change of state on demand. Relay contact positions necessary to show the operability were recorded during the tests.

No mechanical problems occurred during the vertical axis tests. In the side-to-side axis test at lower "g" levels, the two lefthand cabinet-to-base bolts repeatedly loosened and were deformed until it became necessary to replace these with more hardened bolts. During subsequent testing at these levels in the side-to-side axis, these bolts failed completely on the last sine-beat test. Before performing the front-to-back test, twelve additional cabinet-to-base bolts were installed making a total of 24 bolts fastening the cabinet to its base. This change has been incorporated into the SSPS cabinets at DCPP.

The functions monitored by recorders were: undervoltage trip, train trouble, and SI signal. Test switches were operated during the third sine beat simulating a reactor trip

and safeguards actuation, causing a change in amplitude of the recorded signals for under voltage trip and SI.

During the front-to-back axis test, the signal indicated several momentary trips (contact closures) before the test switches were operated. Also, at 7 Hz and 9.5 Hz, this signal indicated a momentary trip and then a permanent change of state (latch up) on the first bounce on the output (slave) relays. The permanent change of state was caused by the armature of the same relays bouncing closed. This closing allowed their mechanical latch mechanism to operate. These maloperations could have initiated safeguards actuation. However, they would not have negated a valid safeguard actuation or reactor trip. Although SI was prematurely actuated, the under voltage coil tripped when called upon to do so.

The duration of the momentary contact closure was probably short enough not to cause a false safety injection signal. The probability of spurious initiation of safety injection due to any earthquake is therefore very small. The seismic tests performed have demonstrated that the postulated seismic event will not prevent a legitimate safety injection signal from being actuated, either during or after the event. Reference 9 presents an analysis of the consequences of seismic-induced actuation of protection system relays by considering the possible actuation of each contact of the relays studied and describing the resulting effect of inadvertent equipment actuation.

The relays which exhibited contact bounce and mechanical latching were replaced by a new type of relay which was seismically qualified by single-axis sine-beat and multiple frequency sine-beat testing. Input levels for the tests were determined from the measured acceleration response at the cabinet during the cabinet tests described in Section 2.5 of Reference 5. Seismic qualification of these replacement relays is documented in Reference 10.

Due to obsolescence issues, the original SSPS printed circuit boards (PCBs) can be replaced with newer vintage boards supplied by Westinghouse. The replacement PCBs have been seismically qualified by Westinghouse. The seismic qualification is documented in Reference 49.

3.10.2.1.3 Process Control and Protection Equipment

Originally, seismic testing was performed using a three-cabinet unit mounted on a common base as defined in Section 2.4 of Reference 5. The three-cabinet test assembly included at least one of each type of module used in all of the various process protection and safeguards actuation channels. Both analog and bistable output signals were recorded. All reactor trips and safeguards actuation signals were continuously recorded and some bistable signals of less importance (e.g., alarms circuits) were monitored with lights. The basis for determining the functional integrity of the reactor trip and safeguards actuation signals was that these signals should remain unchanged during the test and should be capable of changing state after the test if called upon to do so.

DCPP UNITS 1 & 2 FSAR UPDATE

The tripping action of the bistable amplifier circuitry was checked after each series of tests to insure that the seismic test input had not impaired this function.

During front-to-back testing of the circuit board, an internal power supply circuit board disengaged from its connector causing complete failure of the module. Restraining clamps were installed on the circuit board and the test was repeated successfully. These clamps have since been installed on all similar modules. All recorded electrical signals performed properly during and after the tests.

In addition, as part of the overall program to demonstrate the adequacy of the seismic test previously conducted, multiple frequency, multiple axis test (Reference 11) were performed on an entire typical channel, including signal conditioning circuits and the bistables, of the process instrumentation system. The results of the bistable tests show that the electrical functions of each bistable module maintained electrical operability both during and after each seismic event. In addition, no spurious bistable actions were observed.

Subsequently, the Eagle 21 system replaced the Hagan protection system within the existing racks. The Eagle 21 system has been seismically qualified on a generic basis by Westinghouse (see References 40 through 42) in accordance with requirements from References 43 and 44. A site-specific seismic analysis was also performed to ensure that the Eagle 21 generic testing performed by Westinghouse encompasses the DCPP installed condition (see Reference 45), which included the effects of the top entry conduit stiffness.

Subsequently, the Hagan process control system (PCS) in instrument racks 17 through 32 (RNO1A through RNO4E) was replaced with a programmable logic controller based system manufactured by Triconex (DDP 1000000237 and DDP 1000000501). The system chassis, I/O and hardware have been seismically qualified by Triconex (Reference 55). As part of the design change process, a site-specific seismic evaluation and seismic calculation file was completed for the installed condition.

Supporting PCS equipment, such as loop power supplies, signal isolators, circuit breakers, terminal boards and line filters that support safety related equipment, was seismically qualified in accordance References 56, 57 and 58.

3.10.2.1.4 Instrument AC Inverters

A prototype UPS and regulating transformer of the DCPP UPS system was tested as described in PG&E engineering seismic file No. ES-68-1.

The UPS and regulating transformer were tested while loaded at 20 kVA; and the ac output voltage, current and frequency were monitored during the seismic test. The presence of a continuous ac output voltage both during and after the test formed the basis for determining the functional integrity of the UPS system.

DCPP UNITS 1 & 2 FSAR UPDATE

During seismic testing the static inverter maintained structural integrity and functional operability. No variation or loss of 120 Vac output voltage was observed during or after the test. Therefore, the static inverter will perform its safety related functions during and after the postulated DCPD seismic events.

3.10.2.1.5 Pressure and Differential Pressure Transmitters (Westinghouse)

Originally the safety related pressure transmitters provided by Westinghouse for DCPD were installed to sense the following conditions:

- Containment Pressure (CP)
- Reactor Coolant Level using the Reactor vessel Level Instrumentation System (RVLIS)

The transmitters were mounted during seismic qualification to a rigid fixture. The pressure and differential pressure transmitters tested are the following:

<u>Equipment</u>	<u>Function Group</u>	<u>Manufacturer</u>	<u>Model No.</u>
Differential Pressure Transmitter	CP	ITT/Barton	332/351
Differential Pressure Transmitter	RVLIS	ITT/Barton	752

As described in Section 2.8 of Reference 13, the Barton Model 332 transmitter was seismically tested. Subsequently, the containment pressure transmitters were replaced with Rosemount differential pressure transmitter Model 1154 (refer to Section 3.10.2.11 for qualification of this model transmitter). The Barton Model 351 pressure sensors are used in conjunction with the Rosemount transmitter Model 1154 to measure containment pressure.

Seismic testing of the Barton Model 752 differential pressure transmitters is detailed in WCAP-8687, Supplement 2-E04A (Reference 15). Seismic testing was performed using multiple frequency, multiple axis tests. During seismic tests, the transmitters were pressurized to approximately mid-scale with a 2,000-psig static pressure. The output of the transmitters was monitored continuously. The Barton 752 differential pressure transmitters maintain their integrity and performed their safety-related functions as required during and after seismic testing. Subsequently, the RVLIS level transmitters manufactured by Barton were replaced with Rosemount differential pressure-transmitter Model 1153 (refer to Section 3.10.2.11 for qualification of this model transmitter). The RVLIS Rosemount transmitters retain the use of the Barton Model 353 pressure sensors.

3.10.2.1.6 Reactor Trip Switchgear

Seismic testing of a typical reactor trip switchgear was performed as described in Reference 16. The basis for determining the functional integrity of the equipment was the following: (a) the breakers should trip open on loss of voltage to the undervoltage

trip device during the testing sequence, and (b) all breaker outputs, including secondary contact outputs to the various protection system, should maintain proper contact condition of open or closed position.

The electrical functions of the equipment were monitored both during and after the seismic test (Reference 16) to ensure that the equipment was operating properly and performing the required safety related functions. This monitoring consisted of recording output signal voltages, and the input signal voltage to the undervoltage trip. The tripping action of each breaker through the undervoltage trip circuitry was checked during the after each series of test to verify that the simulated earthquake had not impaired this function.

The recordings of all electrical signals indicated proper and complete functioning of the equipment both during and after all testing. No secondary contact chattering, no false breaker closing and no false breaker opening was observed.

The test results show that the functions of this equipment were maintained within the established criteria, both during and after each simulated seismic condition. During seismic testing a modification kit was installed within the reactor trip switchgear to enhance its seismic capabilities. This modification kit has been installed in the DCPP reactor trip switchgear.

3.10.2.1.7 Resistance Temperature Detectors

Resistance temperature detectors (RTDs) are ruggedly built devices designed to withstand the high temperature and pressure of the fluid in the reactor coolant system. They are also designed to withstand severe seismically induced vibration, and the reactor coolant RTDs are designed to withstand the flow-induced vibration from the reactor coolant flow.

The RTDs are mounted in the reactor coolant piping, on the containment sump wall, and on rigid support structures. The reactor coolant RTDs are installed in thermowells mounted into the main coolant piping.

The seismic testing described in Reference 35 was performed on the Weed reactor coolant RTDs. The test inputs were random frequency, biaxial sine wave vibrations for a range of 1 through 1000 Hz. During the test, the RTDs were operated and their input/output signals were monitored. No mechanical damage was observed, and the input/output signals remained within acceptable limits.

The seismic testing described in Reference 36 was performed on the Conax RTDs. The test inputs were random frequency, biaxial sine wave vibrations for a range of 1 through 200 Hz. During the test, the RTDs were operated and their input/output signals were monitored. No mechanical damage was observed, and the input/output signals remained within acceptable limits.

3.10.2.1.8 Safeguards Test Cabinet

As described in Reference 19, sine-beat testing was performed on a typical engineered safeguard test cabinet. The engineered safeguards test cabinet completed seismic testing without sustaining physical damage. The only functional anomaly observed during testing was the momentary opening of the normally closed contacts of certain test selection switches at particular frequencies.

These switches are used to set up and initiate individual tests. The normally closed contacts are used exclusively to reset the blocking relays of the engineered safeguards test cabinet upon completion of a test. When the blocking circuit is not in the test mode, the blocking relay is in the reset state. A momentary opening of the normally closed contacts, therefore, will have no effect on the state of the blocking relay.

Therefore, based on the seismic testing performed, the engineered safeguard test cabinet will perform its safety related function during and after the postulated DCPD seismic events.

3.10.2.1.9 Auxiliary Safeguards Cabinet

The auxiliary safeguards cabinet is structurally identical to the safeguards test cabinet (Section 3.10.2.1.8) and the component layout of the two cabinets is essentially the same. Therefore the results obtained from the test of the safeguards test cabinet were applied to the auxiliary safeguards cabinet.

The auxiliary safeguards cabinet was later analyzed by time history analysis to qualify the use of the rotary relay in the cabinet. This analysis is described in Reference 20.

The rotary relays have been tested separately using single axis, multiple frequency inputs. These tests are described in Reference 10.

The analysis response spectra of the auxiliary safeguards cabinet, at relay mount locations, was found to be enveloped by the relay test response spectra. Therefore both the auxiliary safeguards cabinet and relays will function properly during and after the DCPD postulated seismic event.

3.10.2.2 Main Control Board and Console

The main control board is located within the control room at elevation 140 ft in the auxiliary building. It has two major structures: main control board (MCB) section and control console.

Seismic qualification of the MCB and central console is demonstrated by analysis as described in Reference 21. The analysis consisted of the following tasks:

DCPP UNITS 1 & 2 FSAR UPDATE

- (1) Modeling of the MCB so that its analytical frequencies correlate to those obtained from the field test
- (2) Response spectrum analysis of the model using the given spectra to evaluate structural adequacy
- (3) Modification of MCB to address overstress condition
- (4) Response spectrum analysis of the modified MCB model to compute loads for structural evaluation
- (5) Transient dynamic analysis of the modified model to generate in-equipment response spectra (IERS) for device qualification

The MCB section and central console are modeled using the general purpose finite element computer code, WECAN (Reference 22). The MCB is modeled as a linearly elastic system of beam, plate and lumped mass elements.

In addition, In-situ testing of the unmodified structure was performed to identify local panel modes. This consisted of tap tests of the vertical and bench panels as described in Reference 23.

Response spectrum analyses were performed to compute structural loads using DDE and HE required response spectra. Two dimensional shocks were considered in the evaluation. Maximum elemental stresses were obtained from the two sets of response spectrum analyses.

The structural analyses of the unmodified design indicated some overstress which is a result of the changes in spectra from the original HE loadings. To reconcile the overstressed conditions and simultaneously provide the additional advantage of increasing the overall structural frequencies to above the peak of the floor response spectra, modifications have been done on top of the main control board. These modifications lead to a much lower stress condition and increase the board's overall structural frequencies to values exceeding the peak of the input spectra.

The results of stress analyses for the modified design show that the maximum member stress is about 85 percent of allowable. A comparison of the required and as-built weldments demonstrates that the existing weldments exceed the required weldments. Buckling stability of all MCB structural members has also been evaluated. There exists, at least a factor of safety of three against buckling.

Transient dynamic analyses of the modified structural model and performed to obtain the IERS for use in qualifying board mounted devices. Two sets of transient analyses are performed using two directional seismic excitation with one horizontal and one vertical direction. The synthesized floor excitation is employed in a transient dynamic

DCPP UNITS 1 & 2 FSAR UPDATE

analysis using the modal superposition integration procedure. Five percent of critical damping is assumed in the analyses.

The central console is a U-shaped electrical cabinet consisting of three bolted sections, welded to the main control room floor. The structure is modeled using WECAN, similar to the main control board. Results of modal analyses of the console structural model show the lowest overall fundamental frequency to be 70 Hz.

Since the console model has no frequencies below 33 Hz, it is classified as a rigid structure, and stress evaluations are performed using the static method. Uniform static acceleration equal to the floor response spectra ZPA are applied to the console structural model. Stresses computed by the SRSS method are observed to be well below the allowables. No weldments and buckling evaluations are performed due to the obvious integrity apparent from the low stress conduit.

As all console frequencies are in the rigid range, the IERS for console mounted devices are the floor response spectra.

The IERS obtained from MCB and console analysis were used for seismically qualifying the MCB mounted devices as described in Reference 24. Qualification tests were performed to determine if the structural integrity and functional operability of the devices are maintained for the seismic level.

Devices tested were supplied by PG&E and are representative of all the Design Class I devices used in the MCB. Indicators, recorders, switches, power supply, and light box were tested. The seismic qualification was achieved by subjecting the devices to multiple frequency, multiple axis seismic testing such that the response spectrum envelops the IERS obtained from analysis. It was concluded from the tests that all of the Design Class I devices will maintain their structural integrity and functional operability during and after the postulated seismic event. In addition, three cathode ray tube (CRT) displays have been located in the central console. Seismic tests were performed to insure that these CRTs will not become missile sources.

3.10.2.3 Hot Shutdown Panel

This panel is a backup panel used if the control room must be evacuated and the plant brought to a hot shutdown condition. It contains indicators, control switches, and hand-auto stations for proportional control. These give indication and control over various pumps and valves in the auxiliary feedwater, component cooling water, boration control, and containment fan cooler systems. Additionally, the 10 percent steam dump valves are controlled from the hot shutdown panel, but the control loops for that function are not Design Class I.

3.10.2.3.1 Qualification of the Panel

The panel consists of an enclosure 5 feet 10 inches wide, 6 feet 6 inches high, and 3 feet deep, with two panels inside, one on a vertical plane, the other tilted up 30° from the horizontal. The enclosure is mounted on four channels which are welded to a box comprised of 10-inch WF beams. This box is welded to steel plates embedded in the concrete floor of the auxiliary building at elevation 100 feet.

A three-dimensional response spectra analysis has been performed on a finite element model developed for the hot shutdown control panel. This analysis has shown the subject panel is qualified for DE, DDE, and HE seismic events.

3.10.2.3.2 Qualification of Individual Instruments

The types of components in the panel that are Class 1E are indicators (Westinghouse Model VX252), control switches (Cutler-Hammer Type 10250T), and hand-auto control stations. Other devices (e.g., Westinghouse Type KA-241 indicators) are not Class 1E and have no need to meet seismic qualifications. These devices are separated from Class 1E devices by a barrier.

All required devices (VX252 indicators, W-2 switches, 10250T switches) were qualified by test using multifrequency biaxial shake tests. The devices were mounted to closely simulate their mounting conditions on the panel. The indicator was calibrated before and after the tests to ensure that the tests had not affected the calibration. During the tests, an input was applied that produced a midscale output. The outputs were monitored for fluctuation, and no fluctuation or calibration shift greater than required accuracy was noted.

Replacement valve manual/auto hand stations manufactured by NUS were seismically qualified in accordance with Reference 59, 60 and 61.

The control switches were tested in both the neutral and the "switched" positions. The contacts were monitored for chatter during the event, and were tested for proper operation afterwards. (It should be pointed out that since the safety function of these devices is to give the operator manual control of various devices, and the operator will not be expected to change switch position during the seismic event, no requirement exists to change inputs during the event.) No malfunctions of the switches were noted.

3.10.2.4 Local Instrument Panels

Local instrument panels are used as enclosures for Design Class I and non-Design Class I instrumentation throughout the plant. The panels perform no Design Class I function except to provide support for the Design Class I devices. The panels are supported at the top by fastening them to a wall or other suitable structure. The bottom is fastened to the floor or to the same structure as the top.

DCPP UNITS 1 & 2 FSAR UPDATE

The panels were originally qualified by analysis performed by the panel vendor. The criteria for the panels were that they have a resonant frequency greater than 20 Hz, and that all stresses be below allowables.

Due to the large number of panels requiring qualification, a worst case analytical method was used. It was based on determination of the panel having the highest calculated stresses resulting from simultaneous horizontal and vertical seismic accelerations. Subsequent to their installation in the plant, several of the panels were modified to increase their stiffness.

The qualification of the panels is based on finite element models of several representative panels which include the effect of equipment mounted in the panel. The analysis took into account the various sizes, configurations, and locations, using an envelope of 2 percent DDE and 4 percent HE spectra.

The results of the analyses show that all panel stresses are below allowables. In addition, the panel response at Design Class I transmitter locations was derived for comparison with the test response spectra for Design Class I transmitters in the panels (see Section 3.10.2.11).

3.10.2.5 Instrument Panels PIA, PIB, and PIC

These instrument panels house various devices used to power plant transmitters and perform the necessary signal conditioning to provide alarm functions and send linear signals to indicators on the main control board. The typical parameters involved are CCW flows and heat exchanger DP, and refueling water storage tank (RWST) level, etc. Most of the components in them were originally in the power generation instrument rack (PGIR). The panels are mounted on reinforced concrete columns at about the 132-foot elevation in the cable spreading room.

The panels were originally qualified by analysis. A review of the original stress calculations indicates that nowhere would the stresses (bending or shear) due to postulated seismic loading exceed 50 percent of the yield point of the material.

The relays were qualified by comparison with the same relays installed in the ventilating control panel, physically installed nearby.

The panels were reanalyzed for the current seismic criteria for both the DDE and the HE. In addition, the seismic qualifications of the devices within the panels have been reviewed to the same seismic criteria. The analysis and the review have demonstrated that the instrument panels PIA, PIB, and PIC are seismically qualified to perform their safety function after the postulated seismic conditions.

Subsequent to the original qualification testing, replacement or additional devices to the panels have been installed. These devices are qualified by testing, analyses, or a combination of the two. Their qualification is documented in the engineering seismic files associated with the panels and/or devices.

DCPP UNITS 1 & 2 FSAR UPDATE

Subsequently, design changes 100000237 and 100000501 removed much of the instrumentation in racks PIA, PIB and PIC and transferred their functions to the Process Control System. RWST level control logic relays, CVCS Letdown Heat Exchanger Room high temperature detection/isolation control, and Aux Steam Area K high temperature detection were retained due to interface requirements that could not be incorporated into the PCS. The original Moore direct current alarms (DCAs), thermocouple transmitters (TCTs), square root transmitters (SRTs) and signal conditioners (SCTs) were removed or replaced with new Moore (CPT) PC-programmable temperature transmitter and signal isolators/converters. The Moore CPTs were seismically qualified by NLI per references 56, 57 and 58.

3.10.2.6 Diesel Generator Excitation Cubicle and Control Cabinet

The diesel generator (DG) excitation cubicle and the control cabinet for DGs 1-1, 1-2, 1-3, 2-1, and 2-2, were originally seismically qualified for the DDE by the manufacturer. Subsequently, one excitation cubicle and one control cabinet were shake-table tested and qualified to the 1977 HE requirements.

The seismic qualification has been reviewed to the latest DDE and HE levels described in Section 3.7. Based on this review, it has been demonstrated that both the excitation cubicle and the control cabinet will perform their safety function during and after the specified seismic conditions.

The sixth excitation cubicle and control cabinet for DG 2-3 have been seismically qualified by shake-table testing.

3.10.2.7 Design Class I AC Electrical Distribution Equipment

The following sections describe the seismic qualification of Class 1E ac electrical distribution equipment.

3.10.2.7.1 4160 V Metal-Clad Switchgear

The original 4160 V metal-clad switchgear with General Electric (GE) 250 mVA 4.16 kV magneblast circuit breakers was seismically qualified by a combination of testing and analyses.

Later, it was discovered that 350 mVA circuit breakers should be used in place of the GE 250 mVA 4.16 kV magneblast circuit breakers. GE could not supply such breakers to the same switchgear. Consequently, PG&E decided to procure 350 mVA 4.16 kV breakers from NTS/PDS, which converted Japanese-made Yaskawa SF6 circuit breakers to fit the existing 4 kV switchgear. The new circuit breakers were installed during refueling outages 1R8 and 2R7.

DCPP UNITS 1 & 2 FSAR UPDATE

New circuit breakers were seismically qualified by shake table testing (NTS report No. TR60431-95N-FR). The shake table testing was intended to achieve the following objectives.

- (1) Demonstrate the structural integrity and functionality of the Yaskawa breakers.
- (2) Demonstrate the structural integrity of as-installed 4 kV switchgear cubicles at DCPP with the Yaskawa breakers.
- (3) Demonstrate the functional performance of the existing components (i.e., various relays and switches) installed in the existing 4 kV switchgear cubicles with replacement Yaskawa breakers.
- (4) Instrument the test 4 kV switchgear cubicles with sufficient number of accelerometers to obtain accurate information on the dynamic response (response frequencies, test response spectra) at various cubicle locations. This information is to be used for further/future testing and analyses.
- (5) Take immediate corrective actions to address significant anomalies observed during the test.

The initial seismic testing was performed at Wyle Laboratories in Huntsville, Alabama. Three seismic mock-up 4 kV switchgear cubicles were built to duplicate the design, material, and construction of cubicles G-5, G-12, and G-13 of Unit 1. A total of 18 OBE and SSE test runs were performed, including three runs of resonance search. Test results showed that the new breakers and mock-up cubicles successfully passed the minimum required 5 OBE tests.

For the SSE tests performed at Wyle Laboratories, excessive relay chatter at certain frequencies were noted. The excessive chatter was due to over-testing the equipment, which in turn was a result of Wyle Laboratories being unable to accurately control the test table response at 10 Hz and above due to resonance of the table. The over-test produced a significant amount of relay chatter, which caused the tripping and closing of breakers. The post test functional check showed that the breakers were functioning properly and had no structural damage.

To properly test the relays, supplemental SSE testing was performed at Farwell and Hendricks (F&H) Laboratories. The upper front doors of the G-12 and G-13 cubicles, where a majority of relays are mounted, were mounted on the F&H rigid test fixture. One 1200A breaker and one 2000A breaker, located adjacent to the test table, were fed by the relays. The SSE RRS obtained at relay locations on the G-12 and G-13 cubicles from the previous Wyle testing were reduced with the appropriate scaling factor to eliminate unnecessary over-testing. The supplemental SSE testing was successful. However, certain modifications (such as adding chokes to the breakers and removing

the seal-ins from certain relays) were made when the new breakers were installed in the 4-kV switchgear.

Based on the above, the switchgear and its contents are qualified for the DE, DDE, Hosgri, and LTSP postulated seismic events at DCPP.

3.10.2.7.2 Potential Transformers 4160/120 V

There are a total of four potential transformers associated with each 4 kV vital switchgear. There is a potential transformer for each feeder; auxiliary, startup and the diesel generator and one for the bus itself. Potential transformers are normally an integral mechanical and electrical part of metal clad switchgear. However, the auxiliary and startup potential transformers were removed from the top of the 4160 V metal clad switchgear during the initial qualification testing performed in 1978.

In 1978, a potential transformer representing the auxiliary and startup potential transformer was separately shake-table tested and qualified for the Hosgri earthquake. A potential transformer representing the diesel generator and bus potential transformer was shake-table tested using a mock-up of cubicle H-7.

In 1995, a potential transformer was mounted above a mock-up of cubicle G-12 and a dummy weight, representing the weight of a potential transformer, was mounted above a mock-up of cubicle G-5. These two cubicles were included in the shake-table testing at Wyle Laboratories during the seismic qualification of the new SF6 breakers described in section 3.10.2.7.1.

The auxiliary and startup potential transformers that were originally at the 90-inch level of the vital switchgear have been relocated to rigid stands adjacent to the respective switchgear lineups. Electrically, they are still an integral part of the switchgear. The diesel generator and bus potential transformers located below the 90-inch level are still physically attached to the switchgear, with the exception of the diesel generator potential transformer on Unit 1 Bus F that was also moved to a rigid stand adjacent to the switchgear.

The seismic qualification has been reviewed for the latest DDE and HE levels. The comparison of the earlier test data with current seismic requirements and additional analysis demonstrate that the potential transformers are qualified to perform their safety function during and after the specified seismic conditions.

3.10.2.7.3 Safeguard Relay Boards

Originally, one safeguard relay board from Unit 1 was shake-table tested to qualify the relay boards for the seismic requirements of the DDE. New qualified relays were introduced to replace the ones that exhibited chatter. Relays whose chatter did not impair any safety function were not replaced. As a result of the 1978 HE reevaluation, one relay board of the six installed was shake-table tested to higher levels than the original test.

The qualification of the relay boards has been reviewed to the latest DDE and HE levels. Based on this review, it is concluded that the safeguard relay boards are seismically qualified to perform their safety function.

3.10.2.7.4 Vital 480 V Load Centers

The vital 480 V load centers were originally qualified for the DDE based on seismic tests on similar equipment conducted by the manufacturer. As a result of the 1978 HE reevaluation, the equipment was further qualified by shake-table testing. During the testing, the draw-out modules of the load center were equipped with hold-down brackets to prevent slamming of the modules and subsequent chatter of contacts. Chatter was detected also on the deenergized high-speed contactors of the Unit 2 fan cooler controllers while the low-speed contactor was energized.

As a result, all draw-out modules of the 480 V vital load centers have been equipped with hold-down brackets. The containment fan cooler motor controllers have been equipped with mechanical interlocks that prevent inadvertent closure of the deenergized high-speed contactor when the low-speed contactor is energized, and likewise prevent closure of the low-speed contactor when the high-speed is energized.

The load centers were qualified using a certain type of kickout spring. Subsequently, all load center contactors in question were checked in the field and the proper kickout springs (the one used in the qualification testing) were installed where necessary.

The qualification of the load centers has been reviewed to new 1983 seismic criteria for both the DDE and the postulated HE event described in Section 3.7. The comparison of the earlier test data with current seismic requirements and additional analysis demonstrates that the vital 480 V load centers are seismically qualified to perform their safety function during and after the specified seismic conditions. The qualification meets the requirements of IEEE 344-1975 and RG 1.100.

3.10.2.7.5 Vital Load Center Transformer

The vital load center transformers were originally seismically qualified for the DDE based on shake-table testing of a similar, but larger power transformer. Comparison was made which demonstrated that the test of the 1500-kVA transformers is applicable to qualify the 1000-kVA vital load center transformers installed.

The test results were further reviewed with regard to the 1977 requirements of the HE. It was found then that the earlier testing still qualified the transformer for the HE levels.

A further review of the original test with regard to current seismic requirements for both the DDE and HE concluded that the vital load center transformers are qualified for the above seismic criteria.

3.10.2.7.6 480 V Vital Load Center Auxiliary Relay Panels

The vital load center auxiliary relay panels were originally designed and constructed to meet DDE seismic requirements.

To qualify the panels and electrical components for the 1978 HE requirements, two typical panels were shake-table tested. This requalified all relay panels.

The qualification of the relay panels has been reviewed to current seismic criteria for both the DDE and the HE. The comparison of the earlier test data with the current seismic requirements and additional analysis demonstrates that the vital load center auxiliary relay panels are qualified to perform their safety function.

3.10.2.7.7 Instrument Power AC Panelboards

The instrument power ac panelboards were originally qualified for the DDE by seismic testing which includes multifrequency sine beat test and resonant frequency test. Subsequently, the equipment was requalified to the 1978 HE requirements based on comparison test data from the DDE tests above and shake-table testing for circuit breakers/panelboards of various manufacturers.

The qualification has been reevaluated to the current seismic requirements for both the DDE and the HE. The reevaluation includes the panelboard/component qualification by calculation and by comparison of 1978 shake-table test results to the current seismic criteria. The calculation verifies the equipment structure integrity, and the test results demonstrate that the current seismic criteria are met.

The reevaluation concludes that the instrument power ac panelboards remain seismically qualified.

3.10.2.8 Design Class I DC Electrical Equipment

The following subsections describe the seismic qualification of Class 1E dc electrical equipment.

3.10.2.8.1 Batteries

There are six vital "batteries" at DCPP, three in each unit. Each "battery" consists of 60 battery cells (see Section 8.3.2.3.6.3 for 59-cell configuration). The original Class 1E station batteries were C&D Model LCU-27. They were replaced in 1983 with C&D Model LC-25 battery cells. Currently, all vital batteries are C&D Model LCUN-33 cells.

Each vital battery (60 cells) is located in its own room in the auxiliary building at elevation 115 feet. In each battery room there are currently four battery racks; three are single-tier racks that hold 12 LCUN-33 battery cells each, and the fourth is a two-step rack that holds 24 of the cells.

DCPP UNITS 1 & 2 FSAR UPDATE

The new battery cells (Model LCUN-33) were tested at Wyle Labs in Huntsville, Alabama. A rigid test rack was utilized. The test rack held four LCUN-33 cells. The new battery cells have been qualified by shake table testing for DE, DDE, and Hosgri design basis seismic events. They have also been evaluated for the LTSP requirements and were found to satisfy the LTSP acceptance criteria.

Two separate LCUN-33 tests were performed. First, unaged cells were tested to qualify the cells for installation in outage 1R5 and for a 5-year life. Next, another group of LCUN-33 cells were artificially aged and tested. The second test qualified the LCUN-33 cells for a 15-year life. The qualification was performed using the guidance of IEEE 535-1986 (Reference 51) and NRC Regulatory Guide 1.158 (Reference 52). The qualified life of the C&D LCUN-33 battery was extended to achieve a 20 year mean service life in 2006. Qualified life is determined per IEEE 535-1986 and is documented in the seismic calculation file (Reference 53).

Preventive maintenance is in place to replace the batteries before the expiration of their qualified life.

It is concluded that the station batteries C&D Model LCUN-33 will perform their safety function during and after DCPP design basis seismic events.

3.10.2.8.2 Station Battery Racks

Each vital battery (60 cells – see Section 8.3.2.2.1.3 for 59-cell configuration) is located in its own room in the auxiliary building at elevation 115 feet. In each battery room, there are currently four battery racks. Originally, all battery racks were single-tier racks. Each rack held 15 Model LC-25 cells. Since the new LCUN-33 battery cells are wider than the old cells, the existing single-tier rack would hold only 12 of the new cells. Accordingly, one of the existing single-tier racks was replaced with a new two-step rack that will hold 24 of the new battery cells. Currently, three of the existing racks are single-tier racks that hold 12 LCUN-33 battery cells each. The fourth is a two-step rack that holds 24 of the cells.

The original single-tier racks were supplied by C&D along with the original LCU-27 battery cells. The racks have since been modified by PG&E due to the 1978 Hosgri reevaluation, new stress analysis for the current DDE and Hosgri levels, and finally as a result of replacing the battery cells with the new Model LCUN-33.

Both the single-tier and the two-step racks have been seismically qualified by analysis and are qualified for DCPP design basis seismic events.

3.10.2.8.3 Battery Chargers

Originally, the battery chargers were seismically qualified for the DDE by dynamic testing. As a result of the 1978 HE reevaluation, one of the battery chargers was shake-table tested to qualify all chargers for the HE requirements.

DCPP UNITS 1 & 2 FSAR UPDATE

Further shake table testing has been done on one of the battery chargers to current seismic requirement. The testing demonstrated that the battery charger will perform its safety function during and after the postulated seismic events. The testing qualifies all Class 1E battery chargers for both DDE and HE.

3.10.2.8.4 125 V DC Switchgear

The 125 Vdc switchgear was originally qualified for the DDE based on seismic tests performed on similar equipment conducted by the manufacturer.

As part of the 1978 HE reevaluation, a 125 Vdc switchgear from DCPP was shake-table tested. This switchgear is identical to the other five 125 Vdc vital switchgears installed in the plant. This test demonstrated the adequacy of the equipment's safety function during and after the postulated seismic condition.

The qualification of the dc switchgears has been re-reviewed to current seismic requirements for both the DDE and HE. The review confirms the adequacy of the qualification by comparison of the 1978 equipment test data to the current criteria. Based on the review, it is concluded that the 125 Vdc switchgears are qualified to perform their function during and after the DDE and the HE.

3.10.2.8.5 Motor Controller, 125 Vdc, for Valve FCV 95

The 125 Vdc motor controllers were installed at Units 1 and 2 in 1982. They have been seismically qualified to the seismic requirements of both the DDE and HE described in Section 3.7 by shake-table testing of one unit. The controller met all the test requirements; therefore, it is concluded that the motor controllers will perform their safety function during and after the specified seismic events.

3.10.2.9 Main Annunciator

Originally, the main annunciator cabinets were seismically qualified for the DDE by dynamic analysis. Visual annunciator components similar to those mounted in the cabinets were tested in operation by the supplier. The cabinets were reanalyzed again for the 1978 HE reevaluation. As a result, some bracing was added inside the cabinets. Components of the visual annunciator were shake-table tested and qualified for the HE requirements.

The seismic qualification of the annunciator cabinets and the visual annunciator components have been reviewed to the current requirements of both the DDE and HE. As a result of this review, the annunciator cabinets were further stiffened, particularly in the longitudinal axis. The components were found to meet the new seismic requirements.

The Sequence of Events Recorder (SER) components including the printer have been qualified by shake-table testing. The SER Cathode Ray Tube display and its

DCPP UNITS 1 & 2 FSAR UPDATE

microprocessor were shake-table tested to ensure they would not become a missile hazard but are not required to operate during and after a seismic event.

Subsequently, due to problems obtaining parts for the seismically-qualified printer, PG&E replaced the printer. The printer was replaced with a seismically qualified touch screen and a computer (PC) interfacing with a nonseismically qualified desktop printer. The PC and touch screen were qualified by testing. After a seismic event, the operators will be able to view the alarms on the touch screen. Any compatible desktop printer can be obtained and used to print the data.

The main annunciator communicates via data link to remote multiplexers and visual annunciator drivers associated with the main generator, which are not seismically qualified. There is no failure mechanism of the data link, remote multiplexer, or remote visual annunciator drivers that can adversely impact the function of the main annunciator system following an earthquake. The main generator alarms provided by the multiplexers are Design Class II and are not needed to maintain the plant in a safe shutdown condition or to mitigate the consequences of seismic events (Reference 46).

The main annunciator system is considered to be important to plant operation. However, the main annunciator system is not required for safe shutdown of the reactor. To achieve high reliability, the main annunciator system is designed to remain functional during and after a Hosgri earthquake, and to operate during a momentary or extended loss of offsite power. To meet these performance goals, the main annunciator system was originally classified as a Class I system. However, since the main annunciator system is not designed to meet the single failure criterion, the system was reclassified to Class II.

3.10.2.10 Electrical Penetrations

Electrical penetrations of the containment structure must withstand the forces caused by a LOCA. The header plates are made of forged steel welded to the containment steel liner and therefore have considerably more strength than is needed to meet seismic conditions. The penetrations are approximately 5 feet long and contain insulated electrical conductors of stranded copper. These conductors are supported within the penetration and at the terminal boxes attached to each end of the penetration.

The electrical penetrations were originally seismically qualified for the DDE by static analysis, meeting the requirements of paragraph 3.1.3 of IEEE 344-1971. A further seismic analysis was made for penetration of similar configurations for the Pilgrim 1 and Fitzpatrick 1 units. This analysis was used to qualify the penetration for the 1978 HE reevaluation.

Seismic testing performed by the manufacturer and a new analysis was used to qualify the penetrations to current requirements of the DDE and HE. The analysis demonstrates that the electrical penetrations will perform their safety function during and after the specified seismic conditions.

3.10.2.11 Pressure and Differential Pressure Transmitters

Seismic tests were performed on Barton Model 763 and 764 transmitters and Rosemount Model 1151, 1152, 1153, and 1154 transmitters as part of an environmental test programs conducted by their respective manufacturers. The transmitters were subjected to simultaneous independent biaxial excitation using a random test input. The test included a resonant search, 5-DEs, and 1-DDE, in each of two test positions.

The transmitters were pressurized and operational throughout the test. The output of each transmitter was monitored during the test to verify proper operation. The results of the test verified that the transmitters will operate properly for both DDE and HE excitation.

The seismic qualification of Rosemount Model 1154 transmitters is based on similarity between Model 1154 and Model 1153 Series D transmitters (Reference 37, paragraph 7.2). As documented in References 38 and 39, the Model 1153 Series D transmitters were shake table tested per IEEE 344-1975 to DCPD seismic requirements.

During the seismic testing leak test, calibration check and voltage variation tests were performed.

All tested transmitters successfully met the acceptance criteria. Anomalies observed were determined not to have an impact on the transmitters' qualification (Reference page v in Wyle Test Report No. 45592-3 -- Appendix A of Reference 38). The test response spectra curves enveloped the applicable DCPD-required response spectra curves (Reference 39).

Seismic testing and analysis (Reference 50) was performed to qualify Rosemount 'Smart' transmitter model 3051C for use in Instrument Class IC Systems as defined in Section 7.1 (3). The seismic testing and analysis in Reference 50 also qualifies the use of Rosemount 'Smart' transmitter model 3051N for use in Instrument Class IA Systems as defined in Section 7.1 (1).

Seismic tests were also performed on two typical models of Barton transmitters, Models 368 and 369, pressurized to mid-range operation. The tests were performed at Wyle Laboratories on a biaxial shaking table. Results show that the requirements were met. The transmitters operated throughout the tests without malfunctioning. A helium leak test was made on the pressure boundary of the transmitter after the seismic tests. No leakage was detected. The instruments were qualified in conformance to the requirements of IEEE 344-1971, Paragraph 3, Method 2, simulated seismic test.

Additional seismic qualification tests have been performed on the Barton Model 332 pressure transmitter. These were part of a series of tests, documented in WCAP-8021, where selected types of safety-related essential equipment were subjected to vibration tests in the range of 1 to 35 Hz.

DCPP UNITS 1 & 2 FSAR UPDATE

A preliminary search of the 1 to 35 Hz frequency range, using a sinusoidal input, was performed to identify any resonant condition. Any resonant frequencies found would be included with the test frequencies of the sine beat seismic input. The amplitude of the sine beat was chosen such that it would be at least as great as the maximum acceleration that the equipment would experience during a DE horizontal ground acceleration of 0.4 g, augmented by building structural amplification. Tests were done independently for each of the two horizontal and the one vertical directions of motion. Throughout the duration of the testing, both the test and reference transmitters were energized, measuring a 50 psi input pressure on a 300 psi span. The 4 to 20 mA electric output of the transmitter was monitored during and after the test to check for any loss of function.

Based on the results of these tests, it is concluded that this transmitter will perform its required design function during, as well as following, a seismic event.

3.10.2.12 Raceway Supports

The Class 1E raceway systems (safety-related) consist of conduits, cable trays, and pull boxes supported by approximately 27,000 supports in each unit. The raceway supports are constructed primarily of bolted assemblies of cold-formed channel sections either of "Superstrut" (more than 90 percent) or "Unistrut" (approximately 10 percent) brand, which are spaced at 8-1/2 feet or less, unless otherwise approved by an engineering evaluation. The supports are attached to concrete or structure steel by bolted connections or welding. Based on the similarity of structural configuration, the raceway supports are grouped into more than 400 generic types.

3.10.2.12.1 Design and Acceptance Criteria

The raceway supports are required to withstand loads from DDE or HE. The supports, in their as-built conditions, are evaluated to ensure that they meet the following criteria.

Loading Combination

The horizontal component of seismic load (DDE or HE) either transverse or longitudinal to the raceways that results in the highest stress on the member under consideration is combined, by absolute sum, with the stresses or forces due to dead load and vertical seismic load.

Response Acceleration of Support System

Unless otherwise justified the floor response spectra where supports are located are used for evaluation. The horizontal response is taken as the greater of the building responses due to either the east-west or the north-south ground motion combined by absolute sum, with the corresponding torsional response, as appropriate.

Acceptance Criteria

The specifications used to review the design of the steel members are the AISI "Specification for Design of Cold Formed Steel Structural Members" (Reference 32, Section 3.10.3) and Part 1 of the AISC "Specification for the Design, Fabrication and Erection of Structural Steel for Buildings" (Reference 33, Section 3.10.3) applicable to hot-rolled members. The allowable stress given in the AISC specification is increased by 60 percent as recommended by Standard Review Plan Section 3.8.4 (Reference 34, Section 3.10.2.12.3). The allowable stress for AISI is increased so that the margin against yielding is 1.0 or greater with the allowance for local yielding at connections. The allowable slip-shear capacity of bolted connections on strut members are established by statically testing support connections with various combination of nuts and bolt torque values. The design allowable is based on the support connection containing the type of nut (98 percent of the nuts actually used in the plant exhibit superior behavior) and the bolt torque value (more than 90 percent of the connections have significantly higher values) which very conservatively represent the as-built condition. In addition, a qualification criterion was established by performing dynamic tests on specimens having representative support configuration in determining acceptable shear capacity of the in-situ bolts. In some cases, the slip-shear capacities are based on manufacturer's recommended values. These shear capacities are for appropriate combination of nut types, bolt torque, and strut which have been verified by additional tests.

Permissible loads on conduit clamps are kept below 90 percent of the ultimate values. Clamps are also checked for interaction of pull-out and slip (either in transverse or longitudinal direction). The acceptance limit on fillet welds on cold-formed steel members is 60 percent greater than the allowable given in Section 4.2.1 of the AISI Specification. Spot-welds in composite superstrut channels are checked against allowable shear values developed from a testing program.

3.10.2.12.2 Evaluation

The electrical raceway systems are evaluated for seismic loading in the transverse, longitudinal, and vertical directions by following the methodology stated below.

Transverse Seismic Analysis

Each of the support types are evaluated against the acceptance criteria. The seismic loads used in the evaluation of the supports are based on system frequency of the support and adjacent span of the raceway. The damping value used for conduit supports is 7 percent. For cable tray supports, two separate frequency analyses are made to determine the spectral response. In the first analysis, the system frequency is obtained based on support frequency alone and 7 percent damping is used. In the second analysis, the system frequency is generated by combining the support frequency and the tray frequency. The seismic response is obtained based on

DCPP UNITS 1 & 2 FSAR UPDATE

15 percent damped floor spectra. The second analysis is confirmatory and not a basis for the license. The larger of the two spectral values is used for evaluation.

Each support type is first evaluated for the generic case based on design, which results in maximum support response.

Any support that cannot be qualified for its generic case is investigated for its as-built condition.

Longitudinal Seismic Analysis

All Class 1E raceway systems are walked down and documented. The longitudinal seismic load is generated based on raceway system frequency and 7 percent damping. The peak response acceleration is used if the system frequency is less than 33 Hz; otherwise, the zero period acceleration is used. The seismic load is distributed among the supports in proportion to their longitudinal stiffness. The individual supports are evaluated for structural adequacy.

Vertical Seismic Analysis

The vertical seismic analysis uses the same methodology as the transverse seismic analysis.

3.10.2.13 Fire Pump Controller

The fire pump controllers for the plant interior system were upgraded to Class 1E when the fire protection system was upgraded. One controller was shake-table tested and qualified to 1978 HE seismic requirements.

The qualification has been reviewed to the current seismic criteria for both the DDE and HE. The comparison of earlier test data with the current seismic requirements demonstrates that the fire pump controllers are seismically qualified to perform their safety function during and after the specified seismic conditions.

3.10.2.14 Local Starters

Local starters were originally seismically qualified for the DDE based on shake-table testing by the manufacturer. As a result of the 1978 HE reevaluation, three representative starters were shake-table tested. The testing qualified all local starters for their respective locations. Other starters of different manufacture used for the HVAC systems were qualified by comparison to the starters tested. The qualification of the local starters has been reviewed to current seismic criteria for both the DDE and HE.

For the review of the qualification to current seismic requirements, the local starters were broken down into four groups:

DCPP UNITS 1 & 2 FSAR UPDATE

- (1) Starters located in the auxiliary and fuel handling buildings were qualified by comparison of the 1978 test data to the current seismic criteria. This includes contactors installed since the 1978 shake-table testing.
- (2) Starters located at the turbine building 119-foot elevation were qualified by comparison of the 1978 test data to the current seismic criteria and by comparison to identical starters shake-table tested for the turbine building 140-foot elevation.
- (3) Starters located at the turbine building 140-foot elevation were installed after the 1978 electrical equipment testing program. One of these starters was shake-table tested to qualify the starters for the current seismic criteria.
- (4) Starters located at the auxiliary building 154-foot elevation, some of which are of different manufacture, have been qualified by comparison to the starters tested. The starters tested were qualified to spectra with much higher accelerations than are required for the 154-foot elevation of the auxiliary building.

The aforementioned review of the earlier seismic testing to current criteria for both the DDE and HE and additional testing demonstrates that all local starters are qualified to perform their safety function during and after the specified seismic conditions.

3.10.2.15 Ventilation Control Logic and Relay Cabinet

The ventilation control logic and relay cabinets were originally vibration-tested in July 1973, and seismically qualified for the DDE. The cabinets were found to be rigid. As part of the 1978 HE reevaluation, components of the cabinets were shake-table tested again and qualified for the HE.

The seismic qualification of the ventilating control logic and relay cabinet and their components has been reviewed to the current seismic requirements of both the DDE and the HE. Based on the review, it has been concluded that the ventilation control logic and relay cabinets are seismically qualified to perform their safety function during and after the DDE and the HE.

As part of the Unit 1 and 2 AFHBVS control system replacement, a new programmable logic controller (PLC) system was installed. The seismic qualification of the Plant Operating Vent panels, POV1 and POV2, and their components were reviewed to the current seismic requirements of both the DDE and the HE. The POV panels were evaluated using analytical evaluation and the PLC was shake table tested by the supplier. Based on the review, it was concluded that the POV1 and POV2 cabinets are seismically qualified to perform their intended safety function during and after the DCPP design basis seismic events.

3.10.2.16 Fan Cooler Motors

The fan cooler units were qualified for seismic adequacy by a combination of analysis and testing. A seismic analysis of the fan cooler unit, including the motor, was made to verify that the units will not exceed the allowable stresses or deflections. The response spectrum method of analysis was used.

The fan motor assembly natural frequencies were calculated using a lumped mass model. Because of high natural frequencies (after adding stiffeners to the fan cooler assemblies), this system was analyzed as a rigid structure and equivalent static loads were applied. An additional unbalanced load of 1 g was assumed to occur in all rotating assemblies.

Limit values were in accordance with the elastic provisions of the AISC-69 specification. Bearing limits were taken as failure by brinelling under dynamic load (basic rating) from the manufacturer's catalog.

An analysis and an impact test were also made on an end bell of the motor. Based on these results, Westinghouse concluded that the containment fan-motor-cooler assembly structure could withstand the combination of required loads.

3.10.2.17 Pump Motors

Electric motors for Design Class I pumps were procured with the pumps to equipment specifications that covered the pump/motor assembly as a unit. These equipment specifications required that the equipment be adequately designed to accommodate seismic accelerations appropriate for the DE and DDE.

At the time of procurement of this equipment, there were no industry standards for seismic qualification of electric motors. However, methods and criteria employed in the design of large, integral horsepower electric motors lead to motor designs that are inherently capable of tolerating high seismic loadings without loss of function. Design considerations for motors of this type include maximum torque, critical shaft speed, bearing life, vibration, and cyclical loading. These considerations lead to motor designs that would not be governed by the application of seismic loads in the range of those appropriate for DCPP. Experience with such motors in applications subject to severe vibration and shock provides additional confirmation of seismic adequacy. Based on these considerations, it is the consensus of competent engineering practice that these motors are adequately designed to perform their safety function before, during, and after the DDE or HE.

In the case of the auxiliary saltwater pumps, which are vertically mounted, calculations indicated that seismic bracing in the horizontal direction was necessary to ensure that the first vibrational mode of the pump-and-motor assembly would be in the rigid range of the design spectra. Other pump-and-motor assemblies have natural frequencies well within the rigid range.

Analyses of pump-and-motor assemblies representative of those considered here have been performed and have shown substantial margin in stresses, deflections, and bearing loads for seismic loadings in the range of those appropriate for DCP. Selected pump-and-motor assemblies for DCP have also been analyzed using the appropriate floor response spectra and both static and dynamic analysis methods. For all cases analyzed, seismic adequacy has been verified.

3.10.2.18 Electric Cables

Electric cables interconnecting pieces of equipment depend on raceways for support during seismic activity. Seismic criteria for raceway supports are described in Section 3.10.2.12. These cables are flexible and are fully supported along their entire length in conduit or tray. Adequate slack is provided to impose little or no tension on the wires. Where relative shifts between structures can occur, raceways are provided with flexible joints or are routed with adequate flexibility to ensure that the conductors remain undamaged and their associated supports meet their acceptance criteria. (Note that use of trays for Class 1E circuits is very limited, see Chapter 8.)

3.10.2.19 Motor-Operated Valves

PG&E-purchased motor-operated valves (MOVs) whose only safety function is to maintain a pressure boundary and which are not required to change position during or after an accident (passive valves), and those whose safety function includes both maintaining a pressure boundary and changing position during or after an accident (active valves), were qualified to acceleration levels less than or equal to allowable acceleration levels provided by the vendor or established by analysis. All Westinghouse-purchased MOVs were qualified to acceleration levels less than or equal to allowable acceleration levels provided by Westinghouse.

Limiter MOV operators of the type installed on active Design Class I valves in DCP Units 1 and 2 have been seismically qualified by test. Tests were conducted on various sized operators at g-levels from 3 to 10 g.

Operators were tested both while operating and while energized and not operating. The testing was single axis, performed along each of three mutually perpendicular major axes. Sine sweep testing was utilized over a range from 5 to 35 Hz, and was followed by 1- to 2-minute sinusoidal vibration at 34 Hz or at any resonant frequency below 35 Hz.

The test results for the MOV operators have been considered in the analysis of piping systems. The mass and resonant frequency of the operator is used as input in the piping analysis. The resulting acceleration levels are compared to the allowable levels to verify that the operator will function as required.

3.10.2.20 Control Room Ventilation System

The control relay and power panels are seismically qualified to the current seismic requirements for both the DDE and the HE. The qualification of the power panels is based on: shake-table testing on the similar equipment performed by the manufacturer, onsite resonance frequency test on the similar panelboard, extensive shake-table testing of electro-mechanical equipment containing circuit breakers or circuit breaker panelboards and testing of circuit breakers to the extent of the shake-table limit.

The qualification of the control relay panels is based on the actual shake-table testing of similar ventilation control relay cabinet installed in DCPP, containing the same control relays. Timing relays not found in this shake-test are seismically qualified based on the qualification of 4-kV switchgear equipment in which the identical timing relays were installed.

Test specimens similar to the installed equipment were evaluated for their adequacy of qualification. By comparison of the test data from those shake-table tests to the current seismic requirements, the test results of these equipment demonstrate that the specified seismic criteria are met for both the DDE and HE. It should be noted that the equipment is only needed for the control room ventilation and pressurization (CRVP) after an earthquake and not during the earthquake. Therefore it is concluded that the CRVP control relay and power panels are qualified to perform their safety function after the postulated seismic events such as the DDE and the HE.

The radiation and chlorine monitoring panel has been qualified by seismic simulation testing of a test specimen similar to the panel installed at the DCPP. The panel test specimen was welded to the test table and bolted to an adjacent structure in order to simulate the actual plant mounting conditions. The panel test specimen contained the following instruments: one radiation rate readout (Nuclear Measurements Corporation Model GA-2TMO), one radiation rate readout (Technical Associates Model FML-554), one chlorine analyzer (Capital Controls Model 1030), and one switch reset module. Dummy weights were used to simulate random biaxial seismic simulation tests in accordance with IEEE std. 344-1975. The function of the instruments was verified before and after the testing. The test response spectra have been verified to envelop the DDE and HE required response spectra. The chlorine detection function has been eliminated and the detectors are abandoned in place.

The radiation detector associated with the Nuclear Measurements radiation rate readout described above was also subjected to random biaxial seismic simulation tests. The test specimen was bolted to a rigid steel plate in order to simulate the mounting arrangement used at DCPP. The function of the device was verified before and after the test. The test table response spectra have been verified to envelop the DDE and HE required response spectra.

The radiation detector associated with the Technical Associates radiation readout and the chlorine detector associated with the Capitol Controls chlorine analyzer have also

been submitted to random biaxial seismic simulation tests. These two detectors were mounted into a 14-inch steel duct in order to simulate the mounting arrangement used at the DCP. The function of the detectors was verified before and after the tests. The test response spectra envelops the required response spectra for both the DDE and HE cases. The chlorine detection function has been eliminated and the detectors are abandoned in place.

3.10.2.21 Subcooled Margin Monitors

The subcooled margin monitors (SCMMs) are located in PAM Panels 3 and 4. Subcooled margin is calculated and displayed by the reactor vessel level instrumentation system (RVLIS); therefore, seismic qualification of each SCMM is covered by the seismic qualification of the RVLIS cabinets (see Section 3.10.2.32.1).

Train A of the SCCM provides output to a recorder on PAM1. PAM1 seismic qualification is addressed in Section 3.10.2.22.

Train B of the SCCM provides output to a display on VB2. This display was qualified by testing.

3.10.2.22 Postaccident Monitoring Panels PAM1 and PAM2

These panels are located in the main control room and house various indicators and recorders used for postaccident monitoring. Typical parameters involved are reactor vessel level, containment hydrogen gas concentration, containment gross activity, etc. The panels were manufactured for PG&E by Trayer Engineering, Inc. Design Class I indicators and recorders were manufactured by Westinghouse and other qualified suppliers.

Panel PAM1, with its associated instruments, was qualified by random biaxial seismic simulation tests. The tests were performed at Wyle Laboratories. The function of the devices was verified before and after seismic testing. The test response spectra have been verified to envelop the DDE and HE required response spectra.

Panel PAM2 has been qualified by an analysis that showed that the panel is rigid, with no resonant frequencies below 33 Hz. In addition, a static analysis was performed that showed that the combined seismic stresses do not exceed the allowable limits. The Design Class I instruments mounted in PAM2 have been qualified by seismic simulation tests. The test response spectra obtained from these random biaxial tests have been verified to envelop the DDE and HE spectra.

3.10.2.23 Pilot Solenoid Valves

Pilot solenoid valves are used to control the air supply to air-operated control valves. The pilot valves can be mounted either on or off the control valve actuator. The

DCPP UNITS 1 & 2 FSAR UPDATE

required acceleration level for the pilot valves is 9 g's, which is based on the maximum allowable response for control valve actuators having Design Class I pilot valves.

The pilot solenoid valves have been qualified by tests performed on a variety of valve models by both the vendor, ASCO, and PG&E. The tests consisted typically of sine beat tests performed over the frequency range of 1 to 33 Hz. The minimum acceleration value met or exceeded the required level for the valves except at low frequencies, where the level was limited by testing machine capabilities. The function of the valves was verified before and after the testing.

3.10.2.24 Process Solenoid Valves

Design Class I process solenoid valves are used as containment isolation valves in the post-LOCA sampling system and containment hydrogen monitoring system. The valves were manufactured by Valcor Engineering.

The valves are located both inside and outside of containment. The valves inside containment are mounted to the annulus steel structure. The valves outside of containment are mounted to the exterior of the containment structure. The required acceleration level for the valves is an envelope of the DDE- and HE-required response spectra for both these locations.

The valves were qualified by a test performed by the vendor as part of an environmental qualification program. The test used a random biaxial input, with the devices mounted to the test table simulating an actual installation. The test procedure conformed with IEEE 344-1975. The test levels were sufficient to qualify the valves to their required acceleration level. The function of the valves was verified before and after the testing.

3.10.2.25 Containment Hydrogen Monitoring System

The containment hydrogen monitoring system (CHMS) consists of two redundant systems each consisting of an analyzer panel and a remote control panel. The analyzer panels are anchored to the floor in plant area GE at elevation 100 ft. The remote control panels for both systems are mounted in a panel (RCHMC) located in the post-LOCA sampling room in plant area GE at elevation 85 ft.

The Containment hydrogen monitoring system is Class II, Type C, Category 3, non safety related. The analyzer panels are Class II and anchorage of the analyzer panel has been seismically evaluated. Although the panel inserts for the Containment hydrogen monitor are non-safety related, the remote control panel (RCHMC) is Class I for the Class I circuits powering the related containment isolation valves.

The RCHMC panel has been structurally analyzed which includes the seismic mounting of non-safety related panel inserts. A detailed stress analysis was conducted that showed that the rack assembly is structurally adequate to withstand the DDE and HE loads.

3.10.2.26 Containment Purge Exhaust

Each monitor consists of a detector assembly and a Local Radiation Processor (LRP) located in Area L on the 100 ft elevation. The remote readout is located in the Radiation Monitoring System panel (RNRMS) in the Control Room. The detectors and LRPs are qualified by analysis based on a test simulation performed on similar equipment. The Control Room mounted equipment is qualified based on shaketable tests on the RNRMS panels performed for Victoreen. See Section 3.10.2.1.1.1.

3.10.2.27 Limit Switches

Limit switches are used to detect the position of control valves. Limit switches for motor-operated valves that are an integral part of the actuator are qualified as part of the assembly (see Section 3.10.2.19). Limit switches for air-operated valves and for motor-operated valves that are mounted on the valve actuator are qualified separately. The required acceleration level for these limit switches is 9 g, which is based on the maximum response allowable for valves having Class 1E limit switches.

Class 1E limit switches have been qualified by testing performed on several different styles. Tests have been performed by both the vendor and PG&E. These tests typically consisted of sine beats or sine dwells at 9 g peak acceleration over the frequency range of 1 to 33 Hz. Test acceleration levels met or exceeded the required level except at low frequency ranges where the level was limited to test machine capabilities. The test specimens were functionally tested before and after the vibration testing.

3.10.2.28 Containment High-Range Radiation Monitoring System

The containment high-range radiation monitoring system is used to monitor ambient gamma radiation in the containment following a LOCA. The system consists of two redundant detectors located in the containment at elevation 145 ft and a remote readout located in the postaccident monitoring panel PAM2 in the main control room. The system was supplied and qualified by Victoreen.

The radiation detectors and readouts have been qualified by random biaxial seismic simulation tests that were conducted as part of an environmental qualification test program. The test response spectra have been verified to envelop the required DDE and HE response spectra. There were no malfunctions experienced throughout the seismic tests. The test conformed to IEEE 344-1975.

3.10.2.29 Pressurizer Safety Relief Valve Position Indication

The pressurizer safety relief valve position indication system is an acoustic flow detection system that verifies valve position by sensing flow through the pressurizer relief lines. There are three channels, one for each relief valve. The system consists of four components: detector, charge converter, signal conditioner, and remote readout.

DCPP UNITS 1 & 2 FSAR UPDATE

The detector is an accelerometer attached to the pressurizer relief line by a metal strap. The charge converters for all three channels are housed in a stainless steel enclosure, which is mounted to the wall adjacent to the pressurizer at elevation 145 ft in the containment. The signal conditioner is located in panel RCRM in the main control room. The remote readout is mounted in the main control board. All components of the system were supplied and qualified by Technology for Energy Corporation.

The equipment comprising the system was qualified as part of an environmental qualification program conducted by the vendor. The seismic portion of the testing was conducted in accordance with IEEE 344-1975. All of the system components were qualified by tests consisting of random input, independent triaxial excitation. Tests were conducted at Structural Dynamics Research Corporation. The test response spectra from these tests have been verified to envelop the applicable DDE and HE spectra. The function of the devices was verified before and after the testing.

3.10.2.30 Heating, Ventilating, and Air Conditioning Equipment

The qualification of safety-related heating, ventilating, and air conditioning (HVAC) equipment is reviewed according to DE, DDE, and HE criteria. This HVAC equipment is associated with the following safety-related systems:

- (1) Forced draft shutter
- (2) Diesel generator compartment ductwork
- (3) Auxiliary saltwater compartment ventilation
- (4) 4-kV switchgear ventilation
- (5) 480 Vac switchgear ventilation
- (6) Auxiliary building-fuel handling building ventilation
- (7) Control room ventilation and pressurization system

The equipment and components of Class 1 HVAC systems are listed in Table 3.10-3. They have been reviewed for seismic qualification in accordance with the spectra, defined in Section 3.7.

The equipment listed in the table is organized into qualifying groups consisting of similar types of equipment. The component subject to the worst-case qualifying condition in each group has been reviewed for compliance with acceptance criteria. This worst-case analysis in turn envelops the other components in the respective groups.

All the items in the table were reviewed for identification of the qualifying spectra. Where the most current spectra exceed the conditions under which the component was

previously analyzed, a new analysis was initiated. The results of the analysis confirmed the qualification of the component or identified a physical modification. Where analysis is not appropriate, equipment testing was used to demonstrate the design performed under the qualifying seismic conditions.

3.10.2.30.1 HVAC Duct and Duct Supports

The Class I HVAC duct system consists of ducts and approximately 2,000 supports in both units. HVAC ducts are made of cold-formed steel conforming to ASTM A525, A526, and A527 with the thickness varying depending upon the duct size. The duct supports are mostly structural steel angles. Supports are attached to concrete or structural steel by bolted connections or by welding. The ducts are fastened to the supports by means of screws, rivets, or stitch welds.

3.10.2.30.1.1 Design and Acceptance Criteria

The duct and duct supports are evaluated in their as-built condition to meet the following criteria:

Loading Combination

The ducts are evaluated for the concurrent dead weight, seismic load, and pressure load. The duct supports are evaluated for dead weight and seismic load. The pressure load is the negative operating pressure of the HVAC system and is not included in the evaluation of the duct supports. The seismic loads evaluated are DDE and HE loads. The horizontal component of seismic load (DDE or HE), either transverse or longitudinal to the ducts, that results in the highest stress in the member under consideration is combined, by absolute sum, with the stresses due to vertical seismic load. As an alternative, the seismic loads from each of the three directions are combined by SRSS method.

Response Acceleration of Support System

The applicable floor response spectra where the supports are located are used for evaluation of HVAC duct and duct supports. The corresponding horizontal spectra are combined, by absolute sum, with the corresponding torsional response, as appropriate.

Acceptance Criteria

The AISI "Specification for Design of Cold-formed Steel Structural Members" is used to evaluate the design of cold-formed steel members, and part 1 of the AISC "Specification for the Design, Fabrication, and Erection of Structural Steel for Buildings" is used for the design of hot-rolled members. The allowable stresses given in AISI and AISC Specification are increased by 60 percent.

3.10.2.30.1.2 Evaluation

For duct supports, the seismic loading is evaluated for vertical plus transverse horizontal loads and vertical plus longitudinal horizontal loads. The frequency of the coupled duct and duct support system is used in determining the spectral response. The damping values used are 2 percent for DDE and 7 percent for HE.

3.10.2.31 Electric Hydrogen Recombiner System

The model B electric hydrogen recombiner system (EHRS) is designed to control and reduce post-LOCA containment hydrogen levels. The system consists of three components; control panel, power supply, and recombiner. Two model B EHRSs are provided for the DCPP site.

The recombiner was subjected to multiple frequency multiple axis testing in accordance with IEEE 344-1975. The results of the seismic testing are provided in Reference 25. The recombiner was energized and at operating temperature before, during, and after each seismic test. Following the entire testing, the recombiner was inspected for damage. No disabling damage was found. An air flow test was conducted after testing and the results show no loss of air flow. The test response spectra were checked to envelope the DDE and HE response spectra, to confirm its seismic adequacy.

The power supply and control panel were tested at the same time as documented in Reference 26. Testing was done with conservatively large accelerations over a range of applicable frequencies and conformed to the procedures given in IEEE 344-1971. The peak test input accelerations used in the power supply and control panel tests were checked to verify that they are larger than the requirements derived by DDE and HE loadings.

After each seismic test the power supply was visually inspected for structural integrity and functional operability. Both units were found to operate satisfactorily.

3.10.2.32 Reactor Vessel Level Instrumentation System

The RVLIS consists of the following instrumentation:

- RVLIS/incore thermocouple cabinets (including remote display)
- Reactor coolant level differential pressure transmitters (see Section 3.10.1.5)
- Surface mounted RTDs
- High volume sensors
- Differential pressure indicating switches (hydraulic isolators)

Typical items of the above instrumentation and electronic equipment have been type tested using multiple frequency, multiple axis seismic testing. Testing was performed in accordance with the procedures given in IEEE 344-1975. The test response spectra

obtained from those tests were checked to envelope the DDE and HE response spectra.

3.10.2.32.1 RVLIS/Incore Thermocouple Cabinets

Two RVLIS/incore thermocouple cabinets (PAMs 3 and 4) are provided for DCPP application. Located within each cabinet are the microprocessor electronics, reactor coolant pump (RCP) status panel, and a remote display. The above RVLIS instrumentation is only required to operate normally before and after seismic excitation. The RCP status panel assembly is shown to be operational by the signals recorded during testing and the functional checks made after each simulated SSE. The remote display electronics must function normally by providing microprocessor output display formatted information.

The results of seismic testing of the original RVLIS/incore thermocouple cabinets are provided in Reference 27. The original remote display was not included in the cabinet tested. The original remote display was tested later to worst-case (maximum) in-cabinet response for the RVLIS/incore thermocouple cabinets. The seismic testing of the original remote display is documented in Reference 28.

Because the original Westinghouse-supplied system is obsolete and due to the lack of availability of replacement components, the obsolete RVLIS/incore thermocouple systems were replaced. The replacement processors, signal conditioners, and displays are seismically qualified by testing and analysis as documented in References 47, 48, 54 and PG&E Calculation IS-66.

3.10.2.32.2 Surface Mounted RTDs

There are 14 surface mounted RTDs used in RVLIS to measure the temperature of the reference leg impulse lines. As described in Reference 29, the surface mounted RTDs were subjected to single frequency, multiple axis sinusoidal tests and multiple frequency, multiple axis seismic tests. The RTDs tested were operational throughout all phases of the test sequence. Measurement of performance was by a evaluation of the recorded RTD output, periodic static calibrations, and numerous insulation surface mounted RTDs maintain their structural integrity and functional accuracy required.

3.10.2.32.3 High Volume Sensors

The high volume sensors are bellows designed for large volumetric displacement to accommodate thermal expansion postulated postaccident environment. The safety related performance requirement is that the sensor must maintain this pressure boundary and sensing interface between the process and filled pressure/differential pressure system without introducing any sensing errors.

The results of seismic testing are provided in Reference 30. Based upon the information provided therein, the high volume pressure sensor can successfully fulfill its safety related requirements during and after seismic testing.

3.10.2.32.4 Differential Pressure Indication Switches

The differential pressure indicating switches (hydraulic isolators) are used to seal off full process pressure in either direction and will actuate switches to indicate a unbalanced condition. The safety-related performance requirement for RVLIS is that the switch provide the isolation function without contributing a sensing error to the accuracy of a downstream pressure of differential pressure transmitter.

During the seismic test, adherence to this requirement is verified by monitoring the output of two reference transmitters receiving the pressure signal. While no safety related use is made of the switch contacts in the reactor vessel level indicating system, testing was designed to demonstrate the suitability of indicating switch use for other applications.

Seismic testing of the hydraulic isolators is provided in Reference 31. The hydraulic isolators sustained no physical damage during the seismic testing and performed their process sensing line isolation function successfully, with no leakage of the water fill.

3.10.2.33 Incore Flux Mapping Cabinets and Transfer Device

The incore flux mapping cabinets and flux mapping transfer device are non-safety related but have been seismically qualified for structural integrity for HE loadings.

The incore flux mapping cabinet is structurally identical to the NIS cabinets (see Section 3.10.2.1.1). The weight distribution of equipment within the cabinet would produce essentially the same dynamic results. Therefore the results obtained from the test of the NIS cabinets are applicable for the incore flux mapping cabinet structure.

The flux mapping transfer device is an assembly used to support control equipment to drive detectors into and out of thimbles in the reactor core. The flux mapping transfer device has been evaluated to maintain its structural integrity to withstand the HE for DCPP.

3.10.3 REFERENCES

1. The Institute of Electrical and Electronic Engineers, Inc., IEEE Standard 344-1971, Trial Use Guide For Seismic Qualification of Class I Electric Equipment for Nuclear Power Generating Stations.
2. IEEE Standard 344-1975, Recommended Practices for Seismic Qualification of Class IE Equipment for Nuclear Power Generating Stations.

DCPP UNITS 1 & 2 FSAR UPDATE

3. USNRC RG 1.100, Revision 1, Seismic Qualification of Electrical Equipment for Nuclear Power Plants, August 1977.
4. Description of the Systems Interactions Program for Seismically Induced Events, Revision 4, August 1980.
5. Seismic Testing of Electrical and Control Equipment (PG&E Plants), WCAP-8021, May 1973.
6. Letter No. NS-CE-1609, Eicheldinger (Westinghouse) to Stolz (NRC), Subject: "Drawer Securing Method for NIS Rack," November 1977.
7. Seismic Operability Demonstration Testing of the Nuclear Instrumentation System Bistable Amplifier, WCAP-8830, October 1976.
8. General Method of Developing Multifrequency Biaxial Test Inputs for Bistables, WCAP-8624, September 1975.
9. Consequences of Seismic-Induced Actuation of Protection Systems Relays on the Diablo Canyon Nuclear Plant, Westinghouse Electric Corporation, July 1975.
10. Seismic Qualification of the Rotary Relay for Use in the Solid State Protection System, WCAP-8694, January 1976.
11. Deleted in Revision 21.
12. Deleted.
13. Seismic Testing of Electrical and Control Equipment, High Seismic Plants, WCAP-8921, December 1971.
14. Equipment Qualification Test Report Pressure Sensor, WCAP-8687, Supplement 2-E21A, Revision 1, March 1982.
15. Equipment Qualification Test Report Barton Differential Pressure Transmitter - Qualification Group B, WCAP-8687, Supplement 2-E04A, Revision 2, March 1983.
16. Seismic Testing of Electrical and Control Equipment, Type DB Reactor Trip Switchgear, WCAP-8821, Supplement 4, August 1974.
17. Deleted.
18. Deleted.

DCPP UNITS 1 & 2 FSAR UPDATE

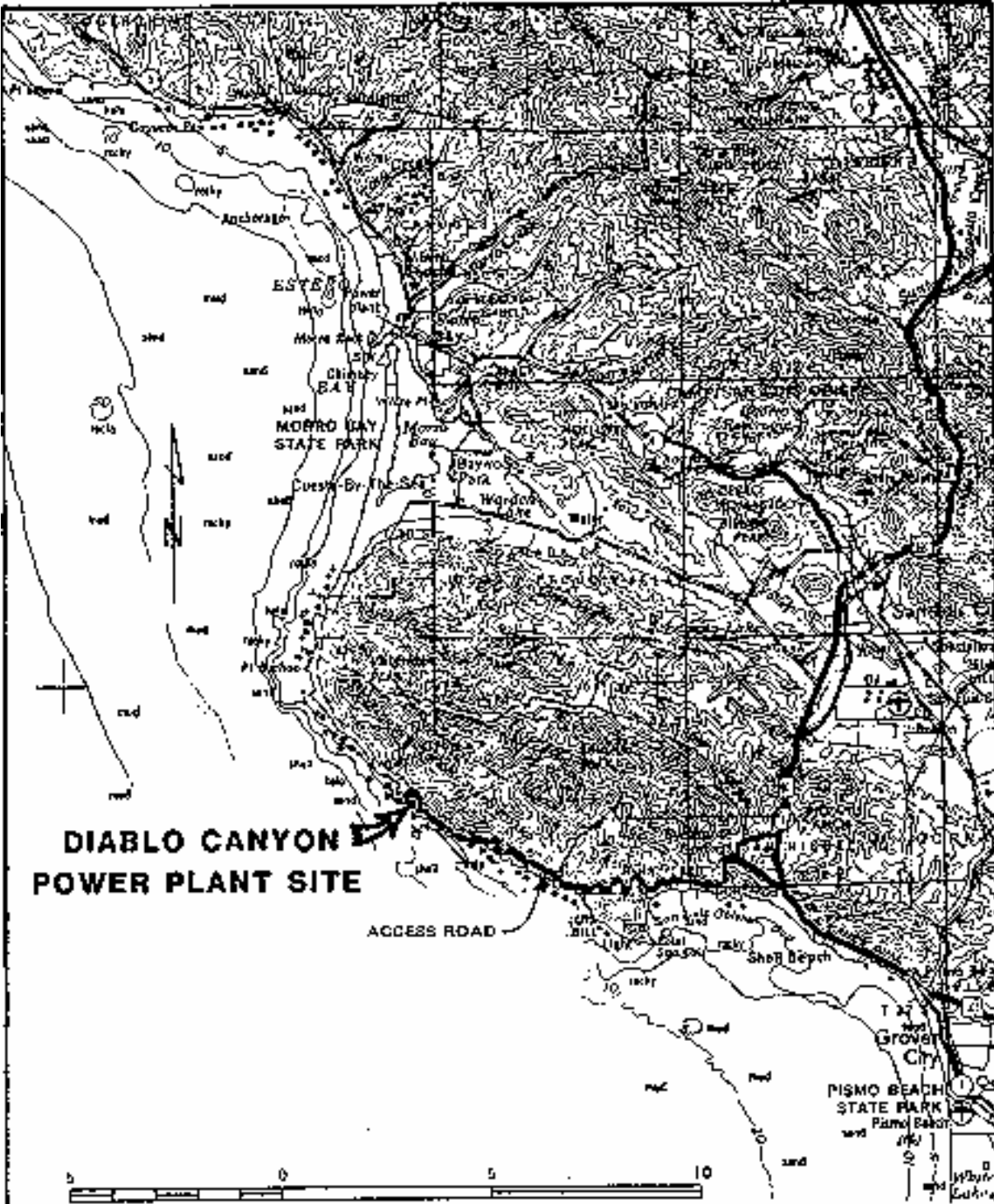
19. Seismic Testing of Electrical and Control Equipment Engineering Safeguards Test Cabinet for PG&E Plants, WCAP-8021, Supplement 1, May 1977.
20. Seismic Qualification of the Rotary Relay for Use in the Trojan and Diablo Canyon Auxiliary Safeguard Cabinets, WCAP-8941, February 1977.
21. Seismic Qualification of the Diablo Canyon Main Control Board, Central Console, WCAP-10358, August 1983.
22. Benchmark Problem Solutions Employed for Verification of the WECAN Code, WCAP-8929, June 1977.
23. Forced Vibration Testing of the Diablo Canyon Unit 1 Main Control Board, ANCO Engineers Inc., Document No. A-000047, May 1983.
24. Seismic Qualification Test Report for Diablo Canyon Main Control Board and Central Console Mounted Class 1E Devices, WCAP-8941, February 1977.
25. Qualification Testing for Model B Electric Hydrogen Recombiner, WCAP-9346, July 1978.
26. Electric Hydrogen Recombiner for PWR Containments Equipment Qualification Report, WCAP-7709-L, Supplement 2, September 1973.
27. Equipment Qualification Test Report, Reactor Vessel Level Instrumentation System/Incore Thermocouple Cabinet With 8080 Microprocessor Electronics and Reactor Cabinet Pump Station Panel, WCAP-8687, Supplement 2-E51A, July 1984.
28. Equipment Qualification Test Report, Remote Digital Display for the 8080 Microprocessor Electronics, WCAP-8687, Supplement 2-E46A, July 1984.
29. Equipment Qualification Test Report, Surface Mounted RTDs, WCAP-8687, Supplement 2-E48A, January 1983.
30. Equipment Qualification Test Report, High Volume Sensor-Group A, WCAP-8687, Supplement 2-E48A, January 1983.
31. Equipment Qualification Test Report, Differential Pressure Indicating Switch-Group, WCAP-8687, Supplement 2-E49A, January 1983.
32. American Iron and Steel Institute, Specification for the Design of Cold-Rolled Steel Structural Members, AISI, Washington, D.C., 1968.

DCPP UNITS 1 & 2 FSAR UPDATE

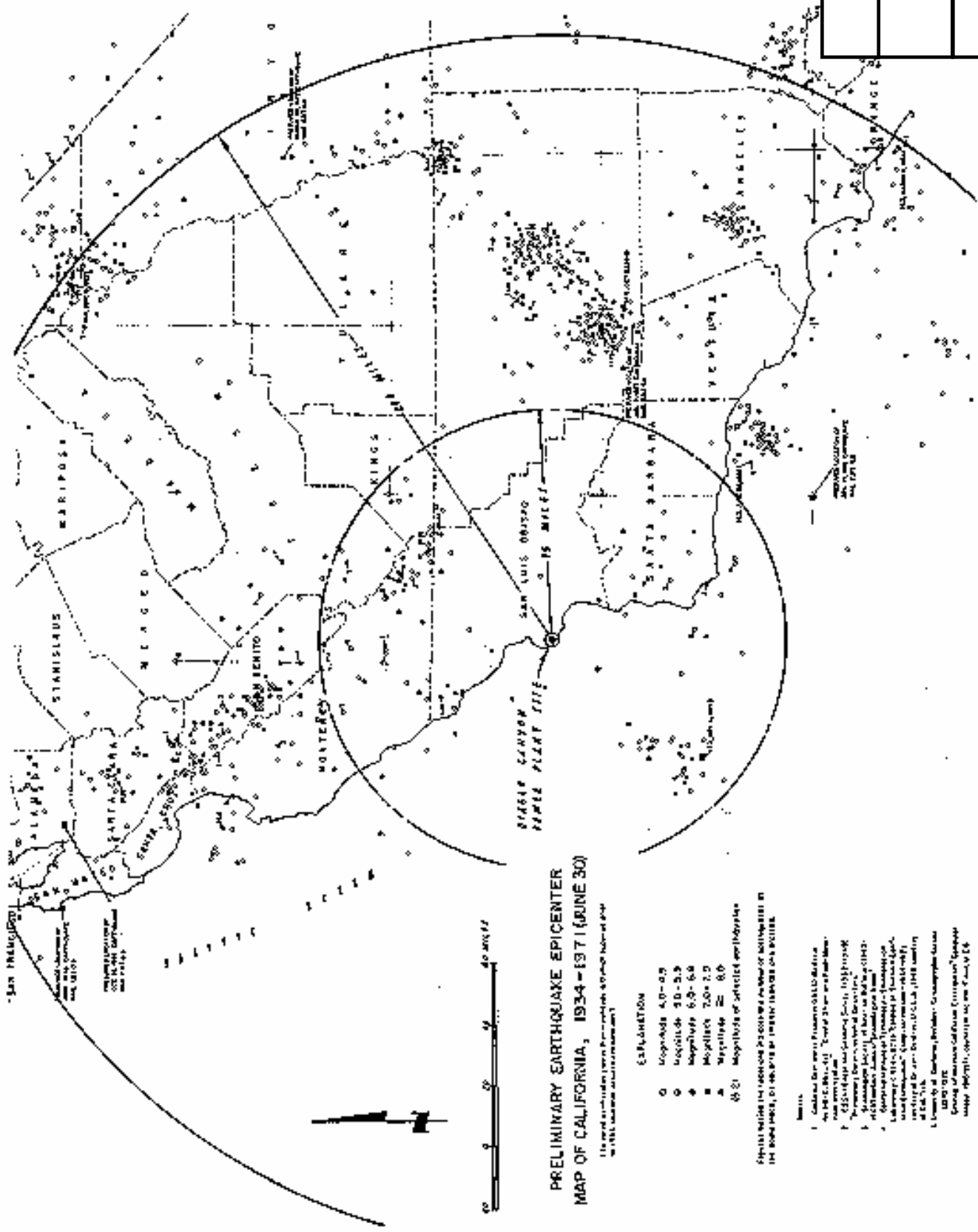
33. American Institute of Steel Construction, *Specification for the Design, Fabrication and Erection of Structural Steel for Buildings*, AISC, Chicago, IL, Seventh Edition.
34. Office of Nuclear Reactor Regulation, *Standard Review Plan*, Section 3.8.4, NRC, Washington, D.C. (November 1975).
35. *Seismic Confirmation of Weed Resistance Temperature Detectors For Diablo Canyon Unit 1 and Unit 2 Bypass Elimination System*, WCAP-12714, Revision 2, February 1993.
36. *Seismic Qualification Test Report of Class IE RTD and Thermocouple Temperature Sensors for Conax Corp.*, Report No. IPS-1165, Rev. A, June 18, 1984.
37. Rosemount Report D8400102, *Qualification Report for Pressure Transmitter Model 1154*, (PG&E DC 6000784-117).
38. Rosemount Report D8300040, *Qualification Report for Pressure Transmitters Rosemount Model 1153 Series D*, (PG&E DC 6000784-7-1).
39. PG&E Seismic Calculation No. IS-35, "Seismic Qualification of Rosemount Transmitters."
40. *Equipment Qualification Test Report, Eagle 21 Process Protection System (Environmental and Seismic Testing)*, WCAP-8687, Supplement 2-E69A, Revision 0, May 1988.
41. *Equipment Qualification Test Report, Eagle 21 Process Protection System (Environmental and Seismic Testing)*, WCAP-8687, Supplement 2-E69B, Revision 0, February 1990.
42. *Equipment Qualification Test Report, Eagle 21 Process Protection System (Environmental and Seismic Testing)*, WCAP-8687, Supplement 2-E69C, Revision 0, February 1991.
43. *Seismic Qualification of Electrical Equipment for Nuclear Power Plants*, NRC Regulatory Guide 1.100, Revision 2, June 1988.
44. *Recommended Practices for Seismic Qualification of Class 1E Equipment for Nuclear Power Generating Stations*, IEEE 344-1987.
45. *Seismic Confirmation of Eagle 21 Digital Process Protection System Upgrade for Pacific Gas and Electric Company Diablo Canyon Power Plant Units 1 and 2*, WCAP-13384, Revision 0, PG&E, September 1992.

DCPP UNITS 1 & 2 FSAR UPDATE

46. PG&E Specification 1021-J-NPG, "Specification for Furnishing and Delivering Remote Multiplexer and Visual Annunciator Equipment Associated with the Main Annunciator Systems for Diablo Canyon Power Plant, Units 1 and 2."
47. Trentec Test Report No. 8Q017.0, dated 11/98.
48. Altran Calculation No. 98250-C-001, Revision 0, dated May 1999.
49. PG&E Seismic Calculation No. ES-66, "Seismic Qualification of Westinghouse Supplied SSPS Cabinets."
50. PG&E Seismic Calculation No. IS-88, "Seismic Qualification of Model 3015C/3015N Rosemount Transmitters."
51. IEEE Standard 535-1986, IEEE Standard for Qualification of Class 1E Lead Storage Batteries for Nuclear Power Generating Stations.
52. USNRC RG 1.158, Revision 0, Qualification of Safety-Related Lead Acid Storage Batteries for Nuclear Power Plants, February 1989.
53. PG&E Seismic Calculation No. ES-15-1, "C&D Model LCUN-33 Vital Batteries and Two Steps Battery Rack."
54. QualTech Test Report No. S1203.0, Revision 0, dated 02/24/2012.
55. Triconex Tricon v10 Seismic Test Report Document No. 9600164-526, Revision 1.
56. Qualification of Rack Mounted Electrical Components at Process Control Racks RNO1A through RNO4D, Specification 10101-M-NPG, Revision 3.
57. NLI Qualification Report QR-01913272-1 Rev. 5(PG&E Document Number 663222-267).
58. NLI Supplemental Qualification Report SQR-01913272-1, Revision 3 (PG&E Document Number 663222-268).
59. Specification for Furnishing and Delivering Manual/Auto Stations for Diablo Canyon Power Plant Units 1 & 2 10083-J-NPG, Rev. 4.
60. AMS826, AMS826/1 and AMS826/2 Qualification Report Rev. 3 (PG&E Document Number 6021767-6).
61. AMS827 Qualification Report Rev. 2 (PG&E Document Number 6021767-8).



FSAR UPDATE
UNITS 1 AND 2 DIABLO CANYON SITE
FIGURE 2.5-1 PLANT SITE LOCATION AND TOPOGRAPHY



PRELIMINARY EARTHQUAKE EPICENTER
MAP OF CALIFORNIA, 1934-1971 (JUNE 30)

1:500,000 scale, U.S. Geological Survey, National Map
1:500,000 scale, U.S. Geological Survey, National Map

- EXPLANATION**
- Magnitude 4.0-4.9
 - Magnitude 5.0-5.9
 - Magnitude 6.0-6.9
 - Magnitude 7.0-7.9
 - ▲ Magnitude 8.0
 - ☆ Magnitude of selected earthquakes

Figures within the circles are dates of earthquakes in
the bold type, or dates of major shocks only.

- NOTES**
1. California Earthquake Catalogue, 1934-1971, U.S. Geological Survey, Bulletin 1450, 1972.
 2. California Earthquake Catalogue, 1934-1971, U.S. Geological Survey, Bulletin 1450, 1972.
 3. California Earthquake Catalogue, 1934-1971, U.S. Geological Survey, Bulletin 1450, 1972.
 4. California Earthquake Catalogue, 1934-1971, U.S. Geological Survey, Bulletin 1450, 1972.
 5. California Earthquake Catalogue, 1934-1971, U.S. Geological Survey, Bulletin 1450, 1972.
 6. California Earthquake Catalogue, 1934-1971, U.S. Geological Survey, Bulletin 1450, 1972.
 7. California Earthquake Catalogue, 1934-1971, U.S. Geological Survey, Bulletin 1450, 1972.
 8. California Earthquake Catalogue, 1934-1971, U.S. Geological Survey, Bulletin 1450, 1972.
 9. California Earthquake Catalogue, 1934-1971, U.S. Geological Survey, Bulletin 1450, 1972.
 10. California Earthquake Catalogue, 1934-1971, U.S. Geological Survey, Bulletin 1450, 1972.

FSAR UPDATE

UNITS 1 AND 2

DIABLO CANYON SITE

FIGURE 2.5-2

EARTHQUAKE EPICENTERS

WITHIN 200 MILES OF PLANT SITE

EXPLANATION

EARTHQUAKE EPICENTER DATA

UNDETERMINATELY LOCATED AND CLASSIFIED SUBSEQUENTLY AS EARTHQUAKE EPICENTERS WITHIN 75 MILES OF THE DIABLO CANYON NUCLEAR PLANT SITE, 1940-1974

SYMBOL	MAGNITUDE
■	7.0-7.9
●	6.0-6.9
○	5.0-5.9
□	4.0-4.9
×	3.0-3.9
+	2.0-2.9

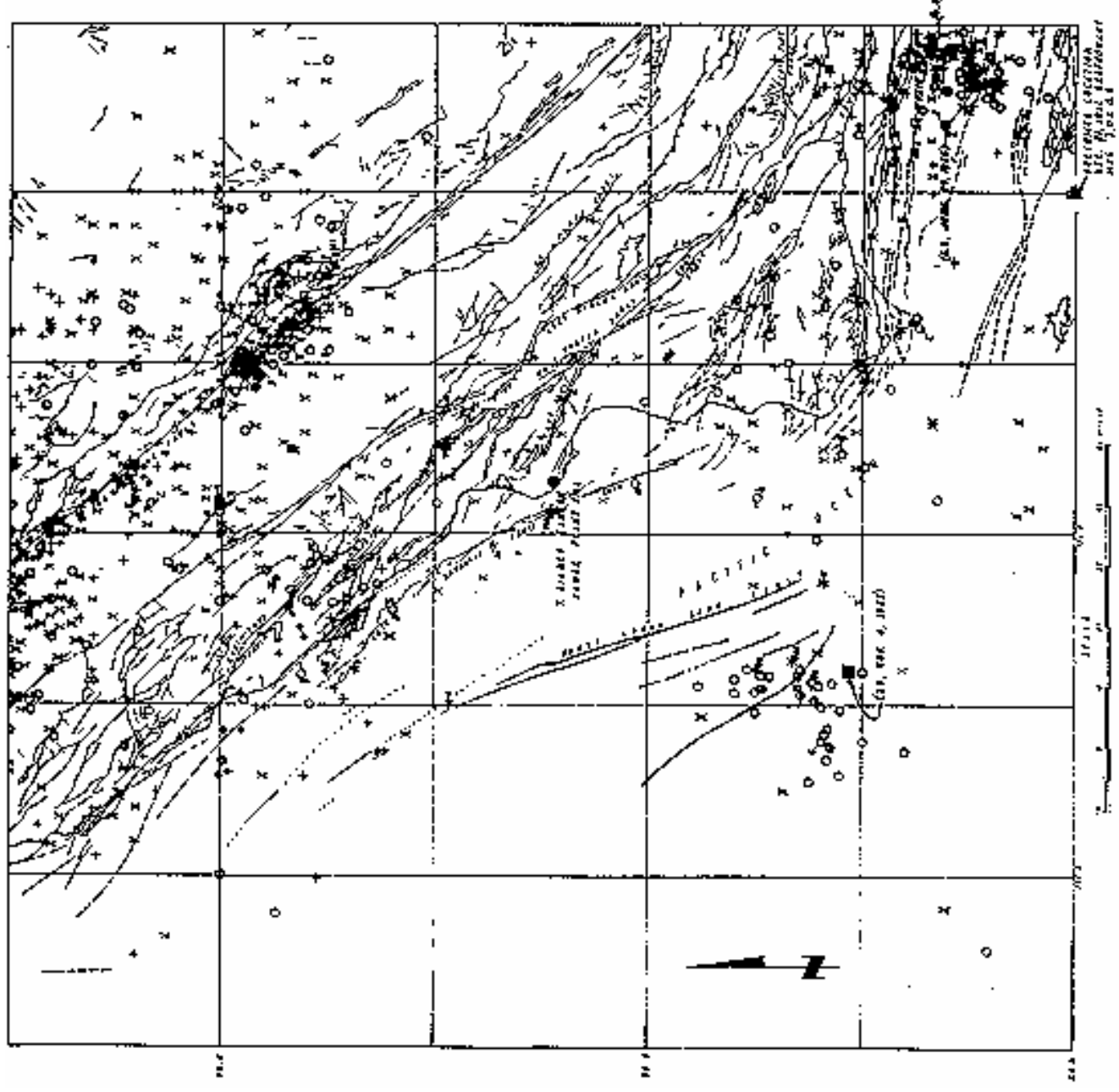
(SYMBOLS WITHIN BRACKETS OF LOCATIONS OF EPICENTERS AT LAMB LOCATION)

BOUNDARIES FOR FAULTS AND EARTHQUAKE EPICENTERS WITH ARE AS FOLLOWS:

1. FAULT LINE FROM JENNINGS, C. W., 1972, GEOTOPIC MAP OF CALIFORNIA, 1:500,000 SCALE, (CALIFORNIA)
2. THE EARTHQUAKE OF 2.0-2.9 MAGNITUDE OCCURRING ALONG THE TONGUE MOUNTAIN FROM JUNE 30, 1974, CALIFORNIA DIVISION OF MINES AND GEOTHERMAL ENERGY, EARTHQUAKE EPICENTER MAP, FILE # 1-100,000, 1974
3. THE EARTHQUAKE OF 2.0-2.9 MAGNITUDE OCCURRING ALONG THE TONGUE MOUNTAIN FROM JUNE 30, 1974, CALIFORNIA DIVISION OF MINES AND GEOTHERMAL ENERGY, EARTHQUAKE EPICENTER MAP, FILE # 1-100,000, 1974
4. THE EARTHQUAKE OF 2.0-2.9 MAGNITUDE OCCURRING ALONG THE TONGUE MOUNTAIN FROM JUNE 30, 1974, CALIFORNIA DIVISION OF MINES AND GEOTHERMAL ENERGY, EARTHQUAKE EPICENTER MAP, FILE # 1-100,000, 1974
5. THE EARTHQUAKE OF 2.0-2.9 MAGNITUDE OCCURRING ALONG THE TONGUE MOUNTAIN FROM JUNE 30, 1974, CALIFORNIA DIVISION OF MINES AND GEOTHERMAL ENERGY, EARTHQUAKE EPICENTER MAP, FILE # 1-100,000, 1974

LOCATIONS OF FAULTS AND EPICENTERS DATA

- A. FAULT DATA BASED ON APPROPRIATE MAPS, FIGURE 5, APPENDIX 2.50
- B. EARTHQUAKE OF 2.0-2.9 MAGNITUDE OCCURRING ALONG THE TONGUE MOUNTAIN FROM JUNE 30, 1974, CALIFORNIA DIVISION OF MINES AND GEOTHERMAL ENERGY, EARTHQUAKE EPICENTER MAP, FILE # 1-100,000, 1974
- C. EARTHQUAKE OF 2.0-2.9 MAGNITUDE OCCURRING ALONG THE TONGUE MOUNTAIN FROM JUNE 30, 1974, CALIFORNIA DIVISION OF MINES AND GEOTHERMAL ENERGY, EARTHQUAKE EPICENTER MAP, FILE # 1-100,000, 1974



FSAR UPDATE

UNITS 1 AND 2

DIABLO CANYON SITE

FIGURE 2.5-3

FAULTS AND EARTHQUAKE EPICENTERS

WITHIN 75 MILES OF PLANT SITE

(FOR EARTHQUAKES WITH ASSIGNED

MAGNITUDES)

EXPLANATION

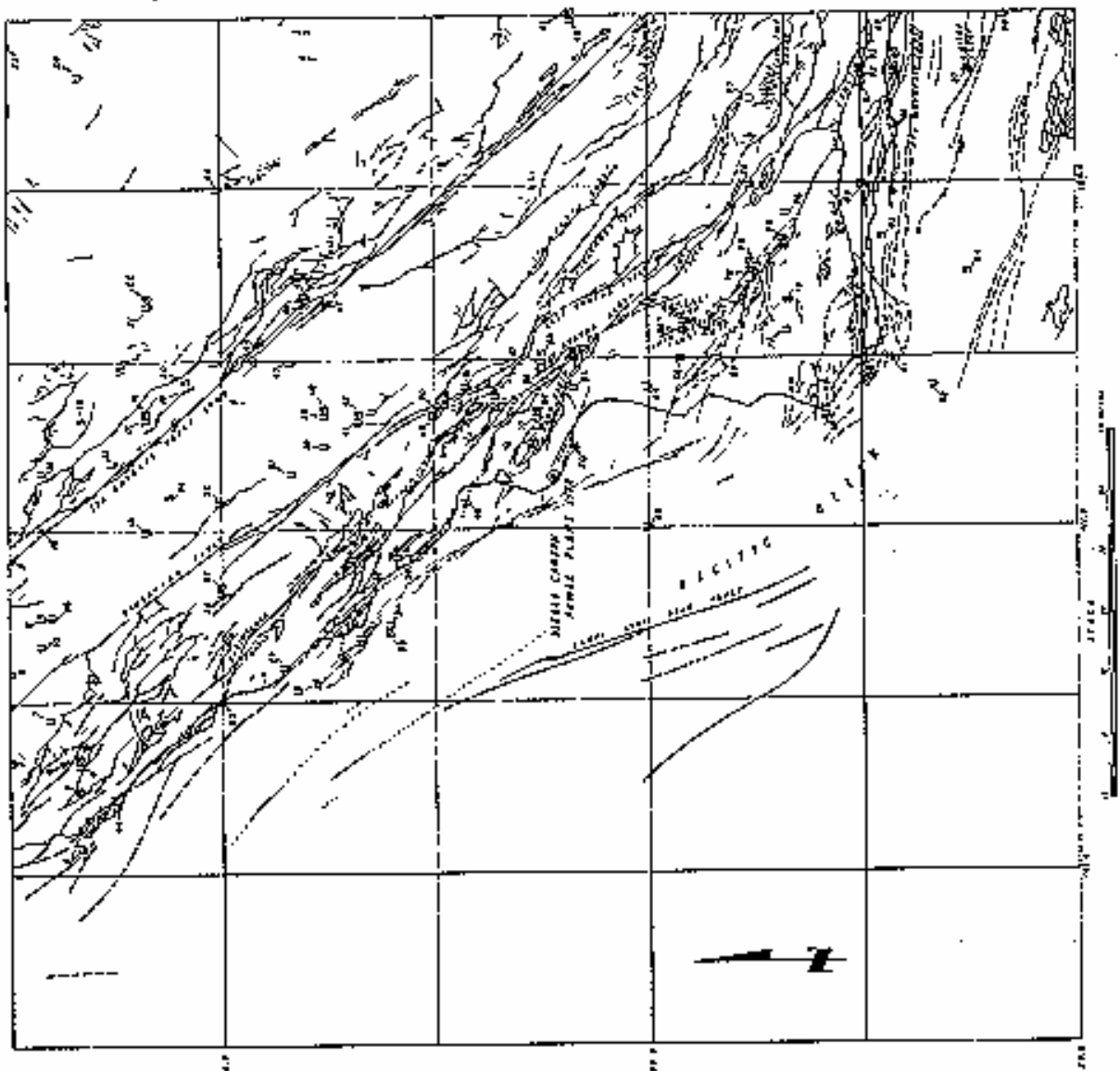
- 1. MAXIMUM INTENSITY 2 III
- 2. MAXIMUM INTENSITY 4 III
- 3. MAXIMUM INTENSITY 5 III
- 4. MAXIMUM INTENSITY 6 III

1. MAXIMUM INTENSITY 2 III
 2. MAXIMUM INTENSITY 4 III
 3. MAXIMUM INTENSITY 5 III
 4. MAXIMUM INTENSITY 6 III

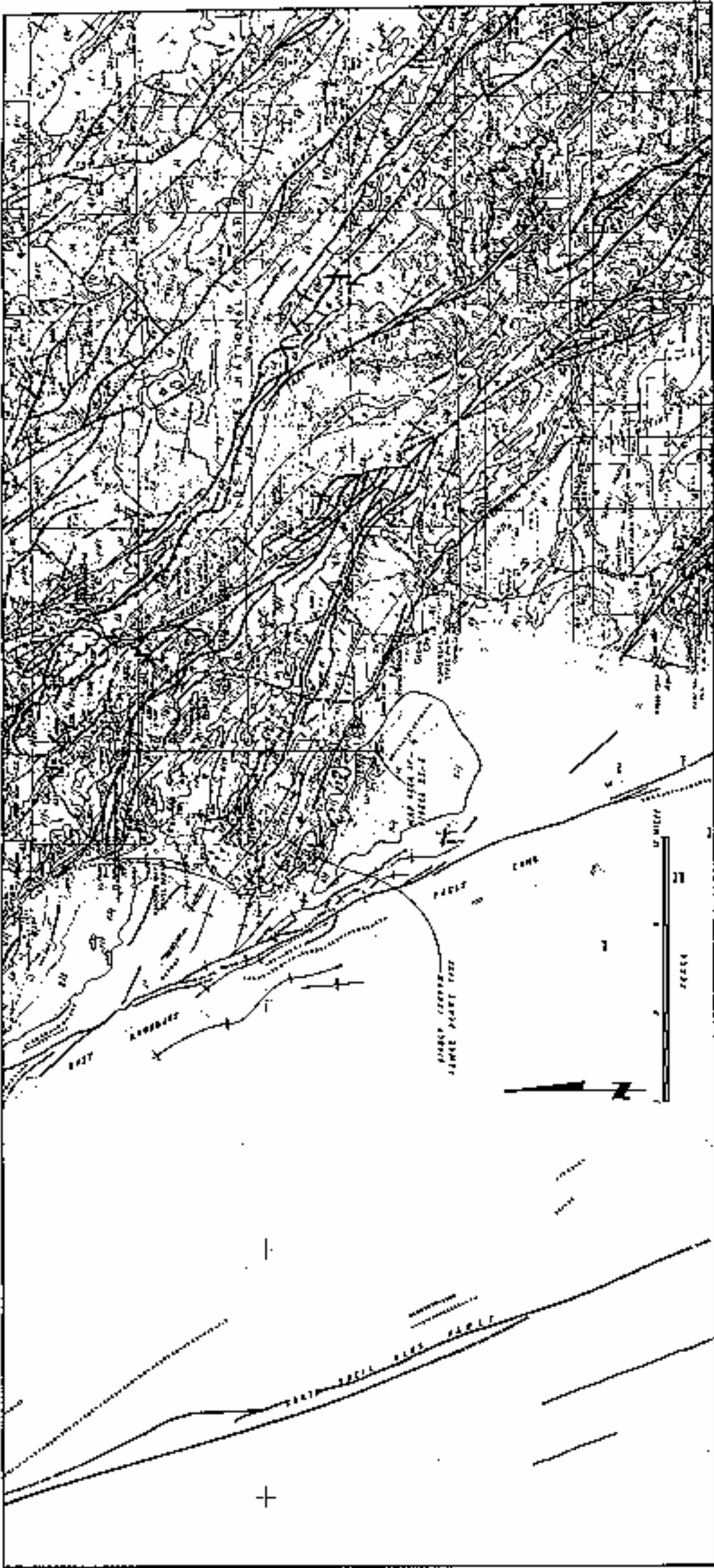
1. MAXIMUM INTENSITY 2 III
 2. MAXIMUM INTENSITY 4 III
 3. MAXIMUM INTENSITY 5 III
 4. MAXIMUM INTENSITY 6 III

1. MAXIMUM INTENSITY 2 III
 2. MAXIMUM INTENSITY 4 III
 3. MAXIMUM INTENSITY 5 III
 4. MAXIMUM INTENSITY 6 III

1. MAXIMUM INTENSITY 2 III
 2. MAXIMUM INTENSITY 4 III
 3. MAXIMUM INTENSITY 5 III
 4. MAXIMUM INTENSITY 6 III



FSAR UPDATE
UNITS 1 AND 2
DIABLO CANYON SITE
FIGURE 2.5-4
FAULTS AND EARTHQUAKE EPICENTERS
WITHIN 75 MILES OF PLANT SITE
(FOR EARTHQUAKES WITH ASSIGNED
INTENSITIES ONLY)



FSAR UPDATE

UNITS 1 AND 2
DIABLO CANYON SITE

FIGURE 2.5-5
GEOLOGIC AND TECTONIC MAP OF
SOUTHERN COAST RANGES IN THE
REGION OF PLANT SITE
(SHEET 1 OF 2)

EXPLANATION

GEOLOGIC UNITS

GEOLGIC

TERTIARILY DEPOSITED AND ROCKS

- Q** MIOCENE AND PLEISTOCENE NORMALIVE (COASTAL ALLUVIAL AND MARINE DEPOSITS, UNDIVIDED)
- Q1** LARKS SANDSTONE, WRECK MAPPER TERRACE
- Q2** DEEP TANK DEPOSIT, WRECK MAPPER TERRACE
- Q3** CLIP-PLATEAU AND ALLUVIAL TERRACE
- P** PLEISTOCENE MARINE
- M** MIOCENE MARINE
- Mc** OCEANIC NORMALIVE
- E** COCENE MARINE
- Ep** PALEOCENE MARINE

PLASCIC ROCKS

- Tp** TERTIARY VOLCANIC ROCKS
- TpP** TERTIARY PORPHYRITIC ROCKS (INCLUDING VOLCANIC MOUNTAIN PLATEAU)
- Tc** TERTIARY INTERTIVE ROCKS

SYMBOLS

GEOLGIC CONTACT, SHOWN WHERE APPROXIMATE OR WHERE QUANTITATIVE DATA ARE AVAILABLE.

Fault (FOLD LINE WHERE LOCATION IS WELL DEFINED; DOTTED LINE WHERE APPROXIMATE OR INFERRED; DOTTED WHERE CONTACTS.

ANTICLINAL AXIS - WITH PLUNGE INDICATED. (SOLID LINE WHERE LOCATION IS WELL DEFINED; DOTTED WHERE APPROXIMATE OR INFERRED; DOTTED WHERE CONTACTS.

SYMBOLIC AXIS - WITH PLUNGE INDICATED. (SOLID LINE WHERE LOCATION IS WELL DEFINED; DOTTED WHERE APPROXIMATE OR INFERRED; DOTTED WHERE CONTACTS.

MESOZOIC

SEDIMENTARY AND METAMORPHIC ROCKS

- Ku** UPPER CRETACEOUS MARINE ROCKS
- Kl** LOWER CRETACEOUS MARINE ROCKS
- Kv** FRANCHISEAN LITHOMARINE (PREDOMINANTLY SEDIMENTARY AND METAMORPHIC ROCKS INCLUDING STRATIGRAPHIC MESSAGES)
- J** JURASSIC MARINE ROCKS (INCLUDING EXTENSIVE FORMATION)
- Ti** METAMORPHIC ROCKS OF PRE-YUCATANIC AGE, UNDIVIDED

METAFASCIC ROCKS

- Mp** MESOZOIC METAFASCIC ROCKS (INCLUDING FRANCHISEAN SEDIMENTARY ROCKS)
- Pl** PLATONIC ROCKS
- Gr** MESOZOIC GRANITIC ROCKS
- Um** MESOZOIC METAMORPHIC ROCKS

NOTES

1. MAP AREA FROM PARTS OF SAN JOSE COUNTY AND SANTA BARBARA COUNTY, U.S. GEOLOGICAL SURVEY (SCALE 1:50,000) AND PARTS OF

2. GEOLGIC DATA FROM:

"GEOLOGIC MAP OF CALIFORNIA" 1:50,000 SCALE 1:50,000, PRELIMINARY, ANNEBOROUGH, CALIFORNIA DIVISION OF MINING AND GEOLOGY (COMPILED BY C.W. JENNINGS) LOCALLY IMPROVED WITH DATA FROM:

BEAULIEU, L.A., 1945, GEOLGIC OF THE COASTAL PARTS OF SAN JOSE COUNTY, SAN JOSE COUNTY, CALIFORNIA, U.S. GEOLOGICAL SURVEY (SCALE 1:50,000); JONES, L.A., 1945, GEOLGIC OF THE DIABLO CANYON AREA, SAN JOSE COUNTY, CALIFORNIA, U.S. GEOLOGICAL SURVEY (SCALE 1:50,000); JONES, L.A., 1945, GEOLGIC OF THE DIABLO CANYON AREA, SAN JOSE COUNTY, CALIFORNIA, U.S. GEOLOGICAL SURVEY (SCALE 1:50,000); TO THE PACIFIC GAS AND ELECTRIC COMPANY.

WALL, C.A., 1971, U.S.G. MAP OF SA, EARTH SCIENCE ASSOCIATES, 1974, OFFSHORE INVESTIGATION,

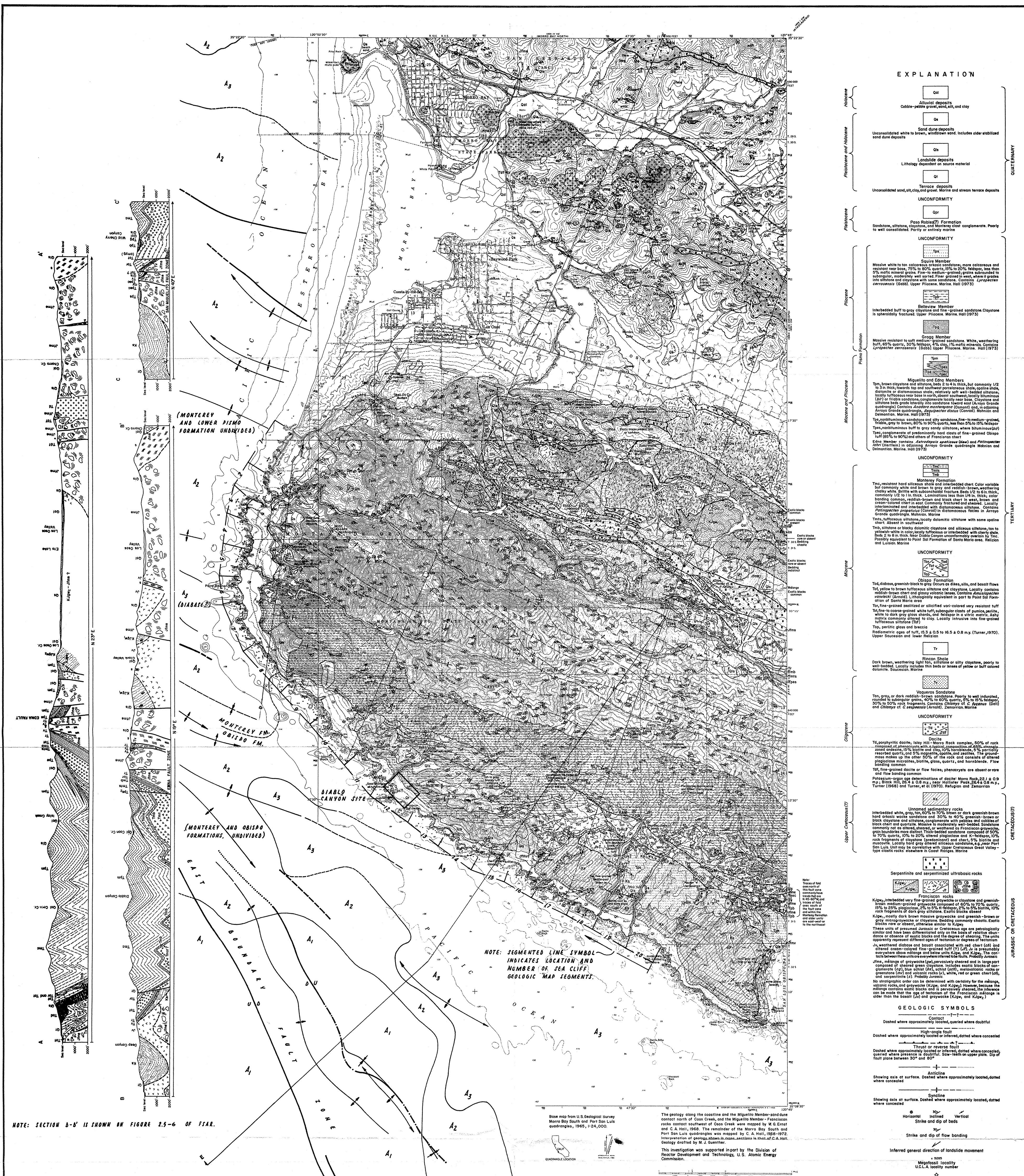
FSAR UPDATE

UNITS 1 AND 2

DIABLO CANYON SITE

FIGURE 2.5-5

GEOLOGIC AND TECTONIC MAP OF SOUTHERN COAST RANGES IN THE REGION OF PLANT SITE (SHEET 2 OF 2)



GEOLOGIC MAP OF THE MORRO BAY SOUTH AND PORT SAN LUIS QUADRANGLES, SAN LUIS OBISPO COUNTY, CALIFORNIA

EXPLANATION FOR GEOLOGIC MAP OF THE OFFSHORE AREA

MAP UNITS

MAP ACOUSTIC UNIT

- A₁
- A₂
- A₃

STRATIGRAPHIC EQUIVALENT

UPPER PART OF DISMO FORMATION (ABOVE MIGUELITO AND EDNA NUMBERS).

MONTEREY FORMATION AND LOWER PART OF DISMO FORMATION (MIGUELITO AND EDNA NUMBERS), INCLUDES OBISPO FORMATION IN THE AREA OFFSHORE FROM DIABLO CANYON.

FRANCISCAN AND GREAT VALLEY SEQUENCE BASEMENT ROCKS, UNDIVIDED. LOCALLY MAY INCLUDE SOME OBISPO FORMATION.

MAP SYMBOLS

- CONTACT, DASHED WHERE POORLY CONTROLLED.
- FAULT, DASHED WHERE POORLY CONTROLLED.
- BURIED FAULT
- ANTICLINE
- SYNCLINE

(ORIGINALLY: PLATE VIII APPENDIX 2.5D)

FSAR UPDATE
UNITS 1 AND 2
DIABLO CANYON SITE

FIGURE 2.5 - 6

GEOLOGIC MAP OF THE MORRO BAY SOUTH AND PORT SAN LUIS QUADRANGLES, SAN LUIS OBISPO COUNTY, CALIFORNIA, AND ADJACENT OFFSHORE AREA.

NOTE: SECTION D-D' IS SHOWN ON FIGURE 2.5-6 OF FSAR.

Base map from U.S. Geological Survey Morro Bay South and Port San Luis quadrangles, 1965, 1:24,000.

The geology along the coastline and the Miguelito Member-Franciscan contact north of Cono Creek, and the Miguelito Member-Franciscan rocks contact southwest of Cono Creek were mapped by R. G. Ernst and C. A. Hall, 1968. The remainder of the Morro Bay South and Port San Luis quadrangles was mapped by C. A. Hall, 1968-1972. Interpretation of geologic observations, sections in this map of a. Hall. Geology drafted by M. J. Guntner.

This investigation was supported in part by the Division of Reactor Development and Technology, U.S. Atomic Energy Commission.

ON-SHORE GEOLOGY AND GEOLOGIC CROSS SECTIONS BY CLARENCE A. HALL, 1973, PUBLISHED AS USGS MAP MF 511, 1973.

OFF-SHORE GEOLOGY BY EARTH SCIENCES ASSOCIATES, 1974.

EXPLANATION

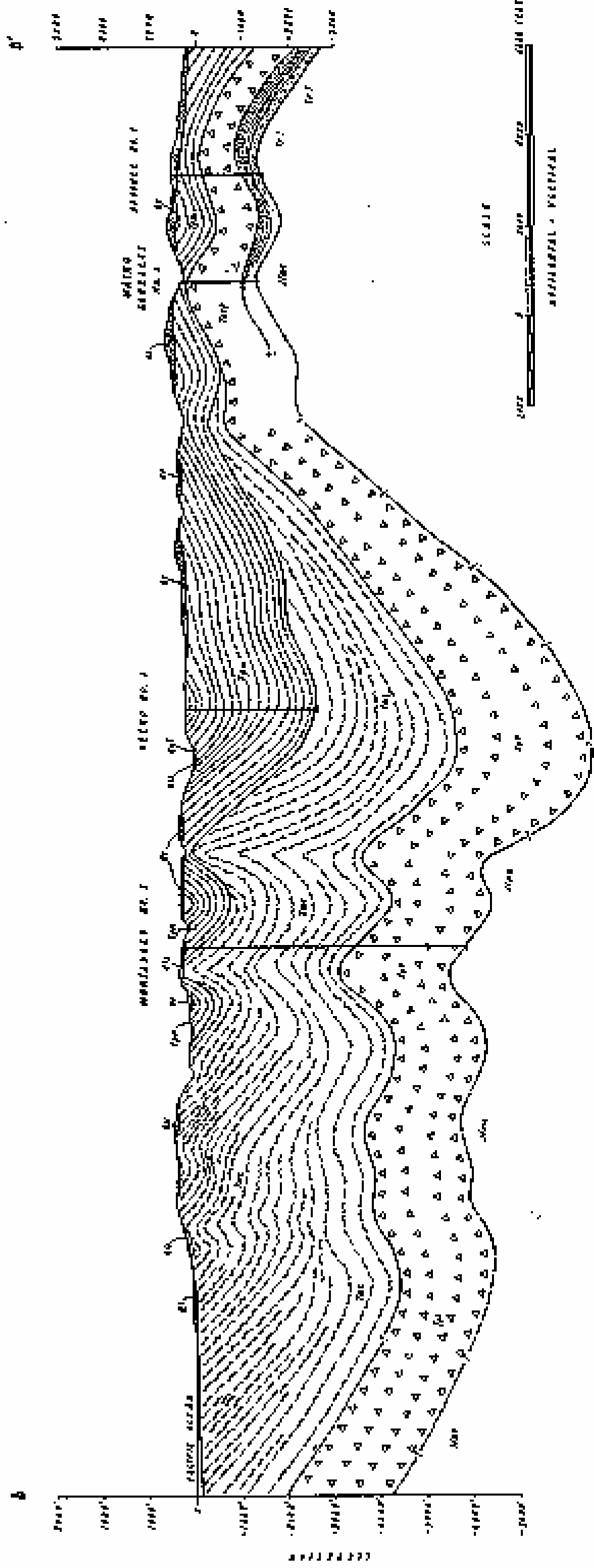
- Quaternary**
 - Q₁ Alluvial deposits: Cobble-pelitic gravel, sand, silt, and clay.
 - Q₂ Sand dune deposits: Unconsolidated white to brown, windblown sand, includes older stabilized sand dune deposits.
 - Q₃ Landslide deposits: Lithology dependent on source material.
 - Q₄ Terrace deposits: Unconsolidated sand, silt, clay, and gravel. Marine and stream terrace deposits.
- UNCONFORMITY**
- Pliocene**
 - P₁ Pass Robles(?) Formation: Sandstone, siltstone, claystone, and Monterey crest conglomerate. Partly to well consolidated. Partly or entirely marine.
- UNCONFORMITY**
- Pleistocene**
 - P₂ Squire Member: Massive white to tan calcareous greenish-gray sandstone, more calcareous and resistant near base. 75% to 80% quartz, 20% to 30% feldspar, less than 5% mica. Well-sorted, moderately well-sorted. Fine grained in west, with a grade into siltstone and claystone with some sandstone. Contains *Lycopodium carolinense* (Gabb), Upper Pliocene. Marine. Hall (1973).
 - P₃ Belmore Member: Interbedded buff to gray claystone and fine-grained sandstone. Claystone is sandstone facies. Upper Pliocene. Marine. Hall (1973).
 - P₄ Groby Member: Massive resistant to soft medium grained sandstone. White, weathering buff to tan. 20% to 30% quartz, 60% to 70% feldspar, less than 5% mica. Well-sorted, moderately well-sorted. Fine grained in west, with a grade into siltstone and claystone with some sandstone. Contains *Lycopodium carolinense* (Gabb), Upper Pliocene. Marine. Hall (1973).
- UNCONFORMITY**
- Miocene and Pliocene**
 - M₁ Miguelito and Edna Members: Tan, brown claystone and siltstone, buff to tan, blocky, but commonly 1/2 to 3/4 inch thick. Contains *Lycopodium carolinense* (Gabb), Upper Pliocene. Marine. Hall (1973).
 - M₂ Monterey Formation: This resistant hard siliceous chert and interbedded chert. Color variable but commonly white and brown to gray and reddish-brown, weathering blocks white. Brittle with subhorizontal fracture. Bed 1/2 to 1 1/2 inch thick. Laminations less than 1/8 inch thick, color ranging from reddish-brown and black to gray, brown, and unconsolidated and overlaid with discontinuous siltstone. Contains *Lycopodium carolinense* (Gabb), Upper Pliocene. Marine. Hall (1973).
 - M₃ Obispo Formation: Tan, siliceous siltstone, locally siliceous siltstone with some opaline chert. Absent in southwest.
- UNCONFORMITY**
- Oligocene**
 - O₁ Obispo Formation: Tan, siliceous or blocky siliceous claystone and siliceous siltstone, has to pinkish-white in color, locally yellowish or interbedded with cherty siltstone. 2 to 3 inch thick. Interbedded with cherty siltstone. Contains *Lycopodium carolinense* (Gabb), Upper Pliocene. Marine. Hall (1973).
 - O₂ Franciscan Formation: Tan, gray, or dark reddish-brown sandstone. Partly to well indurated, rounded to subangular grains. 40% to 60% quartz, 20% to 30% feldspar, 20% to 30% mica. Well-sorted, moderately well-sorted. Fine grained in west, with a grade into siltstone and claystone with some sandstone. Contains *Lycopodium carolinense* (Gabb), Upper Pliocene. Marine. Hall (1973).
- UNCONFORMITY**
- Upper Cretaceous(?)**
 - U₁ Franciscan rocks: Dark brown, weathering light tan, siliceous or silty claystone, partly to well-bedded. Locally includes thin beds or lenses of yellow or buff colored calcareous *Gastropoda* *Marine*.
 - U₂ Franciscan rocks: Tan, gray, or dark reddish-brown sandstone. Partly to well indurated, rounded to subangular grains. 40% to 60% quartz, 20% to 30% feldspar, 20% to 30% mica. Well-sorted, moderately well-sorted. Fine grained in west, with a grade into siltstone and claystone with some sandstone. Contains *Lycopodium carolinense* (Gabb), Upper Pliocene. Marine. Hall (1973).
- JURASSIC OR CRETACEOUS**
 - J₁ Serpentinized and serpentinized ultrabasic rocks.
 - J₂ Franciscan rocks: Kelp, interbedded very fine grained graywacke or claystone and greenish-brown medium-grained graywacke composed of 60% to 70% quartz, 20% to 30% feldspar, 20% to 30% mica. Well-sorted, moderately well-sorted. Fine grained in west, with a grade into siltstone and claystone with some sandstone. Contains *Lycopodium carolinense* (Gabb), Upper Pliocene. Marine. Hall (1973).

GEOLOGIC SYMBOLS

- Dashed where approximately located, queried where doubtful.
- High-angle fault
- Thrust or reverse fault
- Dashed where approximately located or inferred, dashed where concealed, queried where presence is doubtful. Dip to north on upper plate. Dip of fault zone between 30° and 60°.
- Showing axis of surface. Dashed where approximately located, dashed where concealed.
- Syncline
- Showing axis of surface. Dashed where approximately located, dashed where concealed.
- Horizontal
- Inclined
- Vertical
- Strike and dip of bed
- Strike and dip of flow banding
- Inferred general direction of landslide movement
- Megafossil locality
- UCLA locality number
- Abandoned well drilled for oil
- Tuff
- Marker beds

REFERENCES CITED

- Hall, C. A., 1971, Geology of the Morro Bay quadrangle, San Luis Obispo County, California. U.S. Geological Survey Map sheet 1:24,000.
- Tanner, D. L., 1968, Potassium-argon dates concerning the Tertiary igneous rocks of the San Luis Obispo area. U.S. Geological Survey Bulletin 1244, p. 91-129.
- Stearns, R. C., and Hall, C. A., 1970, The Obispo Formation and associated volcanic rocks in central California Coast Ranges - K-40 ages and geochronologic significance. U.S. Geological Survey Bulletin 1244, p. 130-150.



SECTION A-A'
 SHOWING LOCATIONS OF WELLS AND
 GEOLGIC STRATIGRAPHY IN THE SAN LUIS RANGE
 FROM WEST-NORTHWEST

NOTE: THE SYMBOLS A-Z ARE LOCATIONS OF DEPTH
 INTERVALS AND INTERVALS OF STRATA

FSAR UPDATE
UNITS 1 AND 2 DIABLO CANYON SITE
FIGURE 2.5-7 GEOLOGIC SECTION THROUGH EXPLORATORY OIL WELLS IN THE SAN LUIS RANGE



**GEOLOGIC
MAP OF
DIABLO
CANYON
COASTAL
AREA**

**FSAR UPDATE
UNITS 1 AND 2
DIABLO CANYON SITE**

**FIGURE 2.5-8
GEOLOGIC MAP OF DIABLO CANYON
COASTAL AREA**

Prepared by
R.M. EDGELL, INC.
4400 Paseo Blvd., San Francisco, California
Date of Publication: Jan. 2, 1964.

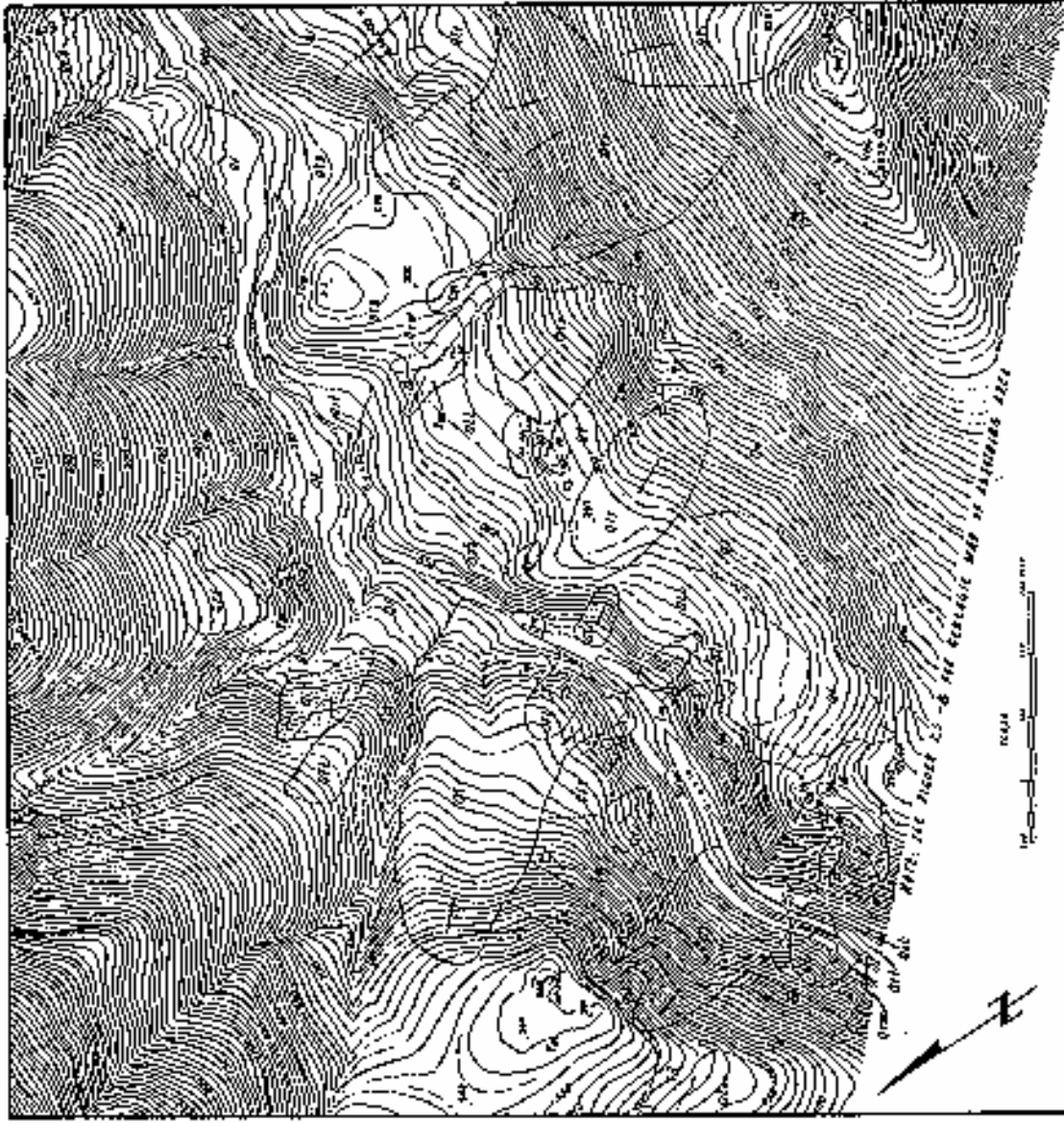
Map is based on California Geologic Survey, June 2
Map 315 (Scale 62,500:1, 1939-41)

SCALE
1:50,000 (VERTICAL SCALE)

EXPLANATION

- 04a Tertiary alluvium.
 - 04b Tills and beach deposits.
 - 04c Sand wash and slope wash deposits.
 - 04d Eolianite deposits.
 - 04f Stream-terrace deposits.
 - 04g Alluvial-terrace deposits.
 - 04h Older fan-terrace deposits.
 - 04i Deposits on terrace wash-out channels.
 - 04j Late Holocene (H) deposits.
 - 04k Beaches (terrestrial beach).
 - 04l Holocene terraces.
 - 04m Shippo loess.
 - 04n Coastal dune and surficial deposits.
 - 04o Sandbar between dune and beach.
 - 04p Beach, showing dip.
 - 04q Shells and top of beach.
 - 04r Shells and top of beach.
 - 04s Highly modified beach.
 - 04t Area of dunes.
 - 04u Boundary between different generations of beach and ridge in the 4 feet thick or more of beach.
 - 04v Surface trace of resistant erosion in 4m.
- Geology mapped by R.M. Edgell
1975/8/1, 8/86, 7/88
Amended by R.M. Edgell on 12/20/94, 1/1/95

FIGURE 2.5-8
Revisions 11 November 1996.



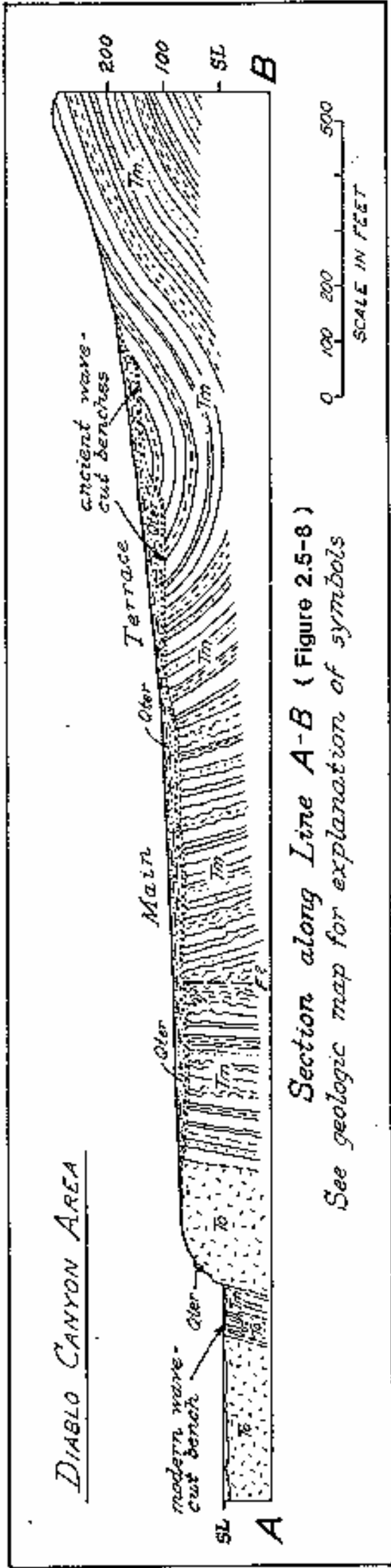
EXPLANATION

Qa2	FRESH-LAND ACCRETION
Qa1	SLOPE SCREE, AND SCOR-MASS DEPOSITS
Qa1	LANDSLIDE DEPOSITS
Qs1	STREAM-TERRACE DEPOSITS
Qf	ALLUVIAL-FAN DEPOSITS
Qp1	SCOR-MASS-TERRACE DEPOSITS
Qp2	DEPOSITS OF MARINE WAVE-CUT TERRACES
Ql3	LAKE-BOTTOM (S) DEPOSITS
Tb	SILTIC INTRUSIVE ROCK
Tm	MONTEREY FORMATION

	CONTACT INVOLVING JURASSIC DEPOSITS
	CONTACT BETWEEN DEBRIS BRILL, SANDS WHICH APPEAR UNLINED, BUTTER WHICH CONCEALED BY DEBR.
	FENCE AND RIP OF DEBR
	TRAIL AND RANGE IN SIB OF BENT (RANGE OF MERRIO ON A SWALE TALE.

GEOL. MAP BY E. G. JARRIS AND A. M. JOHNSON, 1947, SUPPLEMENTED BY J. E. CARRAS, 1969.

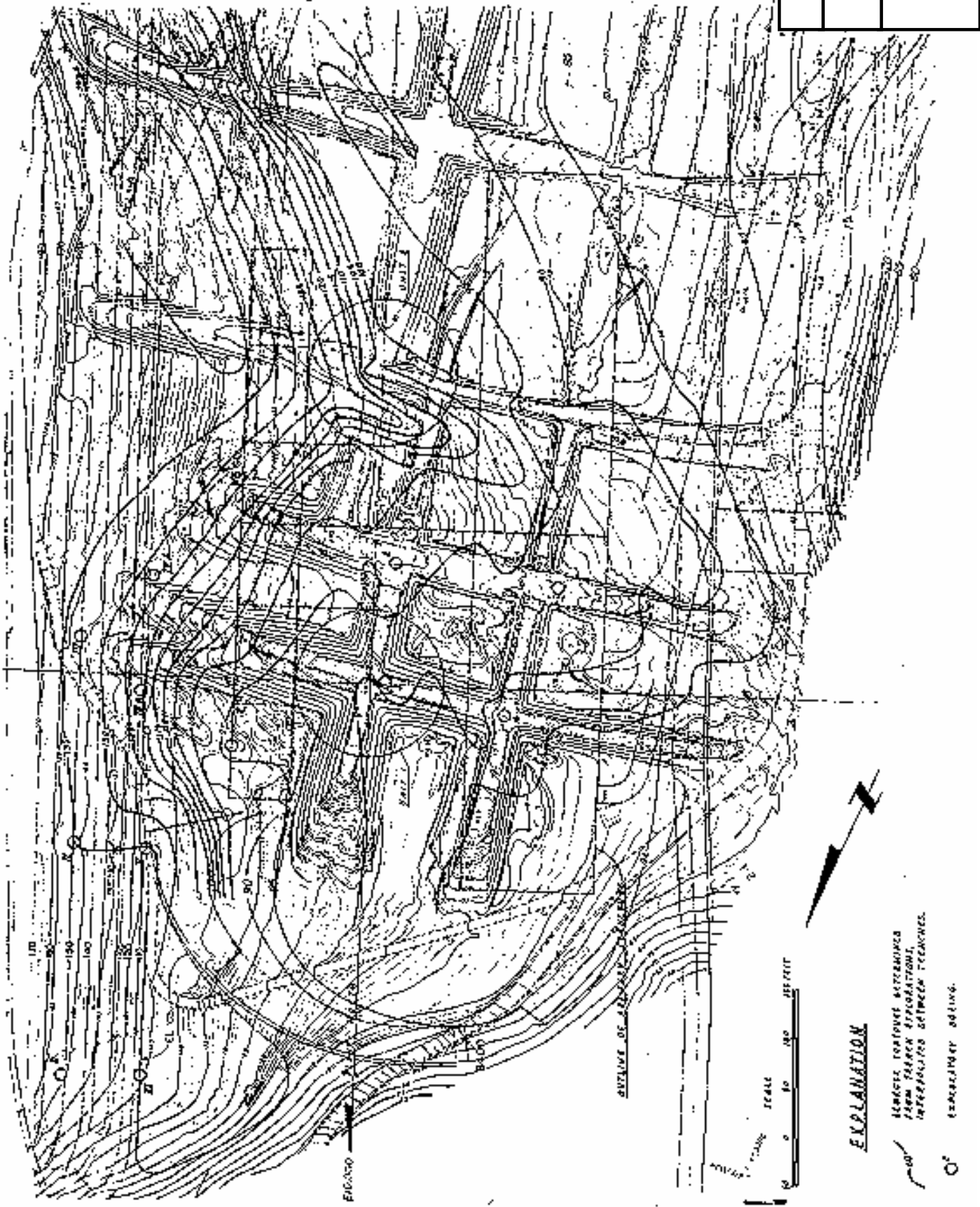
FSAR UPDATE
 UNITS 1 AND 2
 DIABLO CANYON SITE
 FIGURE 2.5-9
 GEOLOGIC MAP OF SWITCHYARD AREA



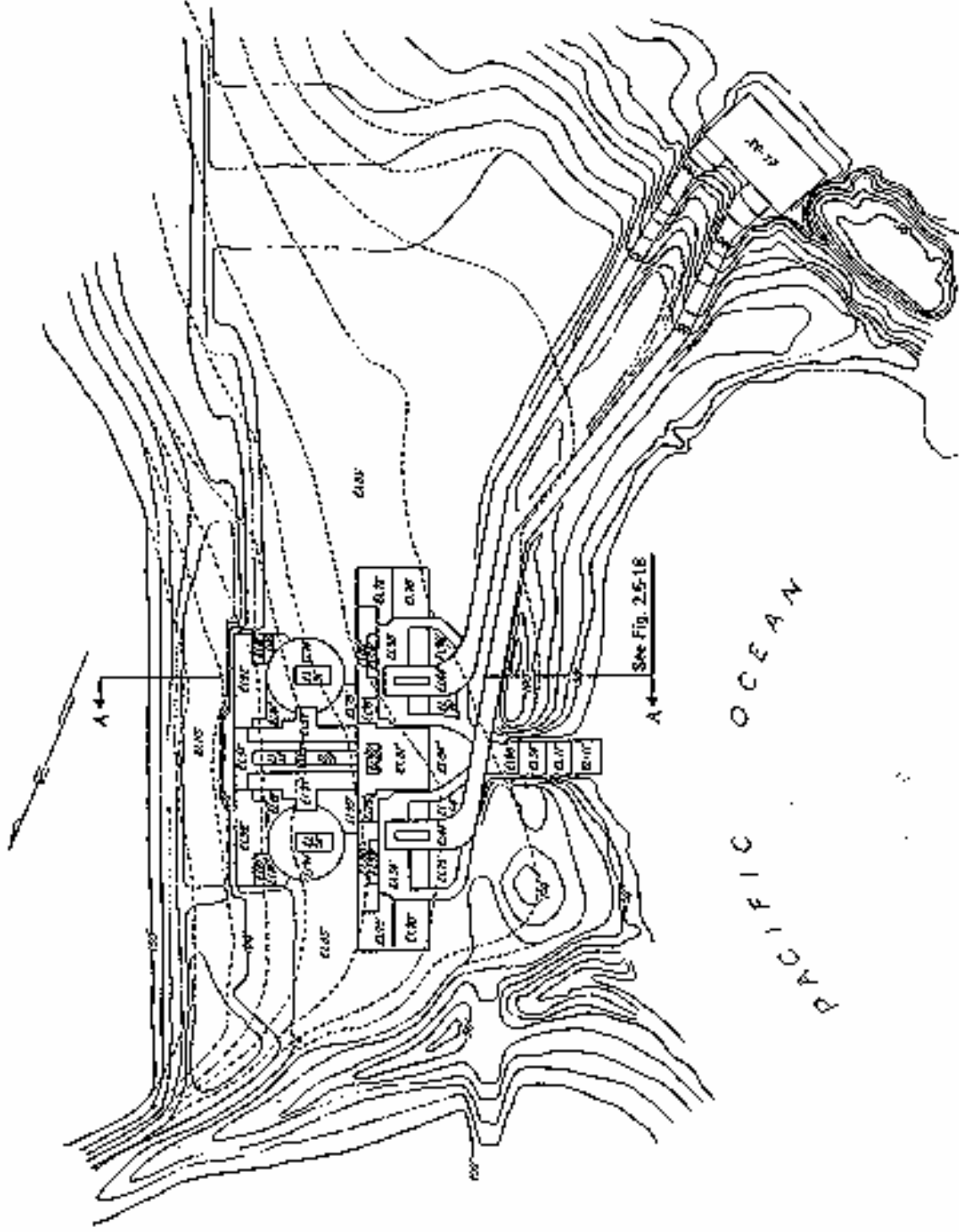
Section along Line A-B (Figure 2.5-8)
 See geologic map for explanation of symbols

FSAR UPDATE
UNITS 1 AND 2 DIABLO CANYON SITE
FIGURE 2.5-10 GEOLOGIC SECTION THROUGH THE PLANT SITE

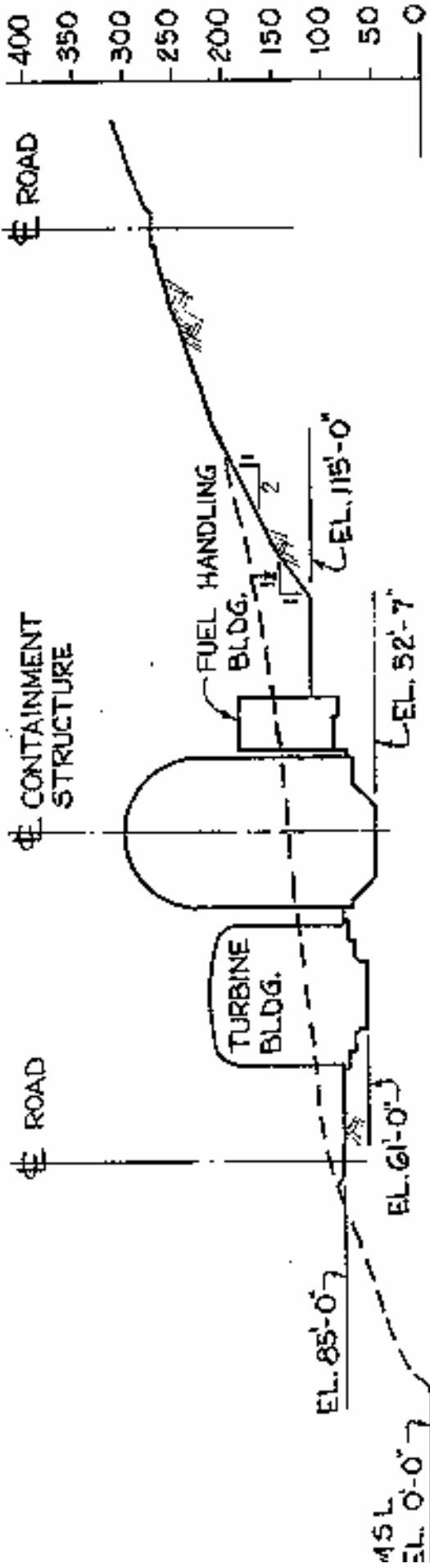
Revision 11 November 1996



FSAR UPDATE
UNITS 1 AND 2 DIABLO CANYON SITE
FIGURE 2.5-11 SITE EXPLORATION FEATURES AND BEDROCK CONTOURS



FSAR UPDATE
UNITS 1 AND 2
DIABLO CANYON SITE
FIGURE 2.5-17
PLAN OF EXCAVATION AND BACKFILL

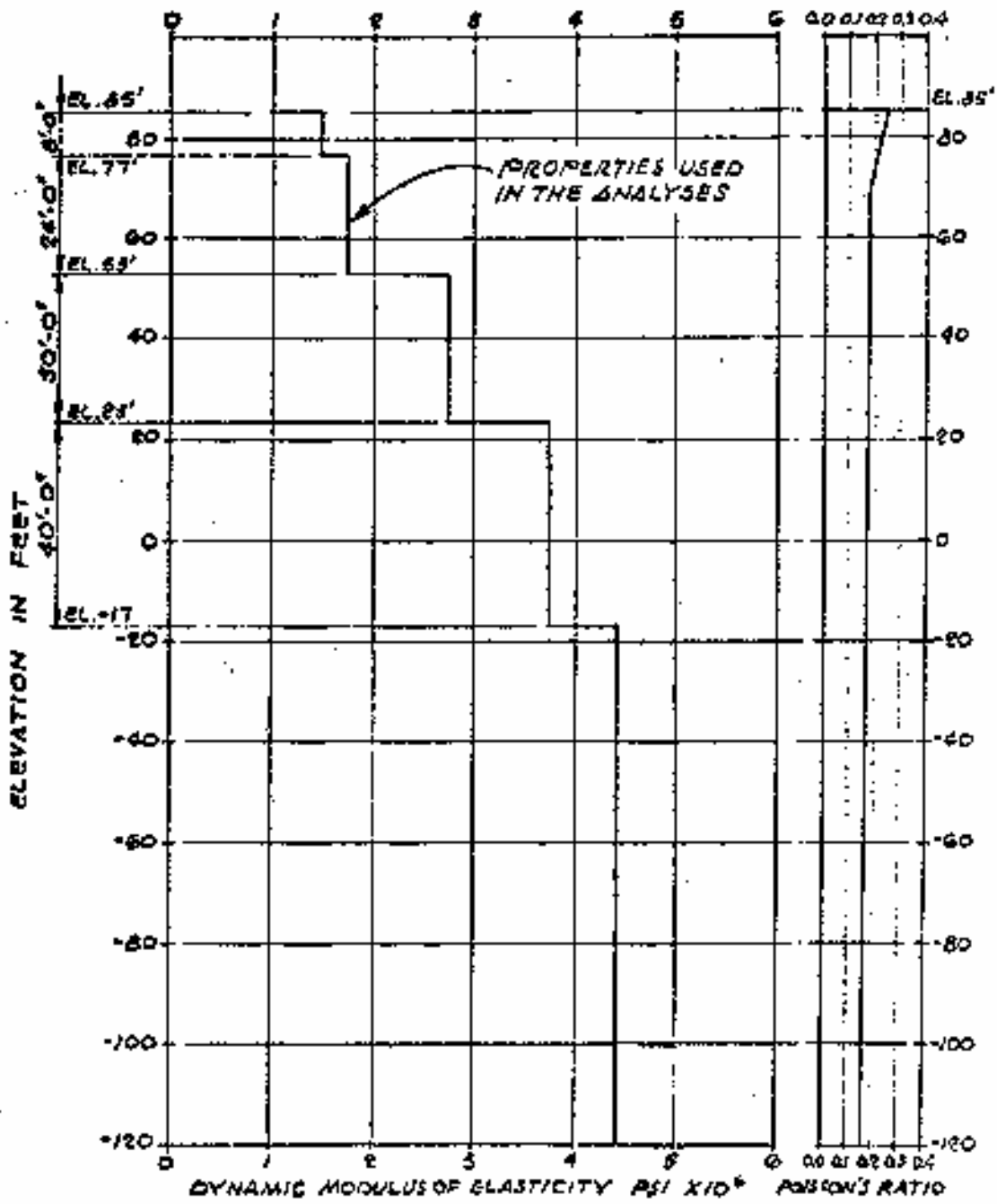


SECTION A-A

FROM FIGURE 2.5-17

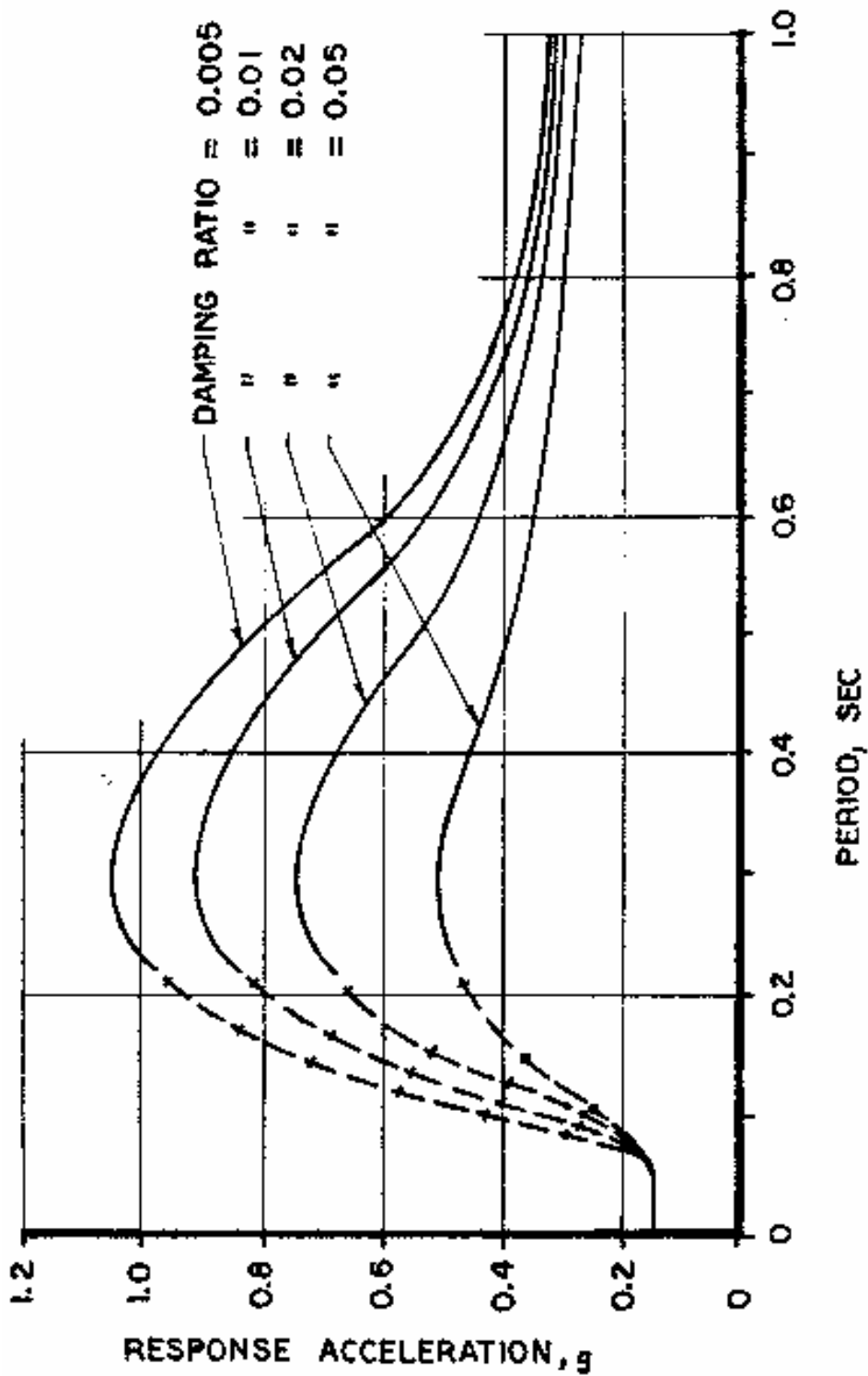
FSAR UPDATE
UNITS 1 AND 2 DIABLO CANYON SITE
FIGURE 2.5-18 SECTION A-A EXCAVATION AND BACKFILL

Revision 11 November 1996

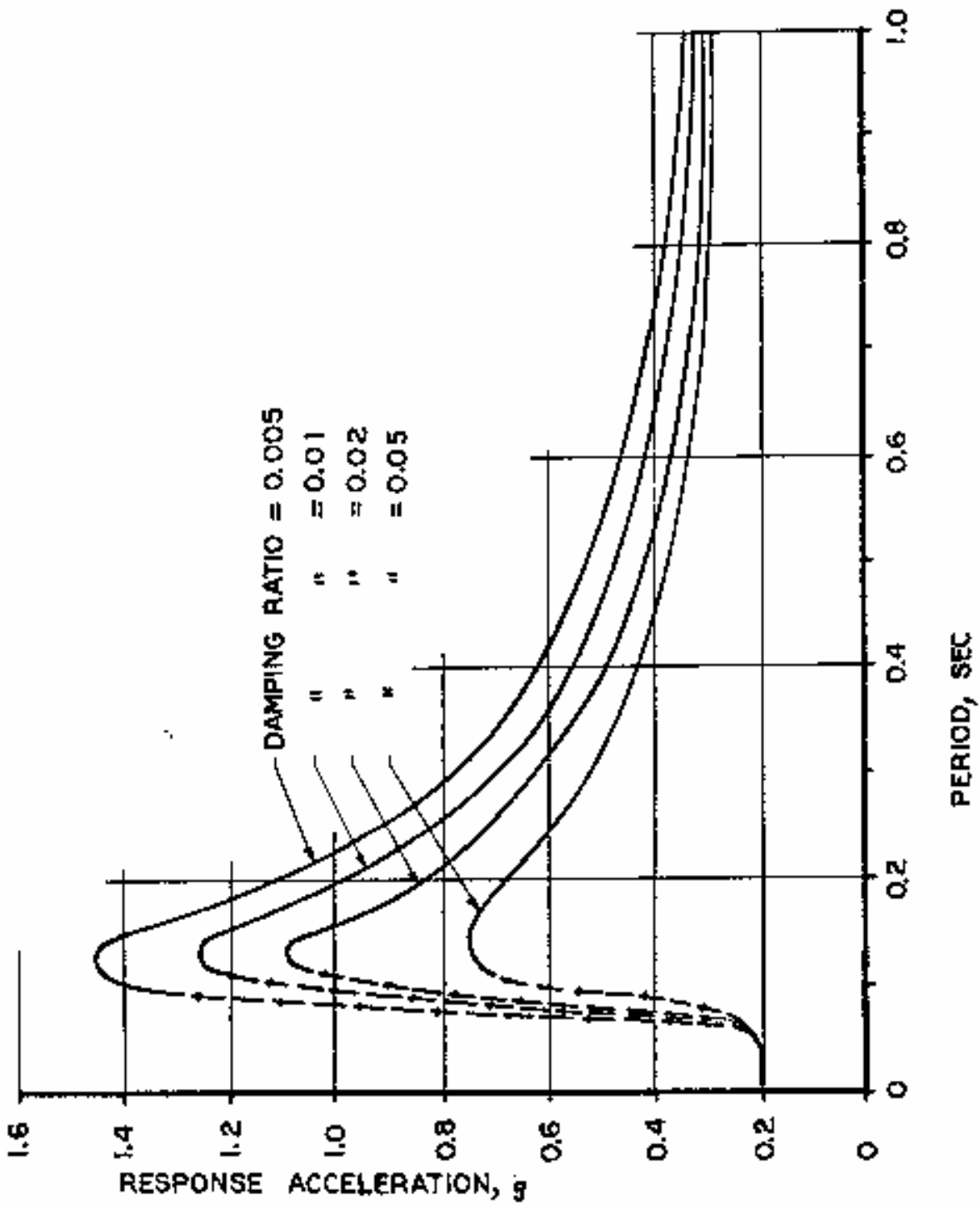


FSAR UPDATE
UNITS 1 AND 2 DIABLO CANYON SITE
FIGURE 2.5-19 SOIL MODULE OF ELASTICITY AND POISSON'S RATIO

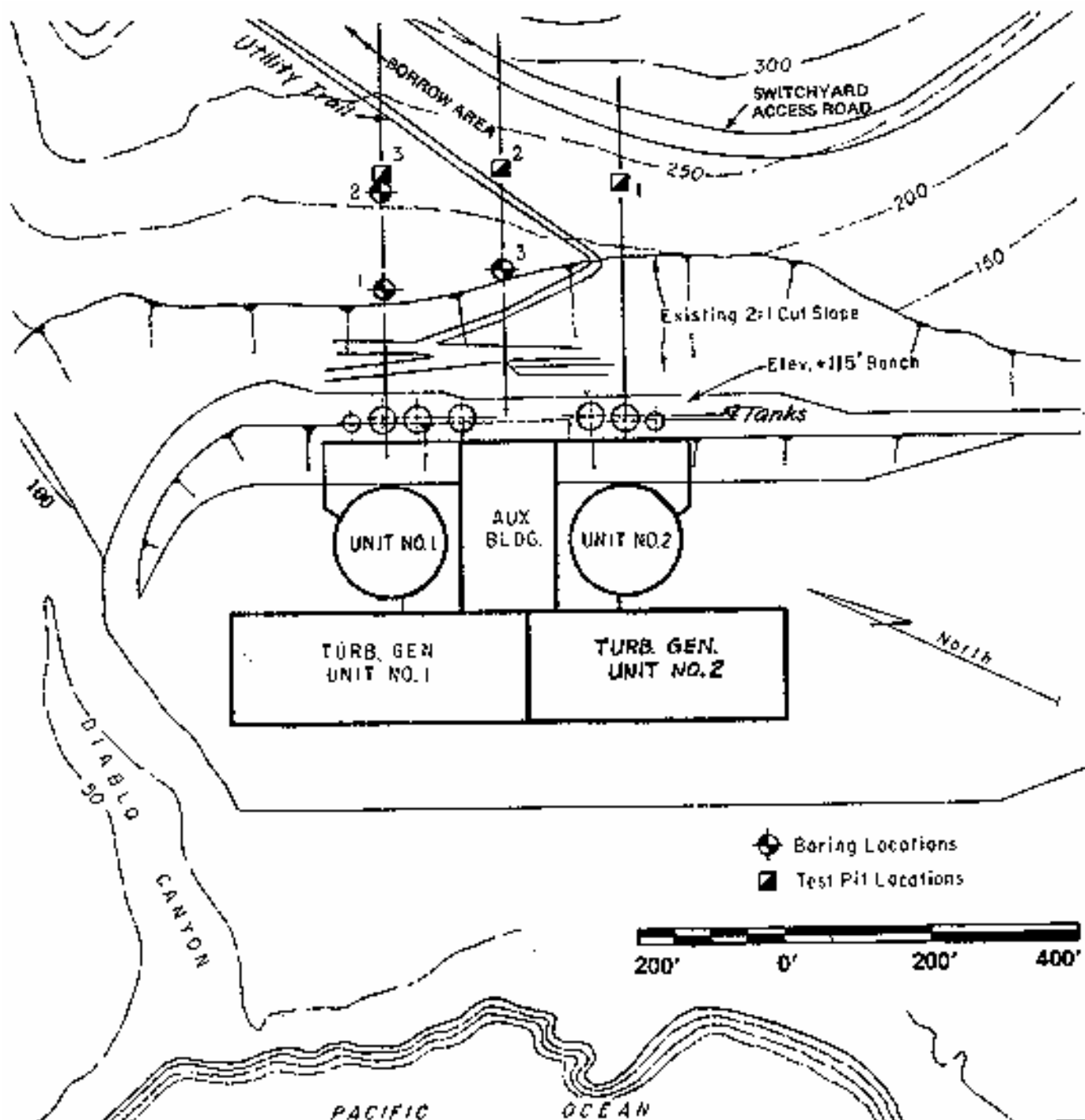
Revision 11 November 1996



FSAR UPDATE
UNITS 1 AND 2 DIABLO CANYON SITE
FIGURE 2.5-20 SMOOTH RESPONSE ACCELERATION SPECTRA - EARTHQUAKE "B"



FSAR UPDATE
UNITS 1 AND 2 DIABLO CANYON SITE
FIGURE 2.5-21 SMOOTH RESPONSE ACCELERATION SPECTRA - EARTHQUAKE "D" MODIFIED



FSAR UPDATE
UNITS 1 AND 2 DIABLO CANYON SITE
FIGURE 2.5-22 POWER PLANT SLOPE PLAN

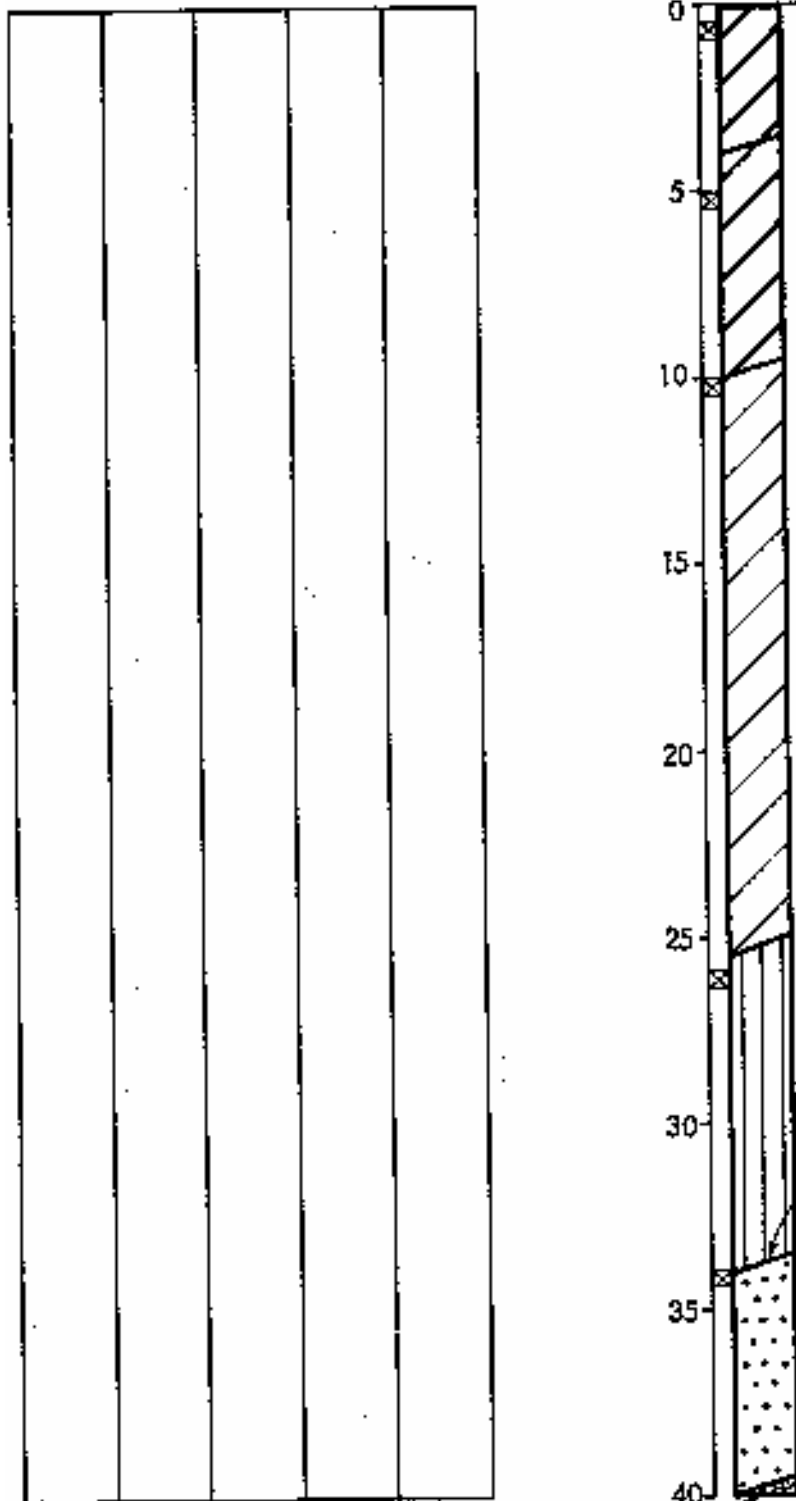
Revision 11 November 1996

LOG OF BORING 1

Shear Strength (lbs/sq ft)

Moisture Content (%)
 Dry Density (pcf)
 Depth (ft)
 Sample

Equipment 24" Flight Auger
 Elevation 170.0 Date 4/7/70



0 BLACK SILTY CLAY (CH)
 soft, moist
 change to medium stiff at 3'

5 GRAY BROWN SANDY SILTY CLAY
 (CH) - medium stiff, moist

10 BROWN SANDY CLAY (CL)
 stiff, moist

15

20

25 BROWN SANDY SILT (ML)
 medium stiff, moist

30 BROWN GRAVELLY SAND (SP)
 loose, moist, well rounded

35

40

FSAR UPDATE

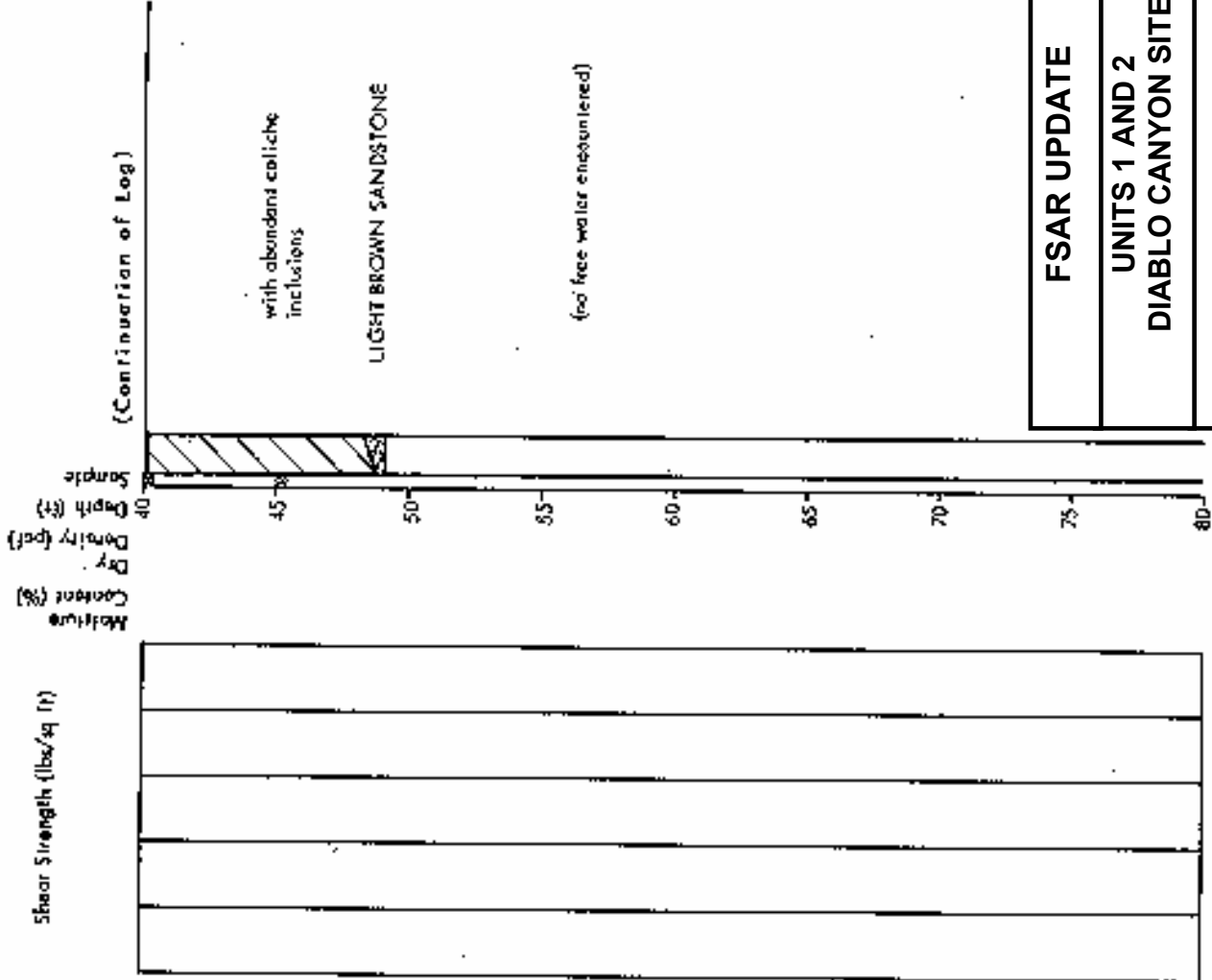
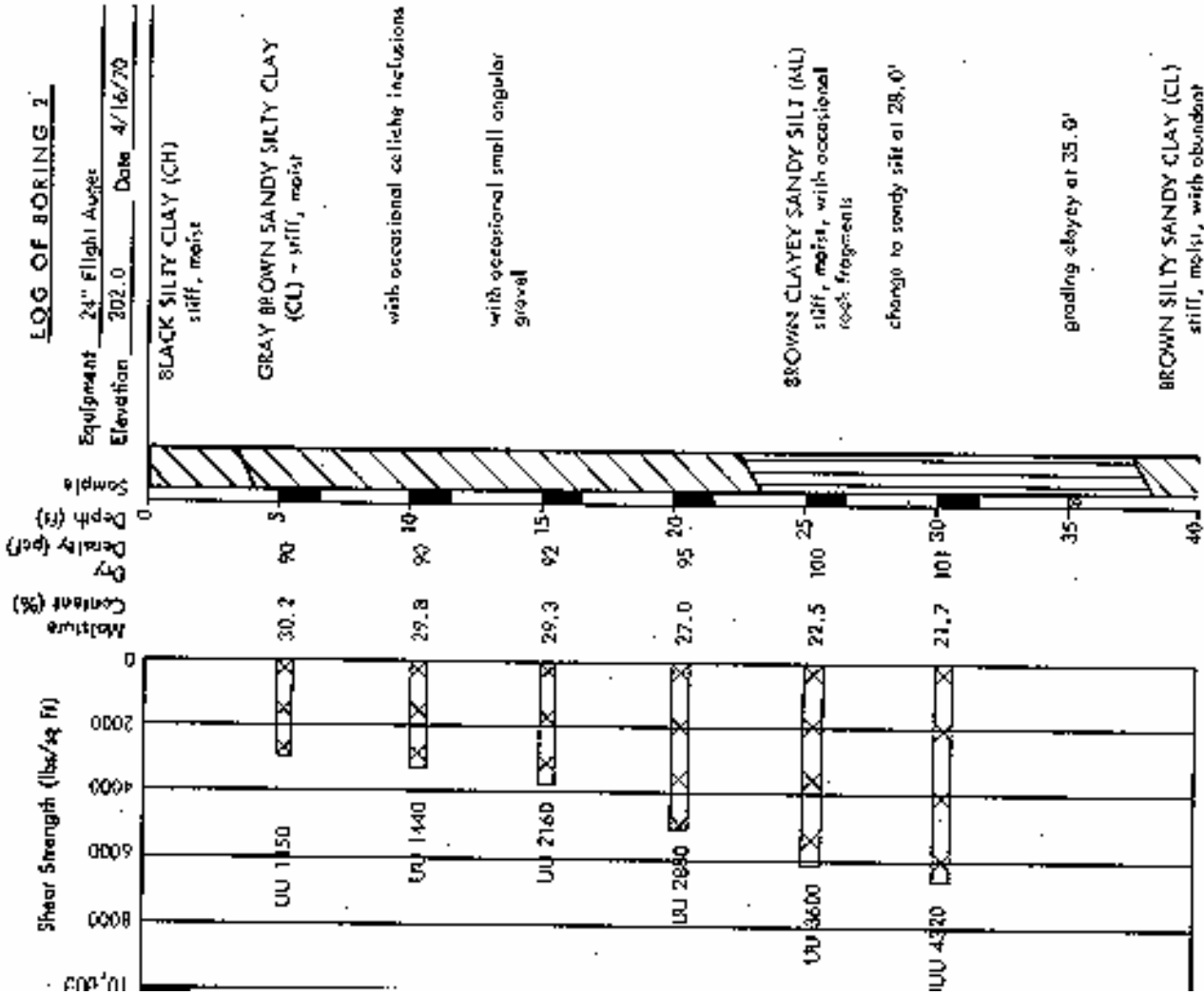
UNITS 1 AND 2
DIABLO CANYON SITE

FIGURE 2.5-23
POWER PLANT SLOPE
LOG OF BORING 1

(no free water encountered) BROWN SANDSTONE

LOG OF BORING 2

Equipment 24" Flight Auger
 Elevation 202.0
 Date 4/16/70



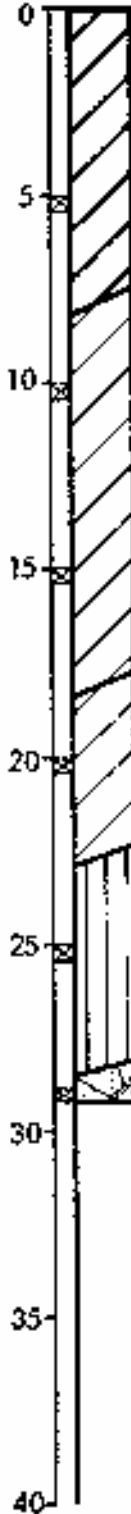
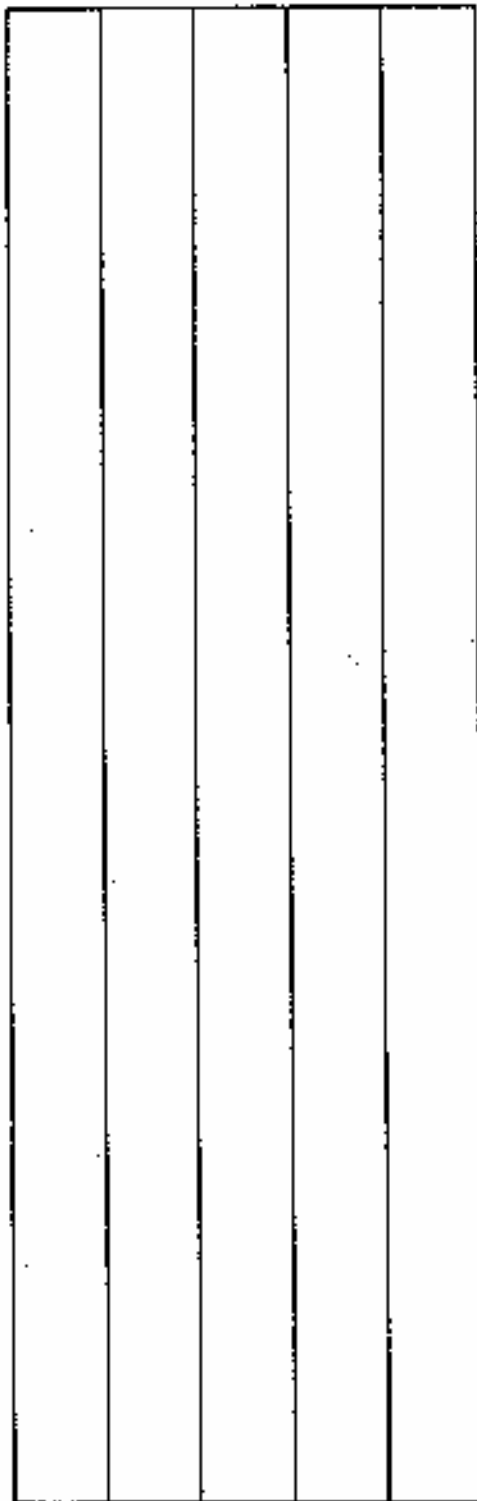
FSAR UPDATE
UNITS 1 AND 2
DIABLO CANYON SITE
FIGURE 2.5-24
POWER PLANT SLOPE
LOG OF BORING 2

LOG OF BORING 3

Shear Strength (lbs/sq ft)

Moisture Content (%)
 Dry Density (pcf)
 Depth (ft)
 Sample

Equipment 24" Flight Auger
 Elevation 178.0 Date 4/16 70



DARK BROWN SANDY CLAY (CH)
 stiff, dry

change to medium stiff at 4'

BROWN SANDY CLAY (CL)
 stiff, moist, with occasional angular gravel

BROWN SANDY CLAYEY SILT (ML)
 medium stiff, moist

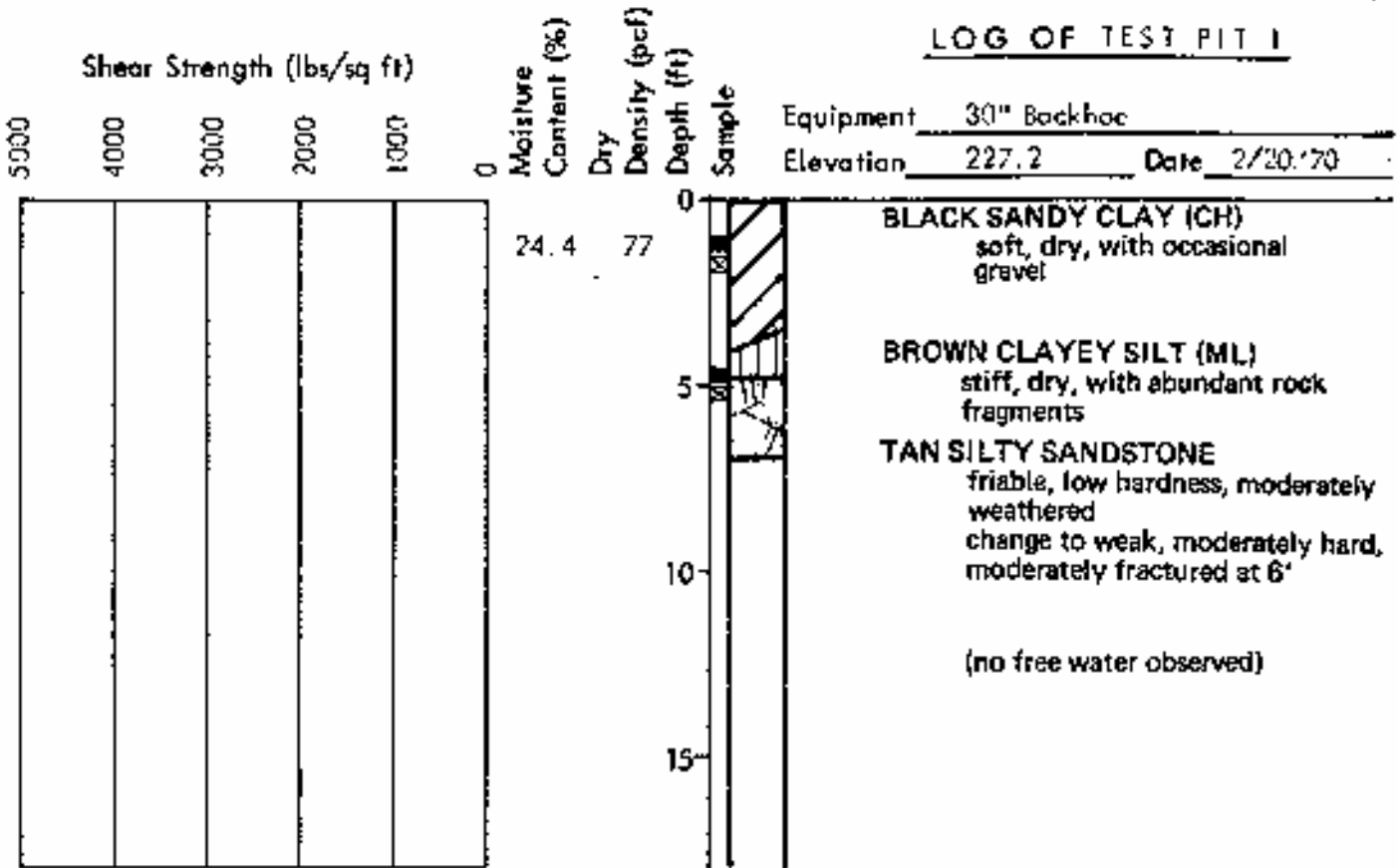
BROWN CLAYEY SANDY SILT (ML)
 medium stiff, moist, with occasional rock fragments

LIGHT BROWN SANDSTONE
 moderately fractured, hard, strong

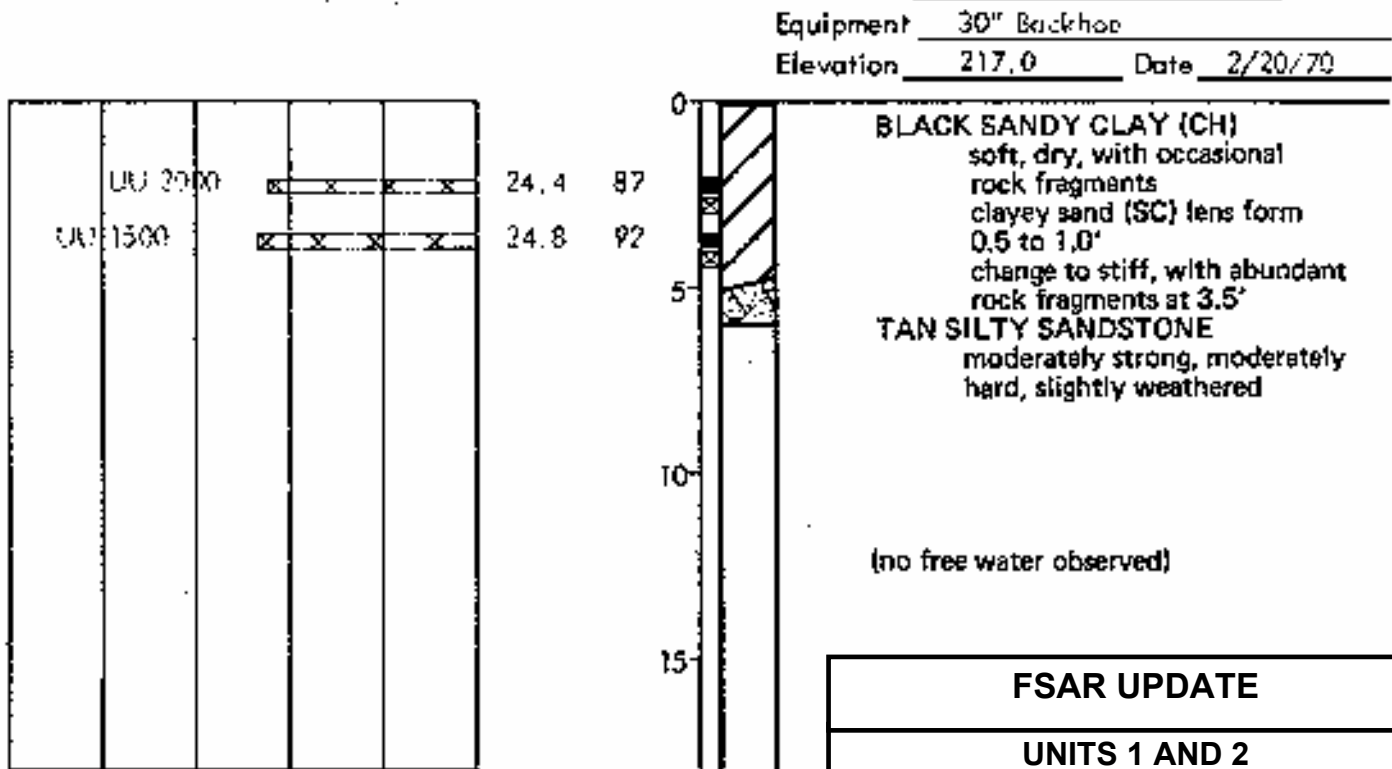
(no free water encountered)

FSAR UPDATE
UNITS 1 AND 2 DIABLO CANYON SITE
FIGURE 2.5-25 POWER PLANT SLOPE LOG OF BORING 3

LOG OF TEST PIT 1

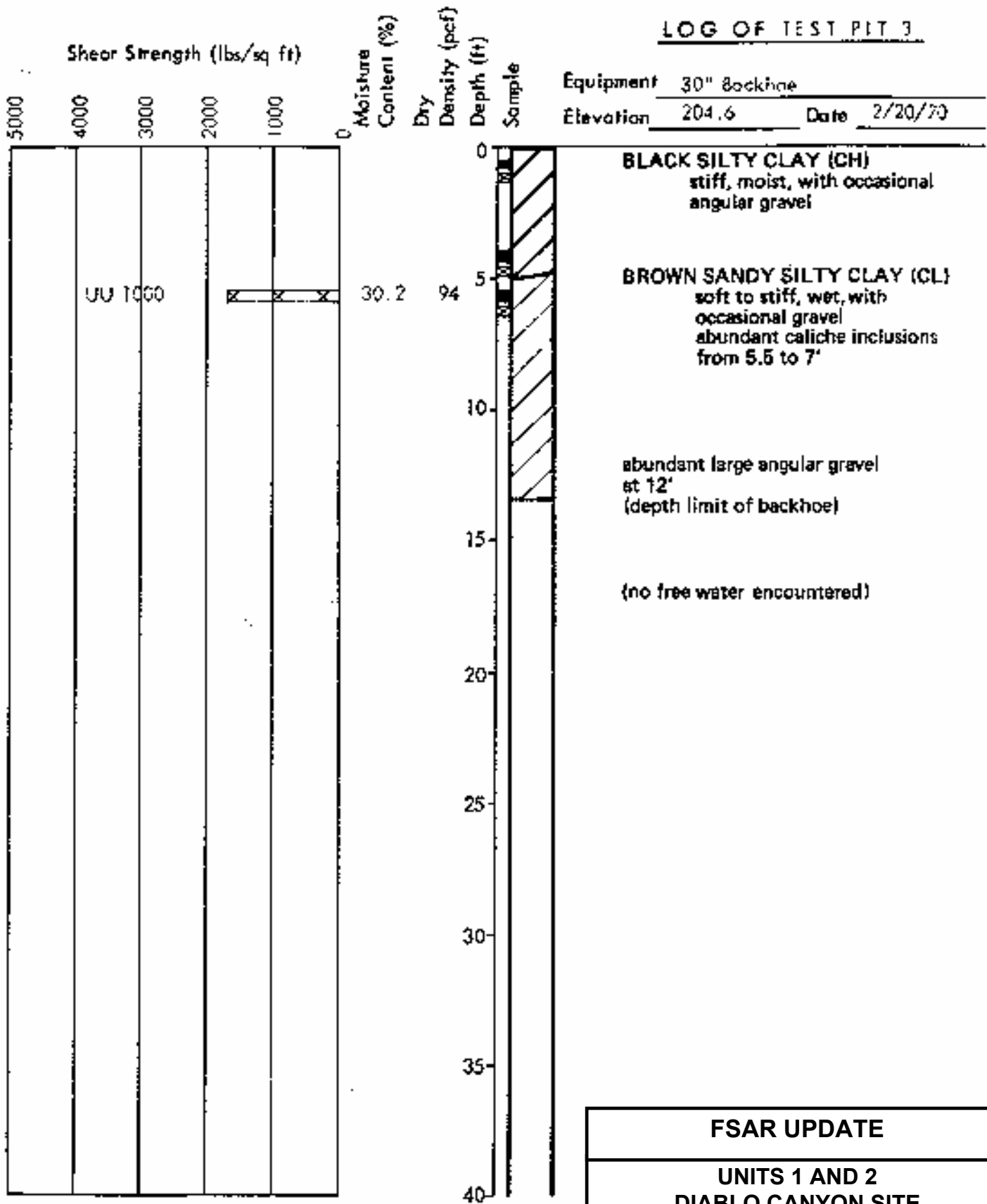


LOG OF TEST PIT 2



FSAR UPDATE
UNITS 1 AND 2
DIABLO CANYON SITE
FIGURE 2.5-26
POWER PLANT SLOPE
LOG OF TEST PITS 1 & 2

LOG OF TEST PIT 3

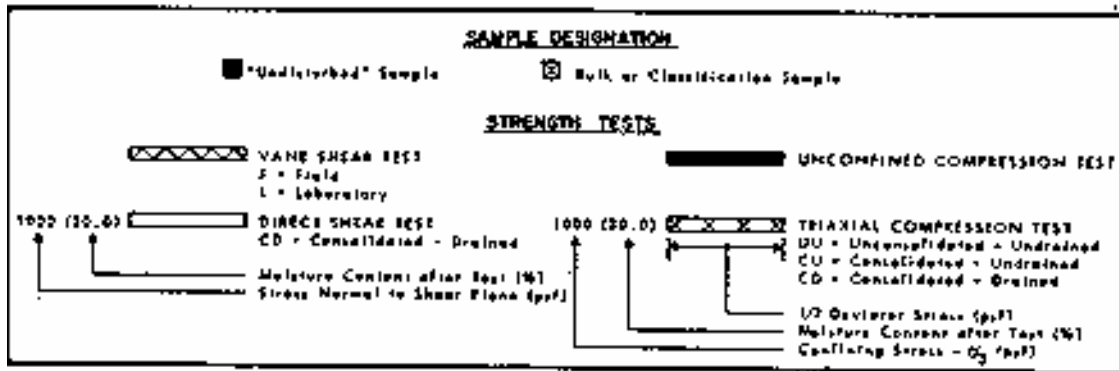


Equipment 30" Backhoe
 Elevation 204.6 Date 2/20/70

FSAR UPDATE
UNITS 1 AND 2
DIABLO CANYON SITE
FIGURE 2.5-27
POWER PLANT SLOPE
LOG OF TEST PIT 3

MAJOR DIVISIONS			TYPICAL NAMES	
COARSE GRAINED SOILS MORE THAN HALF IS LARGER THAN 75µm SIEVE	GRAVELS MORE THAN HALF COARSE FRACTION IS LARGER THAN NO. 4 SIEVE SIZE	CLEAN GRAVELS WITH LITTLE OR NO FINES	GW	WELL GRADED GRAVELS, GRAVEL - SAND MIXTURES
			GP	POORLY GRADED GRAVELS, GRAVEL - SAND MIXTURES
		GRAVELS WITH OVER 12% FINES	GM	SILTY GRAVELS, POORLY GRADED GRAVEL - SAND - SILT MIXTURES
			GC	CLAYEY GRAVELS, POORLY GRADED GRAVEL - SAND - CLAY MIXTURES
	SANDS MORE THAN HALF COARSE FRACTION IS SMALLER THAN NO. 4 SIEVE SIZE	CLEAN SANDS WITH LITTLE OR NO FINES	SW	WELL GRADED SANDS, GRAVELLY SANDS
			SP	POORLY GRADED SANDS, GRAVELLY SANDS
		SANDS WITH OVER 12% FINES	SM	SILTY SANDS, POORLY GRADED SAND - SILT MIXTURES
			SC	CLAYEY SANDS, POORLY GRADED SAND - CLAY MIXTURES
FINE GRAINED SOILS MORE THAN HALF IS SMALLER THAN 75µm SIEVE	SILTS AND CLAYS LIQUID LIMIT LESS THAN 50	ML	INORGANIC SILTS AND VERY FINE SANDS, ROCE FLOUR, SILTY OR CLAYEY FINE SANDS, OR CLAYEY SILTS WITH SLIGHT PLASTICITY	
		CL	INORGANIC CLAYS OF LOW TO MEDIUM PLASTICITY, GRAVELLY CLAYS, SANDY CLAYS, SILTY CLAYS, LEAN CLAYS	
		OL	ORGANIC CLAYS AND ORGANIC SILTY CLAYS OF LOW PLASTICITY	
	SILTS AND CLAYS LIQUID LIMIT GREATER THAN 50	MH	INORGANIC SILTS, ARGILLACIOUS OR ORNITHOMACIOUS FINE SANDY OR SILTY SOILS, FELSIC SILTS	
		CH	INORGANIC CLAYS OF HIGH PLASTICITY, FAT CLAYS	
		OH	ORGANIC CLAYS OF MEDIUM TO HIGH PLASTICITY, ORGANIC SILTS	
		PI	PEAT AND OTHER HIGHLY ORGANIC SOILS	
HIGHLY ORGANIC SOILS				

UNIFIED SOIL CLASSIFICATION SYSTEM

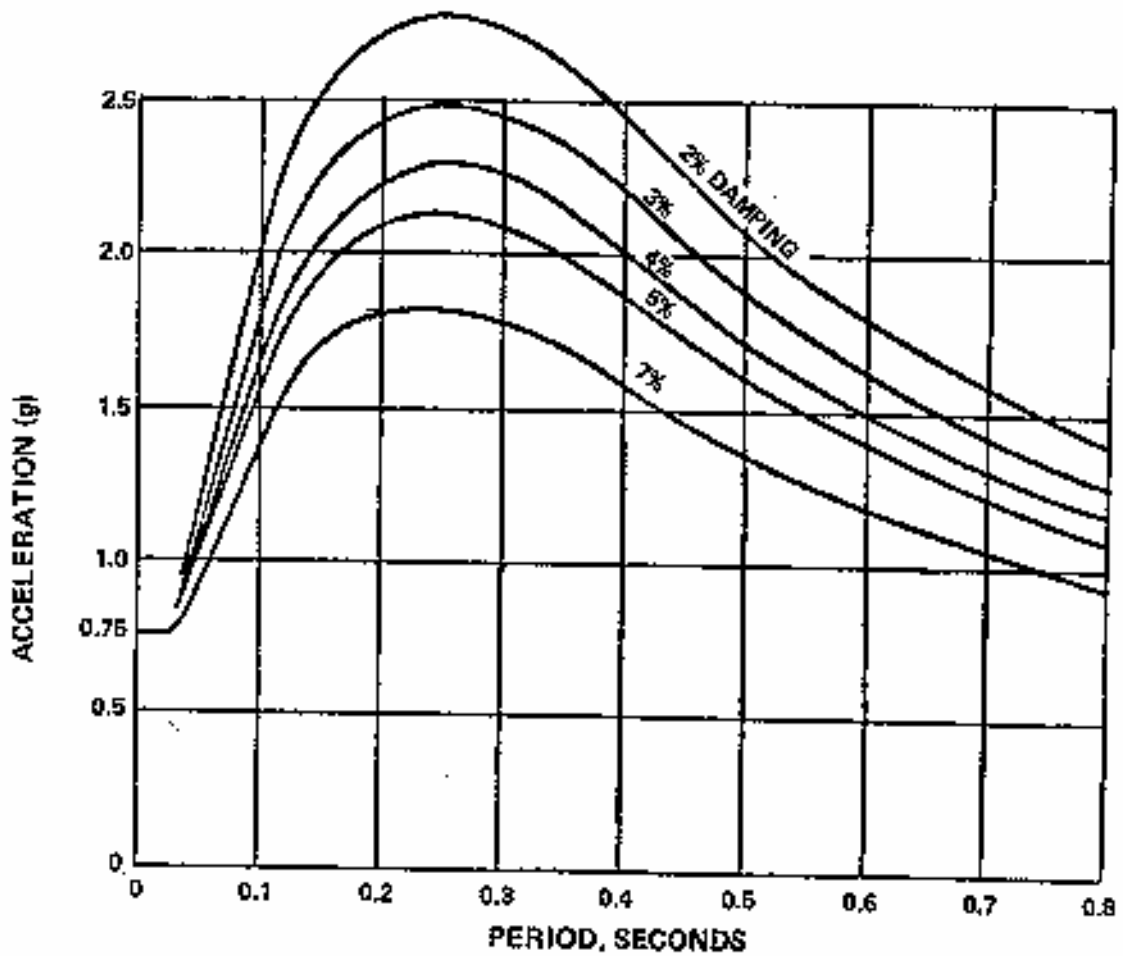


KEY TO TEST DATA

FSAR UPDATE

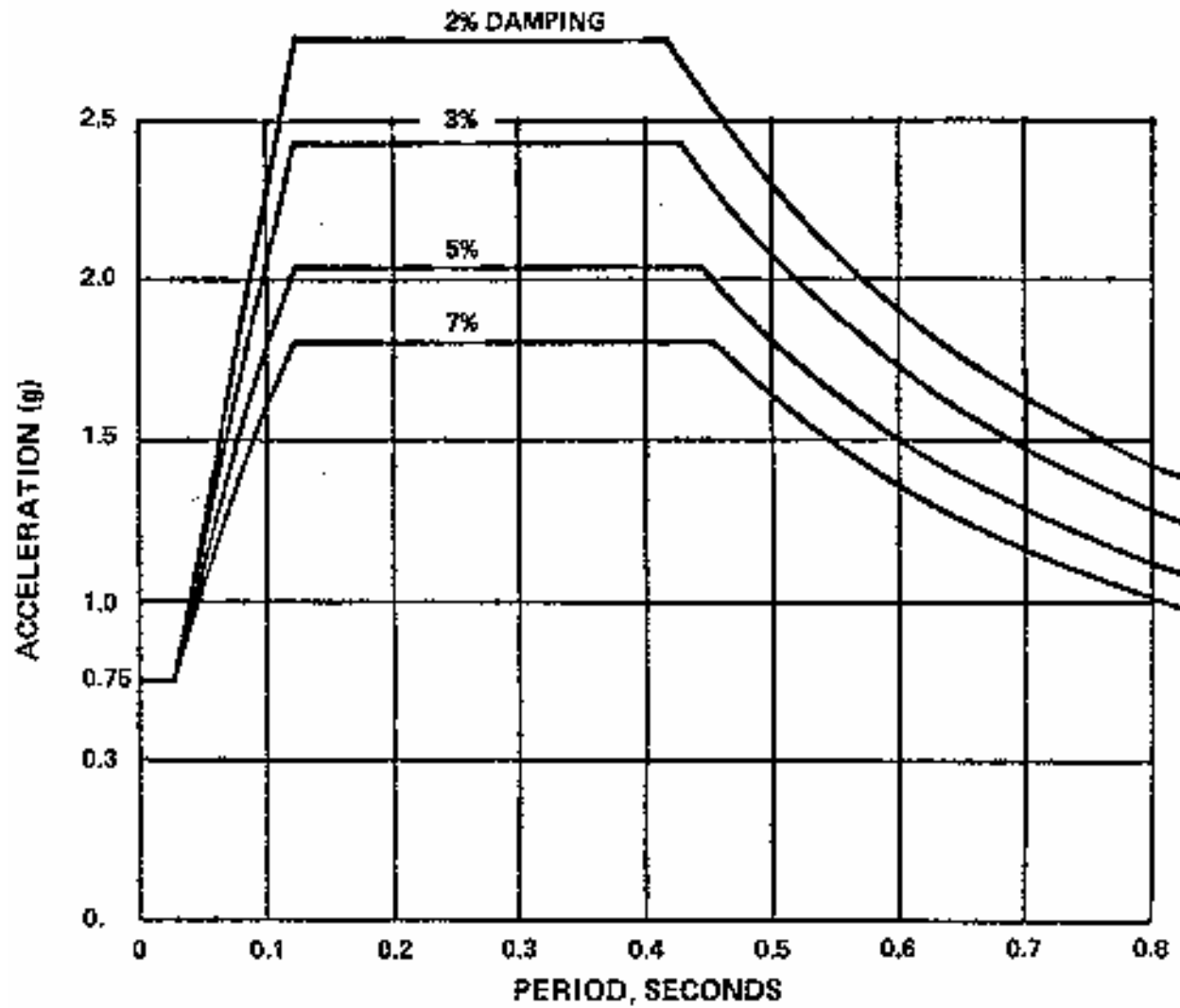
**UNITS 1 AND 2
DIABLO CANYON SITE**

**FIGURE 2.5-28
POWER PLANT SLOPE
SOIL CLASSIFICATION CHART AND
KEY TO TEST AREA**



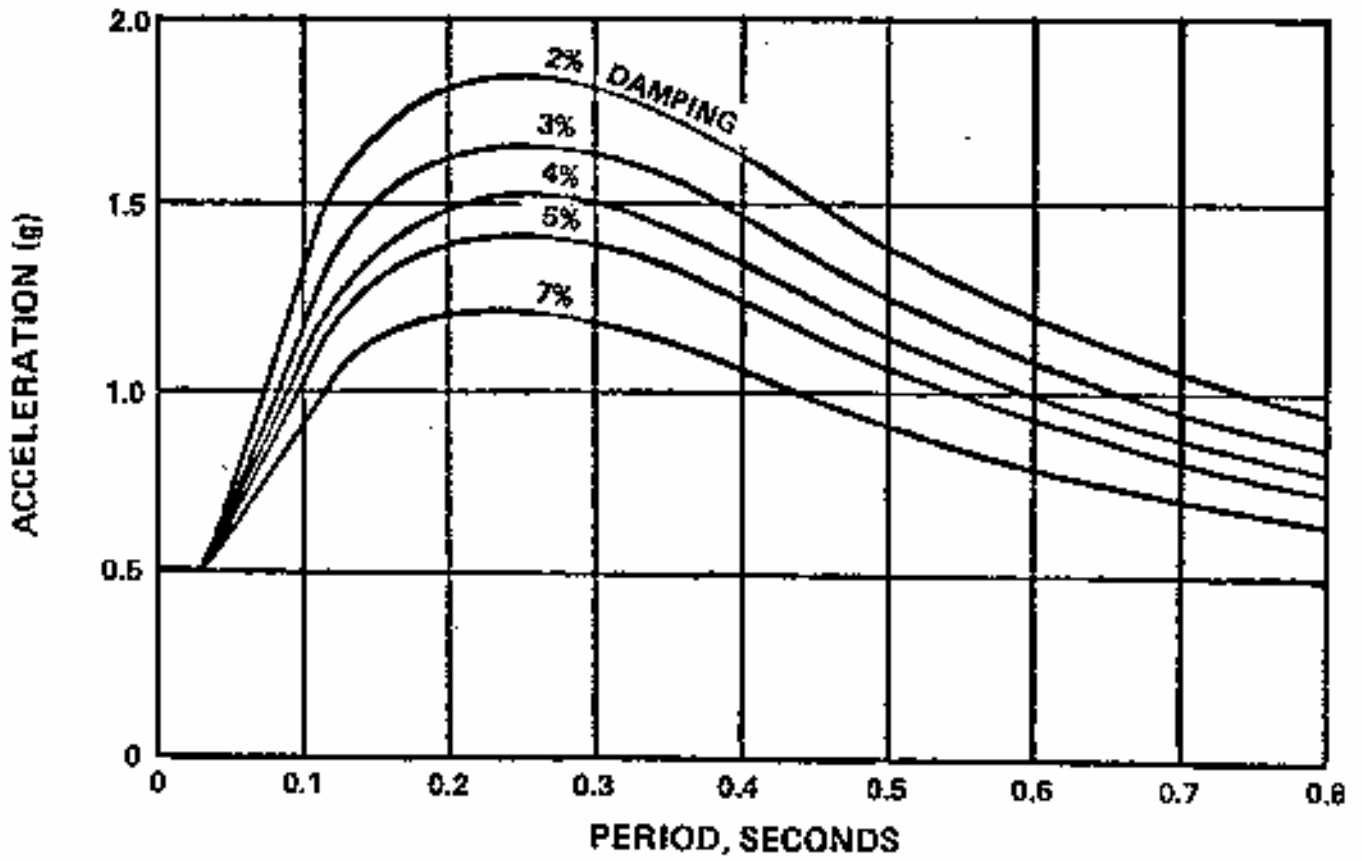
FSAR UPDATE
UNITS 1 AND 2 DIABLO CANYON SITE
FIGURE 2.5-29 FREE FIELD SPECTRA HORIZONTAL HOSGRI 7.5M/BLUME

Revision 11 November 1996



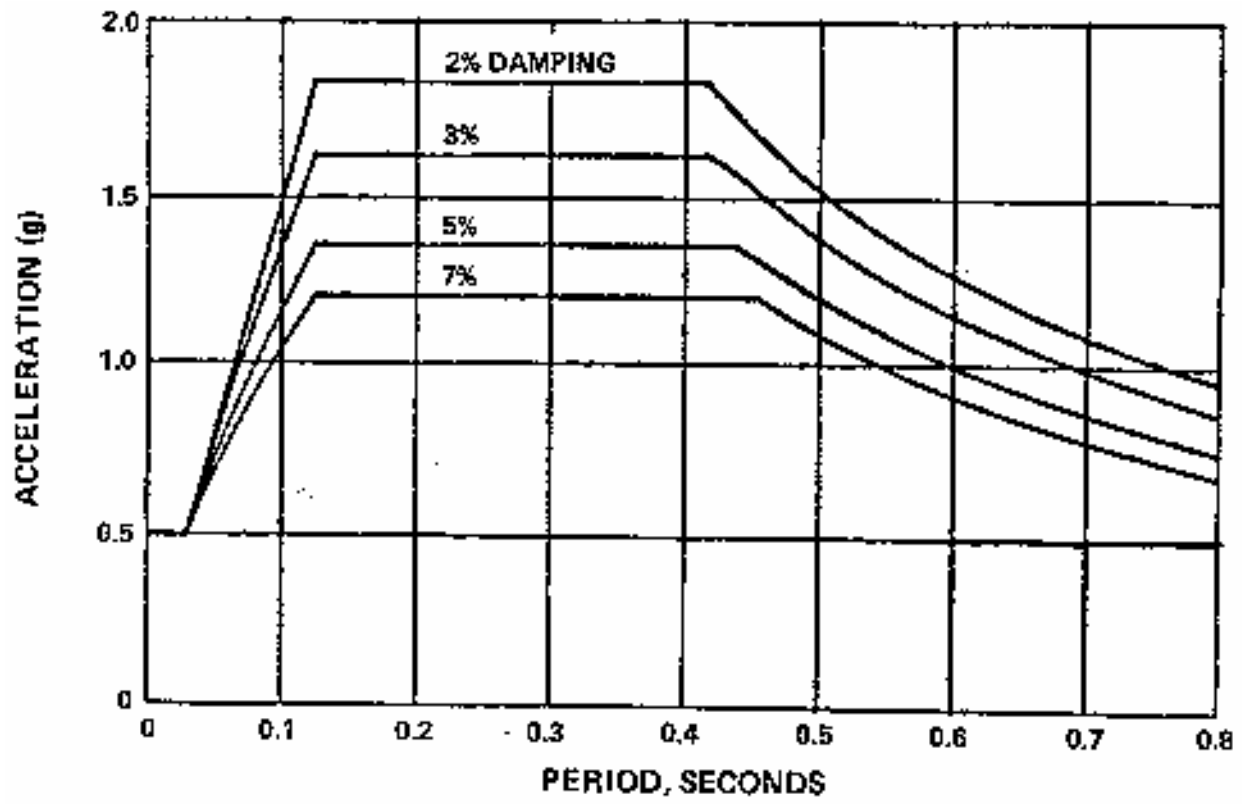
FSAR UPDATE
UNITS 1 AND 2 DIABLO CANYON SITE
FIGURE 2.5-30 FREE FIELD SPECTRA HORIZONTAL HOSGRI 7.5M/NEWMARK

Revision 11 November 1996



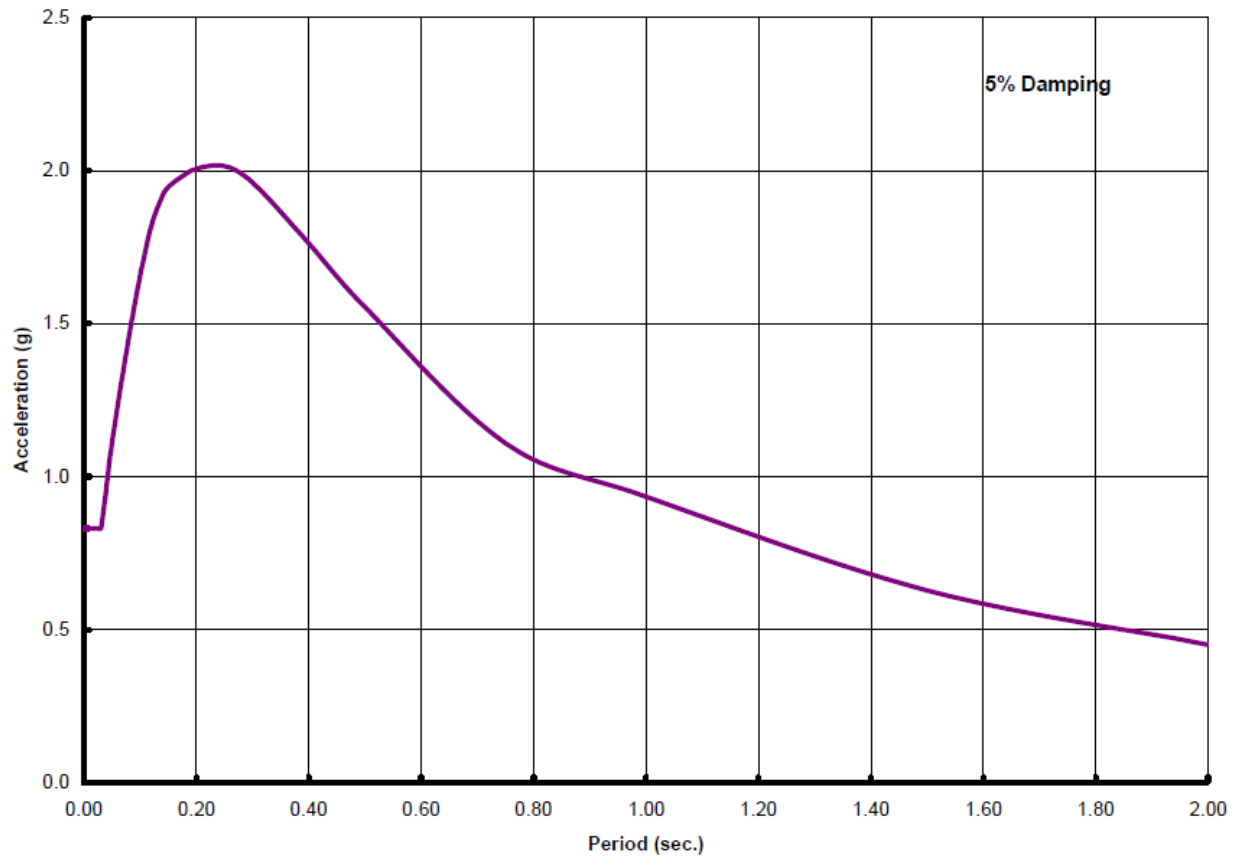
FSAR UPDATE
UNITS 1 AND 2 DIABLO CANYON SITE
FIGURE 2.5-31 FREE FIELD SPECTRA VERTICAL HOSGRI 7.5M/BLUME

Revision 11 November 1996



FSAR UPDATE
UNITS 1 AND 2 DIABLO CANYON SITE
FIGURE 2.5-32 FREE FIELD SPECTRA VERTICAL HOSGRI 7.5M/NEWMARK

Revision 11 November 1996

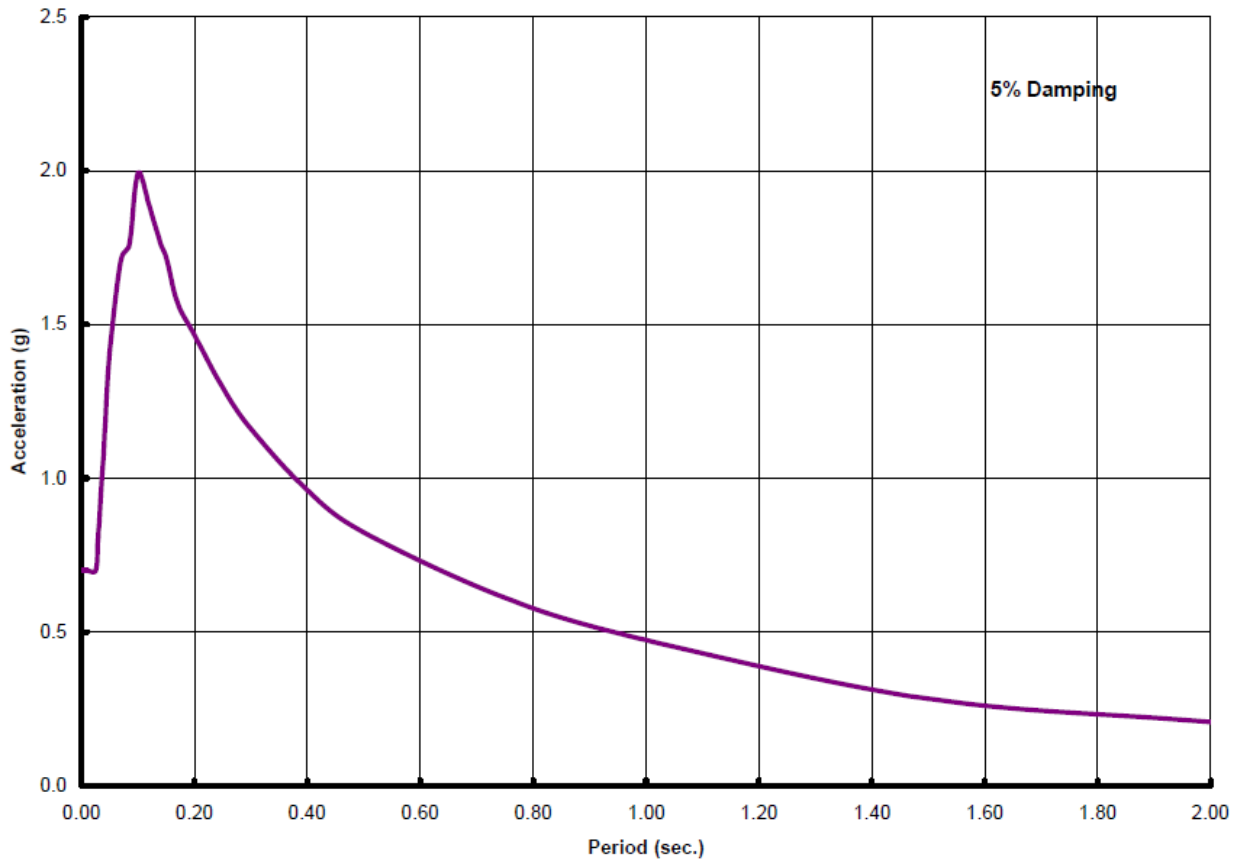


NOTES:

1. This figure is based on Reference 42, Figure 2.4

FSAR UPDATE
UNITS 1 AND 2 DIABLO CANYON SITE
FIGURE 2.5-33 FREE FIELD SPECTRUM HORIZONTAL 1991 LTSP (84TH PERCENTILE NON-EXCEEDANCE) AS MODIFIED PER SSER-34

Revision 21 September 2013

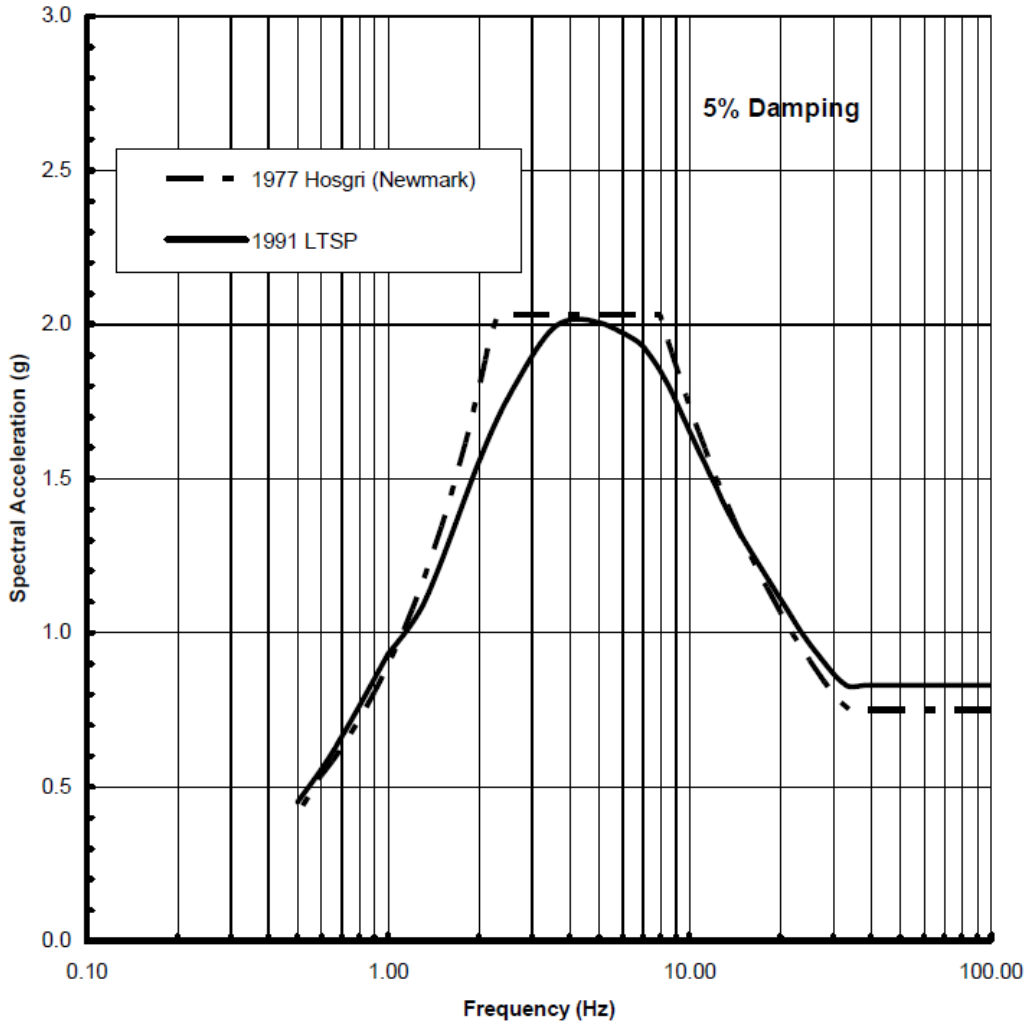


NOTES:

1. This Figure is based on Reference 42, Figure 2.5.

FSAR UPDATE
UNITS 1 AND 2 DIABLO CANYON SITE
FIGURE 2.5-34 FREE FIELD SPECTRUM VERTICAL 1991 LTSP (84TH PERCENTILE NON-EXCEEDANCE) AS MODIFIED PER SSER-34

Revision 21 September 2013



NOTES:

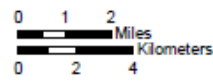
1. This Figure is based on Reference 40, Figure 7-2; however, the LTSP response spectrum has been adjusted in accordance with Reference 42, Figure 2.5.
2. This Figure is for comparison purposes only. Do not use for design.
3. Legend: 1977 Hosgri (Newmark) corresponds to the spectrum shown in Figure 2.5-30
1991 LTSP corresponds to the spectrum shown in Figure 2.5-33

FSAR UPDATE
UNITS 1 AND 2 DIABLO CANYON SITE
FIGURE 2.5-35 FREE FIELD SPECTRA HORIZONTAL LTSP (PG&E 1998) GROUND MOTION VS. HOSGRI (NEWMARK 1977)



LEGEND

- Study area
- Shoreline, Hosgri, San Luis Bay, and Wilmar Avenue faults, dashed where approximate, dotted where concealed

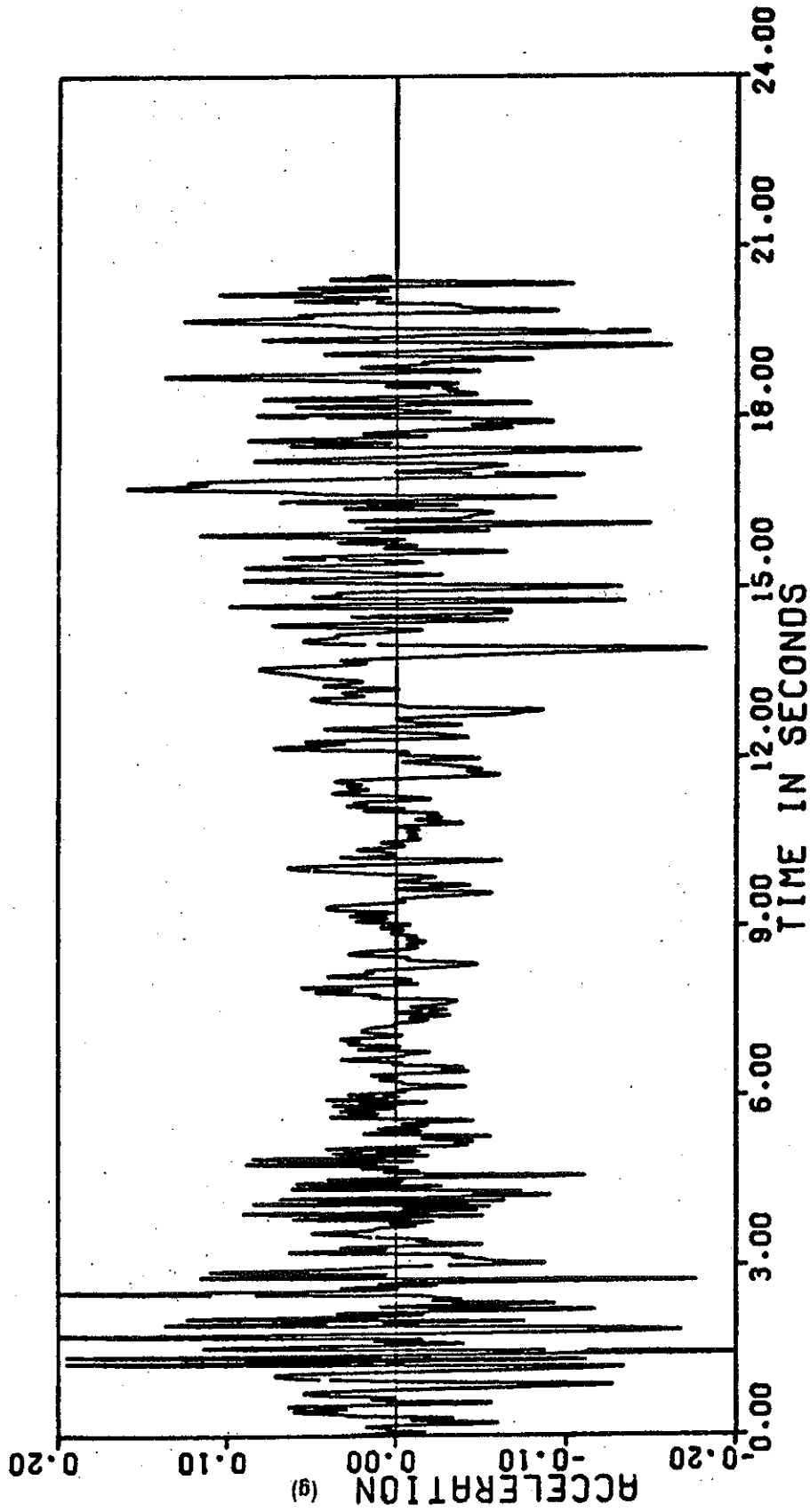


NOTE:

1. This figure is based on Reference 52, Figure 1-1.

FSAR UPDATE
UNITS 1 AND 2 DIABLO CANYON SITE
FIGURE 2.5-36 MAP OF SHORELINE FAULT STUDY AREA

Revision 21 September 2013



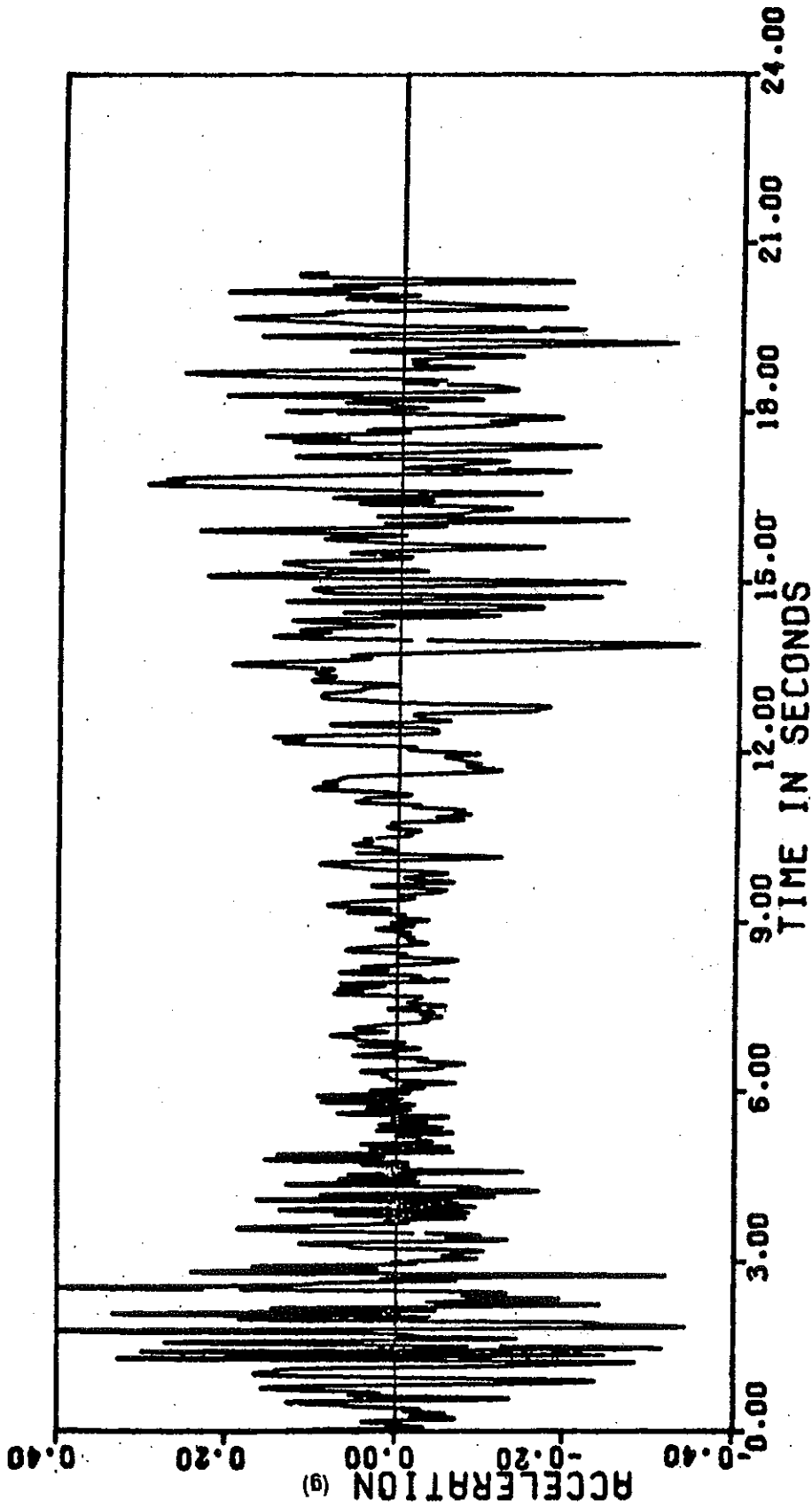
FSAR UPDATE

**UNITS 1 AND 2
DIABLO CANYON SITE**

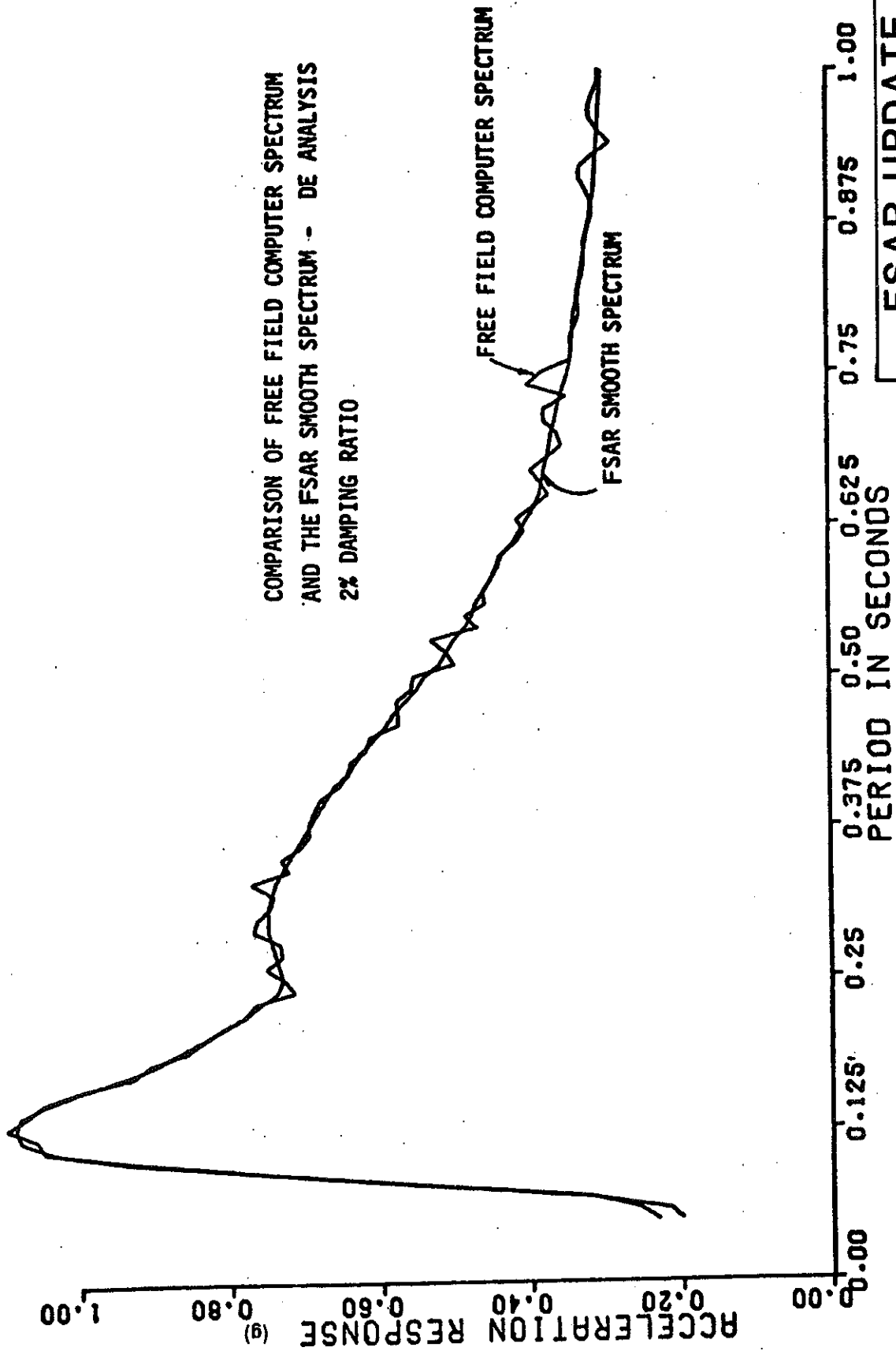
FIGURE 3.7-1

FREE FIELD GROUND MOTION
DE ANALYSIS

Revision 11 November 1996



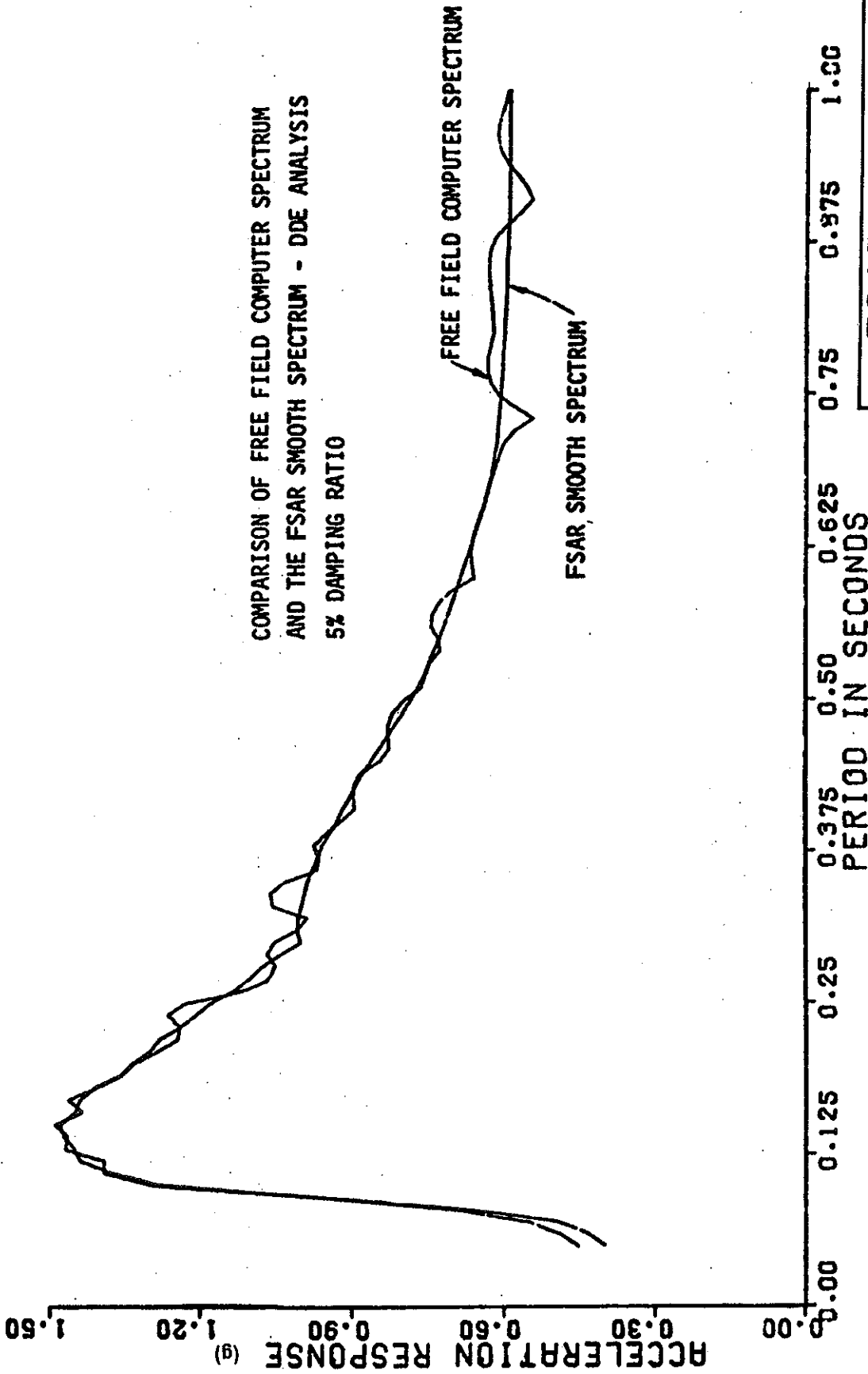
FSAR UPDATE
UNITS 1 AND 2 DIABLO CANYON SITE
FIGURE 3.7-2 FREE FIELD GROUND MOTION DDE ANALYSIS



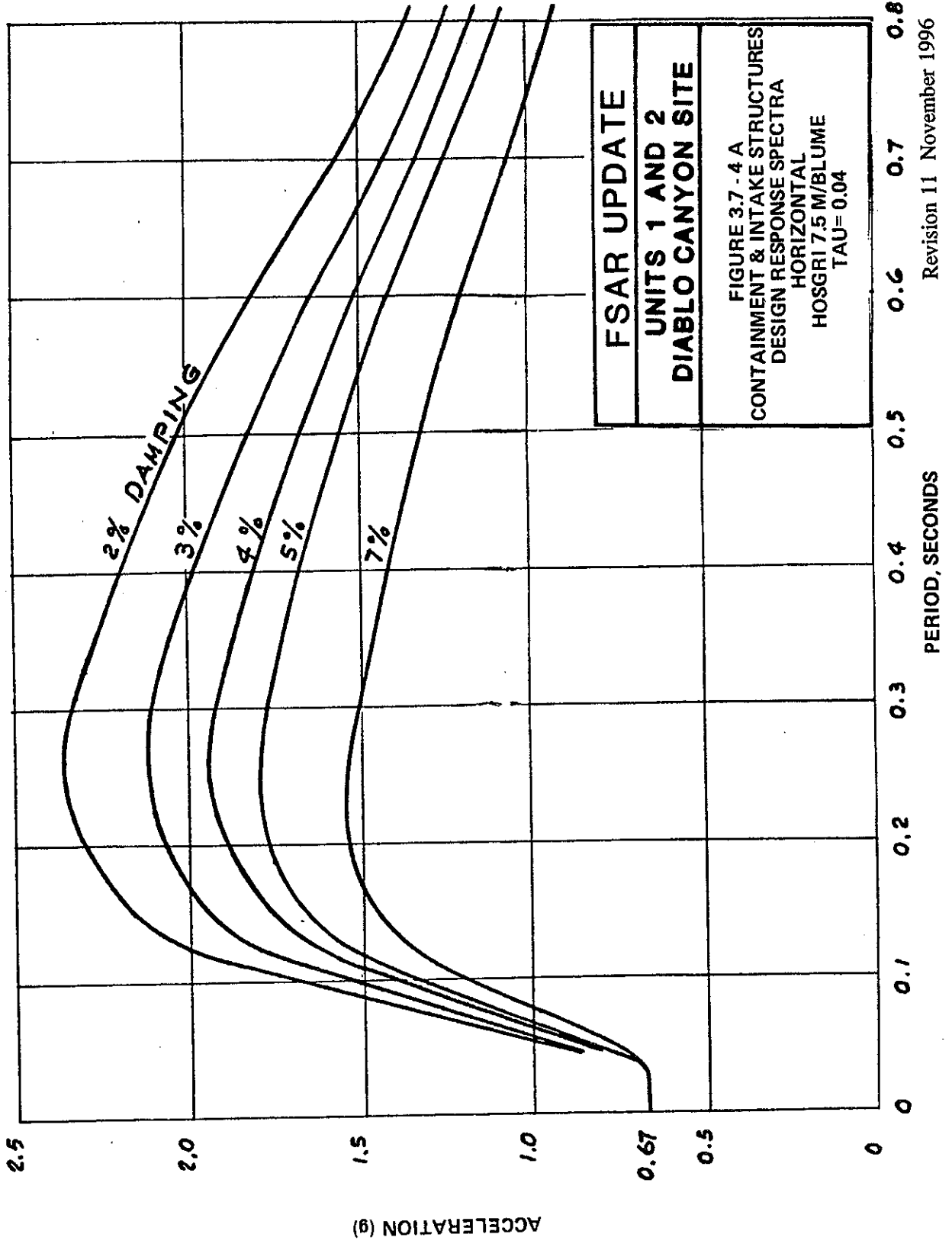
COMPARISON OF FREE FIELD COMPUTER SPECTRUM
AND THE FSAR SMOOTH SPECTRUM - DE ANALYSIS
2% DAMPING RATIO

FREE FIELD COMPUTER SPECTRUM
FSAR SMOOTH SPECTRUM

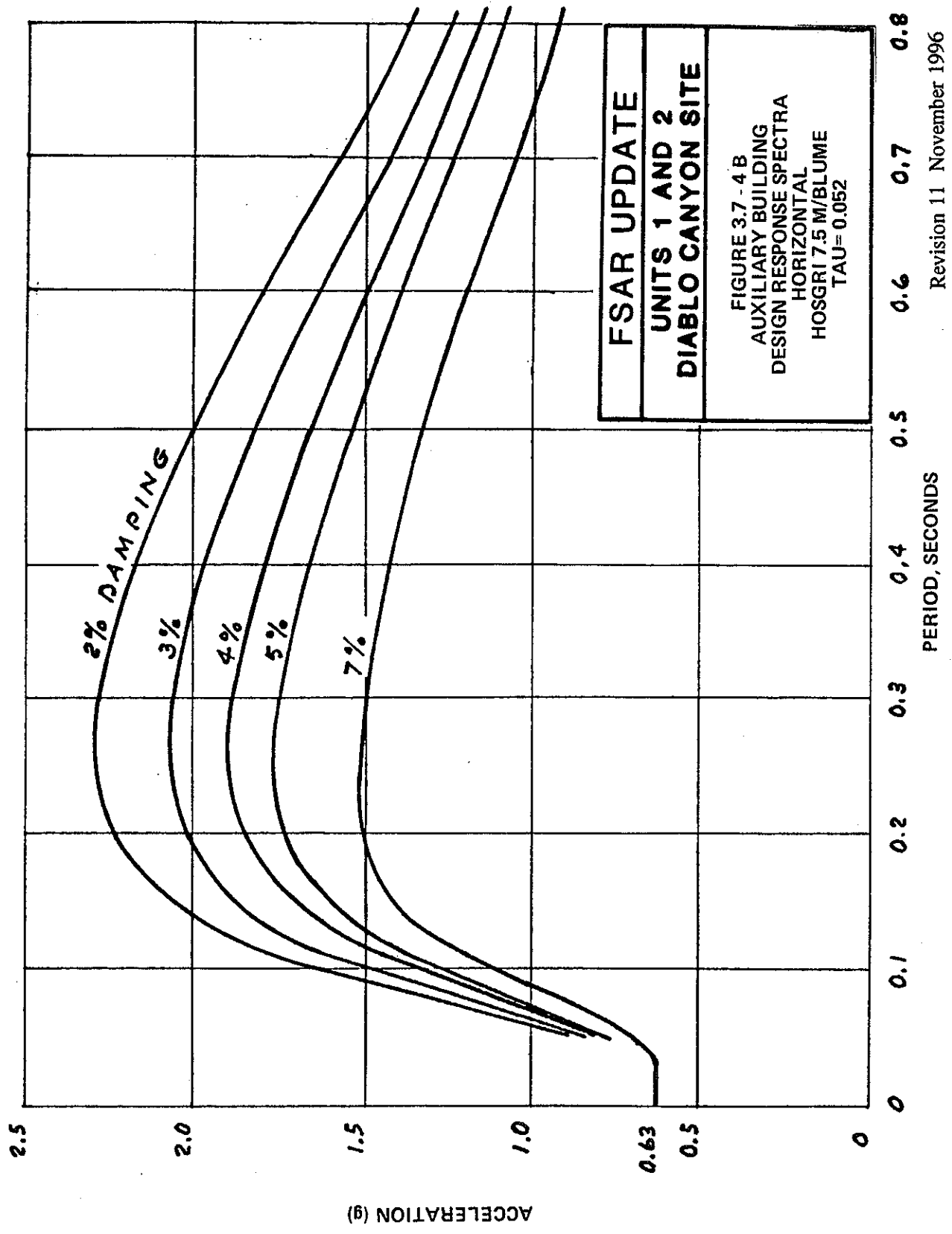
FSAR UPDATE
UNITS 1 AND 2
DIABLO CANYON SITE
FIGURE 3.73 COMPARISON OF SPECTRA 2% DAMPING RATIO



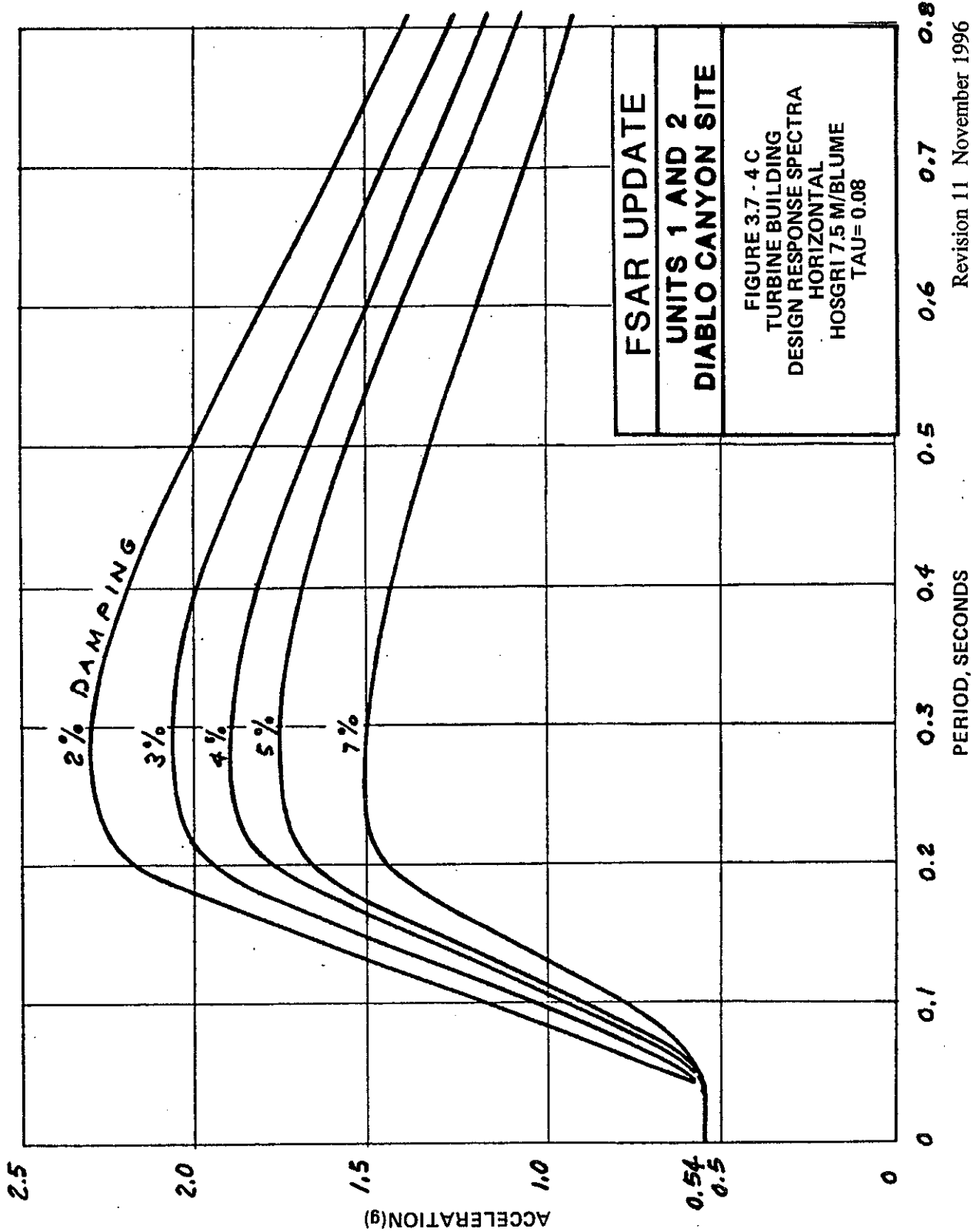
FSAR UPDATE
UNITS 1 AND 2 DIABLO CANYON SITE
FIGURE 3.7-4 COMPARISON OF SPECTRA 5% DAMPING RATIO

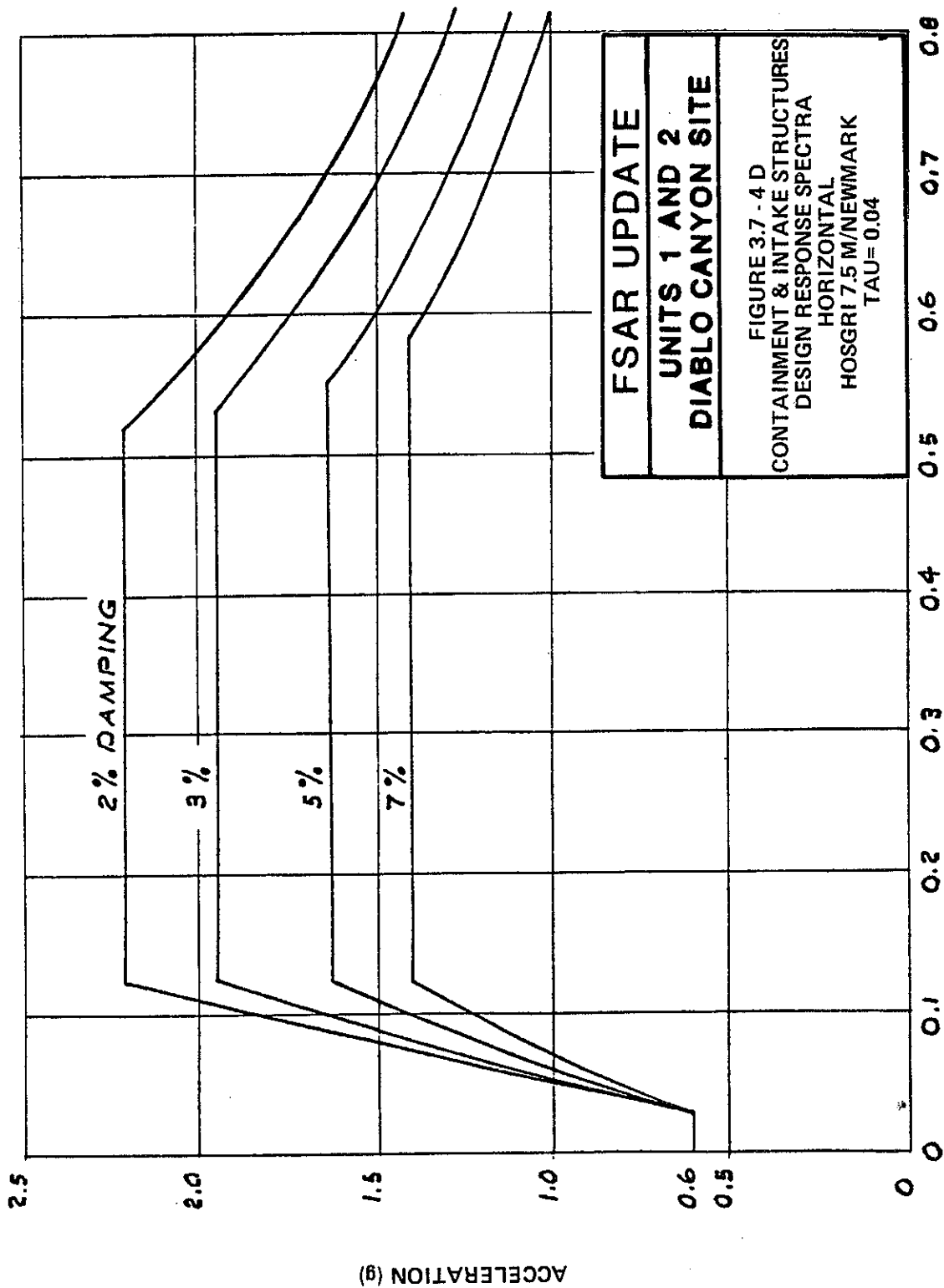


Revision 11 November 1996



Revision 11 November 1996



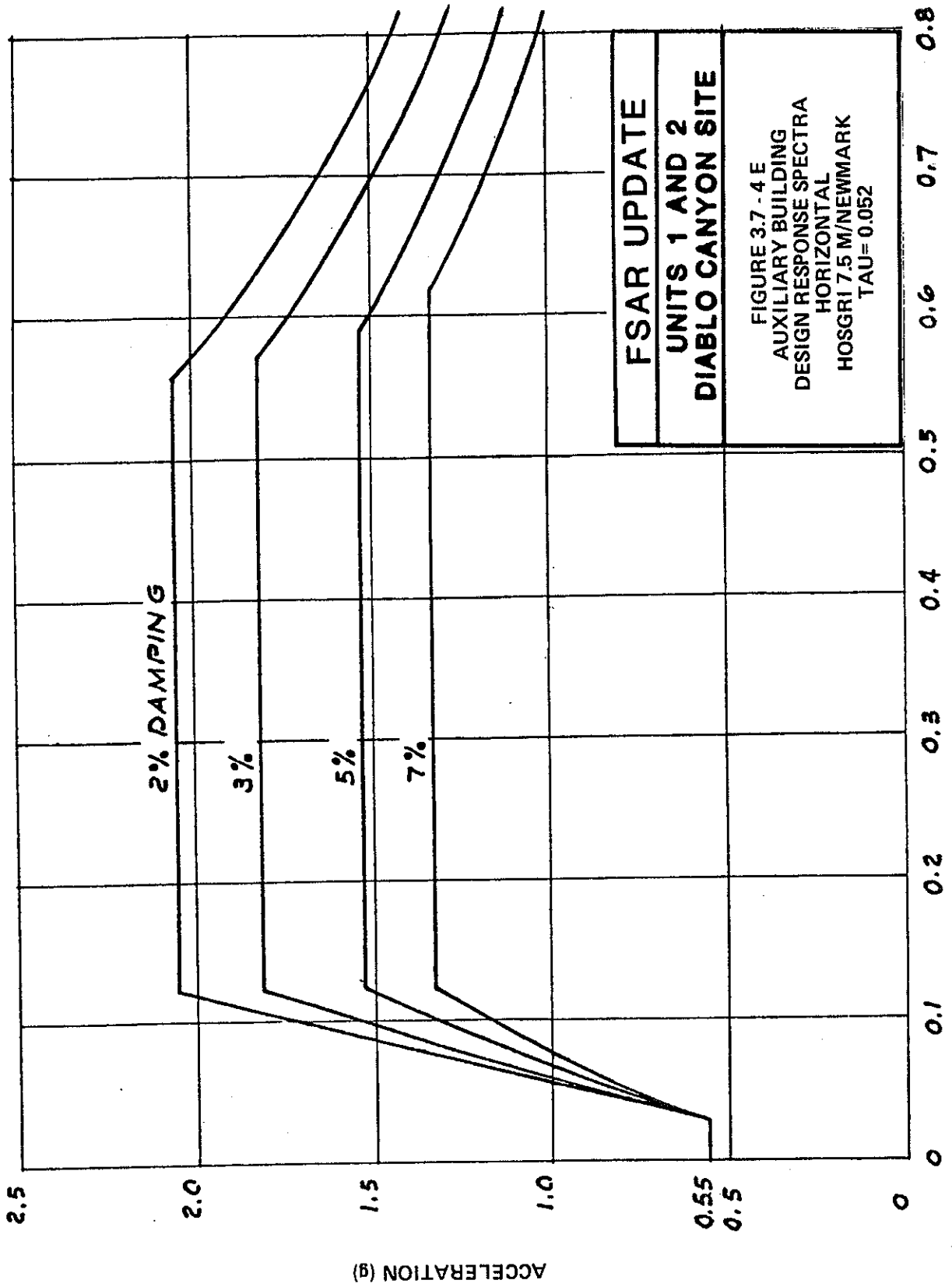


FSAR UPDATE
UNITS 1 AND 2
DIABLO CANYON SITE

FIGURE 3.7 - 4 D
CONTAINMENT & INTAKE STRUCTURES
DESIGN RESPONSE SPECTRA
HORIZONTAL
HOSGRI 7.5 M/NEWMARK
TAU= 0.04

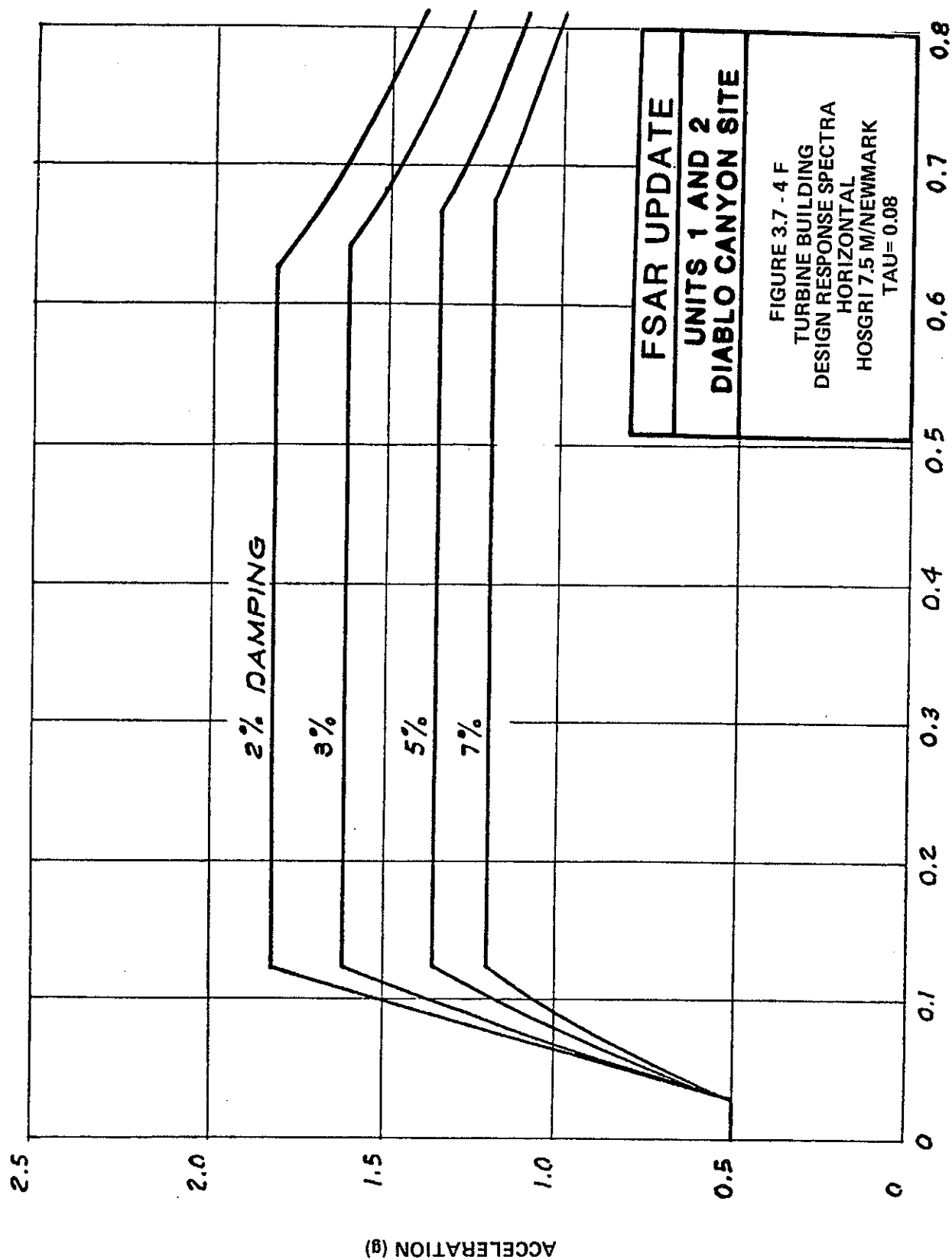
PERIOD, SECONDS

Revision 11 November 1996



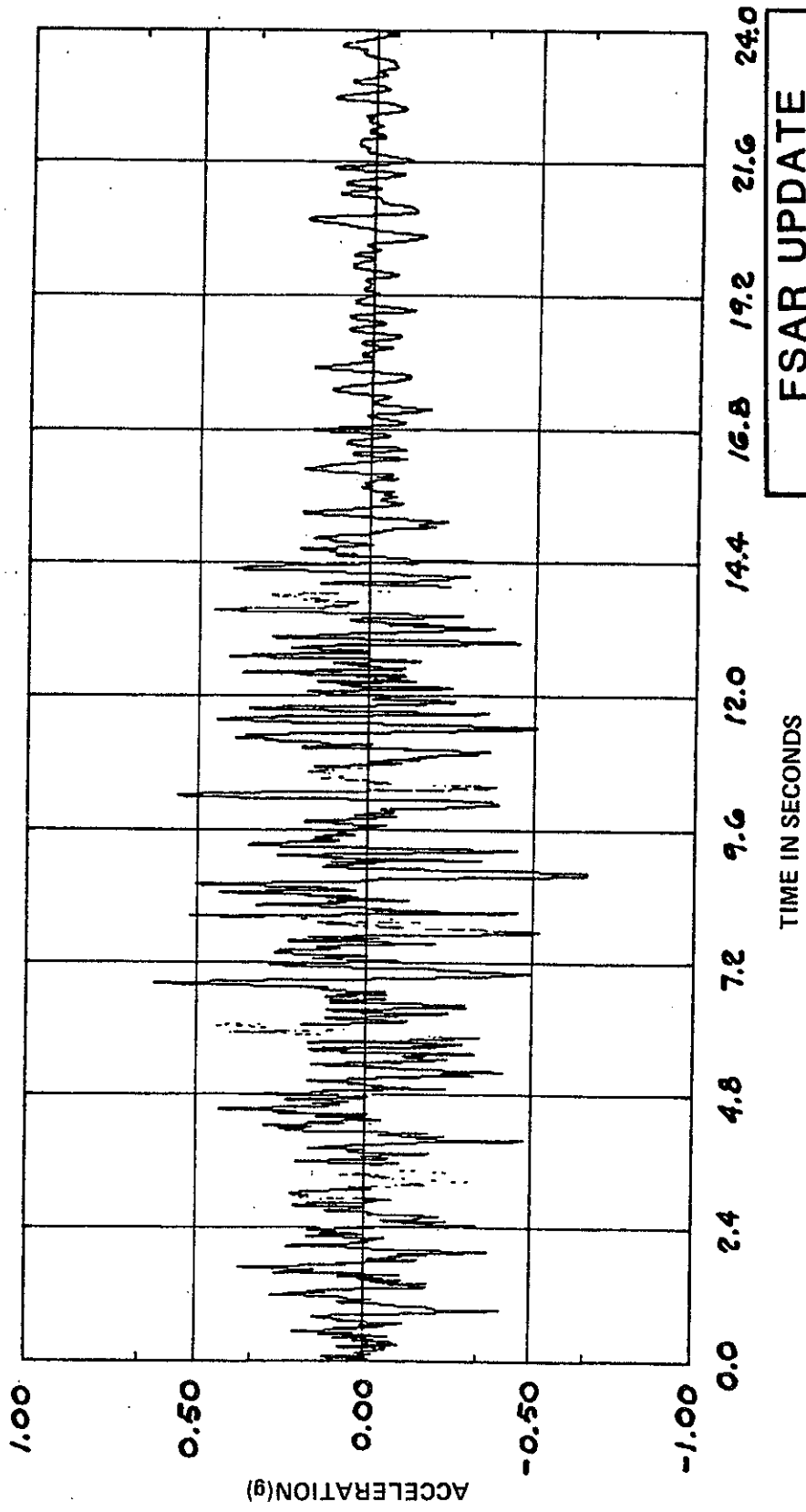
Revision 11 November 1996

PERIOD, SECONDS



FSAR UPDATE
UNITS 1 AND 2
DIABLO CANYON SITE

FIGURE 3.7 - 4 F
 TURBINE BUILDING
 DESIGN RESPONSE SPECTRA
 HORIZONTAL
 HOSGRI 7.5 M/NEWMARK
 TAU=0.08

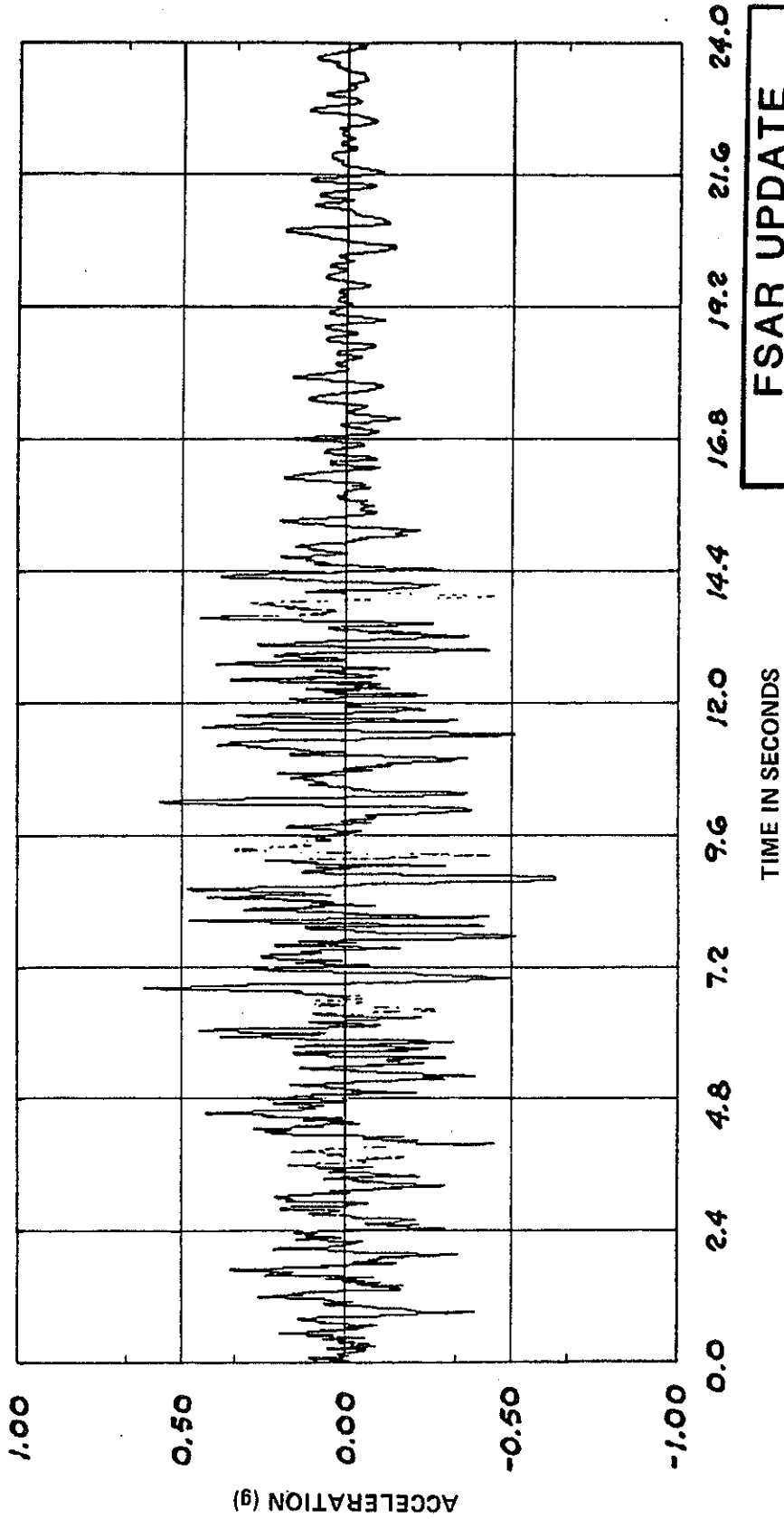


FSAR UPDATE

UNITS 1 AND 2

DIABLO CANYON SITE

FIGURE 3.7 - 4 G
 CONTAINMENT & INTAKE STRUCTURES
 HORIZONTAL TIME - HISTORY
 HOSGRI 7.5M/BLUME
 TAU = 0.04

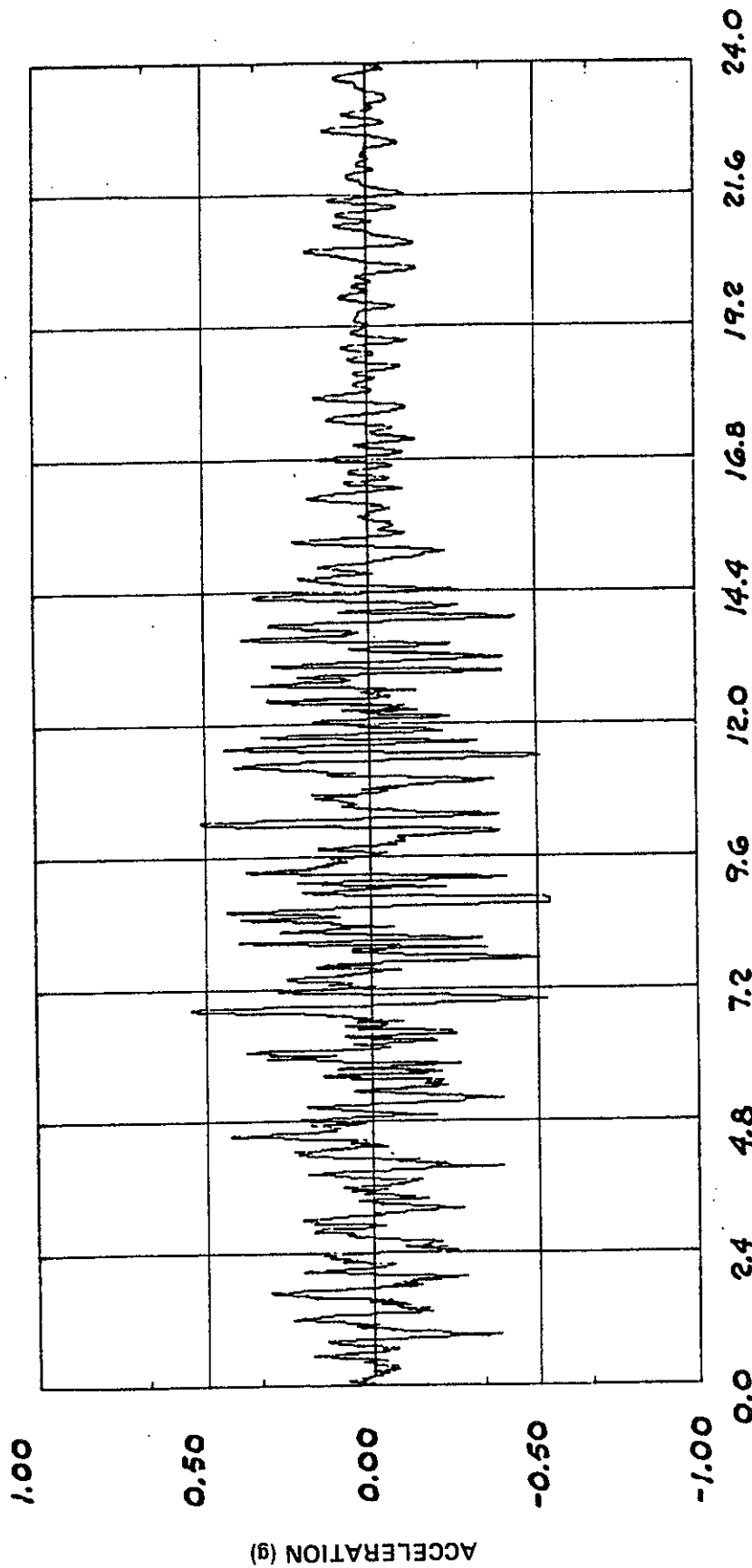


FSAR UPDATE

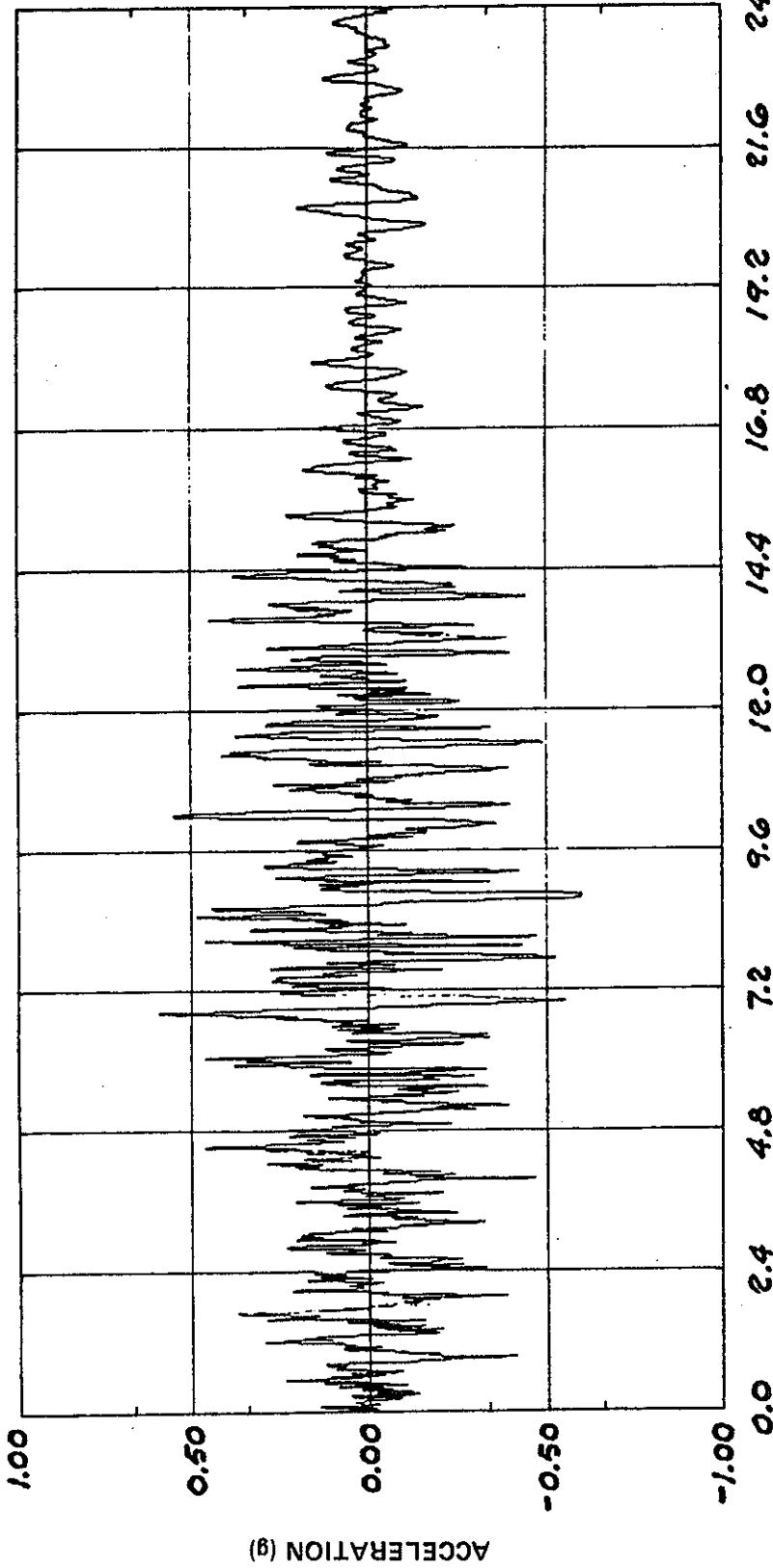
UNITS 1 AND 2

DIABLO CANYON SITE

FIGURE 3.7 - 4 H
AUXILIARY BUILDING
HORIZONTAL TIME - HISTORY
HOSGRI 7.5 M/BLUME
TAU= 0.052



FSAR UPDATE
UNITS 1 AND 2 DIABLO CANYON SITE
FIGURE 3.7 - 4 I TURBINE BUILDING HORIZONTAL TIME - HISTORY HOSGRI 7.5 M/BLUME TAU= 0.080

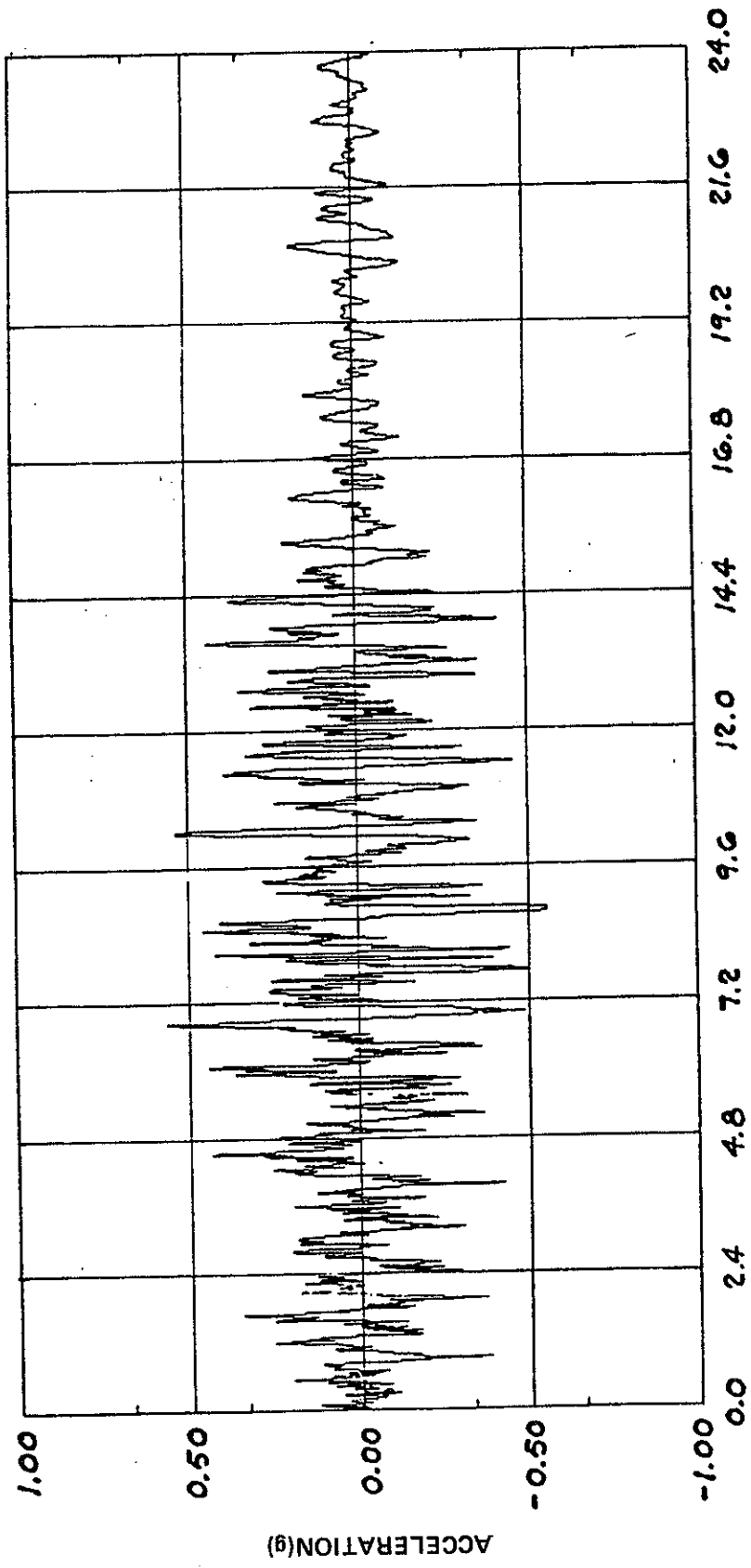


FSAR UPDATE

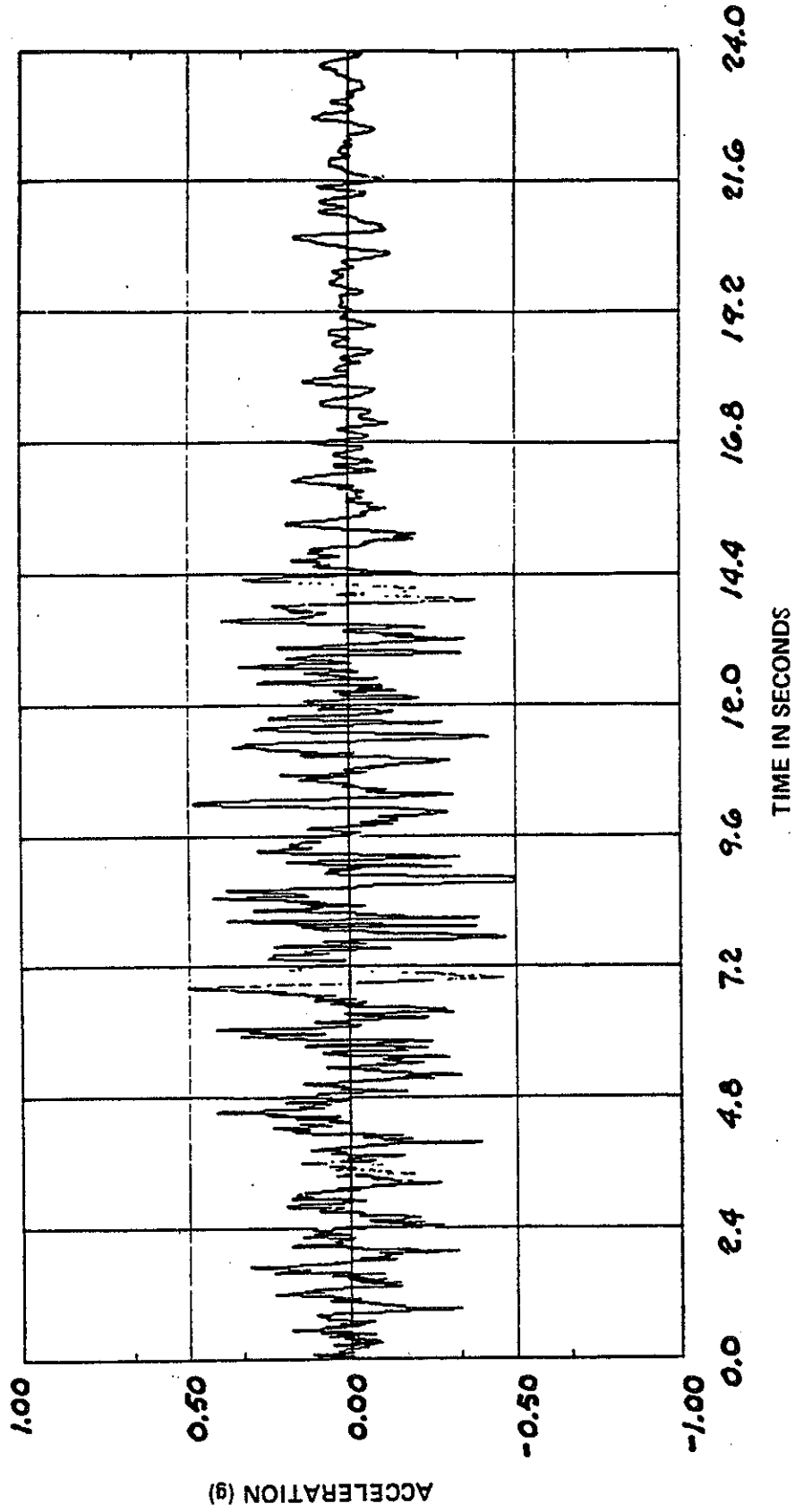
UNITS 1 AND 2

DIABLO CANYON SITE

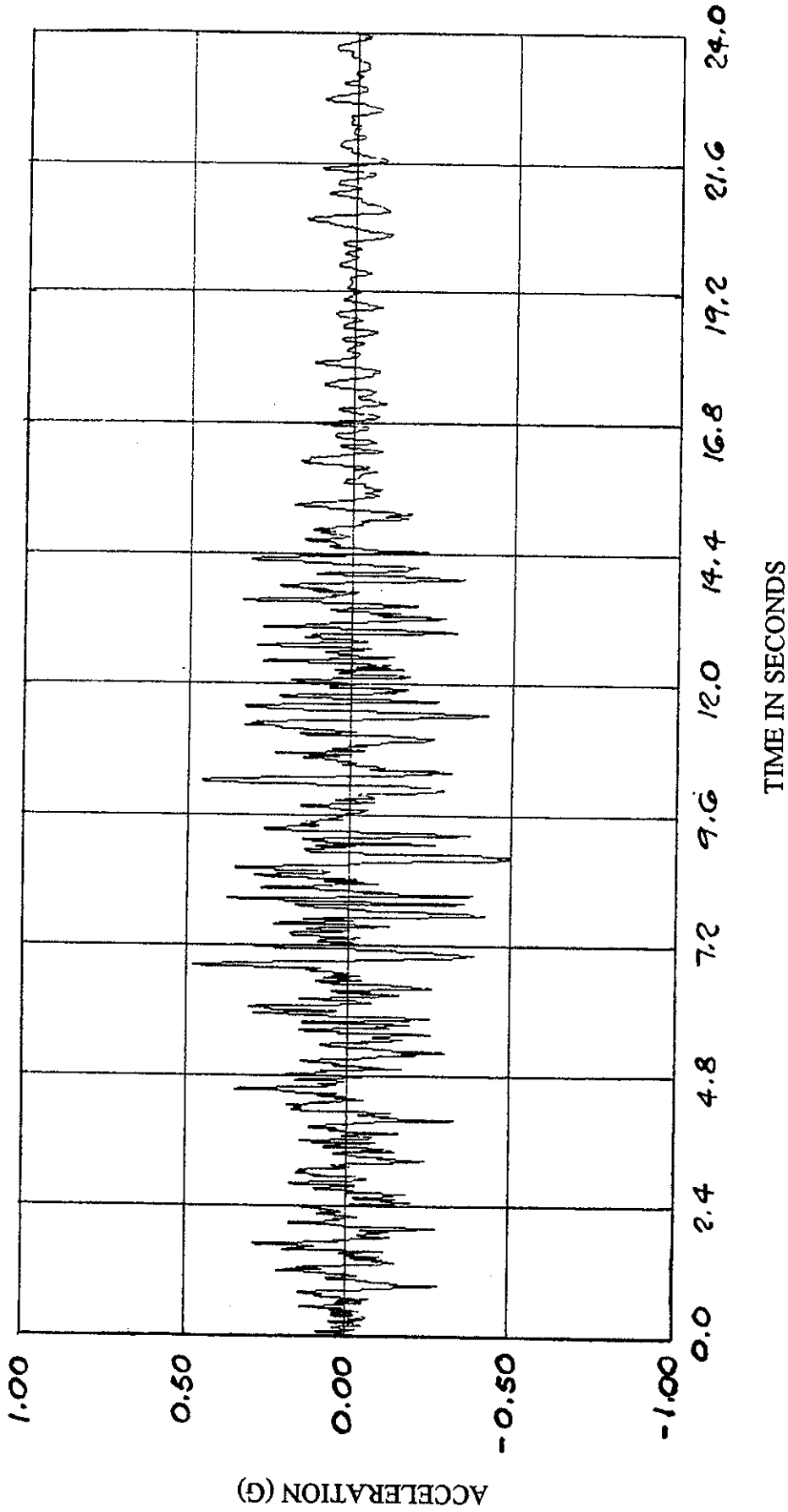
FIGURE 3.7 - 4 J
 CONTAINMENT & INTAKE STRUCTURES
 HORIZONTAL TIME - HISTORY
 HOSGRI 7.5M/NEWMARK
 TAU = 0.04



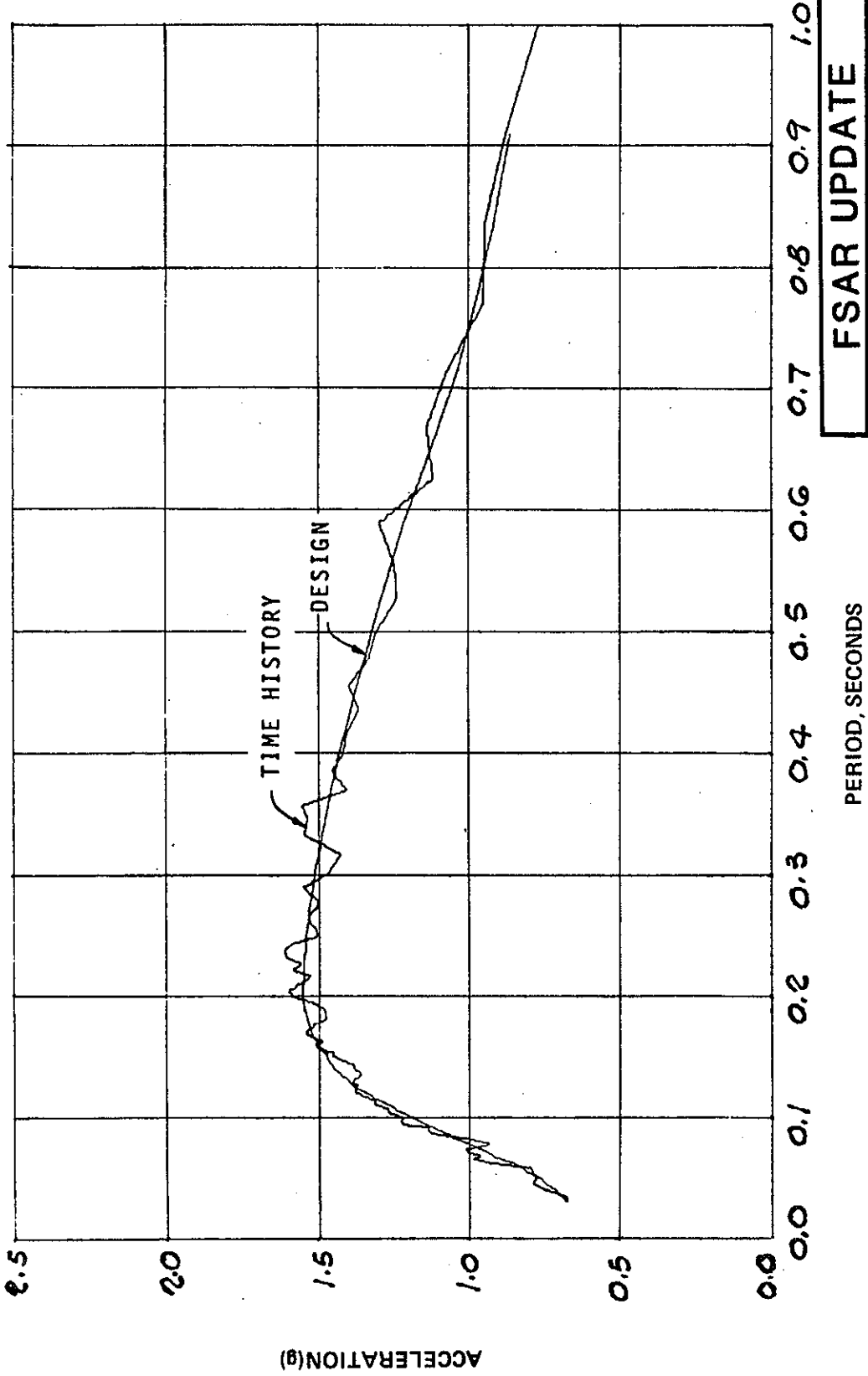
FSAR UPDATE
UNITS 1 AND 2 DIABLO CANYON SITE
FIGURE 3.7 - 4 K AUXILIARY BUILDING HORIZONTAL TIME - HISTORY HOSGRI 75M/NEWMARK TAU= 0.052



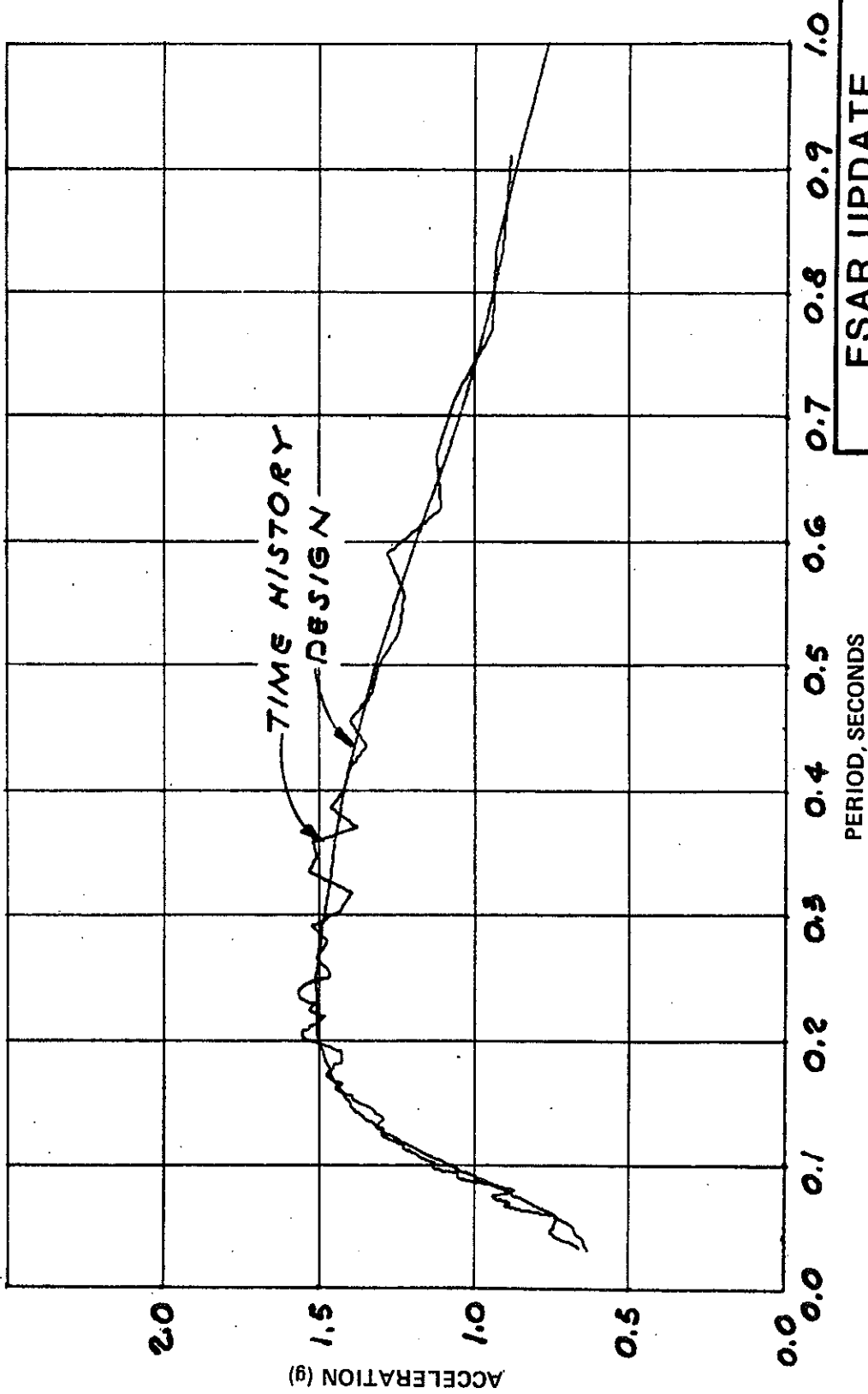
FSAR UPDATE
UNITS 1 AND 2 DIABLO CANYON SITE
FIGURE 3.7 - 4 L TURBINE BUILDING HORIZONTAL TIME - HISTORY HOSGRI 7.5M/NEWMARK TAU = 0.067



FSAR UPDATE
UNITS 1 AND 2
DIABLO CANYON SITE
FIGURE 3.7 - 4 M VERTICAL TIME HISTORY HOSGRI 7.5M/NEWMARK TAU = 0.0



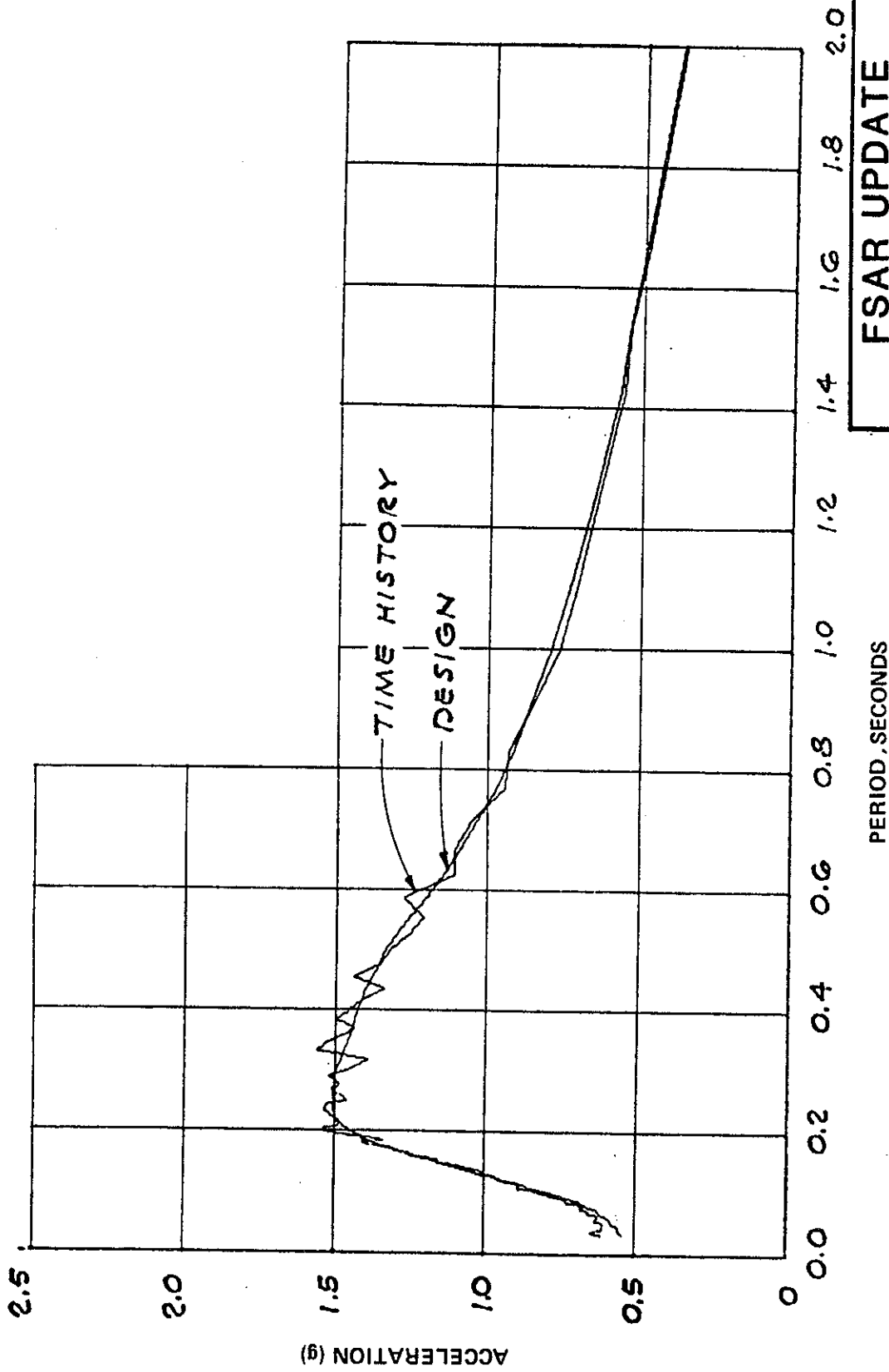
FSAR UPDATE
UNITS 1 AND 2 DIABLO CANYON SITE
FIGURE 3.7 - 4 N CONTAINMENT & INTAKE STRUCTURES COMPARISON OF SPECTRA HORIZONTAL HOSGRI 7.5 M/BLUME TAU= 0.04, 7% DAMPING



FSAR UPDATE

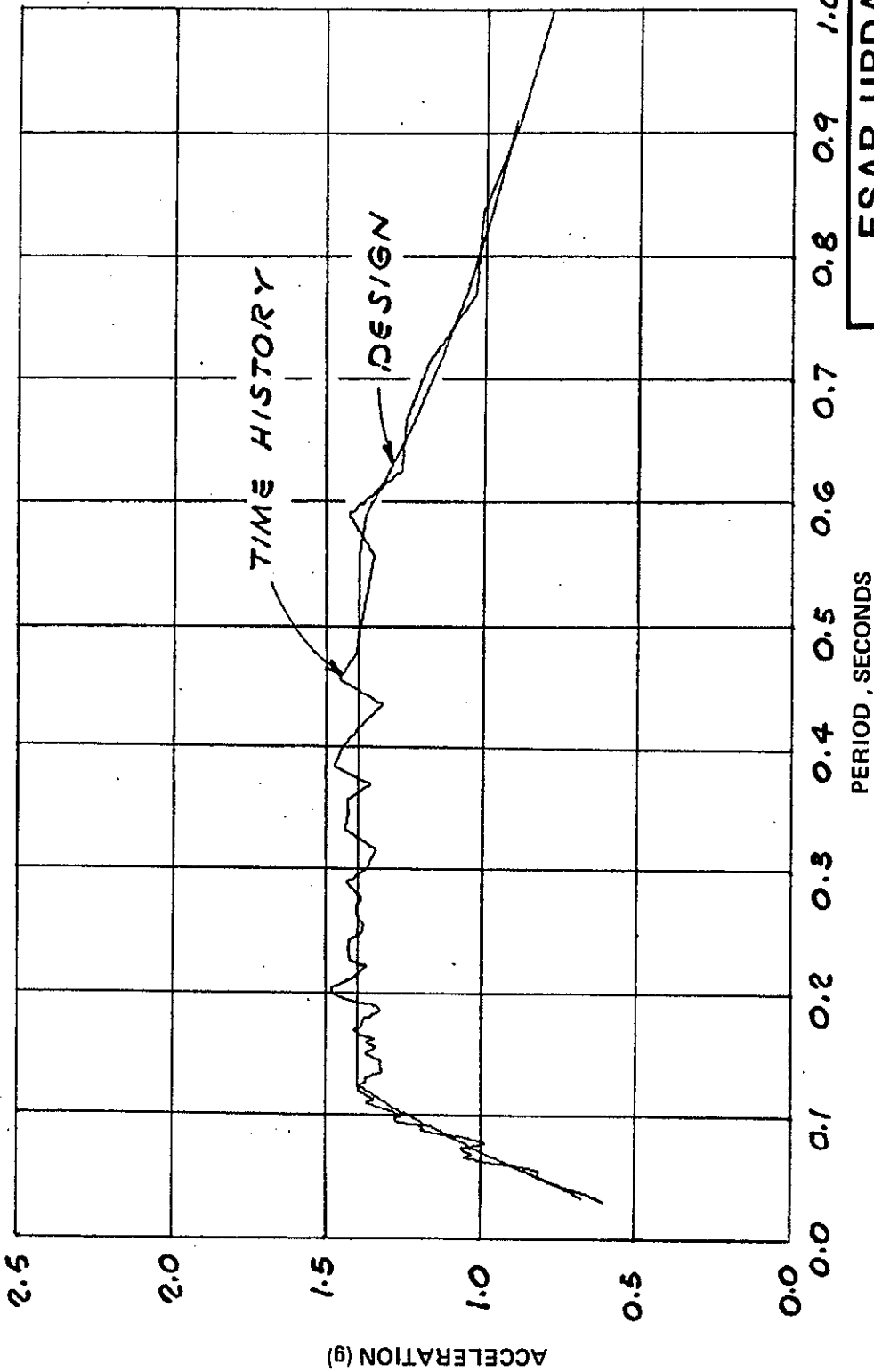
UNITS 1 AND 2
DIABLO CANYON SITE

FIGURE 3.7 - 4 0
AUXILIARY BUILDING
COMPARISON OF SPECTRA
HORIZONTAL
HOSGRI 7.5M/BLUME
TAU= 0.052, 7% DAMPING



FSAR UPDATE
UNITS 1 AND 2
DIABLO CANYON SITE

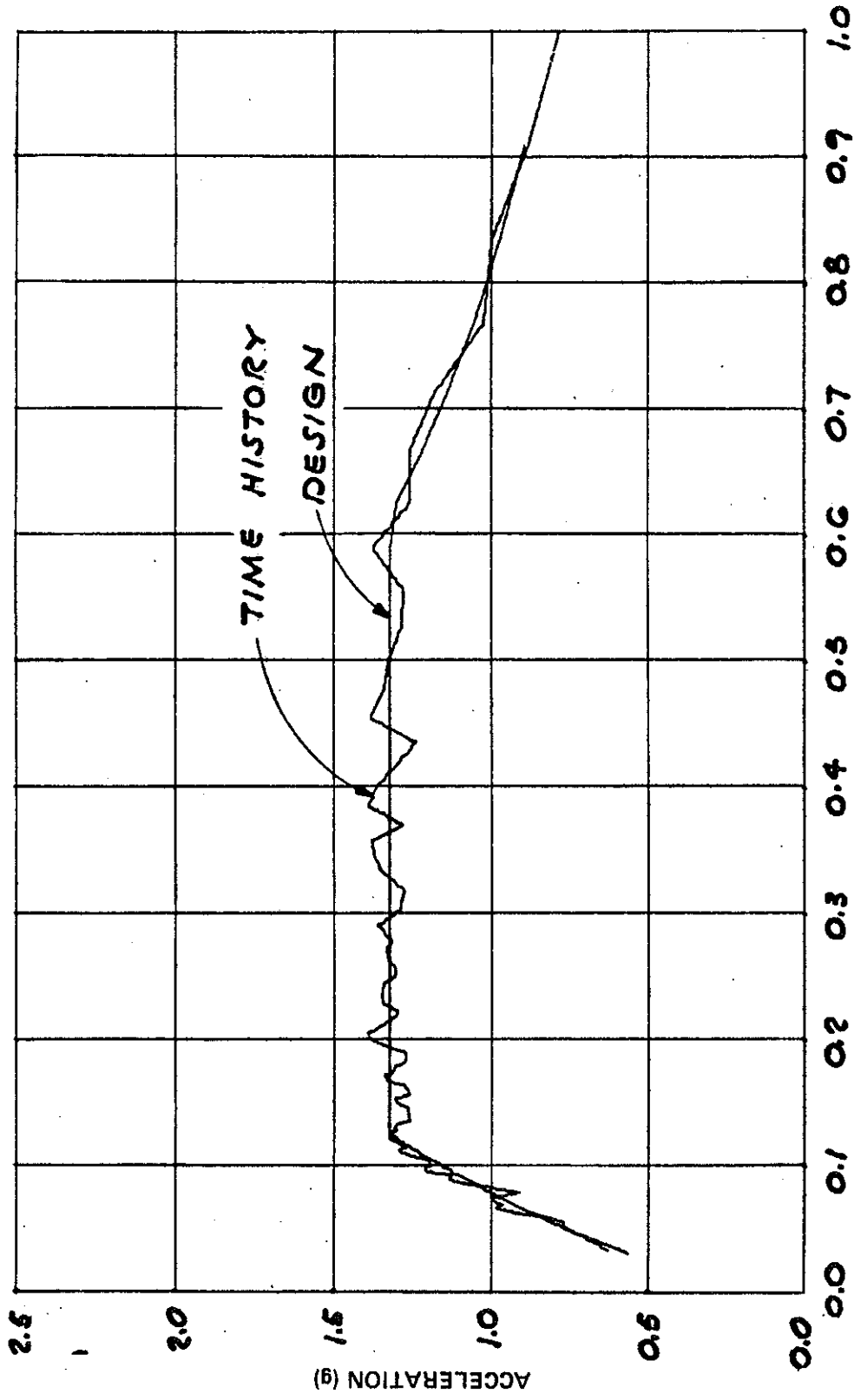
FIGURE 3.7 - 4 P
 TURBINE BUILDING
 COMPARISON OF SPECTRA
 HORIZONTAL
 HOSGRI 7.5 M/BLUME
 TAU = 0.080, 7% DAMPING



FSAR UPDATE

UNITS 1 AND 2
DIABLO CANYON SITE

FIGURE 3.7 - 4 Q
CONTAINMENT AND INTAKE
STRUCTURES
COMPARISON OF SPECTRA
HORIZONTAL
HOSGRI 7.5 M/NEWMARK
TAU = 0.04, 7% DAMPING

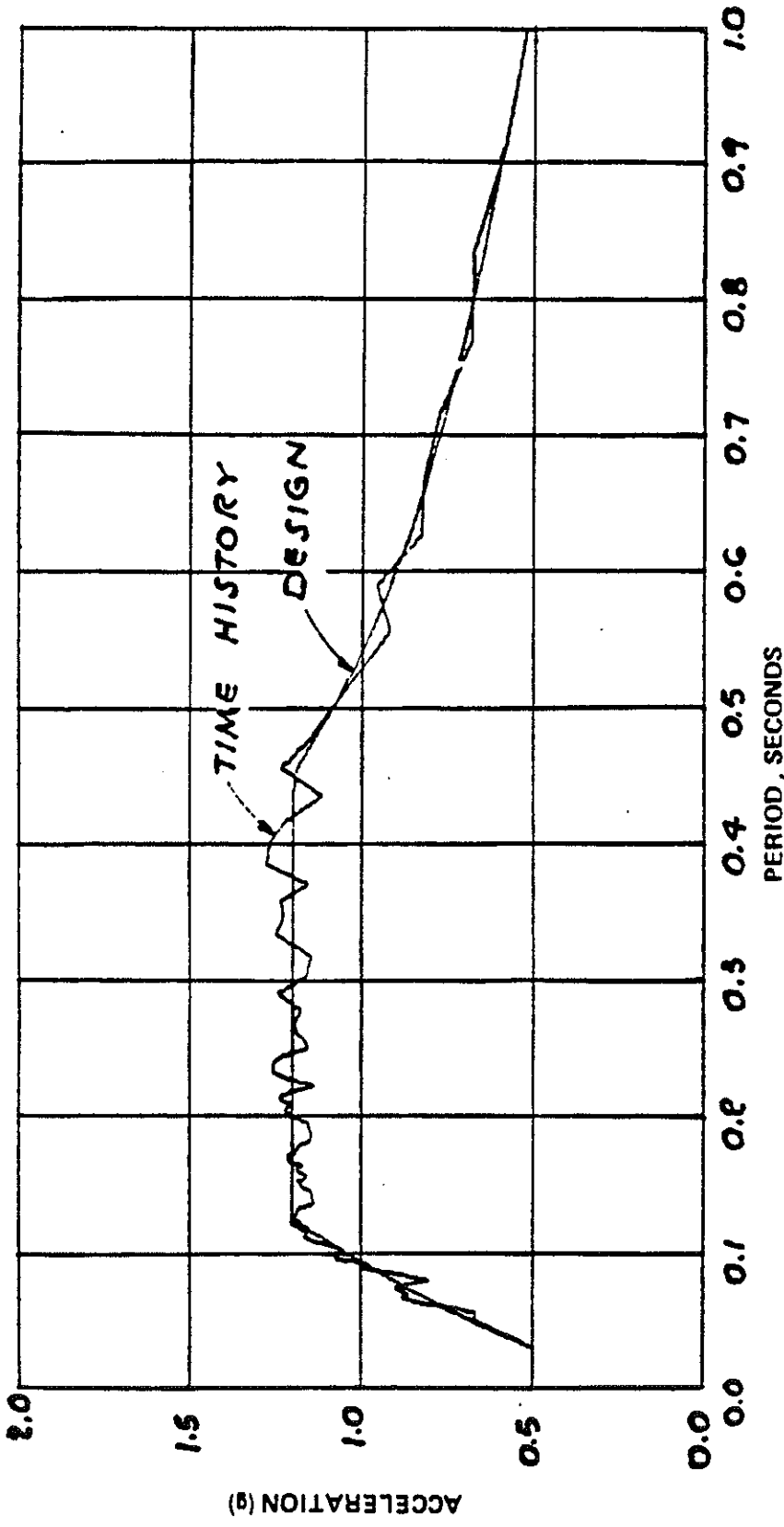


FSAR UPDATE

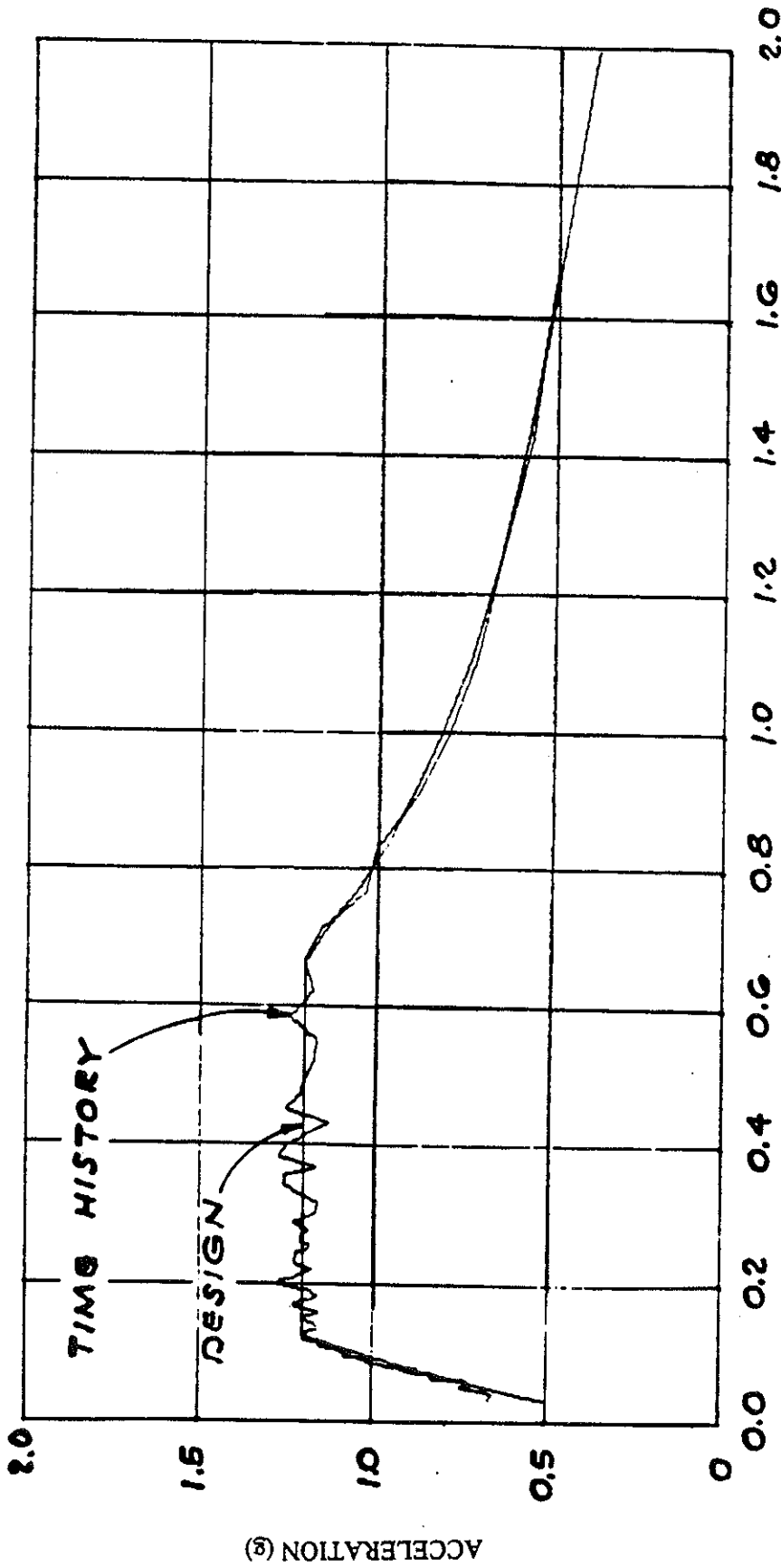
UNITS 1 AND 2

DIABLO CANYON SITE

FIGURE 3.7-4 R
 AUXILIARY BUILDING
 COMPARISON OF SPECTRA
 HORIZONTAL
 HOSGR1 7.5 M/NEWMARK
 TAU= 0.052, 7% DAMPING

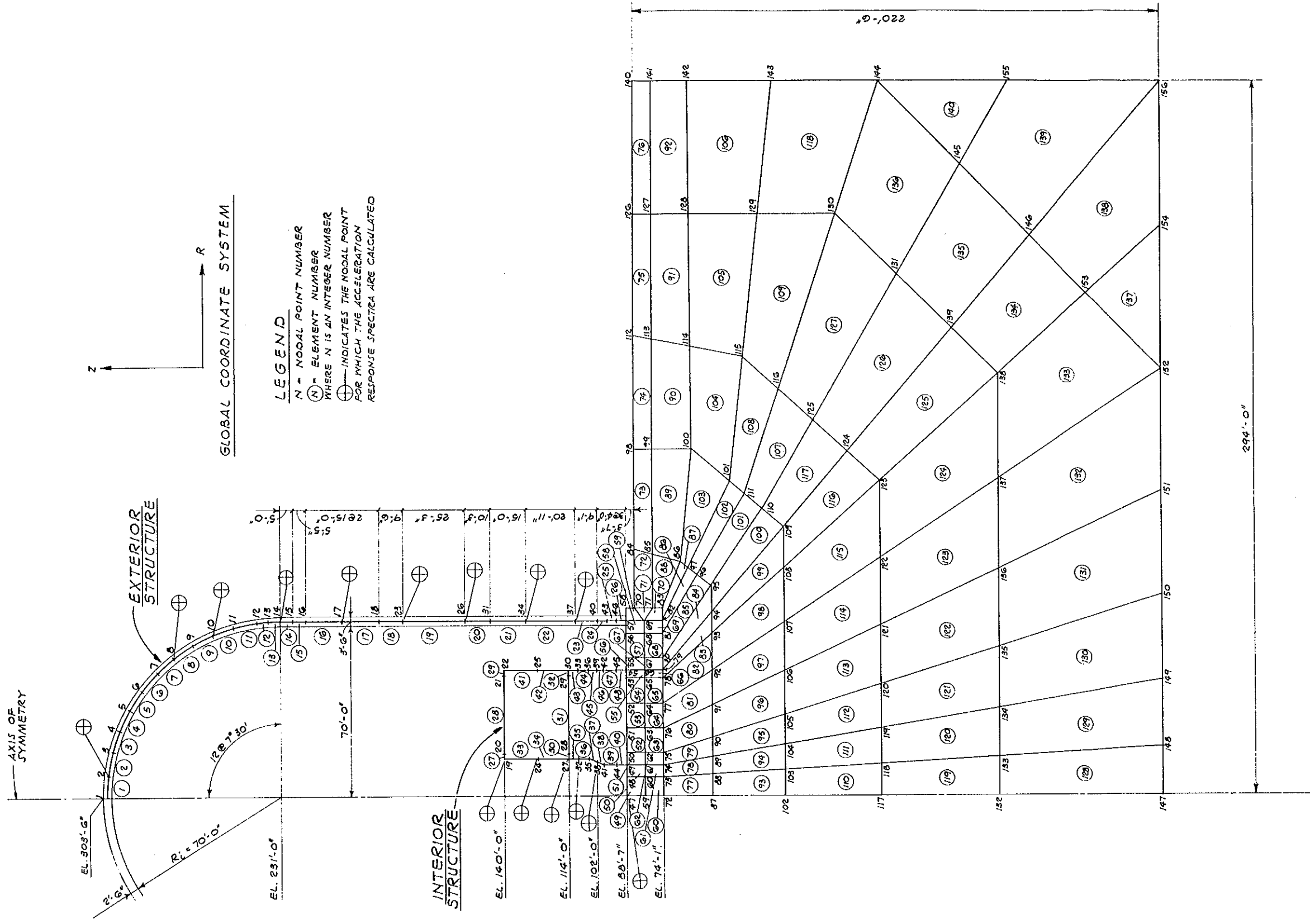


FSAR UPDATE
UNITS 1 AND 2
DIABLO CANYON SITE
FIGURE 3.7 - 4S
COMPARISON OF SPECTRA
VERTICAL
HOSGRI 7.5 M/NEWMARK
TAU = 0.0, 7% DAMPING



PERIOD, SECONDS

FSAR UPDATE
UNIT 1
DIABLO CANYON SITE
FIGURE 3.7 - 4 T TURBINE BUILDING COMPARISON OF SPECTRA HORIZONTAL HOSGRI 7.5M/NEWMARK TAU = 0.067, 7% DAMPING



FSAR UPDATE

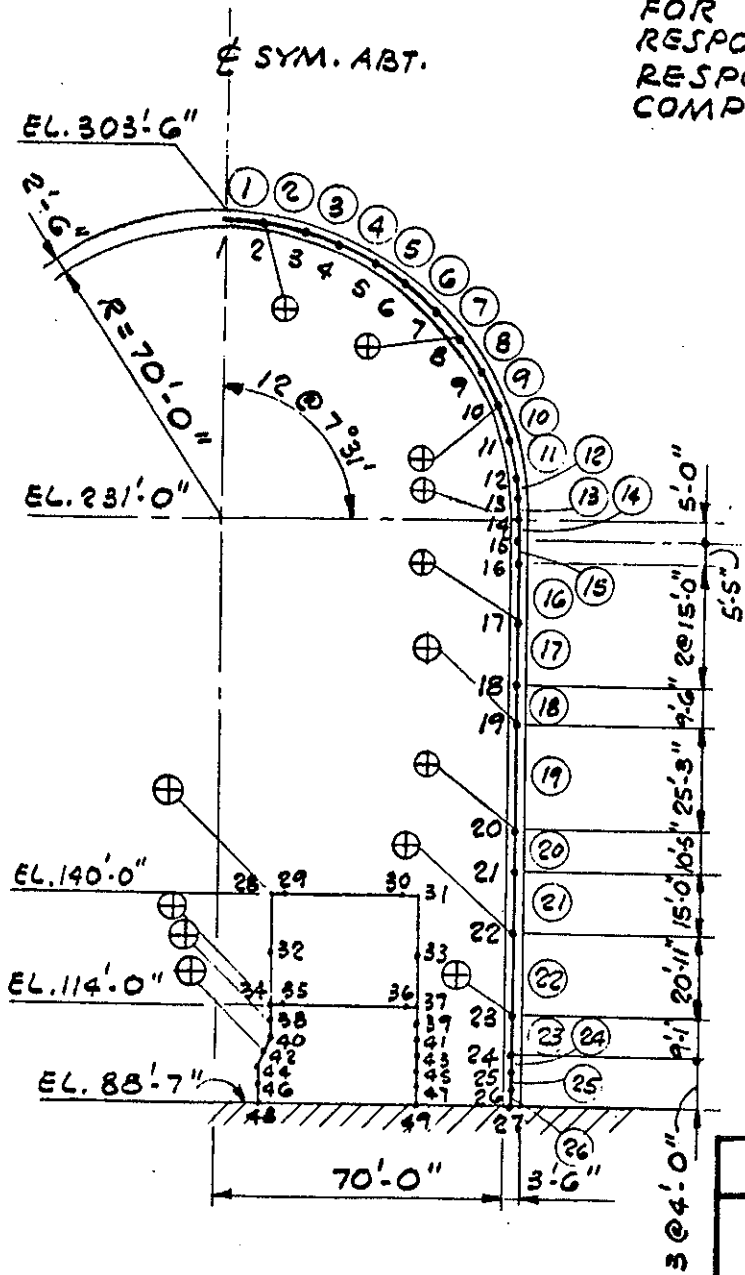
**UNITS 1 AND 2
DIABLO CANYON SITE**

FIGURE 3.7-5

CONTAINMENT STRUCTURE
FINITE ELEMENT MODEL

LEGEND

- 10 NODAL POINT NUMBER
- ⑦ ELEMENT NUMBER
- ⊕ INDICATES NODAL POINTS FOR WHICH STRUCTURE RESPONSES AND ACCELERATION RESPONSE SPECTRA ARE COMPUTED

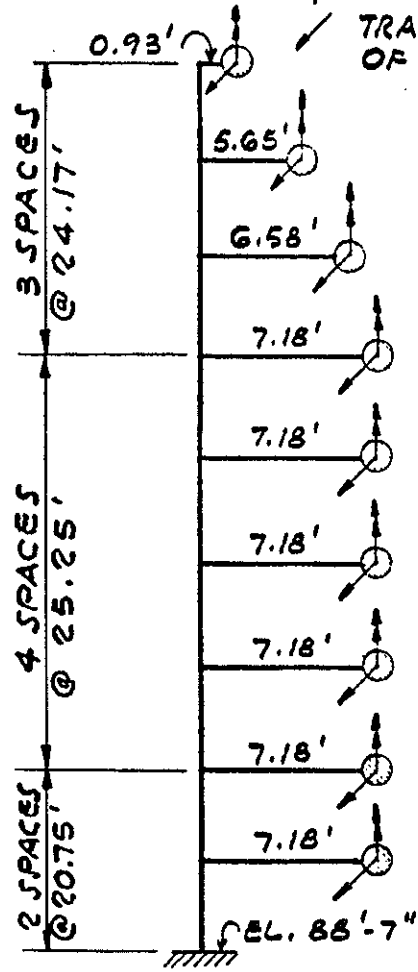


Note: Used for horizontal and vertical analysis of exterior shell and horizontal analysis of internal structure

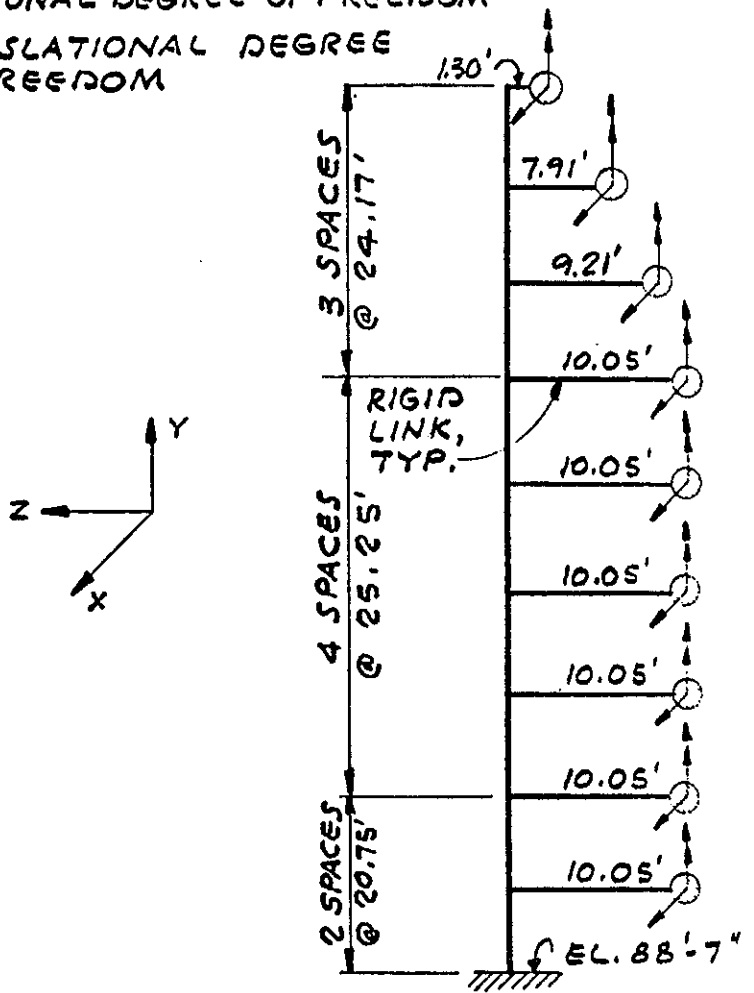
FSAR UPDATE
UNIT 1 DIABLO CANYON SITE
FIGURE 3.7 - 5 A CONTAINMENT STRUCTURE FINITE ELEMENT MODEL

LEGEND

- MASS POINT
- ↑ TORSIONAL DEGREE OF FREEDOM
- ↙ TRANSLATIONAL DEGREE OF FREEDOM



MODEL 1
5% ACCIDENTAL ECCENTRICITY

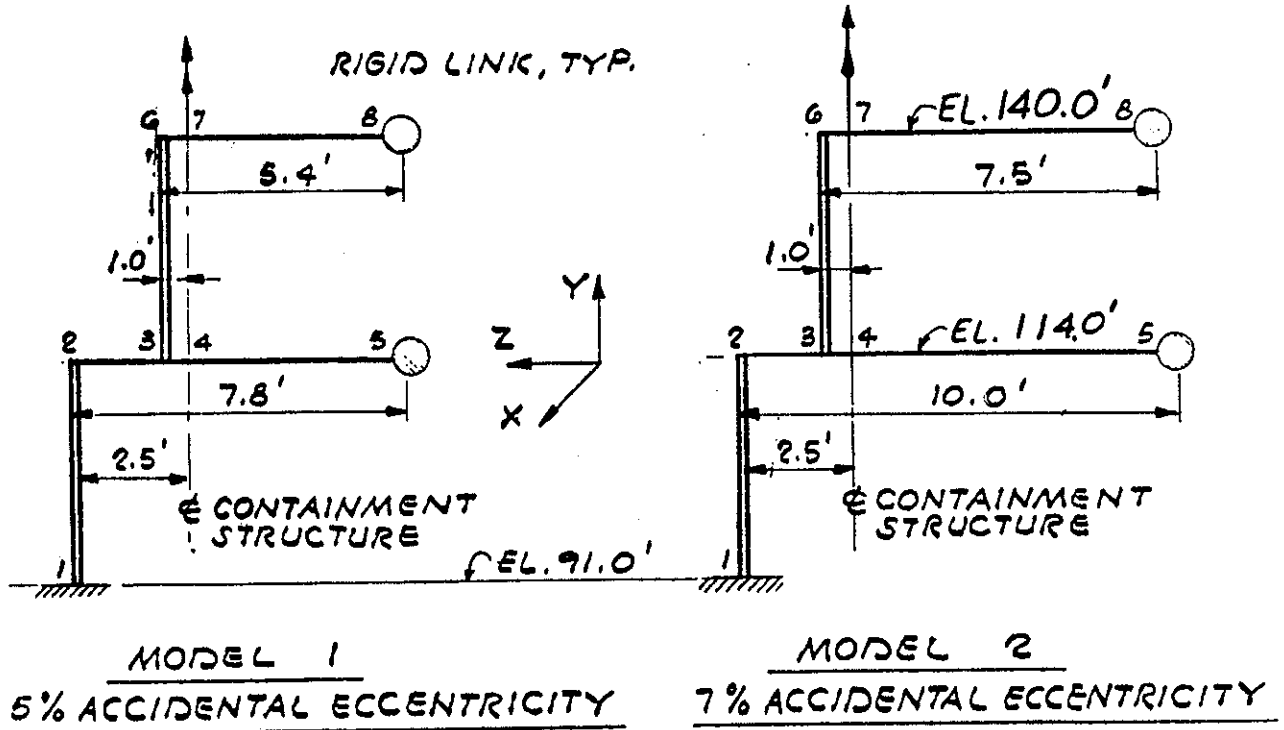


MODEL 2
7% ACCIDENTAL ECCENTRICITY

FSAR UPDATE
UNIT 1
DIABLO CANYON SITE
FIGURE 3.7 - 5 B
CONTAINMENT STRUCTURE EXTERIOR SHELL MATHEMATICAL MODELS FOR TORSIONAL ANALYSIS

LEGEND

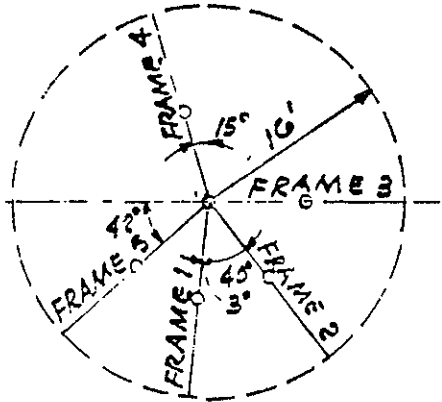
- - MASS POINT
- ↓ - TORSIONAL DEGREE OF FREEDOM
- / - TRANSLATIONAL DEGREE OF FREEDOM



FSAR UPDATE
UNIT 1
DIABLO CANYON SITE
FIGURE 3.7 - 5 C CONTAINMENT INTERIOR STRUCTURE MATHEMATICAL MODEL FOR HORIZONTAL AND TORSIONAL ANALYSIS

CONTAINMENT

CONTAINMENT



LEGEND :

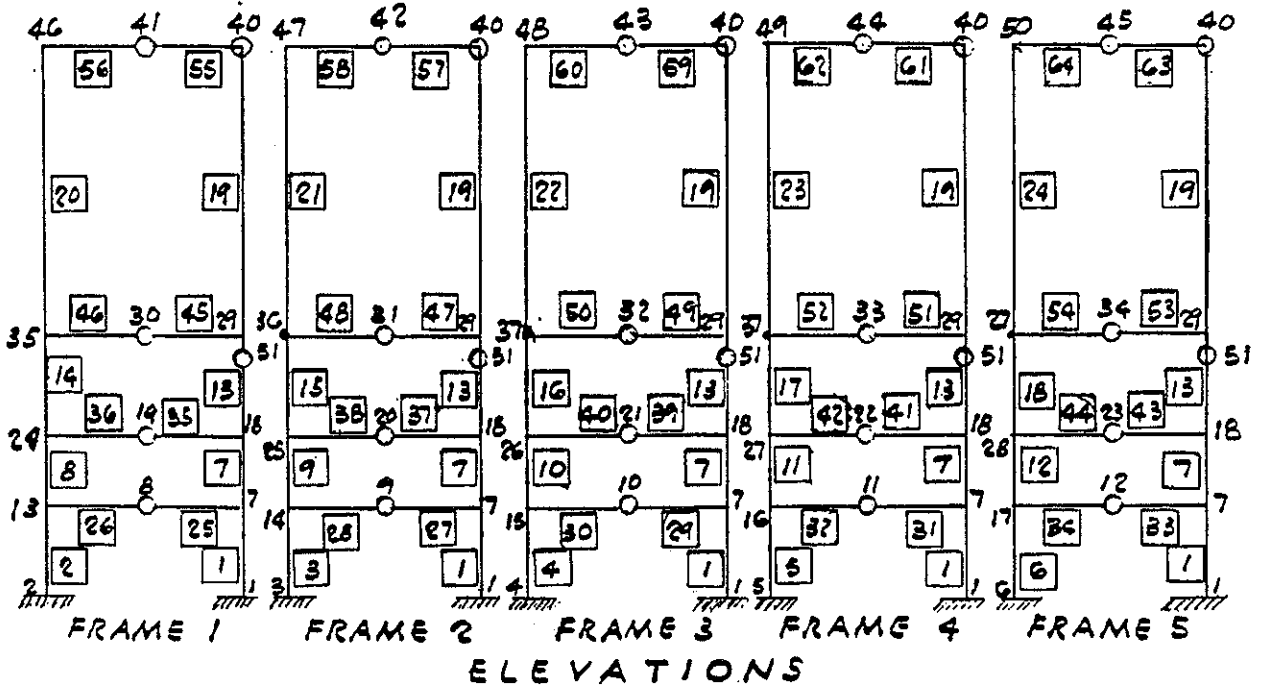
- - ELEMENT NUMBER
- 2 - NODE NUMBER
- - MASS POINT

NOTE :

NODES 1, 7, 18, 29, 40 & 51 ARE ALONG E OF STRUCTURE AND ARE COMMON TO ALL FIVE FRAMES

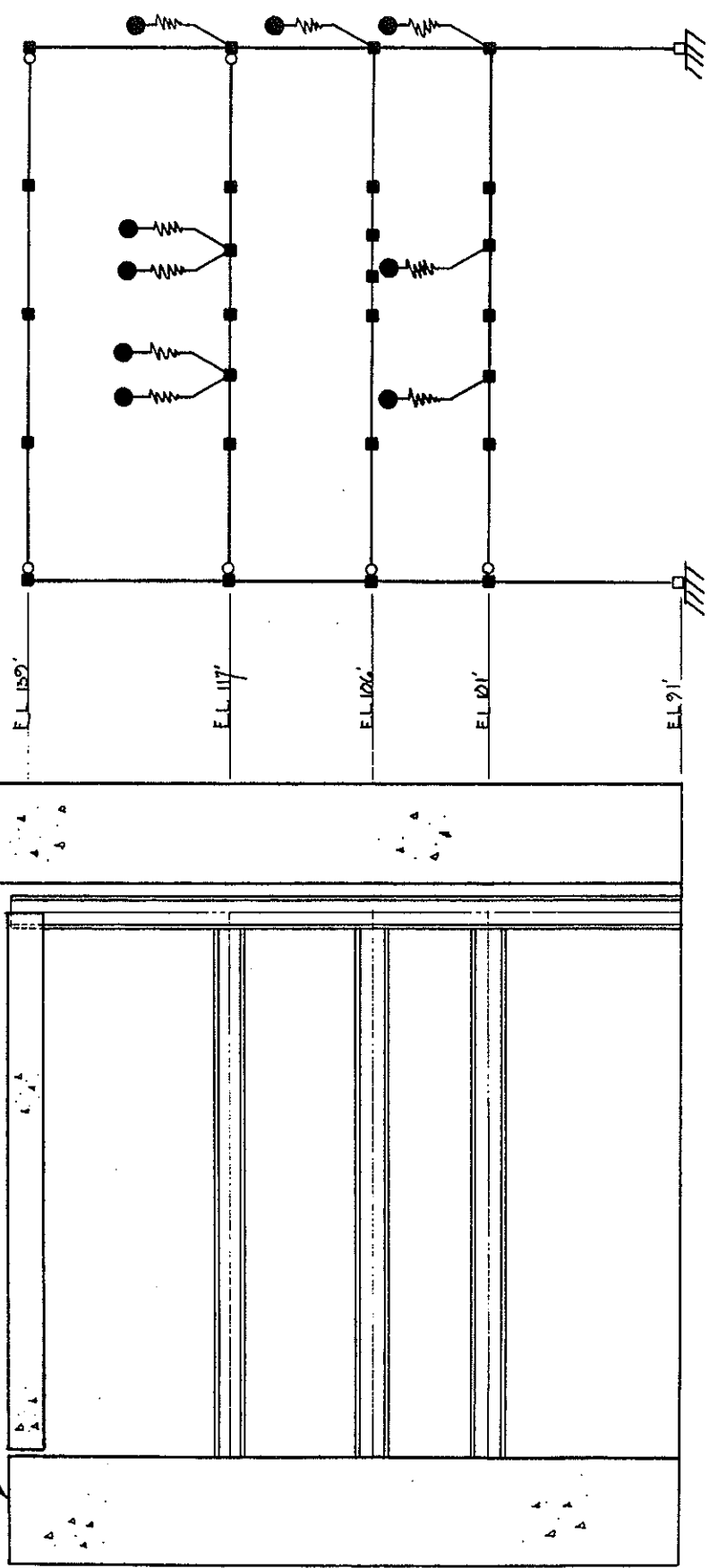
PLAN

UNIT 2



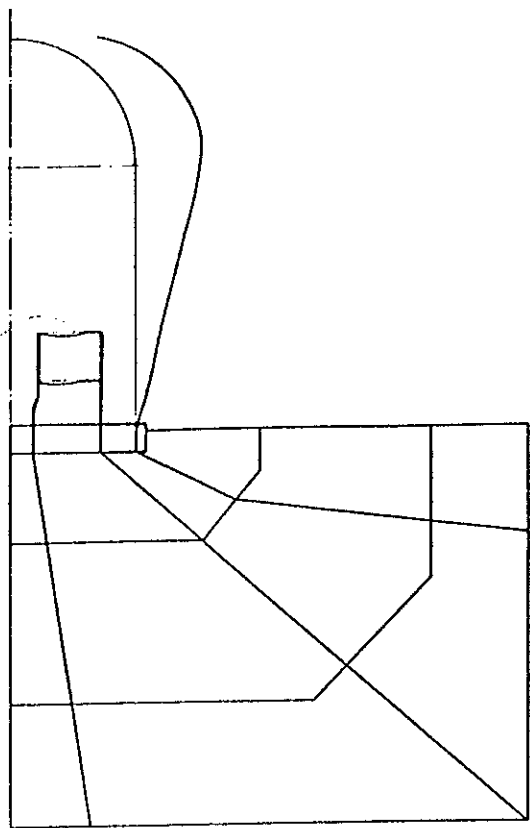
FSAR UPDATE
UNIT 2
DIABLO CANYON SITE
 FIGURE 3.7 - 5 D
 MATHEMATICAL MODEL FOR
 VERTICAL ANALYSIS OF
 CONTAINMENT INTERIOR
 STRUCTURE

CONTAINMENT WALL
CRANE WALL

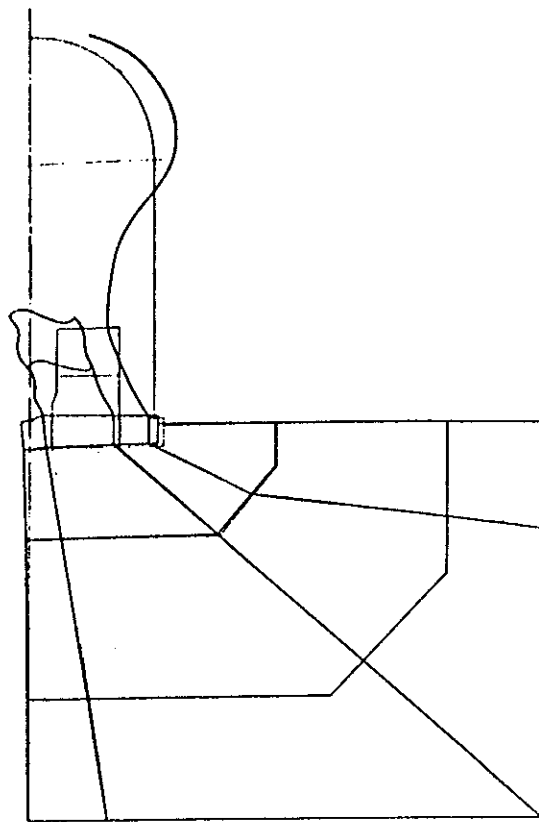


FSAR UPDATE
UNIT 1
DIABLO CANYON SITE
FIGURE 3.7 - 5 E
FRAME ANALYSIS FOR
VERTICAL RESPONSE
COLUMN LINE 6
(FRAME 6)

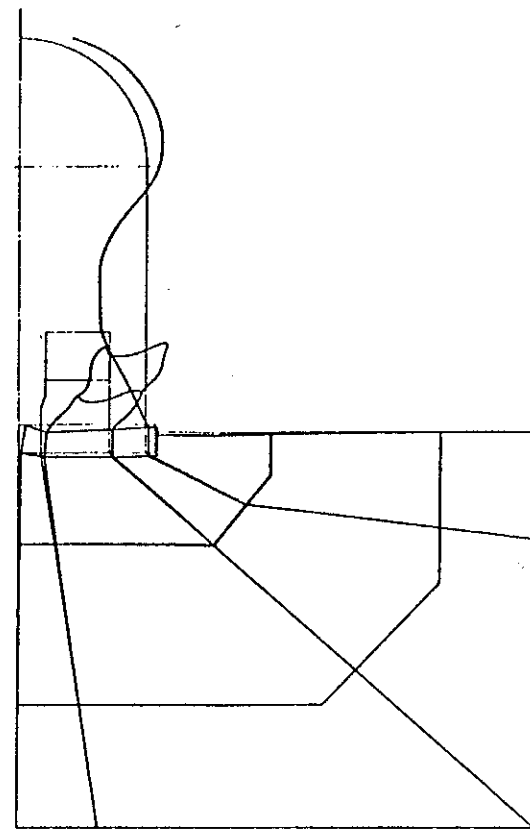
Revision 11 November 1996



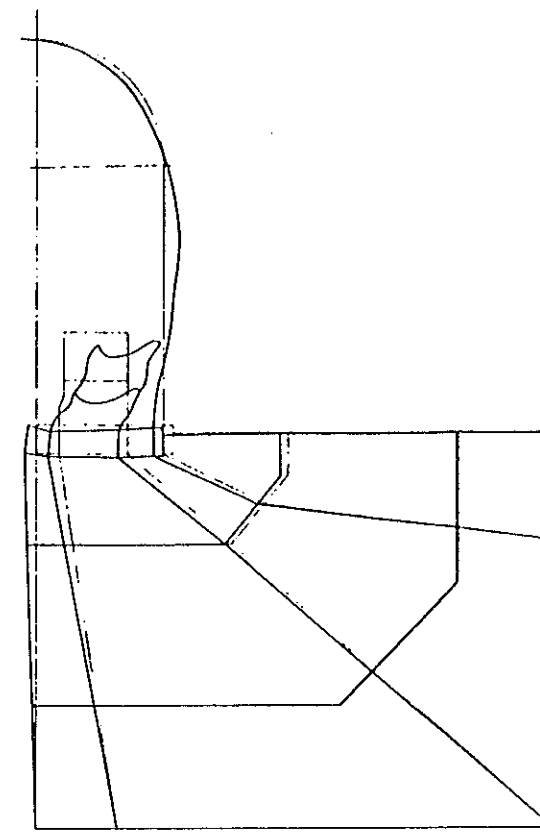
MODE 1
PERIOD = 0.255 SEC.



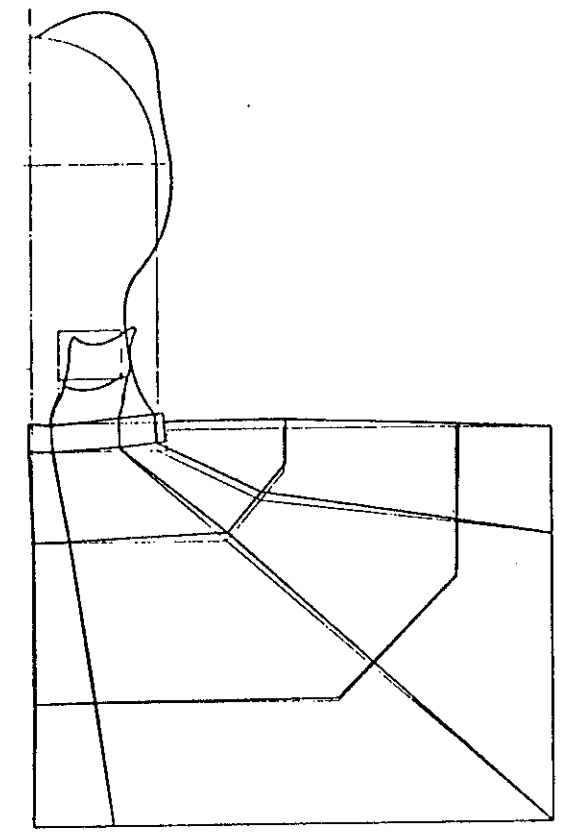
MODE 2
PERIOD = 0.093 SEC.



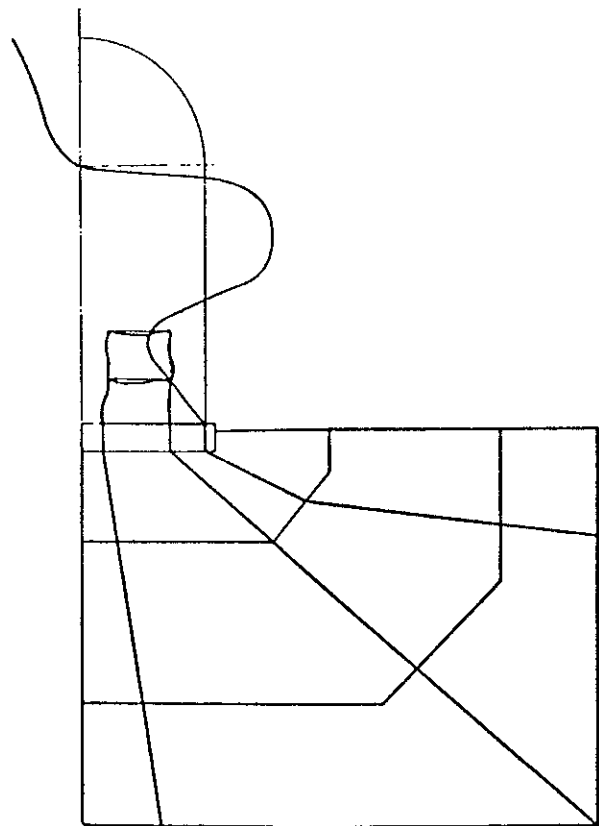
MODE 3
PERIOD = 0.088 SEC.



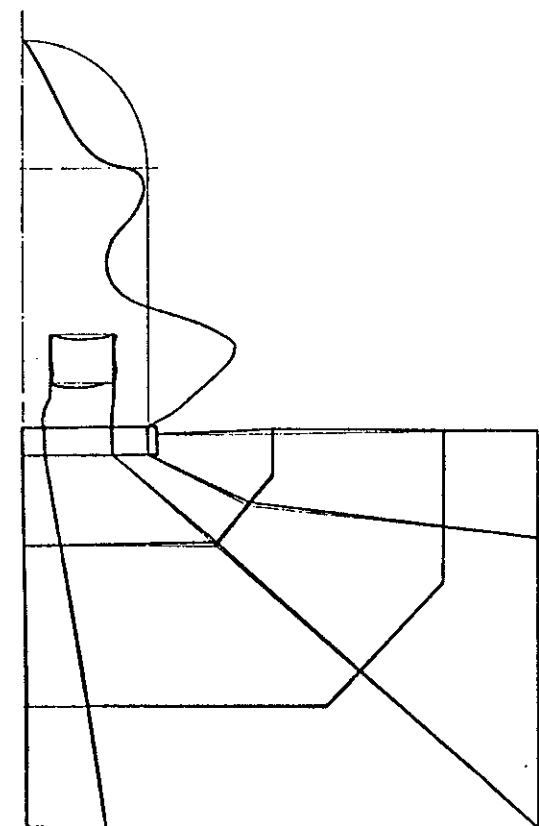
MODE 4
PERIOD = 0.073 SEC.



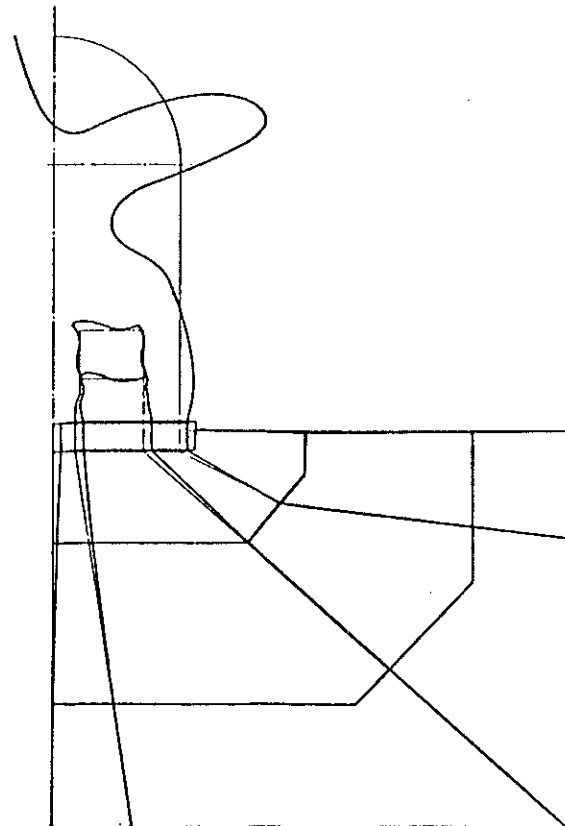
MODE 5
PERIOD = 0.060 SEC.



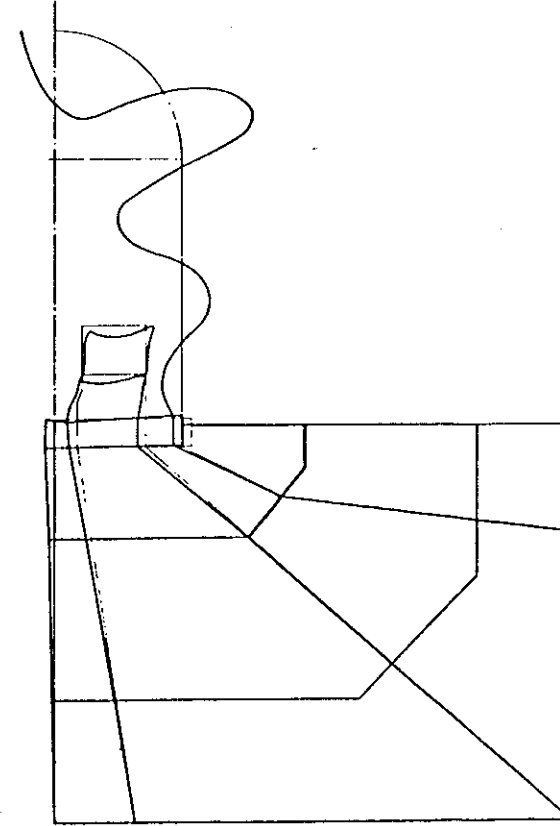
MODE 6
PERIOD = 0.058 SEC.



MODE 7
PERIOD = 0.057 SEC.

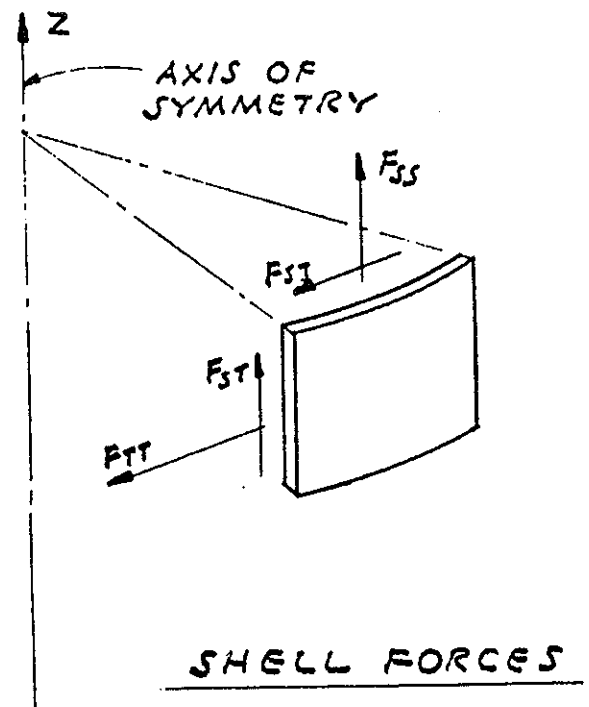
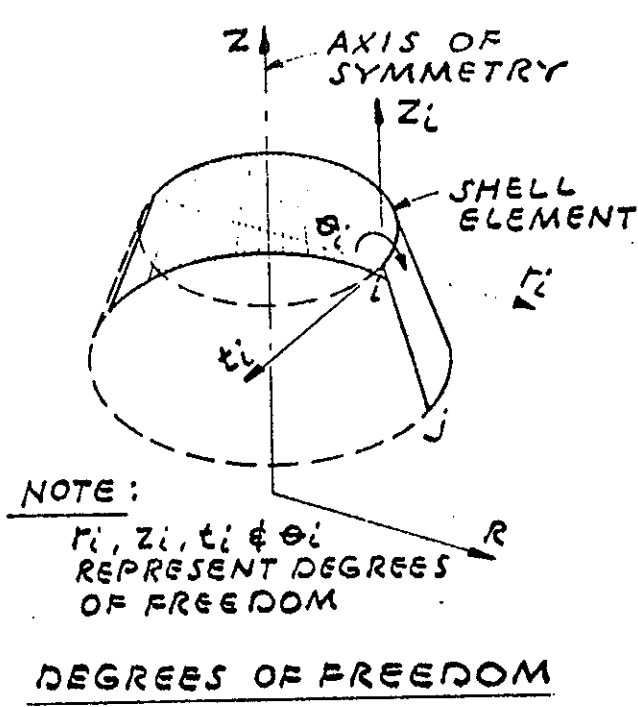


MODE 8
PERIOD = 0.051 SEC.

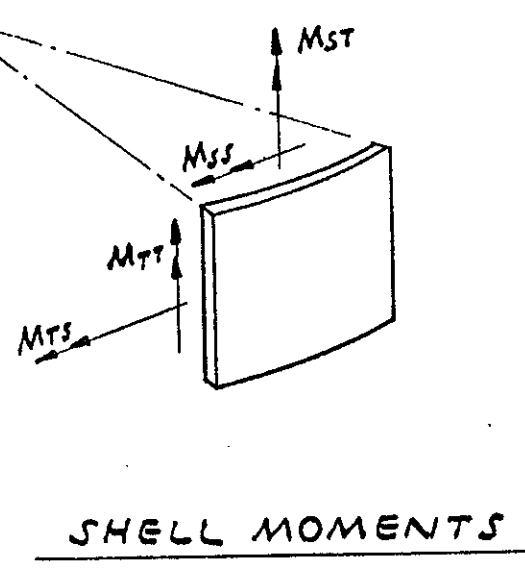


MODE 9
PERIOD = 0.0509 SEC.

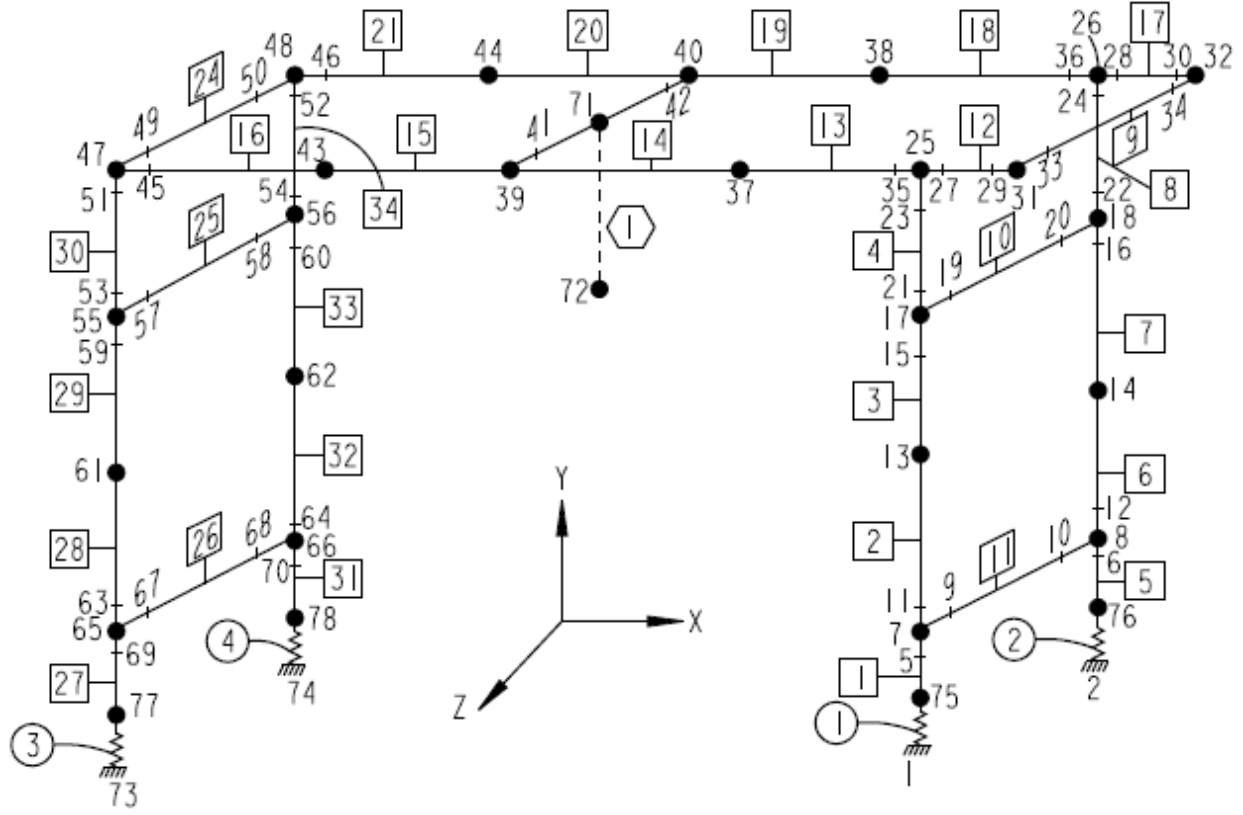
FSAR UPDATE
UNITS 1 AND 2 DIABLO CANYON SITE
FIGURE 3.7-6 CONTAINMENT STRUCTURE MODE SHAPES



- LEGEND:
- F_{SS} - LONGITUDINAL FORCE
 - F_{TT} - HOOP FORCE
 - F_{ST} - SHEAR FORCE
 - M_{SS} - LONGITUDINAL MOMENT
 - M_{TT} - CIRCUMFERENTIAL MOMENT
 - M_{ST} - CROSS MOMENT



FSAR UPDATE
UNITS 1 AND 2
DIABLO CANYON SITE
FIGURE 3.7-7 CONTAINMENT STRUCTURE SHELL FORCES AND MOMENTS AND ELEMENT DEGREES OF FREEDOM



- | --- NODE NUMBER
- --- BEAM ELEMENT
- ⬡ --- TRUSS ELEMENT
- --- GAP ELEMENT

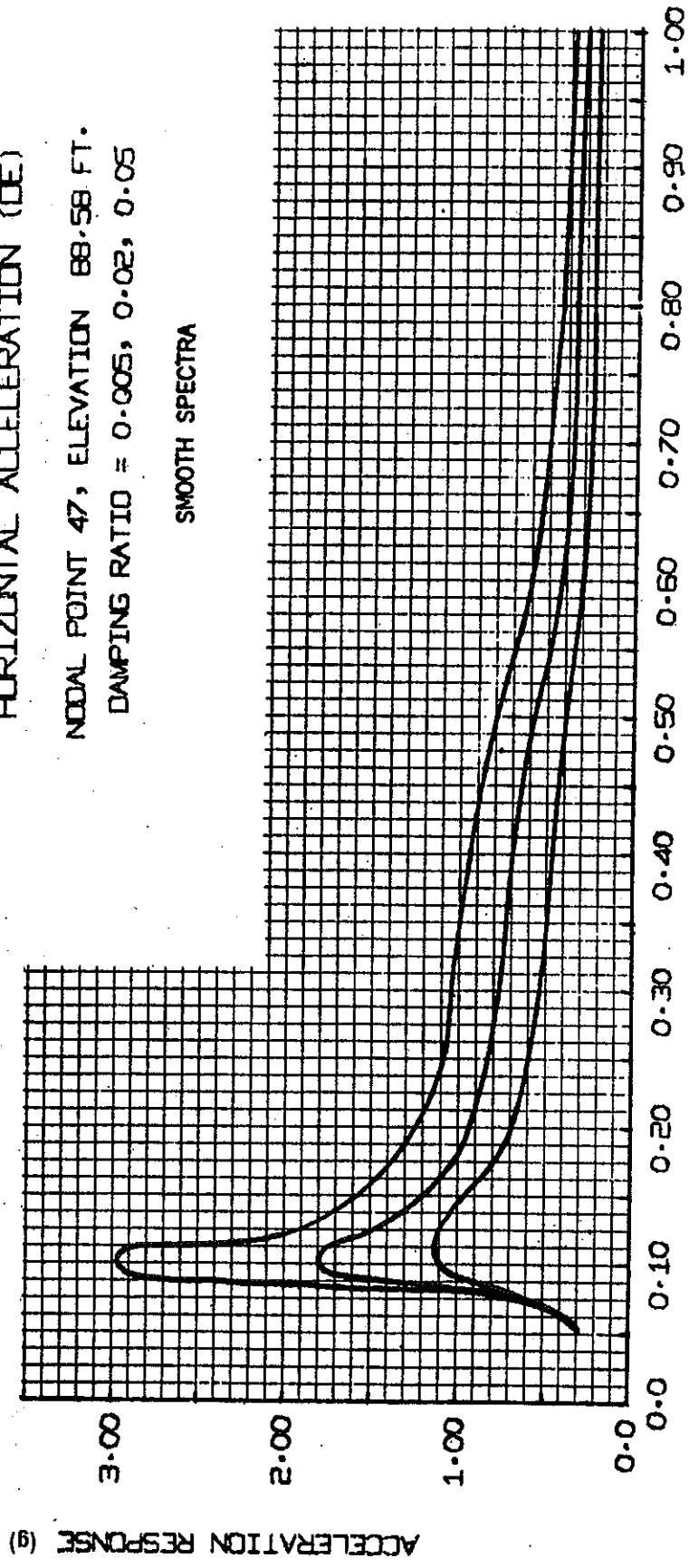
FSAR UPDATE
UNITS 1 AND 2
DIABLO CANYON SITE
FIGURE 3.7-7A
POLAR CRANE THREE DIMENSIONAL NONLINEAR MODEL

Revision 21 September 2013

CONTAINMENT STRUCTURE (FINITE ELEMENT MODEL)
 ACCELERATION RESPONSE SPECTRA
 HORIZONTAL ACCELERATION (DE)

NODAL POINT 47, ELEVATION 88.58 FT.
 DAMPING RATIO = 0.005, 0.02, 0.05

SMOOTH SPECTRA

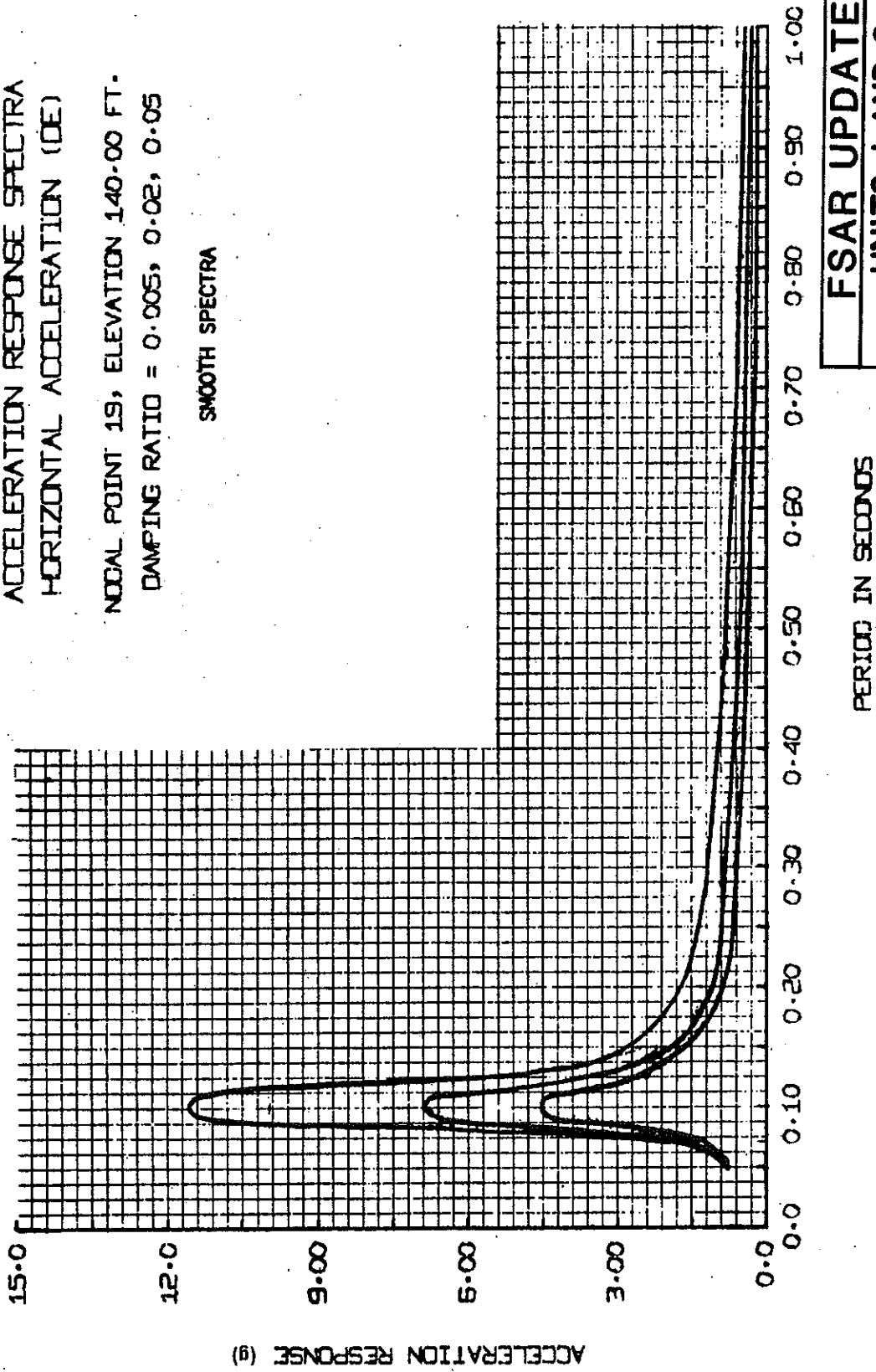


FSAR UPDATE
UNITS 1 AND 2 DIABLO CANYON SITE
FIGURE 3.7-8 CONTAINMENT STRUCTURE TYPICAL SPECTRA

CONTAINMENT STRUCTURE (FINITE ELEMENT MODEL)
 ACCELERATION RESPONSE SPECTRA
 HORIZONTAL ACCELERATION (DE)

NODAL POINT 19, ELEVATION 140.00 FT.
 DAMPING RATIO = 0.005, 0.02, 0.05

SMOOTH SPECTRA

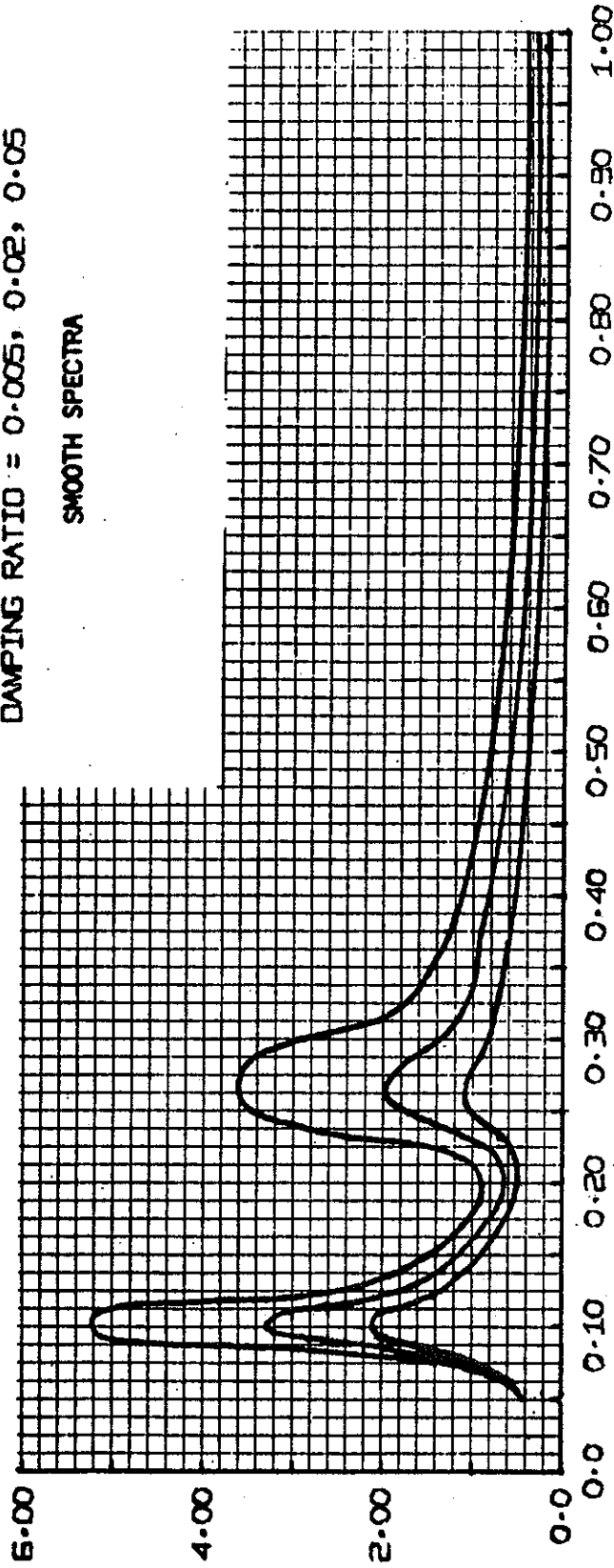


FSAR UPDATE
UNITS 1 AND 2
DIABLO CANYON SITE
FIGURE 3.7 - 9 CONTAINMENT STRUCTURE TYPICAL SPECTRA

CONTAINMENT STRUCTURE (FINITE ELEMENT MODEL)
 ACCELERATION RESPONSE SPECTRA
 HORIZONTAL ACCELERATION (OE)

NODAL POINT 37, ELEVATION 109.67 FT.
 DAMPING RATIO = 0.005, 0.02, 0.05

SMOOTH SPECTRA



ACCELERATION RESPONSE (g)

FSAR UPDATE
UNITS 1 AND 2 DIABLO CANYON SITE
FIGURE 3.7 - 10 CONTAINMENT STRUCTURE TYPICAL SPECTRA

PERIOD IN SECONDS

CONTAINMENT STRUCTURE (FINITE ELEMENT MODEL)

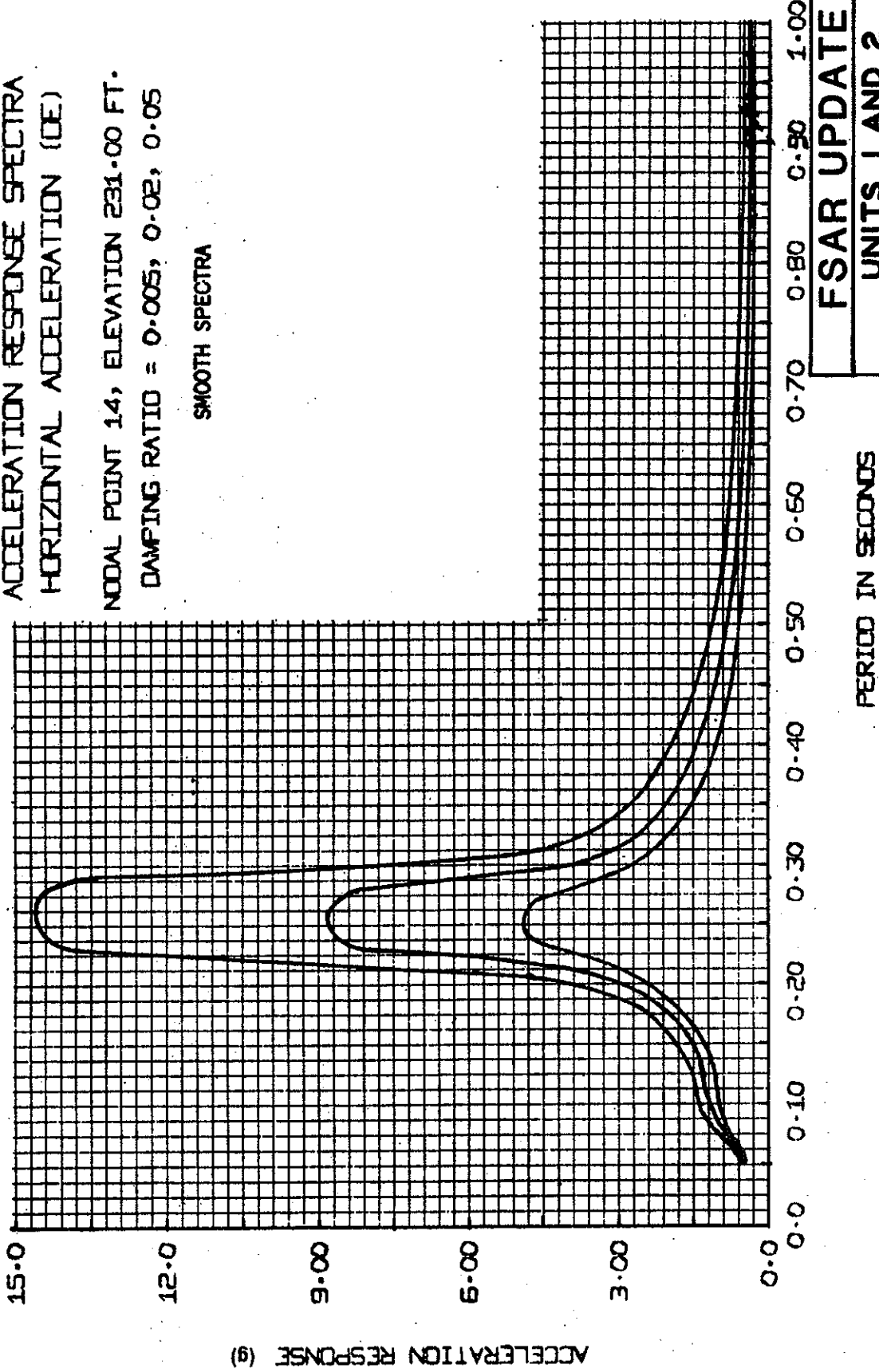
ACCELERATION RESPONSE SPECTRA

HORIZONTAL ACCELERATION (DE)

NODAL POINT 14, ELEVATION 231.00 FT.

DAMPING RATIO = 0.005, 0.02, 0.05

SMOOTH SPECTRA



FSAR UPDATE
UNITS 1 AND 2
DIABLO CANYON SITE

FIGURE 3.7 - 11
CONTAINMENT STRUCTURE
TYPICAL SPECTRA

CONTAINMENT STRUCTURE (FINITE ELEMENT MODEL)

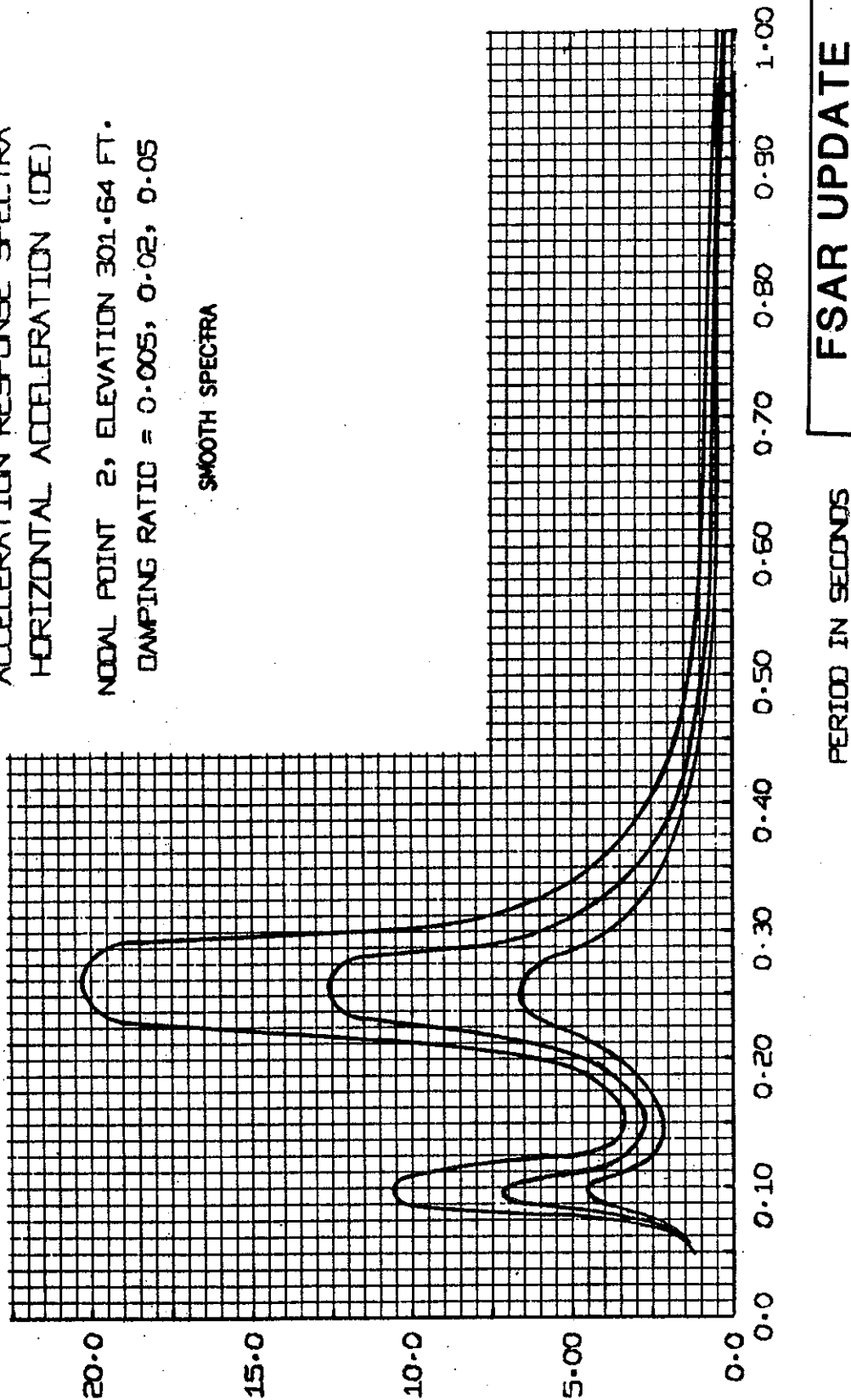
ACCELERATION RESPONSE SPECTRA

HORIZONTAL ACCELERATION (DE)

NODAL POINT 2, ELEVATION 301.64 FT.

DAMPING RATIO = 0.005, 0.02, 0.05

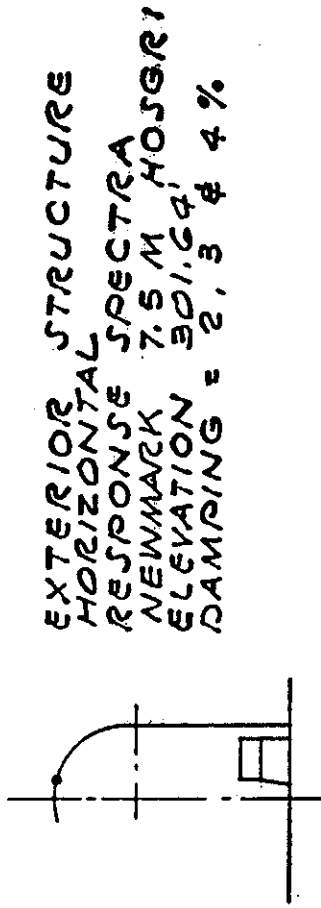
SMOOTH SPECTRA



FSAR UPDATE

UNITS 1 AND 2
DIABLO CANYON SITE

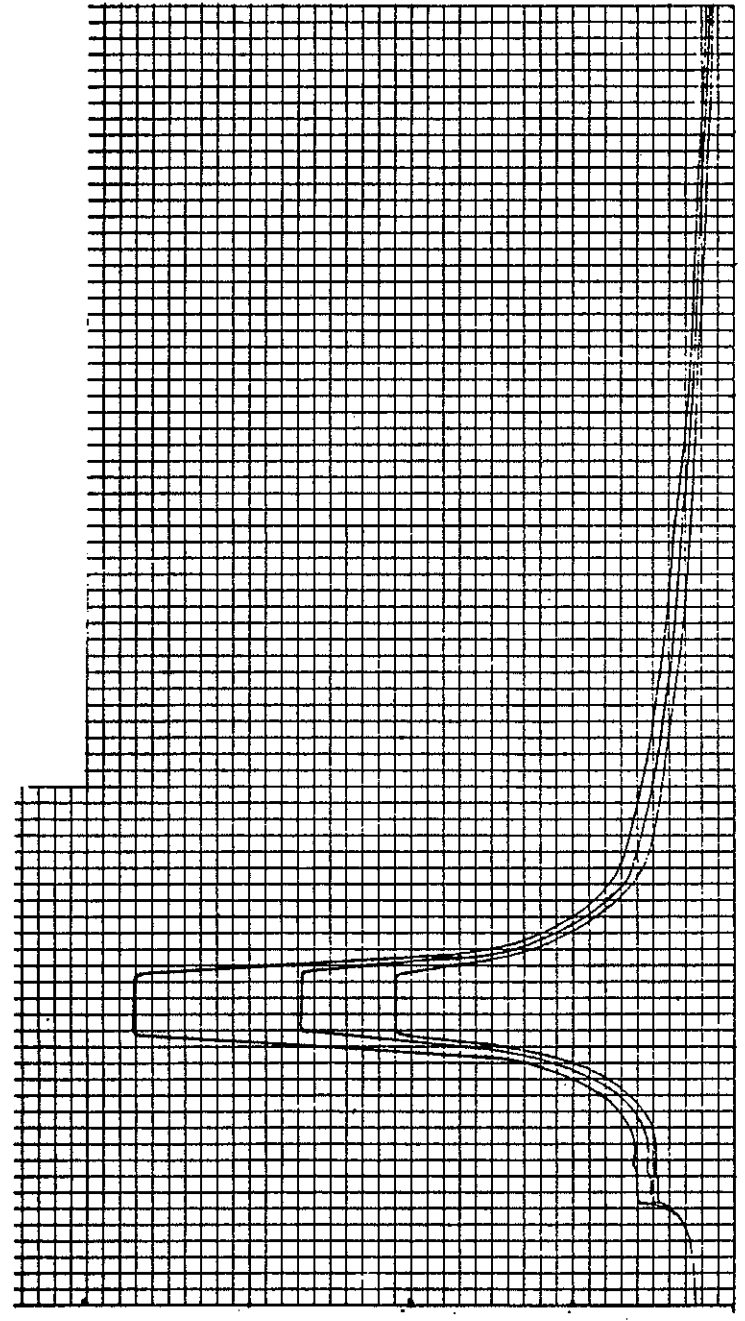
FIGURE 3.7 - 12
CONTAINMENT STRUCTURE
TYPICAL SPECTRA



EXTERIOR STRUCTURE
 HORIZONTAL SPECTRA
 RESPONSE 7.5 M HOSORI
 NEWMARK 301.64'
 ELEVATION = 2, 3 & 4 %
 DAMPING = 2, 3 & 4 %

ACCELERATION RESPONSE IN g UNITS

40
32
24
16
8
0

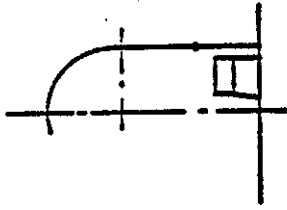


0.0 0.1 0.2 0.3 0.4 0.5 0.6 0.7 0.8 0.9 1.0

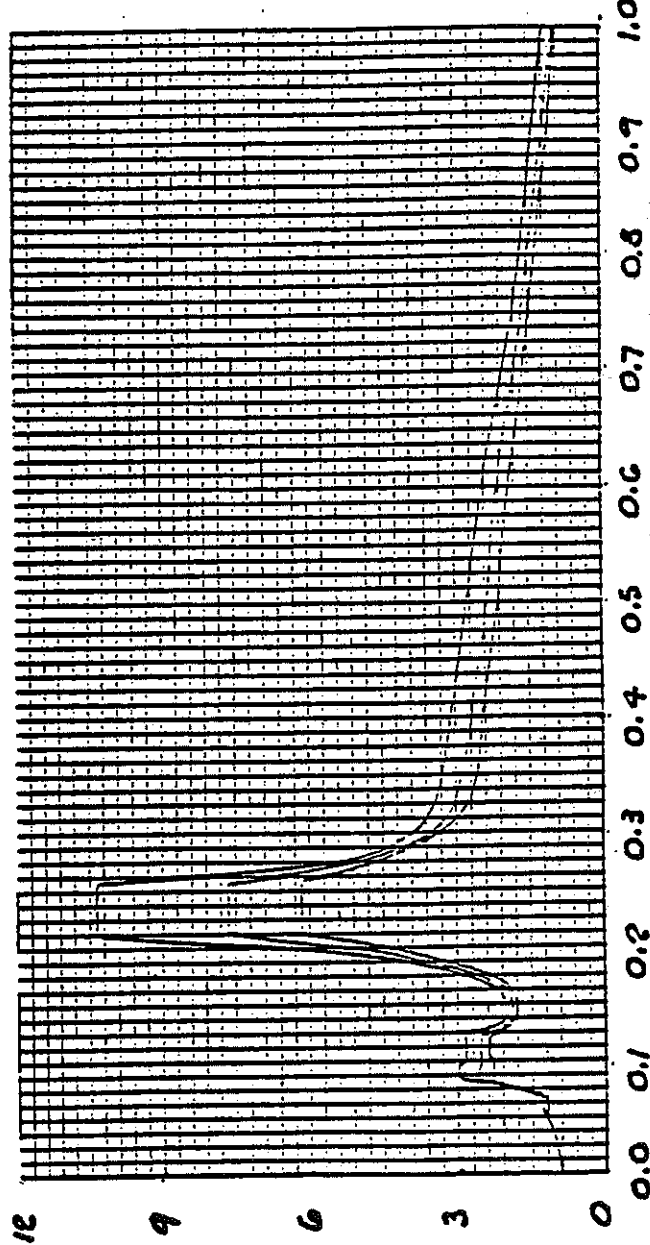
PERIOD IN SECONDS

FSAR UPDATE
UNITS 1 AND 2
DIABLO CANYON SITE
FIGURE 3.7 - 12A
CONTAINMENT STRUCTURE

EXTERIOR STRUCTURE
 HORIZONTAL
 RESPONSE SPECTRA
 NEWMARK 7.5 M, HOSGERI
 ELEVATION 155.83, HOSGERI
 DAMPING = 2.3 & 4%



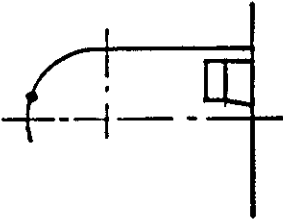
ACCELERATION RESPONSE IN g UNITS



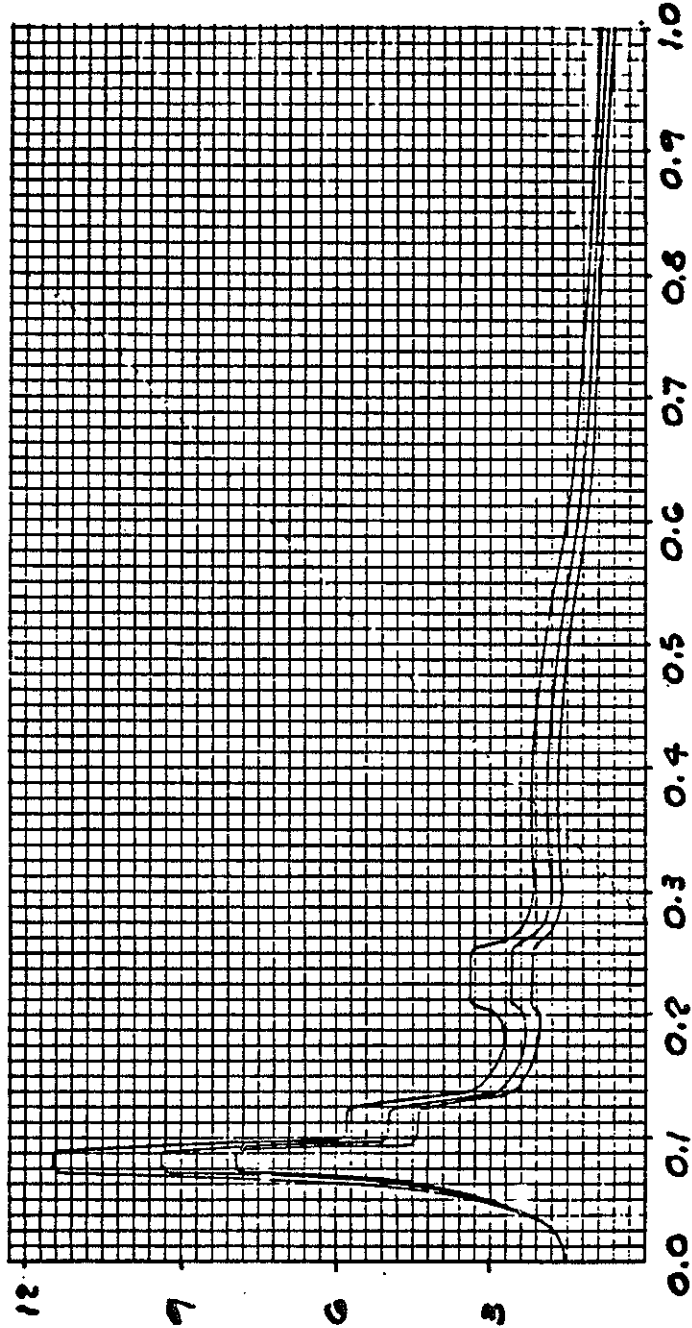
PERIOD IN SECONDS

FSAR UPDATE
UNITS 1 AND 2 DIABLO CANYON SITE
FIGURE 3.7 - 12B CONTAINMENT STRUCTURE

EXTERIOR STRUCTURE
 VERTICAL RESPONSE SPECTRA
 VOLUME 7.5 M HOSGRI
 ELEVATION 301.64' & 4%
 DAMPING = 2, 3 & 4%



ACCELERATION RESPONSE IN g UNITS

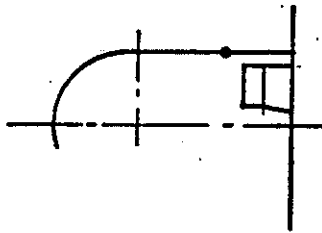


FSAR UPDATE

UNITS 1 AND 2
 DIABLO CANYON SITE

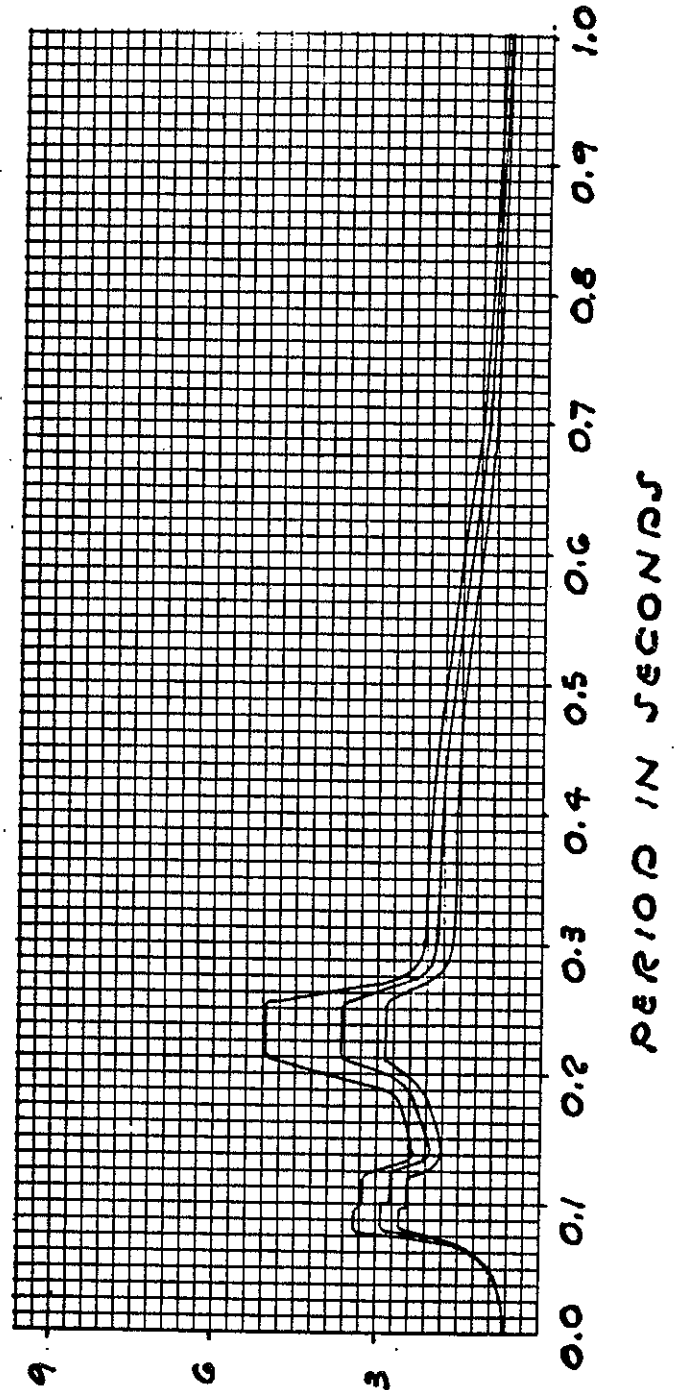
FIGURE 3.7 - 12C
 CONTAINMENT STRUCTURE

PERIOD IN SECONDS

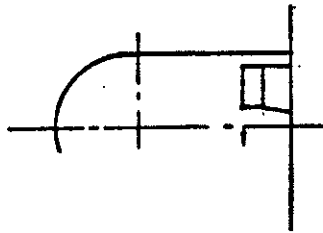


EXTERIOR STRUCTURE
 VERTICAL RESPONSE SPECTRA
 NEWMARK 7.5 M. HOSGRI
 ELEVATION 155.83'
 DAMPING = 2, 3 & 4%

ACCELERATION RESPONSE IN g UNITS

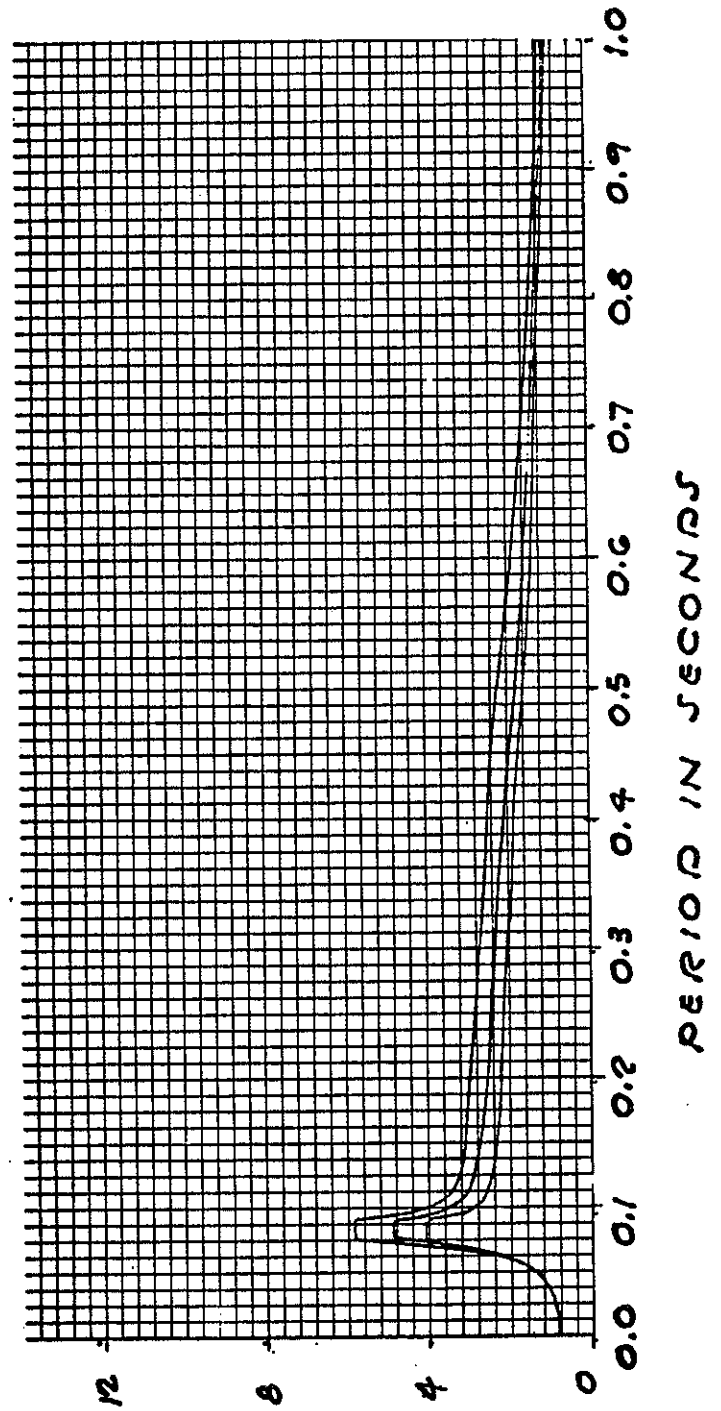


FSAR UPDATE
UNITS 1 AND 2 DIABLO CANYON SITE
FIGURE 3.7 - 12D CONTAINMENT STRUCTURE

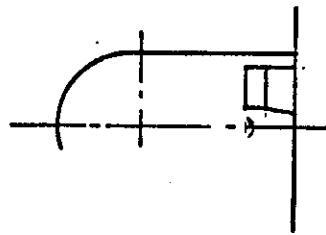


INTERIOR STRUCTURE
 HORIZONTAL SPECTRA
 RESPONSE 7.5 M HOSER
 VOLUME 140.00
 DAMPING = 2, 3 & 4%

ACCELERATION RESPONSE IN G UNITS

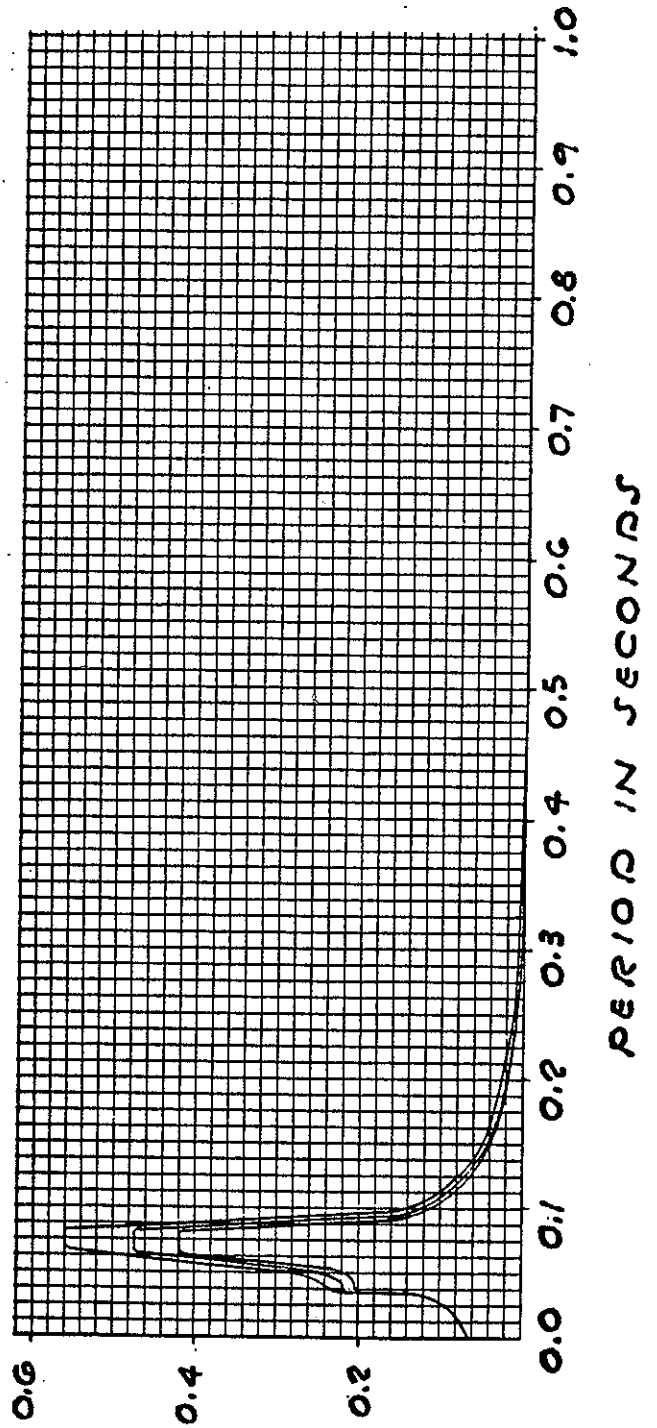


FSAR UPDATE
UNITS 1 AND 2 DIABLO CANYON SITE
FIGURE 3.7 - 12E CONTAINMENT STRUCTURE



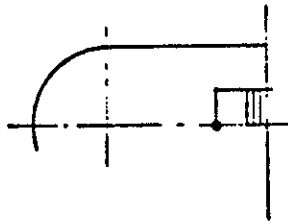
INTERIOR STRUCTURE
 TORSIONAL RESPONSE SPECTRA
 NEWMARK 7.5 M, HOSGRI
 ELEVATION 140.00, # 4%
 DAMPING = 2, 3 & 4%

ACCELERATION RESPONSE IN RAD/SEC²

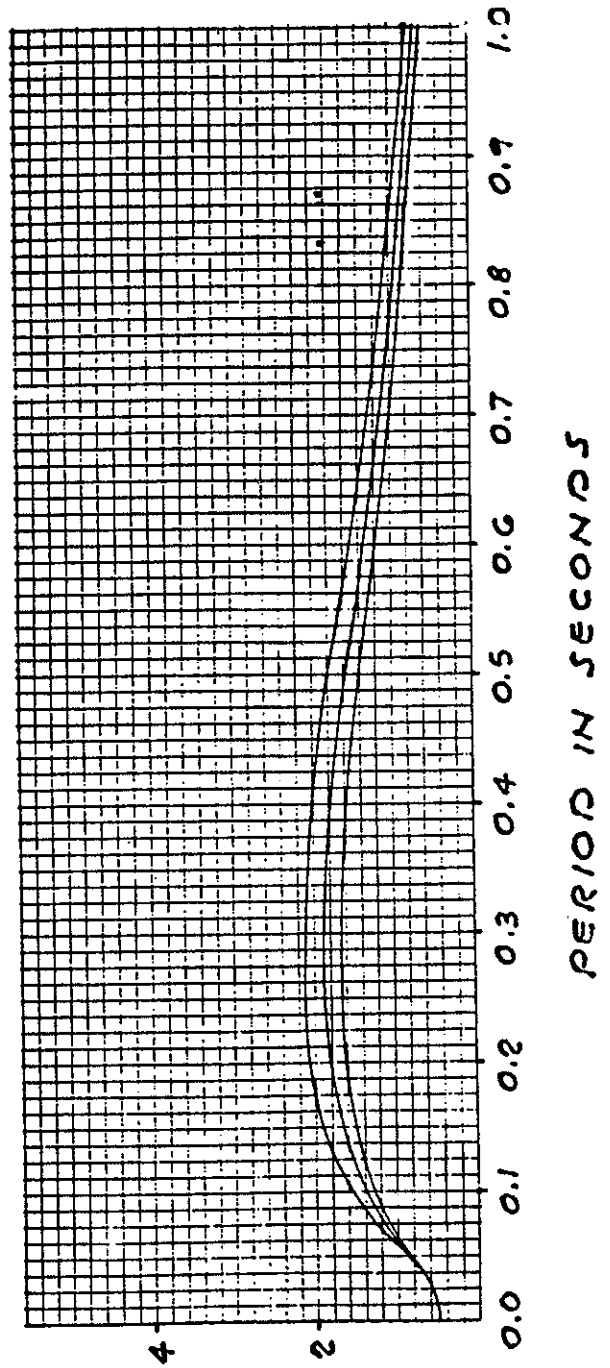


FSAR UPDATE
UNITS 1 AND 2 DIABLO CANYON SITE
FIGURE 3.7 - 12 F CONTAINMENT STRUCTURE

INTERIOR (CONCRETE) STRUCTURE
 VERTICAL
 RESPONSE SPECTRA
 NEWMARK 7.5M HOSGRI.
 NODE NO. 40
 ELEVATION 140.00'



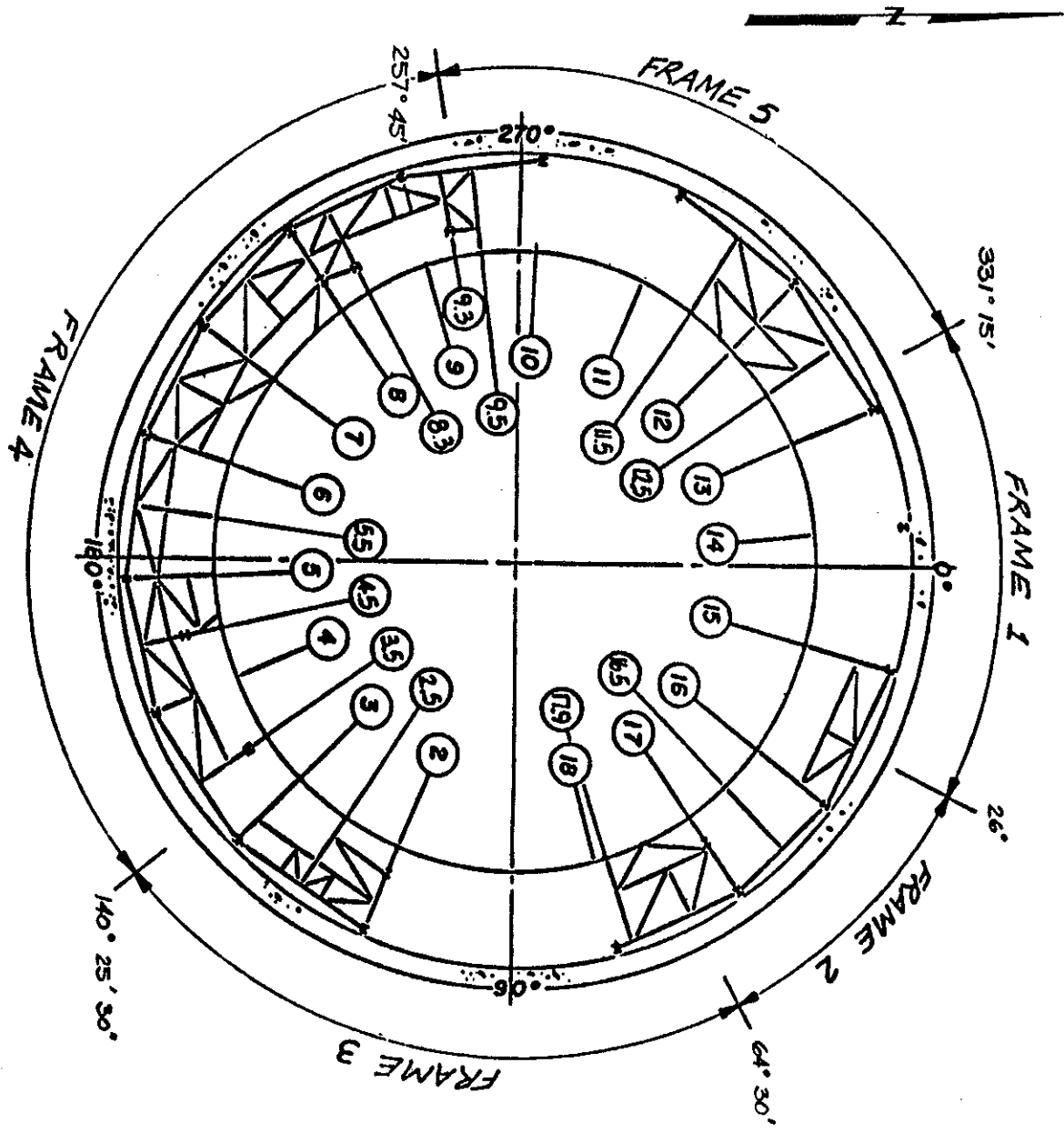
ACCELERATION RESPONSE IN G UNITS



FSAR UPDATE
UNITS 1 AND 2
DIABLO CANYON SITE

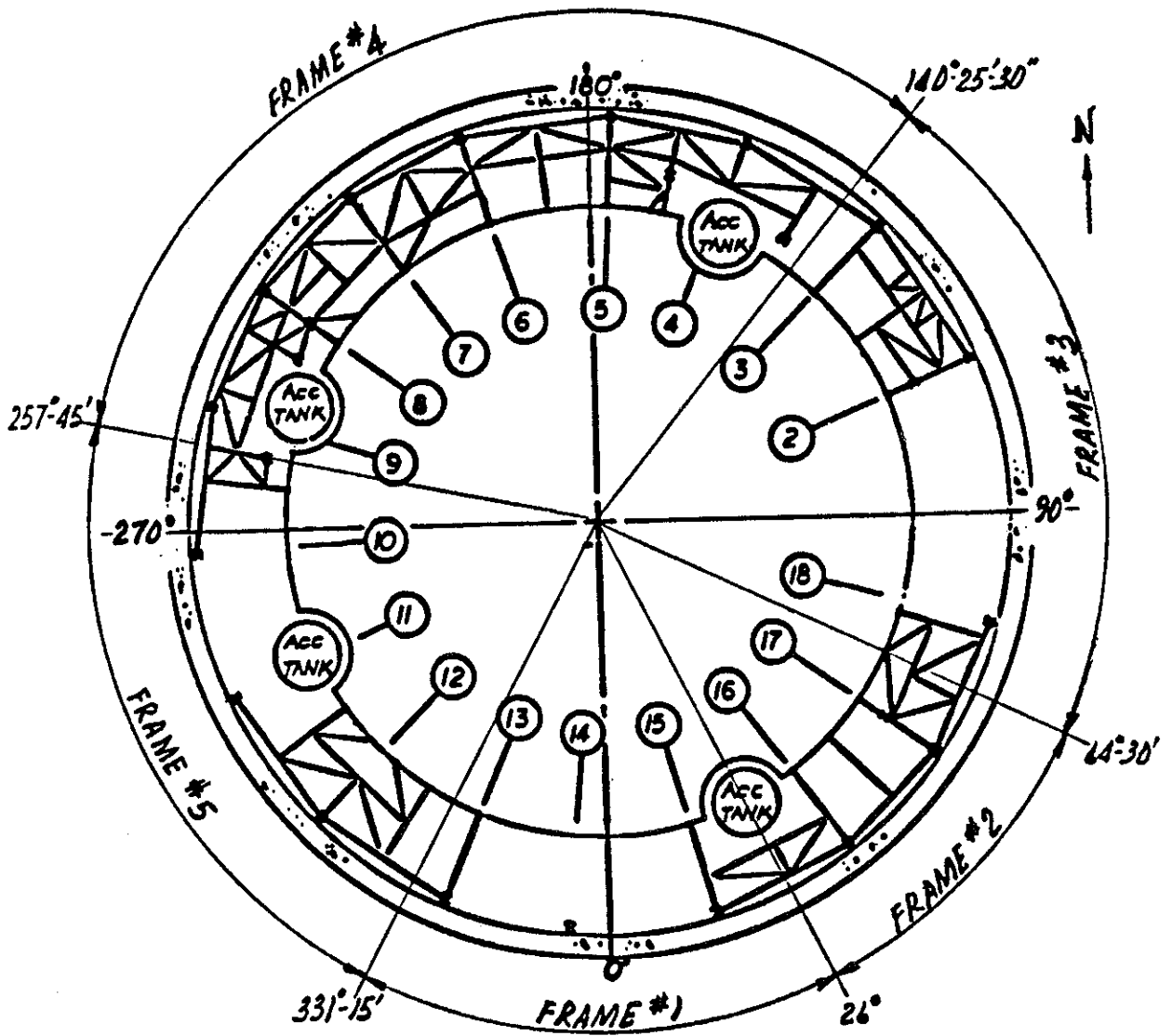
FIGURE 3.7 - 12G
 CONTAINMENT STRUCTURE

Revision 11 November 1996



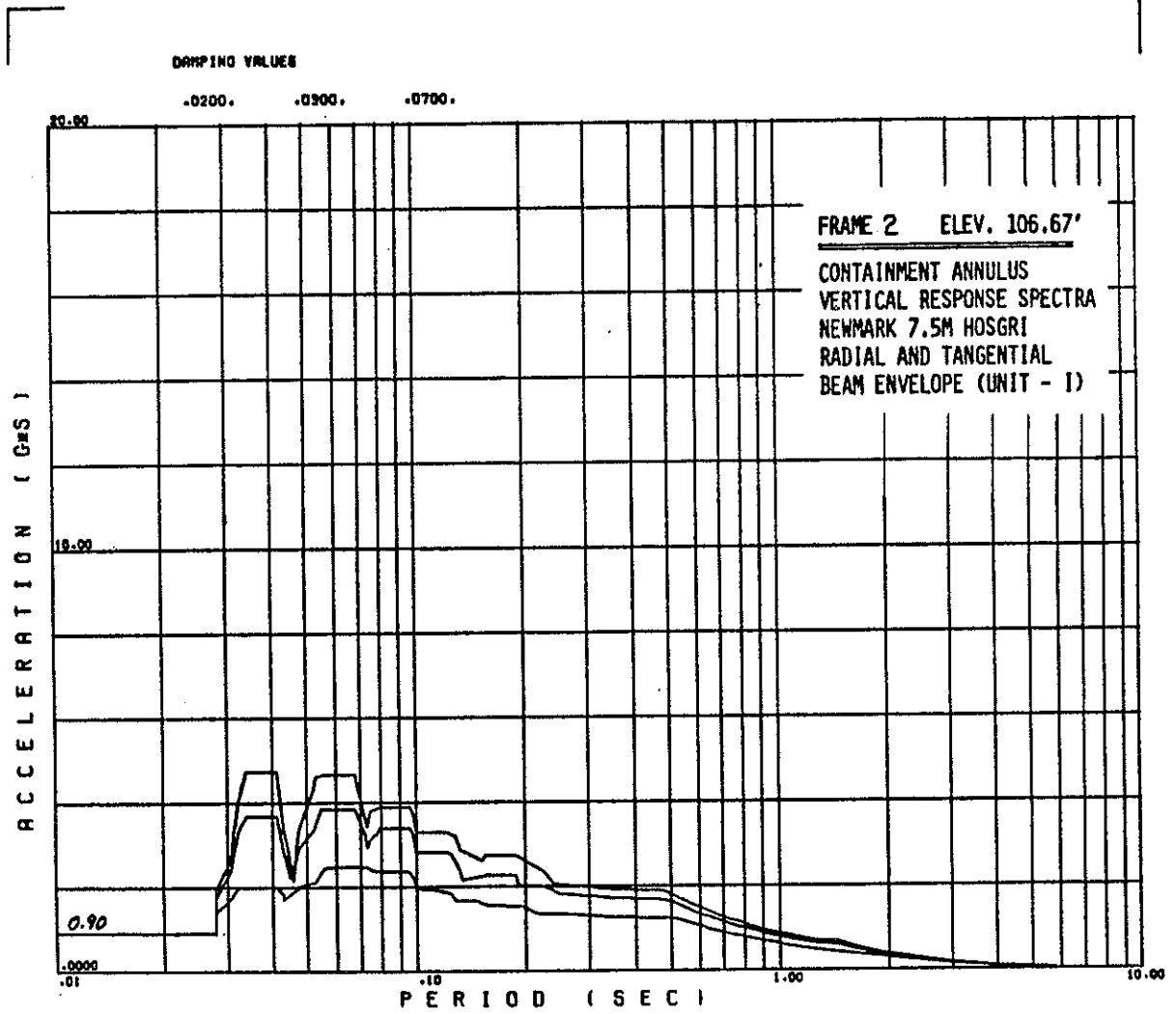
FSAR UPDATE
UNIT 1
DIABLO CANYON SITE
FIGURE 3.7 - 12 H CONTAINMENT - ANNULUS STRUCTURE

Revision 11 November 1996



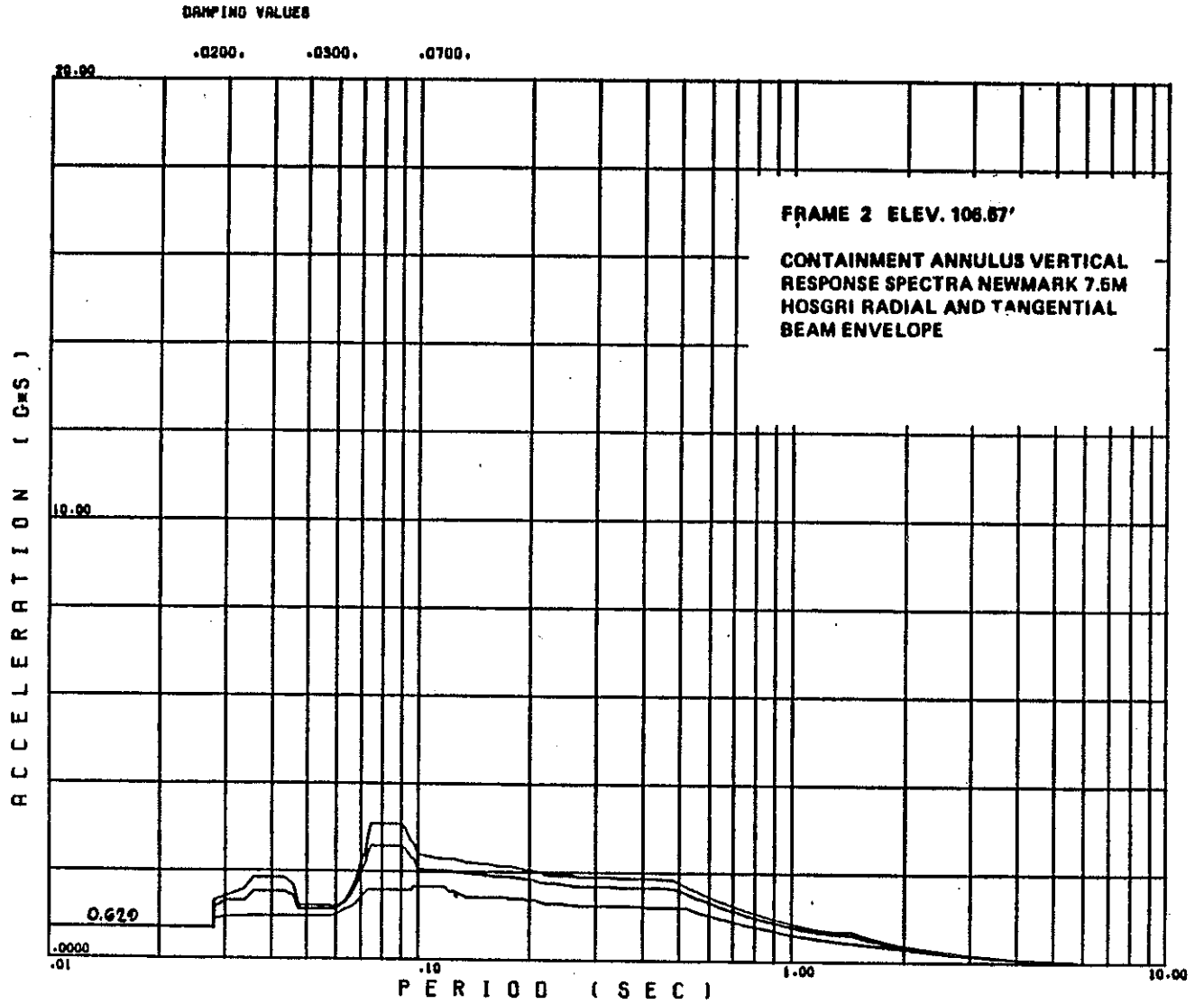
FSAR UPDATE
UNIT 2
DIABLO CANYON SITE
FIGURE 3.7 - 12 I CONTAINMENT - ANNULUS STRUCTURE

Revision 11 November 1996



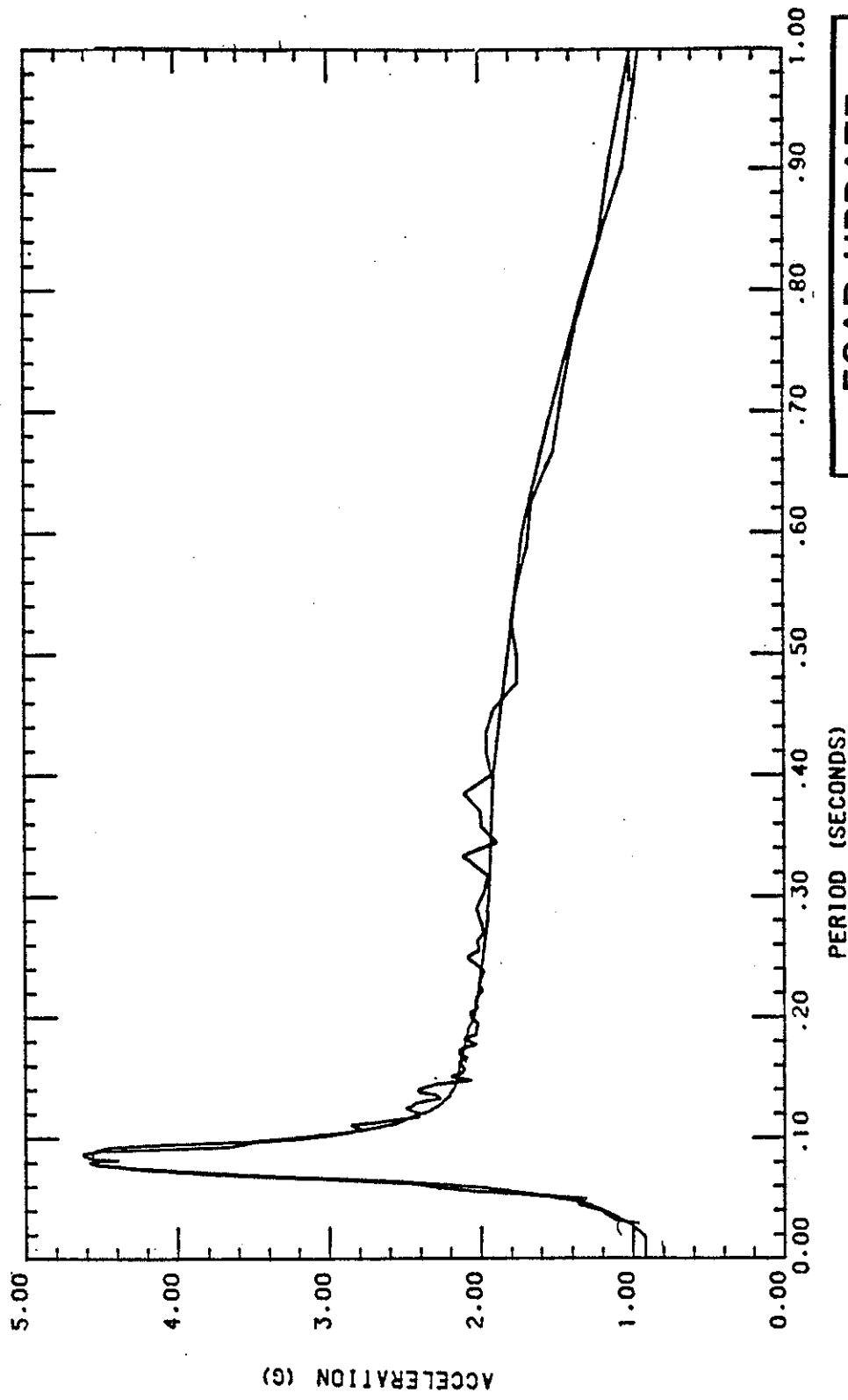
FSAR UPDATE
UNIT 1
DIABLO CANYON SITE
FIGURE 3.7 - 12 J CONTAINMENT ANNULUS SPECTRA

Revision 11 November 1996

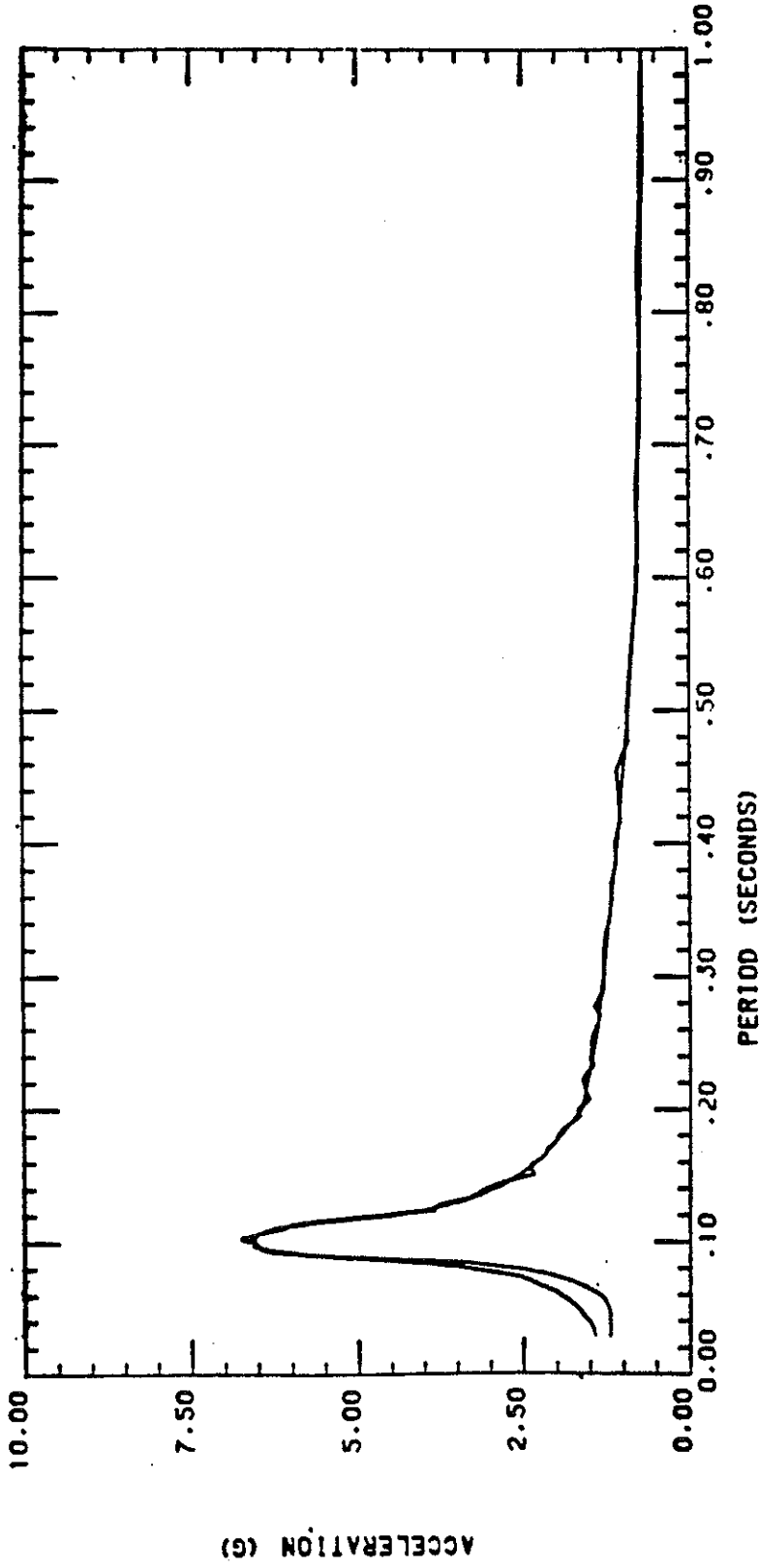


FSAR UPDATE
UNIT 2
DIABLO CANYON SITE
FIGURE 3.7 - 12K CONTAINMENT ANNULUS SPECTRA

Revision 11 November 1996



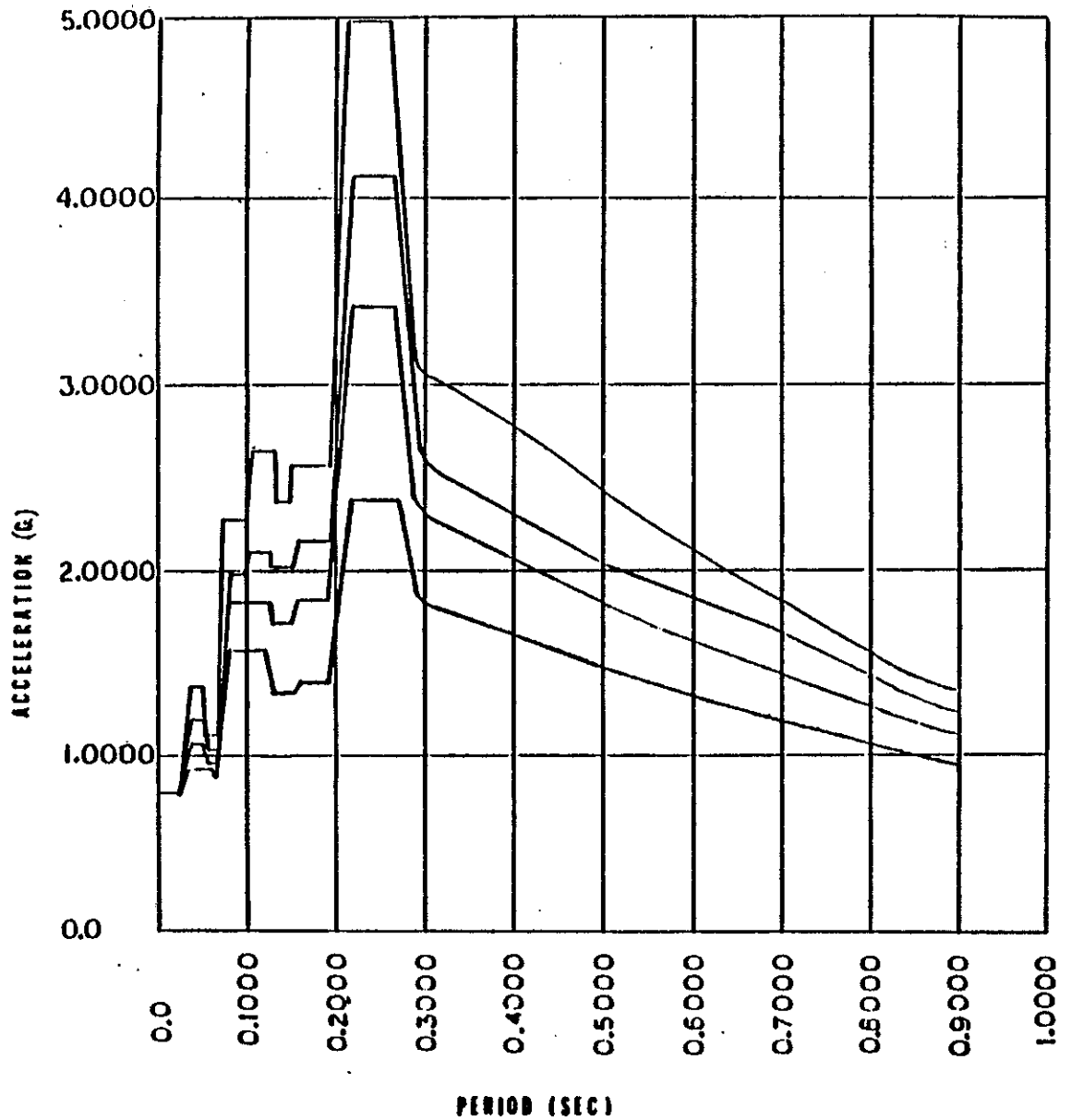
FSAR UPDATE
UNITS 1 AND 2
DIABLO CANYON SITE
FIGURE 3.7 - 12 L POLAR CRANE HOSGRI HORIZONTAL SPECTRUM IN X DIRECTION WITH 4% DAMPING AT EL. 140'



FSAR UPDATE

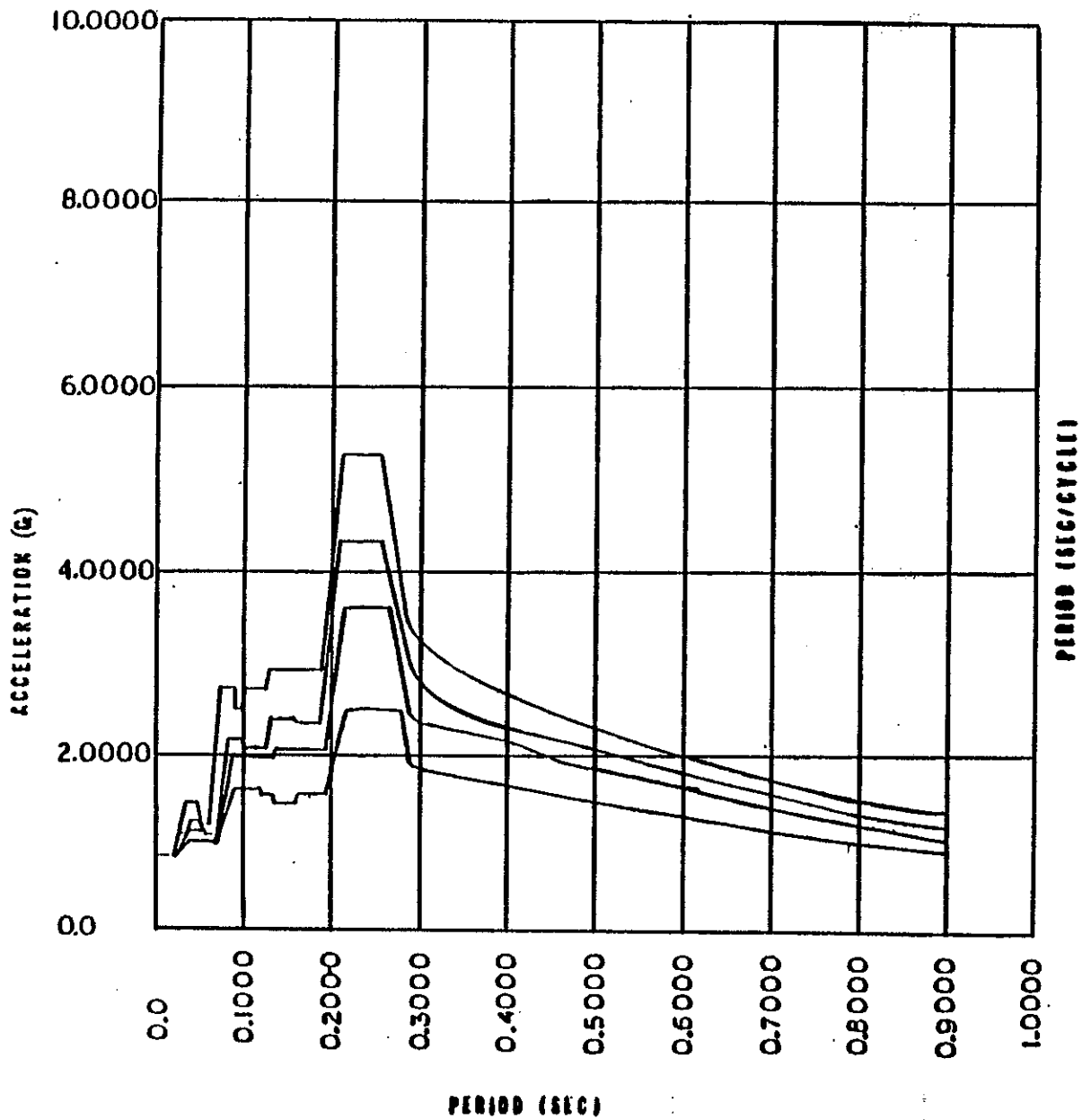
**UNITS 1 AND 2
DIABLO CANYON SITE**

FIGURE 3.7 - 12 M
POLAR CRANE DDE HORIZONTAL
SPECTRUM IN Z DIRECTION
WITH 5% DAMPING AT EL. 140'



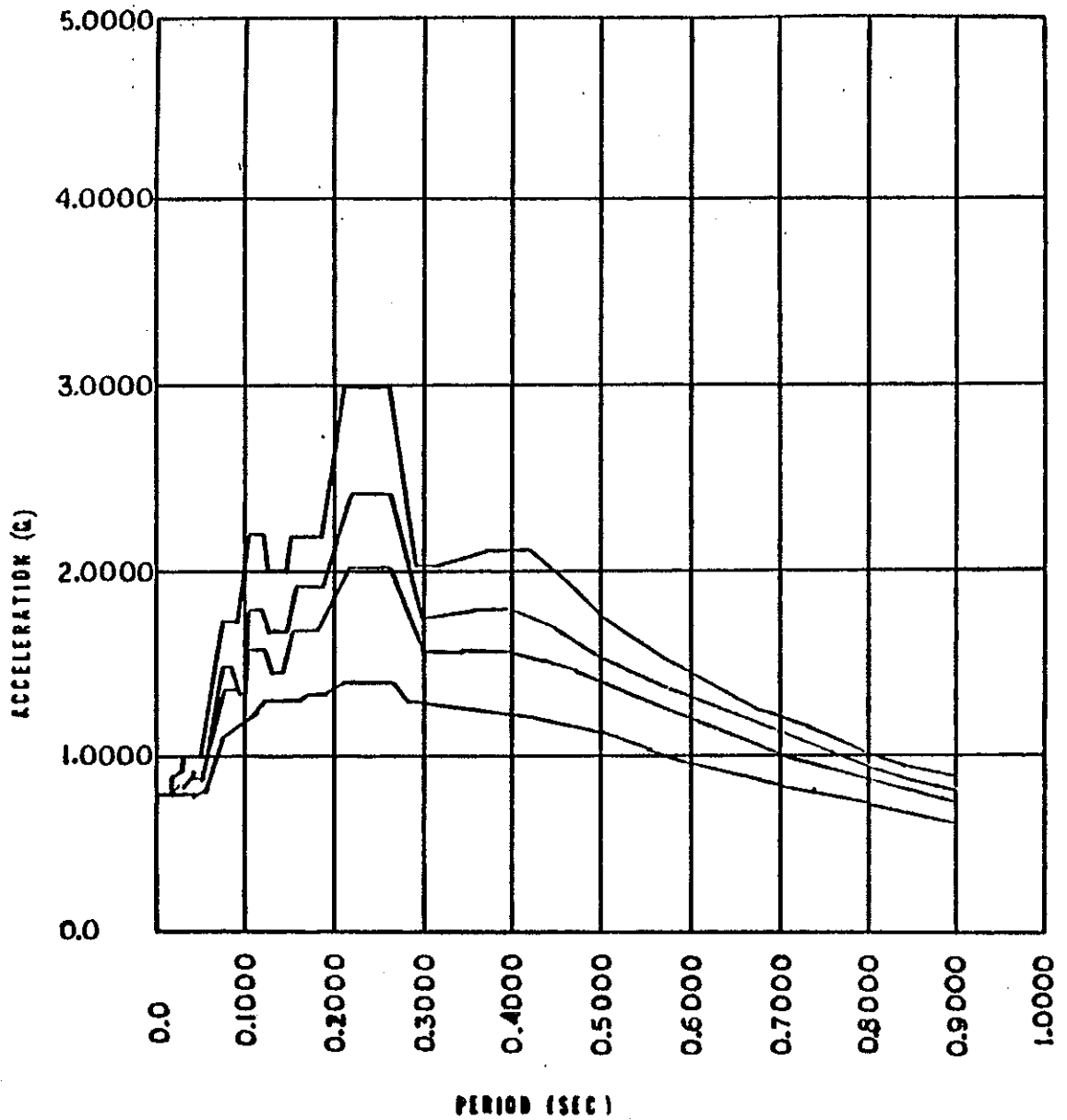
FSAR UPDATE
UNIT 1
DIABLO CANYON SITE
FIGURE 3.7 - 12 N PIPEWAY STRUCTURE HOSGRI BLUME N-S RESPONSE SPECTRA % DAMPING 2,3,4,7 ELEVATION 109'4" NODE 893

Revision 11 November 1996



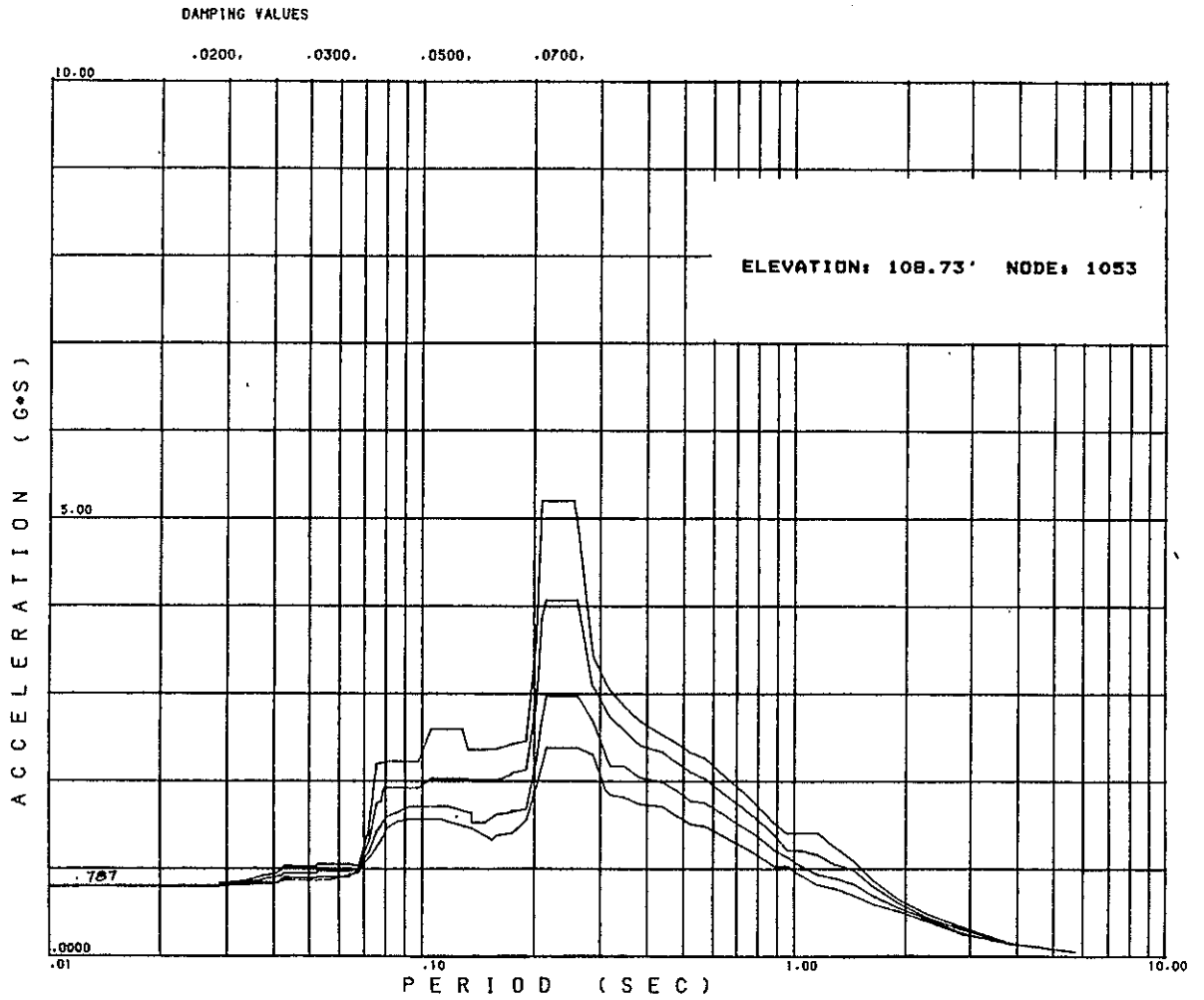
FSAR UPDATE
UNIT 1
DIABLO CANYON SITE
FIGURE 3.7 - 12 O PIPEWAY STRUCTURE HOSGRI BLUME E-W RESPONSE SPECTRA % DAMPING 2, 3, 4, 7 ELEVATION 109'-4" NODE 893

Revision 11 November 1996



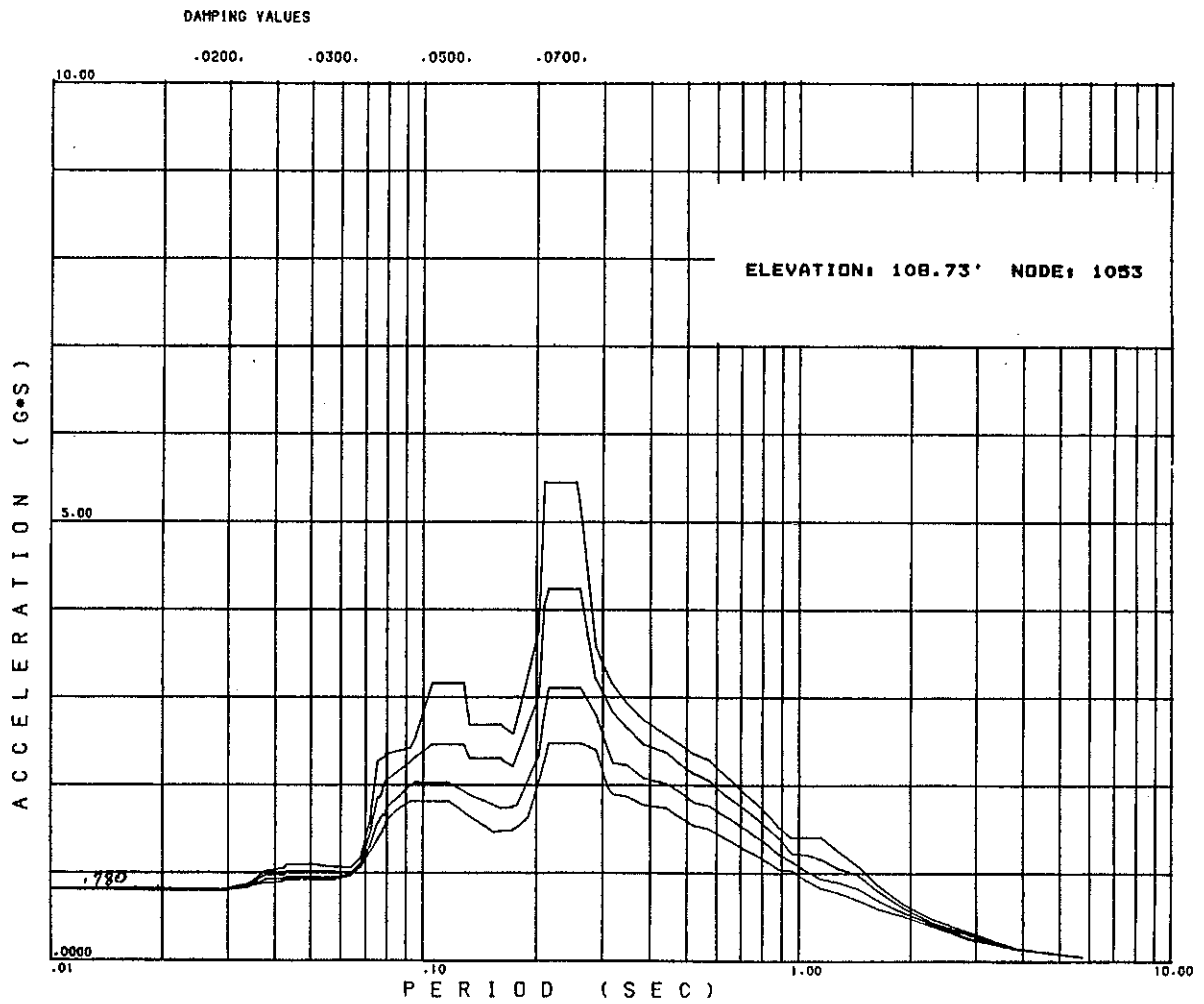
FSAR UPDATE
UNIT 1 DIABLO CANYON SITE
FIGURE 3.7 - 12P PIPEWAY STRUCTURE HOSGRI BLUME VERTICAL RESPONSE SPECTRA % DAMPING 2,3,4,7 ELEVATION 109'-4" NODE 893

Revision 11 November 1996



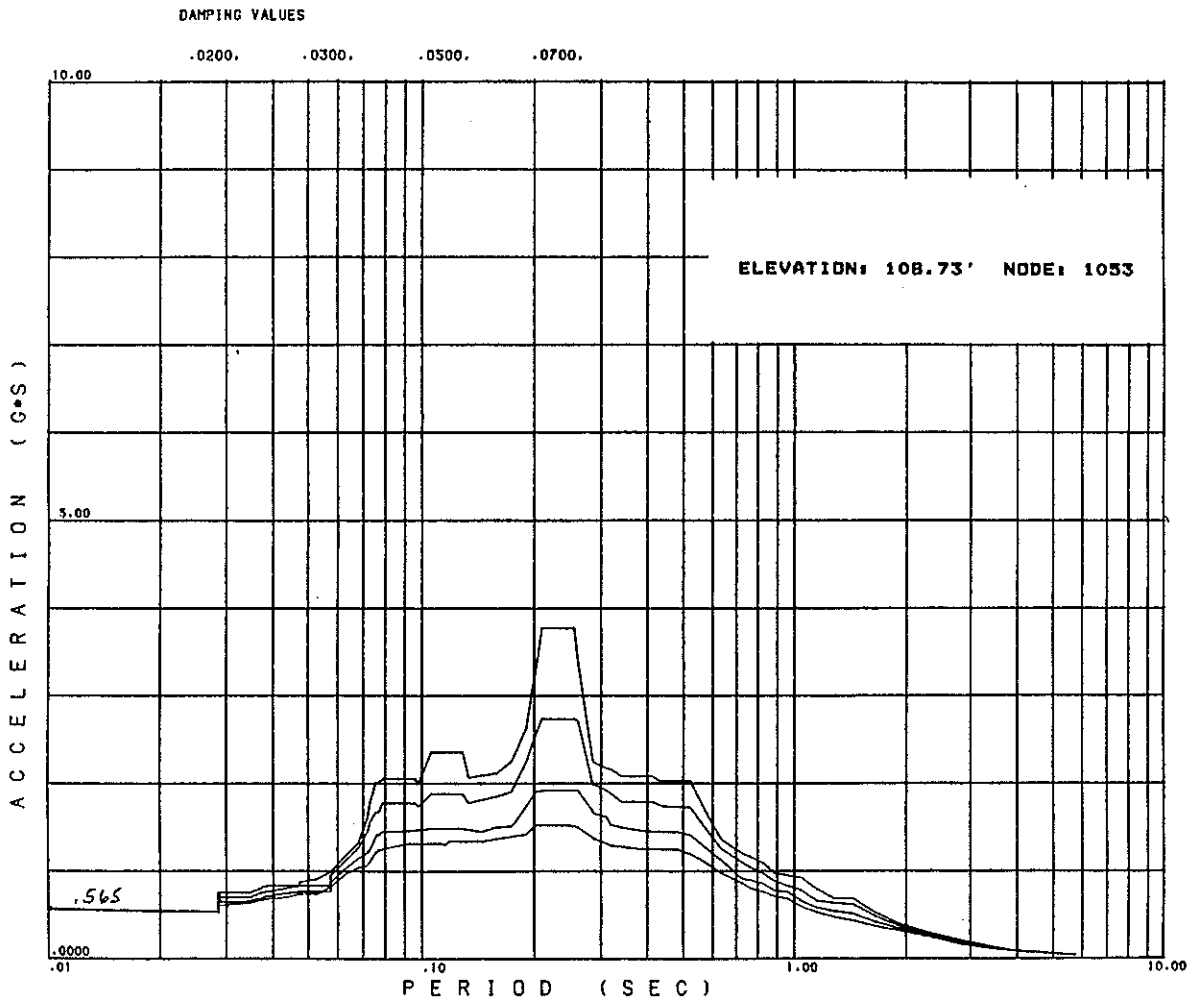
FSAR UPDATE
UNIT 2
DIABLO CANYON SITE
FIGURE 3.7 - 12Q PIPEWAY STRUCTURE HOSGRI BLUME N-S RESPONSE SPECTRA

Revision 11 November 1996



FSAR UPDATE
UNIT 2
DIABLO CANYON SITE
FIGURE 3.7 - 12R PIPEWAY STRUCTURE HOSGRI BLUME E- W RESPONSE SPECTRA

Revision 11 November 1996



FSAR UPDATE
UNIT 2
DIABLO CANYON SITE
 FIGURE 3.7 - 12 S
 PIPEWAY STRUCTURE
 HOSGRI BLUME VERTICAL
 RESPONSE SPECTRA

Revision 11 November 1996

LEGEND:

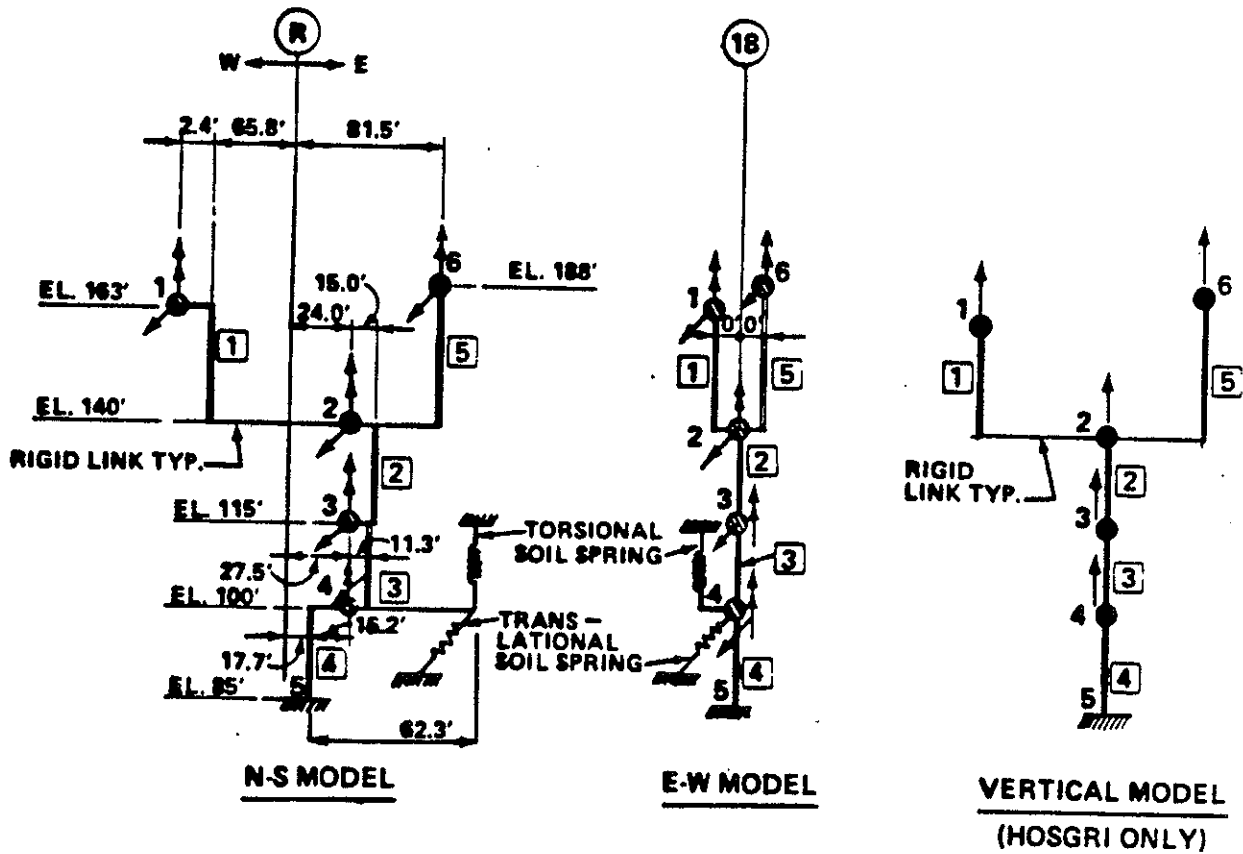
2 - NODE NUMBER

1 - ELEMENT NUMBER

↑ - ROTATIONAL DEGREE OF FREEDOM

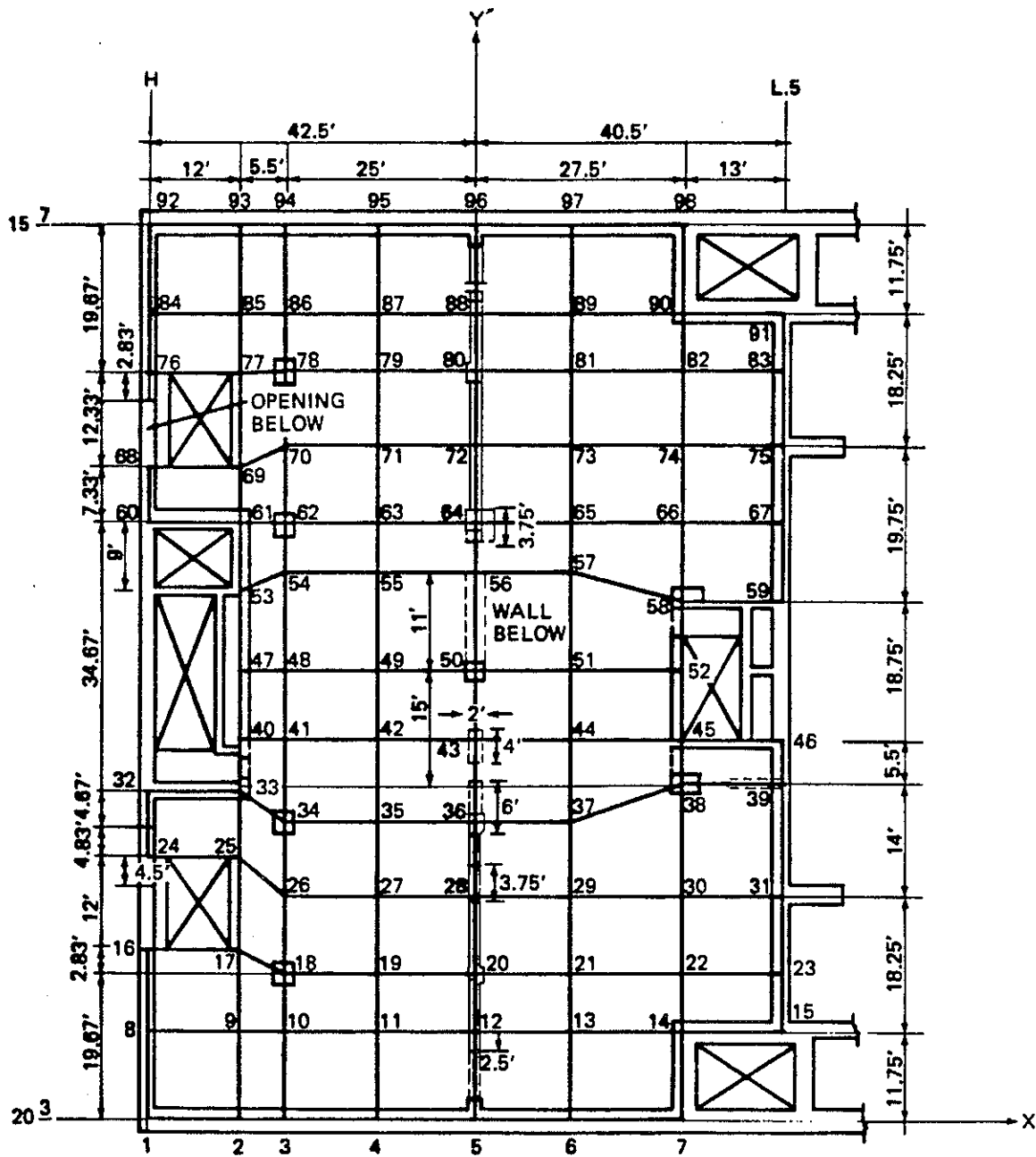
↗ - TRANSLATIONAL DEGREE OF FREEDOM

● - MASS POINT



FSAR UPDATE
UNITS 1 AND 2 DIABLO CANYON SITE
FIGURE 3.7-13 AUXILIARY BUILDING MATHEMATICAL MODEL

Revision 11 November 1996



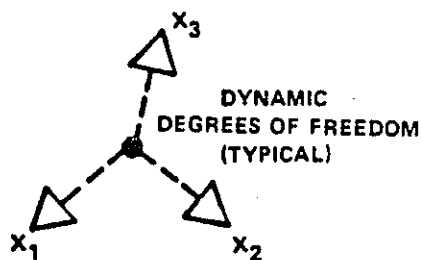
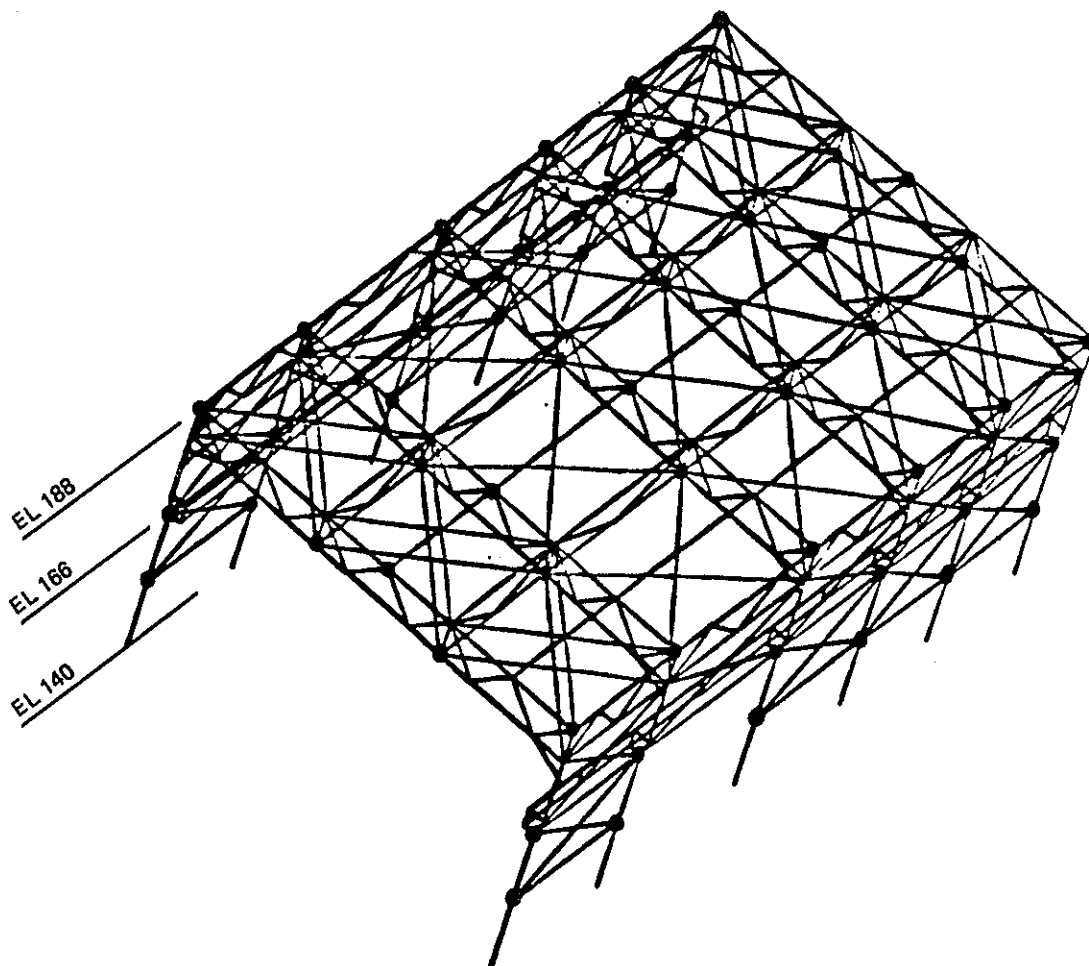
FSAR UPDATE
UNITS 1 AND 2
DIABLO CANYON SITE
 FIGURE 3.7-13A
AUXILIARY BUILDING
FLEXIBLE SLAB MODEL

Revision 11 November 1996

LEGEND:

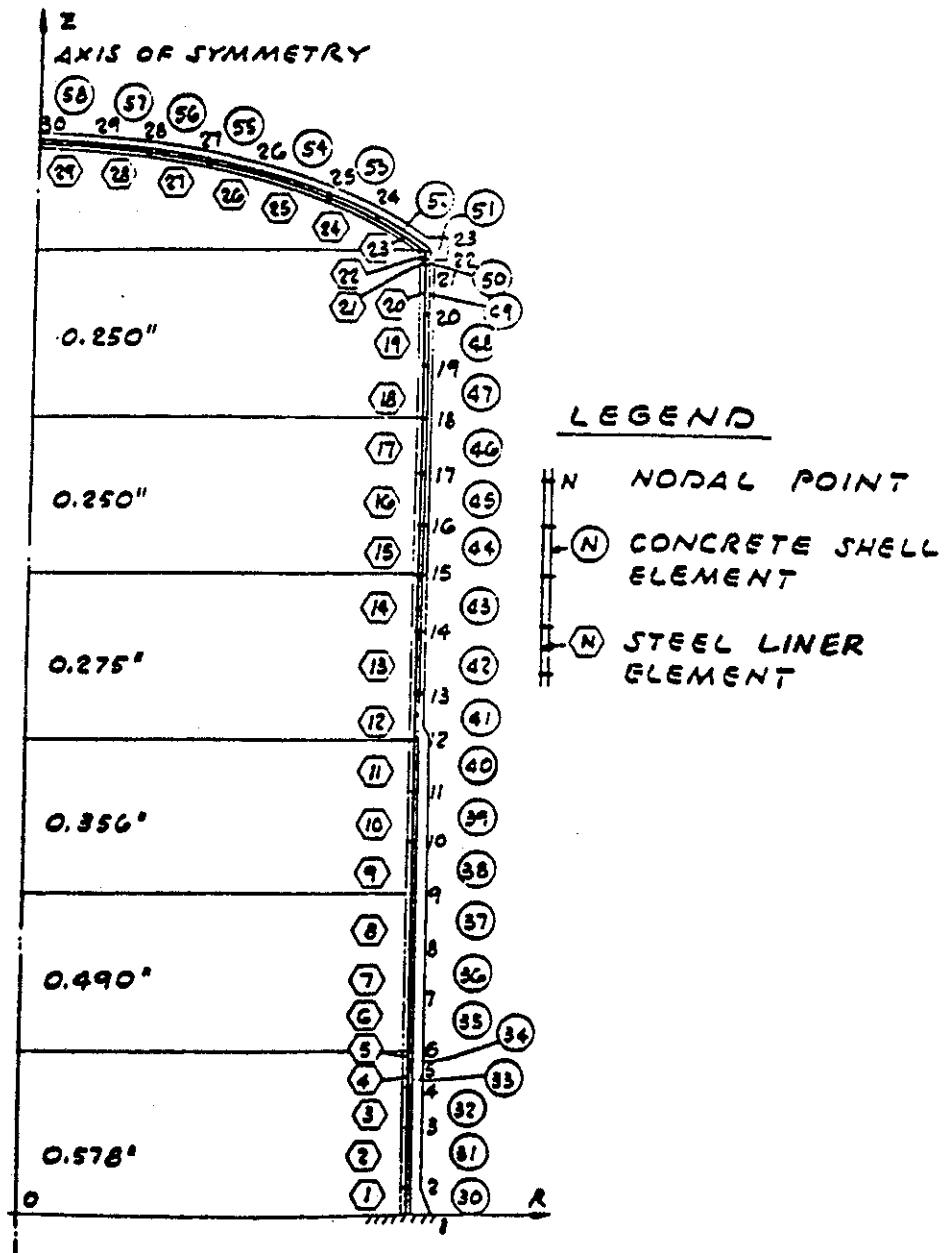
————— SIGNIFICANT STRUCTURAL MEMBER

● DYNAMIC DEGREE OF FREEDOM 162



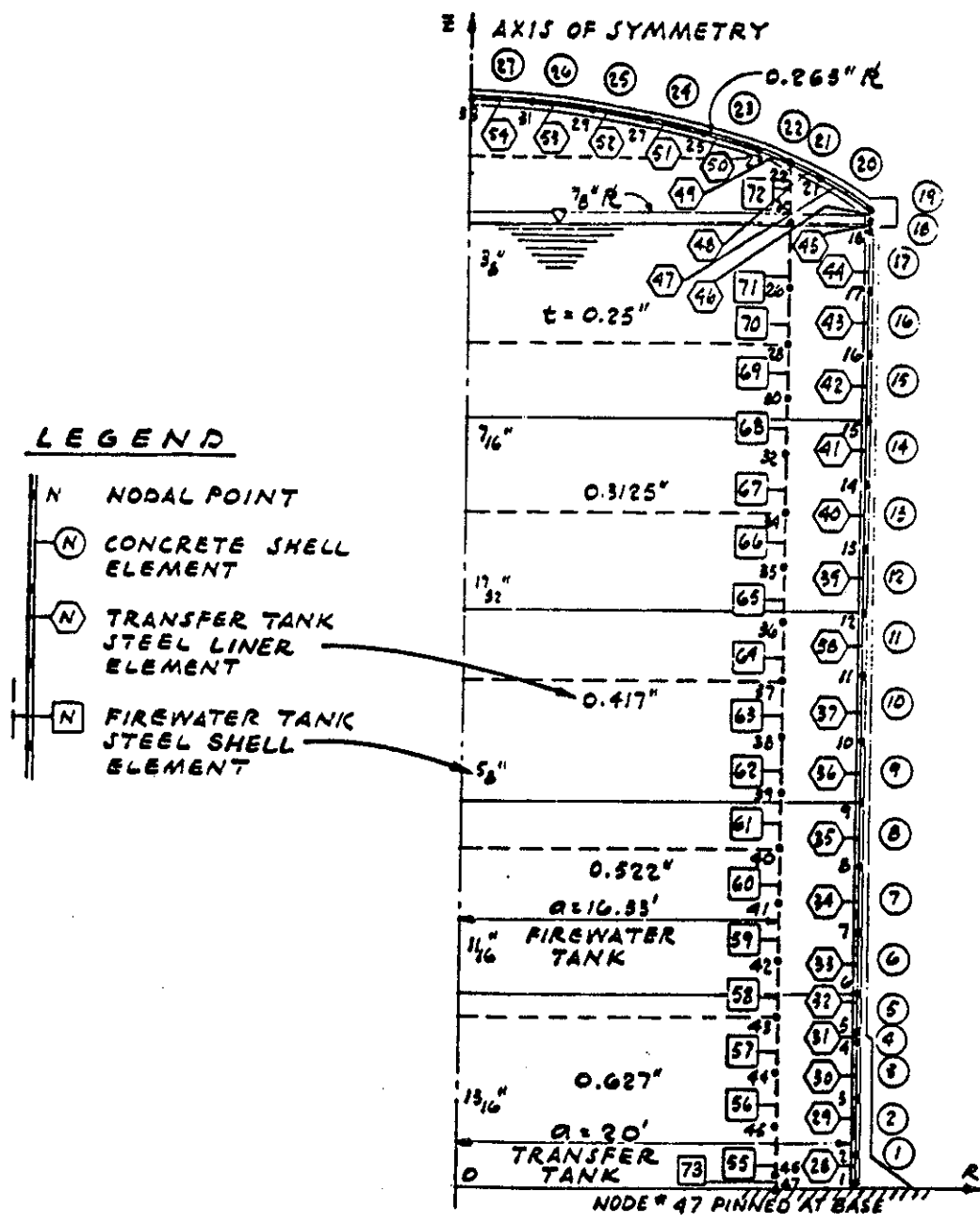
FSAR UPDATE
UNITS 1 AND 2 DIABLO CANYON SITE
FIGURE 3.7-13B AUXILIARY BUILDING FUEL HANDLING CRANE SUPPORT STRUCTURE MODEL NO. 2.2

Revision 11 November 1996



FSAR UPDATE
UNITS 1 AND 2 DIABLO CANYON SITE
FIGURE 3.7-14 OUTDOOR WATER STORAGE TANKS: REFUELING WATER TANK, AXISYMMETRIC MODEL

Revision 11 November 1996



FSAR UPDATE

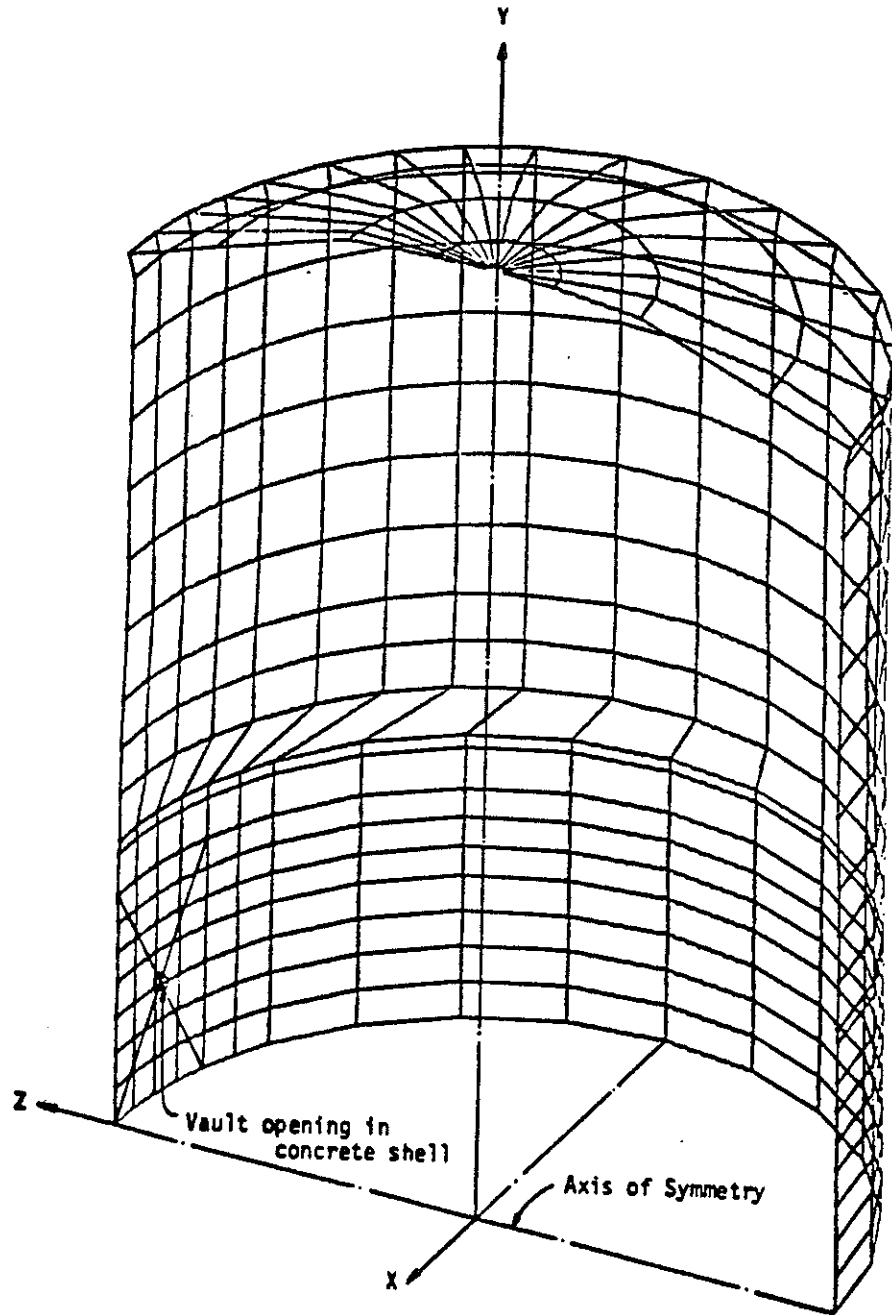
UNITS 1 AND 2

DIABLO CANYON SITE

FIGURE 3.7 - 15

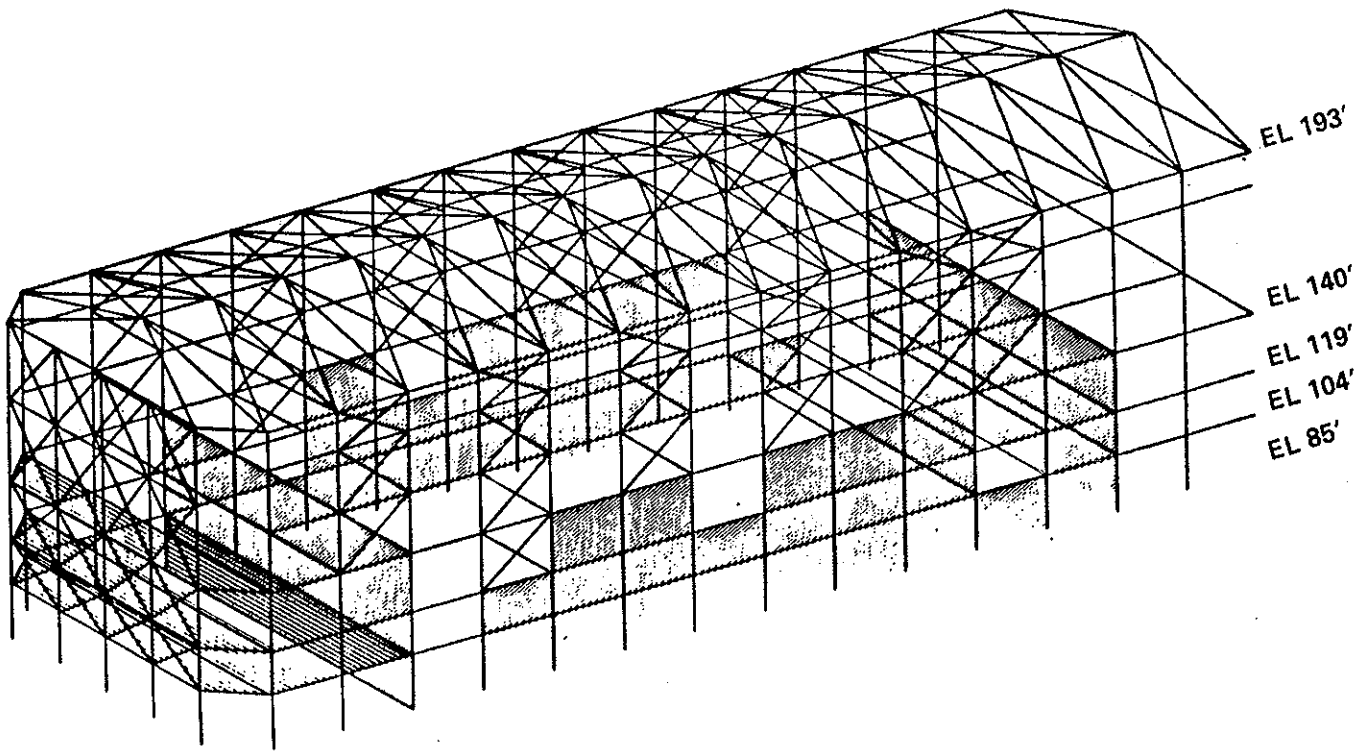
OUTDOOR WATER STORAGE TANKS:
FIREWATER AND TRANSFER TANK,
AXISYMMETRIC MODEL

Revision 11 November 1996



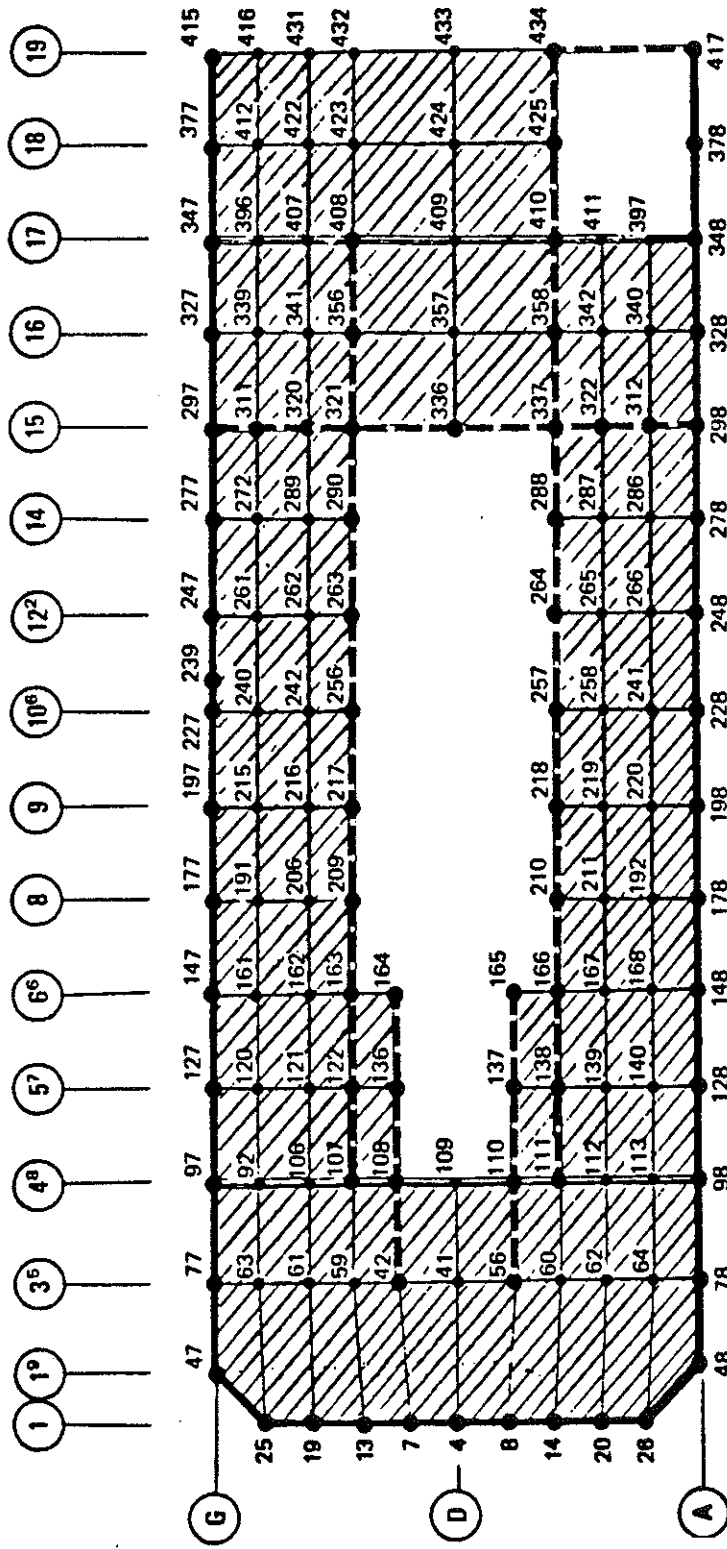
FSAR UPDATE
UNIT 1 DIABLO CANYON SITE
FIGURE 3.7 - 15 A OUTDOOR WATER STORAGE TANKS: REFUELING WATER TANK, PERSPECTIVE VIEW OF HALF-TANK MODEL

Revision 11 November 1996



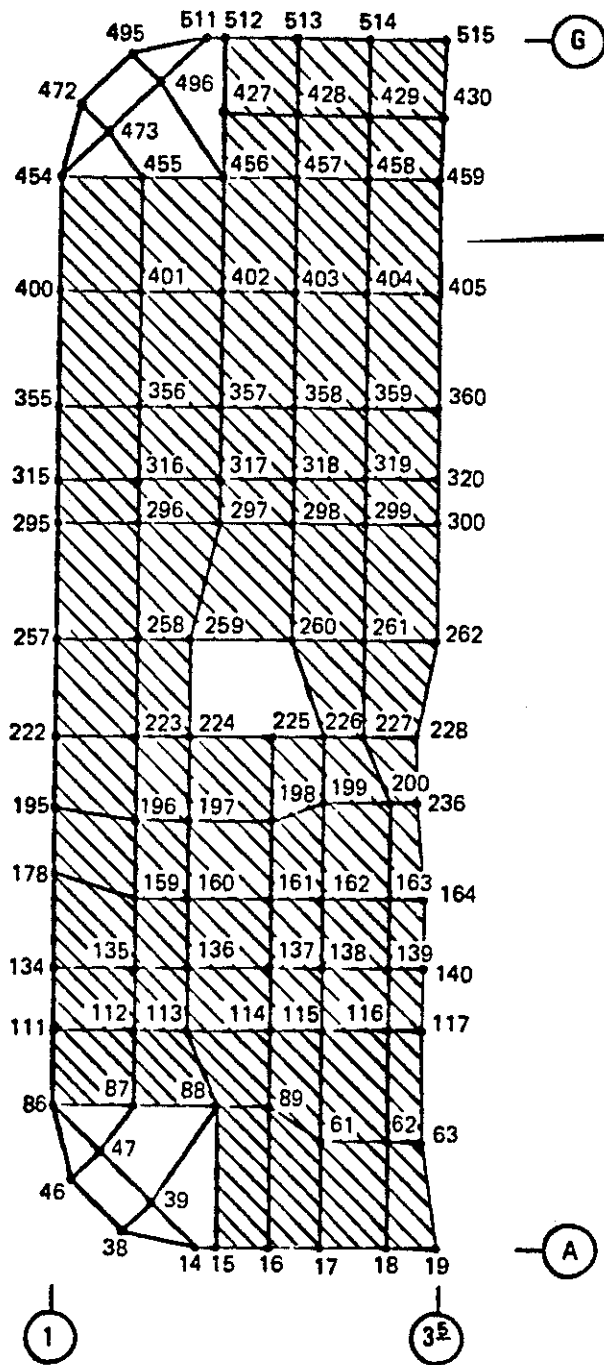
FSAR UPDATE
UNITS 1 AND 2 DIABLO CANYON SITE
FIGURE 3.7 - 15 C TURBINE BUILDING UNIT 1 PORTION HORIZONTAL MODEL ISOMETRIC


Revision 11 November 1996



FSAR UPDATE
UNITS 1 AND 2
DIABLO CANYON SITE
 FIGURE 3.7 - 15 D
 TURBINE BUILDING UNIT 1
 PORTION HORIZONTAL
 MODEL PLAN AT ELEV. 140'

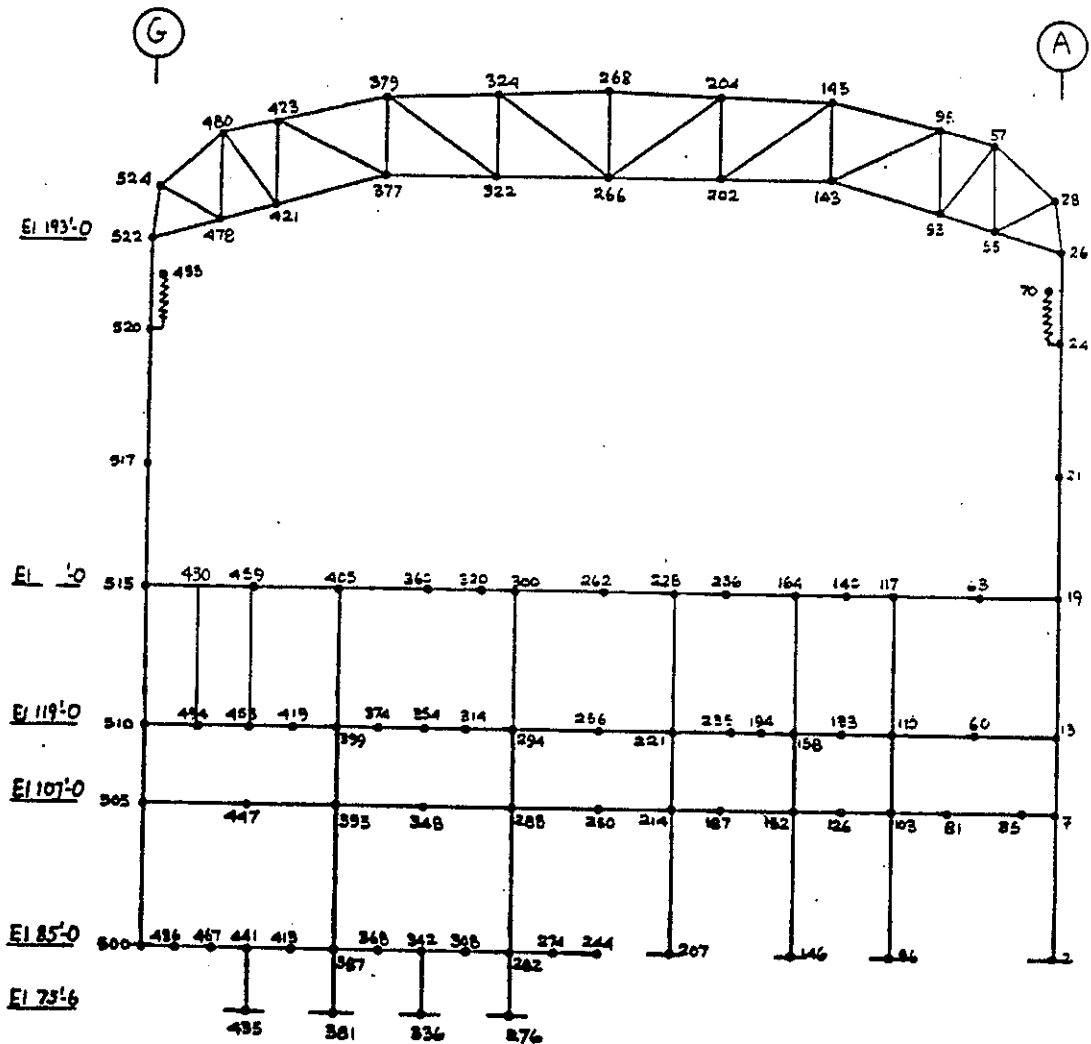
--- TRUSS ELEMENTS
 --- BEAM ELEMENTS
 ▨ PLANE STRESS ELEMENTS



 ELEMENT

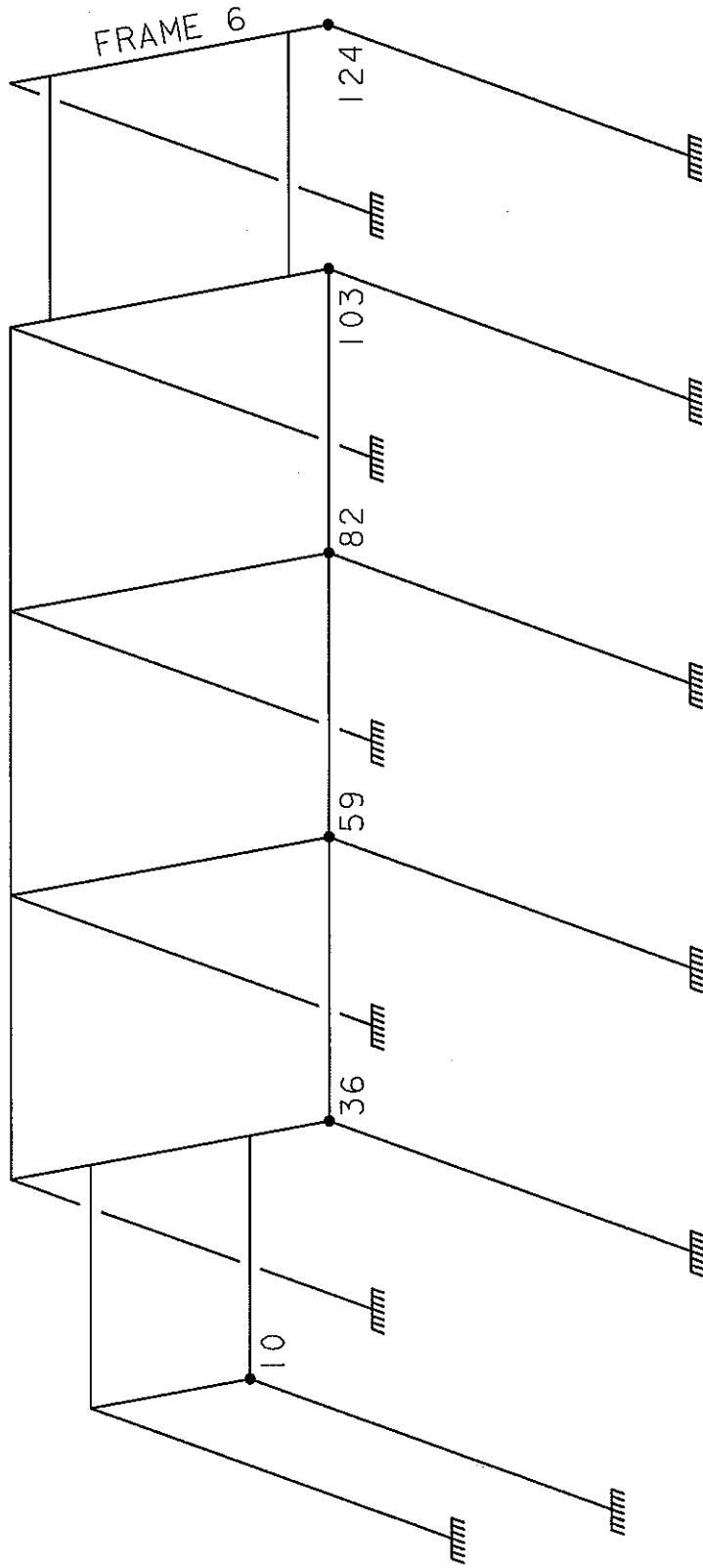
FSAR UPDATE
UNITS 1 AND 2 DIABLO CANYON SITE
FIGURE 3.7 -15E TURBINE BUILDING VERTICAL MODEL NO. 1 PLAN AT ELEVATION 140'

Revision 11 November 1996



FSAR UPDATE
UNIT 1
DIABLO CANYON SITE
 FIGURE 3.7 - 15 F
 TURBINE BUILDING
 VERTICAL MODEL NO.1
 ELEVATION AT LINE 3.5

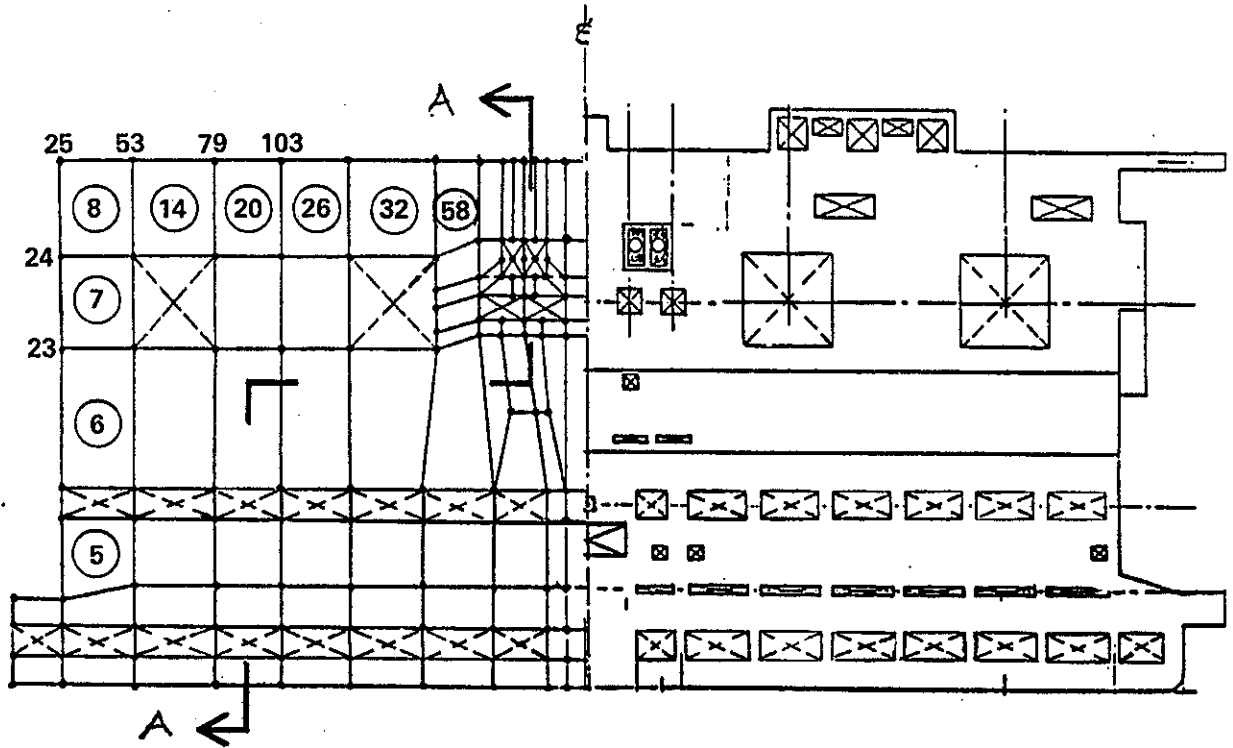
Revision 11 November 1996



TOTAL NUMBER OF ELEMENTS = 208

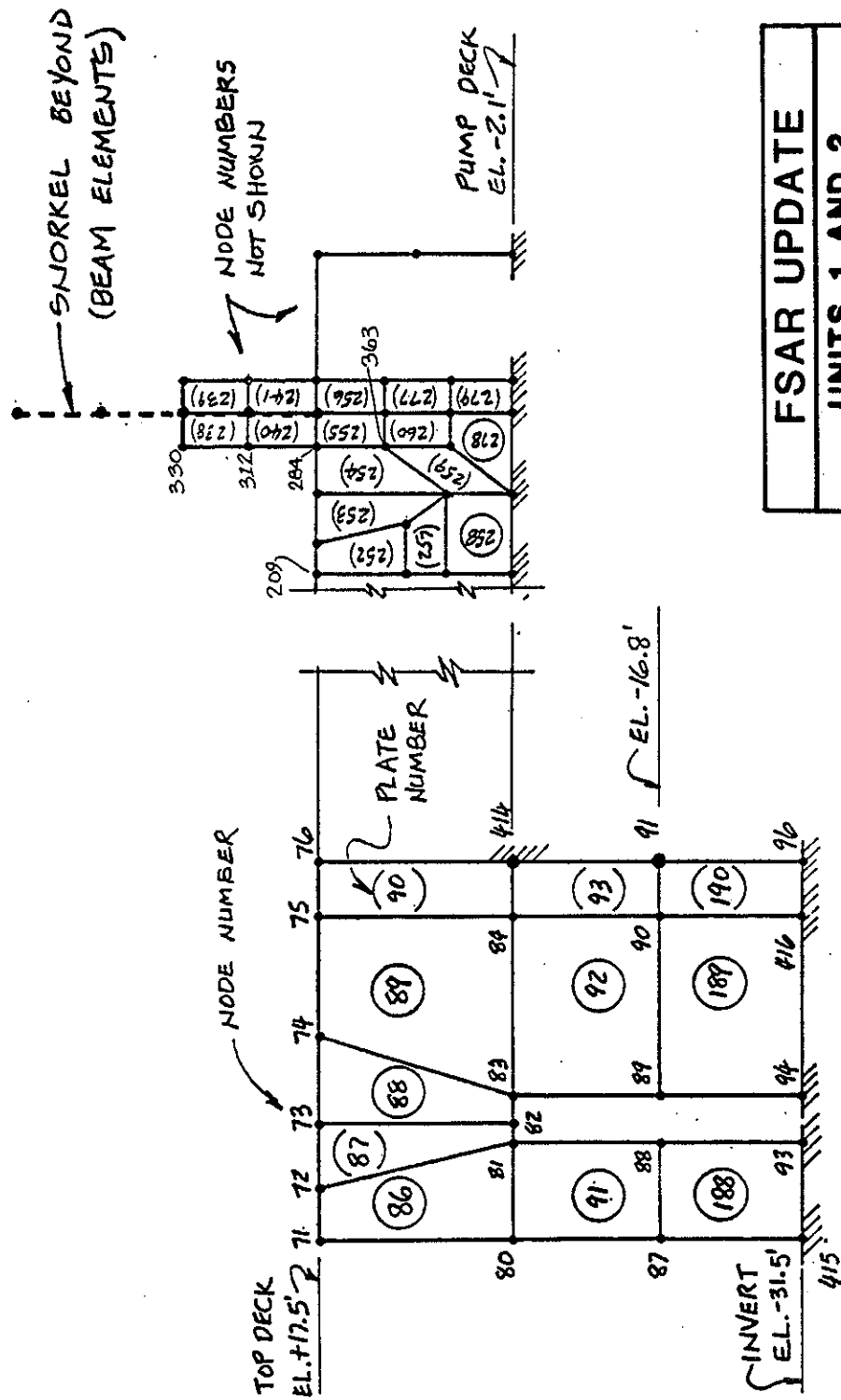
FSAR UPDATE
UNIT 1
DIABLO CANYON SITE
FIGURE 3.7-15G
TURBINE PEDESTAL
SEISMIC ANALYSIS MODEL

Revision 17 November 2006



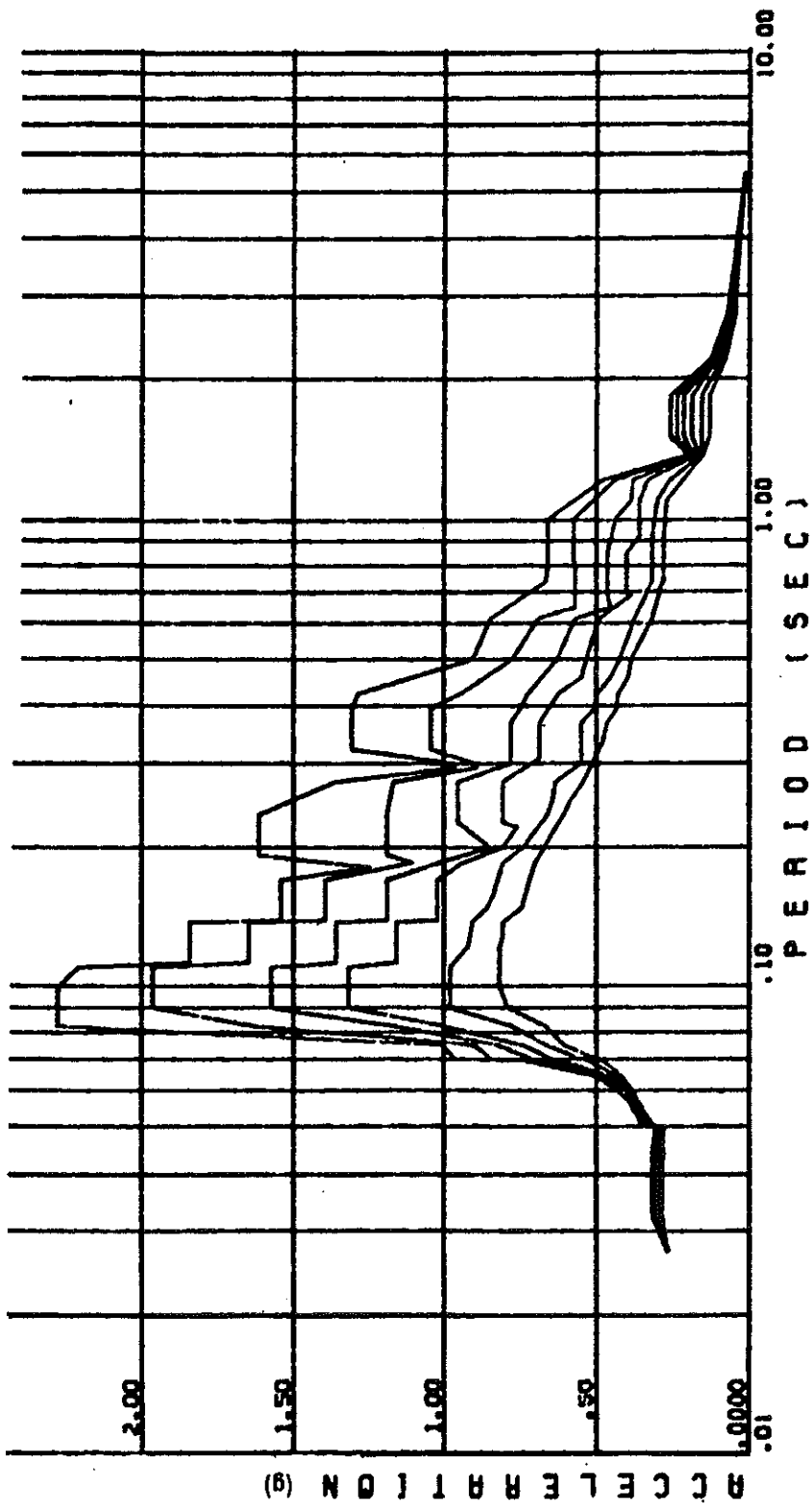
FSAR UPDATE
UNITS 1 AND 2 DIABLO CANYON SITE
FIGURE 3.7 - 15 H INTAKE STRUCTURE TOP DECK MATHEMATICAL MODEL, ELEVATION + 17.5 FT.

Revision 11 November 1996



FSAR UPDATE
UNITS 1 AND 2
DIABLO CANYON SITE
FIGURE 3.7-15 I
INTAKE STRUCTURE
TRANSVERSE SECTION A-A
MATHEMATICAL MODEL

SEE FIG. 3.7-15 H FOR LOCATION OF SECTION A-A

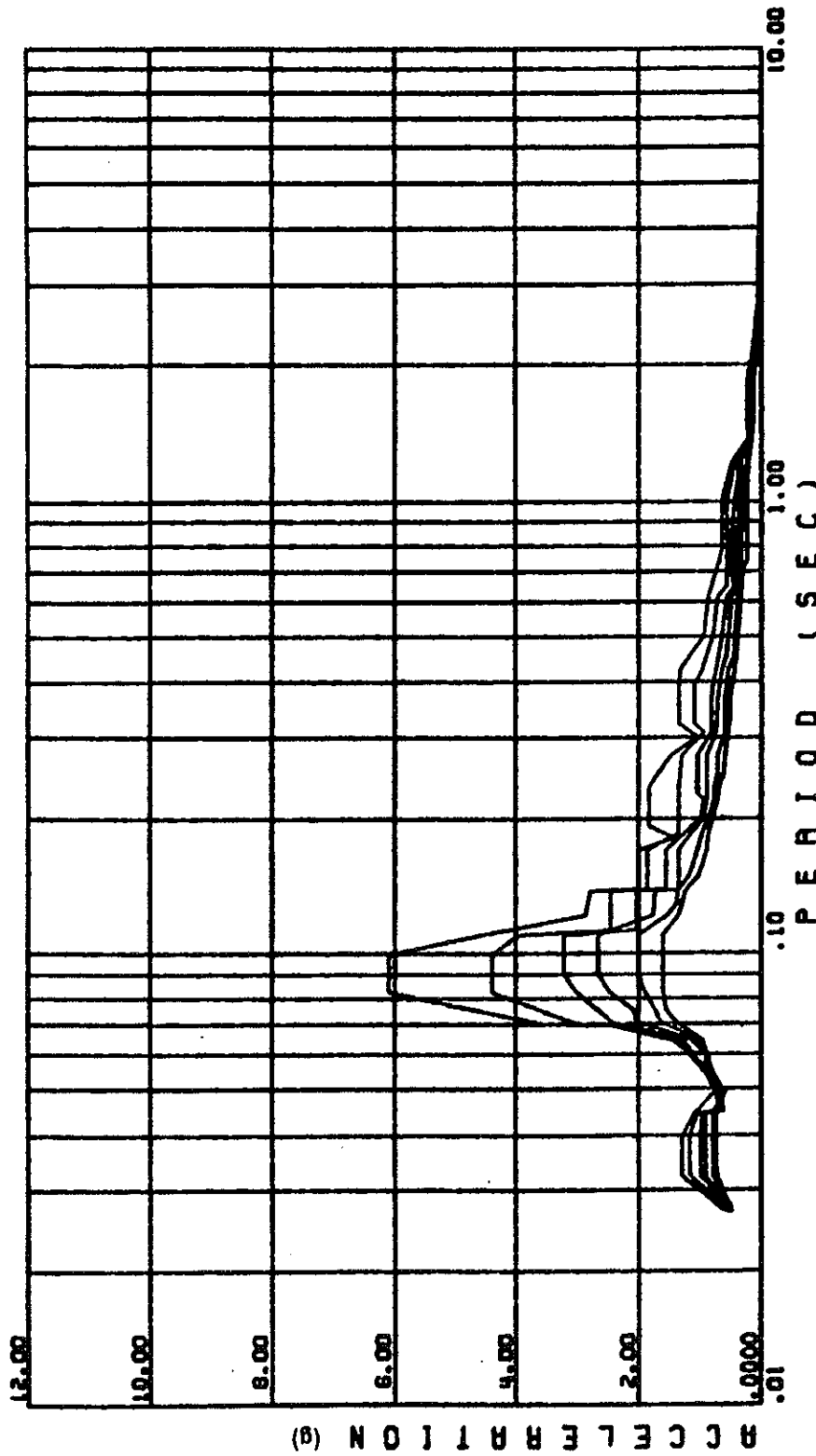


FSAR UPDATE

UNITS 1 AND 2

DIABLO CANYON SITE

FIGURE 3.7.16
 AUXILIARY BUILDING
 FLOOR ELEV. 100'-0" N-S
 HORIZONTAL SPECTRA
 DESIGN EARTHQUAKE
 $\frac{1}{2}$, 1, 2, 3, 5, 7% DAMPING



FSAR UPDATE

UNITS 1 AND 2

DIABLO CANYON SITE

FIGURE 3.7-17

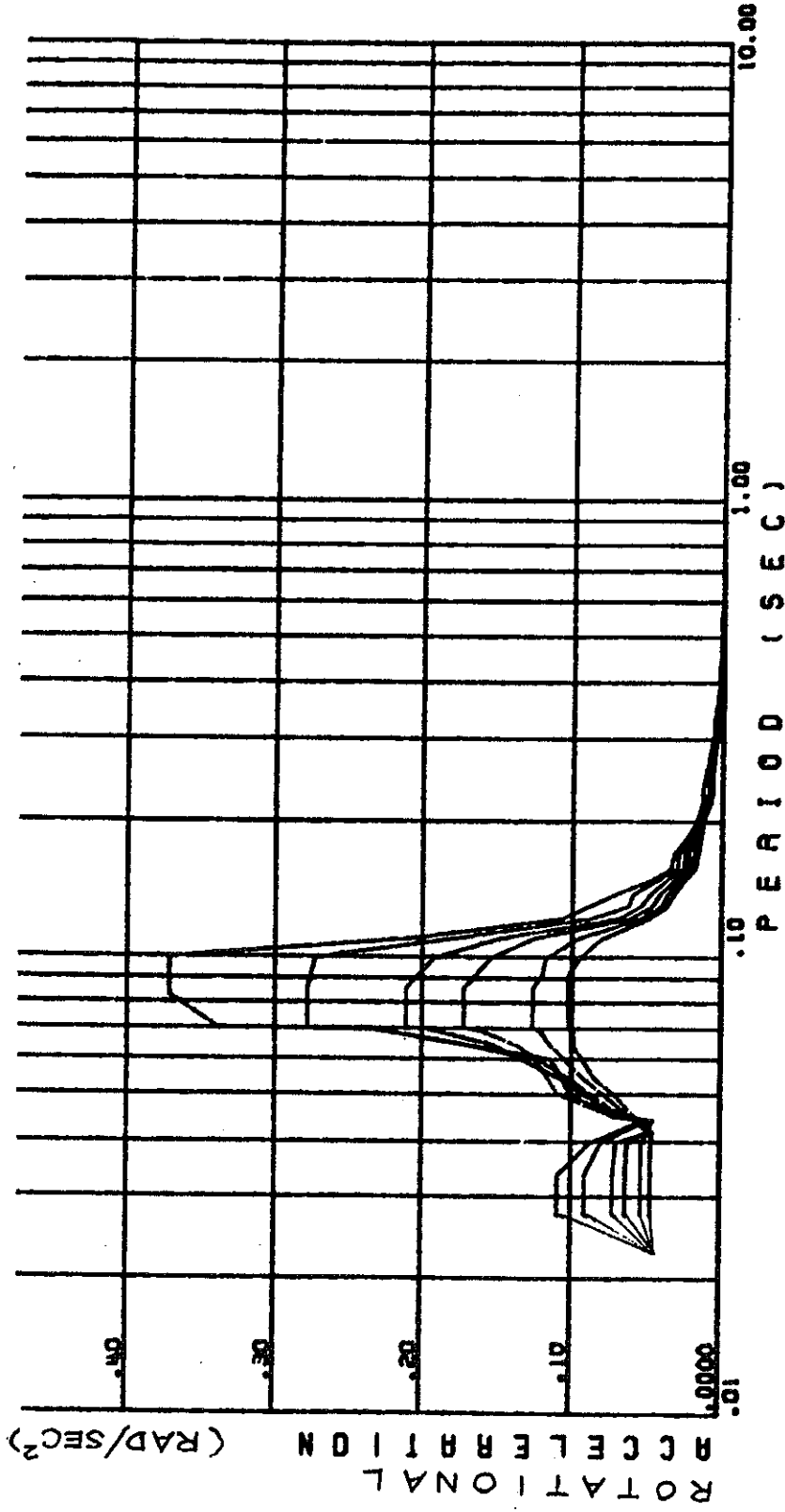
AUXILIARY BUILDING

FLOOR ELEV. 163'-0" N-S

HORIZONTAL SPECTRA

DESIGN EARTHQUAKE

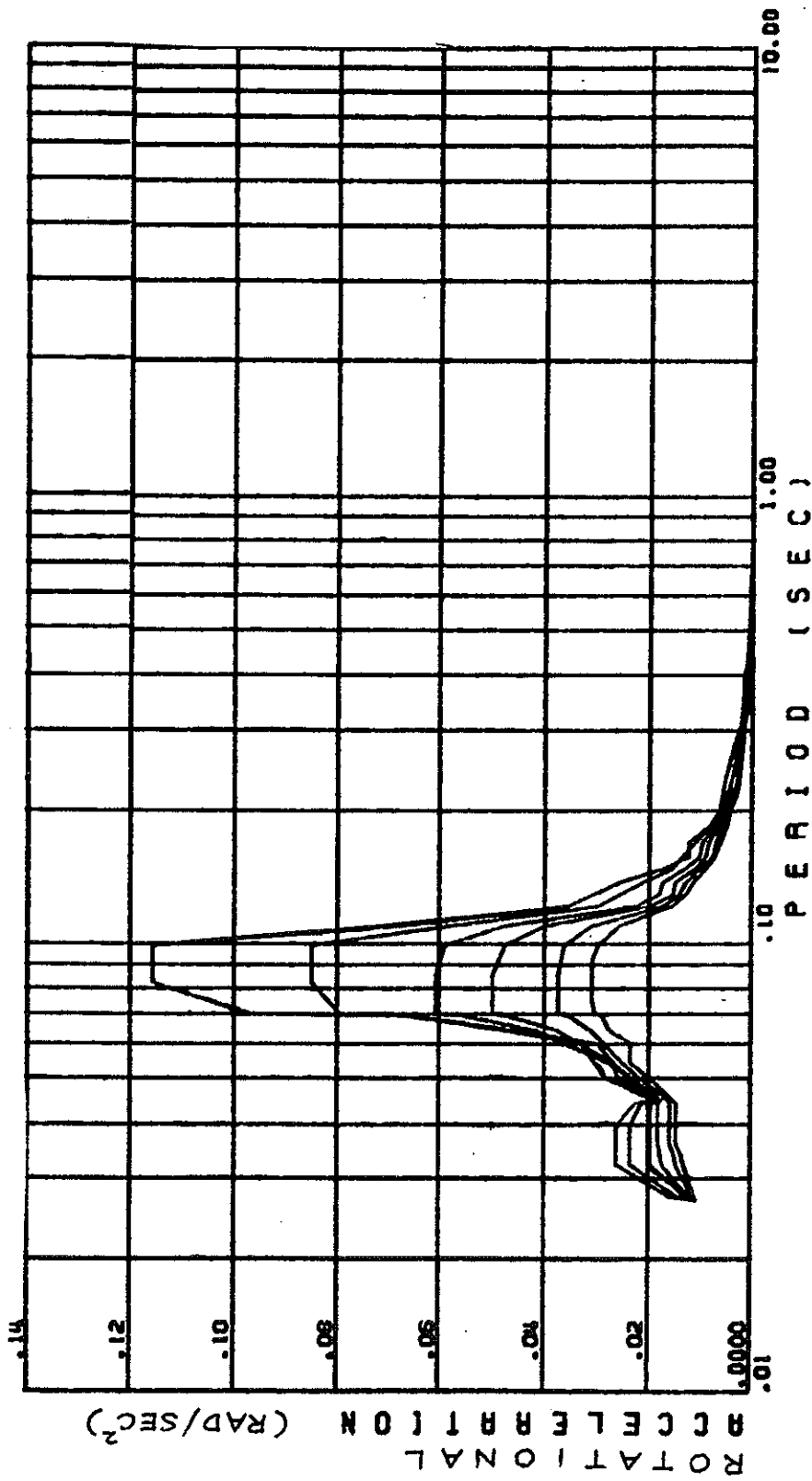
1/2, 1, 2, 3, 5, 7% DAMPING



FSAR UPDATE

**UNITS 1 AND 2
DIABLO CANYON SITE**

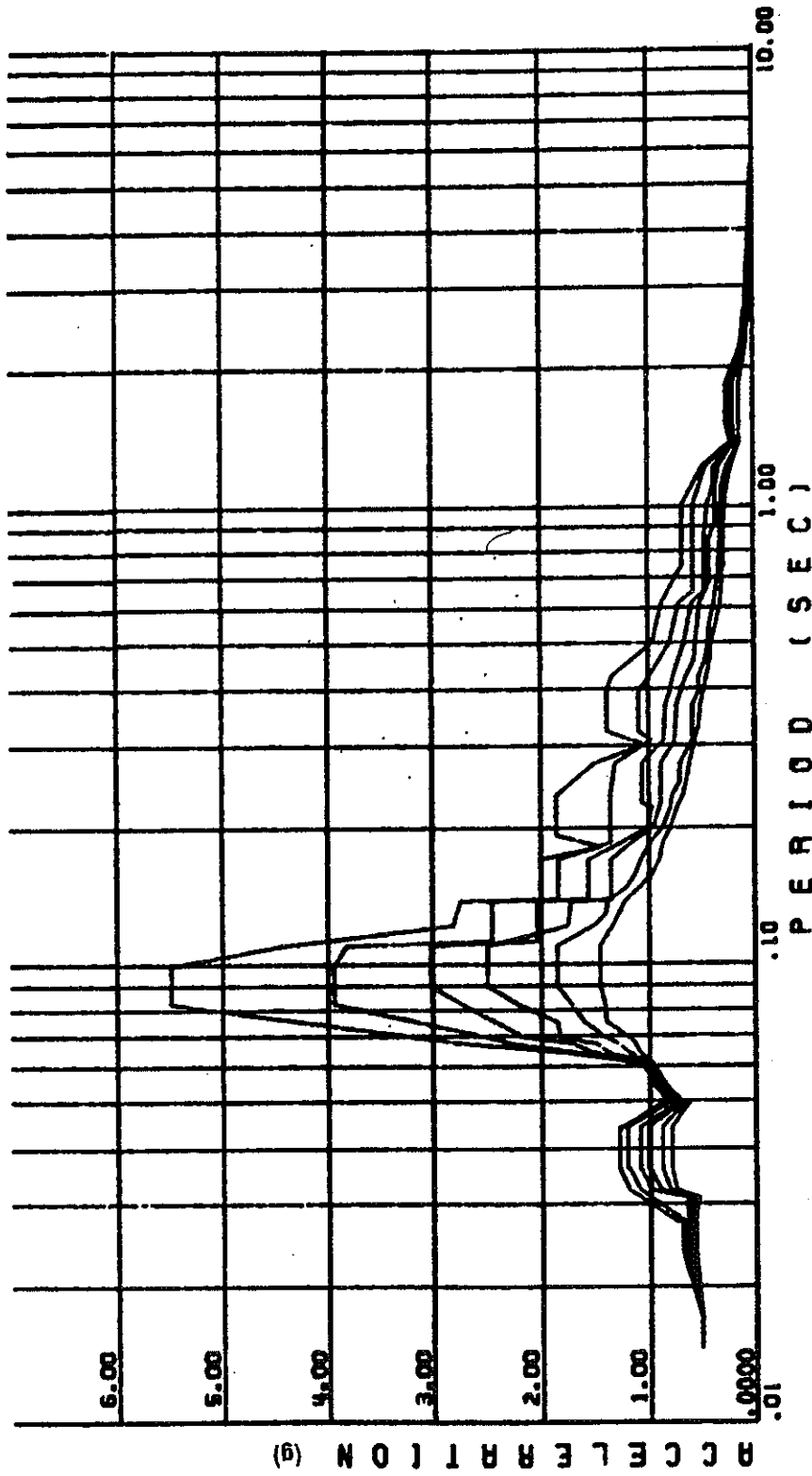
FIGURE 3.7-18
 AUXILIARY BUILDING
 FLOOR ELEV. 163'-0"
 N-S TORSIONAL SPECTRA
 DESIGN EARTHQUAKE
 1/2, 1, 2, 3, 5, 7% DAMPING



FSAR UPDATE

UNITS 1 AND 2
DIABLO CANYON SITE

FIGURE 3.7-19
 AUXILIARY BUILDING
 FLOOR ELEV. 100'-0"
 N-S TORSIONAL SPECTRA
 DESIGN EARTHQUAKE
 1/2, 1, 2, 3, 5, 7% DAMPING



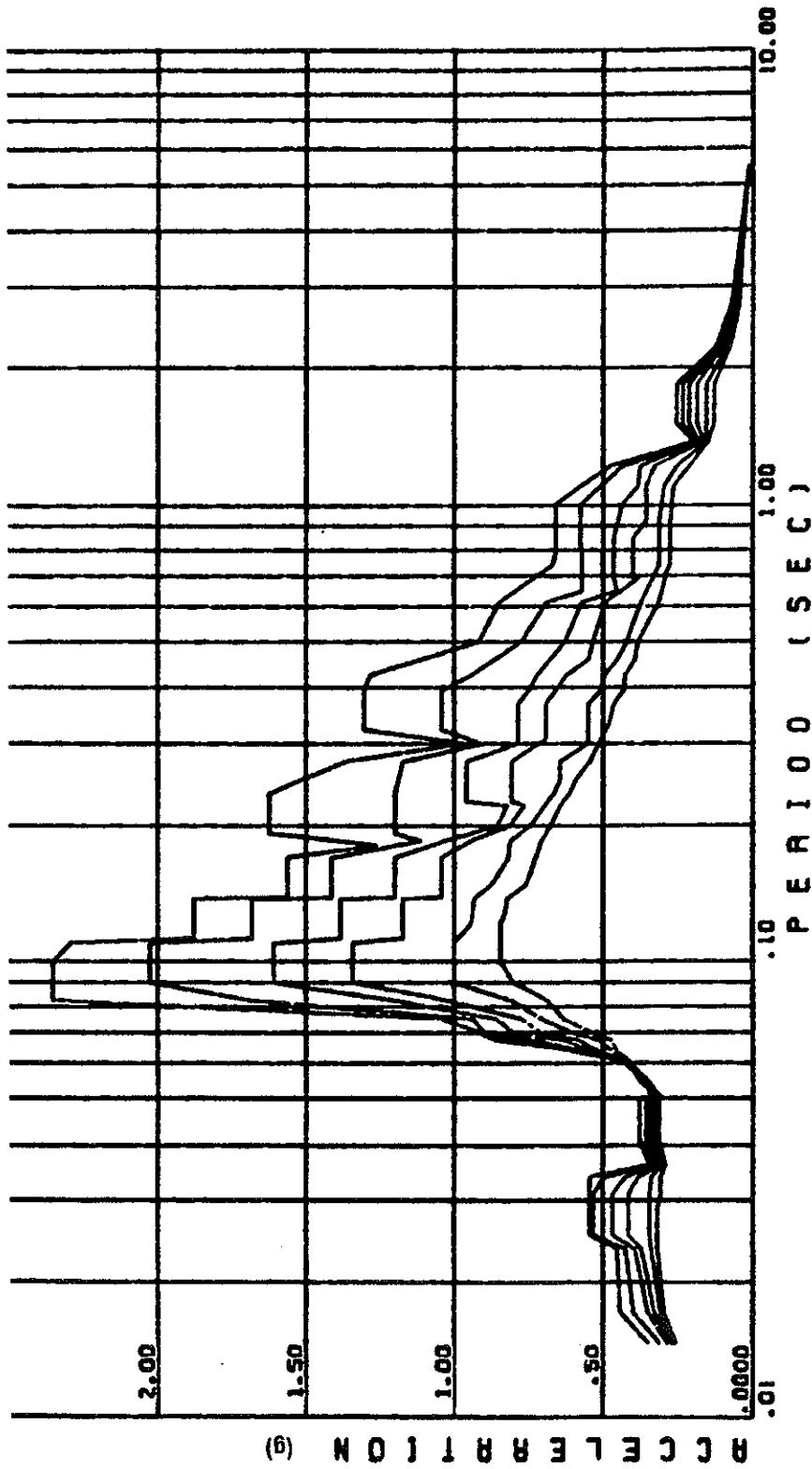
FSAR UPDATE

UNITS 1 AND 2

DIABLO CANYON SITE

FIGURE 3.7-20

AUXILIARY BUILDING
 FLOOR ELEV. 163'-0" E-W
 HORIZONTAL SPECTRA
 DESIGN EARTHQUAKE
 $\frac{1}{2}$, 1, 2, 3, 5, 7% DAMPING



FSAR UPDATE

UNITS 1 AND 2

DIABLO CANYON SITE

FIGURE 3.7-21

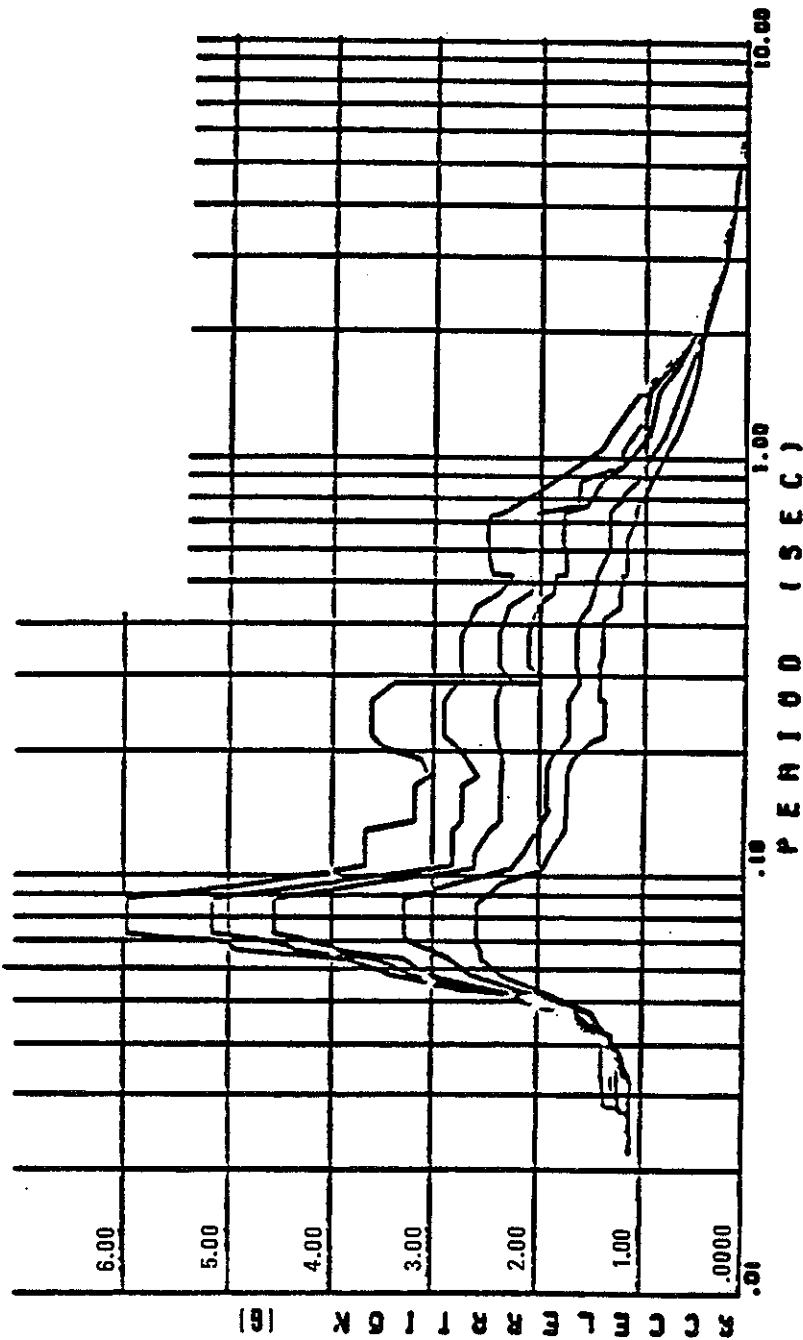
AUXILIARY BUILDING

FLOOR ELEV. 100'-0"

E-W HORIZONTAL SPECTRA

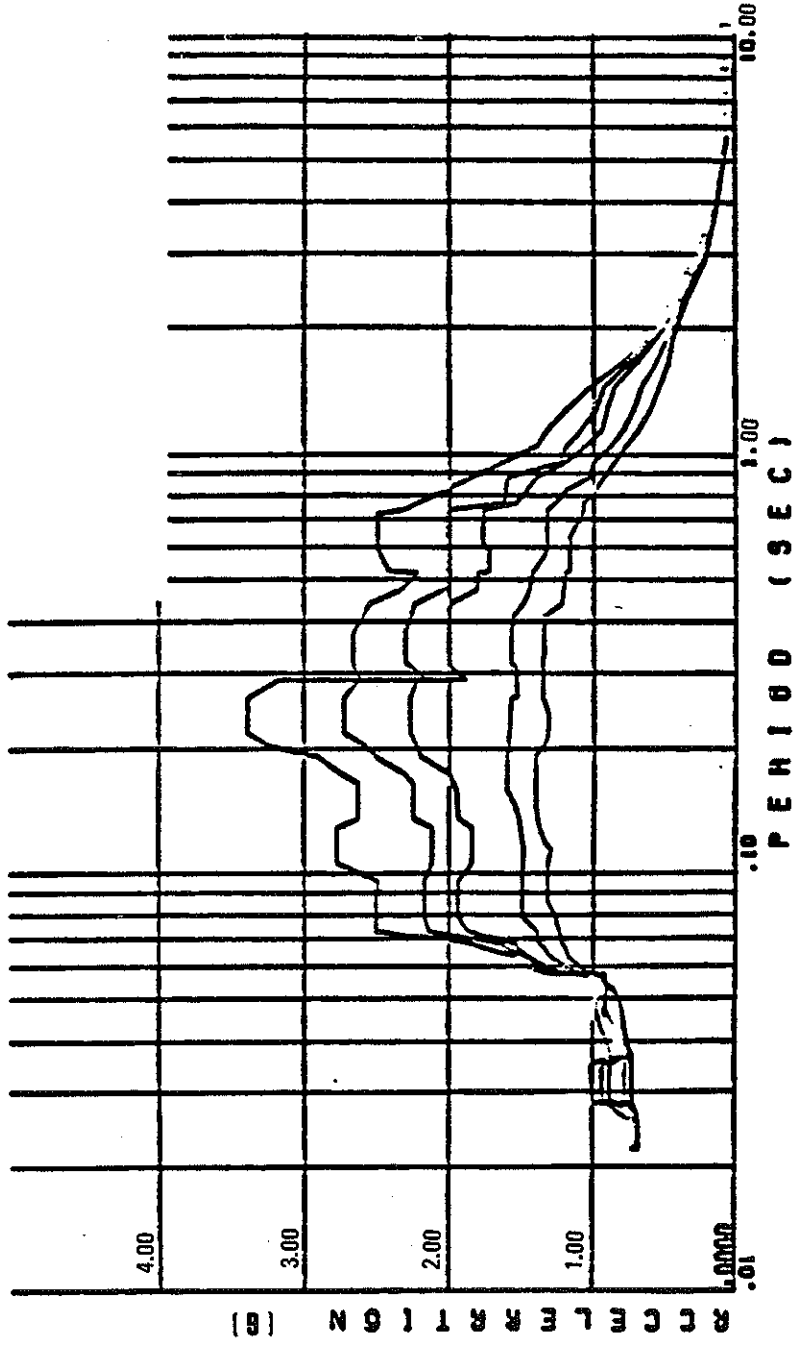
DESIGN EARTHQUAKE

1/2, 1, 2, 3, 5, 7% DAMPING



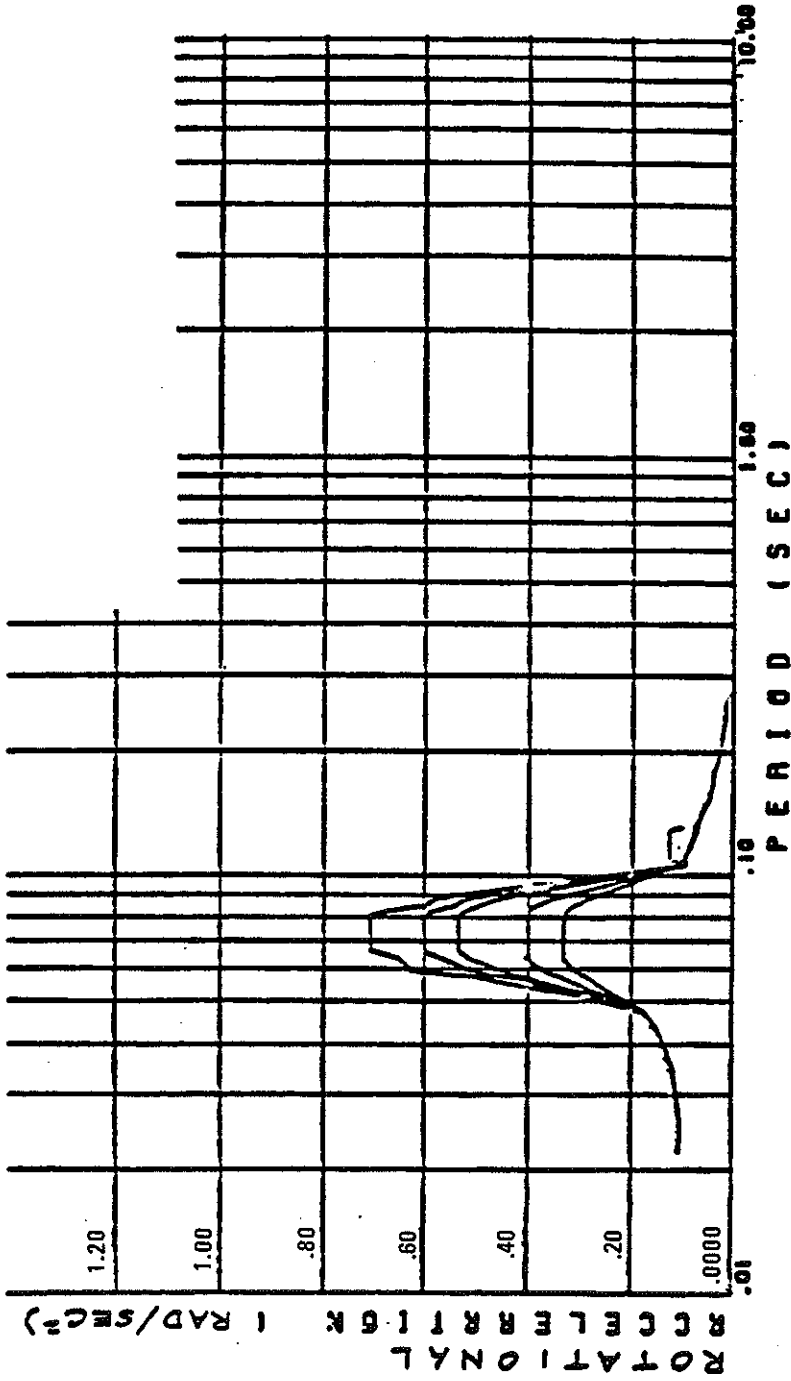
FSAR UPDATE
UNITS 1 AND 2
DIABLO CANYON SITE
 FIGURE 3.7-21A
 AUXILIARY BUILDING
 E-W HOSGR1
 HORIZONTAL FLOOR SPECTRA
 AT EL 140'-0"
 2,3,4,7, AND 10% DAMPING

Revision 11 November 1996



FSAR UPDATE
UNITS 1 AND 2
DIABLO CANYON SITE
 FIGURE 3.7-21B
 AUXILIARY BUILDING
 E-W HOSGRI
 HORIZONTAL FLOOR SPECTRA
 AT EL 100'-0"
 2,3,4,7, AND 10% DAMPING

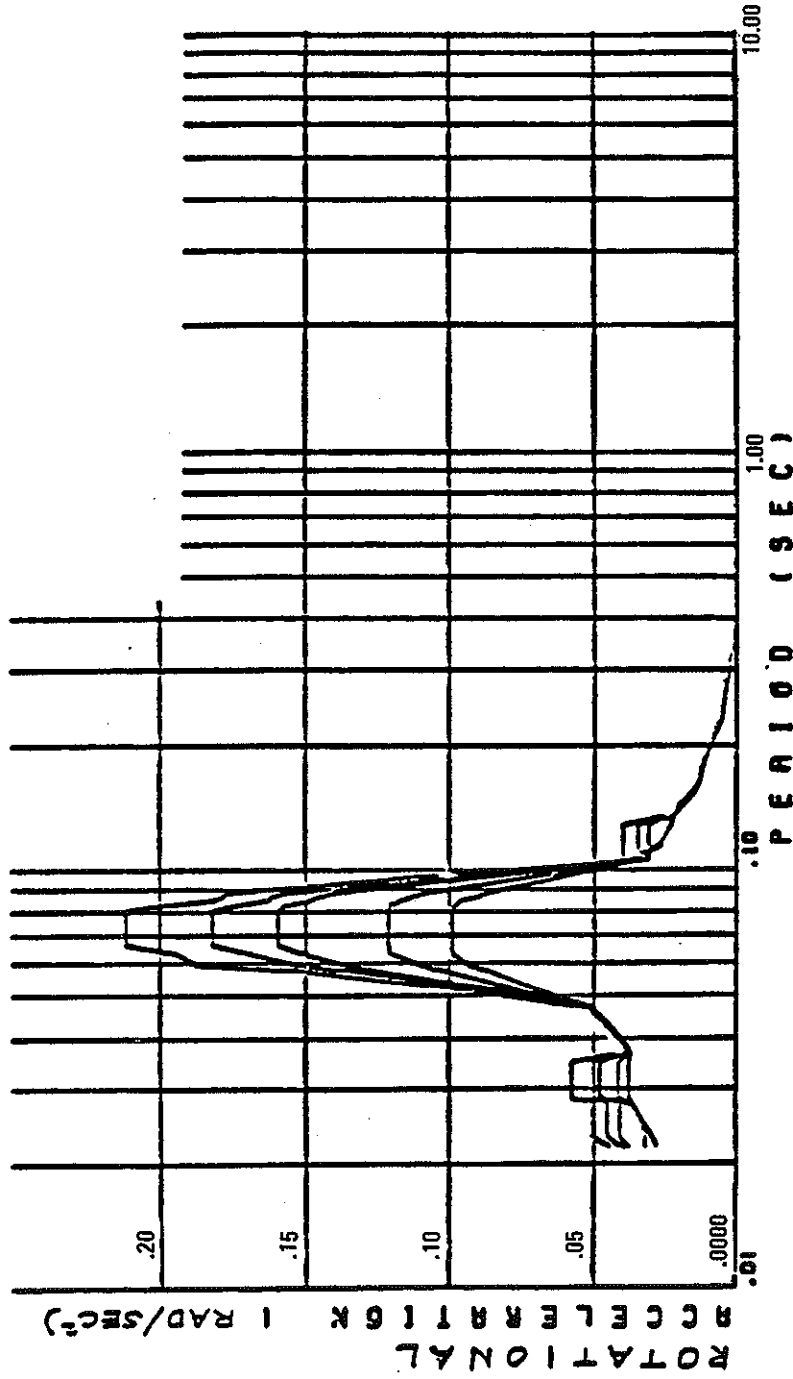
Revision 11 November 1996



FSAR UPDATE

UNITS 1 AND 2
DIABLO CANYON SITE

FIGURE 3.7-21C
AUXILIARY BUILDING
E-W HOSGRI
TORSIONAL FLOOR SPECTRA
AT EL. 140'-0"
2,3,4,7 and 10% DAMPING



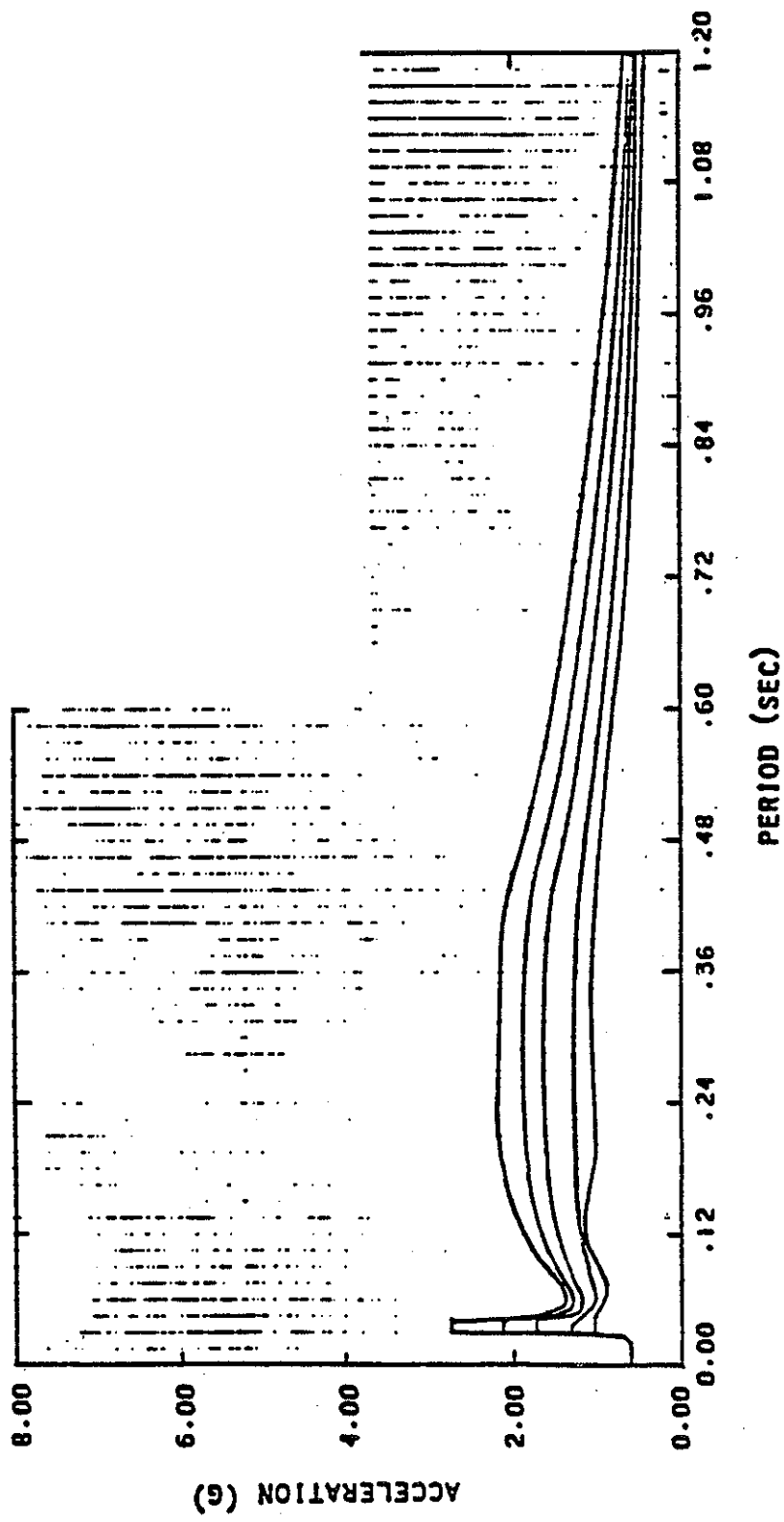
FSAR UPDATE

UNITS 1 AND 2
DIABLO CANYON SITE

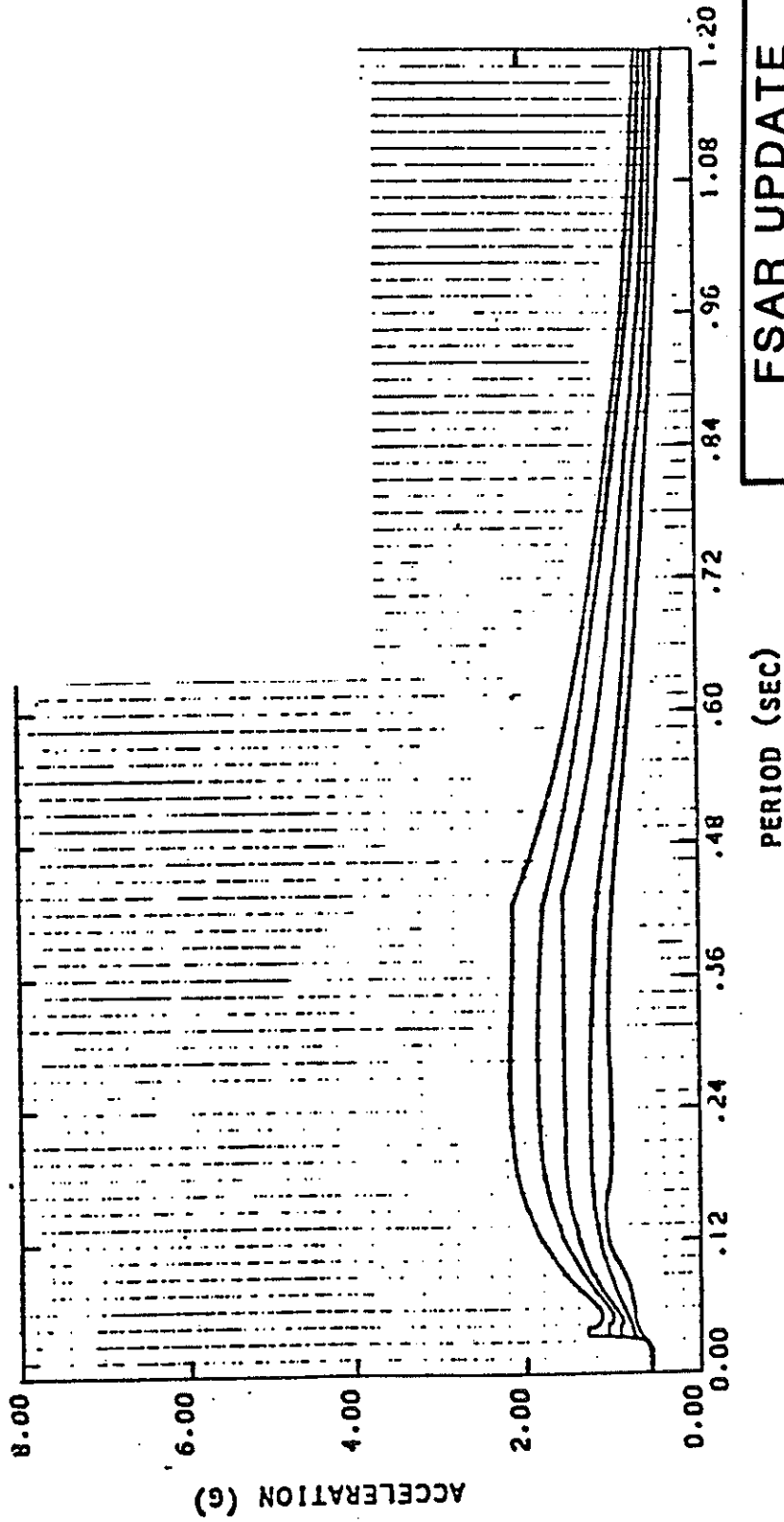
FIGURE 3.7-21D

AUXILIARY BUILDING
E-W HOSGRI
TORSIONAL FLOOR SPECTRA
AT EL 100'-0"
2,3,4,7, AND 10% DAMPING

Revision 11 November 1996



FSAR UPDATE
UNITS 1 AND 2 DIABLO CANYON SITE
FIGURE 3.7-21E AUXILIARY BUILDING HOSGRI VERTICAL SPECTRA AT EL 140'-0" 2,3,4,7, AND 10% DAMPING



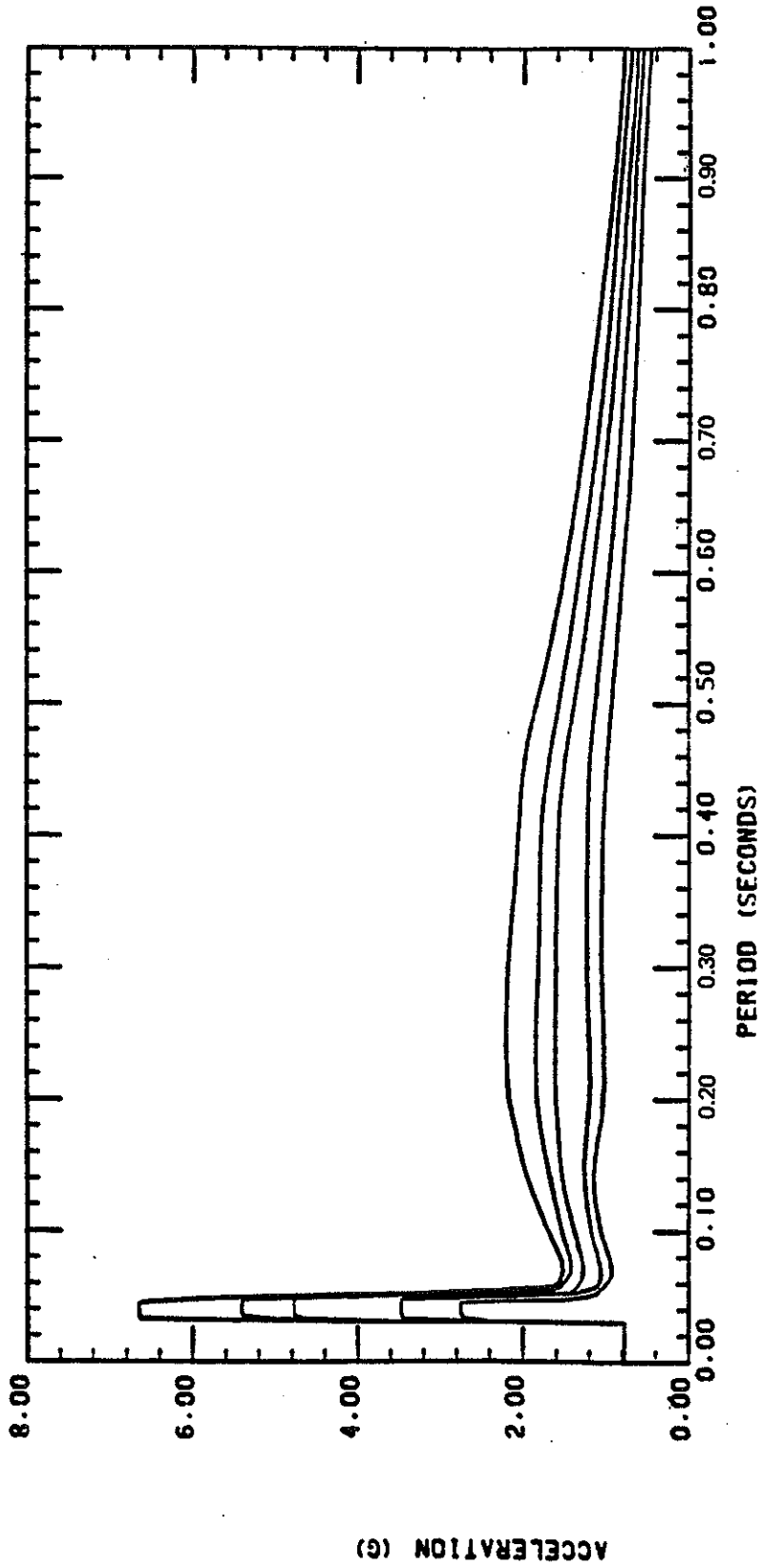
FSAR UPDATE

UNITS 1 AND 2

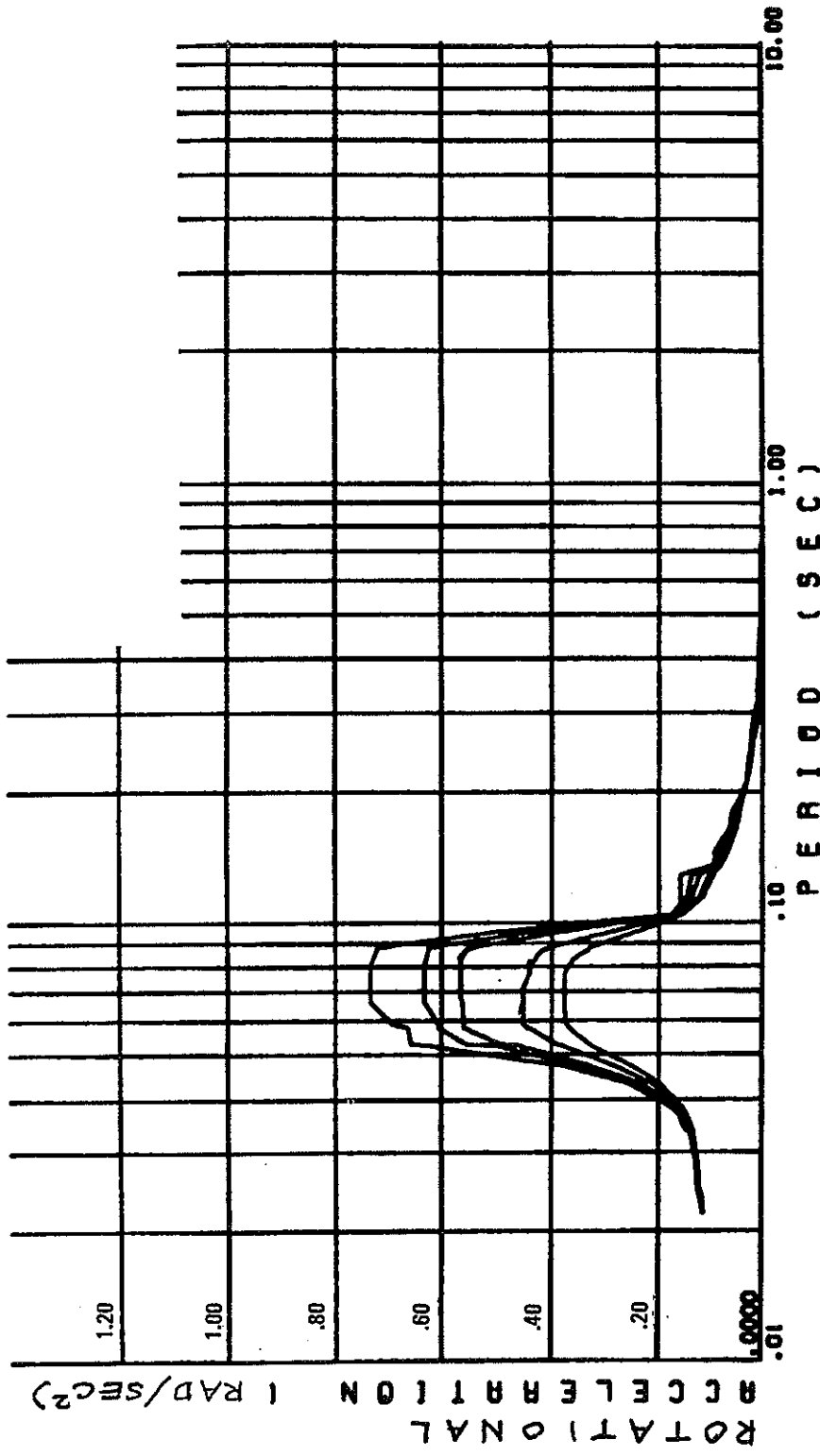
DIABLO CANYON SITE

FIGURE 3.7-21F

AUXILIARY BUILDING
 HOSGRI VERTICAL SPECTRA
 AT EL 100'-0"
 2,3,4,7, AND 10% DAMPING



FSAR UPDATE
UNITS 1 AND 2
DIABLO CANYON SITE
 FIGURE 3.7-21G
 AUXILIARY BUILDING
 HOSGRI VERTICAL SPECTRA
 EL 100'-0" SLAB 2 NODE 51
 2,3,4,7, AND 10%

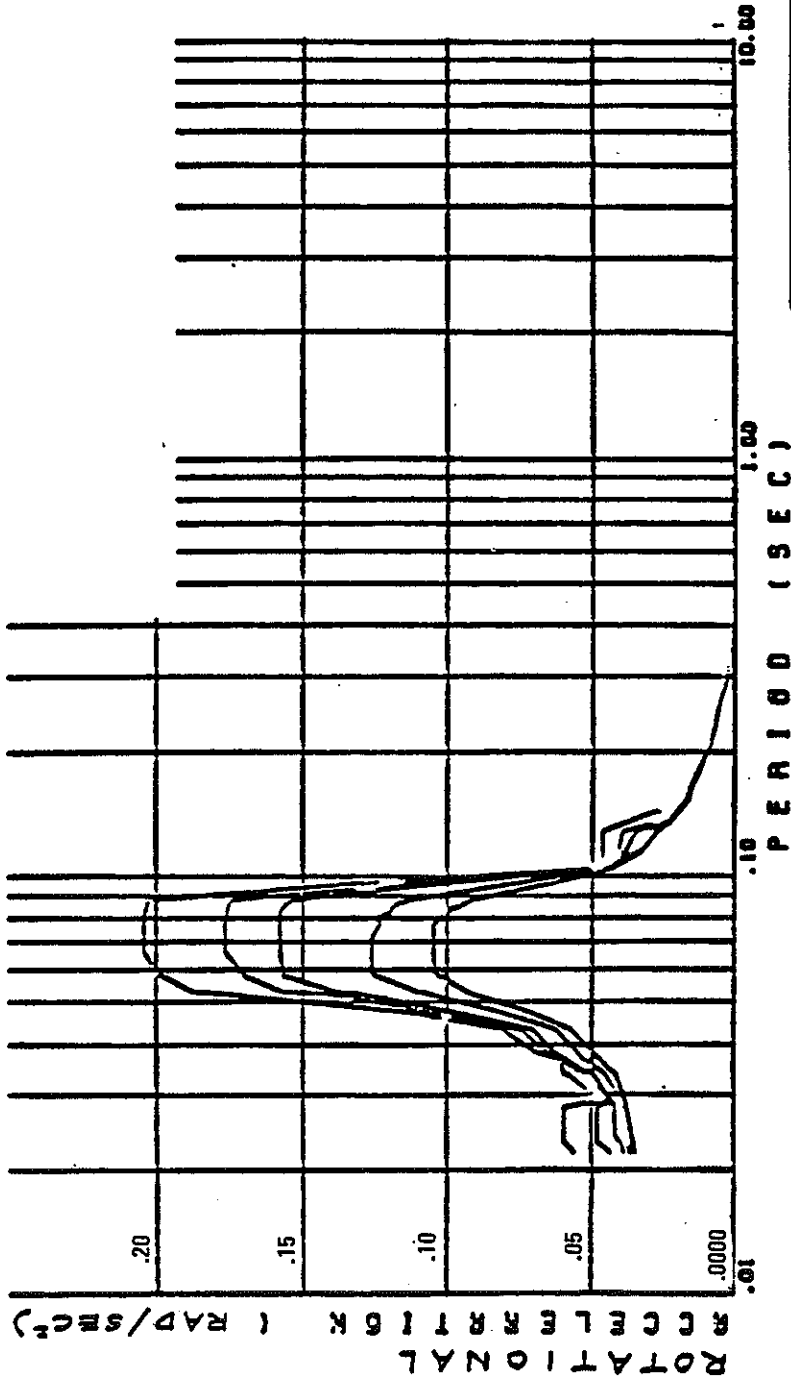


FSAR UPDATE

UNITS 1 AND 2
DIABLO CANYON SITE

FIGURE 3.7-21H

AUXILIARY BUILDING
 N-S HOSGRI
 TORSIONAL FLOOR SPECTRA
 AT EL 140'-0"
 2,3,4,7, AND 10% DAMPING

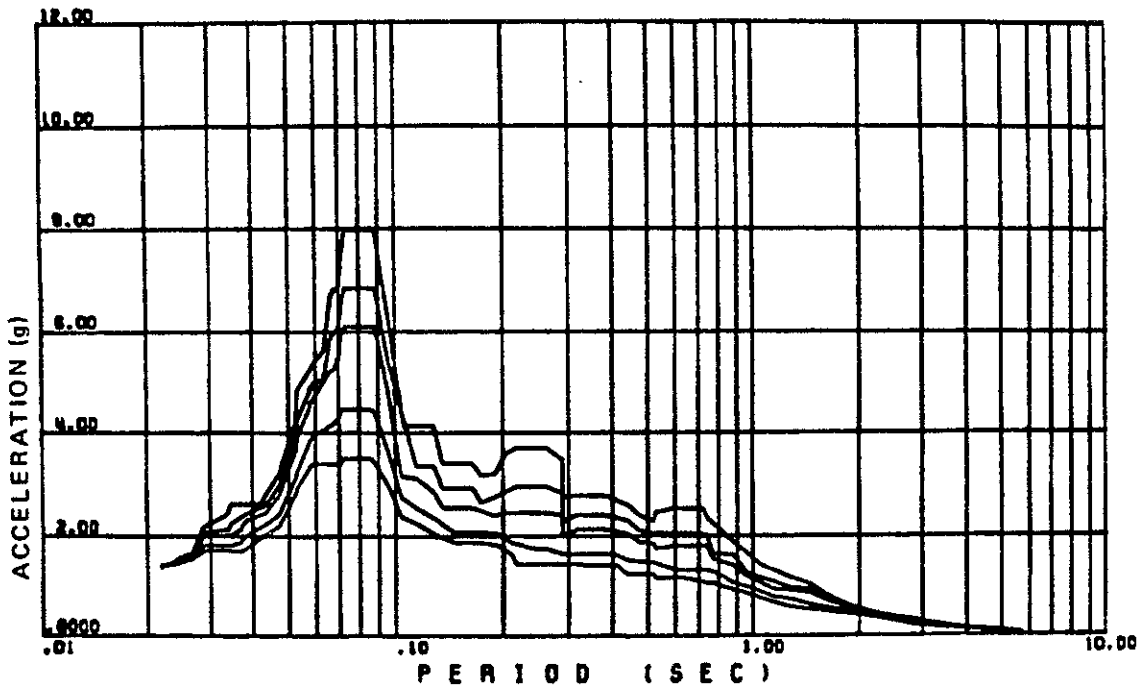


FSAR UPDATE

UNITS 1 AND 2
DIABLO CANYON SITE

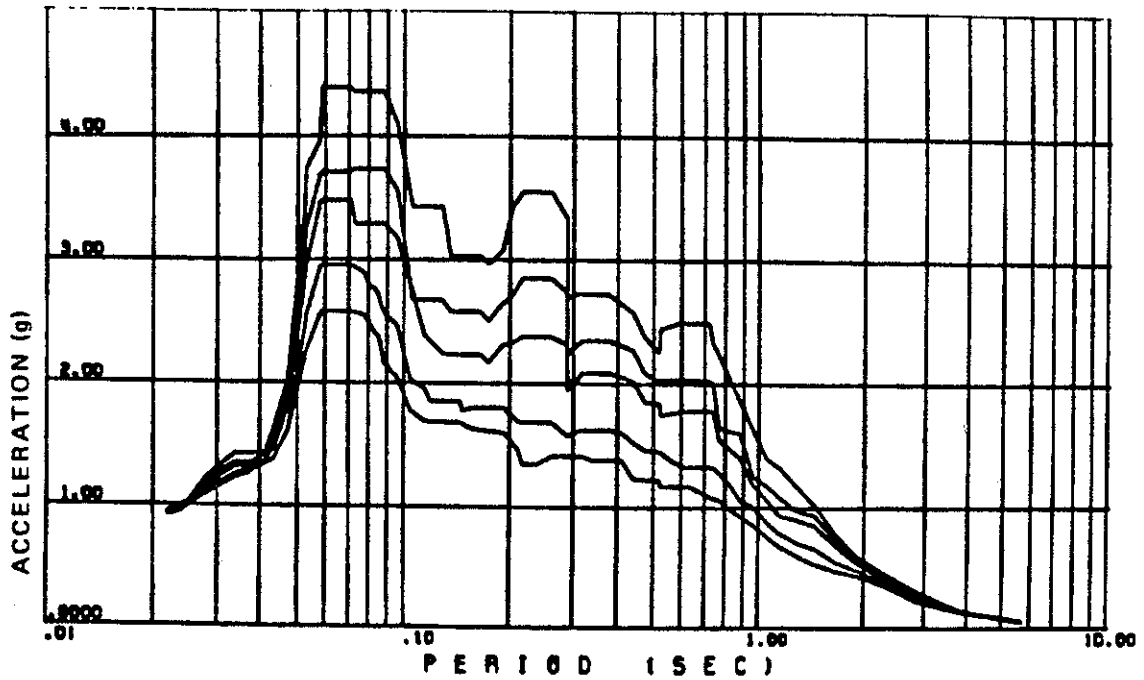
FIGURE 3.7-211

AUXILIARY BUILDING
N-S HOSGRI
TORSIONAL FLOOR SPECTRA
AT EL 100'-0"
2,3,4,7 AND 10% DAMPING



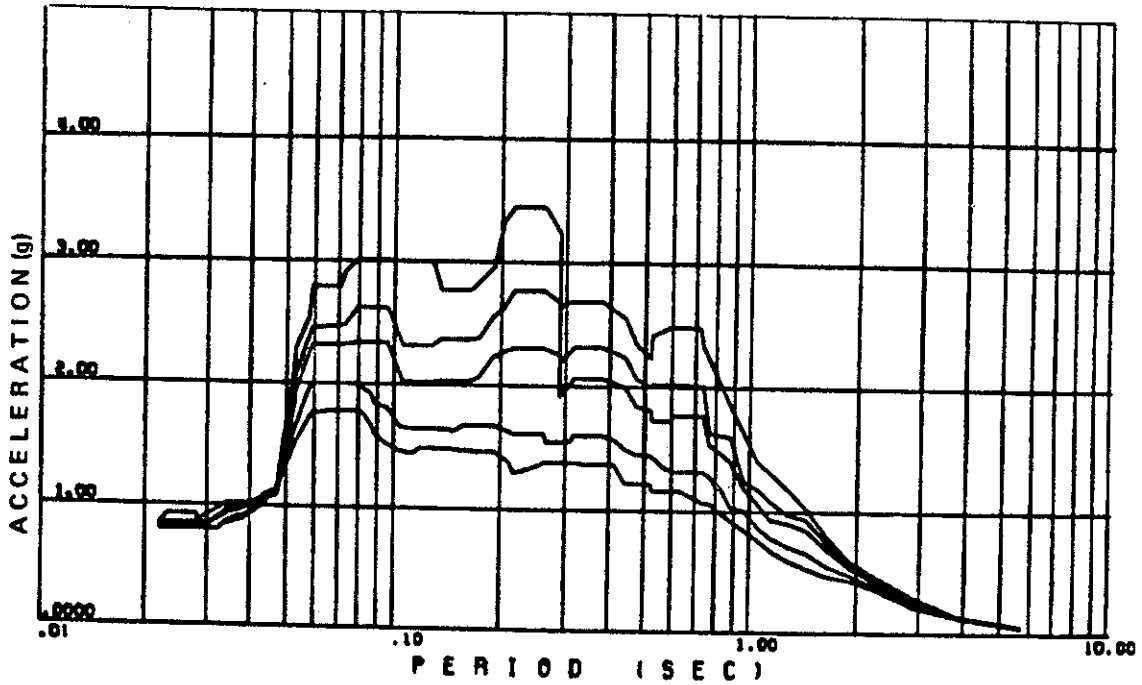
FSAR UPDATE
UNITS 1 AND 2 DIABLO CANYON SITE
FIGURE 3.7-22 AUXILIARY BUILDING N-S HOSGRI HORIZONTAL FLOOR SPECTRA AT EL 163'-0" NODE 1 2, 3, 4, 7, AND 10% DAMPING

Revision 11 November 1996



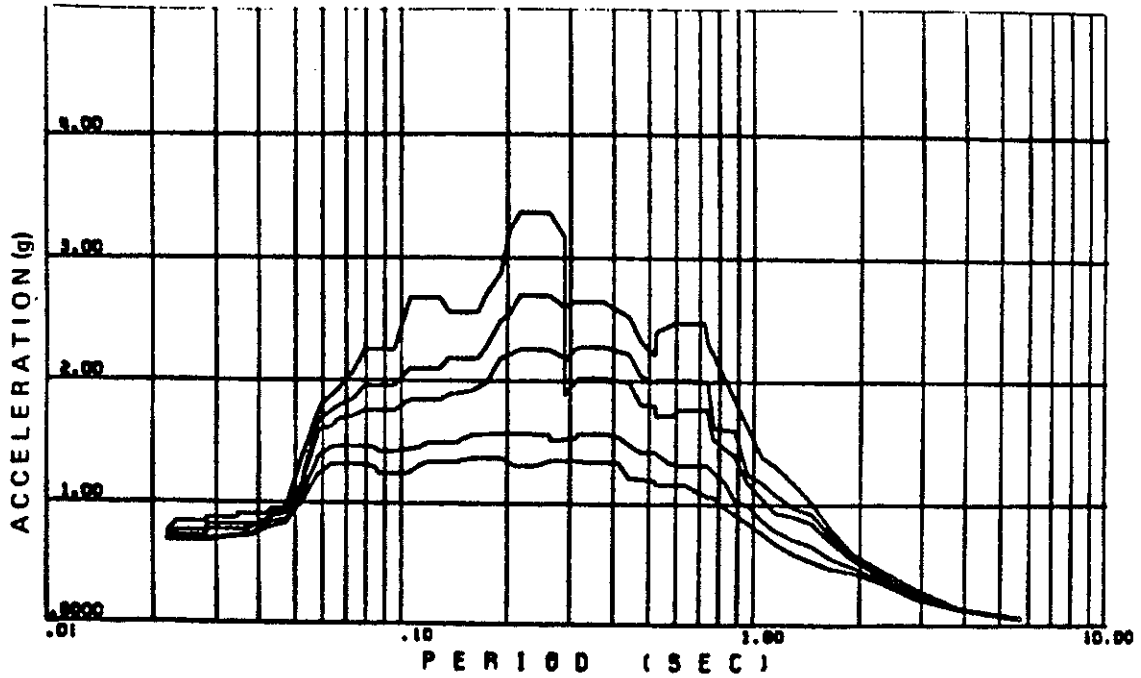
FSAR UPDATE
UNITS 1 AND 2 DIABLO CANYON SITE
FIGURE 3.7-23 AUXILIARY BUILDING N-S HOSGRI HORIZONTAL FLOOR SPECTRA AT EL 140'-0" NODE 2 2, 3, 4, 7, AND 10% DAMPING

Revision 11 November 1996



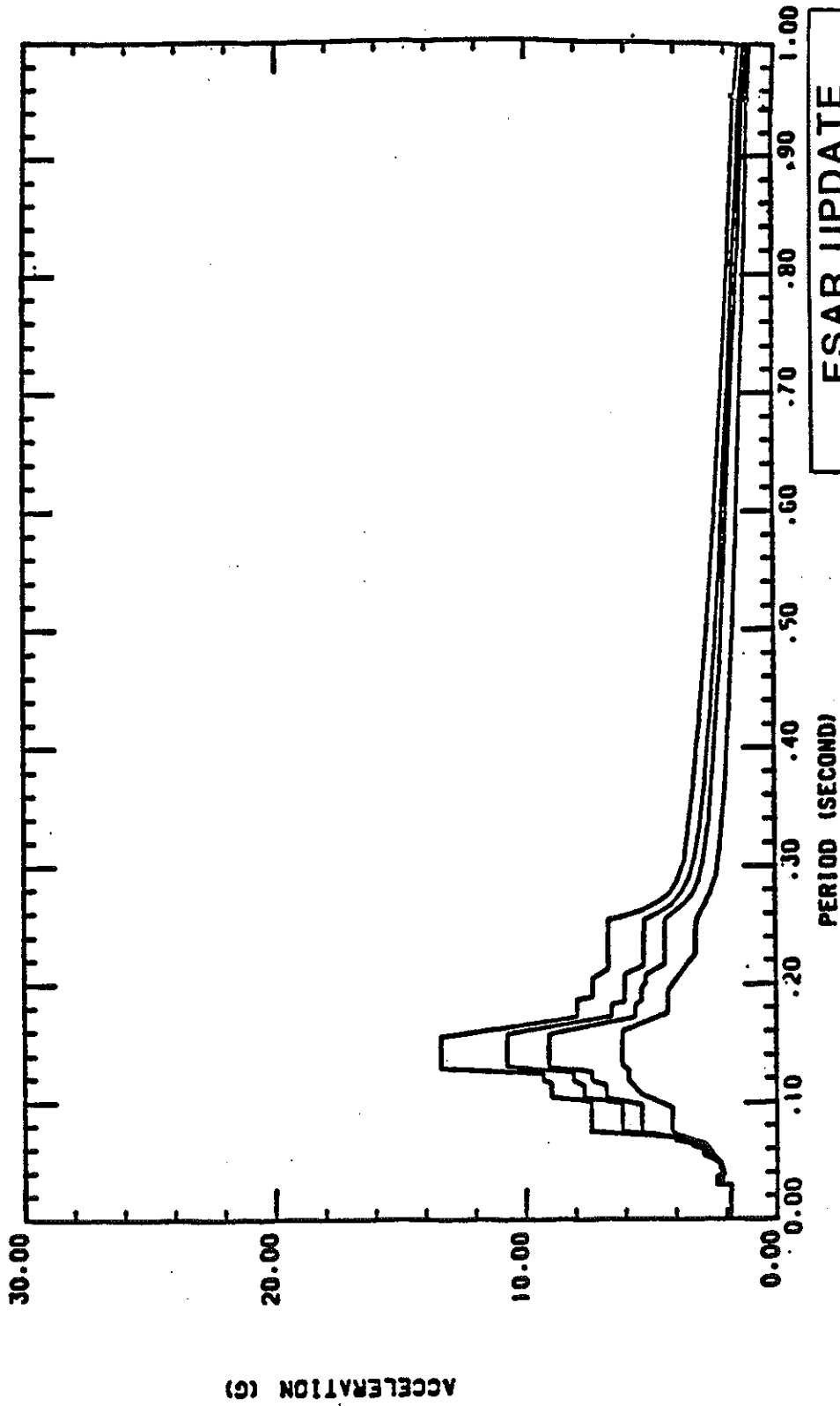
FSAR UPDATE
UNITS 1 AND 2 DIABLO CANYON SITE
FIGURE 3.7-24 AUXILIARY BUILDING N-S HOSGR1 HORIZONTAL FLOOR SPECTRA AT EL 115'-0" NODE 3 2, 3, 4, 7, AND 10% DAMPING

Revision 11 November 1996



FSAR UPDATE
UNITS 1 AND 2 DIABLO CANYON SITE
FIGURE 3.7-25 AUXILIARY BUILDING N-S HOSGRI HORIZONTAL FLOOR SPECTRA AT EL 100'-0" NODE 4 2, 3, 4, 7, AND 10% DAMPING

Revision 11 November 1996

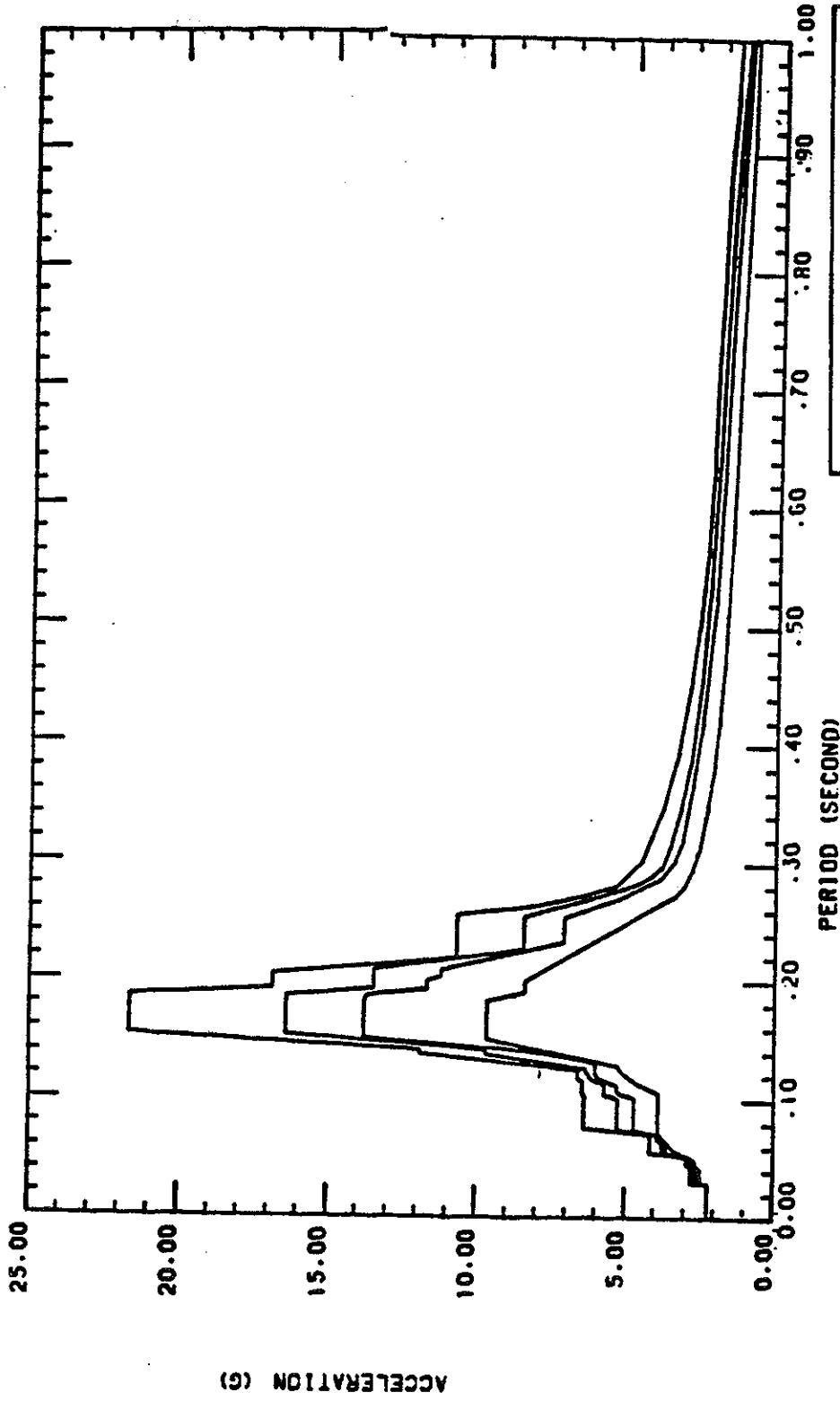


FSAR UPDATE

UNITS 1 AND 2

DIABLO CANYON SITE

FIGURE 3.7 - 25 A
 TURBINE BUILDING
 EL. 119'
 4 KV SWITCHGEAR AREA
 COLUMN LINES 1-4, D-G
 HOSGRI E-W SPECTRA
 2,3,4,7% DAMPING

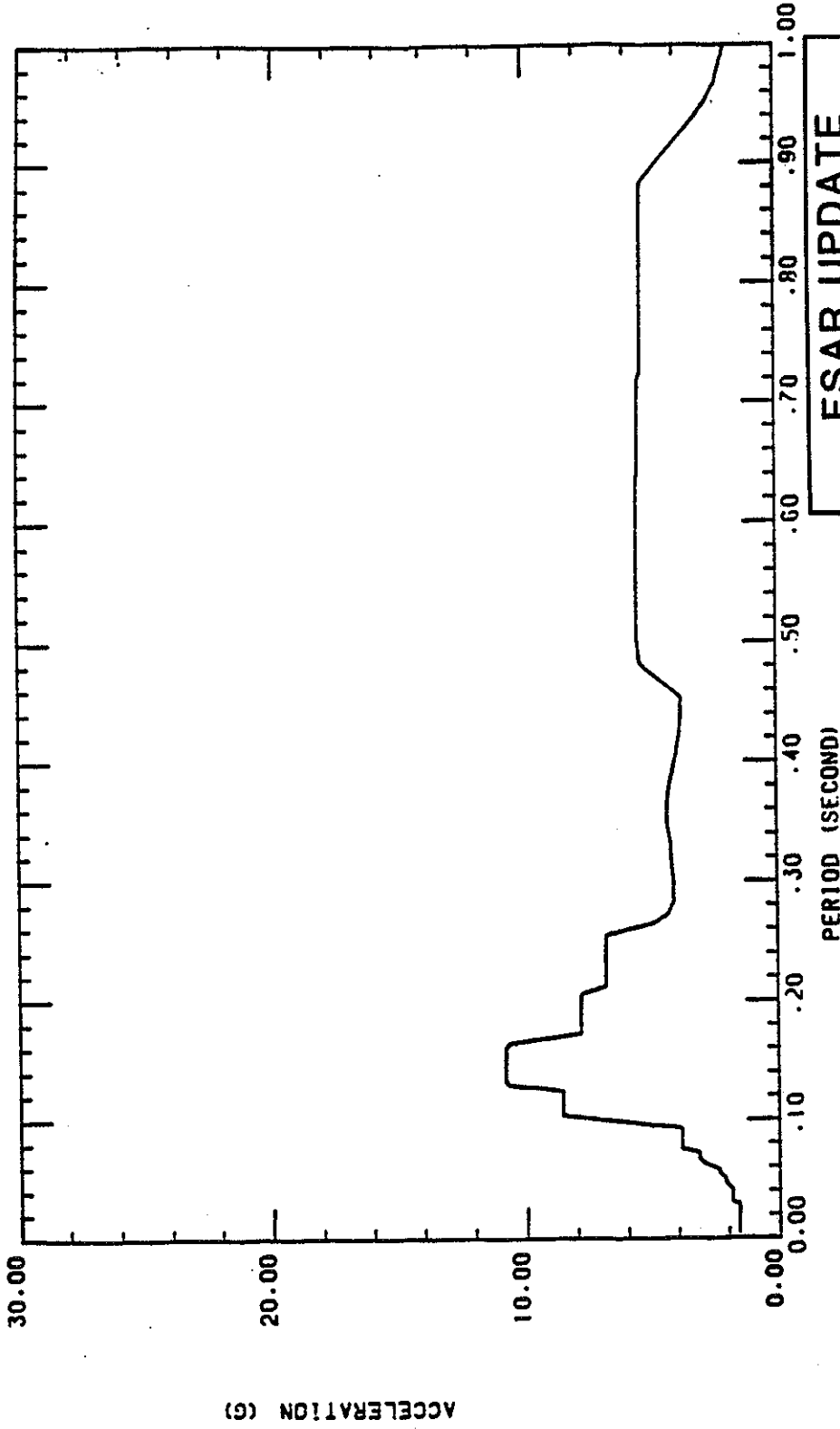


FSAR UPDATE

UNIT 1

DIABLO CANYON SITE

FIGURE 3.7 - 25B
 TURBINE BUILDING EL. 140'
 COLUMN LINES 5-15
 HOSGRI E-W SPECTRA
 2, 3, 4, 7% DAMPING

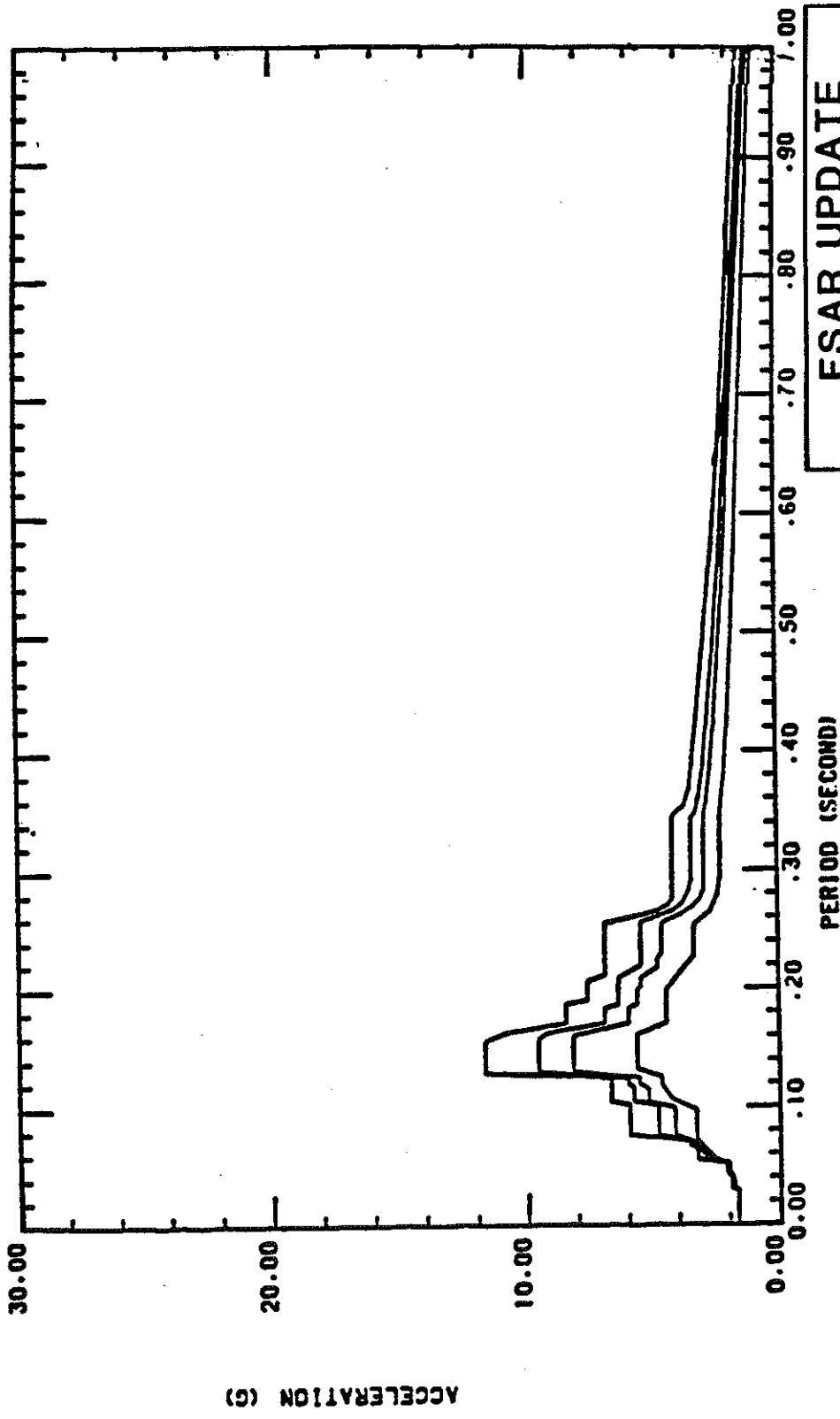


FSAR UPDATE

UNIT 1

DIABLO CANYON SITE

FIGURE 3.7 - 25 C
 TURBINE BUILDING
 ROOF LEVEL
 COLUMN LINES 1 TO 1.9, A-D
 HOSGRI E - W SPECTRA
 3% DAMPING

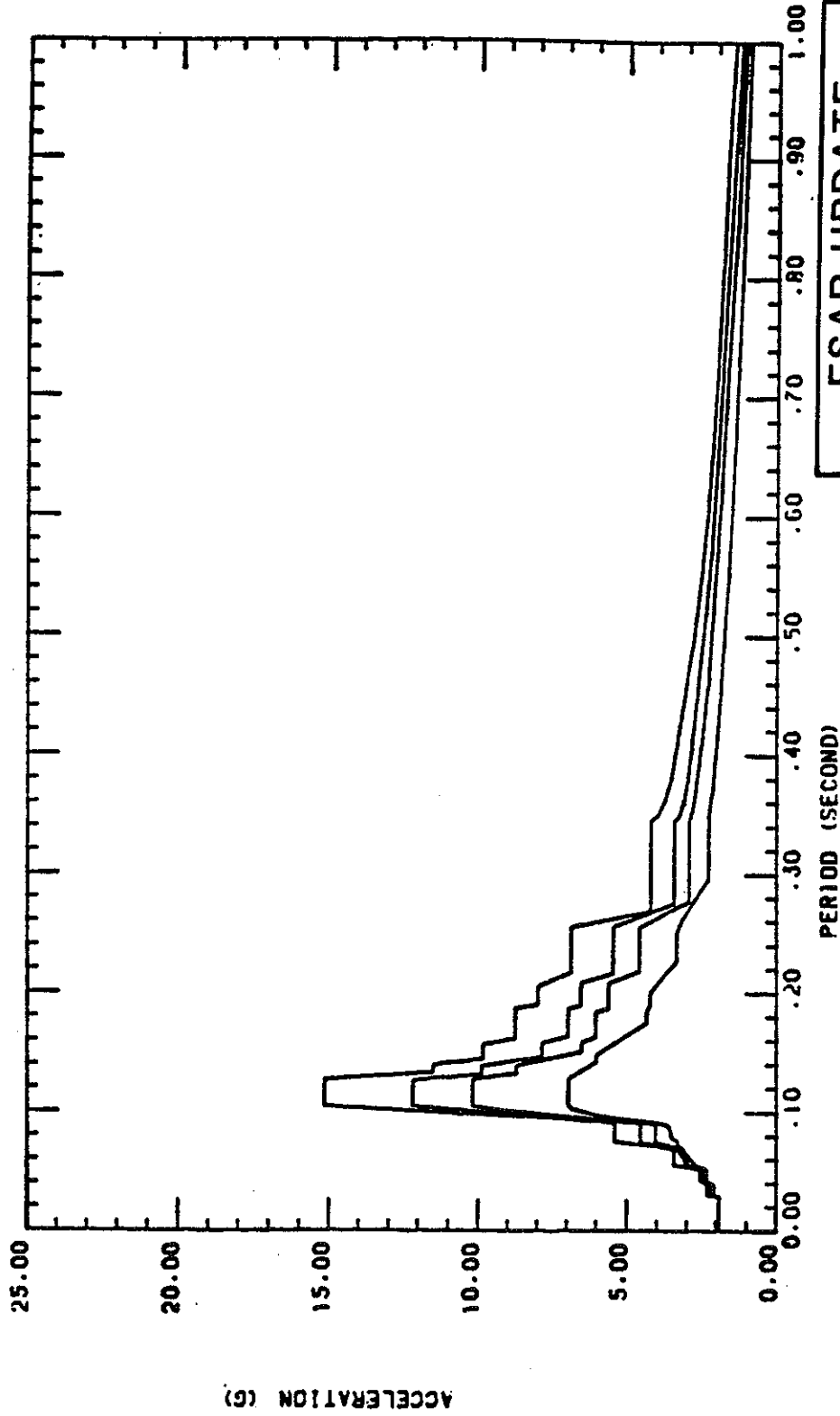


FSAR UPDATE

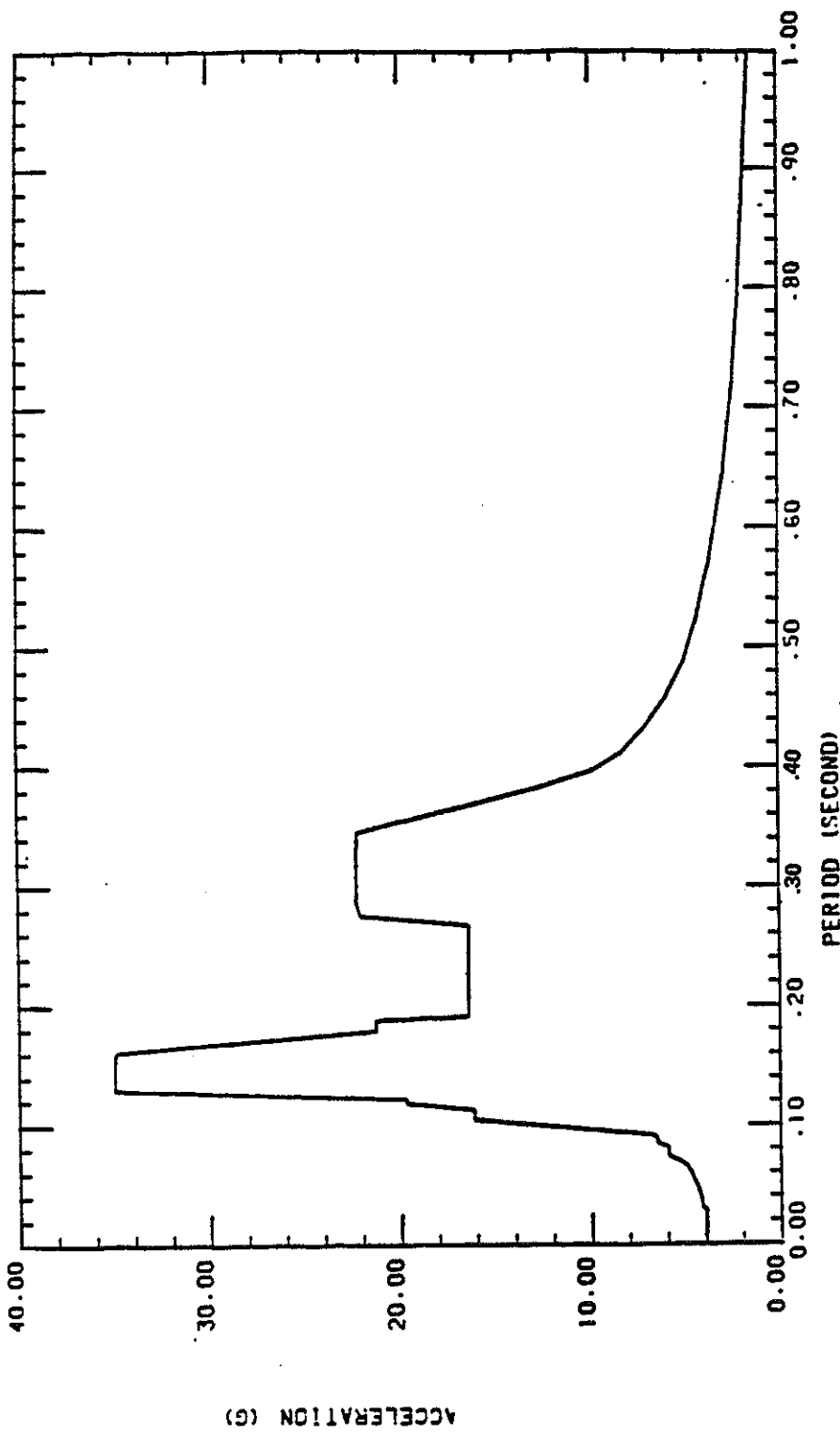
UNITS 1 AND 2

DIABLO CANYON SITE

FIGURE 3.7 - 25 D
 TURBINE BUILDING
 EL. 119'
 4 KV SWITCHGEAR AREA
 COLUMN LINES 1-4, D-G
 HOSGRI N-S SPECTRA
 2, 3, 4, 7% DAMPING



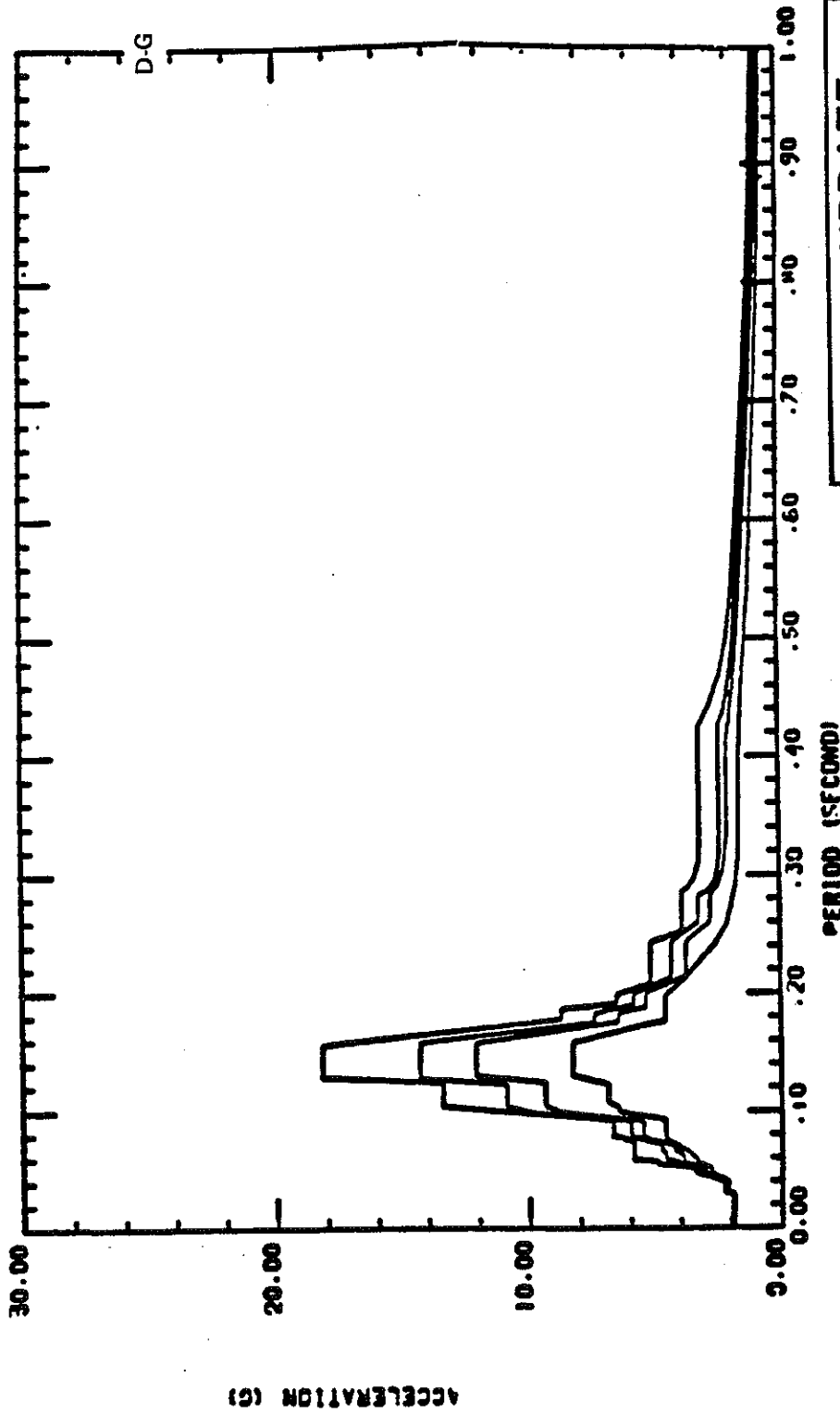
FSAR UPDATE
UNIT 1
DIABLO CANYON SITE
FIGURE 3.7 - 25 E
TURBINE BUILDING
EL. 140'
COLUMN LINES 1-19
HOSGRINS SPECTRA
2, 3, 4, 7% DAMPING



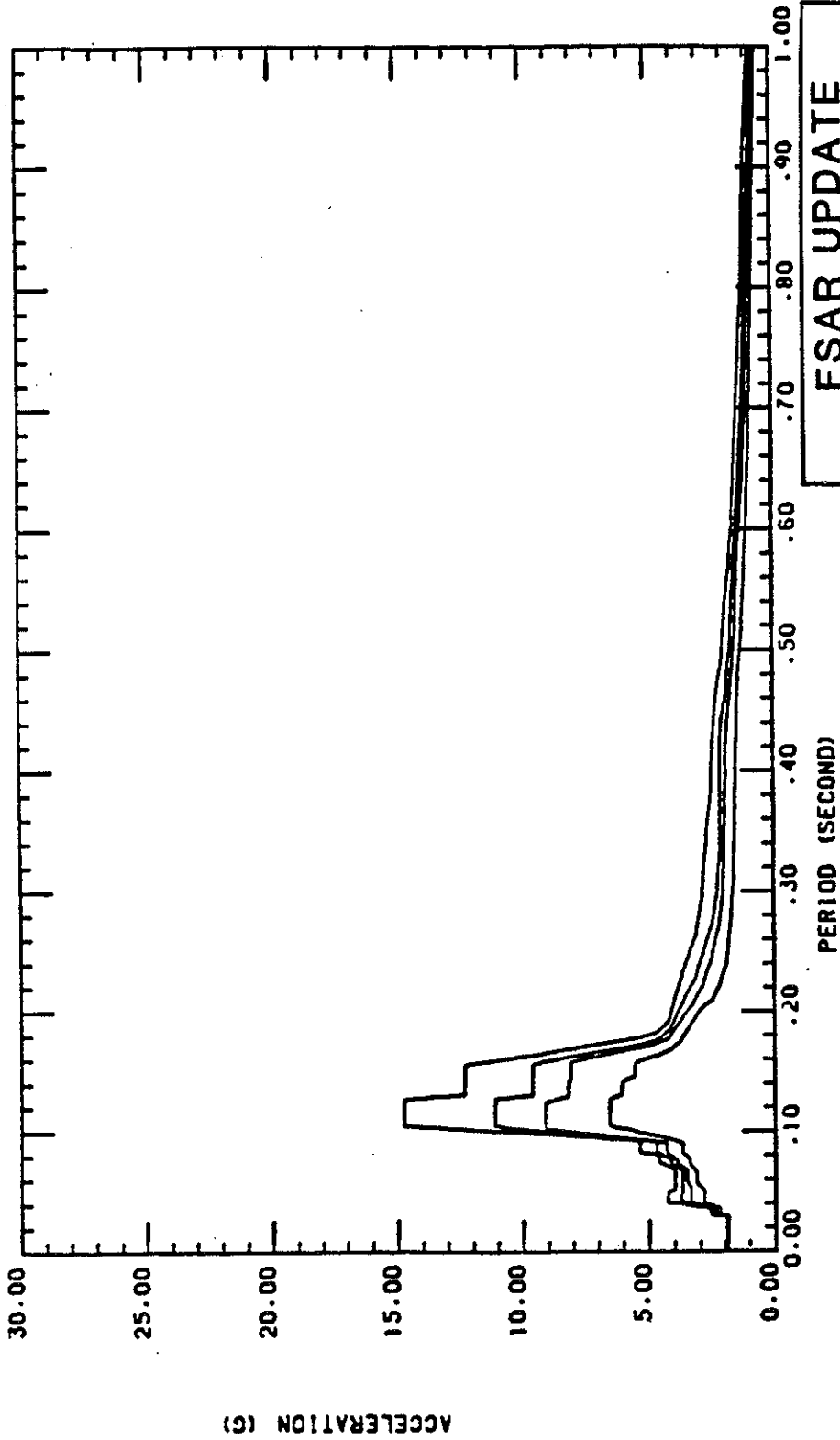
COLUMN LINES 1 & D, EL. 193'
 COLUMN LINES 1 & A', EL. 193'
 COLUMN LINES 1' & A, EL. 193'
 COLUMN LINES 1' & D, EL. 210.69'

*SPECTRUM ENVELOPING THE SPECTRA AT FOUR LOCATIONS:

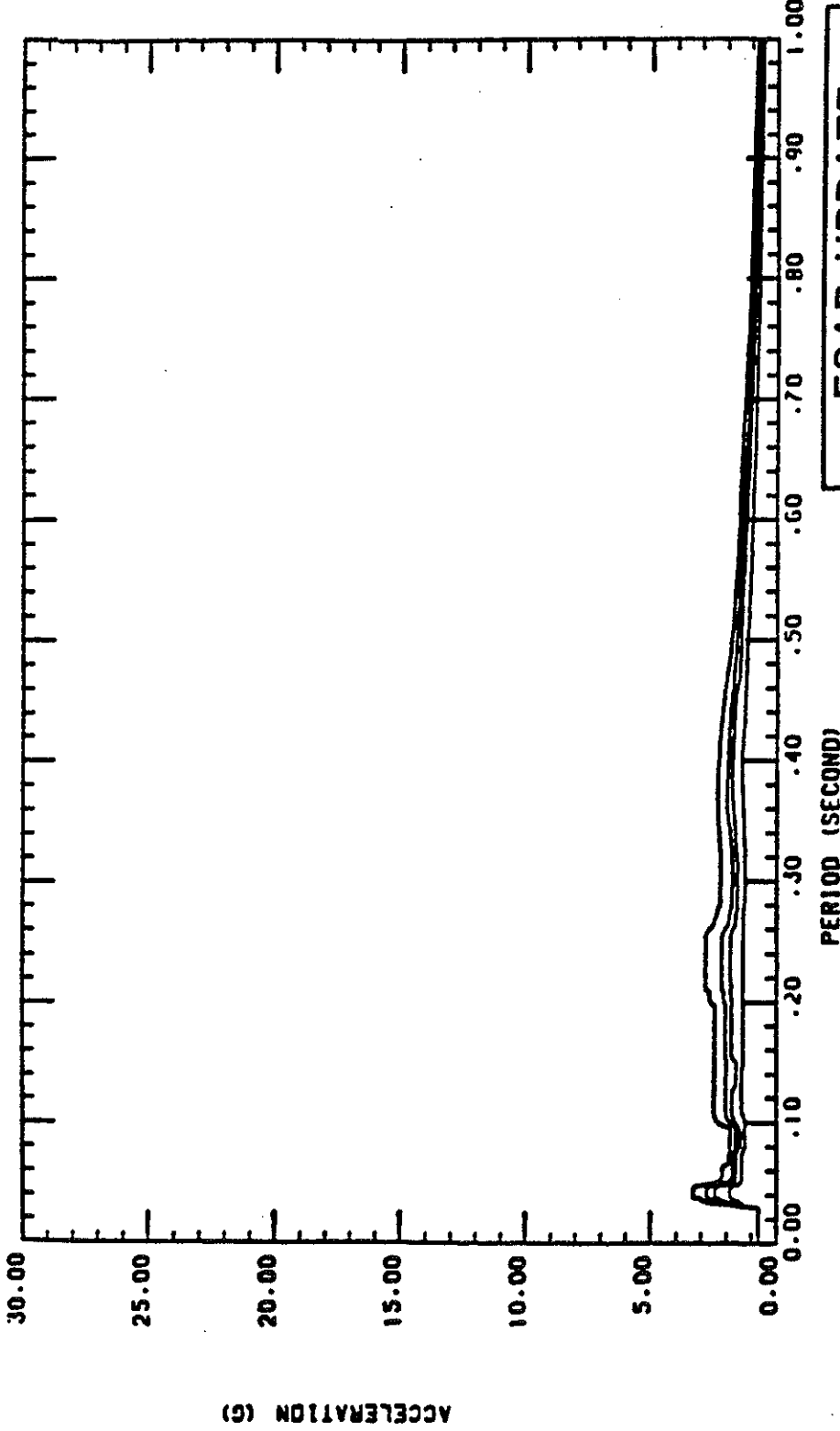
FSAR UPDATE
UNITS 1 AND 2 DIABLO CANYON SITE
FIGURE 3.7 - 25 F TURBINE BUILDING ROOF LEVEL COLUMN LINES 1 to 1.9, A-D HOSGRI N-S SPECTRA 3% DAMPING



FSAR UPDATE
UNITS 1 AND 2 DIABLO CANYON SITE
FIGURE 3.7 - 25 G TURBINE BUILDING EL. 119' COLUMN LINES 1-4 & 32-35 D G 4 KV SWITCHGEAR AREA HOSGRI VERTICAL SPECTRA 2, 3, 4, 7% DAMPING



FSAR UPDATE
UNITS 1 AND 2 DIABLO CANYON SITE
FIGURE 3.7 - 25-H TURBINE BUILDING EL. 140' COLUMN LINES 5-15, 21-31 HOSGRI VERTICAL SPECTRA 2, 3, 4, 7% DAMPING



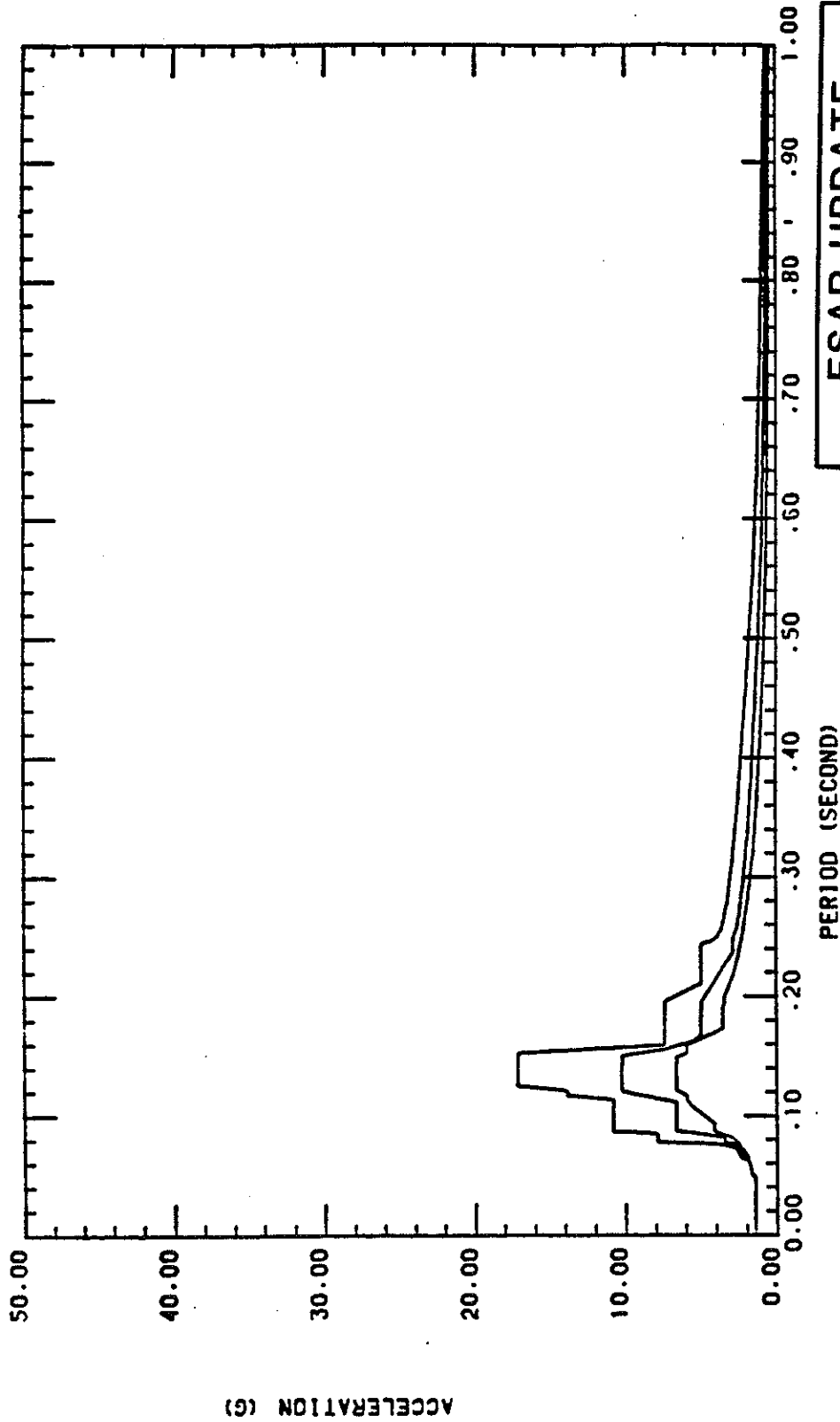
FSAR UPDATE

UNITS 1 AND 2

DIABLO CANYON SITE

FIGURE 3.7 - 25I
 TURBINE BUILDING
 EL. 193'

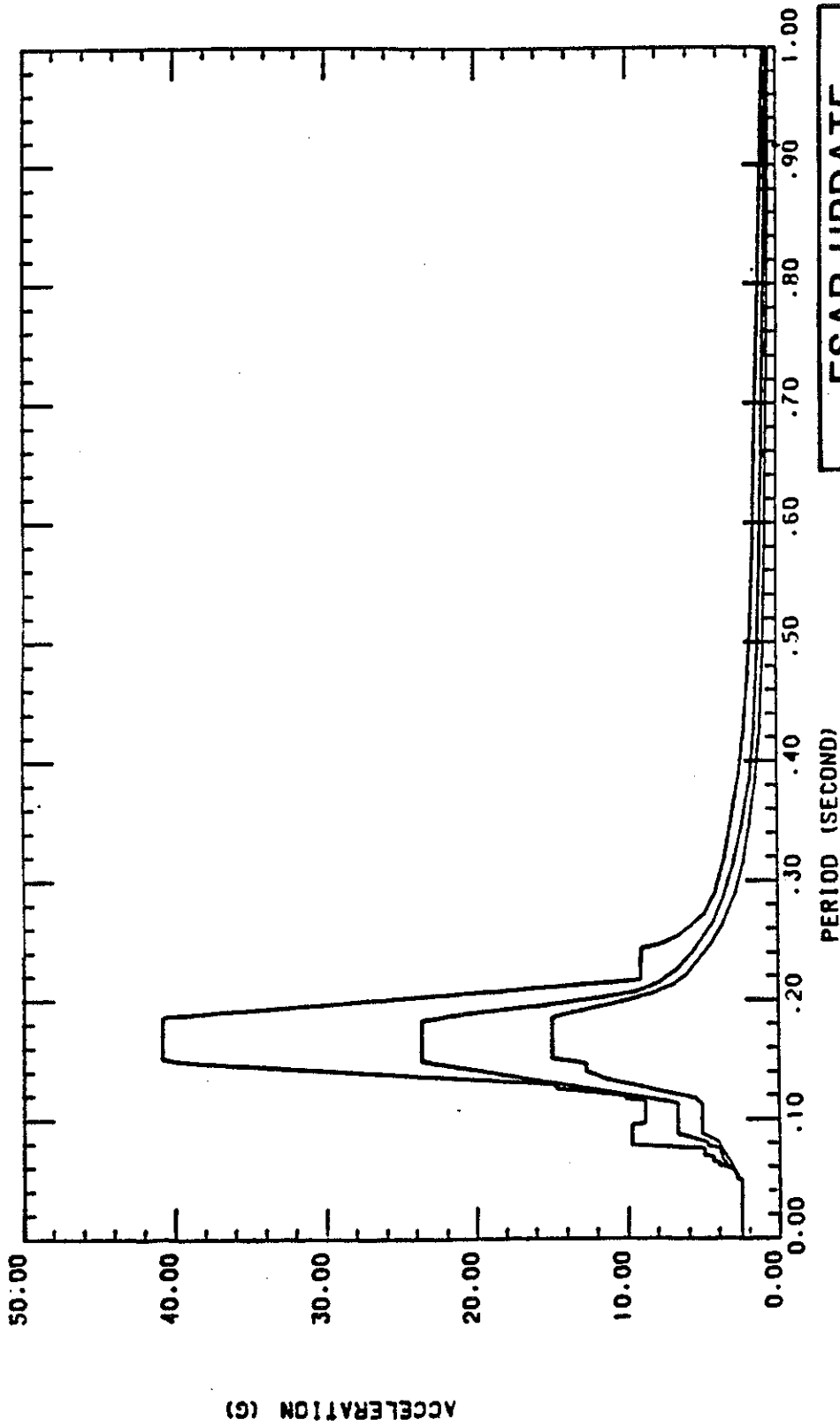
BUILT UP COLUMNS ON LINE
 A&G FROM 5.7 TO 15 & 21 TO 30.3
 HOSGRI VERTICAL SPECTRA
 2, 3, 4, 7% DAMPING



FSAR UPDATE

**UNITS 1 AND 2
DIABLO CANYON SITE**

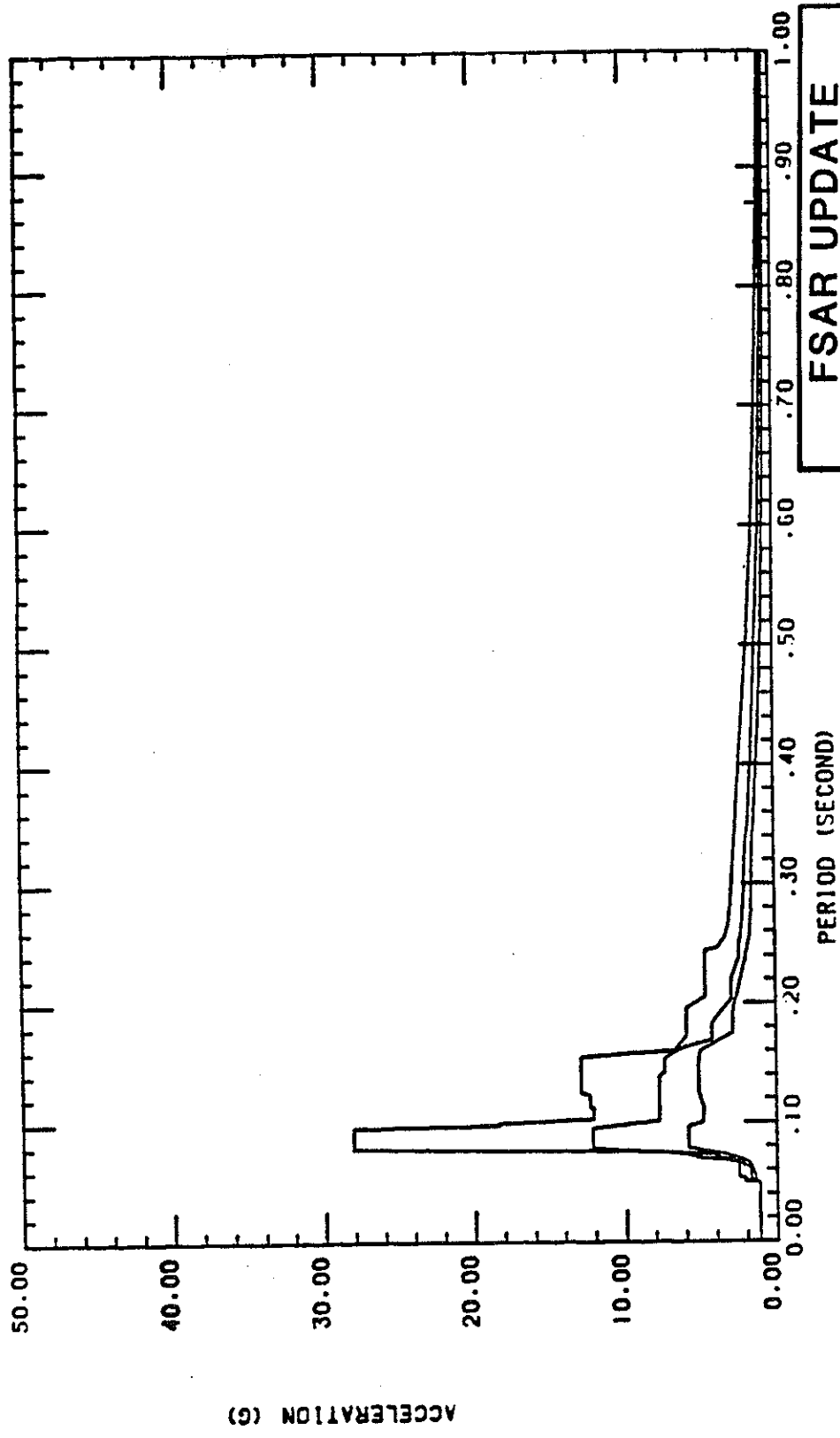
FIGURE 3.7 - 25 J
TURBINE BUILDING
ELEV. 104'
COLUMN LINES 5 TO 15
DDE E-W SPECTRA
1/2, 2, 5% DAMPING



FSAR UPDATE

**UNITS 1 AND 2
DIABLO CANYON SITE**

FIGURE 3.7 - 25 K
TURBINE BUILDING
ELEV. 140'
COLUMN LINES 5-15
DDE E-W SPECTRA
1/2,2.5% DAMPING

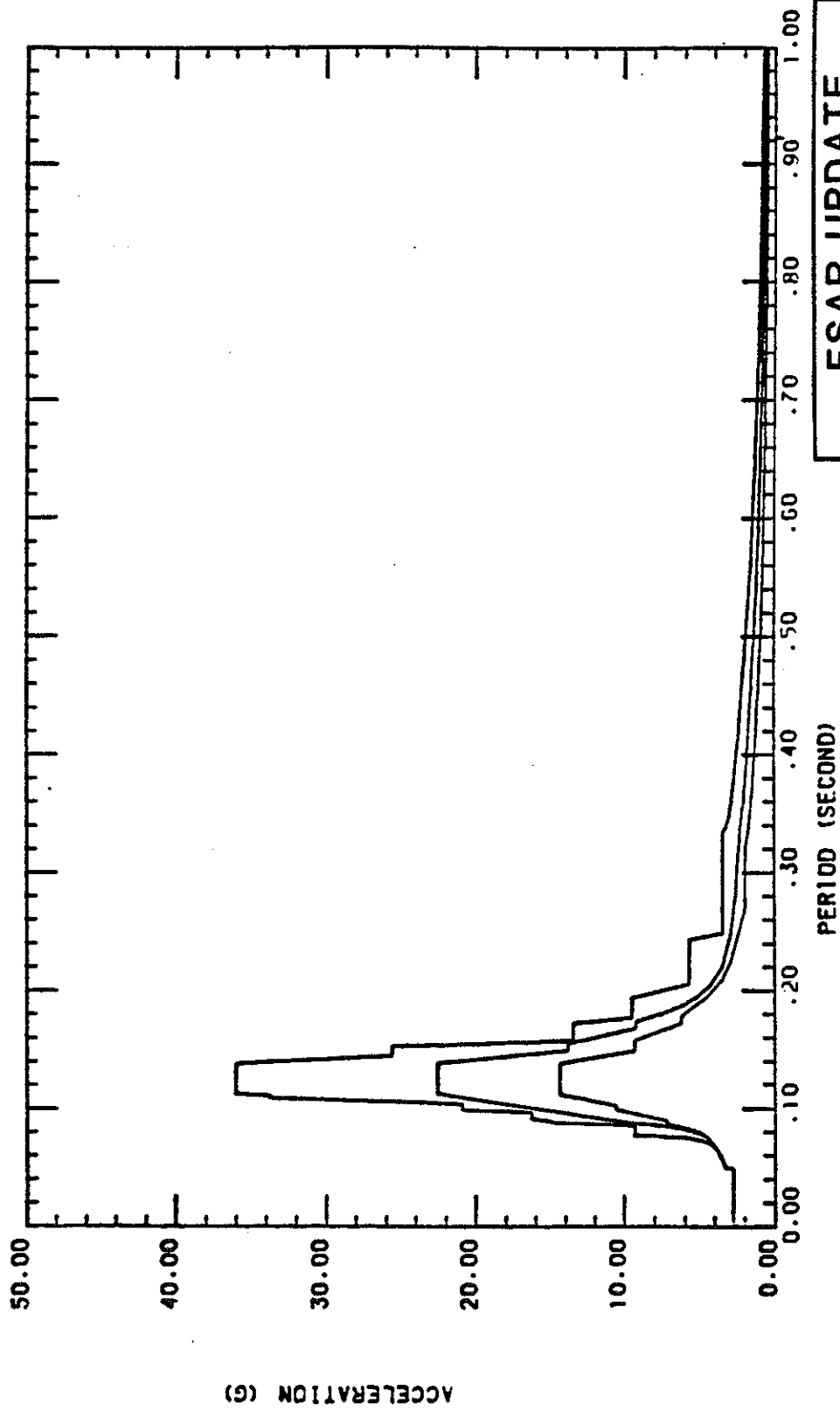


FSAR UPDATE

UNITS 1 AND 2

DIABLO CANYON SITE

FIGURE 3.7 - 25 L
 TURBINE BUILDING
 ELEV 104' & 107'
 COLUMN LINES 1-19
 DDE N-S SPECTRA
 1/2, 2, 5% DAMPING

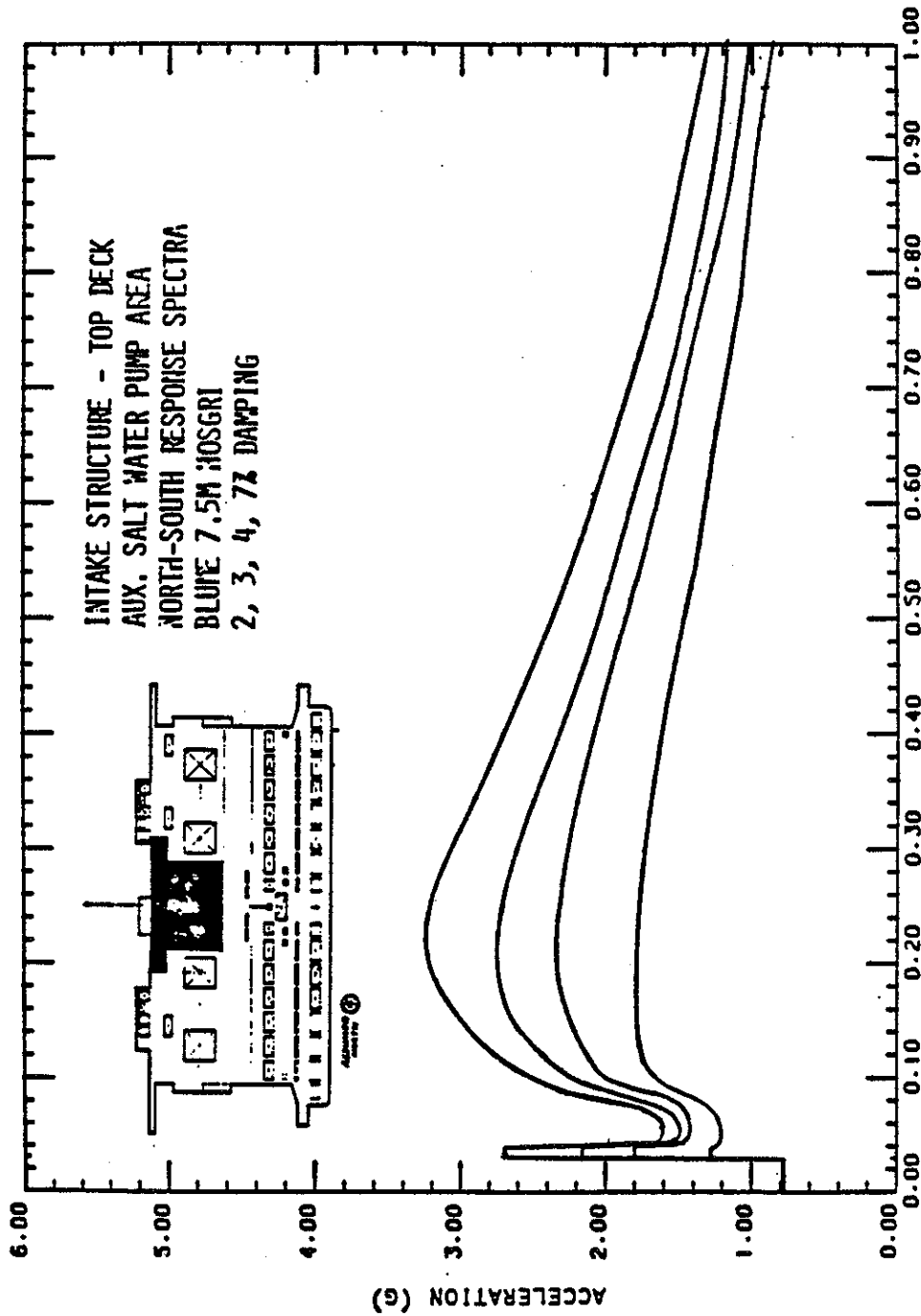


FSAR UPDATE

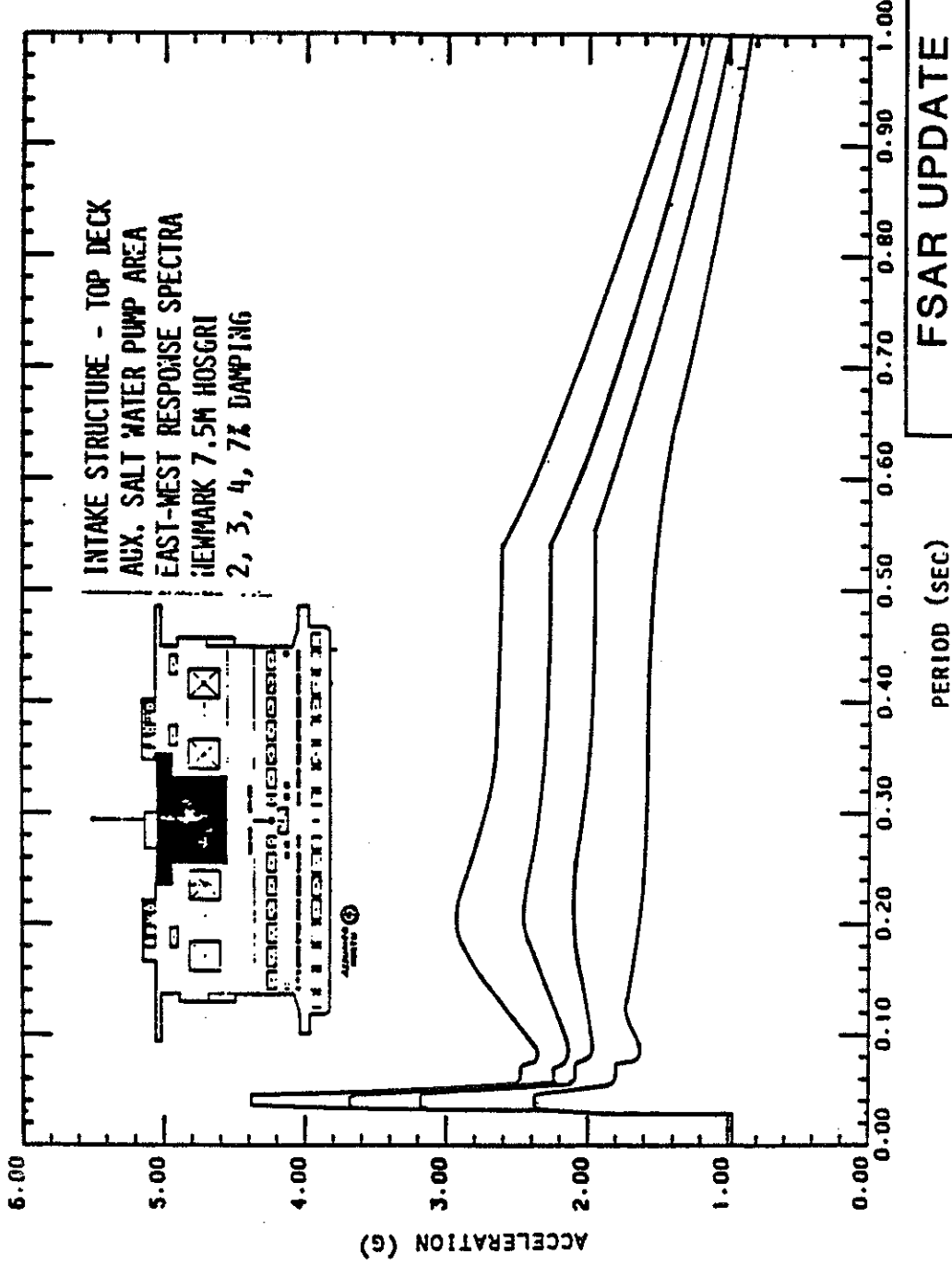
UNITS 1 AND 2

DIABLO CANYON SITE

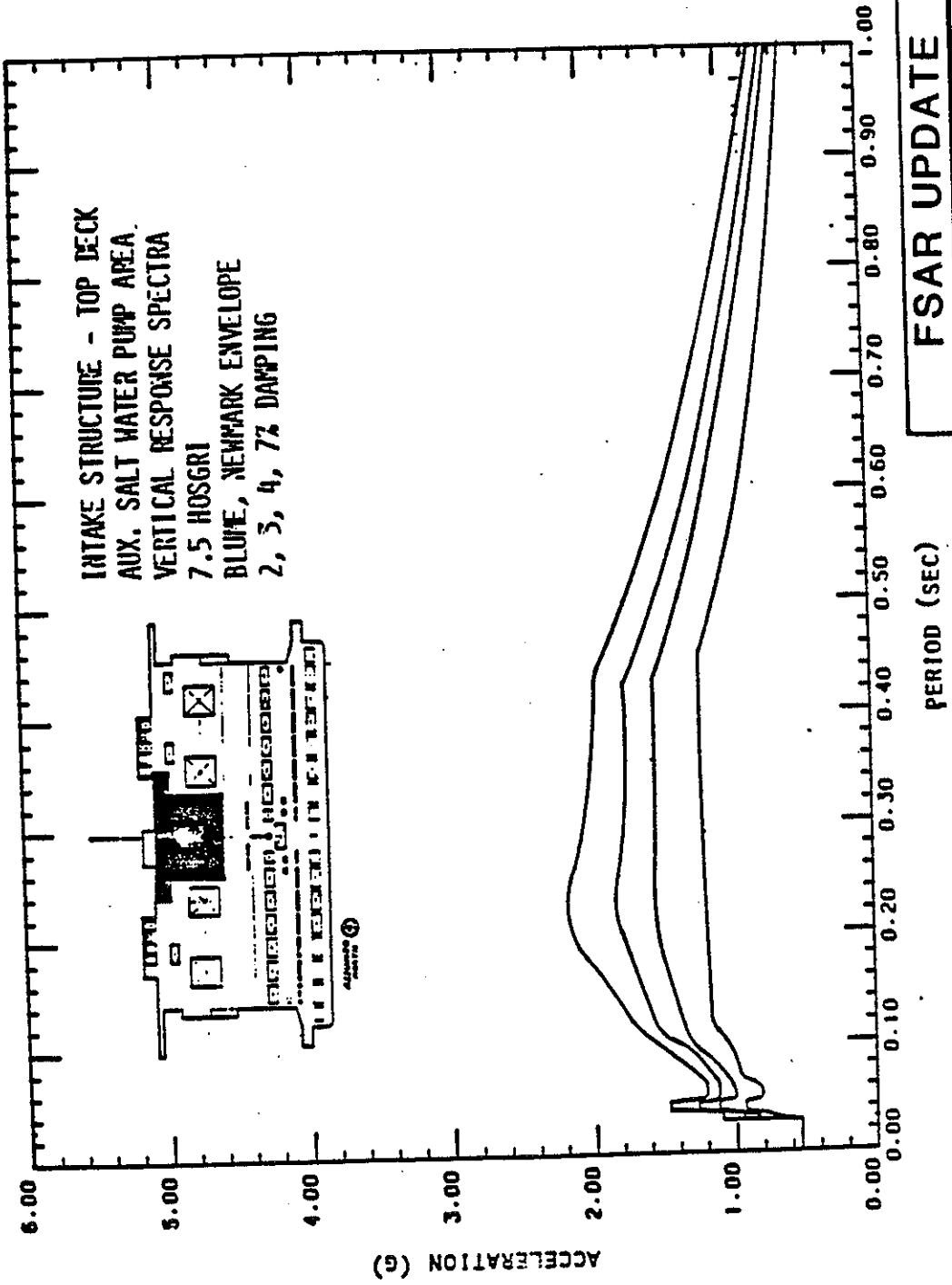
FIGURE 3.7 - 25 M
TURBINE BUILDING
ELEV 140'
COLUMN LINES 1-19
DDE N-S SPECTRA
1/2, 2, 5% DAMPING



FSAR UPDATE
UNITS 1 AND 2
DIABLO CANYON SITE
 FIGURE 3.7 - 25 N
 INTAKE STRUCTURE
 RESPONSE SPECTRA
 BLUME 7.5 M HOSGRI



FSAR UPDATE
UNITS 1 AND 2
DIABLO CANYON SITE
 FIGURE 3.7 - 25.0
 INTAKE STRUCTURE
 RESPONSE SPECTRA
 NEWMARK 7.5 M HOSGRI



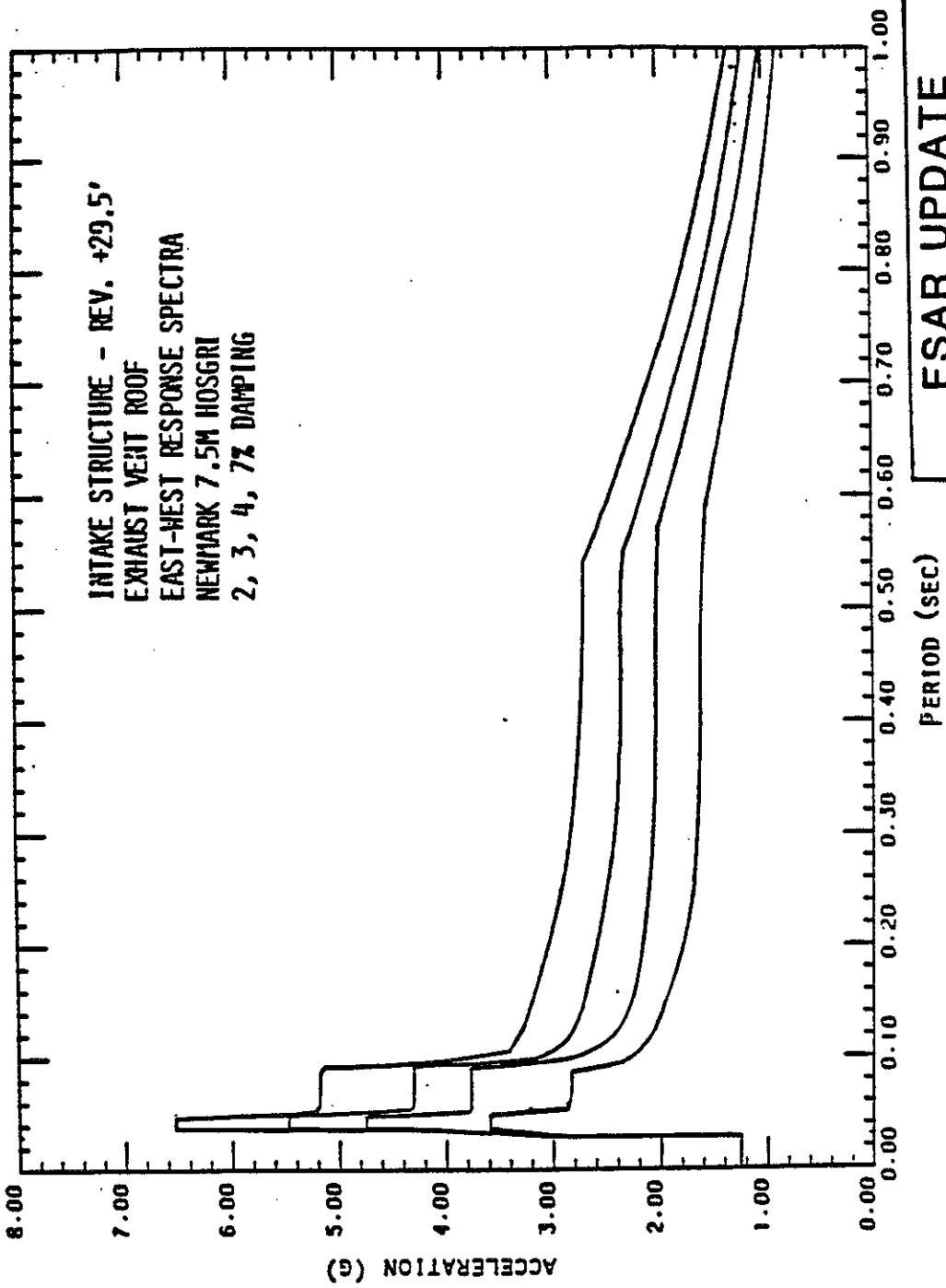
FSAR UPDATE

UNITS 1 AND 2

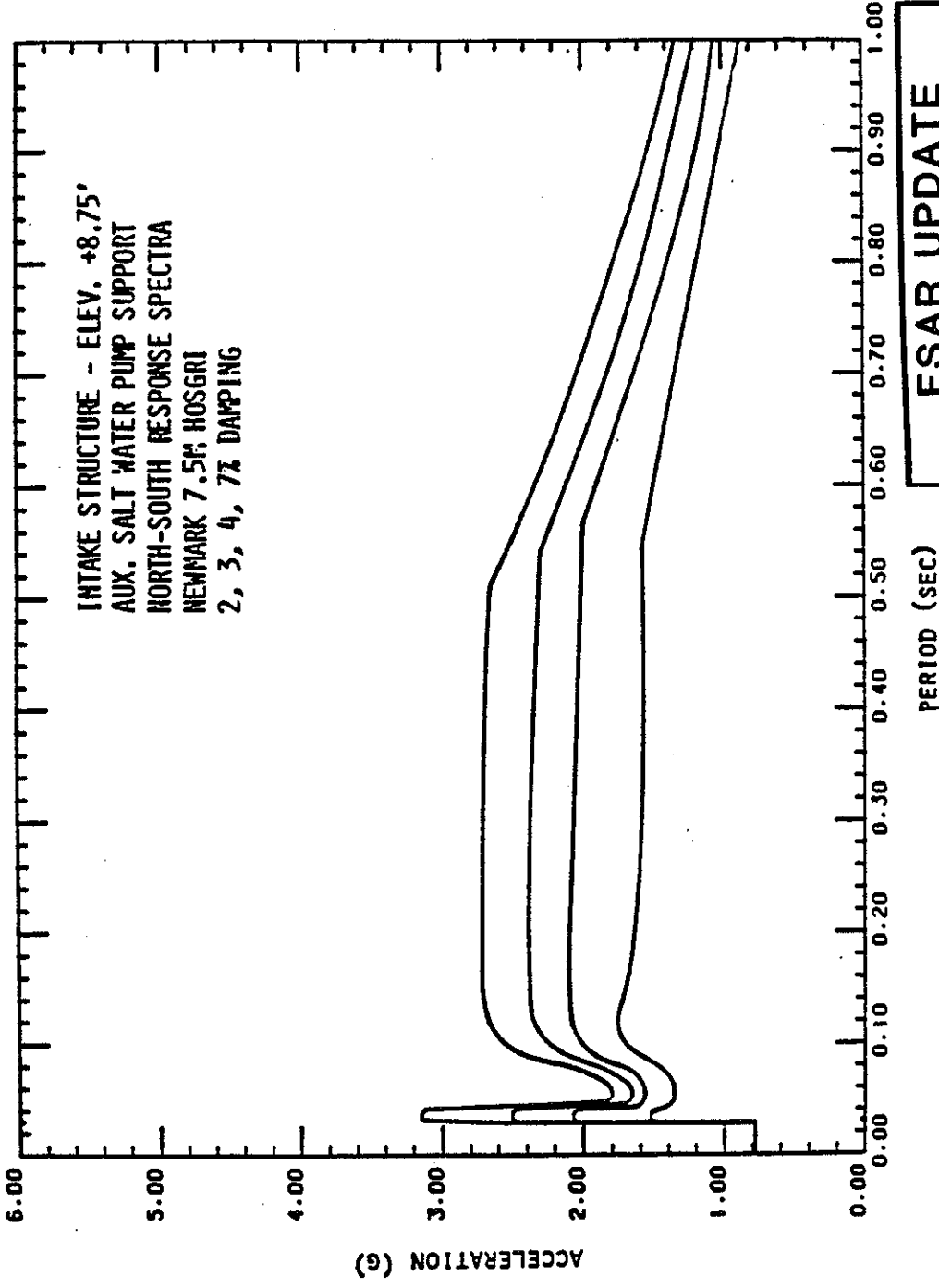
DIABLO CANYON SITE

FIGURE 3.7 - 25 P

INTAKE STRUCTURE VERTICAL
 RESPONSE SPECTRA 7.5M/HOSGRI
 BLUME, NEWMARK ENVELOPE



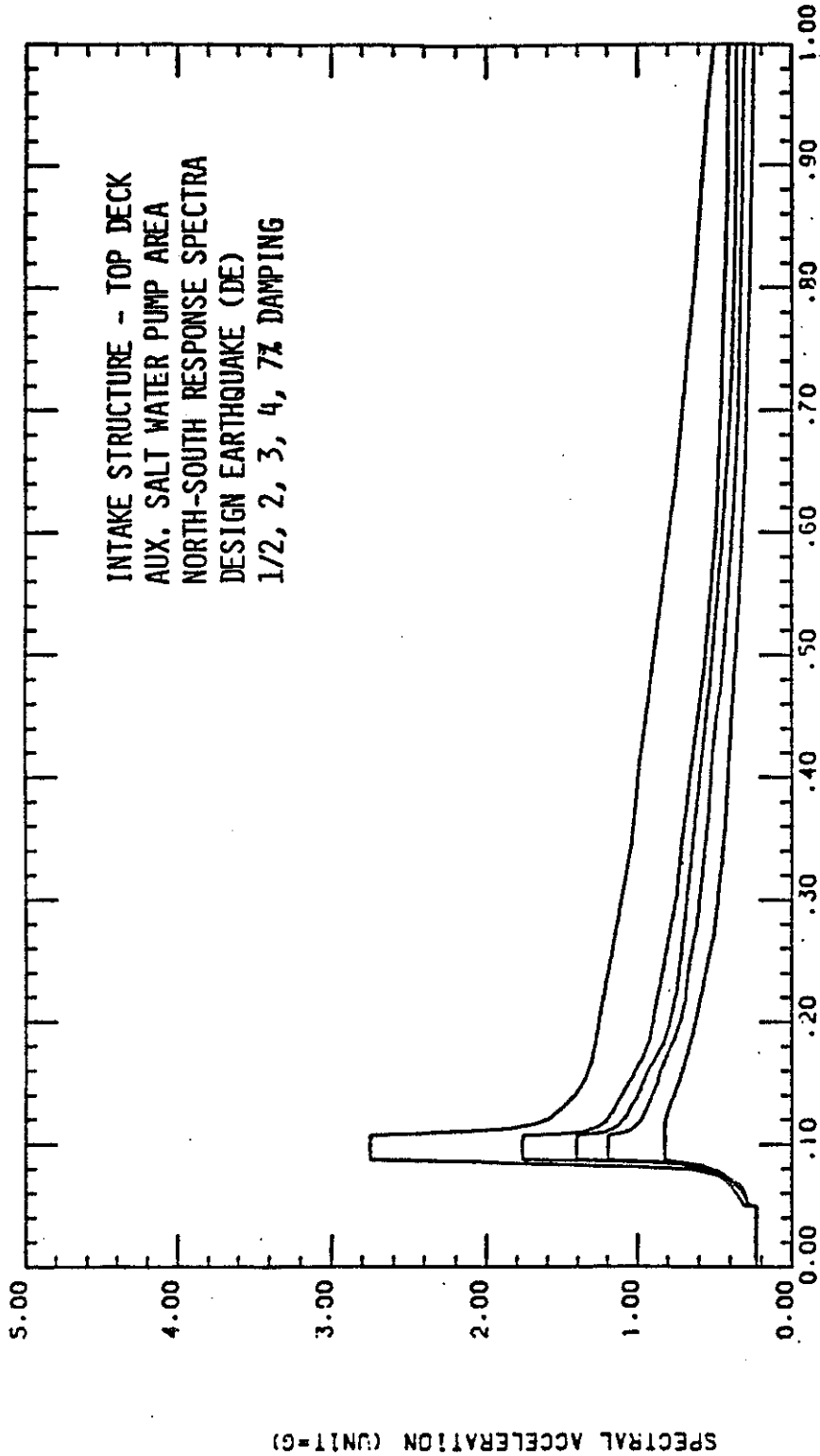
FSAR UPDATE
UNITS 1 AND 2
DIABLO CANYON SITE
 FIGURE 3.7 - 25 Q
 INTAKE STRUCTURE
 RESPONSE SPECTRA
 NEWMARK 7.5 M HOSGRI



FSAR UPDATE

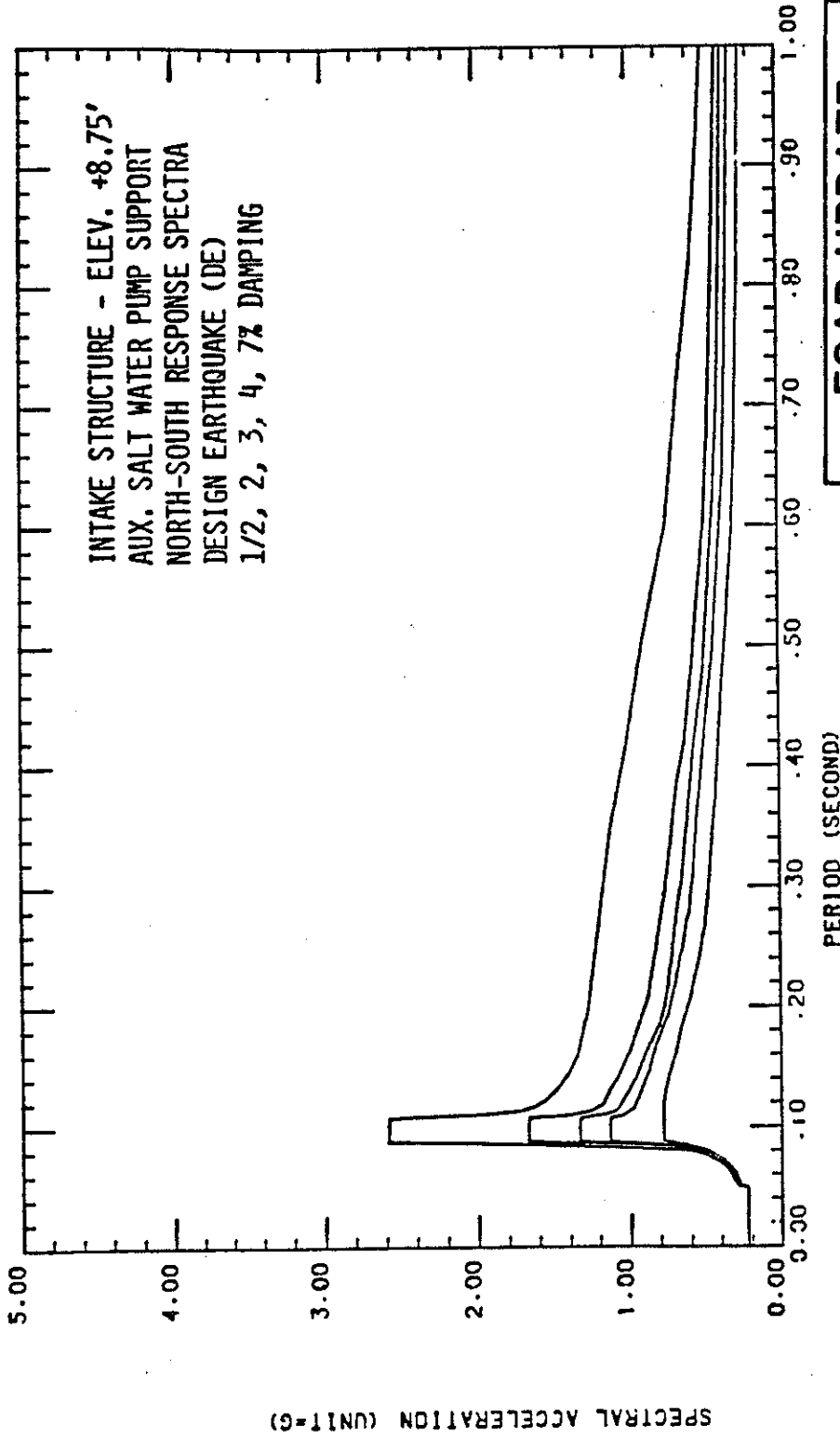
UNITS 1 AND 2
DIABLO CANYON SITE

FIGURE 3.7 - 25 R
 INTAKE STRUCTURE
 RESPONSE SPECTRA
 NEWMARK 7.5 M HOSGRI

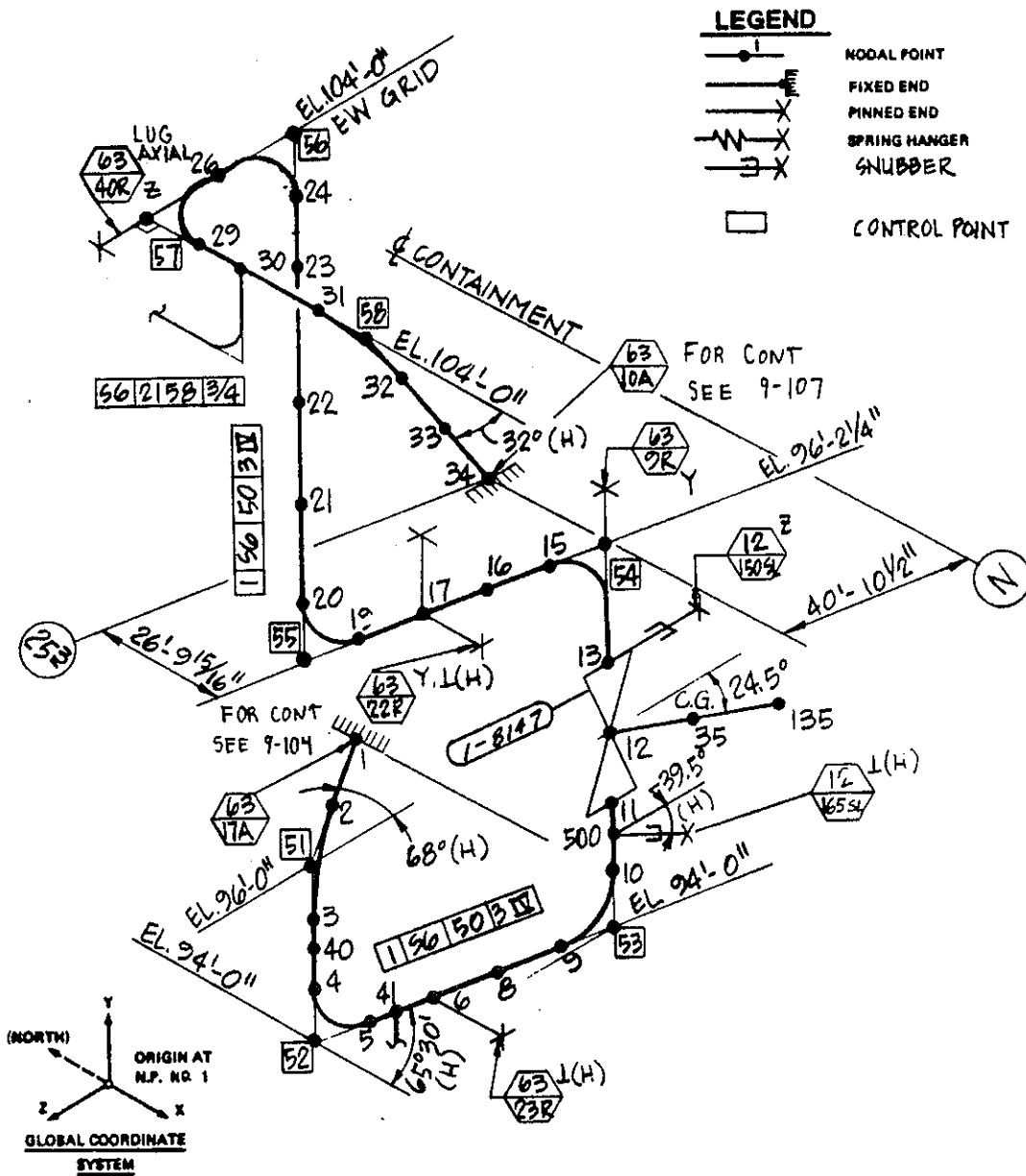


INTAKE STRUCTURE - TOP DECK
 AUX. SALT WATER PUMP AREA
 NORTH-SOUTH RESPONSE SPECTRA
 DESIGN EARTHQUAKE (DE)
 1/2, 2, 3, 4, 7% DAMPING

FSAR UPDATE
UNITS 1 AND 2 DIABLO CANYON SITE
FIGURE 3.7 - 25 S INTAKE STRUCTURE RESPONSE SPECTRA DESIGN EARTHQUAKE (DE)



FSAR UPDATE
UNITS 1 AND 2 DIABLO CANYON SITE
FIGURE 3.7 - 25 T INTAKE STRUCTURE RESPONSE SPECTRA DESIGN EARTHQUAKE (DE)



LEGEND

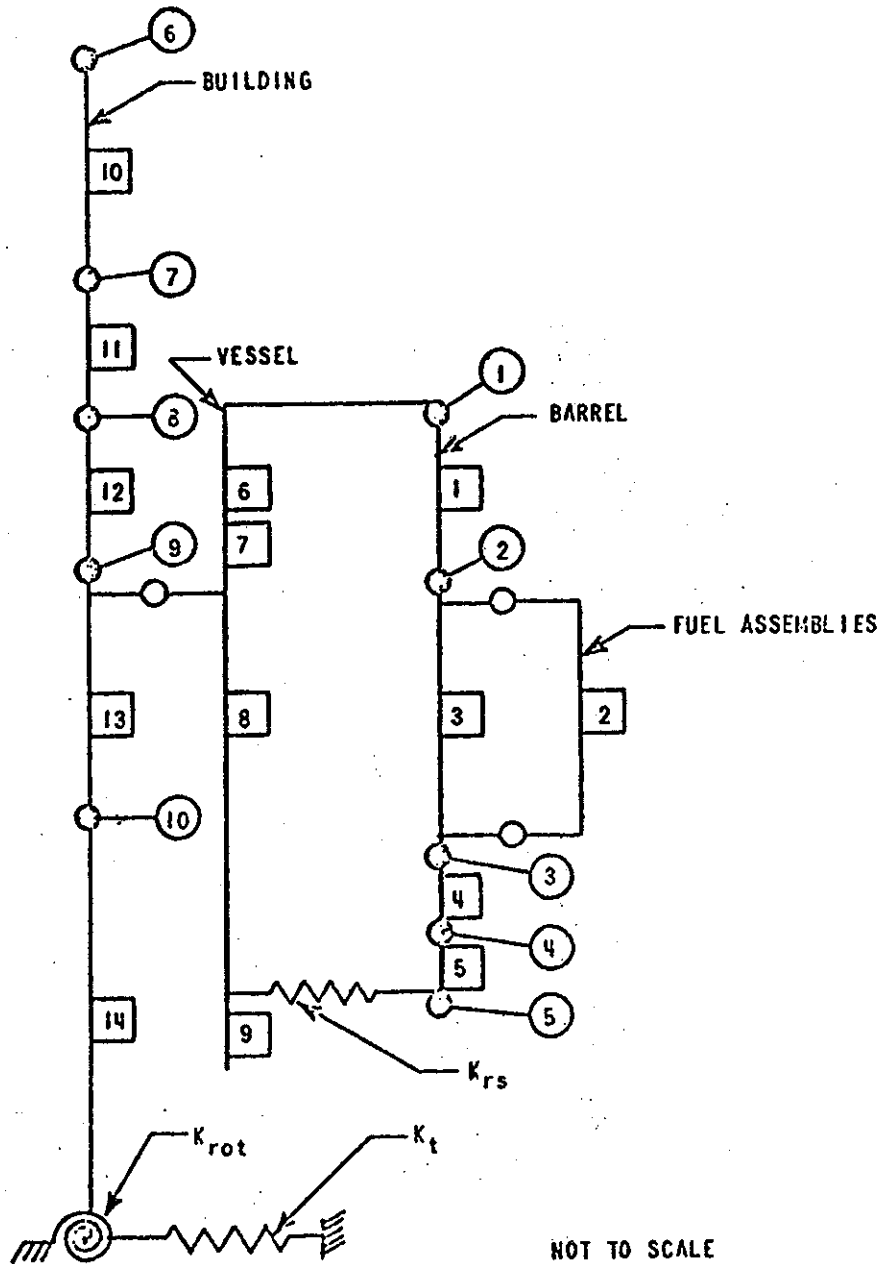
	NODAL POINT
	FIXED END
	PINNED END
	SPRING HANGER
	SNUBBER
	CONTROL POINT

FSAR UPDATE
UNIT 1
DIABLO CANYON SITE

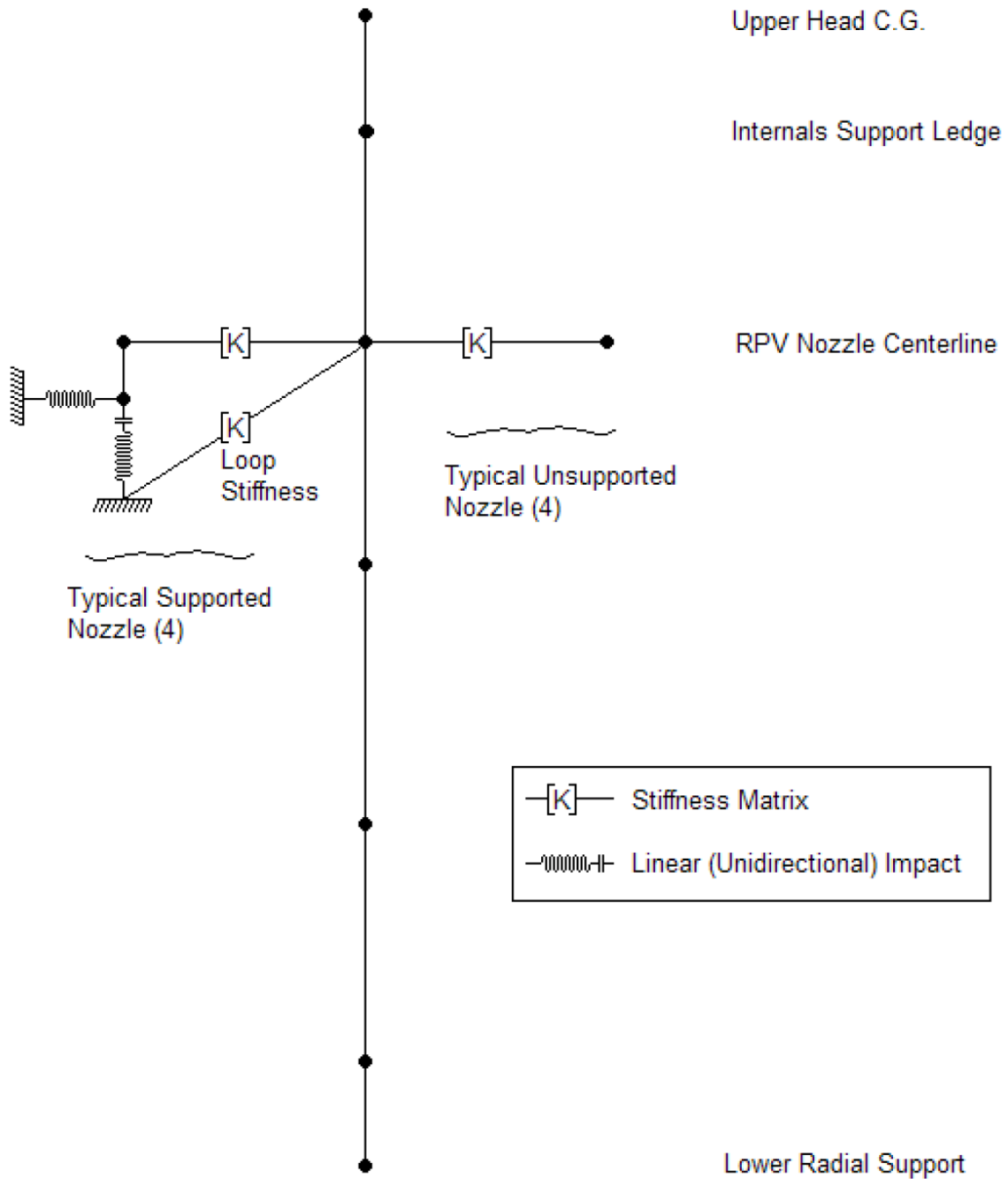
FIGURE 3.7-26
 TYPICAL PIPING
 MATHEMATICAL MODEL

Revision 11 November 1996

K_{rs} = RADIAL SUPPORT SPRING CONSTANT
 K_{rot} = ROTATIONAL GROUND SPRING CONSTANT
 K_t = TRANSLATIONAL GROUND SPRING CONSTANT

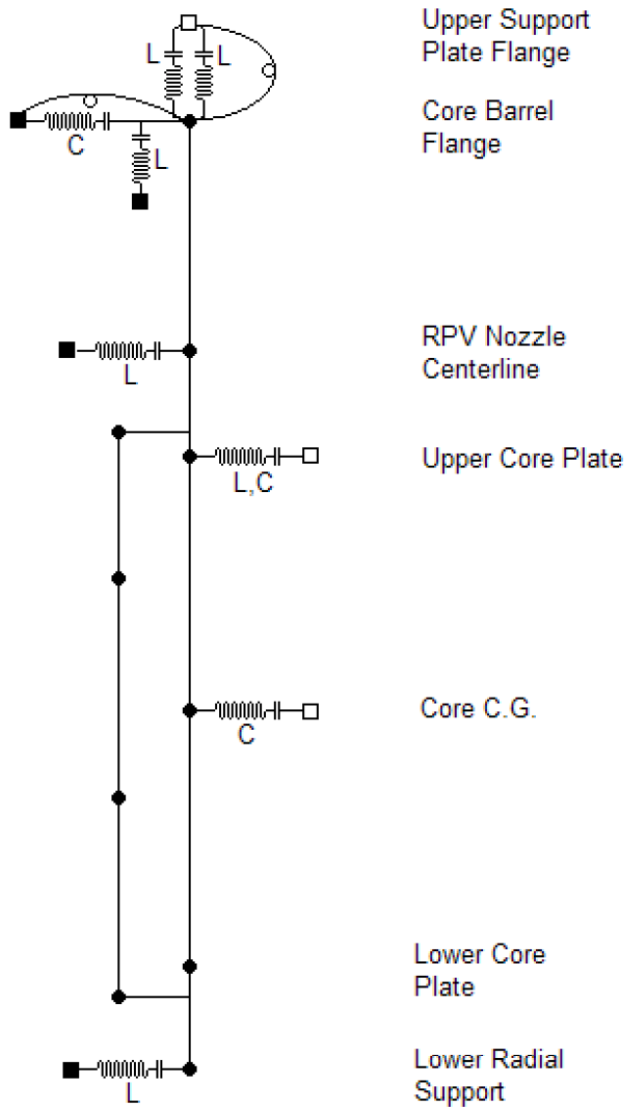


FSAR UPDATE
UNITS 1 AND 2 DIABLO CANYON SITE
FIGURE 3.7 - 27 REACTOR INTERNALS MATHEMATICAL MODELS



FSAR UPDATE
UNITS 1 AND 2
DIABLO CANYON SITE
FIGURE 3.7-27A
REACTOR PRESSURE VESSEL
SHELL SUBMODEL

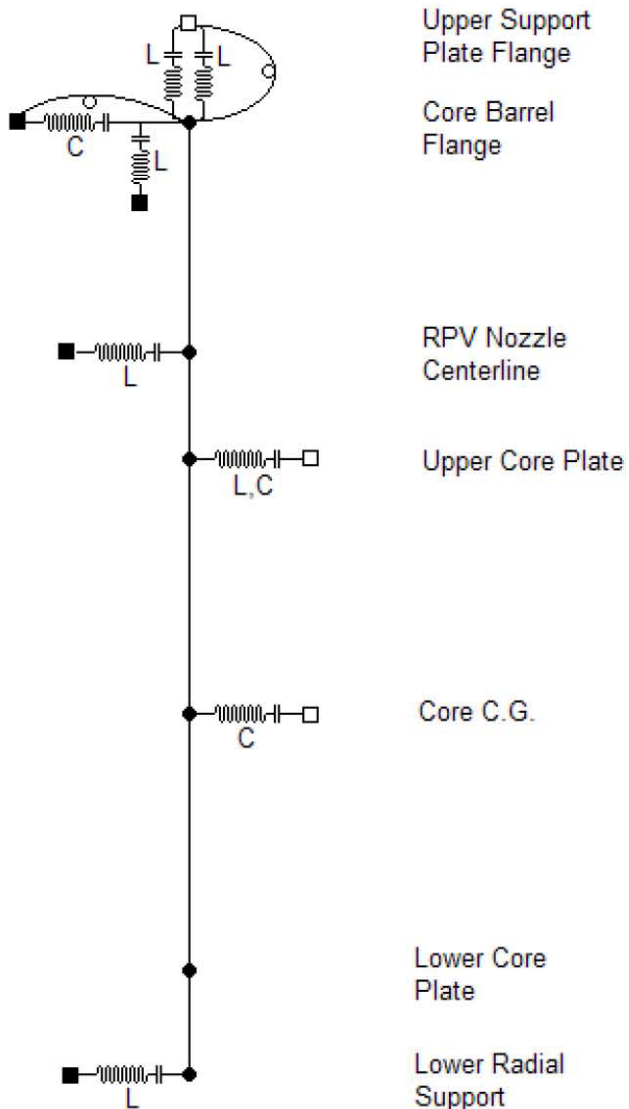
Revision 20 November 2011



	Concentric Impact		Denotes Nodes on RPV Shell Submodel
	Linear (Unidirectional) Impact		Denotes Nodes on Internals Submodel
	Rotational Stiffness		

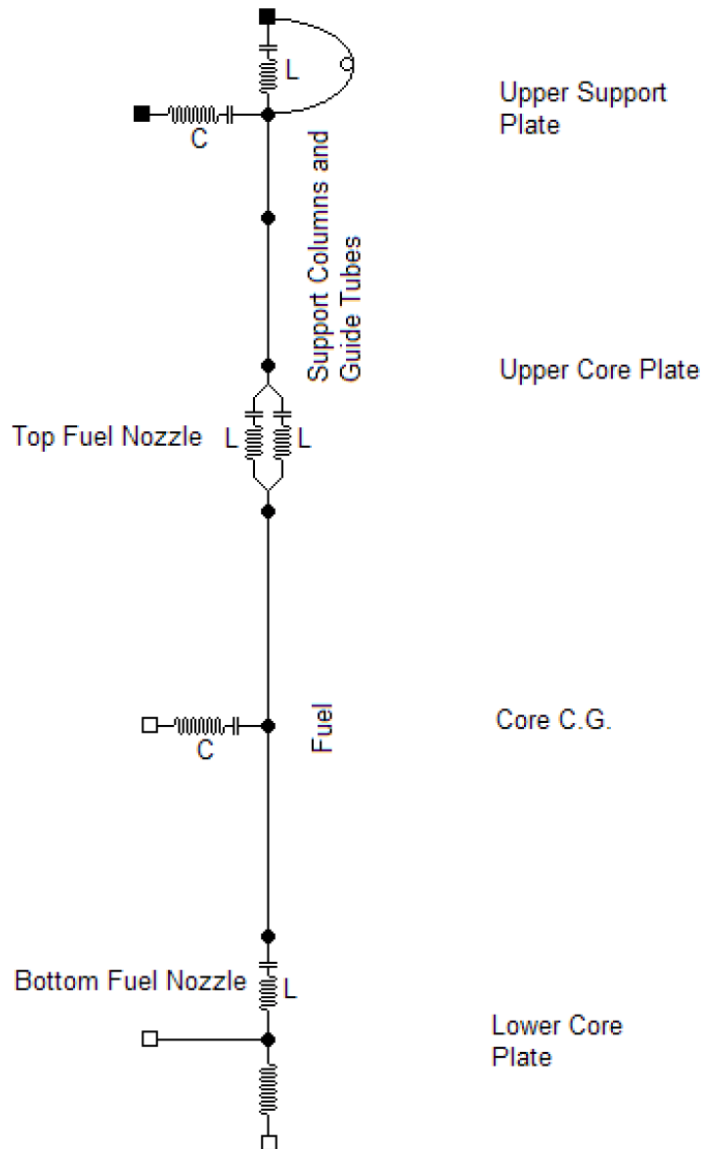
FSAR UPDATE
UNIT 1
DIABLO CANYON SITE
FIGURE 3.7-27B
CORE BARREL SUBMODEL

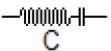

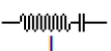
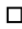
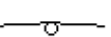
Revision 20 November 2011



	Concentric Impact		Denotes Nodes on RPV Shell Submodel
	Linear (Unidirectional) Impact		Denotes Nodes on Internals Submodel
	Rotational Stiffness		

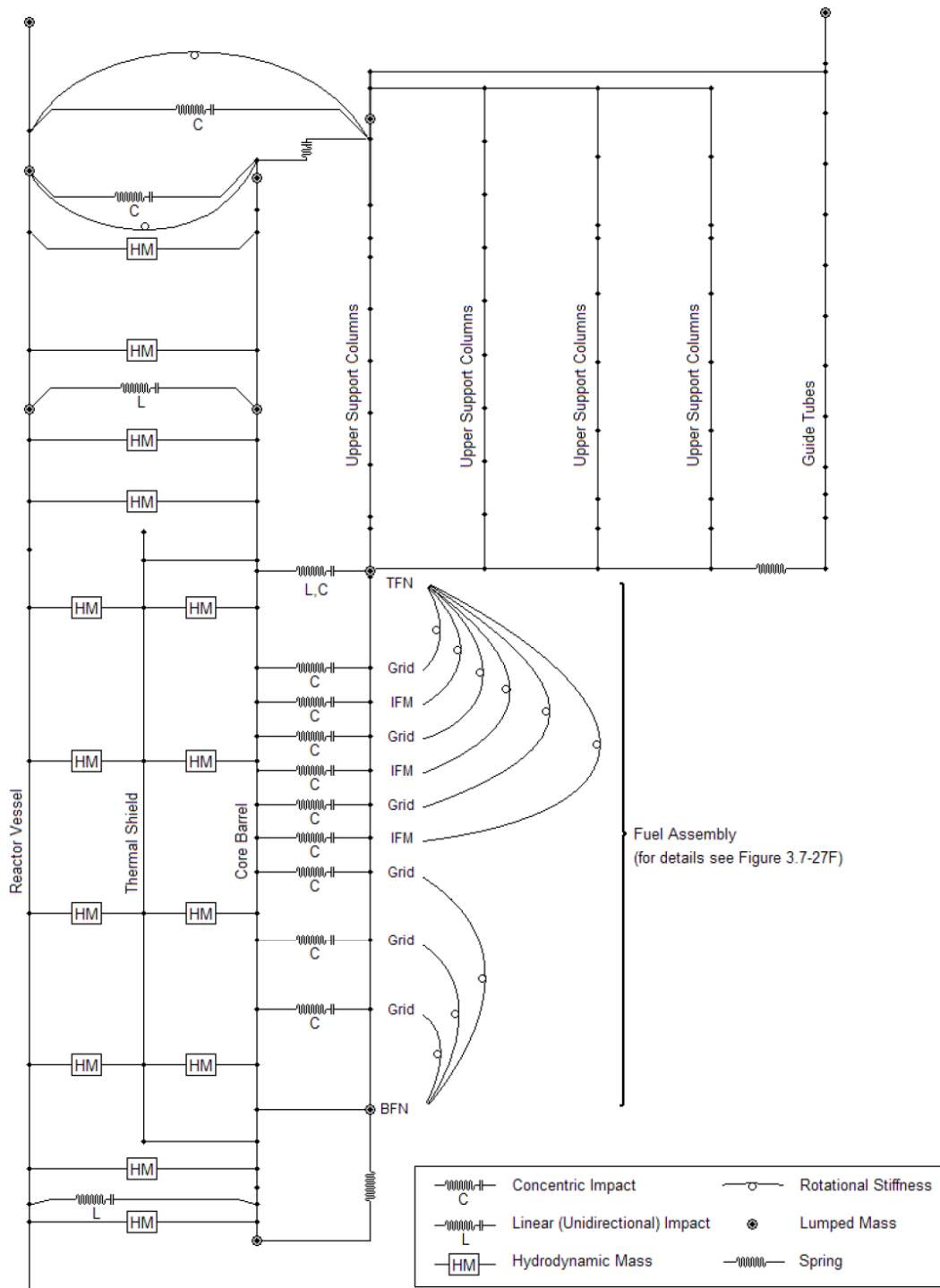
FSAR UPDATE
UNIT 2
DIABLO CANYON SITE
FIGURE 3.7-27C
CORE BARREL SUBMODEL



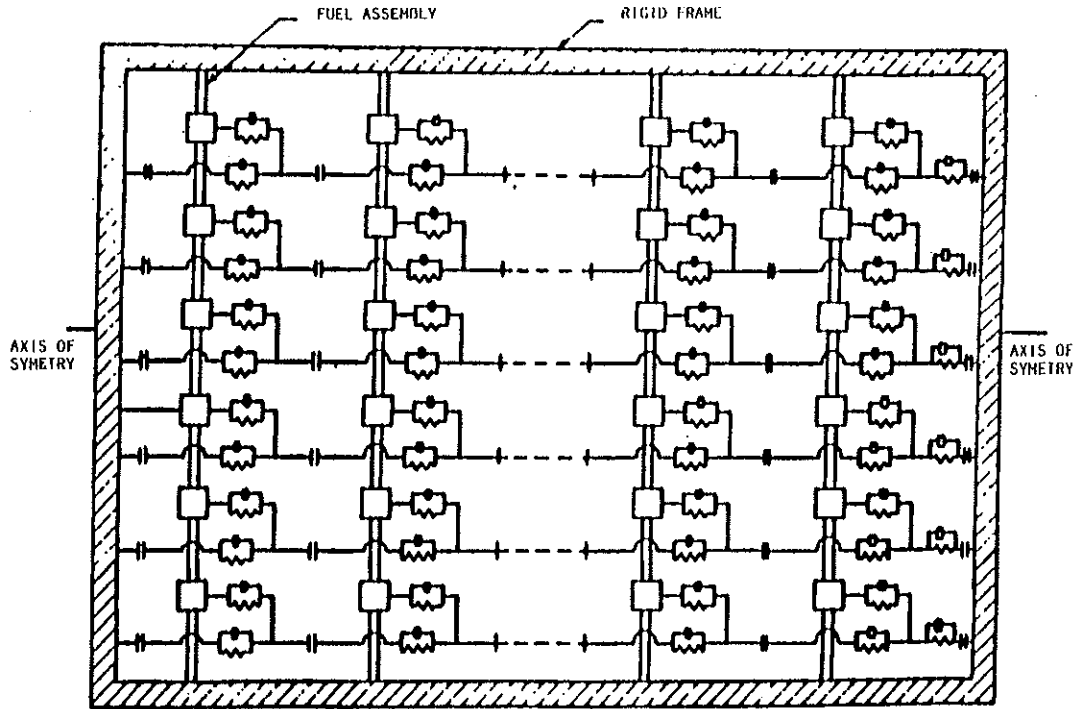
	Concentric Impact		Denotes Nodes on RPV Shell Submodel
	Linear (Unidirectional) Impact		Denotes Nodes on Core Barrel Submodel
	Rotational Stiffness		

FSAR UPDATE
UNITS 1 AND 2
DIABLO CANYON SITE
FIGURE 3.7-27D
INTERNALS (INNERMOST)
SUBMODEL

Revision 20 November 2011

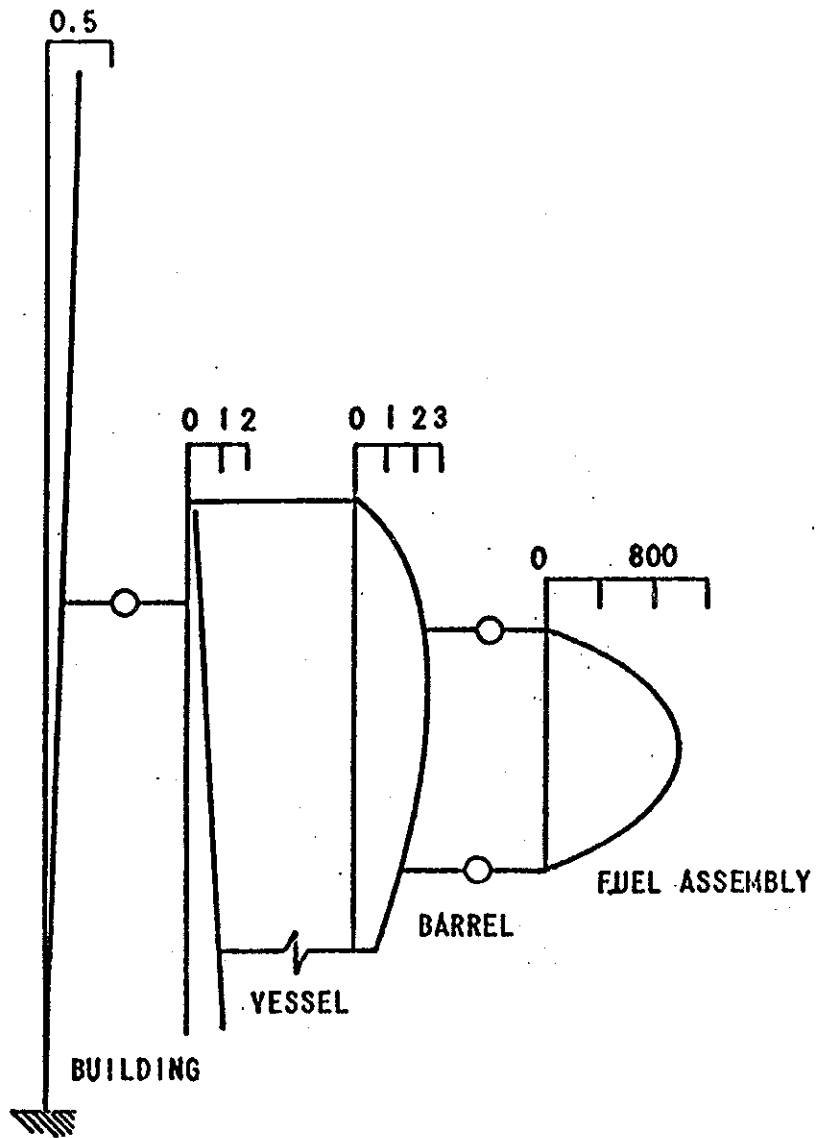


FSAR UPDATE
UNITS 1 AND 2
DIABLO CANYON SITE
FIGURE 3.7-27E
ASSEMBLED FINITE ELEMENT
SYSTEM MODEL

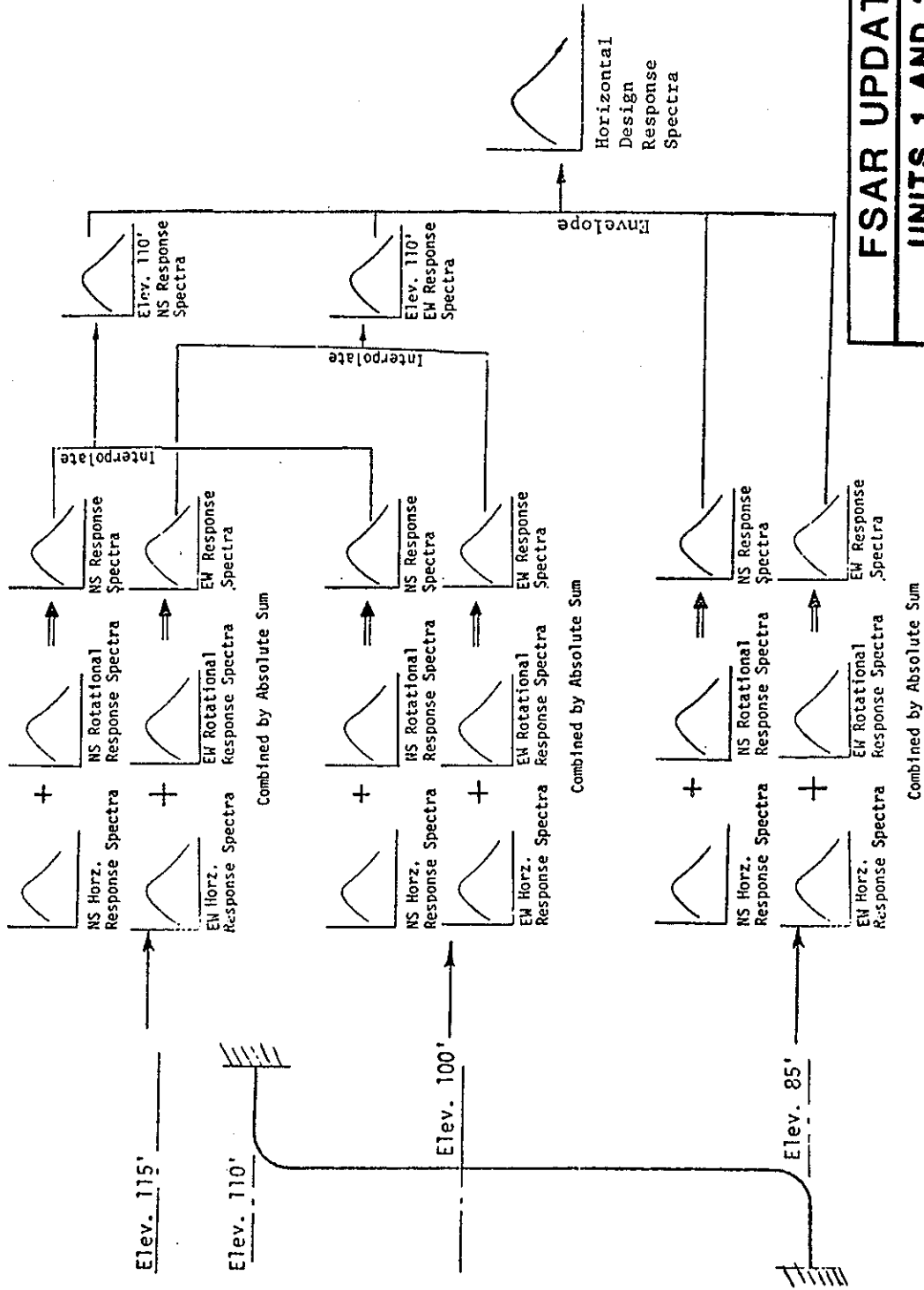


LEGENDO:
 ~ IMPACT SPRING ELEMENT -|- GAP ELEMENT
 ● VISCIOUS DAMPLING ELEMENT □ MASS ELEMENT

FSAR UPDATE
UNITS 1 AND 2 DIABLO CANYON SITE
FIGURE 3.7-27F SCHEMATIC REPRESENTATION OF COMPUTER MODEL USED TO ANALYZE CORE DYNAMIC RESPONSE



FSAR UPDATE
UNITS 1 AND 2
DIABLO CANYON SITE
FIGURE 3.7 -28
REACTOR INTERNALS
FIRST MODE OF VIBRATION



FSAR UPDATE
UNITS 1 AND 2
DIABLO CANYON SITE
 FIGURE 3.7-29
 DERIVATION OF
 DESIGN RESPONSE SPECTRA
 FOR A TYPICAL PIPING SYSTEM

DCPP UNITS 1 & 2 FSAR UPDATE

TABLE 2.5-1

LISTING OF EARTHQUAKES WITHIN 75 MILES OF THE DIABLO CANYON POWER PLANT SITE
SELECTED EARTHQUAKES

MM/DD/YY	HR/MIN/SE	NORTH LAT	WEST LONG	QUALITY	MAG.	STA. REC.	FELT	MAXIMUM INTENSITY - COMMENTS
-?-?-?	-?-?-?	34.50	119.67	D			F	SANTA BARBARA.
03/25/1806	08--?-?	34.50	119.67	D			F	VIII AT SANTA BARBARA.
12/21/1812	18--?-?	34.50	120.00	D			F	VIII AT SAN FERNANDO.
12/21/1812	19--?-?	34.50	120.00	D			F	IX AT SAN FERNANDO.
01/18/1815	-?-?-?	34.50	119.67	D			F	SANTA BARBARA; 5 SHOCKS.
01/30/1815	-?-?-?	34.50	119.67	D			F	SANTA BARBARA.
07/08/1815	-?-?-?	34.50	119.67	D			F	SANTA BARBARA; 6 SHOCKS ON THE EIGHTH AND NINTH.
-?-?-?/1830	-?-?-?	35.25	120.67	D			F	VIII AT SAN LUIS OBISPO.
07/03/1841	-?-?-?	36.30	122.30	D	6.3		F	(CALTECH FILE)
06/13/1851	-?-?-?	35.25	120.67	D			F	V AT SAN LUIS OBISPO.
10/26/1852	-?-?-?	35.67	121.17	D			F	X AT SAN SIMEON; 11 SHOCKS.
12/17/1852	-?-?-?	35.25	120.67	D			F	IX AT SAN LUIS OBISPO; 2 SHOCKS.
01/10/1853	-?-?-?	35.25	120.67	D			F	DANA RANCHO
01/29/1853	-?-?-?	34.50	119.67	D			F	SANTA BARBARA.
02/01/1853	21--?-?	35.67	121.17	D			F	VIII AT SAN SIMEON.
02/14/1853	-?-?-?	35.25	120.67	D			F	SAN LUIS OBISPO.
03/01/1853	-?-?-?	34.50	119.67	D			F	V AT SAN LUIS OBISPO.
04/20/1854	-?-?-?	34.50	119.67	D			F	SANTA BARBARA.
04/29/1854	-?-?-?	34.50	119.67	D			F	III AT SANTA BARBARA.
05/03/1854	13-10--?	34.50	119.67	D			F	SANTA BARBARA; 3 SEVERE SHOCKS.
05/13/1854	-?-?-?	34.50	119.67	D			F	SANTA BARBARA.
05/29/1854	-?-?-?	34.50	119.67	D			F	SANTA BARBARA.
05/31/1854	12-50--?	34.50	119.67	D			F	VI AT SANTA BARBARA; 3 SHOCKS.
01/14/1855	02-30--?	35.75	120.67	D			F	SAN BENITO AND SAN MIGUEL.
06/25/1855	22--?-?	34.50	119.67	D			F	V AT SANTA BARBARA.
01/08/1857	14--?-?	34.50	119.67	D			F	SANTA BARBARA.
01/08/1857	17--?-?	34.50	119.67	D			F	SANTA BARBARA.
01/08/1857	18--?-?	34.50	119.67	D			F	SANTA BARBARA.
01/09/1857	07-20--?	34.50	119.67	D			F	SANTA BARBARA.
01/21/1857	-?-?-?	36.50	121.08	D			F	IX AT SANTA BARBARA.
03/14/1857	23--?-?	34.50	119.67	D			F	III AT A POINT NORTHWEST OF SAN BENITO.
09/02/1858	-?-?-?	36.50	119.67	D			F	V AT MONTECITO AND SANTA BARBARA.
04/03/1860	04--?-?	34.50	121.08	D			F	V AT SANTA BARBARA.
04/17/1860	-?-?-?	34.50	119.67	D			F	VI AT SAN JOSE.
-?-?-?/1862	-?-?-?	34.42	119.63	D			F	SANTA BARBARA.
09/13/1869	-?-?-?	35.25	120.67	D			F	VIII AT GOLETA.
09/14/1869	-?-?-?	35.25	120.67	D			F	V AT SAN LUIS OBISPO.
12/15/1869	-?-?-?	35.25	120.67	D			F	SAN LUIS OBISPO.
02/06/1872	-?-?-?	34.50	119.67	D			F	V AT SAN LUIS OBISPO.
11/07/1875	-?-?-?	36.50	121.08	D			F	SANTA BARBARA; FIRST SINCE APRIL 1860.
12/21/1875	-?-?-?	34.50	119.67	D			F	V IN SAN BENITO COUNTY.
05/10/1876	-?-?-?	34.50	119.67	D			F	SANTA BARBARA.
05/30/1877	-?-?-?	35.67	120.67	D			F	V AT PASO ROBLES.

DCPP UNITS 1 & 2 FSAR UPDATE

TABLE 2.5-1

MM/DD/YY	HR/MIN/SE	NORTH LAT	WEST LONG	QUALITY	MAG.	STA. REC.	FELT	MAXIMUM INTENSITY - COMMENTS
06/24/1877	07-30--?	34.50	119.67	D			F	SANTA BARBARA.
01/08/1878	-?-?-?	34.50	119.67	D			F	SANTA BARBARA.
11/13/1880	06-30--?	34.50	119.67	D			F	SANTA BARBARA.
02/02/1881	-?-?-?	36.37	121.67	D			F	III AT SALINAS.
08/31/1881	03--?-?	34.50	119.67	D			F	III AT SANTA BARBARA.
09/13/1883	22-30--?	34.50	119.67	D			F	IV AT SANTA BARBARA.
08/03/1884	-?-?-?	34.50	119.67	D			F	III AT SANTA BARBARA; NIGHT.
08/04/1884	09--?-?	34.50	119.67	D			F	III AT SANTA BARBARA; 3 SHOCKS.
03/31/1885	-?-?-?	36.30	121.00	D	7.0		F	(CALTECH FILE)
04/07/1885	10--?-?	34.50	119.67	D			F	SANTA BARBARA AND SAN BUENAVENTURA.
04/09/1885	-?-?-?	35.58	121.08	D			F	CAMBRIA.
04/12/1885	04-05--?	36.25	120.80	D			F	IX IN CENTRAL CALIFORNIA; FELT OVER AN AREA OF 125,000 SQ. MI. - EPICENTER PROBABLY EAST OF KING CITY.
04/12/1885	11--?-?	36.33	119.67	D			F	HANFORD.
07/09/1885	09-15--?	34.50	119.67	D			F	V AT SANTA BARBARA.
07/09/1885	16-15--?	34.50	119.67	D			F	V AT SANTA BARBARA; 5 EARTHQUAKES.
10/03/1888	20-52--?	35.75	120.67	D			F	III AT SAN MIGUEL.
10/03/1888	21-02--?	35.75	120.67	D			F	VI AT SAN MIGUEL.
10/04/1888	-?-?-?	35.67	120.67	D			F	PASO ROBLES.
05/01/1889	19-55--?	34.67	120.42	D			F	SUSANVILLE.
05/26/1889	15-13--?	36.50	121.42	D			F	GONZALES; SAN FRANCISCO, AND SANTA CRUZ; RECORDED AT MT. HAMILTON.
07/10/1889	-?-?-?	35.17	120.58	D			F	ARROYO GRANDE; SHOCKS FOR SEVERAL DAYS.
09/30/1889	20-17--?	36.50	119.58	D			F	KINGSBURG.
01/-?/1890	23-30--?	34.50	119.67	D			F	SANTA BARBARA.
11/13/1892	-?-?-?	36.30	122.00	D	6.0		F	(CALTECH FILE)
05/19/1893	-?-35--?	34.17	119.50	D			F	VII FELT FROM SAN DIEGO TO LOMPOC, INLAND TO SAN BERNADINO, MOST SEVERE SE OF VENTURA. POSSIBLY OF SUBMARINE ORIGIN OFF THE COAST OF VENTURA COUNTY.
06/01/1893	12--?-?	34.50	119.67	D			F	VII AT NORDHOFF (OJAI), SANTA BARBARA, AND VENTURA.
06/01/1893	12--?-?	34.50	119.67	D			F	NORDHOFF, SANTA BARBARA, AND VENTURA.
12/06/1893	04-56--?	35.67	121.33	D			F	NORDHOFF, SANTA BARBARA, AND VENTURA.
07/27/1895	-?-10--?	34.50	119.67	D			F	PIEDRAS BLANCAS LIGHTHOUSE.
12/24/1895	05-30--?	34.50	119.67	D			F	SANTA BARBARA.
06/24/1897	14-10--?	34.50	119.67	D			F	SANTA BARBARA.
07/18/1897	-?-?-?	34.50	119.67	D			F	CASTLE PINCKNEY.
07/20/1897	07-45--?	34.50	119.67	D			F	SANTA BARBARA.
05/30/1898	03-03--?	34.50	119.67	D			F	SANTA BARBARA.
06/04/1898	06-20--?	34.67	120.08	D			F	LOS OLIVOS; FELT THROUGHOUT THE SANTA YNEZ VALLEY; AT SANTA BARBARA THE HEAVIEST FOR SOME YEARS.
02/08/1899	04-55--?	36.33	121.92	D			F	POINT SUR LIGHT STATION.
06/05/1899	-?-?-?	35.83	120.83	D			F	BRADLEY.
06/25/1899	-?-?-?	35.75	120.67	D			F	SAN MIGUEL.
06/09/1900	-?-?-?	36.00	120.92	D			F	SAN ARDO.
10/18/1900	-?-?-?	35.25	120.67	D			F	SAN LUIS OBISPO.
03/03/1901	-?-?-?	35.25	120.67	D			F	SAN LUIS OBISPO.

DCPP UNITS 1 & 2 FSAR UPDATE

TABLE 2.5-1

MM/DD/YY	HR/MIN/SE	NORTH LAT	WEST LONG	QUALITY	MAG.	STA. REC.	FELT	MAXIMUM INTENSITY - COMMENTS
03/03/1901	07-45--?	36.08	120.58	D			F	IX AT STONE CANYON - SURFACE CRACKS IN THE GROUND; ALSO FELT AT ADELAIDA, ESTRELLA, PARKFIELD, PASO ROBLES, PORTERVILLE, SAN JOSE, SAN LUIS OBISPO, AND SAN MIGUEL.
03/05/1901	-?-?-?-?	35.67	120.67	D			F	PASO ROBLES.
03/06/1901	-?-?-?-?	36.00	120.92	D			F	SAN ARDO AND SAN LUIS OBISPO.
06/03/1901	-?-?-?-?	35.25	120.67	D			F	SAN LUIS OBISPO.
07/30/1901	19--?-?-?	35.25	120.67	D			F	SAN LUIS OBISPO.
08/14/1901	11-11--?	35.42	120.92	D			F	CAYUCOS, HOLLISTER, SALINAS, SAN LUIS OBISPO, AND SANTA CRUZ.
02/07/1902	-?-?-?-?	34.50	119.67	D			F	SANTA BARBARA.
02/09/1902	15--?-?-?	34.50	119.67	D			F	PINE CREST, SAN LUIS OBISPO, SANTA BARBARA, AND VENTURA.
04/06/1902	-?-?-?-?	35.25	120.67	D			F	SAN LUIS OBISPO.
07/21/1902	-?-?-?-?	34.75	120.00	D			F	PINE CREST.
07/28/1902	06-57--?	34.75	120.25	D			F	IX AT LOMPOC AND LOS ALAMOS; CONFINED TO THE NORTHERN PART OF SANTA BARBARA COUNTY.
07/28/1902	13--8--?	35.25	120.67	D			F	SAN LUIS OBISPO; AFTERSHOCK OF 06-57-?
07/31/1902	09-20--?	34.75	120.25	D			F	IX AT LOS ALAMOS AND SURROUNDING COUNTRY; FISSURES, CRACKS IN THE GROUND, AND LANDSLIDES.
08/01/1902	-?-?-?-?	34.75	120.25	D			F	LOS ALAMOS. SEVERAL SHOCKS.
08/01/1902	03-30--?	34.75	120.25	D			F	VIII AT LOS ALAMOS.
08/02/1902	-?-?-?-?	34.75	120.25	D			F	LOS ALAMOS.
08/03/1902	-?-?-?-?	34.75	120.25	D			F	LOS ALAMOS.
08/04/1902	10-5--?	34.75	120.25	D			F	LOS ALAMOS.
08/04/1902	11-18--?	34.75	120.25	D			F	LOS ALAMOS.
08/04/1902	12-15--?	34.75	120.25	D			F	LOS ALAMOS.
08/04/1902	21-29--?	34.75	120.25	D			F	LOS ALAMOS.
08/04/1902	23-40--?	34.75	120.25	D			F	LOS ALAMOS.
08/05/1902	-?-55--?	34.75	120.25	D			F	LOS ALAMOS.
08/10/1902	-?-?-?-?	34.75	120.25	D			F	LOS ALAMOS; DISTINCT EARTHQUAKE DETONATION AND TREMOR.
08/10/1902	10-40--?	34.75	120.25	D			F	LOS ALAMOS; HEAVY DETONATION FOLLOWED BY TREMBLING.
08/10/1902	22-40--?	34.50	119.67	D			F	SANTA BARBARA.
08/14/1902	10-15--?	34.75	120.25	D			F	LOS ALAMOS.
08/14/1902	11-05--?	34.75	120.25	D			F	LOS ALAMOS.
08/14/1902	11-20--?	34.75	120.25	D			F	LOS ALAMOS; SHOOK GROUND VIOLENTLY.
08/14/1902	21-50--?	34.75	120.25	D			F	LOS ALAMOS.
08/14/1902	23-50--?	34.75	120.25	D			F	LOS ALAMOS.
08/28/1902	-?-?-?-?	35.25	120.67	D			F	SAN LUIS OBISPO.
08/31/1902	-?-?-?-?	35.25	120.67	D			F	SAN LUIS OBISPO.
09/11/1902	05-30--?	34.25	120.25	D			F	V AT LOS ALAMOS.
10/21/1902	21-45--?	34.75	120.25	D			F	LOMPOC AND LOS ALAMOS.
10/21/1902	22-15--?	34.75	120.25	D			F	LOMPOC AND LOS ALAMOS.
10/22/1902	10--?-?-?	34.75	120.25	D			F	LOS ALAMOS.
12/12/1902	-?-?-?-?	34.75	120.25	D			F	VIII AT LOS ALAMOS -3 SHOCKS IN 5 MINUTES; FELT THROUGHOUT THE NORTHERN PART OF SANTA BARBARA COUNTY, ESPECIALLY AT LOMPOC, LOS ALAMOS, SAN LUIS OBISPO, SANTA BARBARA, AND SANTA MARIA.
01/11/1903	-?-?-?-?	35.25	120.67	D			F	SAN LUIS OBISPO.

DCPP UNITS 1 & 2 FSAR UPDATE

TABLE 2.5-1

MM/DD/YY	HR/Min/SE	NORTH LAT	WEST LONG	QUALITY	MAG.	STA. REC.	FELT	MAXIMUM INTENSITY - COMMENTS
03/07/1903	-?-?-?	36.50	121.42	D			F	GONZALES.
03/24/1903	-?-?-?	36.50	121.42	D			F	GONZALES AND SANTA MARGARITA.
04/24/1903	-?-?-?	35.42	120.58	D			F	SANTA MARGARITA.
07/29/1903	07-13--?	35.67	121.33	D			F	V AT POINT PIEDRAS BLANCAS LIGHTHOUSE.
07/29/1903	10-30--?	35.67	121.33	D			F	POINT PIEDRAS BLANCAS LIGHTHOUSE.
08/24/1903	-?-?-?	34.67	120.08	D			F	LOS OLIVOS.
01/22/1904	-?-?-?	34.75	120.25	D			F	LOS ALAMOS.
01/23/1904	-?-?-?	34.75	120.25	D			F	SAN LUIS OBISPO.
09/10/1904	-?-?-?	35.25	120.67	D			F	LOS GATOS, SALINAS, SAN FRANCISCO, SAN LUIS OBISPO, SANTA
05/26/1905	05-49--?	35.25	120.67	D			F	CRUZ AND SOLEDAD.
07/06/1906	-?-?-?	35.25	120.67	D			F	SAN LUIS OBISPO.
07/22/1906	-?-?-?	35.25	120.67	D			F	SAN LUIS OBISPO.
08/01/1906	-?-?-?	35.25	120.67	D			F	SAN LUIS OBISPO.
12/07/1906	06-40--?	35.67	121.33	D			F	VII AT SAN LUIS OBISPO AND SANTA MARIA; DURATION 30
								SECONDS, FOLLOWED BY SECOND SHOCK HALF AN HOUR LATER.
+12/08/1906	06-55--?	35.75	120.67	D			F	SAN MIGUEL.
06/19/1907	12--?-?	36.17	120.67	D			F	PRIEST VALLEY.
07/02/1907	18-10--?	35.25	120.67	D			F	SAN LUIS OBISPO.
07/21/1907	-?-?-?	35.25	120.67	D			F	SAN LUIS OBISPO.
07/29/1907	05-10--?	34.75	120.00	D			F	PINE CREST.
08-?-1907	-?-?-?	34.75	120.00	D			F	PINE CREST AND SANTA BARBARA.
12/27/1907	09-15--?	34.50	119.67	D			F	SANTA BARBARA; ALSO FELT AT VENTURA; REPORTED FROM OJAI
								AND PINE CREST.
04/27/1908	10-50--?	36.00	121.17	D			F	JOLON; PASO ROBLES; PRIEST VALLEY, SAN LUIS OBISPO, SANTA
								MARGARETA, AND SAN MIGUEL.
05/19/1908	-?-?-?	35.25	120.67	D			F	SAN LUIS OBISPO.
09/16/1908	-?-?-?	36.17	120.67	D			F	PRIEST VALLEY.
11-?-1908	19-30--?	36.17	120.67	D			F	PRIEST VALLEY.
01/23/1909	14-58--?	34.50	119.67	D			F	PINE CREST AND SANTA BARBARA.
04/10/1909	-?-?-?	34.50	119.67	D			F	MONO RANCH AND SANTA PAULA CANYON.
06/17/1909	08-20--?	36.42	121.33	D			F	SOLEDAD.
07/03/1909	07--?-?	34.50	119.67	D			F	MONTECITO AND SANTA BARBARA.
07/05/1909	06-10--?	34.50	119.67	D			F	III AT SANTA BARBARA.
07/16/1909	10-28--?	34.50	119.67	D			F	IV AT LOS ANGELES AND SANTA BARBARA.
07/31/1909	19-37--?	34.50	119.67	D			F	IV AT OJAI AND SANTA BARBARA.
08/18/1909	-?-?-?	35.25	120.67	D			F	SAN LUIS OBISPO.
11/24/1909	15--?-?	36.00	121.17	D			F	JOLON.
03/08/1910	09-30--?	36.17	120.67	D			F	PRIEST VALLEY.
04/30/1910	18-25--?	36.17	120.67	D			F	PRIEST VALLEY; 3 SHOCKS, THE SECOND ONE QUITE VIOLENT.
11-?-1910	-?-?-?	34.50	119.67	D			F	SANTA BARBARA; 2 SLIGHT QUAKES DURING NOVEMBER.
02/02/1911	-?-?-?	34.75	120.25	D			F	LOS ALAMOS.
03/22/1911	10-55--?	35.75	120.67	D			F	SAN MIGUEL; QUITE SEVERE.
06/02/1911	-?-?-?	36.17	120.67	D			F	PRIEST VALLEY.
06/18/1912	22-27--?	36.00	121.17	D			F	JOLON. (RECORDED AT BERKELEY.)
10/20/1913	11-25--?	35.25	120.67	D			F	BETTERAVIA, PASO ROBLES, SAN LUIS OBISPO, AND SANTA MARIA.
11/27/1913	19--?-?	34.50	119.67	D			F	MONO RANCH.

DCPP UNITS 1 & 2 FSAR UPDATE

TABLE 2.5-1

MM/DD/YY	HR/IN/SE	NORTH LAT	WEST LONG	QUALITY	MAG.	STA. REC.	FELT	MAXIMUM INTENSITY - COMMENTS
12/26/1913	12--?--?	36.17	121.00	D			F	SAN LUCAS.
11/24/1914	04-25--?	35.25	120.67	D			F	II AT SAN LUIS OBISPO; ABRUPT TREMBLING, LASTING 20 SECONDS.
01/12/1915	-?-?-?-?	34.92	120.50	D			F	BETTERAVIA.
01/12/1915	04-31--?	34.75	120.25	B			F	VIII AT LOS ALAMOS - EPICENTER 2 OR 3 MI. EAST OF LOS ALAMOS; FELT FROM SAN JOSE TO LOS ANGELES; SHAKEN AREA IN EXCESS OF 50,000 SQ. MI. - PRACTICALLY EVERY CHIMNEY DAMAGED AT LOS ALAMOS. VII AT LOMPOC. VI-VII AT SANTA MARIA; V AT SAN LUIS OBISPO AND SANTA BARBARA; IV AT PASO ROBLES, AND II AT LOS ANGELES. WEATHER BUREAU REPORTED V-VI AT SANTA BARBARA; V AT OZENA AND SAN LUIS OBISPO, IV AT PASO ROBLES, III AT OJAI, AND II IN PRIEST VALLEY; ALSO II AT BAKERSFIELD.
01/14/1915	-?-?-?-?	34.92	120.50	D			F	BETTERAVIA.
01/15/1915	-?-?-?-?	34.75	120.25	D			F	LOS ALAMOS.
01/20/1915	-?-?-?-?	34.75	120.25	D			F	LOS ALAMOS.
01/26/1915	-?-?-?-?	34.75	120.25	D			F	LOS ALAMOS.
01/27/1915	-?-?-?-?	34.75	120.25	D			F	LOS ALAMOS.
04/21/1915	09-58--?	35.25	120.67	D			F	IV AT SAN LUIS OBISPO; ALSO FELT 3 MI. NW OF PRIEST VALLEY.
08/23/1915	23-15--?	34.75	119.75	D			F	HILL CAMP.
08/31/1915	21--?-?-?	34.75	119.75	D			F	HILL CAMP.
09/08/1915	12-45--?	35.67	120.67	D			F	V IN REGION EAST OF PASO ROBLES; ANTELOPE - 2 SHOCKS. FIRST THE HEAVIER, OIL CAME UP WITH WATER IN WELL AFTER SHOCK. AT SHANDON A SEATED MAN WAS SHAKEN SO HARD HE THOUGHT A PERSON WAS SHAKING HIM. AT CRESTON THE SHOCK WAS SHORT AND SHARP. A SLIGHT LANDSLIDE AT PORT SAN LUIS. WEATHER BUREAU REPORTS -PASO ROBLES V AND SAN LUIS OBISPO III-IV.
09/14/1915	-?-?-?-?	34.75	119.75	D			F	HILL CAMP; 3 HARD SHOCKS - EARTH TREMBLED FOR 15 MINUTES AFTERWARDS.
02/27/1916	13-26--?	34.75	120.25	D			F	LOS ALAMOS.
03/01/1916	19-15--?	34.75	120.25	D			F	LOS ALAMOS.
05/06/1916	03-45--?	34.75	120.25	D			F	III AT LOS ALAMOS. FELT BY MANY AT EL ROBLAR RANCH, 2 MI. SE OF LOS ALAMOS.
08/06/1916	-?-?-?-?	36.00	121.00		7.0		F	(CALTECH FILE)
10/24/1916	13-03--?	35.25	120.67	D			F	II AT SAN LUIS OBISPO; PROBABLY NEXT SHOCK, WITH TIME ERROR.
10/24/1916	13-30--?	36.00	121.17	D			F	V AT JOLON; III AT A POINT 3.5 MI. NW OF PRIEST VALLEY.
12/01/1916	22-53--?	35.17	120.75	D			F	VII AT AVILA - CONSIDERABLE GLASS BROKEN AND GOODS IN STORES THROWN FROM SHELVES. FELT AT SAN LUIS OBISPO; WATER IN BAY DISTURBED; PLASTER IN COTTAGES JARRED LOOSE. SMOKESTACKS OF UNION OIL CO. REFINERY TOPPLED OVER. SEVERE AT PORT SAN LUIS; III AT SANTA MARIA.
02/01/1917	05-18--?	34.92	120.42	D			F	III AT SANTA MARIA.
04/05/1917	19--?-?-?	34.67	120.33	D			F	IV AT SANTA RITA; ALSO FELT AT LOMPOC.

DCPP UNITS 1 & 2 FSAR UPDATE

TABLE 2.5-1

MM/DD/YY	HR/MIN/SE	NORTH LAT	WEST LONG	QUALITY	MAG.	STA. REC.	FELT	MAXIMUM INTENSITY - COMMENTS
04/13/1917	03-59--?	34.25	119.67	D			F	V I AT SANTA BARBARA CHANNEL REGION; FELT OVER AN AREA OF COAST SOUTH AND EAST OF SANTA BARBARA AS FAR AS VENTURA, AND ON SANTA CRUZ ISLAND.
04/21/1917	06-59--?	34.25	119.67	D			F	V AT SANTA BARBARA CHANNEL; PERCEPTIBLE OVER AN AREA OF PERHAPS 4000 SQ. MI.
07/07/1917	20-57--?	35.25	120.50	D			F	LOPEZ CANYON; ALSO AT SAN LUIS OBISPO.
07/07/1917	21-02--?	35.25	120.50	D			F	LOPEZ CANYON.
07/07/1917	21-15--?	35.25	120.50	D			F	LOPEZ CANYON.
07/08/1917	03-20--?	34.92	120.42	D			F	II AT SANTA MARIA.
07/08/1917	11-29--?	35.25	120.50	D			F	IV IN LOPEZ CANYON.
07/09/1917	22-22--?	35.25	120.50	D			F	VII IN LOPEZ CANYON; IV AT SAN LUIS OBISPO.
07/09/1917	22-38--?	35.25	120.50	D			F	LOPEZ CANYON.
07/10/1917	-?-43--?	35.25	120.50	D			F	LOPEZ CANYON.
07/10/1917	-?-45--?	35.25	120.50	D			F	LOPEZ CANYON.
07/26/1917	08-31--?	34.92	120.42	D			F	V AT SANTA MARIA - FURNITURE MOVED. IV AT LOS OLIVOS - AWAKENED SLEEPERS AT SAN LUIS OBISPO
12/05/1918	02-38--?	35.67	120.67	D			F	IV AT PASO ROBLES; II AT SAN LUIS OBISPO.
12/05/1918	04-30--?	35.25	120.67	D			F	SAN LUIS OBISPO.
03/01/1919	04-19--?	36.17	120.67	D			F	IV IN PRIEST VALLEY.
03/15/1919	07-53--?	35.25	120.67	D			F	SAN LUIS OBISPO.
07/31/1919	21-31--?	36.33	120.67	D			F	V IN SAN BENITO COUNTY; FELT AT IDRIA - ORIGIN SOME DISTANCE FROM IDRIA
08/26/1919	12-12--?	34.50	119.67	D			F	V IN SANTA BARBARA COUNTY - FELT AT OJAI, SAN LUIS OBISPO (3 SHOCKS), SANTA BARBARA.
08/26/1919	14-57--?	34.50	119.67	D			F	V IN SANTA BARBARA COUNTY - THIS SHOCK STRONGER AT SANTA BARBARA THAN PREVIOUS SHOCK. BUILDINGS AND WHARVES SWAYED; FELT AT OJAI.
12/18/1919	07-15--?	35.67	120.67	D			F	PASO ROBLES.
01/30/1920	23-30--?	34.50	119.67	D			F	III AT SANTA BARBARA.
01/30/1920	23-33--?	34.50	119.67	D			F	II AT SANTA BARBARA.
01/30/1920	23-35--?	34.50	119.67	D			F	II AT SANTA BARBARA.
01/30/1920	23-38--?	34.50	119.67	D			F	II AT SANTA BARBARA.
01/31/1920	01--?-?-?	34.50	119.67	D			F	III AT SANTA BARBARA.
01/31/1920	01-03--?	34.50	119.67	D			F	III AT SANTA BARBARA.
01/31/1920	01-07--?	34.50	119.67	D			F	III AT SANTA BARBARA.
03/20/1920	07-04--?	35.25	120.67	D			F	II AT SAN LUIS OBISPO.
05/07/1920	01-59--?	35.25	120.67	D			F	IV AT SAN LUIS OBISPO.
06/28/1920	09-01--?	35.25	120.67	D			F	V AT SAN LUIS OBISPO.
12/01/1920	01-30--?	35.17	119.50	D			F	V I AT TAFT - MANY PEOPLE MADE "SEASICK", DISHES SHAKEN FROM SHELVES. IV AT MARICOPA.
12/05/1920	11-58--?	34.50	119.67	D			F	V IN SANTA BARBARA COUNTY MOUNTAINS, V AT LOMPOC, LOS ALAMOS, MARICOPA, OJAI, AND SANTA BARBARA.
12/06/1920	-?-?-?-?	35.25	120.67	D			F	SAN LUIS OBISPO.
03/10/1922	11-21-20	35.75	120.25	C	6.5	43	F	IX IN CHOLAME VALLEY REGION OF SAN ANDREAS FAULT. FELT OVER AN AREA OF 100,000 SQ. MI. - CRACKS IN THE GROUND AND NEW SPRINGS. VII-VIII AT PARKFIELD AND SHANDON. VI-VII AT SAN LUIS OBISPO AND SIMMLER, AND V AT LOS ANGELES.

DCPP UNITS 1 & 2 FSAR UPDATE

TABLE 2.5-1

MMDD/YY	HR/MIN/SE	NORTH LAT	WEST LONG	QUALITY	MAG.	STA. REC.	FELT	MAXIMUM INTENSITY - COMMENTS
03/16/1922	23-10--?	35.75	120.33	D			F	VI IN CHOLAME VALLEY - RATHER STRONG AFTERSHOCKS, V AT PASO ROBLES AND SAN LUIS OBISPO, AND IV AT ANTELOPE VALLEY; ALSO IV AT SHANDON.
03/19/1922	11--?-?	35.67	120.67	D			F	III AT PASO ROBLES.
03/23/1922	10--?-?	35.67	120.67	D			F	III AT PASO ROBLES.
03/25/1922	12--?-?	35.67	120.67	D			F	III AT PASO ROBLES.
05/31/1922	01-25--?	35.67	120.67	D			F	III AT PASO ROBLES; 2 SHOCKS.
07/05/1922	19--?-?	34.75	120.25	D			F	LOS ALAMOS.
07/09/1922	12--?-?	34.75	120.25	D			F	LOS ALAMOS.
07/11/1922	03--?-?	34.75	120.25	D			F	LOS ALAMOS.
07/11/1922	15-30--?	34.75	120.25	D			F	LOS ALAMOS.
08/18/1922	05-12--?	35.75	120.33	D			F	VII IN CHOLAME VALLEY; V AT PASO ROBLES AND SAN LUIS OBISPO.
08/20/1922	21-14--?	35.50	120.67	D			F	III AT ATASCADERO.
09/04/1922	10-15--?	35.67	120.67	D			F	IV AT PASO ROBLES.
09/05/1922	09-05--?	35.25	120.67	D			F	V AT SAN LUIS OBISPO; 2 SHOCKS.
12/29/1922	11--?-?	35.67	120.67	D			F	III AT PASO ROBLES.
12/29/1922	12--?-?	35.67	120.67	D			F	III AT PASO ROBLES.
03/12/1923	06--?-?	34.75	120.25	D			F	LOS ALAMOS.
05/04/1923	22-45--?	35.25	120.67	D			F	V AT SAN LUIS OBISPO; 2 SHOCKS, SECOND EQUALED INTENSITY II.
05/08/1923	05-02--?	35.75	120.33	D			F	II AT CHOLAME.
06/16/1923	20-40--?	35.67	120.67	D			F	IV AT PASO ROBLES - DURATION 15-20 SECONDS.
06/25/1923	13-21--?	35.25	120.67	D			F	II AT SAN LUIS OBISPO.
12/19/1923	07-35--?	34.92	120.42	D			F	II AT SANTA MARIA - DURATION 20 SECONDS.
07/02/1924	58-02--?	34.50	119.67	D			F	SANTA BARBARA.
12/30/1924	12-17--?	34.50	119.67	D			F	SANTA BARBARA.
12/30/1924	14-15--?	34.50	119.67	D			F	SANTA BARBARA.
06/29/1925	14-42-16	34.30	119.80	B	6.3	1	F	IX AT SANTA BARBARA; FELT OVER AN AREA OF 100,000 SQ. MI. - RECORDED WORLD-WIDE. RUPTURE AT DEPTH ON THE MESA AND RECORDED WORLD-WIDE. RUPTURE AT DEPTH ON THE MESA AND SANTA YNEZ FAULTS (BAILEY WILLIS); A FEW DEATHS, SEVERAL MILLION DOLLARS DAMAGE; IX AT GOLETA, NAPLES, AND SANTA BARBARA; VIII AT GAVIOTA, MIRAMAR, AND SANTA YNEZ, LOS ALAMOS, LOS OLIVOS; VII AT ARROYO GRANDE, NIPOMO, ORCOTT, ALAMOS, LOS OLIVOS; VII AT ARROYO GRANDE, NIPOMO, ORCOTT, PISMO BEACH, SANTA MARIA, AND VENTURA, AND VI AT AVILA, LOMPOC, AND PORT SAN LUIS.
06/29/1925	15-20--?	35.25	120.67	D			F	III AT SAN LUIS OBISPO.
06/29/1925	16-35--?	34.50	119.67	D			F	SANTA BARBARA; II AT OXNARD.
06/29/1925	18-54--?	34.50	119.67	D			F	IV AT SANTA BARBARA; II AT OXNARD - STRONGEST AFTERSHOCK OF THE DAY.
06/30/1925	01-37--?	34.50	119.67	D			F	SANTA BARBARA.
06/30/1925	02-47--?	34.50	119.67	D			F	SANTA BARBARA.
06/30/1925	09-19--?	34.50	119.67	D			F	SANTA BARBARA - VIOLENT; FELT AT OJAI AND OXNARD.

DCPP UNITS 1 & 2 FSAR UPDATE

TABLE 2.5-1

MM/DD/YY	HR/MIN/SE	NORTH LAT	WEST LONG	QUALITY	MAG.	STA. REC.	FELT	MAXIMUM INTENSITY - COMMENTS
07/03/1925	16-38--?	34.50	119.67	D			F	VII AT SANTA BARBARA; III AT PASADENA AND OJAI - STIFF TREMOR AT VENTURA.
07/03/1925	18-21--?	34.50	119.67	D			F	VII AT SANTA BARBARA - STRONGEST AFTERSHOCK; FELT AT LOS ANGELES, OJAI, AND PASADENA.
07/03/1925	18-46--?	34.50	119.67	D			F	SANTA BARBARA.
07/04/1925	19-18--?	34.50	119.67	D			F	SANTA BARBARA - ANOTHER SHOCK FELT LATER IN DAY.
07/05/1925	12--?--?	34.50	119.67	D			F	SANTA BARBARA; 11 SHOCKS IN THE NEXT 19 HOURS.
07/06/1925	21-45--?	34.50	119.67	D			F	SANTA BARBARA - SEVERAL FAIRLY SEVERE SHOCKS.
07/09/1925	--?--?--?	34.50	119.67	D			F	SANTA BARBARA.
07/20/1925	09-50--?	34.50	119.67	D			F	SANTA BARBARA.
07/29/1925	14--?--?	34.50	119.67	D			F	V AT WASIOJA - CEMENT WALK CRACKED.
07/30/1925	09-50--?	34.50	119.67	D			F	SANTA BARBARA.
07/30/1925	12--?--?	34.50	119.67	D			F	SANTA BARBARA.
08/13/1925	11--?--?	34.50	119.67	D			F	SANTA BARBARA - 5 LIGHT SHOCKS DURING NIGHT; THE STRONGEST TOOK PLACE JUST BEFORE 11--?--?.
10/04/1925	--?--50--?	34.50	119.67	D			F	SANTA BARBARA.
10/08/1925	21-30--?	34.50	119.67	D			F	SANTA BARBARA.
10/30/1925	09-45--?	34.50	119.67	D			F	SANTA BARBARA.
10/30/1925	13-30--?	34.50	119.67	D			F	SANTA BARBARA AND VENTURA.
02/18/1926	18-18--?	34.17	119.50	D			F	VII ORIGIN AT SEA, SW OF VENTURA; FELT ALONG COAST FROM SAN LUIS OBISPO ON NW TO SOUTH OF SANTA ANA; A DISTANCE OF 200 MI. AT SANTA BARBARA WINDOWS OF A SCHOOL WERE BROKEN, WATER PIPE IN ROUNDHOUSE WAS BROKEN. THERE WAS DAMAGE TO TELEPHONE EQUIPMENT AT SIMI. ALSO FELT AT LOS ANGELES, PASADENA, SANTA MONICA, SANTA SUSANA, AND VENTURA.
04/29/1926	12-18--?	34.67	120.17	D			F	IV AT BUELLTON.
06/18/1926	--?--?--?	34.50	119.67	D			F	SANTA BARBARA.
06/24/1926	15-30--?	34.50	119.67	D			F	V AT SANTA BARBARA.
06/29/1926	23-21--?	34.50	119.67	D			F	VII-VIII AT SANTA BARBARA - ONE PERSON KILLED BY FALLING CHIMNEY. VI AT BUELLTON AND VENTURA; ALSO FELT AT CAMARILLO, LOS ANGELES, OJAI, OXNARD, PORT HUENEME, AND SANTA PAULA - POSSIBLY SUBMARINE ORIGIN; FELT OVER AN AREA OF 30,000 SQ. MI.
07/03/1926	23--?--?	34.50	119.67	D			F	II AT SANTA BARBARA.
07/06/1926	17-45--?	34.50	119.67	D			F	V AT SANTA BARBARA.
07/25/1926	--?--?--?	36.30	120.30	D			F	(CALTECH FILE)
08/06/1926	17-42--?	34.50	119.67	D			F	IV IN SANTA BARBARA REGION; 2 SHOCKS AT OJAI - LASTED 30 SECONDS AT VENTURA WITH SHARP SHOCK AT SANTA BARBARA.
08/09/1926	04-12--?	34.50	119.67	D			F	V AT SANTA BARBARA; 2 SHOCKS AT VENTURA.
10/22/1926	10-10--?	35.67	120.67	D			F	III AT PASO ROBLES.
10/22/1926	--?--?--?	36.45	122.00	D			F	(CALTECH FILE)
12/09/1926	--?--03--?	35.67	120.67	D			F	IV AT PASO ROBLES - PROBABLY MISTIMED REPORT OF SHOCK AT --? 41--?
12/09/1926	--?--41--?	35.25	120.67	D			F	NE OF SAN LUIS OBISPO; AT SAN LUIS OBISPO DURATION 20 SECONDS; FELT AT COALINGA WITH ORIGIN ABOUT 120 MI. FROM MT HAMILTON.

DCPP UNITS 1 & 2 FSAR UPDATE

TABLE 2.5-1

MM/DD/YY	HR/MIN/SE	NORTH LAT	WEST LONG	QUALITY	MAG.	STA. REC.	FELT	MAXIMUM INTENSITY - COMMENTS
12/27/1926	09-19--?	36.17	120.33	D			F	VI NEAR COALINGA; FELT OVER AN AREA OF 25,000 SQ. MI. FELT AT FIREBAUGH, FRESNO, LOS BANOS, MENDOTA, OAKDALE, OILFIELDS, PORTERVILLE, AND SAN LUIS OBISPO.
11/04/1927	11--?-?	34.58	120.67	D			F	LOMPOC, POINT ARGUELLO, AND SAN LUIS OBISPO.
11/04/1927	11-30--?	34.58	120.67	D			F	LOMPOC.
11/04/1927	13-50-53	34.54	121.40	A	7.3	3	F	X AT SEA, WEST OF POINT ARGUELLO. AREA SHAKEN WITH INTENSITY VI OR GREATER WAS 40,000 SQ. MI. A SMALL SEA WAVE WAS PRODUCED, RECORDED ON TIDE GAUGES AT SAN DIEGO AND SAN FRANCISCO, AND OBSERVED AS 6 FEET HIGH AT SURF; IX AT HONDA, ROBERDS RANCH, SURF, AND WHITE HILLS, VIII AT ARLIGHT, ARROYO GRANDE, BERROS, BETTERAVIA, CAMBRIA, CASMALIA, CAYUCOS, GUADOCEANO, PISMO BEACH, POINT CONCEPTION, SAN JULIAN RANCH, SAN LUIS OBISPO, AND SANTA MARIA. VI-VII AT GUADOCEANO, PISMO BEACH, POINT CONCEPTION, SAN JULIAN RANCH, SAN LUIS OBISPO, AND SANTA MARIA. VI-VII AT ALUPE, HALCYON, HARRISTON, HUASNO, LOMPOC, LOS ALAMOS, LOS OLIVOS, MORRO BAY, NIPOMO, ADELAIDA, ATASCADERO, BAKERSFIELD, BICKNELL, BUTTONWILLOW, CARPINTERIA CHOLAME, CRESTON, EDNA GAVIOTA, GOLETA, HARMONY, KING CITY, LAS CRUCES, NAPLES, OXNARD, PASO ROBLES, REWARD, SANTA BARBARA, SANTA MARGARITA, SANTA YNEZ, SOLVANG, TAFT, TEMPLETON, VENTURA, AND WASIOJA; AND IV-V AT ANNETTE, BIG SUR, CASTROVILLE, COALINGA, FELLOWS, GONZALES, GORMAN, HOLLISTER, LOCKWOOD, LUCIA, MCKITTRICK, MONTEREY, PARKFIELD, PATTIWAY, PORT SAN LUIS, POZO PRIEST, SALINAS, SANGER, SAN LUCAS, SAN SIMEON, SANTA PAULA, SCHEIDECK, SESPE, SIMMLER, SOLEDAD, AND TEHACHAPI. DATA FROM BSSA V. 17, P. 258 AND V. 20, P. 53.
11/04/1927	14-12--?	34.58	120.67	D			F	SANTA MARIA - AFTERSHOCK
11/04/1927	14-14--?	34.58	120.67	D			F	SANTA MARIA - AFTERSHOCK.
11/04/1927	15--?-?	34.58	120.67	D			F	SAN LUIS OBISPO - AFTERSHOCK.
11/04/1927	15-42--?	34.58	120.67	D			F	SANTA MARIA - AFTERSHOCK.
1/05/1927	08-17--?	34.58	120.67	D			F	POINT ARGUELLO - AFTERSHOCK; MILD AT SURF.
11/05/1927	09--?-?	34.58	120.67	D			F	POINT ARGUELLO - AFTERSHOCK; REPORTED FROM PASO ROBLES TO HADLEY TOWER.
11/05/1927	11-37--?	34.58	120.67	D			F	POINT ARGUELLO - AFTERSHOCK; REPORTED FROM SURF TO HADLEY TOWER, AND SOUTH OF SAN LUIS OBISPO.
11/06/1927	-?-06--?	34.67	120.17	D			F	IV AT BUELLTON.
11/06/1927	02-25--?	34.67	120.17	D			F	POINT ARGUELLO - AFTERSHOCK; STRONGEST IMMEDIATE AFTERSHOCK AT LOMPOC.
11/06/1927	03-10--?	34.67	120.17	D			F	IV AT BUELLTON.
11/06/1927	22-10--?	34.67	120.17	D			F	OFF POINT CONCEPTION.
11/06/1927	22-50--?	34.67	120.17	D			F	IV AT BUELLTON.
11/06/1927	23-10--?	34.67	120.17	D			F	OFF POINT CONCEPTION.
11/08/1927	10-10--?	34.67	120.17	D			F	IV AT BUELLTON - SHARP BUMPING AT 10-02--?; AROUSED NEARLY ALL. AT LOMPOC MANY AWAKENED BY SHOCK AT 10-15--?.

DCPP UNITS 1 & 2 FSAR UPDATE

TABLE 2.5-1

MM/DD/YY	HR/MIN/SE	NORTH LAT	WEST LONG	QUALITY	MAG.	STA. REC.	FELT	MAXIMUM INTENSITY - COMMENTS
11/19/1927	03-32--?	34.92	120.42	D			F	VII AT SANTA MARIA - CENTERED TO NW OF ORIGIN OF NOVEMBER 4 QUAKE -WEAKER, YET NEARLY AS STRONG AT SANTA MARIA, AND VI AT BETTERAVIA AND BICKNELL; REPORTED FROM SAN MIGUEL AND PARKFIELD ON THE NORTH TO SANTA BARBARA CHANNEL ON THE SOUTH.
12/05/1927	11-45--?	34.58	120.67	D			F	IV AT POINT ARGUELLO, AND IV AT BUELLTON WITH 2 SHOCKS 15 SECONDS APART; FELT AT GUADALUPE, SANTA MARGARITA, SANTA MARIA AND SURF.
12/31/1927	10-10--?	34.58	120.67	D			F	V AT POINT ARGUELLO.
03/15/1928	12-03--?	34.92	120.42	D			F	SANTA MARIA.
03/15/1928	12-20--?	34.50	119.67	D			F	SANTA BARBARA.
03/16/1928	14-30--?	34.92	120.42	D			F	SANTA MARIA.
03/29/1928	06-25--?	34.92	120.42	D			F	VII AT SANTA MARIA.
06/09/1928	08-22--?	35.17	119.50	D			F	TAFT.
06/09/1928	08-31--?	35.17	119.50	D			F	TAFT.
06/09/1928	12-25--?	35.17	119.50	D			F	TAFT.
09/03/1928	04-01-54	34.50	122.50	D	5.0	1	F	OFF POINT ARGUELLO - LICK OBSERVATORY S-P= 39 SECONDS.
11/02/1928	05--?-?	34.67	120.42	D			F	LOMPOC.
05/28/1929	07-10--?	36.17	120.33	D			F	COALINGA.
07/03/1929	09-24--?	34.50	119.67	D			F	SANTA BARBARA.
07/12/1929	13-10--?	36.17	120.33	D			F	COALINGA.
08/28/1929	18-10--?	34.50	119.67	D			F	SANTA BARBARA.
09/09/1929	05-15--?	34.50	119.67	D			F	SANTA BARBARA.
09/16/1929	03-16--?	35.42	120.92	D			F	GAVIOTA, NAPLES, AND SANTA BARBARA.
09/16/1929	06-15--?	35.42	120.92	D			F	CAYUCOS.
10/05/1929	20-03--?	36.17	120.33	D			F	CAYUCOS.
10/06/1929	21-14--?	36.17	120.33	D			F	COALINGA AND LIGHTHIPE.
10/07/1929	08--?-?	36.17	120.33	D			F	COALINGA.
10/07/1929	11-30--?	34.83	120.42	D			F	COALINGA.
10/11/1929	17-55--?	36.17	120.33	D			F	ORCUTT.
10/15/1929	22-02--?	36.17	120.33	D			F	COALINGA, KETTLEMEN HILLS, OILFIELDS, AND PRIEST VALLEY, HANFORD.
11/07/1929	06-30--?	36.33	119.67	D			F	BITTER WATER, COALINGA, AND MCKITTRICK.
11/09/1929	02-30--?	36.17	120.33	D			F	BITTER WATER.
11/20/1929	22-50--?	36.42	121.00	D			F	BITTER WATER.
11/24/1929	09-54--?	36.42	121.00	D			F	LONOAK, BITTER WATER, AND LEWIS CREEK.
11/26/1929	08-05--?	36.42	121.00	D			F	V AT BITTER WATER AND SAN ARDO; FELT FROM HOLLISTER TO SANTA MARGARITA.
11/26/1929	09--?-?	36.42	120.83	D			F	SANTA MARGARITA.
11/26/1929	18-06--?	36.42	121.00	D			F	HIERNANDEZ.
12/05/1929	07-40--?	36.33	119.67	D			F	BITTER WATER.
03/11/1930	23-59--?	36.42	121.25	D			F	HANFORD.
06/21/1930	05-15--?	34.83	120.50	D			F	PINNACLES.
08/05/1930	11-25--?	34.42	119.50	D			F	CASMALIA.
08/08/1930	16-46--?	34.42	119.67	D			F	NEAR SANTA BARBARA - FELT OVER AN AREA OF 9000 SQ. MI. V-VI AT CARPINTERIA, GOLETA, OJAI, OXNARD, AND SANTA BARBARA.
08/18/1930	13-09--?	34.33	120.58	D			F	SANTA BARBARA AND GOLETA.
							F	OFF POINT CONCEPTION; V OVER A LAND AREA OF 500 SQ. MI. NEAR POINT CONCEPTION.

DCPP UNITS 1 & 2 FSAR UPDATE

TABLE 2.5-1

MM/DD/YY	HR/IN/SE	NORTH LAT	WEST LONG	QUALITY	MAG.	STA. REC.	FELT	MAXIMUM INTENSITY - COMMENTS
08/28/1930	05-15--?	36.42	121.33	D			F	SOLEDAD.
09/02/1930	13-35--?	35.00	121.00	D			F	OFF COAST - FELT AT HALCYON AND SAN LUIS OBISPO.
09/09/1930	05-27--?	34.42	119.50	D			F	SANTA BARBARA.
10/02/1930	14-18--?	34.58	120.67	D			F	OFF POINT ARGUELLO - FELT AT HALCYON.
10/28/1930	13-57--?	35.42	120.92	D			F	OFF COAST NEAR CAYUCOS - FELT AT NIPOMO.
12/08/1930	01-23--?	34.50	119.67	D			F	GOLETA AND SANTA BARBARA.
12/08/1930	01-29--?	34.50	119.67	D			F	GOLETA AND SANTA BARBARA.
02/21/1931	08-10--?	35.67	121.33	D			F	NW OF SAN LUIS OBISPO - FELT AT BRYSON AND PIEDRAS BLANCAS.
02/23/1931	10-01--?	35.83	120.50	D			F	OVER AN AREA OF 5000 SQ. MI.; V AT CAYUCOS, PARKFIELD, AND TEMPLETON.
02/23/1931	10-33--?	35.83	120.50	D			F	SAME AS ABOVE.
04/05/1931	03--?--?	36.17	121.00	D			F	SE OF KING CITY.
07/15/1931	18-40--?	35.00	120.58	D			F	GUADALUPE, NIPOMO, AND SANTA MARGARITA.
07/21/1931	03-25--?	35.25	120.67	D			F	SAN LUIS OBISPO.
07/21/1931	12-08--?	35.25	120.67	D			F	IV AT HALCYON, LOS ALAMOS, NIPOMO, OCEANO, AND TEMPLETON; ALSO FELT AT CAMBRIA, GAVIOTA, PIEDRAS BLANCAS, PORT SAN LUIS, SAN LUIS OBISPO, SANTA MARGARITA, AND SANTA MARIA.
09/03/1931	13-50--?	34.50	119.67	D			F	SANTA BARBARA.
09/10/1931	14-35--?	35.50	120.67	D			F	ATASCADERO.
09/30/1931	14-35--?	35.50	120.67	D			F	ATASCADERO.
10/13/1931	12-25--?	36.33	121.67	D			F	JAMESBURG.
10/18/1931	19-58--?	36.33	121.67	D			F	IV AT HOLLISTER, JAMESBURG, AND SPRECKLES; ALSO FELT AT APTOS, CARMEL, CHUALAR, MOSS LANDING, MONTEREY, PARISO, SALINAS, AND SANTA CRUZ.
12/04/1931	-?-53--?	36.50	121.67	D			F	10 MI. S OF SPRECKLES. FELT AT HOLLISTER, METZ, PIGEON POINT, SPRECKLES, AND SANTA CRUZ.
02/04/1932	16-02-58	34.55	119.73	C	3.0	1	F	SANTA BARBARA AND VENTURA.
02/05/1932	04-14-45	35.83	121.47	C	3.5	1	F	COAST OF MONTEREY COUNTY; FELT AT PIEDRAS BLANCAS LIGHT AND SALMON CREEK.
02/05/1932	06-46-54	35.83	121.47	C	3.5	1	F	COAST OF MONTEREY COUNTY; FELT AT PIEDRAS BLANCAS LIGHT AND SALMON CREEK.
02/05/1932	07-10--?	35.83	121.47	C			F	AFTERSHOCK OF PRECEDING.
02/26/1932	16-58--?	36.00	121.00	C	5.0		F	IV AT APTOS, ASILOMAR, CARMEL, DEL MONTE, GONZALES, METZ, MONTEREY, PACIFIC GROVE, AND PEBBLE BEACH.
03/13/1932	23-09-24	34.44	120.17	B	3.5	1	F	OFF POINT CONCEPTION; FELT AT BUELLTON.
04/21/1932	03-36-20	35.50	120.67	D	3.0		F	ATASCADERO.
05/06/1932	03-37-08	36.00	120.50	C	3.0	1	F	PARKFIELD.
06/27/1932	05-17-25	36.00	122.00	D	4.0		F	COAST OF MONTEREY COUNTY.
10/24/1932	04-45--?	35.75	120.75	D			F	PASO ROBLES.
01/30/1933	17--?--?	34.67	120.42	D			F	LOMPOC.
02/26/1933	09-34-32	36.40	121.30	D			F	III AT HOLLISTER, SALINAS, AND SPRECKLES.
04/12/1933	10-03--?	36.33	121.75	D			F	IV AT PORTERVILLE AND VISALIA.
06/26/1933	06-26--?	34.42	120.50	D			F	V AT BUELLTON AND POINT CONCEPTION.
06/26/1933	06-29--?	34.42	120.50	D			F	V AT BUELLTON AND POINT CONCEPTION.
01/09/1934	12-48--?	35.13	120.08	C	3.0		F	

DCPP UNITS 1 & 2 FSAR UPDATE

TABLE 2.5-1

MMDD/YY	HR/MIN/SE	NORTH LAT	WEST LONG	QUALITY	MAG.	STA. REC.	FELT	MAXIMUM INTENSITY - COMMENTS
01/12/1934	12-50--?	34.45	120.15	D			F	IV AT LOS ALAMOS.
02/01/1934	16-09--?	34.55	119.53	B	3.5		F	II AT SANTA BARBARA.
02/11/1934	15-16--?	34.55	119.53	C	2.0			
03/20/1934	11-48--?	36.00	120.00	D	3.0			
05/06/1934	20-14--?	35.83	120.75	B	3.5			
05/10/1934	11-28--?	34.50	119.58	C	3.0			
05/19/1934	06-37--?	34.58	120.75	D	3.0			
05/24/1934	06-52--?	34.42	119.75	C	2.5			
05/24/1934	09-04--?	34.42	119.75	C	2.5			
05/24/1934	11-18--?	34.42	119.75	C	2.0			
06/05/1934	09-51--?	35.80	120.33	D			F	COALINGA AND KETTLEMAN HILLS; ALSO FELT AT MONTEREY AND SANTA CRUZ.
06/05/1934	11-30--?	35.80	120.33	D			F	SAN MIGUEL AND SHANDON.
06/05/1934	11-47--?	35.80	120.33	B	3.0			
06/05/1934	13-46--?	35.80	120.33	C	3.0			
06/05/1934	21-30--?	35.80	120.33	D			F	SAN MIGUEL.
06/05/1934	21-48--?	35.80	120.33	B	5.0		F	V AT ADELAIDA, PARKFIELD, AND PRIEST, IV AT ATASCADERO, AVENAL, BIG SUR, BRYSON, CARMEL, HANFORD, KING CITY, LEMOORE, LONOK, PARAISO, SAN MIGUEL, SANTA CRUZ, SHANDON, AND TEMPLETON, II AT APTOS, BOULDER CREEK, CAMBRIA, CHUALAR, COALINGA, GONZALES, HOLLISTER, MONTEREY, MORRO BAY, PASO ROBLES, SALINAS, SAN FRANCISCO, SAN JOAQUIN VALLEY, SAN LUIS OBISPO, SOLEDAD, SPRECKLES, ETC.; NOT FELT AT ANTIOCH, ETC., BAKERSFIELD, FRESNO, GILROY, LIVERMORE, LOS GATOS, MARICOPA, MERCED, MODESTO, MORGAN HILL, REDWOOD CITY, SAN JOSE, SANTA MARIA, TULARE, OR WATSONVILLE.
06/05/1934	22-52--?	35.80	120.33	C	4.0		F	VI AT ADELAIDA; IV AT ATASCADERO.
06/05/1934	23-30--?	35.80	120.33	D			F	V AT LEMOORE; ALSO FELT AT CASTROVILLE.
06/06/1934	-?-55--?	35.80	120.33	C	3.0			
06/06/1934	16-40--?	35.80	120.33	C	3.5			
06/06/1934	22-40--?	35.80	120.33	C	3.5		F	ADELAIDA, GRAEAGLE, AND PAYNES CREEK. STONE CANYON.
06/07/1934	22-30--?	35.80	120.33	D			F	IV AT GONZALES AND MCKITTRICK.
06/08/1934	04-15--?	35.80	120.33	D			F	VI TO VII AT CHOLOME RANCH; PARKFIELD, AND STONE CANYON DURATION 30 SECONDS, DAMAGE SLIGHT, V AT ATASCADERO, AT ANTELOPE, BIG SUR, CAMBRIA, CASTROVILLE, DELANO, MONTEREY, PASO ROBLES, SAN LUIS OBISPO, SANTA BARBARASANTA MARGARITA, SANTA MARIA, SOLEDAD, TAFT, VENTURA, VISALIA, ETC., AND III OR LESS AT ARVIN, BAKERSFIELD, FRESNO, KERNVILLE, LOMPOC, LOS ANGELES, MENDOTA, PORTERVILLE, SALINAS, SAN BENITO, SANTA ANA, SANTA BARBARA, TULARE, WATSONVILLE, ETC.; NOT FELT AT BIG BASIN, CAJON, COYOTE, GILROY, HUNTINGTON BEACH, INDEPENDENCE, INYOKERN, LANCASTER, MERCED, POMONA, OR SAN JOSE.
06/08/1934	04-30--?	35.80	120.33	B	5.0		F	IV AT PIEDRAS BLANCAS, SAN LUIS OBISPO, AND SANTA CRUZ; ALSO FELT AT BRYSON AND LOS ALAMOS.
06/08/1934	04-37--?	35.60	121.30	D			F	

DCPP UNITS 1 & 2 FSAR UPDATE

TABLE 2.5-1

MM/DD/YY	HR/IN/SE	NORTH LAT	WEST LONG	QUALITY	MAG.	STA. REC.	FELT	MAXIMUM INTENSITY - COMMENTS
06/08/1934	04-45--?	35.80	120.33	D			F	ATASCADERO, COALINGA, LOCKWOOD, PASO ROBLES, PORT SAN LUIS, PRIEST, SAN MIGUEL, AND WESTHAVEN.
06/08/1934	04-47--?	35.80	120.33	B	6.0		F	WITHIN A RADIUS OF 250 KM FROM THE EPICENTER NEAR THE SOUTHEASTERN ANGLE OF MONTEREY COUNTY: VII TO VIII AT PARKFIELD, VI AT COALINGA, KETTLEMAN CITY, LEMOORE, AND STONE CANYON, V AT ATASCADERO, DUDLEY, HOLLISTER, KING CITY, OILFIELDS, SAN MIGUEL, SEASIDE, SHALE PUMP STATION, AND SHANDON, IV AT ANTELOPE, AVILA, CANOGA PARK, HANFORD, LOS ALAMOS, MARICOPA, MORRO BAY, NIPOMO, PASO ROBLES, PRIEST, SAN LUIS OBISPO, SANTA CRUZ, SANTA MARIA, SOLEDAD, VISALIA ETC., AND III OR LESS AT APTOS, FRESNO, KERNVILLE, LONE PINE, LOS BANOS, MENDOTA, MONTEREY, OAKLAND HARBOR, SALINAS, SAN BENITO, SANTA ANA, TEHACHAPI, TULARE, ETC.
06/08/1934	05--?-?	35.60	121.30	D			F	PIEDRAS BLANCAS LIGHT; ALSO BRYSON, KERNVILLE, LA PANZA, LEMOORE, PARKFIELD, SANDBERG, AND SAN FERNANDO.
06/08/1934	05-20--?	35.80	120.33	D			F	III AT ATASCADERO.
06/08/1934	05-23--?	35.80	120.33	C	3.5		F	ATASCADERO AND SAN MIGUEL.
06/08/1934	05-36--?	35.80	120.33	C	3.0		F	
06/08/1934	05-42--?	35.80	120.33	B	4.5		F	ATASCADERO, BIG SUR, COALINGA, KING CITY, PASO ROBLES, AND WESTHAVEN.
06/08/1934	05-50--?	35.80	120.33	D			F	IV AT ATASCADERO; ALSO FELT AT COALINGA AND SAN LUIS OBISPO.
06/08/1934	09-30--?	35.80	120.33	B	4.0		F	ATASCADERO AND PARKFIELD.
06/08/1934	15-30--?	35.80	120.33	C	3.5		F	
06/08/1934	16-30--?	35.80	120.33	D			F	PARKFIELD.
06/08/1934	23-23--?	35.80	120.33	B	4.0		F	NEAR PARKFIELD.
06/10/1934	06-47--?	35.80	120.33	C	3.0		F	
06/10/1934	08-03--?	35.80	120.33	B	4.5		F	NEAR PARKFIELD; IV AT SAN MIGUEL.
06/10/1934	20-02--?	35.80	120.33	D			F	IV AT SAN MIGUEL; ALSO PARKFIELD AND WOODY.
06/11/1934	03-25--?	35.80	120.33	C	3.0		F	
06/12/1934	10-47--?	35.80	120.33	C	3.5		F	
06/14/1934	14-55--?	35.80	120.33	C	4.0		F	IV AT ATASCADERO; ALSO FELT AT SAN MIGUEL AND TEMPLETON.
06/14/1934	15-54--?	35.80	120.33	C	4.0		F	III AT ATASCADERO AND SAN MIGUEL.
06/14/1934	19-26--?	35.80	120.33	C	4.5		F	ATASCADERO AND TEMPLETON.
06/14/1934	22-02--?	35.80	120.33	C	3.5		F	ATASCADERO.
06/15/1934	04-48--?	35.80	120.33	C	3.0		F	
06/16/1934	23-03--?	36.50	121.00	D	4.0		F	IV AT HOLLISTER AND MONTEREY, AND III AT GONZALES, PARKFIELD, AND SALINAS.
07/02/1934	18-44--?	35.80	120.33	B	3.0		F	
08/04/1934	-?-18--?	35.80	120.33	B	3.0		F	
08/21/1934	03-37--?	36.08	120.58	D			F	IV IN STONE CANYON.
08/25/1934	18-52--?	34.42	119.75	C	2.5		F	
08/26/1934	03-02--?	35.57	119.85	B	3.0		F	
09/06/1934	23-24--?	36.00	120.55	C	3.0		F	
09/16/1934	14-38--?	35.83	120.33	C	3.5		F	
10/07/1934	-?-18--?	34.55	120.78	C	3.5		F	

DCPP UNITS 1 & 2 FSAR UPDATE

TABLE 2.5-1

MMDD/YY	HR/MIN/SE	NORTH LAT	WEST LONG	QUALITY	MAG.	STA. REC.	FELT	MAXIMUM INTENSITY - COMMENTS
10/08/1934	04-57--?	34.50	119.58	C	2.0			
10/10/1934	10-52--?	34.55	120.78	C	3.0			
10/19/1934	15-39--?	35.80	120.33	C	3.0			
11/04/1934	22-17--?	34.53	119.67	B	3.0			
11/21/1934	01-02--?	34.58	119.62	B	2.5			
12/01/1934	13-05--?	36.00	121.50	D			F	15 MI. S OF PARAISO; V AT PIEDRAS BLANCAS LIGHT AND IV AT PARAISO.
12/02/1934	16-07--?	35.97	120.58	C	4.0		F	SAN MIGUEL.
12/03/1934	01-54--?	35.95	121.50	C	4.5		F	IV AT BRYSON, KING CITY, AND PARAISO; ALSO FELT AT PARKFIELD, PASO ROBLES, SAN LUCAS, AND SAN MIGUEL.
12/17/1934	11-10--?	34.58	120.33	B	4.5		F	VI AT LOS ALAMOS.
12/17/1934	13-51--?	34.58	120.33	C	2.5		F	LOS ALAMOS.
12/17/1934	15-16--?	34.55	119.67	C	2.5		F	LOS ALAMOS.
12/17/1934	15-35--?	34.58	120.33	C	2.5		F	LOS ALAMOS.
12/17/1934	03-09--?	34.58	120.33	C	4.0		F	LOS ALAMOS.
12/18/1934	04-34--?	34.58	120.33	C	3.0		F	LOS ALAMOS.
12/18/1934	05-28--?	34.58	120.33	C	3.0		F	LOS ALAMOS.
12/19/1934	20-39--?	34.28	119.50	B	2.5		F	LOS ALAMOS.
12/20/1934	12-37--?	34.58	120.33	C	2.5		F	LOS ALAMOS.
12/20/1934	12-39--?	34.58	120.33	C	3.0		F	LOS ALAMOS.
12/20/1934	22-21--?	34.58	120.33	C	3.0		F	LOS ALAMOS.
12/23/1934	16-08--?	34.58	120.33	C	2.5		F	LOS ALAMOS.
12/24/1934	10-22--?	34.58	120.33	B	3.0		F	LOS ALAMOS.
12/24/1934	16-26--?	35.93	120.48	B	5.0		F	IV AT LOS ALAMOS AND SHANDON; ALSO FELT AT KING CITY TEMPLETON.
12/25/1934	04-03--?	34.58	120.33	C	3.0		F	IV AT PARKFIELD; ALSO FELT AT SHANDON.
01/06/1935	04-04--?	35.98	120.48	C	4.0		F	IV AT PARKFIELD.
01/06/1935	04-25--?	35.90	120.45	D			F	IV AT PARKFIELD AND III AT SHANDON.
01/06/1935	04-40--?	35.98	120.48	C	4.0		F	
01/07/1935	-?-11--?	35.75	119.67	D	3.0		F	
01/23/1935	03-16--?	34.58	120.33	C	3.5		F	IV AT LOS ALAMOS.
01/27/1935	09-49--?	34.50	119.62	C	2.5		F	
02/18/1935	04-02--?	35.93	120.48	C	3.5		F	
02/19/1935	14-17--?	35.93	120.48	D	3.0		F	
02/28/1935	19-06--?	35.80	120.33	C	3.0		F	
03/03/1935	11-26--?	36.42	121.75	C	3.0		F	
03/06/1935	23-14--?	34.43	119.87	C	3.5		F	III AT SANTA BARBARA.
03/19/1935	03-59--?	34.55	120.78	B	4.0		F	OFF POINT ARGUELLO.
04/05/1935	10-13--?	35.93	120.48	C	3.5		F	
05/05/1935	12-58--?	34.58	119.68	C	2.5		F	
05/18/1935	04-36--?	34.58	120.33	B	3.5		F	IV AT LOS ALAMOS.
05/19/1935	03-44--?	34.58	120.33	C	3.0		F	
05/20/1935	23-44--?	34.58	120.33	C	3.0		F	
05/27/1935	16-08--?	35.37	120.97	C	3.0		F	III AT TEMPLETON.
06/10/1935	02-02--?	35.33	119.83	C	3.5		F	
06/18/1935	08-52--?	34.60	119.60	C	2.0		F	
06/23/1935	23-53--?	34.55	119.68	C	3.0		F	

DCPP UNITS 1 & 2 FSAR UPDATE

TABLE 2.5-1

MM/DD/YY	HR/MI/SE	NORTH LAT	WEST LONG	QUALITY	MAG.	STA. REC.	FELT	MAXIMUM INTENSITY - COMMENTS
06/30/1935	23-28--?	36.00	121.00	D	4.0		F	SE OF SALINAS; III AT HOLLISTER.
07/25/1935	04-16--?	35.80	120.33	C	3.0		F	V AT PARKFIELD.
07/28/1935	06--?-?	35.70	121.12	B	4.0		F	SAN SIMEON.
08/06/1935	19-05--?	34.62	119.62	C	3.0		F	SANTA BARBARA.
08/07/1935	22-30--?	34.55	120.78	C	3.5		F	PRIEST VALLEY.
08/09/1935	17-14--?	36.17	120.98	C	3.5		F	
08/31/1935	09-28--?	34.50	119.70	C	2.5		F	IV AT PARKFIELD - AFTERSHOCK.
10/18/1935	09-24--?	35.80	120.70	D	3.5		F	PARKFIELD.
10/22/1935	18-37--?	35.93	120.48	C	4.0		F	13 MI. W OF SOLEDAD; IV AT SAN BENITO.
10/25/1935	19-43--?	36.40	121.55	D			F	AFTERSHOCK.
10/26/1935	10-46--?	35.85	121.40	D	3.0		F	
12/22/1935	06-54--?	34.55	120.78	C	3.0		F	
02/03/1936	09-12--?	34.75	119.75	C	2.5		F	
02/21/1936	23-06--?	34.42	119.67	C	3.0		F	
02/22/1936	-?-18--?	34.42	119.67	C	2.5		F	
02/22/1936	-?-21--?	34.42	119.67	C	3.0		F	
02/22/1936	-?-23--?	34.42	119.67	C	3.0		F	
02/22/1936	04-55--?	34.42	119.67	C	3.0		F	
03/06/1936	03-45--?	35.90	120.40	D	3.0		F	IV AT CHUALAR, HOLLISTER, AND TRES PINOS.
03/17/1936	01-55--?	36.50	120.92	C	4.0		F	
03/18/1936	09-07--?	35.93	120.48	C	2.5		F	
03/27/1936	-?-58--?	34.55	120.78	C	3.0		F	
03/29/1936	09-26--?	34.50	119.62	C	2.5		F	
05/20/1936	17-22--?	35.93	120.48	C	3.0		F	
05/23/1936	04-41--?	36.17	120.92	C	4.0		F	IV AT KING CITY.
05/27/1936	19-55--?	36.50	121.17	C	4.5		F	SAN BENITO COUNTY.
06/24/1936	12-23--?	35.12	120.08	C	3.0		F	SAN LUIS OBISPO CO.; IV AT LOS ALAMOS.
07/13/1936	18-09--?	34.50	119.60	D	2.5		F	
07/22/1936	04-03--?	34.50	119.80	C	2.5		F	
09/07/1936	09-36--?	34.57	119.63	C	3.0		F	
09/07/1936	16-47--?	34.37	120.38	C	3.0		F	
09/09/1936	04-54--?	34.37	120.38	C	4.0		F	
09/10/1936	21-21--?	34.40	120.40	D	3.0		F	LOS ALAMOS.
09/12/1936	13-56--?	34.75	120.33	C	3.5		F	
09/15/1936	-?-09--?	34.50	120.50	D	2.5		F	
10/16/1936	15-30--?	34.83	120.58	C	4.0		F	NEAR CASMALLIA.
10/16/1936	15-36--?	34.83	120.58	C	3.0		F	
10/17/1936	01-17--?	34.83	120.58	C	3.0		F	
10/19/1936	14-01--?	34.83	120.58	C	3.0		F	
11/01/1936	15-10--?	34.55	120.78	B	4.0		F	OFF POINT ARGUELLO.
11/02/1936	01-29--?	34.55	120.78	C	3.0		F	HOLLISTER.
11/05/1936	14-30--?	35.85	121.40	D	3.0		F	
11/08/1936	16-51--?	34.55	120.78	C	3.0		F	
11/08/1936	22-43--?	34.55	120.78	C	3.0		F	
11/18/1936	17-15--?	35.35	120.60	D			F	POZO, SAN LUIS OBISPO, AND SANTA MARGARITA.
11/18/1936	18-02--?	34.70	120.25	C	4.5		F	IV AT ARROYO GRANDE, ATASCADERO, BETTERAVIA, LOS ALAMOS OCEANO, POZO, SAN LUIS OBISPO, AND SANTA MARGARITA.

DCPP UNITS 1 & 2 FSAR UPDATE

TABLE 2.5-1

MM/DD/YY	HR/MIN/SE	NORTH LAT	WEST LONG	QUALITY	MAG.	STA. REC.	FELT	MAXIMUM INTENSITY - COMMENTS
11/22/1936	02-16--?	34.58	120.78	C	3.5			
11/25/1936	21-51--?	34.58	120.78	C	3.0			
12/23/1936	17-16--?	35.93	120.48	B	3.5			
12/26/1936	01-12--?	34.55	119.68	C	2.5			
01/12/1937	15-44--?	34.50	120.80	D	3.0			
01/28/1937	17-36--?	34.43	119.87	C	2.5			
02/16/1937	17-40--?	34.55	120.78	C	4.0			OFF POINT ARGUELLO.
02/17/1937	03-33--?	36.50	121.58	C	4.5		F	9 MI. SE OF PAICINE; FELT AT ANTELOPE, HOLLISTER, AND PANOCHÉ.
02/20/1937	09-58--?	35.93	120.48	C	4.0		F	PARKFIELD AND PASO ROBLES.
02/22/1937	18-10--?	36.17	121.53	C	4.0		F	KING CITY.
02/24/1937	13-37--?	34.50	119.70	C	2.0			
02/25/1937	03-20--?	34.50	119.70	C	2.0			
03/26/1937	21-35--?	34.60	119.70	C	3.5			
03/31/1937	17-43--?	34.50	119.70	C	3.0			
04/17/1937	08-30--?	34.60	119.70	C	2.5			
04/30/1937	08-16--?	34.50	119.70	D	2.5			
05/31/1937	15-33--?	36.50	120.70	C	3.0			
06/02/1937	09-32--?	34.40	119.70	C	2.5			
07/31/1937	14-18--?	34.22	119.55	C	3.0			
07/31/1937	15-14--?	34.22	119.55	C	2.5			
08/15/1937	19-01--?	36.50	120.70	D	3.0			
08/22/1937	01-56--?	35.00	121.00	D	3.5			
09/16/1937	02-48--?	35.93	120.48	B	3.5		F	NEAR PARKFIELD; FELT AT BRADLEY.
09/18/1937	13-29--?	36.50	121.50	D	4.0		F	9 MI. SE OF PAICINES; FELT AT CHUALAR, SALINAS, AND SPRECKLES.
09/22/1937	02-41--?	34.50	119.70	C	3.0			
09/29/1937	22-39--?	34.50	119.70	C	3.0			
10/13/1937	08-32--?	34.40	119.70	C	2.5			
11/01/1937	21-40--?	36.50	121.40	D			F	6 MI. N OF GONZALES.
11/03/1937	10--?--?	36.15	121.00	D			F	V AT SAN LUCAS; FELT ALSO AT KING CITY AND SAN ARDO.
11/22/1937	04-12--?	34.55	120.78	C	4.5		F	POINT D SANTA MARIA, AND IV AT ARLIGHT, BETTERAVIA, BICKNELL, E. GAVIOTA, GUADALUPE, LOMPOC, LOS ALAMOS, LOS OLIVOS, SANTA URF.
11/22/1937	04-51--?	34.55	120.78	C	3.5			
11/28/1937	09-55--?	34.55	120.78	C	3.5			
12/03/1937	15-28--?	34.55	120.78	C	4.0		F	OFF POINT ARGUELLO; FELT AT GAVIOTA AND POINT CONCEPTION.
12/03/1937	21-13--?	34.55	120.78	C	3.5			
12/05/1937	01-36--?	36.00	121.00	D	3.5		F	19 MI. S OF LOS BANOS; V AT LOS BANOS.
12/05/1937	01-37--?	36.00	121.00	D	4.0			SAN BENITO COUNTY.
12/05/1937	02-05--?	36.00	121.00	D	3.0		F	19 MI. S OF LOS BANOS.
12/24/1937	11-57--?	34.50	120.80	D	4.0		F	OFF POINT ARGUELLO. FELT AT CASMALIA, LOS ALAMOS, POINT CONCEPTION.
12/25/1937	13-01--?	36.00	120.00	D	3.0			
01/01/1938	01-59--?	34.55	120.78	C	3.5			

DCPP UNITS 1 & 2 FSAR UPDATE

TABLE 2.5-1

MMDD/YY	HR/MIN/SE	NORTH LAT	WEST LONG	QUALITY	MAG.	STA. REC.	FELT	MAXIMUM INTENSITY - COMMENTS
01/18/1938	04-35--?	34.55	120.78	B	3.5			
01/24/1938	04-38--?	34.55	120.78	C	3.5			
01/25/1938	12-24--?	34.55	120.78	C	3.5			
02/01/1938	18-14--?	34.55	120.78	C	3.5			
02/20/1938	14--?-?	34.55	120.78	C	3.5			
02/21/1938	10-59--?	35.93	120.78	C	3.0			
03/04/1938	15-14--?	34.30	119.57	C	2.5			
03/04/1938	18-25--?	34.30	119.57	C	2.5			
04/12/1938	01-50--?	34.55	120.78	C	3.5		F	BIG SUR, HOLLISTER, KING CITY, PINNACLES, SALINAS, SOLEDAD, SOQUEL, AND TRES PINOS-6 SHOCKS FELT AT PINNACLES.
05/10/1938	10-32--?	36.20	121.30	D	4.5		F	SAN BENITO MONTEREY COUNTY.
05/10/1938	10-41--?	36.20	121.30	D	4.0		F	SANTA BARBARA.
05/13/1938	19-34--?	36.20	121.30	D	4.0		F	PINNACLES.
05/27/1938	22-03--?	36.20	120.00	D	3.5		F	OVER AN AREA OF 9000 SQ. MI. OF WEST-CENTRAL CALIFORNIA, ALONG THE COAST AS FAR NORTH AS PESCADERO AND SOUTH TO SAN LUIS OBISPO. INLAND IT WAS FELT AT COALINGA, MENDOTA, AND STEVENSON, WITH A V AT BIG SUR, BRYSON, CHUALAR, GONZALES, GREENFIELD, HARMONY, HOLLISTER, JOLON, LOCKWOOD, PAICINES, PARAISO, PINNACLES, SAN ARDO, SAN BENITO, SAN LUCAS, SOLEDAD, AND SPRECKLES, AND IV AT BEN LOMOND, CAMBRIA, CARMEL, CASTROVILLE, DOS PALOS, GILROY, KING CITY, LOS BANOS, MENDOTA, MONTEREY, PASO ROBLES, PRIEST, SALINAS, SAN LUIS OBISPO, TRES PINOS, WATSONVILLE, ETC.
06/01/1938	06-17--?	34.55	119.68	D	3.0		F	PAICINES AND PINNACLES. OFF POINT ARGUELLO.
06/06/1938	02-55--?	34.50	119.67	C	3.0		F	SANTA BARBARA AND SUMMERLAND. HOLLISTER AND PINNACLES.
09/16/1938	06-11--?	36.40	121.20	D	4.0		F	
09/27/1938	10-21--?	34.50	119.70	C	2.5		F	
09/27/1938	12-23--?	36.30	120.90	C	5.0		F	
09/27/1938	16-20--?	36.45	121.25	D			F	
09/29/1938	12-12--?	34.55	120.78	C	4.0		F	
10/02/1938	18-45--?	34.33	119.58	C	4.0		F	
10/24/1938	13-40--?	36.45	121.25	D			F	
10/28/1938	10-07--?	35.80	120.33	C	3.5		F	
11/01/1938	22-46--?	35.12	120.08	C	3.0		F	
11/16/1938	13-39--?	35.80	120.33	C	3.0		F	
11/22/1938	15-30--?	35.93	120.48	B	4.5		F	NEAR PARKFIELD; FELT AT ATASCADERO, CAMBRIA, CRESTON, MORRO BAY, PARKFIELD, PASO ROBLES, SAN MIGUEL, AND SHANDON.
01/01/1939	-?-53--?	34.58	120.33	C	3.0		F	PINNACLES.
01/21/1939	07-08--?	36.45	121.25	D			F	
01/22/1939	15-52--?	34.40	119.70	C	2.5		F	
02/05/1939	03-30--?	35.65	120.65	D			F	PASO ROBLES. NEAR PARKFIELD.
02/09/1939	06-44--?	35.93	120.48	C	3.0		F	
02/12/1939	03-12--?	34.42	119.83	B	3.0		F	GOLETA AND SANTA BARBARA.
03/24/1939	02-49--?	34.55	120.78	C	3.5		F	

DCPP UNITS 1 & 2 FSAR UPDATE

TABLE 2.5-1

MM/DD/YY	HR/MIN/SE	NORTH LAT	WEST LONG	QUALITY	MAG.	STA. REC.	FELT	MAXIMUM INTENSITY - COMMENTS
03/25/1939	03-45--?	36.45	121.25	D			F	PINNACLES.
03/30/1939	10-11--?	34.50	119.80	C	2.5		F	IV AT PARKFIELD.
05/02/1939	18-49--?	35.93	120.48	C	4.0		F	
05/03/1939	07-55--?	34.55	120.78	C	3.0		F	PASO ROBLES.
05/03/1939	12-39--?	35.65	120.65	D			F	
05/18/1939	23--?-?	35.80	120.33	C	3.0		F	LOS ALAMOS. REPORTS OF SEVERAL SHOCKS.
06/15/1939	21-12--?	34.50	119.70	C	2.5		F	BRADLEY.
06/17/1939	04-30--?	34.75	120.25	D			F	OVER AN AREA OF 10,000 SQ. MI. IN WEST-CENTRAL CALIFORNIA,
06/24/1939	12-55--?	35.85	120.85	D			F	ALONG THE COAST AS FAR NORTH AS HALF MOON BAY AND
06/24/1939	13-02--?	36.40	121.00	C	5.5		F	SOUTH TO ESTERO BAY. INLAND IT WAS FELT AT COALINGA,
							F	TRANQUILITY, AND VOLTA, WITH A VII AT HOLLISTER, VI AT KING
							F	CITY AND PAICINES, V AT CAYUCOS, SOLEDAD, AND SPRECKLES,
							F	AND IV AT PAICINES, V AT CAYUCOS, SOLEDAD, AND SPRECKLES,
							F	AND IV AT CAMBRIA, CARMEL, CASTROVILLE, CHUALAR, GILROY,
							F	GONZALES, LOCKWOOD, MILPITAS, MONTEREY, NIPOMO, PASO
							F	ROBLES, PINNACLES, SALINAS, SAN ARDO, SAN BENITO, SAN
							F	JUAN, SAN MIGUEL, SAN SIMEON, SANTA CRUZ, TRES PINOS, AND
							F	WATSONVILLE.
07/04/1939	10-49--?	36.40	121.00	C	4.0		F	HOLLISTER, PAICINES, AND SALINAS.
07/10/1939	18-33--?	36.40	121.25	D			F	PINNACLES.
07/24/1939	09-30--?	36.25	121.80	D			F	BIG SUR.
07/24/1939	13--?-?	36.00	121.15	D			F	JOLON.
09/06/1939	01-53-43	34.58	120.42	C	3.0		F	
09/07/1939	02-50-30	35.42	121.08	C	3.0		F	OFF SAN LUIS OBISPO CO.; FELT AT CAMBRIA.
09/08/1939	01-57--?	34.75	120.25	D			F	LOS ALAMOS.
09/08/1939	05--?-?	34.75	120.25	D			F	LOS ALAMOS.
09/12/1939	-?-?-47	34.25	119.75	C	3.0		F	
09/24/1939	11-57-40	36.40	121.00	D	3.5		F	
10/06/1939	04-39--?	35.80	121.50	D	3.5		F	
10/17/1939	19-21-41	34.55	120.78	C	3.5		F	
10/17/1939	20-42-43	34.55	120.78	C	4.0		F	
11/02/1939	14-02--?	34.40	120.50	D			F	OFF POINT ARGUELLO.
11/04/1939	14-11-33	36.20	120.90	D	3.0		F	POINT CONCEPTION LIGHT STATION.
12/14/1939	03-45-18	36.10	120.00	D	3.0		F	SALINAS AND SAN LUCAS.
12/25/1939	15-36-23	34.28	119.83	C	3.5		F	
12/28/1939	12-15-38	35.80	120.33	B	5.0		F	OVER AN AREA OF 15,000 SQ. MI. IN WEST-CENTRAL CALIFORNIA,
							F	ON
							F	THE COAST FROM SANTA CRUZ SOUTH TO POINT ARGUELLO, AND
							F	INLAND TO LOST HILLS AND FRESNO. V AT COALINGA, FRESNO,
							F	GREENFIELD, PRIEST, SAN ARDO, AND SAN LUCAS, AND IV AT
							F	APTOS, ATASCADERO, BIG SUR, CAMBRIA, CARMEL,
							F	CASTROVILLE, CAYUCOS, CHUALAR, GONZALES, HOLLISTER, KING
							F	CITY, MENDOTA, MONTEREY, MORRO BAY, PARKFIELD, PASO
							F	ROBLES, PINNACLES, SALINAS, SAN JUAN BAUTISTA, SAN LUIS
							F	OBISPO, SANTA CRUZ, SOLEDAD, TAFT, ETC.

DCPP UNITS 1 & 2 FSAR UPDATE

TABLE 2.5-1

MMDDYY	HR/MIN/SE	NORTH LAT	WEST LONG	QUALITY	MAG.	STA. REC.	FELT	MAXIMUM INTENSITY - COMMENTS
12/29/1939	04--?-?	36.40	121.25	D			F	PINNACLES.
12/30/1939	15-24-37	35.80	120.33	D	3.5		F	NEAR PARKFIELD. FELT AT SAN LUCAS.
02/27/1940	11-40-25	34.25	119.50	B	3.0		F	
05/21/1940	10-05-34	35.28	120.48	B	4.0		F	ATASCADERO, CAMBRIA, CAYUCOS, MORRO BAY, PASO ROBLES, PISMO BEACH, AND SAN LUIS OBISPO.
06/16/1940	09-25-04	34.55	120.78	C	4.0		F	OFF POINT ARGUELLO; FELT AT GUADALUPE AND LOS ALAMOS.
06/26/1940	08-56--?	36.08	120.32	C	3.5			
06/28/1940	04-06-42	34.55	120.78	C	3.0			
08/13/1940	22-07-29	36.23	120.32	B	4.0			(DEPT. OF WATER RESOURCES DATA.)
08/31/1940	08-52-46	34.55	120.78	B	3.5			
09/07/1940	10-36-30	36.50	121.50	D	3.5			
09/07/1940	10-38-36	36.50	121.50	D	4.5		F	CARMEL AND SALINAS.
09/07/1940	13-02-06	36.50	121.50	D	4.5		F	SANTA BARBARA CHANNEL; FELT AT GOLETA, PARADISE CAMP, AND SANTA BARBARA.
10/20/1940	22-18-45	34.55	120.78	C	3.0			
11/10/1940	10-25-10	34.35	119.77	C	4.0			
11/17/1940	21-23-43	35.00	119.50	C	3.0			
01/29/1941	08-54-01	34.48	119.53	B	3.0			
02/04/1941	03-19-12	34.55	119.68	C	3.0			
02/04/1941	03-42-09	34.55	119.68	C	3.0			
02/08/1941	15-58-50	34.55	119.68	C	3.5		F	SANTA BARBARA.
02/09/1941	23-49-18	34.50	119.70	C	2.0			
02/11/1941	06-43-30	34.27	119.57	B	3.5		F	SANTA BARBARA.
02/12/1941	20-10-24	34.40	119.70	C	3.0			
02/14/1941	22-19-06	34.40	119.70	C	2.5			
05/07/1941	16-17-34	34.55	120.78	C	3.5			
05/15/1941	03-29--?	36.15	120.35	D			F	COALINGA.
05/15/1941	06--?-?	36.15	120.35	D			F	COALINGA.
07/01/1941	07-50-57	34.33	119.58	A	6.0		F	SANTA BARBARA; FELT OVER AN AREA OF 20,000 SQ. MI. VIII AT CARPINTERIA AND SANTA BARBARA, VII AT GOLETA AND VENTURA, VI AT FILLMORE, KEYSTONE, LOS ALAMOS, OJAI, OXNARD, PORT HUENEME, SANTA PAULA, SUMMERLAND, AND WHEELER SPRINGS, AND V AT ACTON, ALTADENA, ARLIGHT, ARTESIA, ARVIN, BETTERAVIA, BUELLTON, BURBANK, CAMARILLO, CANOGA PARK, CASMALIA, CAYUCOS, CHATSWORTH, COMPTON, EL SEGUNDO, GAVIOTA, GLENDALE, HERMOSA BEACH, INGLEWOOD, LA CRESCENTA, LAGUNA BEACH, LANCASTER, LOMITA, LOMPOC, LONG BEACH, LOS ANGELES, LOS OLIVOS, MAYWOOD, MCKITTRICK, MONTALVO, MOORPARK, NEWBURY PARK, NEWPORT, NIPOMO, NORTH HOLLYWOOD, OCEANO, ORCUTT, PASADENA, PATTIWAY, IRU, POINT CONCEPTION, SANDBERG, SAN NICHOLAS ISLAND, SAN PEDRO, SANTA ANA, SANTA MARIA, SANTA MONICA, SANTA YNEZ, SIERRA MADRE, SIMI, STANTON, SUNLAND, SURF, TEHACHAPI, UPPER SESPE MOUNTAINS, VALYERMO, WHEELER RIDGE, AND WHITTIER.
07/01/1941	07-57--?	34.33	119.58	B	3.0			
07/01/1941	07-58--?	34.33	119.58	B	3.5			

DCPP UNITS 1 & 2 FSAR UPDATE

TABLE 2.5-1

MMDDYY	HR/MI/SE	NORTH LAT	WEST LONG	QUALITY	MAG.	STA. REC.	FELT	MAXIMUM INTENSITY - COMMENTS
07/01/1941	08-05--?	34.33	119.58	B	3.0			
07/01/1941	08-07--?	34.33	119.58	B	3.0			
07/01/1941	08-10--?	34.33	119.58	B	3.0			
07/01/1941	08-13--?	34.33	119.58	B	3.0			
07/01/1941	08-15--?	34.33	119.58	B	3.0			
07/01/1941	08-19--?	34.33	119.58	B	4.0		F	AFTERSHOCK OF 07-50-57 (THIS DATE).
07/01/1941	08-21--?	34.33	119.58	B	4.0		F	AFTERSHOCK OF 07-50-57.
07/01/1941	08-25--?	34.33	119.58	B	3.5			
07/01/1941	08-30--?	34.33	119.58	B	4.0		F	AFTERSHOCK OF 07-50-57.
		NORTH	WEST			STA.		
		LAT	LONG	QUALITY	MAG.	REC.	FELT	MAXIMUM INTENSITY - COMMENTS
MMDDYY	HR/MI/SE							
07/01/1941	08-48--?	34.33	119.58	B	4.0		FELT	MAXIMUM INTENSITY - COMMENTS
07/01/1941	08-58--?	34.33	119.58	B	4.0		F	AFTERSHOCK OF 07-50-57.
07/01/1941	09-05--?	34.33	119.58	B	4.0		F	AFTERSHOCK OF 07-50-57.
07/01/1941	09-45--?	34.33	119.58	B	4.0		F	AFTERSHOCK OF 07-50-57.
07/01/1941	10-25--?	34.33	119.58	B	4.0		F	AFTERSHOCK OF 07-50-57.
07/01/1941	12-37--?	34.33	119.58	B	3.0			
07/01/1941	14-22--?	34.33	119.58	B	3.0			
07/01/1941	18-13--?	34.33	119.58	B	3.0			
07/01/1941	18-20--?	34.33	119.58	B	4.0		F	AFTERSHOCK OF 07-50-57.
07/01/1941	19-48--?	34.33	119.58	B	3.0			
07/01/1941	20-15--?	34.33	119.58	B	3.5			
07/01/1941	22-51--?	34.33	119.58	B	3.5			
07/01/1941	23-54--?	34.33	119.58	B	4.5		F	AFTERSHOCK OF 07-50-57; FELT AT FILLMORE, GAVIOTA, LOS ALAMOS, AND SANTA BARBARA.
07/02/1941	-?-17--?	34.33	119.58	B	3.0			
07/02/1941	04-33--?	34.33	119.58	B	3.5			
07/02/1941	08-45--?	34.33	119.58	B	3.5			
07/02/1941	11-41--?	34.33	119.58	B	3.0			
07/02/1941	22-19--?	34.33	119.58	B	4.0		F	AFTERSHOCK OF 07-50-57.
07/03/1941	-?-25--?	34.33	119.58	B	3.5			
07/03/1941	19-26--?	34.33	119.58	B	4.0		F	AFTERSHOCK OF 07-50-57.
07/07/1941	01-06--?	34.33	119.58	B	3.0			
07/07/1941	06-25--?	34.33	119.58	B	3.5			
07/08/1941	19-37--?	34.33	119.58	B	3.0			
07/12/1941	16-18--?	34.33	119.58	B	4.5		F	AFTERSHOCK OF 07-50-57; FELT AT FILLMORE, GLENDALE, MONTRROSE, SATICOY, SAUGUS, AND WHEELER SPRINGS.
07/12/1941	16-41--?	34.33	119.58	B	3.0			
07/12/1941	21-07--?	34.33	119.58	B	3.0			
07/12/1941	21-12--?	34.33	119.58	B	3.0			
07/13/1941	06-11--?	34.33	119.58	B	3.5			
07/16/1941	23-10--?	34.33	119.58	B	3.0			
07/17/1941	18-31--?	34.33	119.58	B	3.0			
07/27/1941	12-44--?	34.33	119.58	B	3.0			
07/31/1941	13-23--?	34.33	119.58	B	3.0			
08/02/1941	12-31-19	34.33	119.58	C	3.0			
08/09/1941	05-05-24	34.33	119.58	C	3.5			

DCPP UNITS 1 & 2 FSAR UPDATE

TABLE 2.5-1

MMDDYY	HR/MIN/SE	NORTH LAT	WEST LONG	QUALITY	MAG.	STA. REC.	FELT	MAXIMUM INTENSITY - COMMENTS
08/12/1941	22-35-24	34.33	119.58	C	3.5			
08/19/1941	10-20-25	34.33	119.58	C	3.0			
08/25/1941	06-58-22	34.33	119.58	C	3.0			
08/27/1941	17-11-02	34.33	119.58	C	3.0			
08/29/1941	08-43-24	34.60	120.30	C	3.0			
09/08/1941	03-12-45	34.33	119.58	B	4.5		F	AFTERSHOCK OF 07/01/41, 07-50-57. V AT GOLETA AND SANTA BARBARA; FELT STRONGLY AT LOS ALAMOS AND SUMMERLAND.
09/08/1941	03-14-23	34.33	119.58	B	4.0		F	TWIN SHOCK OF 03-12-45; SAME "FELT" REPORT.
09/08/1941	04-45-16	34.33	119.58	B	3.5		F	SANTA BARBARA.
09/09/1941	03-23-17	34.33	119.58	B	3.5		F	SANTA BARBARA.
09/09/1941	13-44-46	34.33	119.58	B	3.0		F	SANTA BARBARA.
09/14/1941	01-45-18	34.33	119.58	B	4.0		F	AFTERSHOCK OF 07/01/41, 07-50-57.
09/14/1941	02-20-42	34.33	119.58	B	3.0		F	GOLETA, SANTA BARBARA, AND SUMMERLAND.
09/15/1941	01-37-02	34.33	119.58	B	4.0		F	
09/15/1941	01-55-18	34.33	119.58	B	3.0		F	
09/15/1941	02-49-06	34.33	119.58	B	3.5		F	
09/16/1941	07-27--?	34.33	119.58	B	3.5		F	
09/25/1941	05-12-56	34.33	119.58	B	4.0		F	GOLETA AND SANTA BARBARA.
10/07/1941	12-05-42	34.33	119.58	B	3.0		F	
10/19/1941	23-22-19	34.33	119.58	B	3.0		F	
11/05/1941	16-36--?	35.00	121.00	D	3.5		F	OFF POINT CONCEPTION; FELT AT SAN SIMEON.
11/17/1941	17-30-27	34.33	119.58	C	3.0		F	
11/18/1941	18-08-10	34.33	119.58	C	4.0		F	CARPINTERIA AND SANTA BARBARA.
11/21/1941	16-56-03	34.33	119.58	C	4.0		F	GOLETA AND SANTA BARBARA.
11/25/1941	20-01-48	34.33	119.58	C	3.0		F	
11/28/1941	06-33--?	35.00	120.00	D	3.5		F	
12/08/1941	-?-29-42	36.00	121.00	D	3.5		F	
12/22/1941	-?-54-09	35.93	120.48	C	4.0		F	NEAR PARKFIELD-NOT RECORDED ON BERKELEY NETWORK.
01/06/1942	09-20--?	36.15	120.65	D			F	PRIEST VALLEY-RECORDED AT TINEMAHA.
01/06/1942	09-23--?	36.15	120.65	D			F	PRIEST VALLEY-RECORDED AT TINEMAHA.
01/08/1942	18-21-05	34.13	119.58	C	2.5		F	
01/18/1942	11-35--?	36.40	121.25	D			F	PINNACLES.
01/18/1942	16-50--?	36.40	121.25	D			F	PINNACLES.
02/19/1942	18-33--?	36.40	121.25	D			F	PINNACLES.
03/09/1942	05-57-42	34.30	119.60	D	3.0		F	PINNACLES, LIGHT SHOCK.
03/25/1942	-?-?-?	36.40	121.25	D			F	
04/19/1942	04-02-47	34.30	119.60	D	3.0		F	
04/22/1942	05-32-52	35.30	119.50	D	3.0		F	
05/08/1942	17-19-13	34.33	119.58	C	3.0		F	GOLETA.
06/06/1942	06-42-11	34.35	119.85	C	3.0		F	IV AT CAMBRIA AND SAN LUIS OBISPO.
06/29/1942	21-07-30	35.60	120.80	D	4.0		F	SW OF LLANADA.
07/19/1942	10-42-07	36.40	121.10	D	1.6		F	SW OF KING CITY.
09/15/1942	10-36-33	36.13	122.18	B	3.0		F	IV AT SANTA YNEZ PEAK.
10/04/1942	10--?-?	34.60	120.00	D			F	FORESHOCK OF QUAKE ON OCTOBER 15 AT 13-53-56.
10/11/1942	23-48-23	36.48	121.40	C	1.9		F	IV AT BIG SUR, GONZALES, GREENFIELD, HOLLISTER, SALINAS, AND SOLEDAD.
10/15/1942	13-53-56	36.48	121.40	B	4.3		F	

DCPP UNITS 1 & 2 FSAR UPDATE

TABLE 2.5-1

MM/DD/YY	HR/MIN/SE	NORTH LAT	WEST LONG	QUALITY	MAG.	STA. REC.	FELT	MAXIMUM INTENSITY - COMMENTS
10/18/1942	08--?--?	36.00	121.00	D			F	CAMBRIA.
10/18/1942	12-01-42	36.00	121.00	D			F	V AT CAMBRIA.
10/19/1942	10-23--?	34.50	119.65	D			F	V AT SANTA BARBARA.
10/20/1942	10-25--?	36.00	121.00	D			F	V AT CAMBRIA.
10/26/1942	01-09-01	36.40	121.60	D	1.8		F	DEPTH ABOUT 12 KM.
12/02/1942	11-46--?	34.33	119.58	C	3.5		F	V AT SANTA BARBARA.
12/06/1942	16-57-49	35.93	120.48	C	3.5		F	
01/24/1943	06-55-57	34.33	119.58	C	3.0		F	
03/16/1943	09-27-47	34.28	119.60	C	3.0		F	
04/01/1943	13-39-66	34.68	121.75	B	3.1		F	OFF COAST, WEST OF POINT ARGUELLO.
06/29/1943	02-50-53	36.50	121.10	D	3.1		F	SW OF LLANADA.
07/05/1943	16-30-29	36.38	121.83	C	3.9		F	SOUTH OF SALINAS.
07/15/1943	?-44-42	36.00	120.15	D			F	NEAR AVENAL.
08/07/1943	16-59-47	34.28	119.57	C	3.5		F	
08/12/1943	15-56-33	34.75	121.15	C	3.5		F	
08/27/1943	08-16-53	34.43	119.87	C	3.5		F	IV AT SANTA BARBARA.
09/13/1943	12-40--?	35.65	120.65	D			F	PASO ROBLES, POSSIBLY GUN FIRE.
09/18/1943	17-07-16	34.37	119.58	C	3.0		F	
10/22/1943	12--?--?	36.00	120.90	D			F	SAN ARDO; 2 SHOCKS.
10/26/1943	22-10--?	34.75	120.25	D			F	LOS ALAMOS.
10/31/1943	17-54-06	35.80	120.40	D	3.5		F	
10/31/1943	20--?--?	36.40	121.00	D			F	LONOAK.
11/08/1943	11-33-46	36.00	119.92	C	3.0		F	KETTLEMAN HILLS; FELT AT AVENAL.
11/30/1943	21-57-18	36.30	120.50	D	4.0		F	NEAR COALINGA.
12/01/1943	04-51--?	36.50	121.10	D			F	SAN BENITO.
01/04/1944	18-06-40	34.10	120.40	D	3.3		F	
02/18/1944	16-29-37	34.10	119.52	C	2.1		F	WEST OF PRIEST.
02/21/1944	13--?-11	36.17	120.93	C	3.8		F	NE OF PARAISO.
03/06/1944	21-32-16	36.40	121.25	C	3.4		F	OFF POINT ARGUELLO.
04/03/1944	02-33--?	34.50	121.40	D	4.0		F	OFF CARPINTERIA; FELT EAST OF SANTA BARBARA.
04/12/1944	15-33-10	34.27	119.52	C	4.0		F	NEAR LOMPOC; VI AT LOS ALAMOS AND IV AT SANTA MARIA.
06/13/1944	08-27-32	34.67	120.50	C	4.6		F	AFTERSHOCK OF 08-27-32.
06/13/1944	08-46-43	34.67	120.50	C	4.0		F	AFTERSHOCK OF 08-27-32.
06/13/1944	11-07-24	34.67	120.50	C	4.4		F	AFTERSHOCK OF 08-27-32.
07/11/1944	22-33--?	36.50	121.10	D			F	SAN BENITO.
07/15/1944	19-22-37	34.37	119.62	C	3.1		F	
09/04/1944	02-47-46	35.00	120.00	D	3.4		F	LOS ALAMOS.
09/04/1944	05--?--?	35.00	120.00	D			F	LOS ALAMOS.
09/15/1944	14-12-42	34.70	120.20	D	2.6		F	KETTLEMAN HILLS REGION; FELT AT PARKFIELD.
09/18/1944	01-30--?	35.00	120.00	D	3.5		F	
11/04/1944	08-12-01	36.33	120.08	C	3.4		F	
11/08/1944	16-12-36	34.33	119.72	C	3.1		F	
11/28/1944	10-36--?	35.80	120.00	D	3.3		F	
11/30/1944	18-53-15	34.72	120.42	C	4.1		F	NEAR LOS ALAMOS; FELT AT LOS ALAMOS AND LOS OLIVOS.
12/02/1944	15-09-12	35.80	120.00	D	3.2		F	
01/27/1945	17-50-31	34.75	120.67	C	3.9		F	
02/25/1945	20-18-38	36.00	120.48	C	3.6		F	

DCPP UNITS 1 & 2 FSAR UPDATE

TABLE 2.5-1

MMDDYY	HR/MIN/SE	NORTH LAT	WEST LONG	QUALITY	MAG.	STA. REC.	FELT	MAXIMUM INTENSITY - COMMENTS
04/15/1945	22-59-57	34.13	119.83	C	3.1			
06/11/1945	03-54-52	34.50	120.80	D	3.2			NEAR SAN SIMEON; IV AT CAMBRIA.
07/11/1945	16-13--?	35.67	121.25	D	4.0		F	EAST OF SANTA MARIA; IV AT LOS ALAMOS.
07/28/1945	02-33-48	34.70	120.10	D	4.2		F	
09/04/1945	12-38-31	34.32	119.63	C	3.2		F	NEAR BRADLEY; IV AT CAMBRIA, PARKFIELD, PASO ROBLES, AND SAN MIGUEL.
09/07/1945	11-34-20	35.83	120.75	C	4.2		F	NEAR SOLEDAD.
11/04/1945	-?-46-34	36.38	121.28	C	3.3			
02/09/1946	02-55-28	34.33	119.92	C	2.5			
02/10/1946	11-01-19	36.50	121.00	D	4.2		F	OVER AN AREA OF 2000 SQ. MI. IN WEST CENTRAL CALIFORNIA. V AT SAN BENITO, AND IV AT BIG SUR, CHUALAR, GREENFIELD, HOLLISTER, LONOAK, SAN LUCAS, SAN MIGUEL, SANTA CRUZ, AND SOLEDAD.
02/15/1946	12-07-00	35.90	121.45	D			F	PARKFIELD; LIGHT SHOCK.
04/19/1946	12-50--?	34.00	120.40	D			F	SANTA MARIA.
07/08/1946	19-59-44	34.83	120.53	C	3.2			
08/06/1946	04-55-07	34.95	120.18	C	2.8		F	E OF SANTA MARIA; FELT AT LOS ALAMOS.
09/02/1946	10-09-47	34.18	119.62	C	3.0			
09/09/1946	11-20--?	34.90	120.40	D			F	SANTA MARIA.
09/19/1946	06-35-44	35.83	119.67	C	3.2			
10/24/1946	18-26-50	34.37	119.62	C	2.7			
11/22/1946	09-47-59	34.83	120.68	D	3.0		F	NEAR CAYUCOS; V AT MORRO BAY AND SANTA MARGARITA; ALSO FELT AT ASCADERO, LOS ALAMOS, PISMO BEACH, AND SAN LUIS OBISPO.
11/27/1946	14-44-51	35.50	120.92	C	4.3			
12/13/1946	-?-40-01	34.17	119.53	C	3.5			
01/06/1947	21-05-47	35.85	120.47	C	3.6			
01/13/1947	19-38-31	34.32	119.65	C	2.2			
01/14/1947	20-49-27	34.23	119.65	C	2.7			
01/18/1947	12--?-42	34.20	121.50	D	3.3			
01/19/1947	19-32--?	35.60	120.30	D	3.1		F	PASO ROBLES.
02/05/1947	06-14--?	38.23	120.65	B	5.0		F	VI AT LONOAK. V AT COALINGA, IDRIA, AND KING CITY, AND IV AT BIG SUR, HURON, PARKFIELD, SAN ARDO, AND WESTHAVEN, NEAR COALINGA - AFTERSHOCK OF 2/5/47 OF 06-14--?.
02/25/1947	11-45-18	36.20	120.50	D	4.2			
03/23/1947	16-04-51	35.15	121.30	D	3.7			
03/27/1947	09-16-46	35.00	121.00	D	4.2		F	OFF COAST; V AT LOMPOC.
04/29/1947	07-44--?	34.33	119.55	C	3.2			
06/25/1947	18-39-53	34.25	119.50	C	3.1		F	NEAR CARPINTERIA.
06/25/1947	13-41-21	34.25	119.50	C	3.6		F	NEAR CARPINTERIA.
06/25/1947	18-48-26	34.25	119.50	C	2.5			
06/25/1947	20-55-16	34.25	119.50	C	3.2		F	NEAR CARPINTERIA.
06/25/1947	20-55-54	34.25	119.50	C	3.8			
07/13/1947	05-35--?	36.08	121.10	D	3.4			
07/14/1947	05-40-06	35.92	119.92	C	4.0		F	SOUTH OF KING CITY.
10/6/1947	18-39--?	36.50	121.23	A	3.2			KETTLEMAN HILLS; IV AT KETTLEMAN CITY.
12/14/1947	05-42--?	36.45	121.08	B	3.4			EAST OF GONZALES. SW OF LLANADA.

DCPP UNITS 1 & 2 FSAR UPDATE

TABLE 2.5-1

MM/DD/YY	HR/Min/SE	NORTH LAT	WEST LONG	QUALITY	MAG.	STA. REC.	FELT	MAXIMUM INTENSITY - COMMENTS
12/16/1947	09-21-03	36.25	120.77	C	3.6		F	IV AT SAN LUCAS.
12/18/1947	19-30-06	36.12	120.90	D			F	IV AT PARKFIELD.
12/25/1947	06-05--?	35.60	121.10	D			F	CAMBRIA.
12/25/1947	06-20--?	35.60	121.10	D			F	CAMBRIA.
01/11/1948	05-37-28	36.43	121.48	B	4.3		F	IV AT HOLLISTER.
02/01/1948	17--?-54	34.42	119.92	C	3.0		F	
02/15/1948	08-04-06	35.88	120.37	A	3.4		F	EAST OF PARKFIELD.
03/07/1948	07-46-22	36.10	120.40	D	3.0		F	NEAR COALINGA.
03/10/1948	23-24-34	34.43	119.73	C	2.6		F	
03/18/1948	09-35-05	34.40	119.60	C	2.8		F	IV AT HOLLISTER.
03/29/1948	02-40--?	35.85	121.40	D	3.7		F	
04/23/1948	15-23-43	34.10	120.93	C	2.7		F	WEST OF PRIEST.
05/05/1948	06-47-06	34.45	119.72	B	3.0		F	V AT LOS ALAMOS.
05/07/1948	12--?-32	36.20	121.90	D			F	
05/09/1948	11-10--?	34.75	120.25	D	3.2		F	
07/14/1948	11-05-37	34.67	120.92	C	3.4		F	
07/17/1948	05-26-31	34.55	120.05	C	3.4		F	
07/28/1948	01-30-57	36.05	120.53	C	3.1		F	SE OF PRIEST.
07/29/1948	13-16-23	35.12	120.47	C	3.4		F	
08/04/1948	10-22-57	35.92	120.33	C	3.6		F	
09/03/1948	23-42-26	34.33	119.53	C	3.9		F	SANTA BARBARA.
09/17/1948	15-41-01	34.40	119.62	C	3.1		F	
10/27/1948	03-05--?	34.75	120.25	D			F	IV AT LOS ALAMOS.
10/29/1948	03-04-59	34.10	120.40	D	3.4		F	V AT ARLIGHT AND POINT ARGUELLO LIGHT STATION.
11/02/1948	19-06-45	34.37	119.58	C	2.9		F	
12/04/1948	06-44-20	34.43	119.72	C	2.8		F	
12/04/1948	23-32-51	34.42	119.50	C	2.7		F	
12/20/1948	04-42-46	35.80	121.50	C	4.5		F	OFF COAST NEAR PIEDRAS BLANCAS POINT. III AT SAN SIMEON.
12/31/1948	14-35-46	35.67	121.40	B	4.6		F	ALONG THE COAST FROM LOMPOC TO MOSS LANDING. VI AT SAN SIMEON AND V AT CAYUCOS. CRESTON, MOSS LANDING, AND PIEDRAS BLANCAS LIGHT STATION.
01/25/1949	04-29--?	34.90	120.40	D			F	V AT ORCUTT AND SANTA MARIA.
03/27/1949	06-31-16	34.25	119.62	C	2.6		F	
04/06/1949	14-07--?	35.00	120.00	C	2.6		F	
04/08/1949	13-17-07	34.60	120.35	C	3.2		F	IV AT LOS ALAMOS.
04/14/1949	01-46-12	34.28	119.52	C	2.6		F	
04/23/1949	09-18-09	36.38	121.37	C	3.7		F	NORTH OF PARAISO.
05/06/1949	04-23-46	34.50	121.00	C	3.4		F	
05/10/1949	06-20--?	35.90	120.40	D			F	SANTA MARIA - SLIGHT.
05/10/1949	11--?-?	35.90	120.40	D			F	SANTA MARIA - SLIGHT.
05/16/1949	03-01-03	34.72	120.02	C	3.2		F	IV AT SAN SIMEON.
05/17/1949	23-57-55	35.63	121.15	D	4.1		F	V AT SAN ARDO AND SAN MIGUEL; ALSO FELT AT PASO ROBLES, SAN LUIS OBISPO, AND SANTA MARGARITA.
06/27/1949	10-35-31	35.80	121.10	D	4.5		F	IV AT COALINGA.
07/21/1949	16-50--?	36.15	120.35	D			F	IV AT COALINGA.
07/21/1949	17-01--?	36.15	120.35	D			F	IV AT COALINGA.
07/24/1949	03-04-05	36.00	120.00	D	2.3		F	SE. KINGS CO. AFTER SHOCK AT 06-26--?, MAG. 2.0.

DCPP UNITS 1 & 2 FSAR UPDATE

TABLE 2.5-1

MM/DD/YY	HR/IN/SE	NORTH LAT	WEST LONG	QUALITY	MAG.	STA. REC.	FELT	MAXIMUM INTENSITY - COMMENTS
07/27/1949	18-21-35	34.53	120.37	C	3.6			SOUTH OF KING CITY.
08/01/1949	-?-07-24	36.90	121.20	D	3.0			NO. MONTEREY CO.
08/07/1949	01-38-43	36.50	121.50	D	2.3			CENTRAL SAN BENITO CO.
08/10/1949	09-17-39	36.50	121.00	C	2.6		F	KETTLEMAN HILLS: FIFTH SHOCK IN 2 WEEKS.
08/22/1949	03--?-?	36.00	120.00	D	4.2		F	NEAR POINT CONCEPTION. VI AT ARLIGHT AND SURF. IV AT
08/26/1949	16-52-32	34.50	120.50	D				GUADALUPE, LOMPOC, AND LOS ALAMOS.
08/27/1949	14-15--?	34.50	120.50	D			F	ARLIGHT. SLIGHT SHOCK.
08/27/1949	14-51-46	34.50	120.50	D	4.9		F	NEAR POINT CONCEPTION. VI AT ARLIGHT, LOMPOC, AND
								SUDDEN. V AT COSMALIA, LOS ALAMOS, NIPOMO, SANTA
								BARBARA, AND SURF.
08/29/1949	12-07-20	36.00	120.10	D	3.0		F	IV IN AVENAL AND KETTLEMAN CITY.
10/28/1949	08-07-02	36.80	120.90	C	2.6			NW OF PRIEST.
11/17/1949	05-06-06	34.80	120.70	D	2.8		F	IV AT SANTA MARIA.
12/28/1949	09-17-12	36.20	120.70	D	2.6			NEAR PRIEST.
02/19/1950	08-29-44	34.50	120.70	D	3.5		F	NORTH OF KING CITY; V AT ROBLES DEL RIO.
03/09/1950	23-43-19	36.35	121.22	C	3.2			
03/22/1950	01-31-57	35.97	120.63	C	3.7			
03/29/1950	12-43-20	35.97	120.88	D	3.5			
04/15/1950	11-56-32	35.75	119.62	C	4.6			
								NE OF LOST HILLS; V AT ASH MOUNTAIN, (SEQUOIA NATIONAL
								PARK), KERNVILLE, AND SHAFTER, AND IV AT BUTTONWILLOW,
								JAWBONE AQUEDUCT STATION, LOST HILLS, THREE RIVERS, AND
								VISALIA.
04/21/1950	13-17-29	34.38	119.58	B	3.0		F	IV AT SANTA BARBARA.
04/26/1950	07-23-29	35.20	120.60	C	3.5		F	V AT SANTA MARIA; ALSO FELT AT ORCUTT.
04/26/1950	07-38--?	35.20	120.60	D			F	SANTA MARIA.
05/21/1950	18-59-03	34.57	119.63	C	2.6			
05/21/1950	19-26-48	35.88	119.73	C	3.4			
05/24/1950	01-46-57	36.43	120.77	C	2.9			SE OF LLANADA.
07/13/1950	15-01-47	34.33	119.50	C	2.8		F	OFF CARPINTERIA; V AT MONTECITO; ALSO FELT AT SANTA
								BARBARA AND NEARBY AREAS.
								OFF COAST, WEST OF BIG SUR.
08/01/1950	21-08-43	36.20	122.23	B	2.0			
08/02/1950	06-50-48	34.67	120.63	C	3.3			
08/23/1950	09-10--?	34.40	119.50	D			F	IV AT RINCON POINT; FELT AT CARPINTERIA.
09/24/1950	04-45--?	34.50	120.50	D			F	III AT ARLIGHT.
09/24/1950	12-23--?	34.22	119.58	C	3.3			
09/24/1950	21-51-44	36.20	120.50	D	2.9			EAST OF PRIEST.
10/20/1950	08-23-25	36.33	121.07	C	2.7			SOUTH OF KING CITY.
11/21/1950	04-30--?	30.90	120.40	D			F	SANTA MARIA.
03/02/1951	02-13-44	36.10	120.60	D	3.1			SE OF PRIEST.
03/04/1951	13-32--?	34.90	120.40	D			F	IV AT SANTA MARIA; 2 SHOCKS.
03/05/1951	09-50--?	34.90	120.40	D			F	IV AT SANTA MARIA.
03/10/1951	05-35--?	34.50	120.50	D			F	IV AT ARLIGHT.
03/15/1951	13-50-43	35.02	120.48	C	3.8		F	IV AT LOS ALAMOS.
03/26/1951	06-07-34	34.62	119.50	C	3.5		F	IV AT OJAI AND SUMMERLAND; FELT AT VENTURA.
05/04/1951	03-28-36	36.20	120.20	D	3.1			FORESHOCK OF QUAKE AT 20-08-10.
05/04/1951	20-08-10	36.20	120.20	D	3.2			EAST OF COALINGA.

DCPP UNITS 1 & 2 FSAR UPDATE

TABLE 2.5-1

MMDD/YY	HR/IN/SE	NORTH LAT	WEST LONG	QUALITY	MAG.	STA. REC.	FELT	MAXIMUM INTENSITY - COMMENTS
05/06/1951	03-18-03	36.40	120.40	D	2.8			NORTH OF COALINGA.
05/25/1951	05-11-18	36.30	120.30	D	3.1			NORTH OF COALINGA.
05/29/1951	05-08-24	35.08	119.65	C	3.2		F	ELKHORN HILLS; IV IN CUYAMA VALLEY.
05/31/1951	06-28-42	36.30	120.20	D	2.7			NE OF COALINGA.
06/16/1951	19-01-17	34.40	120.08	C	3.3			
06/19/1951	06-13-47	35.97	120.42	C	3.6			SOUTH OF COALINGA.
07/01/1951	?-13-19	36.20	120.95	B	3.2			EAST OF KING CITY.
07/07/1951	05-53-33	34.75	120.75	C	3.5			
08/02/1951	05-09-25	36.35	121.27	B	3.9		F	NEAR GREENFIELD; IV AT BIG SUR, AT 7 MI. S OF HOLLISTER, AND ROBLES DEL RIO.
08/08/1951	19-42-?	34.80	120.40	D			F	IV AT ORCUTT.
08/09/1951	09-20-48	36.15	121.75	C	2.2			NEAR BIG SUR.
08/25/1951	01-04-10	36.47	121.15	B	3.1			SW OF LLANADA.
08/28/1951	22-12-27	34.60	121.00	D	3.5		F	OFF POINT ARGUELLO; III AT LOS ALAMOS.
09/18/1951	02-30-?	36.25	121.80	D			F	IV AT BIG SUR.
09/19/1951	22-50-?	36.25	121.80	D			F	IV AT BIG SUR.
10/03/1951	13-44-33	35.92	120.52	C	3.8			
10/26/1951	16-25-40	34.42	119.73	C	3.0			
11/17/1951	03-19-48	34.70	120.50	D	2.5		F	NEAR LOMPOC; III AT LOS ALAMOS.
11/25/1951	23-15-39	35.33	119.50	B	3.8			
12/20/1951	04-13-06	36.00	120.05	C	3.7			
01/24/1952	?-32-38	34.18	119.88	C	2.7			NEAR KING CITY.
01/30/1952	11-05-33	36.30	121.13	C	2.7			
01/31/1952	20-09-02	34.18	119.53	C	2.6			
01/31/1952	21-33-12	36.40	121.40	C	3.6			SOUTHEAST OF SOLEDAD.
02/09/1952	22-26-39	34.07	120.75	C	3.6			
03/25/1952	09-18-50	34.18	120.95	C	3.6			
04/02/1952	05-21-10	36.45	121.25	B	3.1			NEAR SOLEDAD.
05/07/1952	05-45-?	34.40	119.60	D			F	IV AT MONTECITO AND SUMMERLAND.
06/18/1952	04-?-?	34.60	120.65	D			F	IV AT POINT ARGUELLO LIFEBOAT STATION.
07/01/1952	15-29-24	34.30	119.80	D	3.1			
07/15/1952	06-07-55	36.42	121.00	C	2.5			
07/27/1952	18-15-14	34.18	119.70	C	3.1			
07/27/1952	20-20-35	34.22	119.67	C	3.2			
07/27/1952	20-30-05	34.20	119.67	B	3.5		F	OFF POINT CONCEPTION; IV AT LOS ALAMOS.
08/07/1952	19-16-12	34.33	120.68	C	3.6			
08/11/1952	21-42-29	34.17	119.67	C	3.1			
08/23/1952	20-10-?	34.85	119.50	D			F	IV AT VENTUCOPA - SECOND SHOCK AT 21-20-?-?
08/30/1952	14-58-11	34.35	119.62	B	3.3			
09/01/1952	12-03-?	34.30	119.60	D	3.0			
09/12/1952	21-?-15	34.25	119.70	C	3.0			
09/14/1952	11-46-06	35.90	120.30	D	3.3			
10/09/1952	14-46-02	34.20	122.20	D	4.6			(DEPT. OF WATER RESOURCES DATA)

DCPP UNITS 1 & 2 FSAR UPDATE

TABLE 2.5-1

MM/DD/YY	HR/MI/SE	NORTH LAT	WEST LONG	QUALITY	MAG.	STA. REC.	FELT	MAXIMUM INTENSITY - COMMENTS
11/22/1952	07-46-37	35.73	121.20	B	6.0		F	6 MI. NORTH OF SAN SIMEON, NEAR BRYSON; FELT OVER AN AREA OF 20,000 SQ. MI. VII AT BRADLEY AND BRYSON, VI AT ARROYO GRANDE, ATASCADERO, CAMBRIA, CAMP COOKE, CARMEL VALLEY, CAYUCOS, CHUALAR, CRESTON, GORDA STATION, GUADALUPE, HARMONY, HEARST RANCH, KING CITY, LOCKWOOD, LONOAK, MORRO BAY, OCEANO, PARKFIELD, PASO ROBLES, PISMO BEACH, SALINAS, SAN ARDO, SAN LUIS OBISPO, SAN SIMEON, SANTA MARGARITA, AND TEMPLETON, AND V AT AVENAL, BEN LOMOND, BIG SUR, BUELLTON, BUTTONWILLOW, CARUTHERS, CASMALIA, CHOLAME, COALINGA, CORCORAN, DOS PALOS, HOLLISTER, HUASNA, KETTLEMAN CITY, LOMPOC, LOST HILLS, LUCIA, MARICOPA, MONTEREY, MOSS LANDING, NIPOMO, ORCUTT, PAICINES, RIVERDALE, SAN MIGUEL, SANTA CRUZ, SANTA MARIA, SHAFTER, STRATFORD, SUDDEN, AND SURF.
11/22/1952	08-02-40	35.73	121.20	B	3.2			SAN SIMEON AFTERSHOCK.
11/22/1952	08-29-47	35.73	121.20	B	3.1			SAN SIMEON AFTERSHOCK.
11/22/1952	08-53-04	35.73	121.20	B	3.4		F	SAN SIMEON AFTERSHOCK; IV AT ARVIN, CALIENTE, JOLON, LOST HILLS, MALIBU, MARICOPA, MCFARLAND, MIRACLE HOT SPRINGS, MORGAN HILL, NIPOMO, PISMO BEACH, AND SHAFTER.
11/22/1952	11-08-44	35.73	121.20	B	3.1			SAN SIMEON AFTERSHOCK.
11/22/1952	11-45-31	35.73	121.20	B	3.1			SAN SIMEON AFTERSHOCK.
11/22/1952	12-34-44	35.73	121.20	B	3.0			SAN SIMEON AFTERSHOCK.
11/22/1952	13-37-31	35.73	121.20	B	4.0		F	SAN SIMEON AFTERSHOCK; V AT CALIENTE, MIRACLE HOT SPRINGS, AND WHEELER SPRINGS.
11/22/1952	19-25-21	35.73	121.20	B	3.9			SAN SIMEON AFTERSHOCK.
11/22/1952	19-36-27	35.70	121.20	D	3.1			SAN SIMEON AFTERSHOCK.
11/22/1952	23-39-20	35.70	121.20	D	3.1			SAN SIMEON AFTERSHOCK.
11/23/1952	09-22-35	36.00	120.90	D	3.2			SAN SIMEON AFTERSHOCK.
11/23/1952	18-40-19	35.67	121.17	C	4.2			20 MI. SE OF KING CITY.
11/25/1952	19-17-54	36.20	120.00	D	3.2			SAN SIMEON AFTERSHOCK.
11/25/1952	20-14-45	35.73	121.20	C	3.6			SAN SIMEON AFTERSHOCK.
11/25/1952	21-59-17	35.73	121.20	C	4.4			SAN SIMEON AFTERSHOCK.
11/26/1952	13-32-09	35.73	121.20	C	3.5			SAN SIMEON AFTERSHOCK.
11/27/1952	17-37-05	35.70	121.20	D	3.3			SAN SIMEON AFTERSHOCK.
11/28/1952	10-22-33	35.90	121.20	D	3.0			SAN SIMEON AFTERSHOCK.
11/29/1952	16--?-?	36.00	121.15	D			F	IV AT JOLON - TIME MAY BE 04--?-? ON 11/30/1952.
11/29/1952	23-15-58	35.70	121.20	D	3.5			SAN SIMEON AFTERSHOCK.
12/05/1952	01-05-57	36.50	120.70	D	3.0			14 MI. SE OF LLANADA.
12/06/1952	23-50--?	35.66	120.65	D			F	IV AT PASO ROBLES; FELT AT ADELAIDA.
12/12/1952	-?-27-07	36.40	120.97	B	3.0		F	17 MI. NE OF KING CITY; III AT LONOAK.
12/25/1952	16-44-10	34.40	121.40	D	3.6			
01/12/1953	13-05-18	35.80	121.10	D	3.2		F	14 MI. NE OF SAN SIMEON.
01/24/1953	-?-?-?	35.90	121.00	D				TEN SHOCKS REPORTED FELT FROM 1/24 TO 1/31 AT BRYSON (E. WEFERLING RANCH).
01/29/1953	20-31-19	35.80	121.10	D	3.1			14 MI. NE OF SAN SIMEON.

DCPP UNITS 1 & 2 FSAR UPDATE

TABLE 2.5-1

MM/DD/YY	HR/IN/SE	NORTH LAT	WEST LONG	QUALITY	MAG.	STA. REC.	FELT	MAXIMUM INTENSITY - COMMENTS
02/03/1953	14-50-18	35.47	120.75	C	4.1		F	12 MI. NNW OF SAN LUIS OBISPO; V AT ATASCADERO, BRYSON, CRESTON, MORRO BAY, SANTA MARGARITA, AND IV AT CAYUCOS, PASO ROBLES, SAN LUIS OBISPO, AND TEMPLETON.
02/05/1953	02-54-12	35.90	121.00	D	2.8		F	IV AT BRYSON (E. WEFERLING RANCH).
02/15/1953	15-30-?	35.90	121.00	D			F	BRYSON (E. WEFERLING RANCH).
02/17/1953	08-06-?	35.90	121.00	D			F	III AT BRYSON (PLEYTO SCHOOL) - SEVERAL MILD SHOCKS REPORTED FELT DAILY SINCE SHOCK OF 11/21/52, 23-46-38 (NOT LISTED).
02/18/1953	14-10-?	35.90	121.00	D			F	BRYSON (E. WEFERLING RANCH) - MILD.
03/01/1953	18-53-?	35.90	121.00	D			F	V AT BRYSON.
03/04/1953	03-40-?	35.90	121.00	D			F	BRYSON (PLEYTO SCHOOL) - LIGHT.
03/15/1953	21--?-32	34.87	121.53	C	3.7		F	
03/18/1953	05-03-?	35.90	121.00	D			F	III AT BRYSON (PLEYTO SCHOOL).
03/29/1953	17-19-48	35.90	120.20	D	3.7		F	
04/08/1953	-?-59-20	34.80	120.60	D	3.6		F	NEAR CASMALIA; IV AT LOS ALAMOS.
04/15/1953	-?-29-10	35.83	121.07	C	3.1		F	14 MI. NNE OF SAN SIMEON; IV AT BRYSON.
04/15/1953	05-30-?	35.90	121.00	D			F	BRYSON - LIGHT.
04/29/1953	05-26-53	36.00	121.15	C	3.5		F	14 MI. S OF KING CITY - USCGS GIVES TIME AS 05-26-52. LOCATION AS N35.8 121.2W, REPORT AS NEAR BRYSON; V AT PLEYTO SCHOOL. 22 MI. NE OF KING CITY.
05/01/1953	22-16-51	36.40	120.80	D	3.0		F	III AT LOMPOC.
05/08/1953	08-15-?	34.65	120.45	D			F	
05/14/1953	03-36-?	36.00	120.00	D	3.3		F	9 MI. NE OF SAN SIMEON - USCGS GIVES N35.52 121.28W, OFF CAMBRIA; V AT BRYSON.
05/14/1953	09-36-09	35.75	121.08	B	3.7		F	IV AT BRYSON (PLEYTO SCHOOL).
05/15/1983	07-15-?	35.90	121.00	D			F	20 MI. SW OF COALINGA; IV AT PASO ROBLES AND III AT SAN MIGUEL.
05/28/1953	03-51-13	35.88	120.50	B	4.3		F	AFTERSHOCK OF 03-51-13; FELT AT SAN MIGUEL.
05/28/1953	07-58-33	35.88	120.50	C	3.5		F	20 MI. SOUTH OF KING CITY.
05/29/1953	10-20-16	35.90	121.20	D	2.9		F	NEAR COALINGA.
05/31/1953	23-51-17	36.10	120.40	D	3.2		F	V AT CRESTON - PROBABLY A BLAST.
06/04/1953	11-40-?	35.50	120.50	D			F	10 MI. SOUTH OF COALINGA.
06/06/1953	20-26-33	36.00	120.30	D	2.9		F	20 MI. EAST OF KING CITY.
06/19/1953	11-24-50	36.30	120.70	D	2.8		F	15 MI. WSW OF COALINGA; FELT AT COALINGA AND PASO ROBLES.
06/22/1953	15-22-35	35.93	120.38	C	4.3		F	OFF POINT ARGUELLO; IV AT POINT ARGUELLO LIGHT STATION.
07/01/1953	22-17-20	34.60	121.35	D	3.2		F	8 MI. NORTH OF COALINGA.
08/14/1953	01-40-06	36.30	120.30	D	2.9		F	20 MI. NORTH OF KING CITY.
08/14/1953	09-22-50	36.50	121.20	D	2.3		F	30 MI. SE OF KING CITY.
09/02/1953	09-41-20	35.90	120.80	D	3.0		F	CRESTON.
09/03/1953	11--?-?	35.50	120.50	D			F	15 MI. SOUTH OF COALINGA; IV AT CRESTON AND PASO ROBLES.
09/04/1953	03-54-25	35.90	120.32	C	3.5		F	NORTH OF KING CITY.
09/22/1953	07-36-58	36.40	121.20	D	3.8		F	NEAR SAN SIMEON; V AT BRYSON.
09/23/1953	06-21-51	35.70	121.10	D	3.5		F	25 MI. S OF MONTEREY; IV AT BIG SUR.
10/01/1953	03-56-15	36.25	121.83	C	3.4		F	SOUTHWEST OF COALINGA.
10/16/1953	03-45-35	35.95	120.53	C	3.4		F	OFF SANTA BARBARA; V AT SANTA BARBARA AND VICINTY, AND IV AT GOLETA AND LOS PRIETOS RANGER STATION.
10/21/1953	16-02-38	34.32	119.70	B	4.0		F	

DCPP UNITS 1 & 2 FSAR UPDATE

TABLE 2.5-1

MM/DD/YY	HR/IN/SE	NORTH LAT	WEST LONG	QUALITY	MAG.	STA. REC.	FELT	MAXIMUM INTENSITY - COMMENTS
07/06/1955	13-18-53	36.50	121.50	D	2.7			SOUTH OF HOLLISTER.
07/28/1955	12-07-52	36.50	121.40	D	2.6			SOUTH OF HOLLISTER.
09/21/1955	18-06-52	36.50	121.00	D	3.3			NORTH OF KING CITY.
10/22/1955	07-04-18	36.22	120.33	C	4.2		F	V AT AND 14 MI. NW OF COALINGA.
11/02/1955	19-40-06	36.00	120.92	A	5.2		F	55 MI. NNW OF SAN LUIS OBISPO; FELT OVER 7000 SQ. MI. OF COASTAL W CENTRAL CALIF. VI AT ADELAIDA RD, (14 MI. W OF PASO ROBLES), BRYSON, KING CITY, PASO ROBLES, SAN ARDO, SAN LUCAS, AND SAN MIGUEL.
11/18/1955	09-03-30	35.90	120.50	D	2.9			SOUTHWEST OF COALINGA.
11/19/1955	07-20--?	34.50	119.65	D			F	REPORTED FELT AT SANTA BARBARA.
11/19/1955	10-59-41	36.03	120.90	C	3.3			SOUTHEAST OF KING CITY.
11/21/1955	21-14-18	36.10	119.90	D	3.5			
12/11/1955	20-10-38	36.27	120.72	C	3.5		F	NORTHWEST OF COALINGA.
12/16/1955	14-43-11	36.03	120.87	C	3.8		F	SOUTHWEST OF KING CITY; FELT AT ATASCADERO, PASO ROBLES, AND SAN MIGUEL.
12/29/1955	13-33-17	36.45	121.25	C	3.4			NORTH OF KING CITY.
02/14/1956	22-15-08	36.50	121.10	D	2.8			SOUTHWEST OF LLANADA.
03/15/1956	15-26-11	36.50	121.20	D	2.6			SOUTHEAST OF HOLLISTER.
04/03/1956	09-26-02	36.45	121.23	B	2.7			SOUTH OF HOLLISTER.
04/10/1956	11-24-21	36.43	121.48	C	2.9			SOUTHEAST OF MONTEREY.
04/10/1956	20-53-21	36.30	121.00	D	2.9			NORTHEAST OF KING CITY.
05/01/1956	15-06-33	36.50	121.00	D	2.5			SOUTH OF HOLLISTER.
05/04/1956	08-16-14	35.75	121.07	B	3.1			NORTHEAST OF SAN SIMEON.
05/15/1956	10-45--?	34.90	120.40	D	3.5		F	REPORTED FELT AT SANTA MARIA.
06/11/1956	-?-48-37	36.00	120.97	C	3.2			SOUTHWEST OF KING CITY.
06/15/1956	23-42-03	36.30	121.80	D	2.8			SOUTH OF MONTEREY.
07/09/1956	23-15--?	35.10	120.50	D			F	III REPORTED FELT NEAR HUASNA.
07/23/1956	08-03-48	36.30	121.30	D	4.7		F	NW OF KING CITY; FELT OVER 4000 SQ. MI. OF COASTAL CENTRAL CALIF. V AT BIG SUR, CHUALAR, GONZALES, GREENFIELD, 7.5 MI. S OF HOLLISTER, KING CITY, PASO ROBLES, SAN BENITO, AND SAN JUAN BAUTISTA.
07/23/1956	08-20-37	36.50	121.40	D	3.1			AFTERSHOCK OF QUAKE AT 08-03-48.
07/31/1956	-?-40-43	34.15	119.60	C	3.2			
07/31/1956	17-25--?	35.10	120.50	D			F	IV REPORTED FELT AT HUASNA.
08/09/1956	-?-08-49	34.37	119.80	B	4.0		F	OFF SANTA BARBARA; IV AT LOS PRIETOS RANGER STATION.
08/10/1956	23-24-03	35.90	121.30	D	3.0			SOUTHWEST OF KING CITY.
08/20/1956	05-10-33	36.48	121.48	B	3.2		F	NEAR GONZALES; IV AT PINNACLES NATIONAL MONUMENT.
09/15/1956	-?-34-37	36.30	120.30	D	2.7			NORTH OF COALINGA.
10/10/1956	20-02-24	34.70	121.00	D	3.8			
11/12/1956	10-13--?	36.30	120.10	C	3.3			
11/16/1956	03-23-09	35.95	120.47	B	5.0		F	SW OF COALINGA; FELT OVER 8000 SQ. MI. FROM HOLY CITY TO BETTERAVIA TO FIREBAUGH. VI AT KING CITY, MEE RANCH (LONOAK) AND SAN LUCAS.
11/19/1956	13-53-53	35.98	120.57	C	3.3		F	SOUTHWEST OF COALINGA; III AT ADELAIDA (15 MI. WEST OF PASO ROBLES).
11/20/1956	03-42-44	34.70	120.50	C	3.6		F	IV AT LOS ALAMOS; III FELT AT 07-42--?, 11/21/1956.

DCPP UNITS 1 & 2 FSAR UPDATE

TABLE 2.5-1

MM/DD/YY	HR/IN/SE	NORTH LAT	WEST LONG	QUALITY	MAG.	STA. REC.	FELT	MAXIMUM INTENSITY - COMMENTS
12/11/1956	10-56-53	35.88	120.47	C	4.1			NEAR PARKFIELD.
12/28/1956	13-39-37	35.90	121.10	D	2.6			NORTHEAST OF SAN SIMEON.
01/01/1957	09-25--?	35.50	120.65	D			F	REPORTED FELT AT ATASCADERO.
01/29/1957	21-19-53	35.87	122.12	C	4.9		F	OFF COAST NW OF SAN SIMEON; FELT OVER 5000 SQ. MI. OF COASTAL CENTRAL CALIF. V AT BIG SUR, CAMBRIA; CARMEL VALLEY, HARMONY, KING CITY, LUCIA, MARINA, AND SEASIDE, AND IV GENERALLY FROM MOSS LANDING TO 20 MI. W OF COALINGA TO SAN LUIS OBISPO.
02/03/1957	07-57-12	34.50	121.20	C	3.9			NORTH OF KING CITY.
02/08/1957	04-45-38	36.50	121.20	D	2.8			SHARP SHOCK FELT MONTEREY PEN. (BSSA).
02/08/1957	21-20--?	36.50	122.00	D			F	IV REPORTED FELT AT ATASCADERO.
02/09/1957	08-10--?	35.50	120.65	D			F	
02/14/1957	-?-31-30	35.10	119.80	D	2.4			
02/14/1957	10-30-27	36.00	120.60	C	3.6			
02/16/1957	11-43-50	34.30	119.53	C	3.5			
03/09/1957	14-38-28	34.70	119.60	C	2.9			
03/09/1957	14-59-21	34.70	119.60	C	2.4			
04/05/1957	-?-40--?	34.75	120.25	D			F	IV REPORTED FELT AT LOS ALAMOS.
06/21/1957	20-46-42	35.10	120.90	D	3.7		F	OFF COAST; FELT AT SAN LUIS OBISPO AND MORRO BAY.
07/02/1957	09-18-22	34.37	119.88	B	3.4		F	W OF SANTA BARBARA; FELT AT SANTA BARBARA.
07/02/1957	12-59-05	34.37	119.88	B	3.3			
07/02/1957	13-58-28	34.37	119.88	B	3.2			
07/21/1957	01-29-20	36.43	121.22	B	3.1			
08/03/1957	09-31-22	36.25	120.88	C	2.5			
08/18/1957	03-05-25	34.47	120.13	C	3.4			
08/18/1957	11-08-23	34.47	120.13	C			F	N OF GAVIOTA; FELT AT CACHUMA RESERVOIR.
08/21/1957	07-36-54	36.47	121.52	C	3.6			NORTHWEST OF KING CITY.
08/28/1957	01-13-57	34.58	121.00	C	3.5			
09/12/1957	21-36--?	35.50	121.00	D			F	II FELT AT P G AND E PLANT, MORRO BAY.
09/21/1957	06-54-26	36.40	121.10	D	2.8			NORTH OF KING CITY.
09/21/1957	15-32--?	35.50	121.00	D			F	II FELT AT P G AND E PLANT, MORRO BAY.
09/25/1957	23-33-31	36.50	121.50	D	2.7			SOUTH OF HOLLISTER.
10/01/1957	12-55-57	36.47	121.23	C	3.3			SOUTHWEST OF LLANADA.
10/05/1957	14-42--?	34.75	120.25	D			F	IV REPORTED FELT AT LOS ALAMOS.
10/19/1957	-?-04-38	36.10	120.87	B	3.3			SOUTHEAST OF KING CITY.
10/28/1957	11-41-02	34.33	120.00	C	2.8			
11/05/1957	23-50-52	34.72	120.33	C	3.4			
11/18/1957	01-11-42	36.38	121.23	C	3.1			NORTHWEST OF KING CITY.
11/18/1957	07-26-32	36.50	121.70	D	3.3			SOUTHWEST OF MONTEREY.
12/31/1957	22-32-55	36.40	121.00	D	2.9			NORTHEAST OF KING CITY.
01/07/1958	17-13-16	35.70	120.80	D	3.0			NORTH OF SAN LUIS OBISPO.
01/18/1958	08-12--?	35.55	120.65	D			F	REPORTED FELT AT PASO ROBLES.
01/21/1958	21-22-08	36.40	120.50	D	2.9			NORTHWEST OF COALINGA.
01/23/1958	07-06-46	34.38	119.58	B	2.6		F	E OF SANTA BARBARA; IV AT SANTA BARBARA.
01/28/1958	07-12-54	36.50	121.10	D	2.2			SOUTHWEST OF LLANADA.
03/26/1958	13-12-30	36.20	120.30	D	2.4			NEAR COALINGA.
03/27/1958	20-26-14	35.90	121.50	D	2.8			NORTHWEST OF SAN SIMEON.

DCPP UNITS 1 & 2 FSAR UPDATE

TABLE 2.5-1

MM/DD/YY	HR/IN/SE	NORTH LAT	WEST LONG	QUALITY	MAG.	STA. REC.	FELT	MAXIMUM INTENSITY - COMMENTS
03/31/1958	17-38-23	36.50	121.10	D	2.7			SOUTHWEST OF LLANADA.
04/10/1958	08-32-33	36.45	121.12	C	2.9			SOUTHWEST OF LLANADA.
06/05/1958	17-12-50	36.40	121.10	D	3.1			NORTH OF KING CITY.
06/15/1958	07-02-33	36.50	121.38	C	2.9			FORESHOCK OF QUAKE AT 07-05-34.
06/18/1958	07-05-34	36.50	121.38	C	3.3			SOUTH OF HOLLISTER.
06/21/1958	01-03-31	36.40	120.40	D	2.1			SOUTHWEST OF FRESNO.
07/02/1958	17-56-26	36.50	121.30	D	2.8			SOUTHWEST OF LLANADA.
08/08/1958	18-43-01	36.30	121.20	D	2.7			FORESHOCK OF 13-43-15 - RECORDS MIXED.
08/08/1958	13-43-15	36.30	121.20	D	3.9		F	NORTHWEST OF KING CITY; IV AT BIG SUR.
08/18/1958	05-30-42	35.80	121.30	D	3.4			NEAR SAN SIMEON.
09/01/1958	11-31-42	36.10	120.80	D	3.2			SOUTHEAST OF KING CITY.
09/21/1958	07-24-55	36.35	121.12	C	4.0		F	NORTH OF KING CITY; VI AT SAN BENITO; ALSO FELT AT SOLEDAD.
09/21/1958	14-23-01	36.50	121.05	C	2.7			SOUTHWEST OF LLANADA.
10/03/1958	04-25-51	34.37	119.50	B	3.7		F	FROM CARPINTERIA TO GOLETA.
10/10/1958	13-05-16	35.93	120.50	B	4.5		F	SOUTHWEST OF LLANADA; FELT OVER AN AREA OF APPROXIMATELY 3500 SQ. MI. OF THE SOUTHWEST-CENTRAL REGION OF CALIFORNIA - APPEARS TO HAVE BEEN FELT MORE STRONGLY AT PARKFIELD THAN ELSEWHERE; V AT ADELAIDA, CAMP ROBERTS, COALINGA, HARMONY, LONE PINE INN, OILFIELD, PARKFIELD, PASO ROBLES, AND SAN ARDO.
10/15/1958	16-16-44	35.50	121.20	D	3.2			NEAR SAN SIMEON.
11/06/1958	20-11-57	36.08	120.88	C	3.1		F	SOUTHEAST OF KING CITY.
11/16/1958	09-34-04	34.50	119.83	C	4.0		F	NW OF SANTA BARBARA; FELT OVER 600 SQ. MI. FROM SANTA YNEZ TO VENTURA; V AT CARPINTERIA, GOLETA, AND SANTA BARBARA.
11/27/1958	06-04-26	36.37	121.15	C	3.9		F	WEST OF LLANADA; FELT SLIGHTLY AT CARMEL.
11/27/1958	13-39-01	36.20	120.80	D	3.1			EAST OF KING CITY.
12/15/1958	14-58-49	36.20	120.40	D	3.0			NEAR COALINGA.
12/15/1958	15-24-01	36.20	120.40	D	3.0		F	NEAR COALINGA; IV AT COALINGA.
12/30/1958	01-34-15	35.92	119.80	C	3.2			
01/11/1959	05-18-26	36.20	120.80	D	2.5			WEST OF COALINGA.
02/07/1959	05-51-02	36.10	120.00	D	3.0			SOUTHEAST OF KING CITY.
02/27/1959	21-35-01	36.25	120.75	C	3.1			SOUTHEAST OF LLANADA.
03/13/1959	02-44-27	35.80	120.30	D	2.5			SOUTH OF COALINGA.
03/14/1959	02-43-41	35.70	121.30	D	3.6			WEST OF SAN SIMEON.
03/20/1959	05-12-09	36.48	121.17	B	2.9			SOUTHWEST OF LLANADA.
03/25/1959	05-34-17	34.25	119.58	C	2.5		F	SANTA BARBARA CHANNEL; IV AT CARPINTERIA.
04/08/1959	07-41-57	36.37	121.20	B	3.4			NORTH OF KING CITY.
04/09/1959	14-03-11	36.38	121.15	C	2.5			NORTH OF KING CITY.
04/21/1959	09-36-23	36.40	120.40	D	3.0			NORTH OF COALINGA.
04/21/1959	12-31-10	36.10	121.10	D	2.2			NEAR KING CITY.
04/22/1959	19-04-25	36.20	120.90	D	2.6			NEAR KING CITY.
05/13/1959	14-28-10	36.48	121.03	C	2.6			SOUTHWEST OF LLANADA.
05/14/1959	01-34-09	36.50	121.20	D	2.4			SOUTHWEST OF LLANADA.
05/20/1959	10-15-55	36.30	120.40	D	2.6			NORTHWEST OF COALINGA.
06/01/1959	03-47-24	36.50	121.23	C	2.4			SOUTHWEST OF LLANADA.
06/20/1959	15-01-17	36.50	121.30	D	2.9			SOUTH OF VINEYARD.

DCPP UNITS 1 & 2 FSAR UPDATE

TABLE 2.5-1

MM/DD/YY	HR/IN/SE	NORTH LAT	WEST LONG	QUALITY	MAG.	STA. REC.	FELT	MAXIMUM INTENSITY - COMMENTS
06/21/1959	09-24-07	34.32	119.67	B	3.3			SOUTH OF VINEYARD.
07/18/1959	01-11-47	36.50	121.30	D	2.5		F	SOUTHEAST OF COALINGA (NEAR PARKFIELD; FELT STRONGEST AT
08/05/1959	03--?-34	35.95	120.48	C	3.5			PARKFIELD; IV FELT AT PASO ROBLES).
09/05/1959	05-45-34	36.50	121.70	D	3.8		F	SOUTHWEST OF VINEYARD.
10/01/1959	04-35-35	34.43	120.57	B	4.5			OFF POINT CONCEPTION; VI AT GAVIOTA PASS AND V AT GAVIOTA, GOLETA, AND LOMPOC.
10/01/1959	05-52-55	34.20	119.50	C	3.2		F	SOUTHWEST OF LLANADA; FELT AT SALINAS.
10/11/1959	02-03-09	36.45	121.12	C	4.1			SOUTH OF HOLLISTER.
10/24/1959	23-12-54	36.47	121.40	C	3.2			SOUTHEAST OF VINEYARD.
10/25/1959	03-33-13	36.50	121.20	D	2.4			SOUTH OF VINEYARD.
10/25/1959	03-34-02	36.50	121.32	C	3.0			SOUTHEAST OF VINEYARD.
10/26/1959	09-56-01	36.40	121.10	D	3.0			SOUTH OF KING CITY.
11/25/1959	09-28-22	35.20	121.20	D	3.5			SOUTH OF VINEYARD.
11/26/1959	07-02-05	36.40	121.40	D	2.7			SOUTHEAST OF VINEYARD.
12/11/1959	05-55-26	35.60	120.60	D	3.5			SOUTHEAST OF VINEYARD.
12/25/1959	20-38-28	36.00	120.60	D	3.1			SOUTHEAST OF VINEYARD.
12/29/1959	14-53-08	35.75	120.30	C	3.5		F	NEAR CHOLAME; FELT AT PASO ROBLES.
01/02/1960	22-51-48	35.40	121.20	D	4.0			NW OF SAN LUIS OBISPO.
01/04/1960	12-18-20	36.20	120.70	D	3.2			WEST OF COALINGA.
02/14/1960	08-34-30	35.80	121.70	D	2.8			WEST OF SAN SIMEON.
02/25/1960	06-34-31	36.50	121.20	D	2.7			SOUTHWEST OF LLANADA.
02/28/1960	02-55-32	34.33	119.95	C	3.1			SOUTHWEST OF LLANADA.
03/21/1960	20-46-39	36.50	120.73	C	2.5			SOUTHWEST OF LLANADA.
03/26/1960	21-39-21	36.22	121.00	C	2.7			EAST OF KING CITY.
03/29/1960	11-46-42	36.50	121.10	C	2.4			SOUTHWEST OF VINEYARD.
03/31/1960	08-35-09	36.40	121.20	D	2.6			SOUTHWEST OF VINEYARD.
04/02/1960	13-02-10	35.97	120.33	C	2.7			SOUTH OF COALINGA.
04/09/1960	19-01-12	36.20	120.60	D	3.4			WEST OF COALINGA.
05/04/1960	09-44-32	36.42	120.72	B	3.6			SOUTHWEST OF LLANADA.
05/15/1960	06-07-23	36.43	121.27	C	2.5			SOUTH OF VINEYARD.
06/11/1960	17-39-48	36.30	120.90	D	3.7			SOUTHWEST OF VINEYARD, DIABLO RANGE.
06/19/1960	19-51-20	36.20	121.90	D	2.6			SOUTHWEST OF BIG SUR.
06/24/1960	18-13-12	36.45	121.22	B	3.5			SOUTHWEST OF VINEYARD.
07/14/1960	03-22-23	35.60	120.40	D	3.0			NORTHEAST OF SAN LUIS OBISPO.
07/20/1960	-?-59-36	35.80	119.80	D	2.8			NORTHEAST OF SAN LUIS OBISPO.
07/30/1960	02-16-29	36.43	120.28	C	2.5			SOUTHWEST OF FRESNO.
08/09/1960	08-59-47	36.20	120.20	D	3.2			EAST OF COALINGA.
08/10/1960	03-03-50	36.47	121.40	D	3.2			SOUTH OF VINEYARD.
08/26/1960	08-57-24	38.33	121.13	C	3.0			SOUTHWEST OF VINEYARD.
09/10/1960	01-18-22	36.47	121.05	C	2.7			SOUTHWEST OF HOLLISTER.
09/10/1960	20-49-12	36.45	121.28	D	2.8			SOUTHWEST OF LLANADA.
10/08/1960	-?-02-29	36.50	121.67	C	3.0			SOUTHWEST OF VINEYARD.
11/03/1960	07-13-40	36.43	121.07	C	2.7			SOUTH-SOUTHWEST OF LLANADA.
11/18/1960	04-36-44	36.38	121.20	C	3.0			NORTH-NORTHWEST OF KING CITY.

DCPP UNITS 1 & 2 FSAR UPDATE

TABLE 2.5-1

MM/DD/YY	HR/IN/SE	NORTH LAT	WEST LONG	QUALITY	MAG.	STA. REC.	FELT	MAXIMUM INTENSITY - COMMENTS
12/01/1960	14-23-49	34.33	119.85	B	3.2			OFF SANTA BARBARA.
12/15/1960	08-28-08	36.40	121.30	D	3.0			SOUTH OF HOLLISTER.
12/27/1960	03-57-55	36.00	121.10	D	3.3			SOUTH OF KING CITY.
01/06/1961	20-46-36	35.80	120.20	D	3.4			SE OF PARKFIELD.
02/02/1961	12-31--?	36.35	121.20	D	2.2			NORTHWEST OF KING CITY.
02/21/1961	15-46-58	34.37	119.53	C	2.8			SE OF SANTA BARBARA.
03/14/1961	04-15--?	36.40	121.20	D	3.4			SOUTHEAST OF VINEYARD.
03/29/1961	16--?-11	36.50	121.50	D	2.5			SOUTH OF VINEYARD.
04/07/1961	12-21-19	36.20	120.40	D	2.9			NORTH OF COALINGA.
04/08/1961	04-55-26	36.00	121.20	D	2.7			SOUTH OF KING CITY.
04/08/1961	09-29-47	36.10	120.43	B	3.4			NEAR COALINGA.
04/08/1961	12-52-16	36.12	120.43	C	2.7			AFTERSHOCK OF QUAKE AT 09-29-47.
04/11/1961	09-08-11	36.00	120.10	D	2.7			SOUTHEAST OF KING CITY.
04/12/1961	04-59-08	35.92	120.50	C	2.6			SOUTHWEST OF COALINGA.
04/19/1961	18-16-35	36.40	121.58	C	3.3			SOUTHWEST OF MONTEREY.
05/25/1961	14-19-05	36.33	121.00	C	3.4			NORTHEAST OF KING CITY.
05/25/1961	14-19-35	36.33	121.00	B	3.4			NORTHEAST OF KING CITY.
06/01/1961	06-47-20	36.33	121.32	B	2.7			NORTHEAST OF KING CITY.
06/01/1961	14-11-30	36.45	121.20	C	2.6			NORTH OF KING CITY.
06/18/1961	12-50-59	36.18	120.83	C	2.1		F	EAST OF KING CITY.
06/25/1961	13-15-26	36.48	121.35	C	3.6			SOUTH OF HOLLISTER; FELT IN HOLLISTER AREA. INTENSITY IV 7.5
06/26/1961	11-30-22	35.77	122.00	C	2.5			MI. SOUTH OF HOLLISTER AT HARRIS RANCH.
07/22/1961	18-01-55	36.40	121.20	C	4.0		F	OFF SAN SIMEON COAST.
07/31/1961	-?-07-09	35.82	120.37	C	4.7		F	NORTHEAST OF PARISO; FELT AT PINNACLES NATIONAL MONUMENT (ABOUT 25 MI. SOUTHEAST OF HOLLISTER).
08/01/1961	06-12-54	36.43	120.85	C	3.1			SAN LUIS OBISPO; FELT OVER AN AREA OF 5000 SQ. MI. OF WEST CENTRAL CALIFORNIA; INTENSITY V AT ATASCADERO, CHOLAME, CRESTON, PARKFIELD, SAN LUIS OBISPO, AND TEMPLETON.
08/17/1961	17-14-45	36.33	120.95	B	3.1			SOUTH OF LLANADA.
09/14/1961	15-12-20	34.32	119.63	C	2.7			NORTH OF SAN SIMEON.
09/14/1961	15-14-38	34.32	119.63	C	2.8			EAST OF PARISO.
09/27/1961	02-02-06	36.33	121.25	C	2.7			EAST OF LLANADA.
09/29/1961	15-39-58	36.33	120.88	B	2.4			SOUTHEAST OF KING CITY.
10/12/1961	06-31-11	35.80	121.30	D	2.3			SOUTH OF MONTEREY.
10/29/1961	11-47-33	36.33	120.92	C	2.0			SOUTHWEST OF LLANADA.
11/05/1961	10-43-57	36.03	120.10	D	2.0			NORTHWEST OF KING CITY.
11/29/1961	04-49-03	35.15	120.13	C	3.0			WEST OF GUADALUPE; FELT OVER AN AREA OF 3000 SQ. MI. V AT ARROYO GRANDE, AVILA BEACH, CASMALIA, GROVER CITY.
12/06/1961	03-27-30	36.43	121.85	B	2.4			GUADALUPE, HALCYON, OCEANO, POINT ARGUELLO, AND SHELL
12/14/1961	07-28-44	36.48	121.08	B	2.1			
01/04/1962	03-56-10	36.40	121.40	C	3.0	11	F	
01/31/1962	08-33-15	34.88	120.68	C	3.6			
02/01/1962	06-37-57	34.88	120.68	C	4.5			
02/01/1962	07-58-12	34.38	120.68	C	3.7			
02/04/1962	11-43-34.1	36.42	121.27	C	3.2	12		

DCPP UNITS 1 & 2 FSAR UPDATE

TABLE 2.5-1

MM/DD/YY	HR/IN/SE	NORTH LAT	WEST LONG	QUALITY	MAG.	STA. REC.	FELT	MAXIMUM INTENSITY - COMMENTS
02/07/1962	13--?-70	34.30	122.10	D	3.9		F	OFF COAST NEAR LOMPOC; V AT MORRO BAY AND PISMO BEACH.
03/05/1962	07-44-01	34.60	121.60	D	4.5			
03/06/1962	03-40-22	34.60	121.60	D	3.6			OFF COAST NEAR LOMPOC.
03/10/1962	08-07-21	34.60	121.60	D	4.2			OFF COAST NEAR LOMPOC.
03/10/1962	13-40-48	34.60	121.60	D	4.0			OFF COAST NEAR LOMPOC.
03/10/1962	15-24-21	34.60	121.60	D	3.5			
03/12/1962	21-32-09	34.60	121.60	D	3.9			
03/23/1962	22-10-18	34.28	120.20	C	2.9			
03/24/1962	03-38-41.8	36.20	119.78	B	3.4	19		SOUTH OF FRESNO.
04/02/1962	03-06-03.2	36.25	120.10	B	3.7	16	F	EAST OF COALINGA; V IN TEHACHAPI.
04/15/1962	08-41-02.3	36.42	120.62	B	4.7	23	F	SOUTHEAST OF LLANADA; V AT IDRIA.
05/04/1962	20-52-32	35.27	119.55	B	2.8			
05/05/1962	-?-55-20	34.20	121.50	D	3.3			
09/03/1962	17-53-33.1	36.47	121.07	C	2.6	8	F	SOUTHWEST OF LLANADA; FELT IN HOLLISTER.
09/11/1962	01-34-31	36.03	121.23	B	3.3	16		SOUTHWEST OF KING CITY.
09/16/1962	18-12-35	34.48	119.68	B	4.0		F	NEAR SANTA BARBARA; V AT LOS PRIETOS.
09/16/1962	18-17-09	34.48	119.68	C	2.2			
09/16/1962	18-31-17	34.52	119.77	B	2.9			
09/21/1962	05-07-18	34.47	119.58	B	3.0			
09/29/1962	19-47-32	34.47	119.70	B	2.9			
10/13/1962	17-49-39.5	36.35	120.42	B	3.7	17		NORTHEAST OF PRIEST.
12/15/1962	-?-40-20.9	36.47	120.63	B	2.9	13		NORTH OF PRIEST.
01/09/1963	06-04-25.7	35.98	120.35	B	3.2	14	F	SE OF PRIEST; III AT WHEELER RIDGE.
02/09/1963	02-52-14.5	35.98	121.69	C	2.8	8		OFF COAST S OF BIG SUR.
02/12/1963	03-44-30.9	36.50	121.32	B	2.6	10		S OF VINEYARD.
02/22/1963	15-56-21.9	35.11	121.44	C	3.3	15		OFF COAST, SW OF MORRO BAY.
02/22/1963	15-56-36.0	35.67	120.83	D	3.6			
04/04/1963	01--?-58	35.80	121.50	C	2.5	6		NW OF SAN SIMEON.
04/10/1963	01-38-56.8	36.42	121.05	C	2.9	11		SW OF LLANADA.
04/11/1963	14-02-31.8	36.20	120.87	B	2.9	13		NW OF PRIEST.
04/20/1963	16-37-33.0	36.38	120.96	C	3.0	14		SOUTH OF LLANADA.
05/10/1963	10-17-57.1	36.37	120.98	C	2.5	9		SOUTH OF LLANADA.
06/01/1963	05-19-0.2	34.33	119.54	B	2.0			
07/02/1963	12--?-24.9	34.86	119.80	C	2.0			
07/04/1963	03-20-41.0	34.77	120.02	C	3.2			
07/06/1963	23-32-30.4	34.78	120.63	B	3.3			
08/15/1963	21-02-32.2	35.97	121.02	C	3.6	15		NEAR JOLON; FORESHOCK OF FOLLOWING--
08/15/1963	21-21-32.1	35.91	121.06	C	3.9	18	F	NEAR JOLON; FELT AT HARRIS RANCH.
08/16/1963	08-12-13.6	36.06	121.01	C	3.2	10		NEAR JOLON; AFTERSHOCK OF PRECEDING.
09/06/1963	03-54-34	36.22	121.48	C	2.6	8		WEST OF PARAISO.
11/01/1963	14-05-56.0	35.56	120.23	C	3.4	9		EAST OF ATASCADERO.
11/01/1963	14-06-0.4	35.75	120.47	C	3.2			
11/18/1963	07-31-38.5	36.22	120.30	C	3.5		F	IV 15 MI. NE OF SAN MIGUEL.
11/18/1963	10-54-45.4	36.38	120.32	C	2.7	11		NE OF COALINGA.
11/19/1963	03-33-09.2	36.42	121.03	C	2.9	10		SW OF LLANADA.
12/12/1963	17-10-48.5	34.98	119.51	C	3.1			
02/10/1964	05-47-25.0	35.75	120.94	C	3.9	19		NE OF PASO ROBLES.

DCPP UNITS 1 & 2 FSAR UPDATE

TABLE 2.5-1

MM/DD/YY	HR/IM/SE	NORTH LAT	WEST LONG	QUALITY	MAG.	STA. REC.	FELT	MAXIMUM INTENSITY - COMMENTS
03/20/1964	13-15-51.0	36.40	121.03		2.6	7		SW OF LLANADA.
04/28/1964	15-01-48.3	36.23	121.08		2.8	7		NEAR KING CITY.
05/07/1964	17-53-58.3	36.43	120.54		2.5	5		N OF PRIEST.
06/06/1964	11-47-39.0	34.63	121.40	D	4.3			
06/20/1964	09-21-51.4	34.13	120.67	C	3.1			
07/24/1964	07-09-35.9	36.47	121.18		2.9	15		NE OF PARAISO.
08/30/1964	03-41-10.4	36.29	121.94		2.9	7		OFF COAST NW OF POINT SUR.
09/12/1964	01-45-53.5	36.08	120.49		3.1	10		SE OF PRIEST.
10/17/1964	23-43-22.6	36.21	120.92		3.3	14		NW OF PRIEST.
11/08/1964	01-19-19.0	36.00	120.00		4.0	15		E OF AVENAL.
11/08/1964	13-45-51.1	36.34	121.32		3.1	16		NEAR PARAISO.
11/18/1964	01-47-34.0	35.98	121.13		2.7	8		SW OF KING CITY.
11/25/1964	12-49-41.8	36.21	120.78		2.8	15		NW OF PRIEST.
12/05/1964	13-55-57.5	36.02	121.08		2.6	12		W OF SAN ARDO.
12/11/1964	03-35-38.8	34.24	119.76	B	3.5			
12/25/1964	11-21-13.2	35.97	121.18		2.6	5		N OF LAKE NACIMIENTO.
12/27/1964	18-58-59.4	36.46	121.06		2.6	7		SW OF LLANDA.
01/13/1965	04-20-48.2	36.45	120.58		2.6	9		NE OF PRIEST.
01/26/1965	08-34-30.7	35.72	120.54		3.0	12		SE OF PRIEST.
01/26/1965	08-36-36.6	35.92	120.27	C	3.1			
01/26/1965	08-38-16.4	36.04	120.26	C	3.1			
02/21/1965	18-39-18.3	35.67	120.43		3.1	12		E OF PASO ROBLES.
03/28/1965	02-32-21.0	36.20	120.40		3.5			(USCGS)
04/06/1965	20-49-24.4	35.95	121.46		2.5	7		N OF SAN SIMEON.
04/08/1965	01-05-40.6	36.03	121.40		3.0	10		N OF SAN SIMEON.
04/09/1965	12-50-19.3	36.03	120.64		3.0	10		S OF PRIEST.
04/18/1965	03-58-52.4	36.50	121.23		2.7	7		NEAR PINNACLES NATIONAL MONUMENT
04/24/1965	07-29-47.1	34.91	120.14	C	3.6			
05/12/1965	17-55-08.7	35.49	121.17		3.0	6		SW OF SAN SIMEON.
06/07/1965	15-06-47.6	36.50	121.13		2.5	10		NEAR PINNACLES NATIONAL MONUMENT.
06/20/1965	02-56-43.5	36.33	120.37		2.7	11		N OF COALINGA.
06/30/1965	15-21-27.7	36.35	120.71		2.5	9		N OF PRIEST.
07/23/1965	05-31-52.7	35.71	121.23		3.4	13		N OF SAN SIMEON.
08/01/1965	15-25-57.4	36.36	120.98		2.5	7		SW OF LLANADA.
08/01/1965	06-47-27.3	36.23	120.85		2.5	7		NW OF PRIEST.
08/01/1965	13-28-32.9	36.23	120.84		2.5	6		AFTERSHOCK OF 06-47-27.3.
08/13/1965	07-36-08.4	36.46	121.08		2.6	9		SW OF LLANADA.
08/13/1965	13-46-16.5	34.35	119.63	B	3.7		F	IV AT CARPINTERIA AND SANTA BARBARA.
08/13/1965	21-28-51.8	36.48	121.13		2.4	8		W OF LLANADA.
08/15/1965	23-06-52.5	36.00	120.20		4.0		F	AT PAICINES.
08/21/1965	20-09-35.4	36.46	121.07		2.5	8		SW OF LLANADA.
09/06/1965	18--?-57.8	35.96	120.36	C	3.4			
09/12/1965	08-50-05.5	36.49	121.12		2.5	7		W OF LLANADA.
09/19/1965	15-42-07.8	35.98	120.34	C	4.8		F	V AT ARMONA, AVENAL, CHOLAME, KETTLEMAN CITY, AND STRATFORD.
10/22/1965	02-29-22	36.00	121.70		2.7	6		OFF COAST. W OF KING CITY.
12/02/1965	22-29-13.0	36.20	121.68		2.8	9		W OF PARAISO.

DCPP UNITS 1 & 2 FSAR UPDATE

TABLE 2.5-1

MMDD/YY	HR/MIN/SE	NORTH LAT	WEST LONG	QUALITY	MAG.	STA. REC.	FELT	MAXIMUM INTENSITY - COMMENTS
01/28/1966	01-49-47.4	35.83	120.45		3.0		F	PARKFIELD SEQUENCE; MC EVILLY, ET AL, (1967) THE PARKFIELD, CALIFORNIA EARTHQUAKE OF 1966, BULL. SEISM. SOC. AM.
02/01/1966	-?-20-44.3	36.03	120.57		2.9			PARKFIELD SEQUENCE - SEE 01/28/1966 AT 01-49-47.4.
02/14/1966	-?-24-03.9	36.02	120.57		2.4			PARKFIELD SEQUENCE - SEE 01/28/1966 AT 01-49-47.4.
02/25/1966	01-34-38.0	36.05	120.63		2.4			PARKFIELD SEQUENCE - SEE 01/28/1966 AT 01-49-47.4.
03/31/1966	21-38-45.2	36.05	120.60		2.5			PARKFIELD SEQUENCE - SEE 01/28/1966 AT 01-49-47.4.
04/05/1966	20-44-58.7	36.24	120.85		2.7	9		10 KM NW OF PRIEST (UC BERKELEY SEISMOGRAPH STATION (SS))
04/12/1966	15-31-39.8	36.07	120.70		2.3			PARKFIELD SEQUENCE.
05/11/1966	17-37-01.1	35.98	120.57		2.3			PARKFIELD SEQUENCE.
05/23/1966	08-07-37.6	36.02	120.57		2.5			PARKFIELD SEQUENCE.
05/27/1966	08-11-07.0	36.02	120.57		2.2			PARKFIELD SEQUENCE.
06/18/1966	15-36-03.7	35.98	120.49		2.7			PARKFIELD SEQUENCE.
06/20/1966	16-32-17.6	35.96	120.53		2.0			PARKFIELD SEQUENCE.
06/24/1966	23-19-18.8	36.33	120.96		2.8	9		NE OF KING CITY.
06/28/1966	21-42-50.4	36.50	120.85		3.1	10		SE OF LLANADA.
06/28/1966	01--?-31.5	35.95	120.52		3.1		F	PARKFIELD SEQUENCE; FELT AT CHOLAME, PARKFIELD, VALLETON, AND WORK RANCH.
06/28/1966	01-14-55	35.95	120.50		1.8			PARKFIELD SEQUENCE.
06/28/1966	04-08-55.2	35.97	120.50		5.1			PARKFIELD SEQUENCE FIRST MAIN SHOCK (FELT REPORTS FOR THE 2 MAIN SHOCKS ARE NOT SEPARATED.) FELT OVER 20,000 SQ. MI., MINOR SURFACE FAULTING ALONG SAN ANDREAS FAULT FROM PARKFIELD TO CHOLAME (20 MI.), MAXIMUM DISPLACEMENT 4 IN. VII AT CHOLAME AND PARKFIELD, VI AT ANNETTE, BITTERWATER VALLEY, COALINGA, HIDDEN VALLEY RANCH, PASO ROBLES, SAN LUIS OBISPO, SAN MIGUEL, SHAFTER, SHANDON, SLACK CANYON, VALLETON, WAITI RANCH, AND WORK RANCH, AND V AT ADELADA, ALPAUGH, ARROYO GRANDE, ATASCADERO, AVILA BEACH, BAKERSFIELD, BAYWOOD PARK, BRYSON, BURREL, BUTTONWILLOW, EARLIMART, FELLOWS, FRAZIER PARK, GREENFIELD, HARMONY, INDIAN VALLEY, KETTLEMAN CITY, KING CITY, LAPANZA, LOST MARICOPA, MEE RANCH, MORRO BAY, MOSS LANDING, MUSICK, NIPOMO, OCEANO, OLD RIVER, PANOCHÉ, PINE CANYON, PISMO BEACH, POZO, PRIEST VALLEY, SAN ARDO, SAN JOAQUIN, SAN LUCAS, SAN SIMEON, SIMMLER, STRATFORD, TEMPLETON, AND VANDENBURG A.F.B.
06/28/1966	04-09-53	35.95	120.50					PARKFIELD SEQUENCE.
06/28/1966	04-18-34.0	35.95	120.53		2.6		F	PARKFIELD SEQUENCE - FELT AT CANTUA CREEK AND SOQUEL.
06/28/1966	04-26-13.4	35.95	120.50		5.5		F	PARKFIELD SEQUENCE - SECOND MAIN SHOCK.
06/28/1966	04-26-28	35.95	120.50					PARKFIELD SEQUENCE.
06/28/1966	04-26-34	35.95	120.50					PARKFIELD SEQUENCE.
06/28/1966	04-27-37	35.95	120.50					PARKFIELD SEQUENCE.
06/28/1966	04-27-58	35.95	120.50					PARKFIELD SEQUENCE.
06/28/1966	04-28-19	35.95	120.50					PARKFIELD SEQUENCE.
06/28/1966	04-28-36	35.95	120.50					PARKFIELD SEQUENCE.
06/28/1966	04-28-46	35.95	120.50		4.5			PARKFIELD SEQUENCE.

DCPP UNITS 1 & 2 FSAR UPDATE

TABLE 2.5-1

MM/DD/YY	HR/IN/SE	NORTH LAT	WEST LONG	QUALITY	MAG.	STA. REC.	FELT	MAXIMUM INTENSITY - COMMENTS
06/28/1966	04-29-13	35.95	120.50					PARKFIELD SEQUENCE.
06/28/1966	04-31-55	35.95	120.50		3.0			PARKFIELD SEQUENCE
06/28/1966	04-32-50	35.95	120.50		3.5		F	PARKFIELD SEQUENCE - FELT AT CANTUA CREEK, CHOLAME, AND HIERNANDEZ
06/28/1966	04-34-59.1	35.81	120.40		3.0			PARKFIELD SEQUENCE.
06/28/1966	04-39-08.1	35.95	120.50		3.0		F	PARKFIELD SEQUENCE - FELT AT PARKFIELD AND WORK RANCH.
06/28/1966	04-42-33.6	35.83	120.38		2.4			PARKFIELD SEQUENCE.
06/28/1966	04-43-54.8	35.95	120.57		2.7			PARKFIELD SEQUENCE.
06/28/1966	04-46-22	35.95	120.50		3.0			PARKFIELD SEQUENCE.
06/28/1966	04-51-43	35.95	120.50		2.4			PARKFIELD SEQUENCE.
06/28/1966	05--?-59.5	35.85	120.40		3.1			PARKFIELD SEQUENCE.
06/28/1966	05-03-44.7	35.88	120.45		2.4			PARKFIELD SEQUENCE.
06/28/1966	05-09-48.3	35.83	120.13		2.5			PARKFIELD SEQUENCE.
06/28/1966	05-12-42.5	35.92	120.47		2.9			PARKFIELD SEQUENCE.
06/28/1966	05-17-05	35.95	120.50		2.1			PARKFIELD SEQUENCE.
06/28/1966	05-21-05	35.95	120.50		2.0			PARKFIELD SEQUENCE.
06/28/1966	05-29-14.9	35.92	120.48		2.1			PARKFIELD SEQUENCE.
06/28/1966	05-37-04.6	35.88	120.44		2.5			PARKFIELD SEQUENCE.
06/28/1966	05-40-19.4	35.94	120.48		2.7			PARKFIELD SEQUENCE.
06/28/1966	05-45-59.1	35.75	120.33		3.2			PARKFIELD SEQUENCE.
06/28/1966	05-48-26	35.95	120.50		2.2			PARKFIELD SEQUENCE.
06/28/1966	05-51-34.0	35.86	120.44		2.1			PARKFIELD SEQUENCE.
06/28/1966	05-52-06	35.95	120.50		2.3			PARKFIELD SEQUENCE.
06/28/1966	05-52-58	35.95	120.50		2.4			PARKFIELD SEQUENCE.
06/28/1966	05-56--?	35.95	120.50		2.1			PARKFIELD SEQUENCE.
06/28/1966	06-11-03.5	35.81	120.35		2.6			PARKFIELD SEQUENCE.
06/28/1966	06-32-17.9	35.94	120.52		3.4		F	PARKFIELD SEQUENCE - FELT AT CHOLAME, COALINGA, AND PARKFIELD
06/28/1966	06-35-11.4	35.80	120.38		3.0			PARKFIELD SEQUENCE.
06/28/1966	06-39-31.2	35.90	120.47		2.2			PARKFIELD SEQUENCE.
06/28/1966	07-01-03.8	35.92	120.48		2.2			PARKFIELD SEQUENCE.
06/28/1966	07-33-52.7	35.90	120.45		2.7			PARKFIELD SEQUENCE.
06/28/1966	07-41-43	35.95	120.50		2.3			PARKFIELD SEQUENCE.
06/28/1966	07-45-48.3	35.90	120.47		3.0		F	PARKFIELD SEQUENCE - FELT AT CHOLAME AND PARKFIELD.
06/28/1966	08-14-48.6	35.83	120.42		2.4			PARKFIELD SEQUENCE.
06/28/1966	08-47-52.4	35.85	120.42		2.0			PARKFIELD SEQUENCE.
06/28/1966	08-54-49.5	35.92	120.50		2.3			PARKFIELD SEQUENCE.
06/28/1966	08-59-52.3	35.85	120.42		2.5			PARKFIELD SEQUENCE.
06/28/1966	09-31-26.5	35.77	120.35		2.4			PARKFIELD SEQUENCE.
06/28/1966	09-35-54.3	35.77	120.36		2.2			PARKFIELD SEQUENCE.
06/28/1966	09-56-09.7	35.83	120.40		2.5			PARKFIELD SEQUENCE.
06/28/1966	10-15-53.3	35.92	120.53		2.1			PARKFIELD SEQUENCE.
06/28/1966	10-20-16.4	35.85	120.42		2.3			PARKFIELD SEQUENCE.
06/28/1966	10-23-22.8	35.55	120.42		2.0			PARKFIELD SEQUENCE.
06/28/1966	10-23-22.8	35.94	120.48		2.5			PARKFIELD SEQUENCE.
06/28/1966	10-46-22.9	35.94	120.50		2.0			PARKFIELD SEQUENCE.
06/28/1966	11-15-13.9	35.85	120.42		2.0			PARKFIELD SEQUENCE.

DCPP UNITS 1 & 2 FSAR UPDATE

TABLE 2.5-1

MM/DD/YY	HR/IN/SE	NORTH LAT	WEST LONG	QUALITY	MAG.	STA. REC.	FELT	MAXIMUM INTENSITY - COMMENTS
06/28/1966	11-28-41.4	35.85	120.38		2.0			PARKFIELD SEQUENCE.
06/28/1966	11-30-14.0	35.90	120.47		2.2			PARKFIELD SEQUENCE.
06/28/1966	12-31-52.1	35.94	120.48		2.5			PARKFIELD SEQUENCE.
06/28/1966	12-52-22.0	35.97	120.53		2.3			PARKFIELD SEQUENCE.
06/28/1966	13-48-22	35.97	120.53		2.7			PARKFIELD SEQUENCE.
06/28/1966	14-13-09.3	35.94	120.48		2.6			PARKFIELD SEQUENCE.
06/28/1966	14-21-36.3	35.94	120.48		2.2			PARKFIELD SEQUENCE.
06/28/1966	14-51-53.6	35.90	120.47		2.3			PARKFIELD SEQUENCE.
06/28/1966	18-12-19.4	35.92	120.50		2.3			PARKFIELD SEQUENCE.
06/28/1966	18-22-32.4	35.92	120.50		2.0			PARKFIELD SEQUENCE.
06/28/1966	18-54-55.3	35.88	120.45		2.5			PARKFIELD SEQUENCE.
06/28/1966	19-59-37.8	35.92	120.47		2.8			PARKFIELD SEQUENCE.
06/28/1966	20--?-38.7	35.92	120.48		2.5			PARKFIELD SEQUENCE.
06/28/1966	20-46-56.4	35.77	120.40		3.1		F	PARKFIELD SEQUENCE - FELT AT BAR B RANCH AND WORK RANCH.
06/28/1966	22-01-13.9	35.85	120.44		2.0			PARKFIELD SEQUENCE.
06/28/1966	22-37-56.7	35.88	120.42		2.0			PARKFIELD SEQUENCE.
06/28/1966	23-57-22.3	35.77	120.35		2.5			PARKFIELD SEQUENCE.
06/29/1966	-?-17-32.6	35.85	120.44		2.3			PARKFIELD SEQUENCE.
06/29/1966	02-19-39.9	35.92	120.52		3.6		F	PARKFIELD SEQUENCE - FELT AT CHOLAME, PARKFIELD, AND WORK RANCH.
06/29/1966	04-06-40.3	35.92	120.53		2.8			PARKFIELD SEQUENCE.
06/29/1966	07-28-59.4	35.92	120.48		2.3			PARKFIELD SEQUENCE.
06/29/1966	08-55-52.4	35.88	120.45		2.9			PARKFIELD SEQUENCE.
06/29/1966	09-20-50.1	35.78	120.36		2.5			PARKFIELD SEQUENCE.
06/29/1966	10-13-44.0	35.97	120.50		2.3			PARKFIELD SEQUENCE.
06/29/1966	10-56-58.8	35.75	120.33		3.0			PARKFIELD SEQUENCE.
06/29/1966	12-30-09.0	35.94	120.50		2.4			PARKFIELD SEQUENCE.
06/29/1966	13-11-59.7	35.82	120.38		3.1		F	PARKFIELD SEQUENCE - FELT AT CHOLAME AND PARKFIELD.
06/29/1966	15-18-38.9	35.95	120.33		2.0			PARKFIELD SEQUENCE.
06/29/1966	15-34-22.2	35.92	120.48		2.3			PARKFIELD SEQUENCE.
06/29/1966	16-03-30.1	35.86	120.45		2.1			PARKFIELD SEQUENCE.
06/29/1966	17-10-28.3	35.82	120.36		2.0			PARKFIELD SEQUENCE.
06/29/1966	19-53-25.9	35.95	120.53		5.0		F	PARKFIELD SEQUENCE - FELT AT ADELAIDA, BITTERWATER, CHOLAME, COALINGA, FRESNO, MEE RANCH, MORRO BAY, SAN LUIS OBISPO, SAN MIGUEL, SANTA MARGARITA, SHANDON, AND WORK RANCH.
06/29/1966	20-44-40.0	35.74	120.28		2.5			PARKFIELD SEQUENCE.
06/29/1966	23-48-12.0	35.74	120.28		2.3			PARKFIELD SEQUENCE.
06/30/1966	01-17-36.1	35.86	120.45		4.1			PARKFIELD SEQUENCE.
06/30/1966	03-36-16.8	35.92	120.47		2.6			PARKFIELD SEQUENCE.
06/30/1966	05-04-12.9	35.88	120.45		2.0			PARKFIELD SEQUENCE.
06/30/1966	06-07-21.5	35.94	120.48		2.4			PARKFIELD SEQUENCE.
06/30/1966	06-23-32.4	35.90	120.47		2.1			PARKFIELD SEQUENCE.
06/30/1966	07-37-12.1	35.90	120.47		2.0			PARKFIELD SEQUENCE.
06/30/1966	08-01-38.4	35.90	120.47		2.9			PARKFIELD SEQUENCE.
06/30/1966	11-07-55.1	35.78	120.33		2.8			PARKFIELD SEQUENCE.

DCPP UNITS 1 & 2 FSAR UPDATE

TABLE 2.5-1

MM/DD/YY	HR/IM/SE	NORTH LAT	WEST LONG	QUALITY	MAG.	STA. REC.	FELT	MAXIMUM INTENSITY - COMMENTS
06/30/1966	13-26-05.7	35.78	120.35		2.3			PARKFIELD SEQUENCE.
06/30/1966	13-29-56.6	35.86	120.40		2.0			PARKFIELD SEQUENCE.
06/30/1966	13-40-50.9	35.83	120.38		2.1			PARKFIELD SEQUENCE.
06/30/1966	16-05-02.7	35.97	120.50		2.3			PARKFIELD SEQUENCE.
06/30/1966	19-06-17.5	35.86	120.42		2.1			PARKFIELD SEQUENCE.
07/01/1966	09-41-21.9	35.94	120.52	3.2			F	PARKFIELD SEQUENCE - FELT AT WORK RANCH.
07/02/1966	12-08-34.8	35.79	120.33		3.7		F	PARKFIELD SEQUENCE - FELT AT PARKFIELD.
07/02/1966	12-16-15.8	35.81	120.35		3.4		F	PARKFIELD SEQUENCE - FELT AT PARKFIELD.
07/02/1966	12-25-06.8	35.80	120.35		3.1		F	PARKFIELD SEQUENCE - FELT AT PARKFIELD.
07/05/1966	18-54-54.5	35.92	120.48		3.0		F	PARKFIELD SEQUENCE - FELT AT PARKFIELD.
07/25/1966	22-49-39	36.40	120.30		2.5	4		NE OF COALINGA.
07/27/1966	08-12-0.2	35.90	120.48		3.0			PARKFIELD SEQUENCE.
08/03/1966	12-39-05.8	35.80	120.38		3.4		F	PARKFIELD SEQUENCE; V AT CHOLAME, PARKFIELD, AND WORK RANCH.
08/04/1966	-?-54-24.5	35.74	121.35		3.0	8		NW OF SAN SIMEON.
08/07/1966	17-03-24.9	35.94	120.55		3.0			PARKFIELD SEQUENCE.
08/19/1966	22-51-20.1	35.90	120.45		3.3			PARKFIELD SEQUENCE.
09/07/1966	-?-20-50.5	35.83	119.94		3.2	9		SE OF COALINGA.
09/18/1966	15-09-55.7	35.74	120.35		3.1			PARKFIELD SEQUENCE.
10/27/1966	12-06-03.9	35.94	120.50		3.8		F	PARKFIELD SEQUENCE; V AT ATASCADERO, AVENAL, COALINGA, PARKFIELD, SAN MIGUEL, TEMPLETON, AND WORK RANCH.
11/05/1966	13-31-31.2	35.94	120.50		3.3			PARKFIELD SEQUENCE.
11/18/1966	23-39-42.3	35.75	120.33		3.3			PARKFIELD SEQUENCE.
12/30/1966	10-23-48	36.47	120.40		2.5	4		N OF COALINGA.
01/08/1967	23-03-50.9	35.90	120.40		2.8	8		35 KM SE OF PRIEST (UC BERKELEY SS).
01/09/1967	23-18-59.5	35.86	120.10		3.1	9		SE OF COALINGA.
02/01/1967	13-55-54.1	35.70	120.25		3.0	8		NE OF SAN LUIS OBISPO.
02/26/1967	15-17-53.9	36.40	121.06		2.5	9		SW OF LLANADA.
03/13/1967	21-59-48.4	36.00	120.61		3.1	8	F	15 KM S OF PRIEST (UC BERKELEY SS), IV AT SAN MIGUEL; FELT AT INDIAN VALLEY AND RANCHITO CANYON.
03/21/1967	02-24-28.3	36.21	120.85		2.8	8		17 KM NW OF PRIEST (UC BERKELEY SS).
03/23/1967	11-39-56.4	36.16	120.18		3.0	5		20 KM E OF COALINGA.
04/13/1967	09-06-42.5	36.15	120.80		2.7	8		13 KM W OF PRIEST (UC BERKELEY SS).
05/17/1967	14-16-52.2	35.95	120.73		3.0	6		30 KM S OF PRIEST (UC BERKELEY SS).
06/03/1967	20-10-53.0	35.71	121.48		2.6	7		OFF COAST NW OF SAN SIMEON.
06/06/1967	06-11-38.5	35.81	120.43		3.0	10	F	40 KM SE OF PRIEST (UC BERKELEY SS); IV AT WORK RANCH; FELT IN INDIAN VALLEY, SOUTHERN MONTEREY COUNTY, AND VINEYARD CANYON.
06/13/1967	12-54-10.7	35.81	121.50		3.3	10		OFF COAST, 35KM NW OF SAN SIMEON.
07/24/1967	07-08-52.9	35.96	120.50		3.7	9		PARKFIELD AREA.
07/28/1967	14-44-40.1	35.75	121.38		3.0	6		NEAR SAN SIMEON.
08/01/1967	22-14-13.0	35.75	121.40		2.7	6		NW OF SAN SIMEON.
08/08/1967	18-11-20.3	36.42	120.42		2.5	7		N OF COALINGA.
08/12/1967	18-57-40.4	35.80	120.45		4.1	18	F	PARKFIELD AREA; V AT ESTRELLA AREA, HOG CANYON ROAD TO PARKFIELD, AND SHANDON, AND IV AT CHOLAME.

DCPP UNITS 1 & 2 FSAR UPDATE

TABLE 2.5-1

MM/DD/YY	HR/Min/Sec	NORTH LAT	WEST LONG	QUALITY	MAG.	STA. REC.	FELT	MAXIMUM INTENSITY - COMMENTS
08/12/1967	23-21-07.8	36.11	120.80		2.8	6		SE OF KING CITY.
08/12/1967	23-22-05.3	36.13	120.76		2.5	7		SE OF KING CITY.
08/17/1967	23-12-02.7	35.91	121.50		2.6	5		NW OF SAN SIMEON.
08/25/1967	02-28-14.4	35.81	121.27		2.7	6		NW OF SAN SIMEON.
08/25/1967	16-35-27.8	36.05	120.00		3.2	7		SE OF COALINGA.
08/25/1967	16-40-50.2	36.01	119.95		3.0	7		SE OF COALINGA.
08/31/1967	18-10-40.4	35.86	121.35		2.8	7		NW OF SAN SIMEON.
09/09/1967	21-35-05.6	35.81	121.63		2.4	3		OFF SHORE SAN SIMEON.
10/14/1967	12-02-43.6	36.50	120.61		2.7	5		NEAR MT. CIERVO.
10/21/1967	12-05-21.8	35.83	120.46		3.1	7		PARKFIELD AREA.
10/25/1967	23-05-30.5	35.73	121.45		2.6	4		NEAR SAN SIMEON.
11/11/1967	22-10-06.8	36.50	120.81		3.3	9		S OF PANOCHO VALLEY.
11/11/1967	22-33-47.5	36.48	120.78		2.8	6		S OF PANOCHO VALLEY.
11/12/1967	07-11-20.4	36.48	120.80		2.6	7		S OF PANOCHO VALLEY.
11/14/1967	-?-?-51.7	35.78	120.53		3.1	3		PARKFIELD.
11/25/1967	15-27-43.4	36.46	121.06		2.5	6		BEAR VALLEY.
12/21/1967	05-13-11.3	35.36	120.85		2.6	3		S OF SAN SIMEON.
12/21/1967	19-08-53.8	35.91	119.53		3.1	5		NW OF DELANO.
12/21/1967	23-58-60.2	35.93	120.56		3.0	3		PARKFIELD.
12/31/1967	23-48-13.5	35.75	120.45		4.3	3	F	PARKFIELD AREA; V AT CRESTON, PARKFIELD, SALINAS DAM, SAN MIGUEL, SHANDON, TEMPLETON, AND WORK RANCH.
02/03/1968	19-07-26.4	35.73	121.25		2.8	5		NEAR SAN SIMEON.
02/23/1968	20-20-57.9	35.86	121.31		2.5	7		EAST OF HOLLISTER.
03/25/1968	11-32-07.4	36.37	120.70		3.6	8	F	SE OF LLANADA; MAXIMUM INTENSITY V.
03/28/1968	04-53-26.5	36.36	120.19		3.1	5	F	SE OF COALINGA; FELT AT AVENAL - INTENSITY IV.
04/14/1968	06-20-54.6	36.18	121.65		2.5	6		SE OF MONTEREY.
04/23/1968	15-09-14.9	35.52	120.82		3.4	7		SE OF SAN SIMEON.
04/27/1968	14-32-37.4	36.22	120.83		2.7	7		NW OF PRIEST (UC BERKELEY SS).
04/28/1968	06-31-32.9	35.46	120.83		3.5	7		NW OF SAN LUIS OBISPO.
05/31/1968	07-07-37.9	35.80	120.60		3.0	5		S OF COALINGA.
06/11/1968	11-43-28.1	35.90	121.70		3.3	9		OFFSHORE, NW OF SAN SIMEON.
06/22/1968	12-50-50.1	36.43	121.04		2.9	9		S OF LLAN.
07/03/1968	17-52-52	35.80	121.50		2.5	7		NW OF SAN SIMEON.
07/29/1968	04-27-51.9	36.38	120.69		2.7	9		N OF PRIEST (UC BERKELEY SS).
07/29/1968	05-29-19.9	36.37	120.70		2.8	9		N OF PRIEST (UC BERKELEY SS).
07/31/1968	-?-49-25.4	36.37	120.70		2.9	9		N OF PRIEST (UC BERKELEY SS).
08/19/1968	16-30-18.2	36.40	121.91		3.3	9		S OF CARMEL.
09/01/1968	21-56-24.4	36.45	121.02		2.7	8		E OF PINNACLES NATIONAL MONUMENT.
11/06/1968	08-58-23.2	35.88	120.45		2.8	10	F	NEAR PARKFIELD; FELT NEAR SAN MIGUEL.
11/10/1968	04-06-03.9	35.70	121.18		3.2	9		NEAR SAN SIMEON.
11/17/1968	01-03-47.0	36.29	120.94		3.0	6		NEAR KING CITY.
11/11/1968	12-19-52.4	35.81	120.48		3.0	6		NEAR PARKFIELD.
12/16/1968	01-14-10.9	36.17	120.85		2.7	7		W OF PRIEST (UC BERKELEY SS).
01/09/1969	09-42-47.2	35.94	120.57		3.8	7	F	CHOLAME VALLEY; FELT IN PARKFIELD AND SLACK CANYON - MAXIMUM INTENSITY V.
02/04/1969	-?-45-25	36.40	120.38		3.0	4		NORTH OF COALINGA.

DCPP UNITS 1 & 2 FSAR UPDATE

TABLE 2.5-1

MM/DD/YY	HR/MIN/SE	NORTH LAT	WEST LONG	QUALITY	MAG.	STA. REC.	FELT	MAXIMUM INTENSITY - COMMENTS
06/19/1969	07-05-08	36.12	119.58		3.5	8	F	NEAR TULARE; FELT IN CORCORAN, DINUBA, HANFORD, IVANHOE, LEMON COVE, STRATHMORE, AND TIPTON. MAXIMUM INTENSITY IV.
06/24/1969	14-25-37	36.42	120.13		3.0	4		SOUTHWEST OF FRESNO.
07/16/1969	04-06-35	35.83	120.28		3.2	7		15 KM SOUTHEAST OF PARKFIELD.
09/06/1969	13-44-45	35.30	121.10		3.8	10	F	50 KM WEST OF SAN LUIS OBISPO.
09/16/1969	03-32-24	36.18	120.80		2.5	8		13 KM WEST OF PRIEST (UC BERKELEY SS).
10/02/1969	06--?-58.9	36.32	120.32		3.3	10		10 KM NORTH OF COALINGA.
11/17/1969	20-49-10.4	36.43	121.05		4.4	10	F	NINE OF KING CITY; FELT IN MONTEREY - SWAYED BUILDINGS IN SALINAS
11/19/1969	06-23-50	36.45	121.52		4.2	8	F	GONZALES AND SALINAS VALLEY; FELT IN SALINAS AND SANTA CRUZ - RATTLED WINDOWS IN MONTEREY.
11/26/1969	-?-06-59	36.48	120.60		2.5	6		50 KM NORTHEAST OF KING CITY.
11/30/1969	15-11-54	35.30	120.90		2.5	10		20 KM EAST OF KING CITY; 2 SMALL FORESHOCKS RECORDED.
12/10/1969	13-25-31	35.75	120.40		3.5	7		40 KM SOUTH OF COALINGA.
12/14/1969	19-07-57	35.92	120.68		3.2	9		20 KM NORTH OF PASO ROBLES.
01/29/1970	02-49-12.9	36.11	120.99		2.5	6		20 KM SOUTHWEST OF KING CITY.
02/01/1970	21-19-45.7	36.41	121.08		2.6	12		30 KM EAST OF PARAISSO.
02/08/1970	-?-14-13.3	36.40	120.97		2.7	13		25 KM SOUTH OF LLANADA.
02/09/1970	16--?-46.1	35.77	120.35		3.1	16		60 KM SOUTH OF PRIEST (UC BERKELEY SS).
02/14/1970	15-44-58.0	36.09	120.64		2.8	14		5 KM SOUTH OF PRIEST (UC BERKELEY SS).
04/18/1970	13-16-53.4	36.49	120.01		3.0	15		35 KM SOUTHWEST OF FRESNO.
04/21/1970	22-29-25.9	35.66	120.43		3.0	8		65 KM SOUTH OF PRIEST (UC BERKELEY SS).
04/23/1970	03-25-18.9	35.97	121.45		2.5	10		25 KM SOUTHWEST OF KING CITY.
05/27/1970	10-42-19.3	35.99	120.91		3.4	8		40 KM SOUTHWEST OF PRIEST (UC BERKELEY SS).
07/20/1970	23-24-55	35.95	121.57		2.5	5		8 KM SOUTH OF LOPEZ POINT - OFFSHORE.
07/21/1970	05-24-16.1	35.99	121.57		2.5	5		5 KM SOUTHEAST OF LOPEZ POINT.
08/05/1970	06-47-36.4	35.82	119.94		2.9	8		KETTLEMAN HILLS.
08/05/1970	16-51-45.7	36.23	121.69		3.0	11		25 KM SOUTHWEST OF PARAISSO.
08/13/1970	05-06-19.8	36.17	121.70		3.7	11		20 KM WEST OF LOPEZ POINT.
09/05/1970	11-29-11	36.20	120.10		3.1	4		EAST-NORTHEAST OF COALINGA.
09/10/1970	23-45-59	36.40	120.50		3.2	11		30 KM NORTHWEST OF COALINGA.
09/11/1970	15-20-08	35.98	120.05		3.3	9		8 KM EAST OF AVENAL.
09/16/1970	18-22-10.7	35.96	121.27		2.6	7		NEAR MILPITAS.
10/07/1970	17-57-06.3	36.30	121.40		2.5	9		30 KM NORTHWEST OF KING CITY.
12/01/1970	06-05-59	35.38	121.13		3.3	7	F	25 KM WEST OF MORRO BAY, INTENSITY V AT BRYSON - NO DAMAGE.
12/12/1970	22-29-20	35.65	121.55		2.5	6		30 KM WEST OF SAN SIMEON.
01/02/71	06-27-37.5	35°55.1'	120°32.2'		3.0			10 km NW of Parkfield
01/16/71	05-33-27.8	36°00'	120°12'		3.1			Kettleman Hills
01/26/71	21-53-53	35°12'	120°42'		3.0			Near San Luis Obispo.
01/31/71	12-22-49.5	35°55.6'	120°30.6'		3.0			NW of Parkfield; sharp, rapid jolting at Shandon.
04/05/71	01-40-34.2	36°24.8'	120°59.0'		3.0			20 km SE of Pinnacles National Monument.
04/19/71	09-35-58.8	36°13.7'	120°50.3'		3.0			25 km E of King City.
04/29/71	02-13-15.7	36°30.3'	120°32.5'		3.0			40 km NW of Coalinga.
06/20/71	12-41-39.8	35°3'	120°20'		3.4			Near Cholame.
07/06/71	09-24-35	35°34'	121°35'		3.0			SW of San Simeon.

DCPP UNITS 1 & 2 FSAR UPDATE

TABLE 2.5-1

MM/DD/YY	HR:MM:SS	NORTH LAT	WEST LONG	QUALITY	MAG.	STA. REC.	FELT	MAXIMUM INTENSITY - COMMENTS
07/21/71	09-14-26.2	36°13.7'	120°50.8'		3.2			Near Coalinga.
08/06/71	20-03-16.3	36°00.8'	120°02.2'		3.0			Near Coalinga.
10/06/71	14-43-30.6	35°51.3'	120°22.5'		3.5			S of Coalinga; intensity IV at Cholame, Parkfield, and Shandon.
10/21/71	22-09-45.4	35°58.8'	120°50.2'		3.7			SE of King City; intensity V at San Ardo (small objects shifted) and intensity IV at Jolon, King City, Lockwood, Pine Canyon, and San Lucas.
11/07/71	14-03-30.4	35°31.2'	119°50.2'		4.0			SE of Coalinga.
11/18/71	04-03-52.4	36°14.5'	120°50.6'		3.4			NE of King City.
11/30/71	09-45-42.8	36°03.6'	119°53.4'		3.0			SE of Coalinga.

END OF SELECTED EARTHQUAKES

END OF QUAKE PROGRAM FOR SELECTION OF EARTHQUAKES

DCPP UNITS 1 & 2 FSAR UPDATE

TABLE 2.5-2

Sheet 1 of 2

SUMMARY, REVISED EPICENTERS OF REPRESENTATIVE SAMPLES OF EARTHQUAKES OFF THE COAST OF CALIFORNIA NEAR SAN LUIS OBISPO

<u>Date</u>	<u>Event Number</u>	<u>Original Hypocenter</u> Revised Hypocenter		<u>Distance</u> <u>Hypocenter</u> <u>Moved, km</u>	<u>Error</u> <u>Ellipse</u> <u>km</u>	<u>Mag., M_L</u>
		<u>Lat.</u>	<u>Long.</u>			
May 27, 1935	1	35.370 35.621	120.960 121.639	66NW	7 x 14	3.0
Sept. 7, 1939	6	35.420 35.459	121.070 121.495	40W	8 x 8	3.0
Oct. 6, 1939	7	35.800 36.232	121.500 121.763	54NW	16 x 31	3.5
July 11, 1945	8	35.670 35.809	121.250 121.408	21NW	7 x 24	4.0
Mar. 23, 1947	12	35.150 34.577	121.300 121.137	66S	12 x 24	3.7
Mar. 27, 1947	15	35.000 34.739	121.000 120.896	32SW	20 x 20	4.2
Dec. 20, 1948	9	35.800 35.683	121.500 121.364	16SE	9 x 38	4.5
Dec. 31, 1948	10	35.670 35.598	121.400 121.226	17SE	8 x 29	4.6
Nov. 22, 1952 Bryson Earthquake	17	35.730 35.830 35.836	121.190 121.170 121.204	U.C. Berkeley Richter (1969) 12N	7 x 24	6.0
Mar. 13, 1954	21	35.000 34.960	120.690 120.490	19E	9 x 18	3.4
Mar. 5, 1955	23	35.600 35.863	121.400 121.149	38NE	15 x 29	3.3
June 21, 1957	25A	35.100 35.255	120.900 120.951	15NW	10 x 19	3.7
Jan. 2, 1960	26	35.400 35.778	121.190 121.066	44NE	15 x 29	4.0
Feb. 1, 1962	52	34.880 35.031	120.670 120.846	22NW	6 x 16	4.5

DCPP UNITS 1 & 2 FSAR UPDATE

TABLE 2.5-2

Sheet 2 of 2

Date	Event Number	Original Hypocenter Revised Hypocenter		Distance Hypocenter Moved, km	Error Ellipse km	Mag., M_L
		Lat.	Long.			
Mar. 5, 1962	54	34.600 34.622	121.590 121.416	17E	8 x 10	4.5
Mar. 10, 1962	54A	34.600 34.667	121.590 121.372	22NE	6 x 20	4.2
Feb. 22, 1963	28	35.110 34.730	121.440 121.400	42S	7 x 28	3.3
Sept. 6, 1969	31	35.300 35.355	121.090 121.033	9NE	5 x 10	3.6
Oct. 22, 1969	56	34.830 34.649	121.340 121.471	23SW	14 x 50	5.4

DISPLACEMENT HISTORY OF FAULTS IN THE SOUTHERN COAST RANGES OF CALIFORNIA

Fault	Distance From Diablo Site, miles	Time of Principal Activity	Youngest Formation Cut By Fault	Oldest Formation Capping Fault
San Andreas	45	Mid-Tertiary - present		Currently active
Faults in ground between San Andreas and Sur-Nacimiento- Rinconada, La Panza, Cuyama, Red Hills, East Huasna	18-45	Tertiary	Pleistocene (possible Holocene) (Ref. 14)	Not Known
Sur-Nacimiento (zone)	18	Late Mesozoic, (Benioff- subduction zone)	Pleistocene (possible Holocene) (Ref. 14)	Late Quaternary terrace deposits (Ref. 11)
West Huasna-Suey	11	Late Tertiary	Post late-Miocene	Late Quaternary terrace deposits (Ref. 36)
Edna	4.5	Late Tertiary	Plio-Pleistocene (Paso Robles Fm)	Late Pleistocene (Ref. 20)
Miguelito	5	Late Tertiary	Early Pliocene (Miguelito Member of Careaga Fm) (Ref. 21)	Poss. capped by mid-Pliocene Squire Member of Careaga Fm; Plio-Pleistocene Paso Robles Fm

TABLE 2.5-3

Fault	Distance From Diablo Site, miles	Time of Principal Activity	Youngest Formation Cut By Fault	Oldest Formation Capping Fault
Faulting in the Mesozoic rocks near Pt. San Luis	4	Mesozoic	Mesozoic	Late Pleistocene (Ref. 20)
Unnamed faults near Pt. San Simeon	35	Probable Tertiary	Not known; possible Holocene	Not known
Offshore structural zone	4.5	Late Tertiary	Possible Holocene (Ref. 19) (northern part)	Holocene-upper Pliocene (Ref. 19) (southern part)
Faults in the Santa Maria Basin	40	Not known	Possible Pleistocene (orcutt Fm) (Ref. 23)	Pleistocene-Holocene

DCPP UNITS 1 & 2 FSAR UDPATE

TABLE 3.10-1

WESTINGHOUSE SUPPLIED CLASS IE INSTRUMENTATION AND ELECTRICAL EQUIPMENT SEISMIC CAPABILITIES

<u>Equipment</u>	<u>Elev./Bldg.</u>	<u>Qualification Method</u>	<u>Qualifying Spectra HE, DDE, DE</u>	<u>FSAR Reference</u>
Nuclear Instrumentation System Cabinet	140'/Aux.	T / A	HE, DDE, DE	3.10.2.1.1
Radiation Monitoring System Cabinets	140'/Aux.	T	HE, DDE, DE	3.10.2.1.1.1
Two-section Power Range Excore Neutron Detector	102'/Cont.	T	HE, DDE, DE	3.10.2.1.1
Solid State Protection System	140'/Aux.	T	HE, DDE, DE	3.10.2.1.2
Process Control and Protection System	128'/Aux.	T / A	HE, DDE, DE	3.10.2.1.3
Cont. Pressure Transmitter - Transmitter - Sensor	109.67'/Cont. Exterior 109.67'/Cont.	T T	HE, DDE, DE HE, DDE, DE	3.10.2.1.5 3.10.2.1.5
Reactor Coolant Level Differential Pressure Transmitter	100'/Aux.	T	HE, DDE, DE	3.10.2.1.5
Reactor Trip Switchgear	115'/Aux.	T	HE, DDE, DE	3.10.2.1.6
Main Coolant Loop Resistance Temperature Detectors	117'/Cont.	T	HE, DDE, DE	3.10.2.1.7
Safeguards Test Cabinet	140'/Aux.	T	HE, DDE, DE	3.10.2.1.8
Aux. Safeguards Cabinet	128'/Aux.	T / A	HE, DDE, DE	3.10.2.1.9
Main Control Board	140'/Aux.	T / A	HE, DDE, DE	3.10.2.2
Electric Hydrogen Recombiner	140'/Cont.	T	HE, DDE, DE	3.10.2.31

DCPP UNITS 1 & 2 FSAR UDPATE

TABLE 3.10-1

<u>Equipment</u>	<u>Elev./Bldg.</u>	<u>Qualification Method</u>	<u>Qualifying Spectra HE, DDE, DE</u>	<u>FSAR Reference</u>
Hydrogen Recombiner Control Panel and Power Supply	100'/Aux.	T	HE, DDE, DE	3.10.2.31
Reactor Vessel Level Instrumentation System/Incore Thermocouple Cabinets (PAMS 3 & 4)	140'/Aux.	T	HE, DDE, DE	3.10.2.32
Surface Mounted Resistance Temperature Detectors	140'/Cont.	T	HE, DDE, DE	3.10.2.32.2
High Volume Sensors	127'/Cont.	T	HE, DDE, DE	3.10.2.32.3
Hydraulic Isolators	89'/GW	T	HE, DDE, DE	3.10.2.32.4
Flux Mapping Transfer Device	127'/Cont.	A	HE	3.10.2.33
Incore Flux Mapping Cabinets	140'/Cont.	A	HE	3.10.2.33

A = Qualification by analysis (Qualification Method Column)

T = Qualification by testing

DE = Design Earthquake

DDE = Double Design Earthquake

HE = Hosgri Earthquake

DCPP UNITS 1 & 2 FSAR UPDATE

TABLE 3.10-2

EQUIPMENT SEISMIC QUALIFICATION RESULTS:
ELECTRICAL, INSTRUMENTATION, AND CONTROLS

<u>Equipment</u>	<u>Bldg./Elev.</u>	<u>Qualification Method</u>	<u>Qualifying Spectra HE, DDE, DE</u>	<u>FSAR Reference</u>
Main annunciator	Aux/128	T / A	HE, DDE, DE	3.10.2.9
Battery chargers	Aux/115	T	HE, DDE, DE	3.10.2.8.3
Station battery	Aux/115	T / A	HE, DDE, DE	3.10.2.8.1
DC switchgear	Aux/115	T / A	HE, DDE, DE	3.10.2.8.4
Diesel generators				
a) Excitation cabinet	Turb/85	T / A	HE, DDE, DE	3.10.2.6
b) Engine control cabinet	Turb/85	T / A		
Electrical penetrations	Cont/Variou	A	HE, DDE, DE	3.10.2.10
Emergency light packs	Various	T	HE, DDE, DE	--
Fire pump controller	Aux/115	T	HE, DDE, DE	3.10.2.13
Hot shutdown panel	Aux/100	T / A	HE, DDE, DE	3.10.2.3
Heat trace distribution panel	Aux/Variou	A	HE, DDE, DE	N/A
Instrument power ac panelboards	Aux/115	T / A	HE, DDE, DE	3.10.2.7.7

DCPP UNITS 1 & 2 FSAR UPDATE

TABLE 3.10-2

<u>Equipment</u>	<u>Bldg./Elev.</u>	<u>Qualification Method</u>	<u>Qualifying Spectra HE, DDE, DE</u>	<u>FSAR Reference</u>
Instrument panels PIA, PIB & PIC	Aux/128	A	HE, DDE, DE	3.10.2.5
Instrument (Panels A & B)	Aux/128	T / A		
Local instrument panels	Various	A	HE, DDE, DE	3.10.2.4
Local starters (LPF 36)	Turb/119	T	HE, DDE, DE	3.10.2.14
Local starters (LPS 96)	Turb/140	T	HE, DDE, DE	3.10.2.14
Local starters (LPG 66) E1 100/J	Aux/ Various	T / A	HE, DDE, DE	3.10.2.14
Local starter 125 Vdc (FCV 95)	Aux/100	T	HE, DDE, DE	3.10.2.8.5
Limit switches	Various	T	HE, DDE, DE	3.10.2.27
P&ΔP transmitters	Various	T	HE, DDE, DE	3.10.2.11
Safeguards relay board	Turb/119	T / A	HE, DDE, DE	3.10.2.7.3
Ventilation control				
a) Logic cabinet (POV1, POV2)	Aux/140	T / A	HE, DDE, DE	3.10.2.15
b) Relay cabinet (RCV1, RCV2)	Aux/128	T / A	HE, DDE, DE	3.10.2.15
c) Electro-mechanical devices	Aux/Various	T / A	HE, DDE, DE	3.10.2.15
Vital load center (480 Vac MCC)	Aux/100	T / A	HE, DDE, DE	3.10.2.7.4

DCPP UNITS 1 & 2 FSAR UPDATE

TABLE 3.10-2

<u>Equipment</u>	<u>Bldg./Elev.</u>	<u>Qualification Method</u>	<u>Qualifying Spectra HE, DDE, DE</u>	<u>FSAR Reference</u>
Vital load center transformer (480 V)	Aux/100	T / A	HE, DDE, DE	3.10.2.7.5
Auxiliary relay panels (SPF, SPG, SPH)	Aux/100	T / A	HE, DDE, DE	3.10.2.7.6
Fan cooler starter	Aux/100	T / A		
Vital switchgear (4.16 kV)	Turb/119	T / A	HE, DDE, DE	3.10.2.7.1
Potential transformers	Turb/119	T / A	HE, DDE, DE	3.10.2.7.2
Air circuit breaker (pressurizer heaters)	Aux/100	A	HE, DDE, DE	--
Solenoid valves	Various	T	HE, DDE, DE	3.10.2.23
Postaccident monitor panels and instrument (PAMs 1 & 2)	Aux/140	T / A	HE, DDE, DE	3.10.2.22
Containment H2 monitors	GW/85 GE/100	T / A	HE, DDE, DE	3.10.2.25
Containment high-range radiation detector	F/145	T	HE, DDE, DE	3.10.2.28
Containment purge exhaust detectors and LRP	L/100	T / A	HE, DDE, DE	3.10.2.26
Instrument AC UPS	Aux/115	T	HE, DDE, DE	3.10.2.1.4

DCPP UNITS 1 & 2 FSAR UPDATE

TABLE 3.10-2

<u>Equipment</u>	<u>Bldg./Elev.</u>	<u>Qualification Method</u>	<u>Qualifying Spectra HE, DDE, DE</u>	<u>FSAR Reference</u>
Control room air supply radiation monitors	H/158	T	HE, DDE, DE	3.10.2.20
Control room pressurization	Turb/145	T	HE, DDE, DE	3.10.2.20
Radiation monitors	H/140	T	HE, DDE, DE	3.10.2.20
Control room vent & press. control & power panels	Various	T / A	HE, DDE, DE	3.10.2.20
Pressurizer SRV	F/146	T	HE, DDE, DE	3.10.2.29
Position margin monitor	H/140			
Sub-cooled margin monitor (calculators)	H/140	T	HE, DDE, DE	3.10.2.21
Process solenoid valves	G/110 GW/110	T	HE, DDE, DE	3.10.2.24

A = Qualification by analysis (Qualification Method Column)
T = Qualification by testing
DE = Design Earthquake
DDE = Double Design Earthquake
HE = Hosgri Earthquake

TABLE 3.10-3

HVAC EQUIPMENT SEISMIC QUALIFICATION SPECTRA RESULTS

<u>Equipment</u>	<u>Location^(c) Building/ Elevation, ft</u>	<u>Qualification Method^(c)</u>	<u>Qualifying Spectra^(c)</u>	<u>Notes</u>
Supply Fan 1 (S-1)	L/85	A	HE, DDE, DE	(b)
Supply Fan 1 (2S-1)	L/85	C	HE, DDE, DE	(b)
Supply Fan 2 (S-2)	L/85	A	HE, DDE, DE	(b)
Supply Fan 2 (2S-2)	L/85	C	HE, DDE, DE	(b)
Supply Fan 31 (S-31)	K/140	A	HE, DDE, DE	(b)
Supply Fan 32 (S-32)	K/140	A	HE, DDE, DE	(b)
Supply Fan 33 (S-33)	K/140	C	HE, DDE, DE	(b)
Supply Fan 34 (S-34)	K/140	C	HE, DDE, DE	(b)
Supply Fan 39 (S-39)	K/156	A	HE, DDE, DE	(b)
Supply Fan 40 (S-40)	K/156	A	HE, DDE, DE	(b)
Supply Fan 41 (S-41)	K/156	C	HE, DDE, DE	(b)
Supply Fan 42 (S-42)	K/156	C	HE, DDE, DE	(b)
Exhaust Fan 1 (E-1)	L/128	A	HE, DDE, DE	(b)
Exhaust Fan 1 (2E-1)	L/128	C	HE, DDE, DE	(b)
Exhaust Fan 2 (E-2)	L/128	A	HE, DDE, DE	(b)
Exhaust Fan 2 (2E-2)	L/128	C	HE, DDE, DE	(b)
Exhaust Fan 4 (E-4)	L/140	A	HE, DDE, DE	(b)
Exhaust Fan 4 (2E-4)	L/140	C	HE, DDE, DE	(b)
Exhaust Fan 5 (E-5)	L/140	A	HE, DDE, DE	(b)
Exhaust Fan 5 (2E-5)	L/140	C	HE, DDE, DE	(b)
Exhaust Fan 6 (E-6)	L/140	A	HE, DDE, DE	(b)
Exhaust Fan 6 (2E-6)	L/140	C	HE, DDE, DE	(b)
Exhaust Fan 101 (E-101)	ISA/15	A	HE, DDE, DE	(b)
Exhaust Fan 102 (E-102)	ISA/15	A	HE, DDE, DE	(b)

DCPP UNITS 1 & 2 FSAR UPDATE

TABLE 3.10-3

Equipment	Location ^(c) Building/ Elevation, ft	Qualification Method ^(c)	Qualifying Spectra ^(c)	Notes
Exhaust Fan 103 (E-103)	ISA/15	A	HE, DDE, DE	(b)
Exhaust Fan 104 (E-104)	ISA/15	A	HE, DDE, DE	(b)
Supply Fan 43 (S-43)	H/163	A	HE, DDE, DE	(b)
Supply Fan 44 (S-44)	H/163	A	HE, DDE, DE	(b)
Supply Fan 45 (S-45)	H/163	C	HE, DDE, DE	(b)
Supply Fan 46 (S-46)	H/163	C	HE, DDE, DE	(b)
Exhaust Fan 43 (E-43)	H/163	A	HE, DDE, DE	(b)
Exhaust Fan 44 (E-44)	H/163	A	HE, DDE, DE	(b)
Exhaust Fan 45 (E-45)	H/163	C	HE, DDE, DE	(b)
Exhaust Fan 46 (E-46)	H/163	C	HE, DDE, DE	(b)
Supply Fan 35 (S-35)	K/157	A	HE, DDE, DE	(b)
Supply Fan 36 (S-36)	K/157	A	HE, DDE, DE	(b)
Supply Fan 37 (S-37)	K/157	C	HE, DDE, DE	(b)
Supply Fan 38 (S-38)	K/157	C	HE, DDE, DE	(b)
Supply Fan 67 (S-67)	A/119	A	HE, DDE, DE	(b)
Supply Fan 67 (2S-67)	A/119	C	HE, DDE, DE	(b)
Supply Fan 68 (S-68)	A/119	A	HE, DDE, DE	(b)
Supply Fan 68 (2S-68)	A/119	C	HE, DDE, DE	(b)
Supply Fan 69 (S-69)	A/119	A	HE, DDE, DE	(b)
Supply Fan 69 (2S-69)	A/119	C	HE, DDE, DE	(b)
Compressor Unit 35 (CP-35)	K/156	A	HE, DDE, DE	(b)
Compressor Unit 36 (CP-36)	K/156	A	HE, DDE, DE	(b)
Compressor Unit 37 (CP-37)	K/156	C	HE, DDE, DE	(b)
Compressor Unit 38 (CP-38)	K/156	C	HE, DDE, DE	(b)
Condenser Unit 35 (CR-35)	K/157	A	HE, DDE, DE	(b)
Condenser Unit 36 (CR-36)	K/157	A	HE, DDE, DE	(b)

DCPP UNITS 1 & 2 FSAR UPDATE

TABLE 3.10-3

Equipment	Location ^(c) Building/ Elevation, ft	Qualification Method ^(c)	Qualifying Spectra ^(c)	Notes
Condenser Unit 37 (CR-37)	K/157	C	HE, DDE, DE	(b)
Condenser Unit 38 (CR-38)	K/157	C	HE, DDE, DE	(b)
Mode Damper 78 in. (1A)	L/128	A	HE, DDE, DE	(b)
Mode Damper 78 in. (2-1A)	L/128	C	HE, DDE, DE	(b)
Mode Damper 78 in. (1B)	L/128	A	HE, DDE, DE	(b)
Mode Damper 78 in. (2-1B)	L/128	C	HE, DDE, DE	(b)
Mode Damper 132x144 (3)	L/122	A	HE, DDE, DE	(b)
Mode Damper 132x144 (2-3)	L/122	C	HE, DDE, DE	(b)
Mode Damper 96x144 (5A)	L/107	A	HE, DDE, DE	(b)
Mode Damper 96x144 (2-5A)	L/107	C	HE, DDE, DE	(b)
Mode Damper 96x144 (5B)	L/107	A	HE, DDE, DE	(b)
Mode Damper 96x144 (2-5B)	L/107	C	HE, DDE, DE	(b)
Mode Damper 108x144 (6)	L/122	A	HE, DDE, DE	(b)
Mode Damper 108x144 (2-6)	L/122	C	HE, DDE, DE	(b)
Mode Damper 108x144 (9)	L/122	A	HE, DDE, DE	(b)
Mode Damper 108x144 (2-9)	L/122	C	HE, DDE, DE	(b)
Backdraft Damper for Supply Fan S-31 96x72	K/146	A	HE, DDE, DE	(b)
Backdraft Damper for Supply Fan S-32 96x72	K/146	A	HE, DDE, DE	(b)
Backdraft Damper for Supply Fan S-33 96x72	K/146	C	HE, DDE, DE	(b)
Backdraft Damper for Supply Fan S-34 96x72	K/146	C	HE, DDE, DE	(b)
Backdraft Damper for Exhaust Fan E-1 90x66	L/121	A	HE, DDE, DE	(b)
Backdraft Damper for Exhaust Fan 2E-1 90x66	L/121	C	HE, DDE, DE	(b)

DCPP UNITS 1 & 2 FSAR UPDATE

TABLE 3.10-3

Equipment	Location ^(c) Building/ Elevation, ft	Qualification Method ^(c)	Qualifying Spectra ^(c)	Notes
Backdraft Damper for Exhaust Fan E-2 90x66	L/121	A	HE, DDE, DE	(b)
Backdraft Damper for Exhaust Fan 2E-2 90x66	L/121	C	HE, DDE, DE	(b)
Backdraft Damper for Exhaust Fan E-4 56x44	L/143	A	HE, DDE, DE	(b)
Backdraft Damper for Exhaust Fan 2E-4 56x44	L/143	A	HE, DDE, DE	(b)
Backdraft Damper for Exhaust Fan E-5 56x44	L/154	A	HE, DDE, DE	(b)
Backdraft Damper for Exhaust Fan 2E-5 56x44	L/154	A	HE, DDE, DE	(b)
Backdraft Damper for Exhaust Fan E-6 56x44	L/154	A	HE, DDE, DE	(b)
Backdraft Damper for Exhaust Fan 2E-6 56x44	L/154	A	HE, DDE, DE	(b)
Forced Draft Shutter Damper 30x48 Forced Draft Shutter Damper 30x48	G/96 G/96	A C	HE, DDE, DE HE, DDE, DE	(b) (b)
Fire Damper 46x14 (FD-4)	H/125	A	HE, DDE, DE	(b)
Fire Damper 46x14 (2FD-4)	H/125	C	HE, DDE, DE	(b)
Fire Damper 46x14 (FD-5)	H/125	A	HE, DDE, DE	(b)
Fire Damper 46x14 (2FD-5)	H/125	C	HE, DDE, DE	(b)
Fire Damper 46x14 (FD-6)	H/125	A	HE, DDE, DE	(b)
Fire Damper 46x14 (2FD-6)	H/125	C	HE, DDE, DE	(b)
Carbon Tray Filters (EFC-1)	L/115	A	HE, DDE, DE	(b)
Carbon Tray Filters (2EFC-1)	L/115	C	HE, DDE, DE	(b)

DCPP UNITS 1 & 2 FSAR UPDATE

TABLE 3.10-3

Equipment	Location ^(c) Building/ Elevation, ft	Qualification Method ^(c)	Qualifying Spectra ^(c)	Notes
Carbon Tray Filters (EFC-5)	L/148	A	HE, DDE, DE	(b)
Carbon Tray Filters (2EFC-5)	L/148	C	HE, DDE, DE	(b)
Carbon Tray Filters (EFC-6)	L/148	A	HE, DDE, DE	(b)
Carbon Tray Filters (2EFC-6)	L/148	C	HE, DDE, DE	(b)
Astrocel-Hepa Filters (EFH-1)	L/126	A	HE, DDE, DE	(b)
Astrocel-Hepa Filters (2EFH-1)	L/126	C	HE, DDE, DE	(b)
Astrocel-Hepa Filters (EFH-2a)	L/126	A	HE, DDE, DE	(b)
Astrocel-Hepa Filters (2EFH-2a)	L/126	C	HE, DDE, DE	(b)
Astrocel-Hepa Filters (EFH-2b)	L/105	A	HE, DDE, DE	(b)
Astrocel-Hepa Filters (2EFH-2b)	L/105	C	HE, DDE, DE	(b)
Astrocel-Hepa Filters (EFH-4)	L/150	A	HE, DDE, DE	(b)
Astrocel-Hepa Filters (2EFH-4)	L/150	C	HE, DDE, DE	(b)
Astrocel-Hepa Filters (EFH-5)	L/148	A	HE, DDE, DE	(b)
Astrocel-Hepa Filters (2EFH-5)	L/148	C	HE, DDE, DE	(b)
Astrocel-Hepa Filters (EFH-6)	L/148	A	HE, DDE, DE	(b)
Astrocel-Hepa Filters (2EFH-6)	L/148	C	HE, DDE, DE	(b)
Varicel-Roughing Filter (EFR-4)	L/154	A	HE, DDE, DE	(b)
Varicel-Roughing Filter (2EFR-4)	L/154	C	HE, DDE, DE	(b)
Varicel-Roughing Filter (EFR-5)	L/154	A	HE, DDE, DE	(b)
Varicel-Roughing Filter (2EFR-5)	L/154	C	HE, DDE, DE	(b)
Varicel-Roughing Filter (EFR-6)	L/154	A	HE, DDE, DE	(b)
Varicel-Roughing Filter (2EFR-6)	L/154	C	HE, DDE, DE	(b)
Filter Housing With Filters (FU-39)	K/155	A	HE, DDE, DE	(b)
Filter Housing With Filters (FU-41)	K/155	C	HE, DDE, DE	(b)

DCPP UNITS 1 & 2 FSAR UPDATE

TABLE 3.10-3

Equipment	Location ^(c) Building/ Elevation, ft	Qualification Method ^(c)	Qualifying Spectra ^(c)	Notes
Filter Box (FB-29)	H/163	A	HE, DDE, DE	(b)
Filter Box (2FB-29)	H/163	C	HE, DDE, DE	(b)
Electric Duct Heater (EH-30)	L/137	A	HE, DDE, DE	(b)
Chromalox Model TDH-54C (2EH-30)	J/138	C	HE, DDE, DE	(b)
Supply Fan 96 for CRPS (OS-96)	A/140	C	HE, DDE, DE	(b)
Supply Fan 97 for CRPS (OS-97)	A/140	C	HE, DDE, DE	(b)
Supply Fan 98 for CRPS (OS-98)	A/140	A	HE, DDE, DE	(b)
Supply Fan 99 for CRPS (OS-99)	A/140	A	HE, DDE, DE	(b)
Mode Damper 72 in. ϕ and Actuator (2A)	L/132	A	HE, DDE, DE	(b)
Mode Damper 72 in. ϕ and Actuator (2-2A)	L/132	C	HE, DDE, DE	(b)
Mode Damper 72 in. ϕ and Actuator (2B)	L/132	A	HE, DDE, DE	(b)
Mode Damper 72 in. ϕ and Actuator (2-2B)	L/132	C	HE, DDE, DE	(b)
Mode Damper 90x66 and Actuator (7)	L/102	A	HE, DDE, DE	(b)
Mode Damper 90x66 and Actuator (2-7)	L/102	C	HE, DDE, DE	(b)
Mode Damper 10 in. ϕ (13A)	K/97	A	HE, DDE, DE	(b)
Mode Damper 10 in. ϕ (2-13A)	K/97	C	HE, DDE, DE	(b)
Mode Damper 10 in. ϕ (13B)	K/97	A	HE, DDE, DE	(b)
Mode Damper 10 in. ϕ (2-13B)	K/97	C	HE, DDE, DE	(b)
Mode Damper 10 in. ϕ (14A)	GE/81	A	HE, DDE, DE	(b)
Mode Damper 10 in. ϕ (2-14A)	GE/81	C	HE, DDE, DE	(b)
Mode Damper 10 in. ϕ (14B)	GE/81	A	HE, DDE, DE	(b)
Mode Damper 10 in. ϕ (2-14B)	GE/81	C	HE, DDE, DE	(b)
Mode Damper 14 in. ϕ (15A)	GE/70	A	HE, DDE, DE	(b)

DCPP UNITS 1 & 2 FSAR UPDATE

TABLE 3.10-3

Equipment	Location ^(c) Building/ Elevation, ft	Qualification Method ^(c)	Qualifying Spectra ^(c)	Notes
Mode Damper 14 in. ϕ (2-15A)	GE/70	C	HE, DDE, DE	(b)
Mode Damper 14 in. ϕ (15B)	GE/70	A	HE, DDE, DE	(b)
Mode Damper 14 in. ϕ (2-15B)	GE/70	C	HE, DDE, DE	(b)
Mode Damper 48 in. ϕ (35)	L/107	A	HE, DDE, DE	(b)
Mode Damper 48 in. ϕ (2-35)	L/107	C	HE, DDE, DE	(b)
Mode Damper 54 in. ϕ and Actuator (29)	L/150	A	HE, DDE, DE	(b)
Mode Damper 54 in. ϕ and Actuator (2-29)	L/150	C	HE, DDE, DE	(b)
Mode Damper 54 in. ϕ and Actuator (30)	L/150	A	HE, DDE, DE	(b)
Mode Damper 54 in. ϕ and Actuator (2-30)	L/150	C	HE, DDE, DE	(b)
Mode Damper 54 in. ϕ and Actuator (31)	L/150	A	HE, DDE, DE	(b)
Mode Damper 54 in. ϕ and Actuator (2-31)	L/150	C	HE, DDE, DE	(b)
Mode Damper 72x100 (4A)	L/107	A	HE, DDE, DE	(b)
Mode Damper 72x100 (2-4A)	L/107	C	HE, DDE, DE	(b)
Mode Damper 72x100 (4B)	L/107	A	HE, DDE, DE	(b)
Mode Damper 72x100 (2-4B)	L/107	C	HE, DDE, DE	(b)
Mode Damper 72x75 (8A)	L/133	A	HE, DDE, DE	(b)
Mode Damper 72x75 (2-8A)	L/133	C	HE, DDE, DE	(b)
Mode Damper 72x75 (8B)	L/115	A	HE, DDE, DE	(b)
Mode Damper 72x75 (2-8B)	L/115	C	HE, DDE, DE	(b)
Mode Damper 90x66 (10)	L/110	A	HE, DDE, DE	(b)
Mode Damper 90x66 (2-10)	L/110	C	HE, DDE, DE	(b)
Mode Damper 40x84 (12)	K/90	A	HE, DDE, DE	(b)
Mode Damper 40x84 (2-12)	K/90	C	HE, DDE, DE	(b)
Mode Damper 46x40 (16A)	K/95	A	HE, DDE, DE	(b)

DCPP UNITS 1 & 2 FSAR UPDATE

TABLE 3.10-3

Equipment	Location ^(c) Building/ Elevation, ft	Qualification Method ^(c)	Qualifying Spectra ^(c)	Notes
Mode Damper 46x40 (2-16A)	K/95	C	HE, DDE, DE	(b)
Mode Damper 46x40 (16B)	K/95	A	HE, DDE, DE	(b)
Mode Damper 46x40 (2-16B)	K/95	C	HE, DDE, DE	(b)
Mode Damper 26x54 (17A)	K/94	A	HE, DDE, DE	(b)
Mode Damper 26x54 (2-17A)	K/94	C	HE, DDE, DE	(b)
Mode Damper 26x54 (17B)	K/94	A	HE, DDE, DE	(b)
Mode Damper 26x54 (2-17B)	K/94	C	HE, DDE, DE	(b)
Mode Damper 96x72 (20)	K/146	A	HE, DDE, DE	(b)
Mode Damper 96x72 (2-24)	K/146	C	HE, DDE, DE	(b)
Mode Damper 96x72 (21)	K/146	A	HE, DDE, DE	(b)
Mode Damper 96x72 (2-21)	K/146	C	HE, DDE, DE	(b)
Mode Damper 54x100 (22A)	K/141	A	HE, DDE, DE	(b)
Mode Damper 54x100 (2-22A)	K/141	C	HE, DDE, DE	(b)
Mode Damper 54x100 (22B)	K/132	A	HE, DDE, DE	(b)
Mode Damper 54x100 (2-22B)	K/132	C	HE, DDE, DE	(b)
Mode Damper 40x40 (23)	K/135	A	HE, DDE, DE	(b)
Mode Damper 40x40 (2-23)	K/135	C	HE, DDE, DE	(b)
Mode Damper 40x40 (23B)	K/135	A	HE, DDE, DE	(b)
Mode Damper 40x40 (2-23B)	K/135	C	HE, DDE, DE	(b)
Mode Damper 14x44 (24)	K/111	A	HE, DDE, DE	(b)
Mode Damper 14x44 (2-24)	K/111	C	HE, DDE, DE	(b)
Mode Damper 14x44 (24B)	K/111	A	HE, DDE, DE	(b)
Mode Damper 14x44 (2-24B)	K/111	C	HE, DDE, DE	(b)
Mode Damper 48x40 (26A)	K/87	A	HE, DDE, DE	(b)
Mode Damper 48x40 (2-26A)	K/87	C	HE, DDE, DE	(b)
Mode Damper 48x40 (26B)	K/87	A	HE, DDE, DE	(b)
Mode Damper 48x40 (2-26B)	K/87	C	HE, DDE, DE	(b)
Mode Damper 30x48 (25)	K/95	A	HE, DDE, DE	(b)
Mode Damper 30x48 (2-25)	K/95	C	HE, DDE, DE	(b)
Mode Damper 30x48 (25B)	K/95	A	HE, DDE, DE	(b)

DCPP UNITS 1 & 2 FSAR UPDATE

TABLE 3.10-3

<u>Equipment</u>	<u>Location^(c) Building/ Elevation, ft</u>	<u>Qualification Method^(c)</u>	<u>Qualifying Spectra^(c)</u>	<u>Notes</u>
Mode Damper 30x48 (2-25B)	K/95	C	HE, DDE, DE	(b)
Mode Damper 42x64 (33)	L/108	A	HE, DDE, DE	(b)
Mode Damper 42x64 (2-33)	L/108	C	HE, DDE, DE	(b)
Mode Damper 42x64 (34)	L/105	A	HE, DDE, DE	(b)
Mode Damper 42x64 (2-34)	L/105	C	HE, DDE, DE	(b)
Backdraft Damper for Supply Fan S-1 64x42	L/95	A	HE, DDE, DE	(b)
Backdraft Damper for Supply Fan 2S-1 64x42	L/95	C	HE, DDE, DE	(b)
Backdraft Damper for Supply Fan S-2 64x42	L/95	A	HE, DDE, DE	(b)
Backdraft Damper for Supply Fan 2S-2 64x42	L/95	C	HE, DDE, DE	(b)
Backdraft Damper 14 in. ϕ (OBD-1)	A/149	A	HE, DDE, DE	(b)
Backdraft Damper 14 in. ϕ (OBD-2)	A/149	A	HE, DDE, DE	(b)
Backdraft Damper 14 in. ϕ (OBD-3)	A/149	C	HE, DDE, DE	(b)
Backdraft Damper 14 in. ϕ (OBD-4)	A/149	C	HE, DDE, DE	(b)
Quadrant Damper (QD 10 in. ϕ)	K/110	A	HE, DDE, DE	(b)
Quadrant Damper (QD 20 in. ϕ)	K/82	A	HE, DDE, DE	(b)
Quadrant Damper (QD 14 in. ϕ)	K/82	A	HE, DDE, DE	(b)
Quadrant Damper (QD 14 in. ϕ)	K/111	A	HE, DDE, DE	(b)
Quadrant Damper (QD 16 in. ϕ)	K/111	A	HE, DDE, DE	(b)
Quadrant Damper (QD 12 in. ϕ)	K/112	A	HE, DDE, DE	(b)
Quadrant Damper (QD 12 in. ϕ)	K/130	A	HE, DDE, DE	(b) (e)
Quadrant Damper (QD 10 in. ϕ)	K/132	A	HE, DDE, DE	(b) (e)

DCPP UNITS 1 & 2 FSAR UPDATE

TABLE 3.10-3

Equipment	Location ^(c) Building/ Elevation, ft	Qualification Method ^(c)	Qualifying Spectra ^(c)	Notes
Quadrant Damper (QD 14 in. φ)	K/132	A	HE, DDE, DE	(b) (e)
Quadrant Damper (QD 12 in. φ)	K/134	A	HE, DDE, DE	(b) (e)
Quadrant Damper (QD 16 in. φ)	K/134	A	HE, DDE, DE	(b) (e)
Quadrant Damper (QD 16 in. φ)	K/131	A	HE, DDE, DE	(b) (e)
Quadrant Damper (QD 20 in. φ)	K/134	A	HE, DDE, DE	(b) (e)
Quadrant Damper (QD 14 in. φ)	K/134	A	HE, DDE, DE	(b) (e)
Quadrant Damper (QD 14 in. φ)	K/70	A	HE, DDE, DE	(b)
Quadrant Damper (QD 14 in. φ)	GE/70	A	HE, DDE, DE	(b)
Quadrant Damper (QD 14 in. φ)	H/79	A	HE, DDE, DE	(b)
Quadrant Damper (QD 14 in. φ)	H/65	A	HE, DDE, DE	(b)
Quadrant Damper (QD 20 in. φ)	J/132	A	HE, DDE, DE	(b)
Quadrant Damper (QD 28 in. φ)	L/141	A	HE, DDE, DE	(b)
Quadrant Damper (QD 16 in. φ)	GE/70	A	HE, DDE, DE	(b)
Quadrant Damper (QD 14 in. φ)	GE/70	A	HE, DDE, DE	(b)
Quadrant Damper (QD 18 in. φ)	K/132	C	HE, DDE, DE	(b)
Quadrant Damper #52 (QD 48x24)	J/111	A	HE, DDE, DE	(b)
Quadrant Damper #2-52 (QD 48x24)	J/111	A	HE, DDE, DE	(b)
Quadrant Damper #54 (QD 42x42)	J/134	A	HE, DDE, DE	(b)
Quadrant Damper #2-54 (QD 42x42)	J/134	A	HE, DDE, DE	(b)
Quadrant Damper #46 (QD 38x14)	J/123	A	HE, DDE, DE	(b)
Quadrant Damper #2-46 (QD 38x14)	J/123	A	HE, DDE, DE	(b)
Quadrant Damper #33 (QD 40x40)	K/135	A	HE, DDE, DE	(b)
Quadrant Damper #2-33 (QD 40x40)	K/135	A	HE, DDE, DE	(b)
Quadrant Damper #34 (QD 14x10)	K/136	A	HE, DDE, DE	(b)
Quadrant Damper #2-34 (QD 14x10)	K/136	A	HE, DDE, DE	(b)
Quadrant Damper #35 (QD 46x14)	K/134	A	HE, DDE, DE	(b)
Quadrant Damper #2-35 (QD 46x14)	K/134	A	HE, DDE, DE	(b)
Quadrant Damper #24 (QD 14x14)	K/109	A	HE, DDE, DE	(b)
Quadrant Damper #2-24 (QD 14x14)	K/109	A	HE, DDE, DE	(b)
Quadrant Damper #31 (QD 54x100)	K/132	A	HE, DDE, DE	(b)
Quadrant Damper #2-31 (QD 54x100)	K/132	C	HE, DDE, DE	(b)

TABLE 3.10-3

Equipment	Location ^(c) Building/ Elevation, ft	Qualification Method ^(c)	Qualifying Spectra ^(c)	Notes
Quadrant Damper #25 (QD 14x30)	K/111	A	HE, DDE, DE	(b)
Quadrant Damper #2-25 (QD 14x30)	K/111	A	HE, DDE, DE	(b)
Quadrant Damper #66 (QD 24x44)	K/92	A	HE, DDE, DE	(b)
Quadrant Damper #2-67 (QD 24x44)	K/92	A	HE, DDE, DE	(b)
Quadrant Damper #5 (QD 58x32)	K/81	A	HE, DDE, DE	(b)
Quadrant Damper #2-5 (QD 58x32)	K/81	C	HE, DDE, DE	(b)
Quadrant Damper #64 (QD 44x32)	K/81	A	HE, DDE, DE	(b)
Quadrant Damper #2-64 (QD 44x32)	K/81	A	HE, DDE, DE	(b)
Quadrant Damper #6 (QD 24x32)	K/81	A	HE, DDE, DE	(b)
Quadrant Damper #2-6 (QD 24x32)	K/81	A	HE, DDE, DE	(b)
Quadrant Damper #4 (QD 44x26)	K/82	A	HE, DDE, DE	(b)
Quadrant Damper #2-4 (QD 44x26)	K/82	A	HE, DDE, DE	(b)
Quadrant Damper #53 (QD 72x100)	L/100	A	HE, DDE, DE	(b)
Quadrant Damper #2-53 (QD 72x100)	L/100	C	HE, DDE, DE	(b)
Volume Damper (VD 24x24)	H/123	A	HE, DDE, DE	(b)
Volume Damper (VD 24x24)	H/124	A	HE, DDE, DE	(b)
Volume Damper (VD 27x21)	H/124	A	HE, DDE, DE	(b)
Quadrant Damper #19 (QD 38x44)	K/96	A	HE, DDE, DE	(b)
Quadrant Damper #2-19 (QD 38x44)	K/96	A	HE, DDE, DE	(b)
Quadrant Damper #15 (QD 20x12)	K/97	A	HE, DDE, DE	(b)
Quadrant Damper #2-15 (QD 20x12)	K/97	A	HE, DDE, DE	(b)
Quadrant Damper #20 (QD 20x44)	K/97	A	HE, DDE, DE	(b)
Quadrant Damper #2-20 (QD 20x44)	K/97	A	HE, DDE, DE	(b)
Quadrant Damper #14 (QD 72x24)	K/96	A	HE, DDE, DE	(b)
Quadrant Damper #2-14 (QD 72x24)	K/96	A	HE, DDE, DE	(b)
Quadrant Damper #28 (QD 18x16)	K/113	A	HE, DDE, DE	(b)
Quadrant Damper #2-28 (QD 18x16)	K/113	A	HE, DDE, DE	(b)
Quadrant Damper #29 (QD 16x18)	K/112	A	HE, DDE, DE	(b)
Quadrant Damper #2-29 (QD 16x18)	K/112	A	HE, DDE, DE	(b)

DCPP UNITS 1 & 2 FSAR UPDATE

TABLE 3.10-3

Equipment	Location ^(c) Building/ Elevation, ft	Qualification Method ^(c)	Qualifying Spectra ^(c)	Notes
Quadrant Damper #37 (QD 32x30)	K/132	A	HE, DDE, DE	(b)
Quadrant Damper #2-37 (QD 32x30)	K/132	A	HE, DDE, DE	(b)
Quadrant Damper #45 (QD 38x38)	J/120	A	HE, DDE, DE	(b)
Quadrant Damper #2-45 (QD 38x38)	J/120	A	HE, DDE, DE	(b)
Quadrant Damper (QD 24x24)	H/130	C	HE, DDE, DE	(b) (f)
Quadrant Damper (QD 18x24)	H/130	C	HE, DDE, DE	(b) (f)
Quadrant Damper #36 (QD 22x30)	K/131	A	HE, DDE, DE	(b)
Quadrant Damper #2-36 (QD 22x30)	K/131	A	HE, DDE, DE	(b)
Quadrant Damper #10 (QD 46x30)	K/78	A	HE, DDE, DE	(b)
Quadrant Damper #2-10 (QD 46x30)	K/78	A	HE, DDE, DE	(b)
Quadrant Damper #11 (QD 18x30)	K/79	A	HE, DDE, DE	(b)
Quadrant Damper #2-11 (QD 18x30)	K/79	A	HE, DDE, DE	(b)
Quadrant Damper #12 (QD 6x30)	K/79	A	HE, DDE, DE	(b)
Quadrant Damper #2-12 (QD 6x30)	K/79	A	HE, DDE, DE	(b)
Quadrant Damper #3 (QD 20x32)	K/69	A	HE, DDE, DE	(b)
Quadrant Damper #2-3 (QD 20x32)	K/69	A	HE, DDE, DE	(b)
Quadrant Damper #55 (QD 30x12)	H/61	A	HE, DDE, DE	(b)
Quadrant Damper #2-55 (QD 30x12)	H/61	A	HE, DDE, DE	(b)
Quadrant Damper #40 (QD 16x40)	J/152	A	HE, DDE, DE	(b)
Quadrant Damper #2-40 (QD 16x40)	J/152	A	HE, DDE, DE	(b)
Quadrant Damper #27 (QD 40x42)	K/110	A	HE, DDE, DE	(b)
Quadrant Damper #2-27 (QD 40x42)	K/110	A	HE, DDE, DE	(b)

DCPP UNITS 1 & 2 FSAR UPDATE

TABLE 3.10-3

Equipment	Location ^(c) Building/ Elevation, ft	Qualification Method ^(c)	Qualifying Spectra ^(c)	Notes
Quadrant Damper #26 (QD 36x42)	K/110	A	HE, DDE, DE	(b)
Quadrant Damper #2-26 (QD 36x42)	K/110	A	HE, DDE, DE	(b)
Quadrant Damper #18 (QD 40x26)	K/97			
Quadrant Damper #2-18 (QD 40x26)	K/97	A	HE, DDE, DE	(b)
Quadrant Damper #2 (QD 30x66)	H/69	A	HE, DDE, DE	(b)
Quadrant Damper #2-2 (QD 30x66)	H/69	A	HE, DDE, DE	(b)
Quadrant Damper #1 (QD 24x72)	K/69	A	HE, DDE, DE	(b)
Quadrant Damper #2-1 (QD 24x72)	K/69	A	HE, DDE, DE	(b)
Quadrant Damper #43 (QD 86x48)	K/132	A	HE, DDE, DE	(b)
Quadrant Damper #2-43 (QD 86x48)	K/132	C	HE, DDE, DE	(b)
Quadrant Damper #42 (QD 36x18)	K/132	A	HE, DDE, DE	(b)
Quadrant Damper #2-42 (QD 36x18)	K/132	A	HE, DDE, DE	(b)
Quadrant Damper #8 (QD 36x18)	K/81	A	HE, DDE, DE	(b)
Quadrant Damper #2-8 (QD 36x18)	K/81	A	HE, DDE, DE	(b)
Quadrant Damper #9 (QD 36x18)	K/81	A	HE, DDE, DE	(b)
Quadrant Damper #2-9 (QD 36x18)	K/81	A	HE, DDE, DE	(b)
Quadrant Damper #41 (QD 56x50)	L/143	A	HE, DDE, DE	(b)
Quadrant Damper #2-41 (QD 56x50)	L/143	C	HE, DDE, DE	(b)
Quadrant Damper #65 (QD 60x30)	J/152	A	HE, DDE, DE	(b)
Quadrant Damper #2-65 (QD 60x30)	J/152	C	HE, DDE, DE	(b)
Quadrant Damper #49 (QD 38x30)	J/156	A	HE, DDE, DE	(b)
Quadrant Damper #2-49 (QD 38x30)	J/156	C	HE, DDE, DE	(b)
Quadrant Damper #7 (QD 84x72)	K/85	A	HE, DDE, DE	(b)
Quadrant Damper #2-7 (QD 84x72)	K/85	C	HE, DDE, DE	(b)
Quadrant Damper #13 (QD 54x48)	K/86	A	HE, DDE, DE	(b)

DCPP UNITS 1 & 2 FSAR UPDATE

TABLE 3.10-3

Equipment	Location ^(c) Building/ Elevation, ft	Qualification Method ^(c)	Qualifying Spectra ^(c)	Notes
Quadrant Damper #2-13 (QD 54x48)	K/86	C	HE, DDE, DE	(b)
Quadrant Damper #32 (QD 37x78)	K/131	A	HE, DDE, DE	(b)
Quadrant Damper #2-32 (QD 37x78)	K/131	A	HE, DDE, DE	(b)
Motorized Damper 24 in. ϕ (2)	H/156	A	HE, DDE, DE	(b)
Motorized Damper 24 in. ϕ (2-2)	H/156	A	HE, DDE, DE	(b)
Motorized Damper 24 in. ϕ (2A)	H/160	A	HE, DDE, DE	(b)
Motorized Damper 24 in. ϕ (2-2A)	H/160	A	HE, DDE, DE	(b)
Motorized Damper 18 in. ϕ (3)	H/156	A	HE, DDE, DE	(b)
Motorized Damper 18 in. ϕ (2-3)	H/156	A	HE, DDE, DE	(b)
Motorized Damper 18 in. ϕ (3A)	H/160	A	HE, DDE, DE	(b)
Motorized Damper 18 in. ϕ (2-3A)	H/160	A	HE, DDE, DE	(b)
Motorized Damper 24 in. ϕ (7)	H/161	A	HE, DDE, DE	(b)
Motorized Damper 24 in. ϕ (2-7)	H/161	A	HE, DDE, DE	(b)
Motorized Damper 24 in. ϕ (7A)	H/159	A	HE, DDE, DE	(b)
Motorized Damper 24 in. ϕ (2-7A)	H/159	A	HE, DDE, DE	(b)
Motorized Damper 18 in. ϕ (8)	H/163	A	HE, DDE, DE	(b)
Motorized Damper 18 in. ϕ (2-8)	H/163	A	HE, DDE, DE	(b)
Motorized Damper 18 in. ϕ (8A)	H/163	A	HE, DDE, DE	(b)
Motorized Damper 18 in. ϕ (2-8A)	H/163	A	HE, DDE, DE	(b)
Motorized Damper 14 in. ϕ for CRPS (1)	A/143	A	HE, DDE, DE	(b)
Motorized Damper 14 in. ϕ for CRPS (2-1)	A/143	C	HE, DDE, DE	(b)
Motorized Damper 14 in. ϕ for CRPS (1A)	A/149	A	HE, DDE, DE	(b)
Motorized Damper 14 in. ϕ for CRPS (2-1A)	A/149	C	HE, DDE, DE	(b)
Motorized Damper 14 in. ϕ for CRPS (1B)	A/143	A	HE, DDE, DE	(b)
Motorized Damper 14 in. ϕ for CRPS (2-1B)	A/143	C	HE, DDE, DE	(b)
Motorized Damper 14 in. ϕ for CRPS (1C)	A/149	A	HE, DDE, DE	(b)
Motorized Damper 14 in. ϕ for CRPS (2-1C)	A/149	C	HE, DDE, DE	(b)
Limitorque Actuator for	H/156	T	HE, DDE, DE	(b)

DCPP UNITS 1 & 2 FSAR UPDATE

TABLE 3.10-3

Equipment	Location ^(c) Building/ Elevation, ft	Qualification Method ^(c)	Qualifying Spectra ^(c)	Notes
Motorized Damper (2)	H/156	T	HE, DDE, DE	(b)
Limitorque Actuator for Motorized Damper (2-2)	H/160	T	HE, DDE, DE	(b)
Limitorque Actuator for Motorized Damper (2A)	H/160	T	HE, DDE, DE	(b)
Limitorque Actuator for Motorized Damper (2-2A)	H/156	T	HE, DDE, DE	(b)
Limitorque Actuator for Motorized Damper (3)	H/156	T	HE, DDE, DE	(b)
Limitorque Actuator for Motorized Damper (2-3)				
Limitorque Actuator for Motorized Damper (3A)	H/160	T	HE, DDE, DE	(b)
Limitorque Actuator for Motorized Damper (2-3A)	H/160	T	HE, DDE, DE	(b)
Limitorque Actuator for Motorized Damper (7)	H/160	T	HE, DDE, DE	(b)
Limitorque Actuator for Motorized Damper (2-7)	H/159	T	HE, DDE, DE	(b)
Limitorque Actuator for Motorized Damper (7A)	H/159	T	HE, DDE, DE	(b)
Limitorque Actuator for Motorized Damper (2-7A)	H/163	T	HE, DDE, DE	(b)
Limitorque Actuator for Motorized Damper (8)	H/163	T	HE, DDE, DE	(b)
Limitorque Actuator for Motorized Damper (2-8)	H/163	T	HE, DDE, DE	(b)
Limitorque Actuator for Motorized Damper (8A)	H/163	T	HE, DDE, DE	(b)
Limitorque Actuator for Motorized Damper (2-8A)				
Motorized Damper 18x16 (4)	H/163	A	HE, DDE, DE	(b)
Motorized Damper 18x16 (2-4)	H/163	C	HE, DDE, DE	(b)
Motorized Damper 36x24 (5)	H/163	A	HE, DDE, DE	(b)

DCPP UNITS 1 & 2 FSAR UPDATE

TABLE 3.10-3

Equipment	Location ^(c) Building/ Elevation, ft	Qualification Method ^(c)	Qualifying Spectra ^(c)	Notes
Motorized Damper 36x24 (2-5)	H/163	C	HE, DDE, DE	(b)
Motorized Damper 36x24 (6)	H/159	A	HE, DDE, DE	(b)
Motorized Damper 36x24 (2-6)	H/159	C	HE, DDE, DE	(b)
Motorized Damper 70x16 (9)	H/159	A	HE, DDE, DE	(b)
Motorized Damper 70x16 (2-9)	H/159	C	HE, DDE, DE	(b)
Motorized Damper 70x16 (9A)	H/159	A	HE, DDE, DE	(b)
Motorized Damper 70x16 (2-9A)	H/159	C	HE, DDE, DE	(b)
Motorized Damper 70x20 (10)	H/157	A	HE, DDE, DE	(b)
Motorized Damper 70x20 (2-10)	H/157	C	HE, DDE, DE	(b)
Motorized Damper 70x20 (10A)	H/157	A	HE, DDE, DE	(b)
Motorized Damper 70x20 (2-10A)	H/157	C	HE, DDE, DE	(b)
Motorized Damper 70x16 (11)	H/159	A	HE, DDE, DE	(b)
Motorized Damper 70x16 (2-11)	H/159	C	HE, DDE, DE	(b)
Motorized Damper 70x16 (11A)	H/159	A	HE, DDE, DE	(b)
Motorized Damper 70x16 (2-11A)	H/159	C	HE, DDE, DE	(b)
Motorized Damper 70x20 (12)	H/157	A	HE, DDE, DE	(b)
Motorized Damper 70x20 (2-12)	H/157	C	HE, DDE, DE	(b)
Motorized Damper 70x20 (12A)	H/157	A	HE, DDE, DE	(b)
Motorized Damper 70x20 (2-12A)	H/157	C	HE, DDE, DE	(b)
Motorized Damper 22x12 (13)	H/159	A	HE, DDE, DE	(b)
Motorized Damper 22x12 (2-13)	H/159	C	HE, DDE, DE	(b)
Motorized Damper 22x12 (14)	H/159	A	HE, DDE, DE	(b)
Motorized Damper 22x12 (2-14)	H/159	C	HE, DDE, DE	(b)
Balancing Damper 14 in. ϕ (1-15)	H/163	A	HE, DDE, DE	(b)
Balancing Damper 14 in. ϕ (2-15)	H/163	C	HE, DDE, DE	(b)
Balancing Damper 14 in. ϕ (1-16)	A/141	A	HE, DDE, DE	(b)
Balancing Damper 14 in. ϕ (2-16)	A/141	C	HE, DDE, DE	(b)
Shut-off Damper (48X48) (HD-43)	H/168	A	HE, DDE, DE	(b)
Shut-off Damper (48X48) (HD-44)	H/168	A	HE, DDE, DE	(b)
Shut-off Damper (48X48) (HD-45)	H/168	C	HE, DDE, DE	(b)
Shut-off Damper (48X48) (HD-46)	H/168	C	HE, DDE, DE	(b)

DCPP UNITS 1 & 2 FSAR UPDATE

TABLE 3.10-3

Equipment	Location ^(c) Building/ Elevation, ft	Qualification Method ^(c)	Qualifying Spectra ^(c)	Notes
Back Draft Damper (E-21)	GW/96	A	HE, DDE, DE	(b)
Back Draft Damper (48X48) (BDD-43)	H/168	A	HE, DDE, DE	(b)
Back Draft Damper (48X48) (BDD-44)	H/168	A	HE, DDE, DE	(b)
Back Draft Damper (48X48) (BDD-45)	H/168	C	HE, DDE, DE	(b)
Back Draft Damper (48X48) (BDD-46)	H/168	C	HE, DDE, DE	(b)
Barber Colman Actuator for Motorized Damper 4	K/166	T	HE, DDE, DE	(b)
Barber Colman Actuator for Motorized Damper 2-4	K/166	C	HE, DDE, DE	(b)
Barber Colman Actuator for Motorized Damper 5	K/166	T	HE, DDE, DE	(b)
Barber Colman Actuator for Motorized Damper 2-5	K/166	C	HE, DDE, DE	(b)
Barber Colman Actuator for Motorized Damper 6	K/166	T	HE, DDE, DE	(b)
Barber Colman Actuator for Motorized Damper 2-6	K/166	C	HE, DDE, DE	(b)
Barber Colman Actuator for Motorized Damper (9)	K/159	T	HE, DDE, DE	(b)
Barber Colman Actuator for Motorized Damper (2-9)	K/159	T	HE, DDE, DE	(b)
Barber Colman Actuator for Motorized Damper (9A)	K/159	T	HE, DDE, DE	(b)
Barber Colman Actuator for Motorized Damper (2-9A)	K/159	T	HE, DDE, DE	(b)
Barber Colman Actuator for Motorized Damper (10)	H/157	T	HE, DDE, DE	(b)
Barber Colman Actuator for Motorized Damper (2-10)	H/157	T	HE, DDE, DE	(b)
Barber Colman Actuator for Motorized Damper (10A)	H/157	T	HE, DDE, DE	(b)

DCPP UNITS 1 & 2 FSAR UPDATE

TABLE 3.10-3

<u>Equipment</u>	<u>Location^(c) Building/ Elevation, ft</u>	<u>Qualification Method^(c)</u>	<u>Qualifying Spectra^(c)</u>	<u>Notes</u>
Barber Colman Actuator for Motorized Damper (2-10A)	H/157	T	HE, DDE, DE	(b)
Barber Colman Actuator for Motorized Damper (11)	K/159	T	HE, DDE, DE	(b)
Barber Colman Actuator for Motorized Damper (2-11)	K/159	T	HE, DDE, DE	(b)
Barber Colman Actuator for Motorized Damper (11A)	K/159	T	HE, DDE, DE	(b)
Barber Colman Actuator for Motorized Damper (2-11A)	K/159	T	HE, DDE, DE	(b)
Barber Colman Actuator for Motorized Damper (12)	H/157	T	HE, DDE, DE	(b)
Barber Colman Actuator for Motorized Damper (2-12)	H/157	T	HE, DDE, DE	(b)
Barber Colman Actuator for Motorized Damper (12A)	H/157	T	HE, DDE, DE	(b)
Barber Colman Actuator for Motorized Damper (2-12A)	K/159	T	HE, DDE, DE	(b)
Barber Colman Actuator for Motorized Damper (13)	K/159	T	HE, DDE, DE	(b)
Barber Colman Actuator for Motorized Damper (2-13)	K/159	T	HE, DDE, DE	(b)
Barber Colman Actuator for Motorized Damper (14)	K/159	T	HE, DDE, DE	(b)
Barber Colman Actuator for Motorized Damper (2-14)	K/159	T	HE, DDE, DE	(b)
Limitorque Actuator for Motorized Damper (1)	A/143	T	HE, DDE, DE	(b)
Limitorque Actuator for Motorized Damper (2-1)	A/143	C	HE, DDE, DE	(b)
Limitorque Actuator for Motorized Damper (1A)	A/149	T	HE, DDE, DE	(b)
Limitorque Actuator for Motorized Damper (2-1A)	A/149	C	HE, DDE, DE	(b)
Limitorque Actuator for Motorized Damper (1B)	A/143	T	HE, DDE, DE	(b)
Limitorque Actuator for Motorized Damper (2-1B)	A/143	C	HE, DDE, DE	(b)

DCPP UNITS 1 & 2 FSAR UPDATE

TABLE 3.10-3

<u>Equipment</u>	<u>Location^(c) Building/ Elevation, ft</u>	<u>Qualification Method^(c)</u>	<u>Qualifying Spectra^(c)</u>	<u>Notes</u>
Motorized Damper (2-1B) Limitorque Actuator for Motorized Damper (1C) Limitorque Actuator for Motorized Damper (2-1C)	A/149 A/149	T C	HE, DDE, DE HE, DDE, DE	(b) (b)
Pneumatic Contromatics Operator for Fan S-1 Pneumatic Contromatics Operator for Fan 2S-1 Pneumatic Contromatics Operator for Fan S-2 Pneumatic Contromatics Operator for Fan 2S-2 Pneumatic Contromatics Operator for Fan S-31 Pneumatic Contromatics Operator for Fan S-33 Pneumatic Contromatics Operator for Fan S-32 Pneumatic Contromatics Operator for Fan S-34 Pneumatic Contromatics Operator for Fan E-1 Pneumatic Contromatics Operator for Fan 2E-1 Pneumatic Contromatics Operator for Fan E-2 Pneumatic Contromatics Operator for Fan 2E-2	L/91 L/91 L/91 L/91 K/150 K/150 K/150 K/150 L/135 L/135 L/135 L/135	T C T C T C T C T C T C T C T C T C	HE, DDE, DE HE, DDE, DE HE, DDE, DE HE, DDE, DE HE, DDE, DE HE, DDE, DE HE, DDE, DE HE, DDE, DE HE, DDE, DE HE, DDE, DE HE, DDE, DE HE, DDE, DE HE, DDE, DE HE, DDE, DE HE, DDE, DE HE, DDE, DE HE, DDE, DE HE, DDE, DE	(b) (b) (b) (b) (b) (b) (b) (b) (b) (b) (b) (b) (b) (b) (b) (b) (b) (b) (b)
Pneumatic Contromatics Operator for Fan E-4 Pneumatic Contromatics Operator for Fan 2E-4	L/146 L/146	T C	HE, DDE, DE HE, DDE, DE	(b) (b)

DCPP UNITS 1 & 2 FSAR UPDATE

TABLE 3.10-3

<u>Equipment</u>	<u>Location^(c) Building/ Elevation, ft</u>	<u>Qualification Method^(c)</u>	<u>Qualifying Spectra^(c)</u>	<u>Notes</u>
Pneumatic Contromatics Operator for Fan E-5	L/146	T	HE, DDE, DE	(b)
Pneumatic Contromatics Operator for Fan 2E-5	L/146	C	HE, DDE, DE	(b)
Pneumatic Contromatics Operator for Fan E-6	L/146	T	HE, DDE, DE	(b)
Pneumatic Contromatics Operator for Fan 2E-6	L/146	C	HE, DDE, DE	(b)
Fire Damper 12x14 (FD-128)	K/73	A	HE, DDE, DE	(b)
Fire Damper 12x14 (2FD-128)	K/73	C	HE, DDE, DE	(b)
Motor for Supply Fan OS-96 (CRPS)	A/140'	A	HE, DDE, DE	(b)
Motor for Supply Fan OS-97 (CRPS)	A/140'	A	HE, DDE, DE	(b)
Motor for Supply Fan OS-98 (CRPS)	A/140'	A	HE, DDE, DE	(b)
Motor for Supply Fan OS-99 (CRPS)	A/140'	A	HE, DDE, DE	(b)
Fire Damper 46x14 (FD-1)	H/111	A	HE, DDE, DE	(b)
Fire Damper 46x14 (2FD-1)	H/111	C	HE, DDE, DE	(b)
Fire Damper 46x14 (FD-2)	H/111	A	HE, DDE, DE	(b)
Fire Damper 46x14 (2FD-2)	H/111	C	HE, DDE, DE	(b)
Fire Damper 46x14 (FD-3)	H/110	A	HE, DDE, DE	(b)
Fire Damper 46x14 (2FD-3)	H/110	C	HE, DDE, DE	(b)
Fire Damper 32x68 (FD-24)	J/100	A	HE, DDE, DE	(b)
Fire Damper 32x68 (2FD-24)	J/100	C	HE, DDE, DE	(b)
Motors for Fans E-43, E-44, S-43 and S-44	H/163	A	HE, DDE, DE	(b)
Motors for Fans E-45, E-46, S-45 and S-46	H/163	C	HE, DDE, DE	(b)

DCPP UNITS 1 & 2 FSAR UPDATE

TABLE 3.10-3

Equipment	Location ^(c) Building/ Elevation, ft	Qualification Method ^(c)	Qualifying Spectra ^(c)	Notes
Fire Damper 42x24 (FD-25)	A/135	A	HE, DDE, DE	(b)
Fire Damper 42x24 (2FD-25)	A/135	C	HE, DDE, DE	(b)
Fire Damper 42x24 (FD-26)	A/135	A	HE, DDE, DE	(b)
Fire Damper 42x24 (2FD-26)	A/135	C	HE, DDE, DE	(b)
Fire Damper 42x24 (FD-27)	A/135	A	HE, DDE, DE	(b)
Fire Damper 42x24 (2FD-27)	A/135	C	HE, DDE, DE	(b)
Fire Damper 36x39 (FD-19)	A/140	A	HE, DDE, DE	(b)
Fire Damper 36x39 (2FD-19)	A/140	C	HE, DDE, DE	(b)
Fire Damper 36x39 (FD-20)	A/140	A	HE, DDE, DE	(b)
Fire Damper 36x39 (2FD-20)	A/140	C	HE, DDE, DE	(b)
Fire Damper 36x39 (FD-21)	A/140	A	HE, DDE, DE	(b)
Fire Damper 36x39 (2FD-21)	A/140	C	HE, DDE, DE	(b)
Fire Damper 14x10 (FD-26)	H/151	T	HE, DDE, DE	(b)
Fire Damper 14x10 (2FD-26)	H/151	T	HE, DDE, DE	(b)
Fire Damper 20x10 (FD-27)	H/153	T	HE, DDE, DE	(b)
Fire Damper 20x10 (2FD-27)	H/153	T	HE, DDE, DE	(b)
Fire Damper 12x12 (FD-28)	H/158	T	HE, DDE, DE	(b)
Fire Damper 12x12 (2FD-28)	H/158	T	HE, DDE, DE	(b)
Varicel-Roughing Filter (EFR-1)	L/120	A	HE, DDE, DE	(b)
Varicel-Roughing Filter (2EFR-1)	L/120	C	HE, DDE, DE	(b)
Varicel-Roughing Filter (EFR-2a)	L/122	A	HE, DDE, DE	(b)
Varicel-Roughing Filter (2EFR-2a)	L/122	C	HE, DDE, DE	(b)
Varicel-Roughing Filter (EFR-2b)	L/104	A	HE, DDE, DE	(b)
Varicel-Roughing Filter (2EFR-2b)	L/104	C	HE, DDE, DE	(b)
Electric Duct Heater (EH-27)	H/163	A	HE, DDE, DE	(b)
Electric Duct Heater (2EH-27)	H/163	A	HE, DDE, DE	(b)
Electric Duct Heaters (OEH-28A & 28B)	Tech. Support Center/109	A	HE, DDE, DE	(a) (b)

DCPP UNITS 1 & 2 FSAR UPDATE

TABLE 3.10-3

<u>Equipment</u>	<u>Location^(c) Building/ Elevation, ft</u>	<u>Qualification Method^(c)</u>	<u>Qualifying Spectra^(c)</u>	<u>Notes</u>
Mode Damper 8 in. dia (0-17)	Tech. Support Center/109	A	HE, DDE, DE	(a) (b)
Ceiling Registers & Diffusers	Aux./Varies	A	HE, DDE, DE	(b)
Wall Registers & Diffusers(Unit 1)	Aux./Varies	A, C	HE, DDE, DE	(b)
Ceiling Registers & Diffusers	Aux./Varies	A	HE, DDE, DE	(b)
Wall Registers & Diffusers (Unit 2)	Aux./Varies	C	HE, DDE, DE	(b)
Aluminum Air Outlets (26" wide or less) "Metalaire"	Aux./Varies			
Aluminum Air Outlets (26" wide or less) "Metalaire" for Unit 2				
Air Monitors (AM FE-5001, 5013, 5015, 5016, 5018A, 5018B, 5019 and 5020) and Flow Evaluators (FE-5014, 5017A and 5017B)	Aux./Varies	A	HE, DDE, DE	(b)
Air Monitors (AM 2-FE-5001, 5002, 5003, 5004, 5005, 5006, 5007, 5008, 5009, 5010, 5011, 5012, 5013, 5015, 5019 and 5020) and Flow Evaluators (2-FE-5014, 5017A, 5017B, 5018A, 5018B).	Aux./Varies	C	HE, DDE, DE	(b)
Air Flow Controllers Johnson Service R-317-1 for Fans	Aux./Varies	T	HE, DDE, DE	(b)
Pressure Reducing Valve Johnson Service R-130-A for Fan & Dampers	Aux./Varies	T	HE, DDE, DE	(b) (g)
Restrictors Johnson Service T-5210-100 for Fans	Aux./Varies	T	HE, DDE, DE	(b)

DCPP UNITS 1 & 2 FSAR UPDATE

TABLE 3.10-3

<u>Equipment</u>	<u>Location^(c) Building/ Elevation, ft</u>	<u>Qualification Method^(c)</u>	<u>Qualifying Spectra^(c)</u>	<u>Notes</u>
Solenoid Valves ASCO HT-8316-B15, C15 and D45; HT-8320-A20, A24 and A185; and HT-8331-A45 for Fans & Dampers	Aux./Varies	T	HE, DDE, DE	(b)
Speed Controllers ASCO VO221 Speed Controllers ASCO V0222 and VO223	Aux./Varies Aux./Varies	T C	HE, DDE, DE HE, DDE, DE	(b) (b)
Position Switches NAMCO D-2400-X-R2-WS for Dampers Brandt Air Flow Controller (Pi-DPT-2000)	Aux./Varies Aux./Varies	T, C T, A	HE, DDE, DE HE, DDE, DE	(b) (b)
Portion of Refrigerant Piping with Solenoid Valve Exp. Valve with Sight Glass	H/158	T	HE, DDE, DE	(b)
Position Switches Allen-Bradley 802T-HW1 for Dampers Position Switches Allen-Bradley 802T-HW1 for Dampers	Aux./Varies Aux./Varies	T C	HE, DDE, DE HE, DDE, DE	(b) (b)
Air Flow Switches Dwyer 1638 & 1640 for Fans	Aux./Varies, Turbine bldg., Technical Support Center/Varies	T, A	HE, DDE, DE	(a) (b)
Air Flow Switches McDonald-Miller AF1-S for Fans	Aux./Varies	T, A	HE, DDE, DE	(a) (b)
Thermostats Barber Colman TC-1191	H/145	T	HE, DDE, DE	(b)
Thermostats Penn A28AA	K/145	T	HE, DDE, DE	(b)

DCPP UNITS 1 & 2 FSAR UPDATE

TABLE 3.10-3

<u>Equipment</u>	<u>Location^(c) Building/ Elevation, ft</u>	<u>Qualification Method^(c)</u>	<u>Qualifying Spectra^(c)</u>	<u>Notes</u>
Thermostats Penn T26J-2	A/124	T	HE, DDE, DE	(b)
Thermostats Penn T26S-18	A/124	C	HE, DDE, DE	(b)
Thermostats Johnson Controls T26S-18C	A/124	C	HE, DDE, DE	(h)
Control Relay Cabinets for CRC-1 and CRC-3	H/157	T, A	HE, DDE, DE	(b)
Control Relay Cabinets for CRC-6 and CRC-8	H/157	T, A	HE, DDE, DE	(b)
Common Control Relay Cabinets for CCRC-2	H/157	T, A	HE, DDE, DE	(b)
Common Control Relay Cabinets for CCRC-7	H/157	T, A	HE, DDE, DE	(b)
Control Panels for Compressors CP-35 & CP-36	H/156	T	HE, DDE, DE	(b)
Control Panels for Compressors CP-37 & CP-38	H/156	T	HE, DDE, DE	(b)
Heating Relay in Cabinet 3	H/157	T	HE, DDE, DE	(b)
Thermostat Honeywell Model T675A1565 & T6031A1029	H/154	T	HE, DDE, DE	(b)
Motors for Fans S-1, S-2, S-31, S-32, S-39, S-40, E-1, E-2, E-4, E-5, E-6, E-101, E-102, E-103 and E-104	Aux./Varies Intake Structure/Varies	T	HE, DDE, DE	(b)
Motors for Fans 2S-1, 2S-2, S-33, S-34, S-41, S-42,	Aux./Varies Intake Structure/Varies	C	HE, DDE, DE	(b)

DCPP UNITS 1 & 2 FSAR UPDATE

TABLE 3.10-3

<u>Equipment</u>	<u>Location^(c) Building/ Elevation, ft</u>	<u>Qualification Method^(c)</u>	<u>Qualifying Spectra^(c)</u>	<u>Notes</u>
2E-1, 2E-2, 2E-4, 2E-5 and 2E-6				
Motors for Fans CR-35, CR-36, S-35, S-36, S-67, S-68, S-69	Aux./Varies & Turbine /Varies	T, C, A	HE, DDE, DE	(b)
Motors for Fans CR-37, CR-38, S-37, S-38, 2S-67, 2S-68, 2S-69	Aux./Varies & Turbine/Varies	C, A	HE, DDE, DE	(b)
Flex connection in 48-in. ϕ Purge Air Supply Duct FC-1 & FC-2	L/Varies	A	HE, DDE, DE (Bldg. Displ. Per DCM C-28)	(b)
Flex connection in 48-in. ϕ Purge Air Supply Duct 2FC-1 & 2FC-2	L/Varies	C	HE, DDE, DE (Bldg. Displ. per DCM C-28)	(b)
Flex connection in 12-in. ϕ Excess Pressure Relief Duct FC-3 & FC-4	L/Varies	A	HE, DDE, DE (Bldg. Displ. per HE, DDE, DE (Bldg. Displ. per DCM C-28)	(b)
Flex connection in 12-in. ϕ Excess Pressure Relief Duct 2FC-3 & 2FC-4	L/Varies	C	HE, DDE, DE (Bldg. Displ. per HE, DDE, DE (Bldg. Displ. per DCM C-28)	(b)
Flex Connections in 14-in. Pipes OFC-11, through OFC-16, OFC-18 through OFC-21	Turbine bldg. /varies	A	HE, DDE, DE (Bldg. Displ. per DCM C-28)	(b)
Flex Connection in 14-in. Pipe OFC-17	Between Aux. bldg. & Turbine bldg./ 167	A	HE, DDE, DE (Bldg. Displ. per DCM C-28)	(b)
Flex Connection in 14-in. Pipe OFC-22	Aux. bldg./163	A	HE, DDE, DE (Bldg. Displ. Per DCM C-28)	(b) (d)
Flex Connection in 14-in. Pipe OFC-22 Unit 2	Aux. bldg./163	A	HE, DDE, DE (Bldg. Displ. Per DCM C-28)	(b) (d)

DCPP UNITS 1 & 2 FSAR UPDATE

TABLE 3.10-3

<u>Equipment</u>	<u>Location^(c) Building/ Elevation, ft</u>	<u>Qualification Method^(c)</u>	<u>Qualifying Spectra^(c)</u>	<u>Notes</u>
Nutherm/Cleveland Airflow Switches Model AFS-951-1 for over heater in CRPS	H/169	T, A	HE, DDE, DE	(a) (b)
Motors for Compressors CP-35 and CP-36	H/154	A	HE, DDE, DE	(b)
Motors for Compressors CP-37 and CP-38	H/154	C	HE, DDE, DE	(b)
Fire Damper 24x12 (FD-7)	H/110	A	HE, DDE, DE	(b)
Fire Damper 24x12 (2FD-7)	H/110	C	HE, DDE, DE	(b)
Fire Damper 24x12 (FD-8)	H/110	A	HE, DDE, DE	(b)
Fire Damper 24x12 (2FD-8)	H/110	C	HE, DDE, DE	(b)
Fire Damper 24x12 (FD-9)	H/110	A	HE, DDE, DE	(b)
Fire Damper 24x12 (2FD-9)	H/110	C	HE, DDE, DE	(b)
Fire Damper (FD-34)	H/127	T	HE, DDE, DE	(b)
Fire Damper (2FD-34)	H/127	C	HE, DDE, DE	(b)
Fire Damper (FD-36)	H/127	T	HE, DDE, DE	(b)
Fire Damper (2FD-36)	H/127	C	HE, DDE, DE	(b)
Fire Damper (FD-38)	H/126	T	HE, DDE, DE	(b)
Fire Damper (FD-39)	H/126	T	HE, DDE, DE	(b)
Fire Damper (FD-40)	H/123	T	HE, DDE, DE	(b)
Fire Damper (FD-43)	A/119	T	HE, DDE, DE	(b)
Fire Damper (2FD-43)	A/119	C	HE, DDE, DE	(b)
Fire Damper (FD-44)	A/119	T	HE, DDE, DE	(b)
Fire Damper (2FD-44)	A/119	C	HE, DDE, DE	(b)
Fire Damper (FD-45)	A/119	T	HE, DDE, DE	(b)
Fire Damper (2FD-45)	A/119	C	HE, DDE, DE	(b)
Fire Damper (FD-10)	H/121	A	HE, DDE, DE	(b)
Fire Damper (2FD-10)	H/121	C	HE, DDE, DE	(b)

DCPP UNITS 1 & 2 FSAR UPDATE

TABLE 3.10-3

Equipment	Location ^(c) Building/ Elevation, ft	Qualification Method ^(c)	Qualifying Spectra ^(c)	Notes
Fire Damper (FD-11)	H/121	A	HE, DDE, DE	(b)
Fire Damper (2FD-11)	H/121	C	HE, DDE, DE	(b)
Fire Damper (FD-12)	H/121	A	HE, DDE, DE	(b)
Fire Damper (2FD-12)	H/121	C	HE, DDE, DE	(b)
Smoke Damper (SD-26)	H/151	A	HE, DDE, DE	(b)
Smoke Damper (2SD-26)	H/151	C	HE, DDE, DE	(b)
Smoke Damper (SD-27)	H/151	A	HE, DDE, DE	(b)
Smoke Damper (2SD-27)	H/151	C	HE, DDE, DE	(b)
Smoke Damper (SD-35)	H/127	A	HE, DDE, DE	(b)
Smoke Damper (2SD-35)	H/127	C	HE, DDE, DE	(b)
Smoke Damper (SD-37)	H/127	A	HE, DDE, DE	(b)
Smoke Damper (2SD-37)	H/127	C	HE, DDE, DE	(b)
Pneumatic Bettis Actuator for Damper (4A)	Aux/Varies	T	HE, DDE, DE	(b)
Pneumatic Bettis Actuator for Damper (2-4A)	Aux/Varies	T	HE, DDE, DE	(b)
Pneumatic Bettis Actuator for Damper (4B)	Aux/Varies	T	HE, DDE, DE	(b)
Pneumatic Bettis Actuator for Damper (2-4B)	Aux/Varies	T	HE, DDE, DE	(b)
Pneumatic Bettis Actuator for Damper (8A)	Aux/Varies	T	HE, DDE, DE	(b)
Pneumatic Bettis Actuator for Damper (2-8A)	Aux/Varies	T	HE, DDE, DE	(b)
Pneumatic Bettis Actuator for Damper (8B)	Aux/Varies	T	HE, DDE, DE	(b)
Pneumatic Bettis Actuator for Damper (2-8B)	Aux/Varies	T	HE, DDE, DE	(b)
Pneumatic Bettis Actuator for Damper (10)	Aux/Varies	T	HE, DDE, DE	(b)
Pneumatic Bettis Actuator for Damper (2-10)	Aux/Varies	T	HE, DDE, DE	(b)

DCPP UNITS 1 & 2 FSAR UPDATE

TABLE 3.10-3

Equipment	Location ^(c) Building/ Elevation, ft	Qualification Method ^(c)	Qualifying Spectra ^(c)	Notes
Power Regulator Co. Actuator for Damper (12)	Aux/Varies	T	HE, DDE, DE	(b)
Power Regulator Co. Actuator for Damper (16A)	Aux/Varies	T	HE, DDE, DE	(b)
Power Regulator Co. Actuator for Damper (2-16A)	Aux/Varies	C	HE, DDE, DE	(b)
Power Regulator Co. Actuator for Damper (16B)	Aux/Varies	T	HE, DDE, DE	(b)
Power Regulator Co. Actuator for Damper (2-16B)	Aux/Varies	C	HE, DDE, DE	(b)
Power Regulator Co. Actuator for Damper (17A)	Aux/Varies	T	HE, DDE, DE	(b)
Power Regulator Co. Actuator for Damper (2-17A)	Aux/Varies	C	HE, DDE, DE	(b)
Power Regulator Co. Actuator for Damper (17B)	Aux/Varies	T	HE, DDE, DE	(b)
Power Regulator Co. Actuator for Damper (2-17B)	Aux/Varies	C	HE, DDE, DE	(b)
Power Regulator Co. Actuator for Damper (20)	Aux/Varies	T	HE, DDE, DE	(b)
Power Regulator Co. Actuator for Damper (2-20)	Aux/Varies	C	HE, DDE, DE	(b)
Power Regulator Co. Actuator for Damper (21)	Aux/Varies	T	HE, DDE, DE	(b)
Power Regulator Co. Actuator for Damper (2-21)	Aux/Varies	C	HE, DDE, DE	(b)
Power Regulator Co. Actuator for Damper (22A)	Aux/Varies	T	HE, DDE, DE	(b)
Power Regulator Co. Actuator for Damper (2-22A)	Aux/Varies	C	HE, DDE, DE	(b)
Power Regulator Co. Actuator for Damper (22B)	Aux/Varies	T	HE, DDE, DE	(b)
Power Regulator Co. Actuator for Damper (2-22B)	Aux/Varies	C	HE, DDE, DE	(b)
Power Regulator Co. Actuator		T	HE, DDE, DE	(b)

DCPP UNITS 1 & 2 FSAR UPDATE

TABLE 3.10-3

Equipment	Location ^(c) Building/ Elevation, ft	Qualification Method ^(c)	Qualifying Spectra ^(c)	Notes
for Damper (23A)	Aux/Varies	C	HE, DDE, DE	(b)
Power Regulator Co. Actuator for Damper (2-23)				
Power Regulator Co. Actuator for Damper (23B)	Aux/Varies	T	HE, DDE, DE	(b)
Power Regulator Co. Actuator for Damper (2-23B)				
Power Regulator Co. Actuator for Damper (24A)	Aux/Varies	C	HE, DDE, DE	(b)
Power Regulator Co. Actuator for Damper (2-24)				
Power Regulator Co. Actuator for Damper (24B)	Aux/Varies	T	HE, DDE, DE	(b)
Power Regulator Co. Actuator for Damper (2-24B)				
Power Regulator Co. Actuator for Damper (25A)	Aux/Varies	C	HE, DDE, DE	(b)
Power Regulator Co. Actuator for Damper (2-25)				
Power Regulator Co. Actuator for Damper (25B)	Aux/Varies	T	HE, DDE, DE	(b)
Power Regulator Co. Actuator for Damper (2-25B)				
Power Regulator Co. Actuator for Damper (26A)	Aux/Varies	C	HE, DDE, DE	(b)
Power Regulator Co. Actuator for Damper (2-26A)				
Power Regulator Co. Actuator for Damper (26B)	Aux/Varies	T	HE, DDE, DE	(b)
Power Regulator Co. Actuator for Damper (2-26B)				
Power Regulator Co. Actuator for Damper (33)	Aux/Varies	C	HE, DDE, DE	(b)
Power Regulator Co. Actuator for Damper (2-33)				
Power Regulator Co. Actuator for Damper (34)	Aux/Varies	T	HE, DDE, DE	(b)

DCPP UNITS 1 & 2 FSAR UPDATE

TABLE 3.10-3

Equipment	Location ^(c) Building/ Elevation, ft	Qualification Method ^(c)	Qualifying Spectra ^(c)	Notes
Power Regulator Co. Actuator for Damper (2-34)	Aux/Varies	C	HE, DDE, DE	(b)
Pneumatic Parker-Hannifin Actuator for Mode Damper (1A)	L/127	A	HE, DDE, DE	(b)
Pneumatic Parker-Hannifin Actuator for Mode Damper (2-1A)	L/127	A	HE, DDE, DE	(b)
Pneumatic Parker-Hannifin Actuator for Mode Damper (1B)	L/131	C	HE, DDE, DE	(b)
Pneumatic Parker-Hannifin Actuator for Mode Damper (2-1B)	L/131	C	HE, DDE, DE	(b)
Pneumatic Parker-Hannifin Actuator for Damper (13A)	K/97	A	HE, DDE, DE	(b)
Pneumatic Parker-Hannifin Actuator for Damper (2-13A)	K/97	C	HE, DDE, DE	(b)
Pneumatic Parker-Hannifin Actuator for Damper (13B)	K/97	A	HE, DDE, DE	(b)
Pneumatic Parker-Hannifin Actuator for Damper (2-13B)	K/97	C	HE, DDE, DE	(b)
Pneumatic Parker-Hannifin Actuator for Damper (14A)	K/81	A	HE, DDE, DE	(b)
Pneumatic Parker-Hannifin Actuator for Damper (2-14A)	K/81	C	HE, DDE, DE	(b)
Pneumatic Parker-Hannifin Actuator for Damper (14B)	K/81	A	HE, DDE, DE	(b)
Pneumatic Parker-Hannifin Actuator for Damper (2-14B)	K/81	C	HE, DDE, DE	(b)
Pneumatic Parker-Hannifin Actuator for Damper (15A)	Aux/70	A	HE, DDE, DE	(b)
Pneumatic Parker-Hannifin Actuator for Damper (2-15A)	Aux/70	C	HE, DDE, DE	(b)
Pneumatic Parker-Hannifin Actuator for Damper (15B)	Aux/70	A	HE, DDE, DE	(b)
Pneumatic Parker-Hannifin Actuator for Damper (2-15B)	Aux/70	C	HE, DDE, DE	(b)

TABLE 3.10-3

<u>Equipment</u>	<u>Location^(c) Building/ Elevation, ft</u>	<u>Qualification Method^(c)</u>	<u>Qualifying Spectra^(c)</u>	<u>Notes</u>
Position Switches NAMCO SL-3B1W & SL-170D for Dampers	L/115	T	HE, DDE, DE	(b)

- (a) Turbine building, Unit 2, response spectra applicable for Qualification Spectra of equipment in the Technical Support Center.
- (b) Envelope of 4% HE and 2% DDE Acceleration used in Qualification Spectra. Per DCM T-10 acceptance criteria, DE stresses shall not exceed the maximum allowable stress values specified in building codes (Uniform Building Code, 1973 and AISI, 1969). Increase in allowable stresses, permitted by code for seismic loads, shall not be used. In lieu of these, DDE and Hosgri stresses shall not exceed 90% of the yield strength and 150% of the AISI allowable stress, respectively.

(c) Legend:

- ISA = Intake structure area
- A = Qualification Spectra by analysis (Qualification Method column)
- T = Qualification Spectra by testing
- C = Comparison with similarly qualified equipment
- DE = Design Earthquake
- DDE = Double Design Earthquake
- HE = Hosgri Earthquake

The letters in the Location column refer to standard area designations as defined in Figure 1.2-3, Piping and Mechanical Area Location Plan.

- (d) Tag number of flexible connection OFC-22 has been duplicated.
- (e) Quadrant dampers supported on flexible slab.
- (f) Applicable to Units 1 and 2.
- (g) Due to obsolescence of Johnson air pressure reducing regulators, Fisher 67CSR regulators may be installed.
- (h) Due to obsolescence of Penn thermostats, Johnson Controls T26S-18C thermostats may be installed.

DCPP UNITS 1 & 2 FSAR UPDATE

TABLE 3.7-1

CONTAINMENT AND AUXILIARY BUILDING
CRITERIA COMPARISON

<u>Parameters</u>	<u>HE</u>	<u>DE</u>	<u>DDE</u>
Seismic input, horizontal	0.75g	0.2g	0.4g
Seismic input, vertical	2/3 of horizontal dynamic amplification considered	Static - 2/3 of horizontal ground spectra	Static-2/3 of horizontal ground spectra
Accidental torsion	5% and 7% eccentricity	Not considered	Not considered
Foundation filtering	Tau = 0.040 ^(a)	Not applicable	Not applicable
Response combination	3-D SRSS	2-D ABSUM	2-D ABSUM
Damping values	7%	2% concrete ^(b) 2% steel	5% concrete 2% steel
Ductility	Allowed in some areas	Not considered	Not considered
Material properties	Based on test values	Min specified values	Min specified values
Response spectra broadening (based on frequency)	+5%, -15%	±10%	±10%
Response spectra peaks clip		10% (for containment only)	10% (for containment only)

(a) 0.052 for auxiliary building.

(b) 5% for auxiliary building.

DCPP UNITS 1 & 2 FSAR UPDATE

TABLE 3.7-1A

TURBINE BUILDING
CRITERIA COMPARISON

<u>Parameters</u>	<u>HE</u>	<u>DE and DDE^(a)</u>
Seismic input, horizontal	0.75g	0.2g (DE) 0.4g (DDE)
Seismic input, vertical	2/3 of horizontal dynamic amplification Considered	Static - 2/3 of horizontal ground spectra
Accidental torsion	5% and 7% eccentricity, or equivalent Note (b)	Not considered
Foundation filtering	Tau = 0.080 (Blume input) Tau = 0.067 (Newmark input)	Not applicable
Response combination	3-D SRSS	2-D ABSUM
Damping values	7%	5% concrete 2% steel
Ductility	Concrete 1.3 Steel 3 (6 locally)	Not considered
Material properties	Based on test values	Min specified values
Response spectra broadening (based on frequency)	+5%, -15%	±10%
Response spectra peaks clip		10%

(a) DE and DDE analysis is performed only to generate response spectra for systems qualification.

(b) Equivalent method is used as described in Section 3.7.2.10.

DCPP UNITS 1 & 2 FSAR UPDATE

TABLE 3.7-1B

INTAKE STRUCTURE
CRITERIA COMPARISON

<u>Parameters</u>	<u>Hosgri</u>	<u>DE and DDE for Systems Qualifications Only</u>
Seismic input, horizontal	Hosgri 7.5M	DE (0.20g) DDE (0.40g)
Seismic input, vertical	2/3 of horizontal spectra with Tau = 0.0 Dynamic amplification Considered	Static 2/3 of ground horizontal spectra
Accidental torsion	Horizontal floor response spectra increased by 10%	Not considered
Foundation filtering	Tau - 0.04	Not applicable
Response combination	3-D-SRSS	Not applicable
Damping values % critical	7%	5%
Ductility	Concrete 1.3; Steel 3, with up to 6 locally ^(a)	Not considered
Material properties	Based on test values	Minimum specified values
Floor response spectra broadening (based on frequency)	+5%, -15%	Structural peaks clipped 10% and widened by ± 10%

(a) Or as may be required to demonstrate that function of Design Class I equipment will not be adversely affected.

DCPP UNITS 1 & 2 FSAR UPDATE

TABLE 3.7-1C

OUTDOOR STORAGE TANKS
CRITERIA COMPARISON

<u>Parameters</u>	<u>Hosgri</u>	<u>DE and DDE</u>
Seismic input, horizontal	Hosgri 7.5M	DE (0.20g) DDE (0.40g)
Seismic input, vertical	2/3 ZPA (0.75g) of horizontal spectra with Amplification considered Tau = 0.0	Static 2/3 ZPA of horizontal ground spectra
Accidental torsion	Not applicable	Not applicable
Response combination	3-D SRSS	2-D ABSUM
Damping	7%-All tanks with concrete cover 4%-Firewater tank without concrete cover	5%-All tanks with concrete cover 1%-Firewater tank without concrete cover
Material properties	Based on test values	Minimum specified values

DCPP UNITS 1 & 2 FSAR UPDATE

TABLE 3.7-2

CONTAINMENT STRUCTURE
PERIODS OF VIBRATION

<u>Mode No.</u>	<u>Period, T, in sec</u>
1	0.255
2	0.093
3	0.088
4	0.073
5	0.060
6	0.058
7	0.057
8	0.051
9	0.051

DCPP UNITS 1 & 2 FSAR UPDATE

Table 3.7-3

CONTAINMENT STRUCTURE
MAXIMUM ABSOLUTE ACCELERATIONS

<u>Structure</u>	<u>Nodal Point^(a)</u>	<u>Elevation, ft</u>	<u>Maximum Absolute Acceleration, g</u>	
			<u>DE Analysis</u>	<u>DDE Analysis</u>
Exterior structure	2	301.64	1.275	2.083
	8	274.37	1.032	1.736
	10	258.27	0.907	1.567
	14	231.00	0.743	1.177
	17	205.58	0.837	1.358
	23	181.08	0.911	1.369
	26	155.83	0.866	1.292
	34	130.58	0.713	1.080
	37	109.67	0.492	0.793
Interior structure	19-22	140.00	0.735	1.195
	24	127.00	0.597	0.982
	27-30	114.00	0.478	0.773
	32	110.00	0.455	0.726
	38	102.00	0.384	0.601
Base slab	47-58	88.58	0.291	0.483

(a) See Figure 3.7-5.

DCPP UNITS 1 & 2 FSAR UPDATE

Table 3.7-4

CONTAINMENT STRUCTURE
MAXIMUM DISPLACEMENTS

<u>Structure</u>	<u>Nodal Point^(a)</u>	<u>Elevation, ft</u>	<u>Maximum Displacement Inches</u>	
			<u>DE Analysis</u>	<u>DDE Analysis</u>
Exterior structure	2	301.64	0.666	1.063
	8	274.37	0.602	0.967
	10	258.27	0.562	0.911
	14	231.00	0.480	0.807
	17	205.58	0.389	0.695
	23	181.08	0.314	0.587
	26	155.83	0.248	0.459
	34	130.58	0.180	0.327
	37	109.67	0.115	0.212
Interior structure	19-22	140.00	0.083	0.139
	24	127.00	0.069	0.114
	27-30	114.00	0.056	0.090
	32	110.00	0.053	0.084
	38	102.00	0.043	0.068
Base slab	47-58	88.58	0.030	0.050

(a) See Figure 3.7-5.

DCPP UNITS 1 & 2 FSAR UPDATE

Table 3.7-5

CONTAINMENT STRUCTURE MAXIMUM SHELL FORCES AND MOMENTS^(a) - DE ANALYSIS

Nodal ^(b) Point	Elevation, ft	Shell Moments, kip-ft/ft			Shell Forces, kips/ft		
		M_{SS}	M_{TT}	M_{ST}	F_{SS}	F_{TT}	F_{ST}
2	301.64	0.21	0.21	28.99	2.74	3.84	3.75
8	274.37	0.33	0.44	2.96	14.47	32.07	23.85
10	258.27	1.76	0.91	1.63	21.04	40.91	32.80
14	231.00	9.17	2.94	0.36	37.68	42.73	48.97
17	205.58	5.74	1.26	0.27	63.59	33.27	66.44
23	181.08	7.58	2.54	0.31	91.25	37.79	79.59
26	155.83	5.69	1.49	0.50	110.72	36.31	91.43
34	130.58	4.31	1.01	0.27	151.69	31.20	108.65
37	109.67	8.26	2.75	0.19	174.13	18.99	122.66
57	88.58	1.01	0.14	2.23	209.79	63.73	127.22

(a) See Figure 3.7-7.

(b) See Figure 3.7-5.

DCPP UNITS 1 & 2 FSAR UPDATE

Table 3.7-6

CONTAINMENT STRUCTURE MAXIMUM SHELL FORCES AND MOMENTS^(a) - DDE ANALYSIS

Nodal ^(b) Point	Elevation, ft	Shell Moments, kip-ft/ft			Shell Forces, kips/ft		
		M_{SS}	M_{TT}	M_{ST}	E_{SS}	E_{TT}	E_{ST}
2	301.64	0.36	0.37	47.17	4.30	6.33	6.04
8	274.37	0.62	0.76	4.77	22.00	53.37	39.37
10	258.27	2.71	1.46	2.63	32.58	67.71	54.58
14	231.00	15.29	4.92	0.50	60.01	71.93	83.06
17	205.58	8.14	1.64	0.37	103.39	53.31	110.30
23	181.08	11.39	3.96	0.45	154.79	56.72	132.95
26	155.83	8.27	2.21	0.77	190.50	54.24	162.53
34	130.58	6.07	1.36	9.42	251.35	46.24	195.36
37	109.67	15.95	5.31	0.34	282.88	30.75	217.34
57	88.58	1.74	0.23	4.18	338.73	110.90	220.62

(a) See Figure 3.7-7.

(b) See Figure 3.7-5.

DCPP UNITS 1 & 2 FSAR UPDATE

Table 3.7-7

CONTAINMENT STRUCTURE
MAXIMUM TOTAL SHEARS

<u>Structure</u>	<u>Associated^(a) Nodel Point</u>	<u>Elevation, ft</u>	<u>Maximum Shears, kips x 10³</u>	
			<u>DE Analysis</u>	<u>DDE Analysis</u>
Exterior structure	2	301.64	0.19	0.66
	8	274.37	5.81	9.38
	10	258.27	8.49	13.91
	14	231.00	11.39	19.55
	17	205.58	15.00	25.02
	23	181.08	17.95	29.98
	26	155.83	20.63	36.66
	34	130.58	24.53	44.18
	37	109.67	27.83	49.42
	57	88.58	29.55	51.39
Interior structure	19 & 22	140.00	8.06	13.23
	27 & 30	114.00	10.27	16.87
	49 & 54	88.58	18.85	30.96
Total base shear	49, 54, & 57	88.58	35.05	59.99

(a) See Figure 3.7-5.

DCPP UNITS 1 & 2 FSAR UPDATE

Table 3.7-8

CONTAINMENT STRUCTURE
MAXIMUM TOTAL OVERTURNING MOMENTS

<u>Structure</u>	<u>Associated^(a) Nodel Point</u>	<u>Elevation, ft</u>	<u>Maximum Overturning Moment kips-ft x 10⁶</u>	
			<u>DE Analysis</u>	<u>DDE Analysis</u>
Exterior structure	2	301.64	0.00	0.00
	8	274.37	0.12	0.18
	10	258.27	0.27	0.41
	14	231.00	0.61	0.97
	17	205.58	1.03	1.67
	23	181.08	1.48	2.50
	26	155.83	1.79	3.08
	34	130.58	2.45	4.07
	37	109.67	2.82	4.58
	57	88.58	3.39	5.48
Interior structure	19 & 22	140.00	0.06	0.10
	27 & 30	114.00	0.20	0.33
	49 & 54	88.58	0.76	1.24
Total O.T.M. at base	49, 54 & 57	88.58	3.48	5.62

(a) See Figure 3.7-5.

DCPP UNITS 1 & 2 FSAR UPDATE

TABLE 3.7-8A

PERIODS OF VIBRATION AND PERCENT PARTICIPATION FACTORS

Mode No	Translational ^(a) Horizontal Model		Containment Exterior Structure Coupled Translation ^(b) Plus Torsion Model		Vertical Model	
	Period (sec)	Percent Participation Factor	Period (sec)	Percent Participation Factor	Period (sec)	Participation Factor
1	0.225	44.97	0.217	58.85	0.081	51.72
2	0.081	22.75	0.109	0.32	0.051	16.72
3	0.053	3.73	0.074	25.86	0.046	2.62
4	0.053	7.88	0.041	12.35	0.046	3.81
5	0.047	1.96	0.039	5.63	0.044	11.84
6	0.045	0.043			0.043	0.05
7	0.043	9.91			0.040	7.96
8	0.041	1.66			0.038	3.15
9	0.037	1.70			0.035	1.25
10	0.036	1.71			0.035	0.88
11	0.033	1.18				
12	0.032	2.12				

(a) Axisymmetric model (see Figure 3.7-5A).

(b) Lumped-mass model with 5% accidental eccentricity (see Figure 3.7-5B).

DCPP UNITS 1 & 2 FSAR UPDATE

TABLE 3.7-8B

CONTAINMENT EXTERIOR STRUCTURE
MAXIMUM ABSOLUTE HORIZONTAL AND VERTICAL ACCELERATIONS

Node ^(b) Point	Elevation (ft)	Absolute Horizontal Acceleration (g)		Absolute Vertical Acceleration (g)	
		Blume-Hosgri Horizontal Input	Vertical Input	Blume-Hosgri Horizontal Input	Vertical Input
2	301.64	2.21	0.02	0.075	1.600
8	274.37	2.07	0.15	0.450	1.020
10	258.27	1.95	0.28	0.511	0.882
14	231.00	1.70	0.28	0.532	0.810
17	205.58	1.44	0.11	0.475	0.759
19	181.08	1.23	0.14	0.416	0.703
20	155.83	1.00	0.17	0.334	0.633
22	130.58	0.80	0.18	0.228	0.575
23	109.67	0.75	0.16	0.122	0.538

(a) Effective horizontal acceleration at containment shell due to absolute sum of horizontal response and torsional response from 5% eccentricity.

(b) See Figure 3.7-5A.

DCPP UNITS 1 & 2 FSAR UPDATE

TABLE 3.7-8C

CONTAINMENT EXTERIOR STRUCTURE
MAXIMUM HORIZONTAL AND VERTICAL DISPLACEMENTS

Nodal ^(a) Point	Elevation (ft)	Horizontal Displacement (in.)		Vertical Displacement (in.)	
		Blume-Hosgri Horizontal Input	Vertical Input	Blume-Hosgri Horizontal Input	Vertical Input
2	301.64	1.120	0.002	0.032	0.108
8	274.37	1.012	0.009	0.198	0.076
10	258.27	0.943	0.020	0.228	0.066
14	231.00	0.802	0.020	0.240	0.056
17	205.58	0.642	0.008	0.221	0.049
19	181.08	0.515	0.009	0.195	0.041
20	155.83	0.379	0.011	0.158	0.031
22	130.58	0.253	0.012	0.109	0.020
23	109.67	0.151	0.012	0.058	0.010

(a) See Figure 3.7-5A.

DCPP UNITS 1 & 2 FSAR UPDATE

TABLE 3.7-8D

CONTAINMENT EXTERIOR STRUCTURE
MAXIMUM SHELL FORCES AND MOMENTS

Node ^(b) Point	Elevation (ft)	Shell Forces (kip/ft) ^(a)						Shell Moments (kip-ft/ft) ^(a)					
		Blume-Hosgri Horizontal Input			Vertical Input			Blume-Hosgri Horizontal Input			Vertical Input		
		F_{SS}	F_{HI}	F_{SI}	F_{SS}	F_{HI}	F_{SI}	M_{SS}	M_{HI}	M_{SI}	M_{SS}	M_{HI}	M_{SI}
2	301.64	4.48	7.35	6.85	26.04	10.32	0	0.80	0.39	57.55	3.68	2.94	0
8	274.37	23.05	59.90	44.80	27.97	28.90	0	0.72	0.86	5.87	2.66	1.09	0
10	258.27	34.80	77.10	53.15	31.00	28.24	0	2.85	1.59	3.24	3.12	1.36	0
14	231.00	65.60	86.55	101.00	42.95	9.45	0	17.40	5.42	0.64	11.24	1.24	0
17	205.58	118.00	51.40	143.00	57.41	13.38	0	7.80	1.27	0.23	5.86	1.12	0
19	181.08	185.50	47.00	73.50	63.95	11.60	0	11.75	3.86	0.32	3.14	1.40	0
20	155.83	235.00	40.15	200.00	65.85	7.89	0	12.40	2.96	0.69	3.51	1.37	0
22	130.58	325.50	37.80	219.50	66.95	10.76	0	5.99	1.13	0.27	2.08	2.32	0
23	109.67	376.00	36.25	240.50	67.06	0	0	19.05	6.26	0.26	6.99	2.78	0

(a) See Figure 3.7-7.

(b) See Figure 3.7-5A.

DCPP UNITS 1 & 2 FSAR UPDATE

TABLE 3.7-8E

CONTAINMENT EXTERIOR STRUCTURE
 MAXIMUM TOTAL SHEARS AND MAXIMUM OVERTURNING MOMENTS

Nodal ^(b) Point	Elevation (ft)	Maximum Shear Force (kips x 10 ³) ^(a)		Maximum Overturning Moment (kip-ft x 10 ⁶) ^(a)	
		Blume-Hosgri Horizontal Input	Blume-Hosgri Horizontal Input	Blume-Hosgri Horizontal Input	Blume-Hosgri Horizontal Input
2	301.64	0.34	--	--	--
8	274.37	10.50	0.18	0.18	0.18
10	258.27	15.94	0.44	0.44	0.44
14	231.00	23.67	1.06	1.06	1.06
17	205.58	32.49	1.91	1.91	1.91
19	181.08	39.44	3.00	3.00	3.00
20	155.83	45.39	3.80	3.80	3.80
22	130.58	49.70	5.26	5.26	5.26
23	109.67	55.05	6.08	6.08	6.08
27	88.58	55.81	7.31	7.31	7.31

(a) Vertical Input does not produce a net shear force.

(b) See Figure 3.7-5A.

DCPP UNITS 1 & 2 FSAR UPDATE

TABLE 3.7-8F

CONTAINMENT EXTERIOR STRUCTURE
MAXIMUM TOTAL TORSIONAL MOMENTS AND AXIAL FORCES

<u>Nodal^(b) Point</u>	<u>Elevation (ft)</u>	<u>Blume-Hosgri Total Torsional Moment (kip-ft x 10³)^(a) Horizontal Input</u>	<u>Axial Force(kips x 10³)^(c)</u>
2	301.64	5.49	1.52
8	274.37	67.61	9.93
10	258.27	136.94	12.82
14	231.00	216.36	19.36
17	205.58	293.17	25.88
19	181.08	353.32	28.83
20	155.83	400.00	29.69
22	130.58	427.78	30.18
23	109.67	439.99	30.23

(a) Vertical input does not produce a net torque.

(b) See Figure 3.7-5A.

(c) Due to vertical input.

DCPP UNITS 1 & 2 FSAR UPDATE

TABLE 3.7-8G

CONTAINMENT INTERIOR STRUCTURE
 MAXIMUM ABSOLUTE HORIZONTAL ACCELERATIONS AND DISPLACEMENTS

Nodal ^(a) Point	Elevation (ft)	Newmark-Hosgri			
		Horizontal Acceleration (g)	Torsional Acceleration (rad/sec ²)	Displacement (in.)	Rotation (rad x 10 ⁻⁵)
28	140.00	0.92	0.07	0.06	1.21
34	114.00	0.70	0.05	0.03	0.82

(a) See Figure 3.7-5A.

DCPP UNITS 1 & 2 FSAR UPDATE

TABLE 3.7-8H

CONTAINMENT INTERIOR STRUCTURE
 MAXIMUM TOTAL SHEARS, OVERTURNING MOMENTS,
 AND TORSIONAL MOMENTS^(a)

Nodal ^(b) Point	Elevation (ft)	Shear (kips x 10 ³)		Overturning Moment (kip-ft x 10 ³)		Torsional Moment ^(c) (kip-ft x 10 ³)	
		Blume- Hosgri	Newmark- Hosgri	Blume- Hosgri	Newmark- Hosgri	Blume- Hosgri	Newmark- Hosgri
34	114.00	6.52	6.64	74.55	78.82	136.68	146.48
37	114.00	10.80	11.23	227.89	239.55		
48	88.58	10.08	10.40	219.60	229.31	266.06	283.99
49	88.58	13.26	13.73	544.10	560.76		

(a) Due to horizontal input only.

(b) See Figure 3.7-5A.

(c) Values obtained from lumped-mass model shown in Figure 3.7-5C.

DCPP UNITS 1 & 2 FSAR UPDATE

TABLE 3.7-8I

UNIT 1
 VERTICAL DYNAMIC ANALYSIS - FRAME NO. 6
 SUMMARY OF MODAL PARTICIPATION FACTORS AND FREQUENCIES

<u>Mode</u>	<u>Frequency</u>	<u>X-Direction</u>	<u>Y-Direction</u>	<u>Z-Direction</u>	<u>X-Rotation</u>	<u>Y-Rotation</u>	<u>Z-Rotation</u>
1	11.4	0.00	0.00	0.71	0.0	-541.0	0.0
2	16.8	0.00	0.00	0.09	0.0	-63.0	0.0
3	20.6	0.00	0.00	-0.08	0.0	54.0	0.0
4	21.9	0.00	0.00	0.09	0.0	-65.0	0.0
5	24.1	0.00	0.00	0.03	0.0	-31.0	0.0
6	24.4	0.00	0.00	-0.01	0.0	13.0	0.0
7	24.9	0.00	0.00	-0.03	0.0	22.0	0.0
8	26.2	0.00	0.00	-0.01	0.0	-5.0	0.0
9	28.4	0.00	0.00	-0.50	0.0	304.0	0.0
10	29.3	0.00	0.00	0.20	0.0	-124.0	0.0
11	33.2	0.00	0.00	-0.04	0.0	30.0	0.0

NOTE: X is in the Radial direction.
 Y is in the Longitudinal direction.
 Z is in the Vertical direction.

DCPP UNITS 1 & 2 FSAR UPDATE

TABLE 3.7-8J

UNIT 2
 VERTICAL DYNAMIC ANALYSIS - ANNULUS FRAME 6
 SUMMARY OF MODAL PARTICIPATION FACTORS AND FREQUENCIES

<u>Mode</u>	<u>Frequency</u>	<u>X-Direction</u>	<u>Y-Direction</u>	<u>Z-Direction</u>	<u>X-Rotation</u>	<u>Y-Rotation</u>	<u>Z-Rotation</u>
1	11.6	.00	0.70	.00	.00	.00	82.0
2	16.0	.00	-0.09	.00	.00	.00	-7.7
3	16.46	.00	0.07	.00	.00	.00	6.6
4	22.9	.00	-0.07	.00	.00	.00	-13.0
5	23.87	.00	0.02	.00	.00	.00	-2.0
6	24.0	.00	0.00	.00	.00	.00	7.0
7	27.8	.00	0.00	.00	.00	.00	-8.1
8	32.28	.00	0.08	.00	.00	.00	-15.0

NOTE: X is in the Radial direction.
 Y is in the Longitudinal direction.
 Z is in the Vertical direction.

DCPP UNITS 1 & 2 FSAR UPDATE

TABLE 3.7-8K

CONTAINMENT ANNULUS STRUCTURES UNITS 1 AND 2
NATURAL FREQUENCIES FOR HORIZONTAL
SEISMIC GROUND MOTION

<u>Unit</u>	<u>Elevation</u>	<u>Mode</u>	<u>Frequency (cps)</u>
1	101	1	20.95
		2	21.69
	106	1	20.16
		2	21.47
	117	1	20.24
		2	22.78
2	101	1	22.46
		2	22.79
	106	1	19.98
		2	22.20
	117	1	19.98
		2	25.79

TABLE 3.7-8L

POLAR GANTRY CRANE
 MIXIMUM DISPLACEMENTS, HOSGRI
 (UNIT 1)

<u>Condition</u>	<u>Node</u>	<u>Longitudinal Direction (in.)</u>	<u>Transverse Direction (in.)</u>	<u>Vertical Direction (in.)</u>
Unloaded	31	6.16	6.11	1.77
	32	6.29	6.11	2.10
	39	6.16	5.27	1.49
	40	6.30	5.28	1.47
	47	6.16	5.40	1.71
	48	6.29	5.40	1.81
	75	-	-	1.57
	76	-	-	1.92
	77	-	-	1.71
	78	-	-	1.81
Loaded, 200 tons	31	6.61	5.22	1.69
	32	6.67	5.22	1.74
	39	6.62	4.76	2.12
	40	6.68	4.76	2.09
	47	6.62	4.56	1.12
	48	6.67	4.56	1.24
	75	-	-	1.49
	76	-	-	1.34
	77	-	-	1.12
	78	-	-	1.26

Notes:

1. All displacements are measured relative to base of crane.
2. For node numbers, refer to Figure 3.7-7A.
3. See PG&E Calculation No. 2252C-2 (Reference 37).

TABLE 3.7-8L

POLAR GANTRY CRANE
 MAXIMUM DISPLACEMENTS, HOSGRI
 (UNIT 2)

<u>Condition</u>	<u>Node</u>	<u>Longitudinal Direction (in.)</u>	<u>Transverse Direction (in.)</u>	<u>Vertical Direction (in.)</u>
Unloaded	31	6.16	6.11	1.77
	32	6.29	6.11	2.10
	39	6.16	5.27	1.49
	40	6.30	5.28	1.47
	47	6.16	5.40	1.71
	48	6.29	5.40	1.81
	75	-	-	1.57
	76	-	-	1.92
	77	-	-	1.71
	78	-	-	1.81
Loaded, 200 tons	31	6.61	5.22	1.69
	32	6.67	5.22	1.74
	39	6.62	4.76	2.12
	40	6.68	4.76	2.09
	47	6.62	4.56	1.12
	48	6.67	4.56	1.24
	75	-	-	1.49
	76	-	-	1.34
	77	-	-	1.12
	78	-	-	1.26

Notes:

1. All displacements are measured relative to base of crane.
2. For node numbers, refer to Figure 3.7-7A.
3. See Civil Calculation 2252C-4 (Reference 39).

TABLE 3.7-8M

POLAR GANTRY CRANE
MAXIMUM FORCES,
HOSGRI - UNLOADED CONDITION
(UNIT 1)

Type of Element	Element	Node	Axial Force (kips)	Bending Moment About Axis Y (kip-in.)	Bending Moment About Axis Z (kip-in.)
Girder Beam	13	35	212	111,700	17,950
Girder Beam	18	36	172	122,900	18,100
Gantry Leg	2	11	679	23,240	15,810
Gantry Leg	3	15	637	24,660	81,950
Gantry Leg	6	12	635	24,020	16,270
Gantry Leg	7	16	575	25,060	86,170
Gantry Leg	29	59	646	27,740	81,400
Gantry Leg	28	63	720	26,000	16,140
Gantry Leg	33	60	679	26,140	80,930
Gantry Leg	32	64	703	24,080	16,590
Sill Beam	11	9	38	28,800	2,652
Sill Beam	26	68	39	29,470	2,914
Leg Tie BM	10	20	15	28,640	7,176
Leg Tie BM	25	57	6	26,750	4,227
Girder Tie BM	9	34	9	8,853	12,080
Girder Tie BM	24	50	8	14,280	13,480
Trolley	22	71	56	23,280	3,480

Notes:

1. For node and element numbers, refer to Figure 3.7-7A.
2. See PG&E Calculation No. 2252C-3 (Reference 38).
3. Y-axis represents the major axis of cross section. Z-axis represents the minor axis.

TABLE 3.7-8M

POLAR GANTRY CRANE
MAXIMUM FORCES,
HOSGRI - UNLOADED CONDITION
(UNIT 2)

Type of Element	Element	Node	Axial Force (kips)	Bending Moment About Axis Y (kip-in.)	Bending Moment About Axis Z (kip-in.)
Girder Beam	13	35	212	111,700	17,950
Girder Beam	18	36	172	122,900	18,100
Gantry Leg	2	11	679	23,240	15,810
Gantry Leg	3	15	637	24,660	81,950
Gantry Leg	6	12	635	24,020	16,270
Gantry Leg	7	16	575	25,060	86,170
Gantry Leg	29	59	646	27,740	81,400
Gantry Leg	28	63	720	26,000	16,140
Gantry Leg	33	60	679	26,140	80,930
Gantry Leg	32	64	703	24,080	16,590
Sill Beam	11	9	38	28,800	2,652
Sill Beam	26	68	39	29,470	2,914
Leg Tie BM	10	20	15	28,640	7,176
Leg Tie BM	25	57	6	26,750	4,227
Girder Tie BM	9	34	9	8,853	12,080
Girder Tie BM	24	50	8	14,280	13,480
Trolley	22	71	56	23,280	3,480

Notes:

1. For node and element numbers, refer to Figure 3.7-7A.
2. See PG&E Calculation No. 2252C-4 (Reference 39).
3. Y-axis represents the major axis of cross section. Z-axis represents the minor axis.

TABLE 3.7-8N

POLAR GANTRY CRANE
MAXIMUM FORCES,
HOSGRI - LOADED CONDITION
(UNIT 1)

Type of Element	Element	Node	Axial Force (kips)	Bending Moment About Axis Y (kip-in.)	Bending Moment About Axis Z (kip-in.)
Girder Beam	14	39	190	210,700	25,310
Girder Beam	19	40	181	219,000	25,570
Gantry Leg	3	15	824	27,550	105,000
Gantry Leg	4	21	698	10,750	114,700
Gantry Leg	7	16	881	28,290	107,000
Gantry Leg	8	22	675	10,380	115,700
Gantry Leg	30	51	670	11,710	149,700
Gantry Leg	29	59	762	26,430	113,900
Gantry Leg	34	52	681	11,570	147,900
Gantry Leg	33	60	738	25,230	112,100
Sill Beam	11	9	45	34,760	2,410
Sill Beam	26	68	47	30,560	2,370
Leg Tie BM	10	20	15	36,710	7,683
Leg Tie BM	25	58	6	24,640	4,626
Girder Tie BM	9	33	9	11,530	13,550
Girder Tie BM	24	50	7	15,900	14,850
Trolley	22	71	57	88,950	3,269

Notes:

1. For node and element numbers, refer to Figure 3.7-7A.
2. See PG&E Calculation No. 2252C-3 (Reference 38).
3. Y-axis represents the major axis of cross section. Z-axis represents the minor axis.

TABLE 3.7-8N

POLAR GANTRY CRANE
MAXIMUM FORCES,
HOSGRI - LOADED CONDITION
(UNIT 2)

Type of Element	Element	Node	Axial Force (kips)	Bending Moment About Axis Y (kip-in.)	Bending Moment About Axis Z (kip-in.)
Girder Beam	14	39	190	210,700	25,310
Girder Beam	19	40	181	219,000	25,570
Gantry Leg	3	15	824	27,550	105,000
Gantry Leg	4	21	698	10,750	114,700
Gantry Leg	7	16	881	28,290	107,000
Gantry Leg	8	22	675	10,380	115,700
Gantry Leg	30	51	670	11,710	149,700
Gantry Leg	29	59	762	26,430	113,900
Gantry Leg	34	52	681	11,570	147,900
Gantry Leg	33	60	738	25,230	112,100
Sill Beam	11	9	45	34,760	2,410
Sill Beam	26	68	47	30,560	2,370
Leg Tie BM	10	20	15	36,710	7,683
Leg Tie BM	25	58	6	24,640	4,626
Girder Tie BM	9	33	9	11,530	13,550
Girder Tie BM	24	50	7	15,900	14,850
Trolley	22	71	57	88,950	3,269

Notes:

1. For node and element numbers, refer to Figure 3.7-7A.
2. See PG&E Calculation No. 2252C-4 (Reference 39).
3. Y-axis represents the major axis of cross section. Z-axis represents the minor axis.

DCPP UNITS 1 & 2 FSAR UPDATE

TABLE 3.7-80

FUEL HANDLING CRANE SUPPORT STRUCTURE
MAXIMUM ABSOLUTE ACCELERATIONS

<u>Load Case</u>	<u>Location</u>	<u>Acceleration,^(a)g</u>		
		<u>NS</u>	<u>EW</u>	<u>Vertical</u>
HE	EI 188 ft	1.7	1.6	1.1
	Columns, EI 166 ft	1.6	1.3	0.6
DE	EI 188 ft	0.8	0.5	(b)
	Columns, EI 166 ft	0.7	0.4	(b)

(a) Accelerations are average of accelerations from models 2.1 and 2.2.

(b) DE vertical equivalent static analysis coefficient is 0.13 g.

DCPP UNITS 1 & 2 FSAR UPDATE

TABLE 3.7-8P

FUEL HANDLING CRANE SUPPORT STRUCTURE
MAXIMUM RELATIVE DISPLACEMENTS

<u>Load Case</u>	<u>Location</u>	<u>Displacements^(a), in.</u>	
		<u>NS</u>	<u>EW</u>
HE	EI 188 ft	2.0	8.8
	Columns, EI 166 ft	1.8	7.1
DE	EI 188 ft	0.9	2.8
	Columns, EI 166 ft	0.9	2.3

(a) Displacements are from static analysis of detailed fuel handling crane support structure model described in Section 3.8.2.4. Displacements are relative to elevation 140 ft.

DCPP UNITS 1 & 2 FSAR UPDATE

TABLE 3.7-9

AUXILIARY BUILDING
PERIODS OF VIBRATION - DE ANALYSIS

<u>Mode No.</u>	<u>N-S Direction</u>		<u>W Direction</u>	
	<u>Period, T, (sec)</u>	<u>Translational Participation Factor</u>	<u>Period, T, (sec)</u>	<u>Translational Participation Factor</u>
1 ^(a)	0.641	0.0	0.688	8.6
2 ^(a)	0.327	8.9	0.641	0.0
3	0.073	48.1	0.072	68.7
4	0.059	48.7	0.065	0.0
5	0.037	20.0	0.040	20.6
6	0.031	1.5	0.031	0.0

(a) Steel superstructure modes (one translational and the other torsional).

DCPP UNITS 1 & 2 FSAR UPDATE

TABLE 3.7-10

AUXILIARY BUILDING HORIZONTAL MODEL
PERIODS AND PARTICIPATION FACTORS - HE ANALYSIS

Mode No.	North-South Model with 5% Eccentricity to East			North-South Model with 5% Eccentricity to West			East-West Model with 5% Eccentricity		
	Period (sec)	Translation Participation Factor		Period (sec)	Translation Participation Factor		Period (sec)	Translation Participation Factor	
1 ^(a)	.641	-0.0		.641	0.0		.688	8.6	
2 ^(a)	.327	8.9		.327	8.9		.641	0.0	
3	.070	-41.2		.075	-47.6		.074	60.2	
4	.061	54.7		.056	49.4		.062	33.2	
5	.036	-19.7		.037	-19.4		.039	-20.8	
6	.030	-3.8		.030	7.0		.030	3.1	
7	.025	-15.3		.026	14.6		.028	-17.9	
8	.024	19.6		.023	-19.2		.023	14.8	
9	.015	2.8		.016	7.8		.017	11.3	
10	.014	13.9		.014	-11.7		.014	9.0	

(a) Steel superstructure modes (one translational and the other torsional).

DCPP UNITS 1 & 2 FSAR UPDATE

TABLE 3.7-11

AUXILIARY BUILDING VERTICAL MODEL
PERIODS AND PARTICIPATION FACTORS - HE ANALYSIS

Mode Number ^(a)	Period (sec)	Participation Factor
1 ^(b)	0.085	-6.0
2	0.033	67.9

(a) Only modes below 33 Hz are listed.

(b) Steel superstructure roof mode.

DCPP UNITS 1 & 2 FSAR UPDATE

TABLE 3.7-11A

FUEL HANDLING CRANE SUPPORT STRUCTURE
HORIZONTAL MODELS FREQUENCIES OF VIBRATION^(a)

DE, DDE, AND HE ANALYSES

First ^(b) Fundamental Modal Direction	Model 2.1		Model 2.2	
	Frequency (cps)	Modal Effective Mass %	Frequency (cps)	Modal Effective Mass (%)
E-W	1.6	85.0	1.6	86.0
N-S	3.1	88.0	2.7 ^(a)	92.0

(a) For Model 2.2 see Figure 3.7-13B. Model 2.1 represents six end bay frames and is similar.

(b) Other modes have insignificant contributions, and are not included.

DCPP UNITS 1 & 2 FSAR UPDATE

TABLE 3.7-11B

FUEL HANDLING CRANE SUPPORT STRUCTURE
VERTICAL MODEL FREQUENCIES OF VIBRATION^{(a)(b)}

DE, DDE, AND HE ANALYSES

Frequency <u>(hz)</u>	<u>Model 2.1</u>	Frequency <u>(hz)</u>	<u>Model 2.2</u>
	Modal Effective Mass <u>(% of roof)</u>		Modal Effective Mass <u>(% of roof)</u>
10.6	19	10.1	23
16.9	23	16.6	26
20.7	2	22.8	1

- (a) Only significant modes with frequencies less than 33 hz are shown. For models 2.1 and 2.2, 99 modes and 105 modes were extracted, respectively, with frequencies up to 105 hz.
- (b) For model 2.2, see Figure 3.7-13B. Model 2.1 represents six end bay frames and is similar.
-

DCPP UNITS 1 & 2 FSAR UPDATE

TABLE 3.7-12

AUXILIARY BUILDING
 MAXIMUM ABSOLUTE ACCELERATIONS-DE ANALYSIS

Mass ^(a) Point	Elevation, ft	Maximum Absolute Accelerations		
		N-S Direction		E-W Direction
		Horizontal Acceleration, g	Rotational Acceleration rad/sec ²	Horizontal Acceleration, g
6	188.0	0.554	0.0004	0.313
1	163.0	0.375	0.0217	0.435
2	140.0	0.300	0.0187	0.324
3	115.0	0.259	0.0115	0.291
4	100.0	0.230	0.0055	0.257

(a) See Figure 3.7-13.

DCPP UNITS 1 & 2 FSAR UPDATE

TABLE 3.7-13

AUXILIARY BUILDING
 MAXIMUM RELATIVE DISPLACEMENTS-DE ANALYSIS

Mass ^(a) Point	Elevation, ft	Maximum Relative Displacement		
		N-S Direction		E-W Direction
		Horizontal Translation, in.	Rotation radians x 10 ⁻⁶	Horizontal Translation, in.
6	188.0	0.575	1.624	1.447
1	163.0	0.022	4.087	0.025
2	140.0	0.015	3.308	0.018
3	115.0	0.009	2.014	0.012
4	100.0	0.004	0.975	0.006

(a) See Figure 3.7-13.

DCPP UNITS 1 & 2 FSAR UPDATE

TABLE 3.7-14

AUXILIARY BUILDING
MAXIMUM STORY SHEARS-DE ANALYSIS

<u>Element^(a)</u>	Maximum Story Shears, kips x 10 ³	
	<u>N-S Direction</u>	<u>E-W Direction</u>
5	1.3	0.7
1	3.8	4.8
2	26.3	24.6
3	40.0	42.7
4	28.5	28.4

(a) See Figure 3.7-13.

DCPP UNITS 1 & 2 FSAR UPDATE

TABLE 3.7-15

AUXILIARY BUILDING
MAXIMUM OVERTURNING MOMENTS-DE ANALYSIS

<u>Element</u> ^(a)	Maximum O.T. Moments, kips - ft x 10 ⁶	
	<u>N-S Direction</u>	<u>E-W Direction</u>
5	0.06	0.04
1	0.08	0.10
2	0.74	0.68
3	1.32	1.30
4	1.76	1.74

(a) See Figure 3.7-13.

DCPP UNITS 1 & 2 FSAR UPDATE

TABLE 3.7-16

AUXILIARY BUILDING
MAXIMUM TORSIONAL MOMENTS DUE TO
EARTHQUAKE IN N-S DIRECTION-DE ANALYSIS

<u>Element^(a)</u>	<u>Maximum Torsional Moments, kip - ft x 10⁵</u>
5	0.004
1	0.265
2	14.080
3	19.810
4	9.139

(a) See Figure 3.7-13.

DCPP UNITS 1 & 2 FSAR UPDATE

TABLE 3.7-17

AUXILIARY BUILDING
 MAXIMUM ABSOLUTE ACCELERATIONS - HE ANALYSIS
 EARTHQUAKE IN N-S DIRECTION

Mass ^(a) Point	Elevation, ft	Blume-Hosgri Horizontal Acceleration, g		Newmark-Hosgri Horizontal Acceleration, g		Blume-Hosgri Rotational Acceleration, rad/sec ²		Newmark-Hosgri Rotational Acceleration, rad/sec ²	
		5% E	5% W	5% E	5% W	5% E	5% W	5% E	5% W
6	188.0	1.57	1.56	1.37	1.36	-	-	-	-
1	163.0	1.13	1.10	1.25	1.21	.0981	.1477	.1102	.1646
2	140.0	0.84	0.77	0.90	0.84	.0604	.0895	.0710	.1018
3	115.0	0.71	0.70	0.72	0.66	.0370	.0516	.0431	.0590
4	100.0	0.67	0.66	0.58	0.61	.0175	.0239	.0206	.0275

(a) See Figure 3.7-13.

DCPP UNITS 1 & 2 FSAR UPDATE

TABLE 3.7-18

AUXILIARY BUILDING
 MAXIMUM ABSOLUTE ACCELERATIONS - HE ANALYSIS
 EARTHQUAKE IN E-W DIRECTION

Mass ^(a) Point	Elevation, ft	Blume-Hosgri Horizontal Acceleration, g	Newmark-Hosgri Horizontal Acceleration, g	Blume-Hosgri Rotational Acceleration, rad/sec ²	Newmark-Hosgri Rotational Acceleration, rad/sec ²
6	188.0	1.11	1.24	.0015	.0017
1	163.0	1.11	1.22	.1162	.1292
2	140.0	0.94	1.00	.0769	.0881
3	115.0	0.72	0.75	.0452	.0527
4	100.0	0.66	0.62	.0213	.0246

(a) See Figure 3.7-13.

DCPP UNITS 1 & 2 FSAR UPDATE

TABLE 3.7-19

AUXILIARY BUILDING
 MAXIMUM RELATIVE DISPLACEMENTS - HE ANALYSIS
 EARTHQUAKE IN N-S DIRECTION

Mass ^(a) Point	Elevation, ft	Blume-Hosgri Horizontal Translation, in.		Newmark-Hosgri Horizontal Translation, in.		Blume-Hosgri Rotation radians x 10 ⁻⁶ 5% E		Newmark-Hosgri Rotation radians x 10 ⁻⁶ 5% E	
		5% E	5% W	5% E	5% W	5% E	5% W	5% E	5% W
6	188.0	1.63	1.62	1.42	1.42	-	-	-	-
1	163.0	0.06	0.06	0.06	0.07	9.589	18.901	10.961	21.001
2	140.0	0.04	0.04	0.04	0.04	8.034	14.091	9.135	15.472
3	115.0	0.02	0.02	0.02	0.02	4.785	8.530	5.468	9.361
4	100.0	0.01	0.01	0.01	0.01	2.256	4.044	2.576	4.444

(a) See Figure 3.7-13.

DCPP UNITS 1 & 2 FSAR UPDATE

TABLE 3.7-20

AUXILIARY BUILDING
 MAXIMUM RELATIVE DISPLACEMENTS - HE ANALYSIS
 EARTHQUAKE IN E-W DIRECTION

Mass ^(a) Point	Elevation, ft	Blume-Hosgri Horizontal Translation, in.	Newmark-Hosgri Horizontal Translation in.	Blume-Hosgri Rotation radians x 10 ⁻⁶	Newmark-Hosgri Rotation radians x 10 ⁶
6	188.0	5.08	5.63	6.153	6.897
1	163.0	0.07	0.07	14.616	16.354
2	140.0	0.05	0.05	11.219	12.484
3	115.0	0.03	0.03	7.078	7.873
4	100.0	0.02	0.02	3.471	3.854

(a) See Figure 3.7-13.

DCPP UNITS 1 & 2 FSAR UPDATE

TABLE 3.7-21

AUXILIARY BUILDING
MAXIMUM STORY SHEARS - HE ANALYSIS

Element ^(a)	Earthquake in N-S Direction				Earthquake in E-W Direction			
	Blume-Hosgri		Newmark-Hosgri		Blume-Hosgri		Newmark-Hosgri	
	5% E	5% W	5% E	5% W	5% E	5% W	5% E	5% W
5	3.6	3.6	3.2	3.2	2.6	2.6	2.9	2.9
1	12.4	12.4	13.7	13.6	12.3	12.3	13.6	13.6
2	65.6	58.4	71.9	63.3	71.0	71.0	76.2	76.2
3	106.2	100.0	115.2	101.5	115.0	115.0	122.5	122.5
4	84.5	86.7	90.2	85.8	75.8	75.8	80.2	80.2

(a) See Figure 3.7-13.

DCPP UNITS 1 & 2 FSAR UPDATE

TABLE 3.7-22

AUXILIARY BUILDING
MAXIMUM OVERTURNING MOMENTS - HE ANALYSIS

Element ^(a)	Earthquake in N-S Direction			Earthquake in E-W Direction		
	Blume-Hosgri Moment kips x 10 ⁶		Newmark-Hosgri Moment kips x 10 ⁶	Blume-Hosgri Moment kips x 10 ⁶		Newmark-Hosgri Moment kips x 10 ⁶
	5% E	5% W	5% E	5% W	±5%	±5%
5	0.18	0.17	0.15	0.15	0.12	0.14
1	0.27	0.27	0.30	0.29	0.27	0.29
2	1.85	1.66	2.05	1.74	1.96	2.11
3	3.41	3.12	3.73	3.21	3.65	3.90
4	4.68	4.42	5.11	4.46	4.80	5.15

(a) See Figure 3.7-13.

DCPP UNITS 1 & 2 FSAR UPDATE

TABLE 3.7-23

AUXILIARY BUILDING
MAXIMUM TORSIONAL MOMENTS - HE ANALYSIS

Element ^(a)	Earthquake in N-S Direction			Earthquake in E-W Direction		
	Blume-Hosgri		Newmark-Hosgri	Blume-Hosgri		Newmark-Hosgri
	Torsional Moment kips x 10 ⁵	5% W	Torsional Moment kips x 10 ⁵	Torsional Moment kips x 10 ⁵	Torsional Moment kips x 10 ⁵	Torsional Moment kips x 10 ⁵
5	0.01	0.02	0.01	0.01	0.01	0.02
1	0.82	1.71	0.89	1.88	1.30	1.45
2	35.36	60.41	39.93	66.53	44.98	50.14
3	48.24	85.27	55.16	93.73	68.81	76.67
4	21.14	38.00	24.14	41.73	32.59	36.19

(a) See Figure 3.7-13.

DCPP UNITS 1 & 2 FSAR UPDATE

TABLE 3.7-23A

Sheet 1 of 2

TURBINE BUILDING HORIZONTAL MODEL (LOADED CRANE CASE 2)^(a)
 FREQUENCIES OF VIBRATION^(b) - HE ANALYSIS^(d)

Mode No.	Frequency Hz	Participation Factor	
		North-South	East-West
1 ^(c)	1.39	0.00	3.01
4 ^(c)	3.32	2.59	0.00
18	5.81	-4.75	0.77
19	5.86	-0.02	-3.32
21	6.03	-0.32	-2.29
22	6.19	0.76	-2.60
23	6.37	-1.16	0.81
24	6.43	-2.66	-0.66
26	6.78	0.24	-1.74
27	7.10	-2.02	0.50
28	7.18	1.08	-1.32
29	7.32	-2.13	0.62
30	7.36	1.02	-0.03
31	7.43	-1.51	-0.61
32	7.57	0.44	-2.59
33	7.62	1.83	1.42
36	7.99	-2.04	-0.95
38	8.32	-1.70	-0.94
39	8.38	-3.16	-0.70
40	8.47	2.47	1.17
44	9.09	0.30	-1.78
56	10.71	0.28	-1.54
65	11.52	1.54	-0.14
82	13.10	-0.39	2.02
83	13.15	0.29	-1.43
89	14.02	0.01	1.79
92	14.32	-0.11	1.87
93	14.78	0.33	1.04
100	16.60	-0.31	1.54
101	16.74	0.13	2.00
102	16.81	0.52	-1.78
103	17.03	1.65	-0.22
104	17.26	-1.46	-0.54
111	18.16	0.12	1.11
115	18.93	-1.68	-0.10
147	22.29	1.00	-0.41
165	23.89	-0.89	0.49

DCPP UNITS 1 & 2 FSAR UPDATE

TABLE 3.7-23A

Sheet 2 of 2

-
- (a) For Case 2, the Unit 1 crane has a 15-ton load and is located at column line 9, and the Unit 2 crane has a 50-ton load and is located at column line 12.2.
- (b) 210 modes were extracted with frequencies ranging from 1.39 Hz to 33.01 Hz. Shown above are the modes with the twenty highest participation factors in each direction. The cumulative modal masses of the 210 modes represent 95% of the total weight of the building.
- (c) Modes 1 and 4 are the principal modes of the superstructure.
- (d) Note that the results in this table correspond with the seismic analysis performed for the operating license review (Reference 18) and may not reflect the latest as-built configuration of the turbine building.
-

DCPP UNITS 1 & 2 FSAR UPDATE

TABLE 3.7-23B

TURBINE BUILDING VERTICAL MODEL NO. 1
 FREQUENCIES OF VIBRATION^(a) - HE ANALYSIS^(c)

Mode No.	Frequency Hz	Participation Factor
1 ^(b)	2.80	0.65
2 ^(b)	2.80	0.38
5 ^(b)	5.07	-0.48
15	7.48	2.00
17	7.75	-1.55
21	8.71	1.04
23	9.16	-0.55
33	10.70	-0.40
35	10.87	0.52
40	11.38	0.53
54	13.34	-0.36
59	14.02	0.43
61	14.23	0.57
62	14.40	0.31
63	14.46	-0.87
64	14.56	0.28
78	16.68	0.30
83	17.36	-0.65
89	18.29	0.48
115	22.03	-0.29

(a) 187 modes were extracted, ranging from 2.80 Hz to 33.01 Hz. Shown above are the modes with the 20 highest participation factors. The cumulative modal mass of the 187 modes represents 94% of the total weight of the building.

(b) Modes 1, 2, and 5 represent significant modes for the superstructure and overhead crane.

(c) Note that the results in this table correspond to the seismic analysis performed for the operating license review (Reference 18) and may not reflect the latest as-built configuration of the turbine building.

TABLE 3.7-23C

TURBINE BUILDING MODEL
LOADED CRANE CASES
MAXIMUM ABSOLUTE ACCELERATIONS - HE ANALYSIS^(b)

Elevation, ft	Location		Acceleration ^(a) , g		
			N-S	E-W	Vertical
104 & 107	1 to 5	A-G	--	1.16	1.54
	5 to 15	A-G	--	1.18	1.99
	15 to 17	A-G	--	1.06	2.49
	17 to 19	A-G	--	1.11	--
	1 to 19	A-G	1.22	--	--
119 & 123	1 to 5	A-G	--	1.84	2.16
	5 to 15	A-G	--	2.08	2.35
	15 to 17	A-G	--	1.83	2.43
	17 to 19	A-G	--	1.68	1.30
	1 to 19	A-G	2.20	--	--
140	1 to 5	A-G	--	1.37	1.68
	5 to 15	A-G	--	2.19	1.91
	15 to 17	A-G	--	1.24	1.29
	17 to 19	A-G	--	1.11	1.32
	1 to 19	A-G	1.91	--	--
159	1.9 to 4.8	G	--	1.29	0.73
	5.7 to 15	G	--	2.51	0.70
	16 to 19	G	--	1.51	0.59
	1.9 to 19	G	1.57	--	--
193	1.9 to 4.8	A, G	--	--	0.91
	5.7 to 15	A, G	--	--	0.70
	16 to 19	A, G	--	--	0.59
Roof	1 to 1.9	A-D	3.97	1.60	

-
- (a) Acceleration values are zero period accelerations of floor response spectra. At and below elevation 140 feet, values are for the case of a single unloaded crane; values for the case of two cranes with one crane loaded are similar.
- (b) Note that the results in this table correspond to the seismic analysis performed for the operating license review (Reference 18) and may not reflect the latest as-built configuration of the turbine building.
-

DCPP UNITS 1 & 2 FSAR UPDATE

TABLE 3.7-23D

TURBINE BUILDING MODELS
 LOADED CRANE CASES
 MAXIMUM RELATIVE DISPLACEMENTS - HE ANALYSIS^(b)

Elevation, ft	Location		Displacement ^(a) , in.		
	Bent	Line	N-S	E-W	Vertical
104 & 107	1 to 5	A-G	0.08	0.07	0.25
	5 to 15	A-G	0.07	0.16	0.75
	15 to 17	A-G	0.04	0.13	1.31
	17 to 19	A-G	0.06	0.68	--
119, 123, & 125	1 to 5	A-G	0.25	0.23	0.52
	5 to 15	A-G	0.60	0.42	0.82
	15 to 17	A-G	0.80	0.35	0.62
	17 to 19	A-G	0.90	1.02	0.45
140	1 to 5	A-G	0.22	0.18	0.37
	5 to 15	A-G	0.20	0.58	0.03
	15 to 17	A-G	0.20	0.28	0.13
	17 to 19	A-G	0.20	0.83	0.42
159	1 to 5	G	0.42	2.06	0.39
	5 to 15	G	0.42	3.22	0.31
	15 to 17	G	0.41	2.97	0.06
	17 to 19	G	0.42	3.98	--
193	1 to 5	A-G	1.92	5.89	0.13
	5 to 15	A-G	1.09	8.76	0.05
	15 to 17	A-G	1.21	9.64	0.08
	17 to 19	A-G	1.32	11.46	--
Roof	1 to 1.9	A-D	2.60	3.64	--

(a) Displacement values are based on response spectrum analysis.

(b) Note that the results in this table correspond to the seismic analysis performed for the operating license review (Reference 18) and may not reflect the latest as-built configuration of the turbine building.

DCPP UNITS 1 & 2 FSAR UPDATE

TABLE 3.7-23E

TURBINE PEDESTAL MODEL
 FREQUENCIES OF VIBRATION^(a) - HE ANALYSIS

Mode No.	Frequency (Hz)	Participation Factor		
		N-S	E-W	Vertical
1	3.09	--	27.2	--
2	3.54	--	3.6	--
3	4.23	27.6	--	0.4
11	15.14	0.3	--	-14.1
12	15.96	-0.3	--	8.0
23	20.94	-0.5	--	12.1
25	21.69	--	--	-9.1
27	22.06	--	4.0	--
30	23.36	-0.2	--	-8.0
36	26.11	--	-3.4	--
45	30.34	2.1	--	2.2
46	30.54	2.4	--	-5.2
47	30.94	-2.7	--	4.0
49	31.89	-3.5	--	3.0
50	32.14	--	2.7	--

(a) 50 modes were extracted, ranging in frequency from 3.09 Hz to 32.14 Hz. Shown above are the modes with the five highest participation factors for each direction.

DCPP UNITS 1 & 2 FSAR UPDATE

TABLE 3.7-23F

TURBINE PEDESTAL MODEL
MAXIMUM RELATIVE DISPLACEMENTS - HE ANALYSIS

Nodal Point ^(a)	North-South Direction (in.)	East-West Direction (in.)	Vertical Direction (in.)
9	.71	1.30	0.006
35	.73	1.22	0.006
58	.74	1.40	0.006
81	.75	1.63	0.006
102	.76	1.59	0.005
123	.76	1.67 ^(c)	0.005

(a) Nodal points are identified in Figure 3.7-15G.

(b) Vertical displacement includes dead load displacement.

(c) Effects of load redistribution are included.

DCPP UNITS 1 & 2 FSAR UPDATE

TABLE 3.7-23G

SIGNIFICANT PERIODS OF VIBRATION AND PERCENT PARTICIPATION FACTORS
INTAKE STRUCTURE

Mode Number	North-South Model		Period (sec)	East-West Vertical Model		Vertical Percent Participation Factor
	Period (sec)	Percent Participation Factor		East-West Percent Participation Factor	Vertical Percent Participation Factor	
2	0.081	0.5	0.081	0.0	0.1	
3	0.081	0.1	0.081	0.0	0.0	
4	0.081	0.2	0.081	0.0	0.0	
5	0.080	1.1	0.080	0.0	0.0	
6	0.079	2.5	0.079	0.0	0.3	
7	0.078	0.8	0.078	0.0	0.1	
9	0.069	0.1	0.065	0.1	0.1	
10	0.066	2.1	0.065	0.4	0.0	
11	0.065	3.5	0.064	0.2	0.0	
12	0.064	0.2	0.064	0.0	0.0	
13	0.064	0.4	0.064	0.0	0.0	
14	0.064	0.0	0.064	0.0	0.0	
15	0.064	0.2	0.063	0.4	0.1	
17	0.063	0.0	0.063	0.1	0.1	
18	0.063	0.3	0.062	0.4	0.0	
19	0.060	0.7	0.060	0.1	0.9	
21	0.049	0.8	0.049	1.7	0.7	
22	0.049	1.4	0.048	2.1	0.6	
23	0.048	1.1	0.048	0.3	0.0	
24	0.047	2.7	0.047	2.4	0.6	
25	0.047	2.1	0.046	3.4	1.4	
33	0.034	1.4	0.033		7.4	
35	0.032	1.6	0.032	3.0	5.4	
36	0.031	3.4	0.031	1.3	4.7	

DCPP UNITS 1 & 2 FSAR UPDATE

TABLE 3.7-23H

MAXIMUM RELATIVE DISPLACEMENTS AND
MAXIMUM ABSOLUTE ACCELERATIONS (HOSGRI)
INTAKE STRUCTURE

Nodal Point ^(a)	Elevation (ft)	North-South Displacement (in.)	East-West Displacement (in.)	Vertical Displacement (in.)	North-South Acceleration (g)	East-West Acceleration (g)	Vertical Acceleration (g)
330	+32.0	0.025	0.044	0.010	2.36	2.15	0.65
312	+24.4	0.016	0.029	0.008	1.50	1.55	0.65
71	+17.5	0.120	0.011	0.010	1.58	0.66	0.61
73	+17.5	0.065	0.011	0.007	0.94	0.66	0.54
74	+17.5	0.058	0.011	0.005	0.85	0.66	0.51
284	+17.5	0.009	0.019	0.007	0.64	1.00	0.62
363	+11.0	0.008	0.012	0.003	0.64	0.87	0.54
80	-2.1	0.133	0.007	0.010	1.71	0.70	0.59
83	-2.1	0.066	0.005	0.006	0.98	0.71	0.52
87	-16.8	0.251	0.003	0.005	3.14	0.72	0.52
89	-16.8	0.050	0.002	0.003	1.12	0.73	0.50

(a) See Figure 3.7-15F.

DCPP UNITS 1 & 2 FSAR UPDATE

TABLE 3.7-23I

OUTDOOR WATER STORAGE TANKS
SUMMARY OF SIGNIFICANT PERIODS AND PERCENT PARTICIPATION FACTORS
REFUELING WATER STORAGE TANK

Mode No.	Period (sec)	Modal Participation Factor %
1	0.132	50.7
2	0.052	22.6

DCPP UNITS 1 & 2 FSAR UPDATE

TABLE 3.7-23J

OUTDOOR WATER STORAGE TANKS
SUMMARY OF SIGNIFICANT PERIODS AND PERCENT PARTICIPATION FACTORS
FIREWATER AND TRANSFER TANK

<u>Mode No.</u>	<u>Load Case 1^(a)</u>		<u>Load Case 2^(b)</u>	
	<u>Period (sec.)</u>	<u>Modal Participation Factor %</u>	<u>Period (sec.)</u>	<u>Modal Participation Factor %</u>
1	0.12124	54.91	0.1234	48.4
2	0.04985	21.26	0.06318	6.21

(a) Load Case 1: Inner and outer tanks are filled with water up to design level

(b) Load Case 2: Inner tank is filled to design level, outer tank is empty

DCPP UNITS 1 & 2 FSAR UPDATE

Table 3.7-24

FUNDAMENTAL MODE FREQUENCY RANGES
FOR RCL PRIMARY EQUIPMENT

	<u>Frequency, Hz</u>
Steam Generator	6.7 – 9.0
Reactor coolant pump	6.7 - 7.2
Reactor pressure vessel	16.8 - 17.0
